Edited by P. Andrew Evans

WILEY-VCH

Modern Rhodium-Catalyzed Organic Reactions

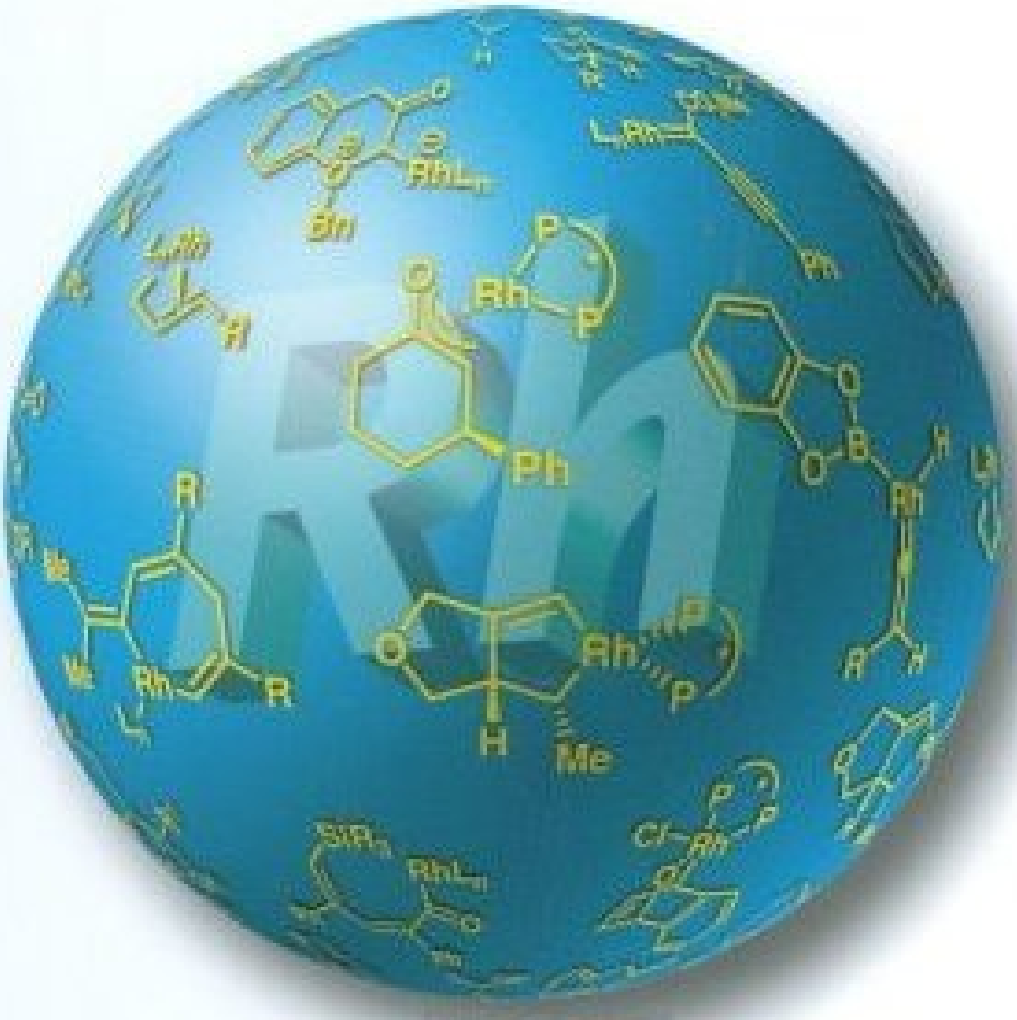

Modern Rhodium-Catalyzed Organic Reactions

Edited by
P. Andrew Evans

Modern Rhodium-Catalyzed Organic Reactions. Edited by P. Andrew Evans

ISBN: 3-527-30683-8

Further Reading from WILEY-VCH

S.-I. Murahashi (Ed.)

Ruthenium in Organic Synthesis

2004. ISBN 3-527-30692-7

M. Beller, C. Bolm (Eds.)

Transition Metals for Organic Synthesis
2nd Edition, 2 Volumes

2004. ISBN 3-527-30613-7

A. de Meijere, F. Diederich (Eds.)

Metal-Catalyzed Cross-Coupling Reactions
2nd Edition, 2 Volumes

2004. ISBN 3-527-30518-1

R. Mahrwald (Ed.)

Modern Aldol Reactions
2 Volumes

2004. ISBN 3-527-30714-1

Modern Rhodium-Catalyzed Organic Reactions

Edited by
P. Andrew Evans

WILEY-VCH Verlag GmbH & Co. KGaA

Editor:

Prof. P. Andrew Evans
Department of Chemistry
Indiana University
Bloomington, IN 47405
USA

Library of Congress Card No.: applied for
A catalogue record for this book is available from the British Library.

Bibliographic information published by Die Deutsche Bibliothek
Die Deutsche Bibliothek lists this publication in the Deutsche Nationalbibliografie; detailed bibliographic data is available in the Internet at http://dnb.ddb.de.

Printed in the Federal Republic of Germany
Printed on acid-free paper

Typesetting K+V Fotosatz GmbH, Beerfelden
Printing Strauss GmbH, Mörlenbach
Bookbinding Buchbinderei J. Schäffer GmbH & Co. KG, Grünstadt

ISBN-13: 978-3-527-30683-1

ISBN-10: 3-527-30683-8

To Rebecca and Sarah

Foreword

The extensive application of transition metal-catalysts to organic synthesis over the last 40 years has dramatically changed the manner in which organic compounds are now prepared. Among the many transition metal-catalysts used in organic synthesis, the noble metal triad, namely palladium, ruthenium and rhodium, has played an increasingly important role in this regard. Hence, it is not an exaggeration to say that the present day is the golden age of these noble metals, which of course have their own characteristic features. Currently, palladium represents the most widely used and versatile metal, given its synthetic utility for carbon-carbon and carbon-heteroatom bond formation. More recently, ruthenium-catalysts have provided exquisite functional group tolerance and selectivity in olefin metathesis and the asymmetric hydrogenation of carbonyl compounds.

Organorhodium chemistry on the other hand has a long history, which dates back to its emergence as the metal of choice in carbonylation processes. Historically, commercial hydroformylation was carried out using a cobalt carbonyl complex as the catalyst. However, this catalyst was gradually replaced by a more active rhodium catalyst, which remains the one predominantly utilized today. A noteworthy example is the Monsanto process, which is a rhodium-catalyzed carbonylation reaction that was developed in early 1970's for the production of acetic acid from methyl iodide. The discovery of the Wilkinson complex by Wilkinson in the mid 1960's proved to be the harbinger of the development of modern organorhodium chemistry, since its discovery opened the new field of homogeneous hydrogenation. This development ultimately led to the remarkable progress in asymmetric hydrogenation, as exemplified by the commercial production of L-Dopa by a rhodium-catalyzed asymmetric hydrogenation developed in 1974 by Monsanto. Notwithstanding the early developments in hydroformylation and the discovery of the Wilkinson complex, progress in organorhodium chemistry seemed to be somewhat slower than that of organopalladium chemistry. Nonetheless, organorhodium chemistry is now rapidly emerging in organic synthesis as the number of useful synthetic methods increases. A number of new rhodium-catalyzed reactions, including several new types of cycloadditions have been discovered, offering unique synthetic methods that are often complimentary to those of palladium and ruthenium. More recent advances have come from the rhodium-catalyzed decomposition of diazo compounds to generate metal carbenoids, which in the presence of alkenes afford cyclopropanes and other derivatives. Indeed, these studies have paved the way for the recent advances in C–H activation, which facilitates the selective formation of carbon-carbon and carbon-nitrogen bonds.

Modern Rhodium-Catalyzed Organic Reactions. Edited by P. Andrew Evans

ISBN: 3-527-30683-8

Although numerous rhodium-catalyzed reactions have now been reported, frankly speaking it has been somewhat difficult to often categorize them in a systematic manner. From this standpoint, a book that summarizes the newer aspects of modern organorhodium chemistry is clearly overdue. The publication of this book, edited by Professor P. Andrew Evans, is both timely and worthwhile. The editor, in the first attempt to summarize the field of organorhodium chemistry, brings together nearly twenty topics, covering almost all known aspects of rhodium-catalyzed reactions. This book covers the following asymmetric rhodium-catalyzed organic reactions: hydrogenation (Zhang), hydroboration (Brown), conjugate addition (Hayashi), olefin isomerization and hydroacylation (Fu), hydroformylation, hydrosilylation and silylformylation (Leighton and Matsuda), cycloisomerization and cyclotrimerization (Ojima), Alder-ene (Brummond), allylic substitution (Evans and Fagnou), carbocyclizations (Jeong, Robinson and Wender), cyclopropanation and carbon-hydrogen insertion (Davies, Doyle and Taber), oxidative amination (Du Bois), ylide rearrangements (West), 1,3-dipolar cycloadditions (Austin), in which each of the chapters is clearly written by an expert in the field.

Overall, this book clearly illustrates "what we can do in organic synthesis using rhodium catalysis" and I have no doubt that it will serve as an excellent reference text for both graduate students and synthetic chemists at all levels in academia and industry. Moreover, I anticipate that this book will stimulate additional research in the area of organorhodium chemistry, and serve to inspire those involved in the development and application of new synthetic methodology.

November 2004

Jiro Tsuji
Professor Emeritus
Tokyo Institute of Technology

Preface

Although there are countless examples of rhodium-catalyzed organic reactions in the chemical literature, it is often very difficult to categorize and thereby appreciate the full impact of this transition metal within the context of target directed synthesis. *Modern Rhodium-Catalyzed Organic Reactions* provides the first comprehensive account of some of the most exciting and seminal advances in this rapidly developing field, and also serves as a historical guide to the origin of many of these impressive advances. I have tried to match internationally recognized scholars within each of the individual areas covered, while trying to be as inclusive as possible, to provide a fairly comprehensive overview of the field. However, as with any project of this nature, there are additional topics that could have been included. This book represents the contributions that utilize two of the most common oxidation states, namely rhodium(I) and (II), as catalysts and pre-catalysts for synthetic applications.

The chapters highlight the synthetic utility of the various transformations, covering each reaction from inception to its development as a synthetically useful process that is capable of achieving exquisite selectivity with excellent efficiency. Throughout each chapter the authors describe rhodium-catalyzed reactions in terms of the scope, selectivity, and mechanism, thereby providing important insight into each transformation. I think it is fair to say that many of these contributions are quite unique since they have not been previously reviewed. Moreover, the most striking feature of each contribution is the underlying difference in chemical reactivity of the rhodium-catalyzed version of a specific transformation to that involving an alternative metal-complex. Indeed, having read all the chapters the reader is left with the notion that rhodium-catalysis is unique, since it provides unparalleled levels of chemo-, regio- and stereoselectivity for many synthetic reactions. The chapters also provide a brief summary and outlook for the continued development of each of the transformations, which will be helpful to individuals already active in this area as well as those planning on breaking into the field. It is my hope that this book will provide an excellent resource for graduate students, and be a suitable reference text for a graduate level course. I also believe that this book will serve practicing synthetic chemists in academia and industry, by providing an up-to-date account of the field that given the current state-of-the-art will provide an indication of where the specific challenges remain.

I would like to dedicate this book to my loving daughters Rebecca and Sarah, in the hope that they will one day understand all the hard work required to provide a wonderful life full of opportunities. I also acknowledge my parents for their unwavering strength and encouragement to pursue my dreams irrespective of the outcome.

Modern Rhodium-Catalyzed Organic Reactions. Edited by P. Andrew Evans

ISBN: 3-527-30683-8

I would like to sincerely thank David K. Leahy, Erich W. Baum, and Santosh J. Gharpure for their assistance with the proofreading of the various chapters. I would especially like to thank and acknowledge the efforts of James R. Sawyer, who gave a significant amount of his time to painstakingly assist in the editing of the manuscript. I sincerely thank Katie for her love, support and understanding throughout what was often a very difficult time. Finally, this book would not have be possible without the participation of the authors; I am deeply indebted to each of them for taking the time out of their busy schedules, and their enduring patience throughout this project.

November 2004 *P. Andrew Evans*

Contents

Modern Rhodium-Catalyzed Organic Reactions. Edited by P. Andrew Evans

ISBN: 3-527-30683-8

List of Contributors

David J. Austin
Yale University
Department of Chemistry
225 Prospect Street
New Haven, CT 06520
USA

John M. Brown
University of Oxford
Chemical Research Center
Oxford OX1 3TA
United Kingdom

Kay M. Brummond
University of Pittsburgh
Department of Chemistry
Pittsburgh, PA 15260
USA

Yongxiang Chi
Pennsylvania State University
Department of Chemistry
104 Chemistry Building
University Park, PA 16802
USA

Huw M. L. Davies
State University of New York
University at Buffalo
Department of Chemistry
Buffalo, NY 14260-3000
USA

Michael P. Doyle
University of Maryland
Department of Chemistry
and Biochemistry
College Park, MD 20742
USA

Justin Du Bois
Stanford University
Department of Chemistry
Stanford, CA 94305-5080
USA

Christine G. Espino
Stanford University
Department of Chemistry
Stanford, CA 94305-5080
USA

P. Andrew Evans
Indiana University
Department of Chemistry
800 E. Kirkwood Avenue
Bloomington, IN 47405
USA

Keith Fagnou
University of Ottawa
Department of Chemistry
10 Marie Curie
Ottawa, Ontario K1N 6N5
Canada

Modern Rhodium-Catalyzed Organic Reactions. Edited by P. Andrew Evans

ISBN: 3-527-30683-8

Gregory C. Fu
Massachusetts Institute of Technology
Department of Chemistry
77 Massachusetts Avenue
Cambridge, MA 02139
USA

Masaki Fujiwara
Central Glass Co., Ltd.
Chemical Research Center
2805 Imafuku-Nakadai Kawagoe-shi
Saitama 350-1151
Japan

Gabriel G. Gamber
Stanford University
Department of Chemistry
121 S.G. Mudd
Stanford, CA 94305-5080
USA

Tamio Hayashi
Kyoto University
Graduate School of Science
Department of Chemistry
Sakyo, Kyoto 606-8502
Japan

Nakcheol Jeong
Korea University
Department of Chemistry
310 Asan Science Building
Seoul 136-701
Korea

Pramod V. Joshi
University of Delaware
Department of Chemistry
and Biochemistry
Newark, DE 19716
USA

David K. Leahy
Bristol-Myers Squibb
One Squibb Drive
New Brunswick, NJ 08903
USA

James L. Leighton
Columbia University
Department of Chemistry
3000 Broadway, Mail Code 3117
New York, NY 10027
USA

Isamu Matsuda
Nagoya University
Graduate School of Engineering
Chikusa, Nagoya 464-8603
Japan

Jamie M. McCabe
University of Pittsburgh
Department of Chemistry
Pittsburgh, PA 15260
USA

Iwao Ojima
State University of New York
Department of Chemistry
Stony Brook, NY 11794
USA

John E. Robinson
Array BioPharma
3200 Walnut Street
Boulder CO 80301
USA

Ruben M. Savizky
Yale University
Department of Chemistry
225 Prospect Street
New Haven, CT 06520
USA

Douglass F. Taber
University of Delaware
Department of Chemistry
and Biochemistry
Newark, DE 19716
USA

Wenjun Tang
Scripps Research Institute
Department of Chemistry
10550 North Torrey Pines Road
La Jolla, CA 92037
USA

Abbas M. Walji
State University of New York
University at Buffalo
Department of Chemistry
Buffalo, NY 14260-3000
USA

Paul A. Wender
Stanford University
Department of Chemistry
121 S.G. Mudd
Stanford, CA 94305-5080
USA

Frederick G. West
University of Alberta
Department of Chemistry
W5-67 Gunning-Lemieux Chemistry
Centre
Edmonton, Alberta T6G 1T7
Canada

Travis J. Williams
Stanford University
Department of Chemistry
121 S.G. Mudd
Stanford, CA 94305-5080
USA

Kazuhiro Yoshida
Chiba University
Faculty of Science
Department of Chemistry
Yayoi-cho, Ingae-ku, Chiba 263-8522
Japan

Xumu Zhang
Pennsylvania State University
Department of Chemistry
104 Chemistry Building
University Park, PA 16802
USA

1
Rhodium-Catalyzed Asymmetric Hydrogenation

Yongxiang Chi, Wenjun Tang, and Xumu Zhang

1.1
Introduction

Molecular chirality plays a very important role in science and technology. For example, the biological activity of many pharmaceuticals and agrochemicals is often associated with a single enantiomer. The increasing demand for enantiomerically pure pharmaceuticals, agrochemicals, and fine chemicals has therefore driven the development of asymmetric catalytic technologies [1, 2]. Asymmetric hydrogenation, using molecular hydrogen to reduce prochiral olefins, ketones, and imines, has become one of the most efficient, practical, and atom-economical methods for the construction of chiral compounds [3]. During the last few decades of the 20th century, significant attention was devoted to the discovery of new asymmetric catalysts, in which transition metals bound to chiral phosphorous ligands have emerged as preferential catalysts for asymmetric hydrogenation. Thousands of efficient chiral phosphorous ligands with diverse structures have been developed, and their application to asymmetric hydrogenation has been established. Indeed, many represent the key step in industrial processes for the preparation of enantiomerically pure compounds. The immense significance of asymmetric hydrogenation was recognized when the Nobel Prize in Chemistry was awarded to Knowles and Noyori.

In this chapter, we focus on the rhodium-catalyzed hydrogenation and the development of chiral phosphorous ligands for this process. Although there are other chiral phosphorous ligands, which are effective for ruthenium-, iridium-, platinum-, titanium-, zirconium-, and palladium-catalyzed hydrogenation, they are not discussed in this account. However, this does not preclude complexes of other transition metals as effective catalysts for asymmetric hydrogenation. Fortunately, there are numerous reviews and books that discuss this particular aspect of asymmetric hydrogenation [3].

1.2
Chiral Phosphorous Ligands

The invention of efficient chiral phosphorous ligands has played a critical role in the development of asymmetric hydrogenation. To a certain extent, the development of asymmetric hydrogenation parallels that of chiral phosphorous ligands.

Modern Rhodium-Catalyzed Organic Reactions. Edited by P. Andrew Evans

ISBN: 3-527-30683-8

The introduction of Wilkinson's homogeneous hydrogenation catalyst, $[RhCl(PPh_3)_3]$ [4], prompted the development of the analogous asymmetric hydrogenation by Knowles [5] and Horner [6] using chiral monodentate phosphine ligands, albeit with poor enantioselectivity. Kagan and Knowles each demonstrated that improved enantioselectivities could be obtained using bidentate chiral phosphine ligands. For example, Kagan and Knowles independently reported the C_2-symmetric bisphosphine ligands, DIOP [7] and DIPAMP [8], for rhodium-catalyzed asymmetric hydrogenation. Due to its high catalytic efficiency in rhodium-catalyzed asymmetric hydrogenation of dehydroamino acids, DIPAMP was employed in the industrial production of L-DOPA [9]. Subsequently to this work, several other successful chiral phosphorous ligands were developed, as exemplified by Kumada's ferrocene ligand BPPFOH [10] and Achiwa's BPPM ligand [11].

The mechanism of the asymmetric hydrogenation is fairly well established, due to the seminal work of Halpern [12] and Brown [13]. Indeed, much of the early work in this area focused on the development of chiral rhodium catalysts, rather than expanding the reaction's substrate scope, which was limited to α-dehydroamino acids. In 1980, Noyori and Takaya reported an atropisomeric C_2-symmetric bisphosphine ligand, BINAP [14, 15]. This ligand was first used in rhodium-catalyzed asymmetric hydrogenation of α-(acylamino)acrylic acids, in which high selectivities were reported for certain substrates [16]. The discovery that the Ru–BINAP system could efficiently and selectively affect the asymmetric hydrogenation of various functionalized olefins [17], functionalized ketones [18], and unfunctionalized ketones [19] led to the development of other atropisomeric biaryl bisphosphine ligands, as exemplified by Miyashita's BICHEP ligand [20] and Schmid's BIPHEMP/MeO-BIPHEP [21, 22] ligands.

Achiwa has successfully developed the modified DIOP ligands, MOD-DIOP and Cy-DIOP, by varying their electronic and steric properties; MOD-DIOP was applied to the asymmetric hydrogenation of itaconic acid derivatives with up to 96% enantioselectivity [23]. A series of modified BPPM ligands such as BCPM and MCCPM were also developed by Achiwa [24], and some excellent chiral 1,2-bisphosphane ligands such as NORPHOS [25] and PYRPHOS (DEGUPHOS) [26] have been developed for the rhodium-catalyzed asymmetric hydrogenation. Several 1,3-bisphosphane ligands, such as BDPP (SKEWPHOS) [27], have been prepared and examined.

Hayashi and Ito developed the (aminoalkyl)ferrocenylphosphine ligand **L1**, which was successfully applied to the rhodium-catalyzed hydrogenation of trisubstituted acrylic acids [28]. In the early 1990s, significant progress was achieved with the application of the chiral bisphosphorous ligands, DuPhos and BPE developed by Burk *et al.* [29, 30], to the enantioselective hydrogenation of α-(acylamino)acrylic acids, enamides, enol acetates, β-keto esters, unsaturated carboxylic acids, and itaconic acids. Scheme 1.1 shows the several important chiral phosphine ligands studied before the early 1990s.

Inspired by the excellent results of chiral ligands such as BINAP and DuPhos, many research groups have devoted their efforts to designing and discovering new efficient and selective chiral phosphorous ligands. A major feature in the design of the new chiral phosphorus ligands is the ability to tune the steric and electronic properties of ligands within a given scaffold. These new ligands, which have proven efficient and selective for the asymmetric rhodium-catalyzed hydrogenation, can be divided into several different categories.

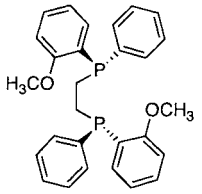

(*S*,*S*)-DIPAMP

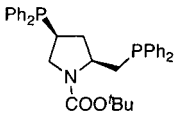

(*S*,*S*)-BPPM

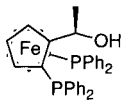

(*R*,*S*)-BPPFOH

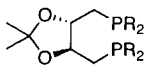

(*S*,*S*)-DIOP: R = Ph
(*S*,*S*)-Cy-DIOP: R = Cy
(*S*,*S*)-MOD-DIOP:
R = 3, 5-(Me)$_2$-4-(MeO)C$_6$H$_2$

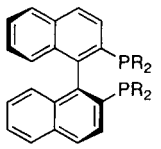

(*S*)-BINAP: R = Ph
(*S*)-TolBINAP: R = 4-MeC$_6$H$_4$
(*S*)-XylBINAP: R = 3,5-(Me)$_2$C$_6$H$_3$

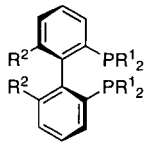

(*S*)-BICHEP: R^1 = Cy; R^2 = CH$_3$
(*S*)-BIPHEMP: R^1 = Ph; R^2 = CH$_3$
(*S*)-BIPHEP: R^1 = Ph; R^2 = OCH$_3$

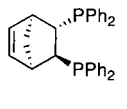

(*S*,*S*)-NORPHOS

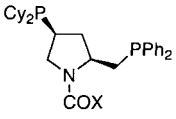

(*S*,*S*)-BCPM: X = O^{t}Bu
(*S*,*S*)-MCCPM: X = NHMe

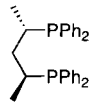

(*S*,*S*)-BDPP

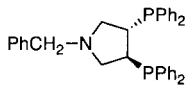

(*S*,*S*)-PYRPHOS

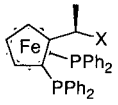

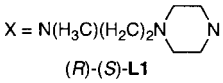

(*R*)-(*S*)-**L1**

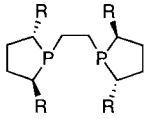

(*S*,*S*)-Me-BPE: R = Me
(*S*,*S*)-Et-BPE: R = Et
(*S*,*S*)-^{i}Pr-BPE: R = ^{i}Pr

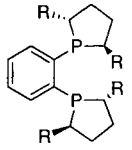

(S,*S*)-Me-DuPhos: R = Me
(*S*,*S*)-Et-DuPhos: R = Et
(*S*,*S*)-^{i}Pr-DuPhos: R = ^{i}Pr

Scheme 1.1

1.2.1
Atropisomeric Biaryl Bisphosphine Ligands

Modification of the electronic and steric properties of BINAP, BIPHEMP, and MeO-BIPHEP led to the development of new efficient atropisomeric ligands. Although most of them are efficient for ruthenium-catalyzed asymmetric hydrogenation [3], Zhang *et al.* have recently reported an *ortho*-substituted BIPHEP ligand, *o*-Ph-HexaMeO-BIPHEP, for the rhodium-catalyzed asymmetric hydrogenation of cyclic enamides (Scheme 1.2) [31].

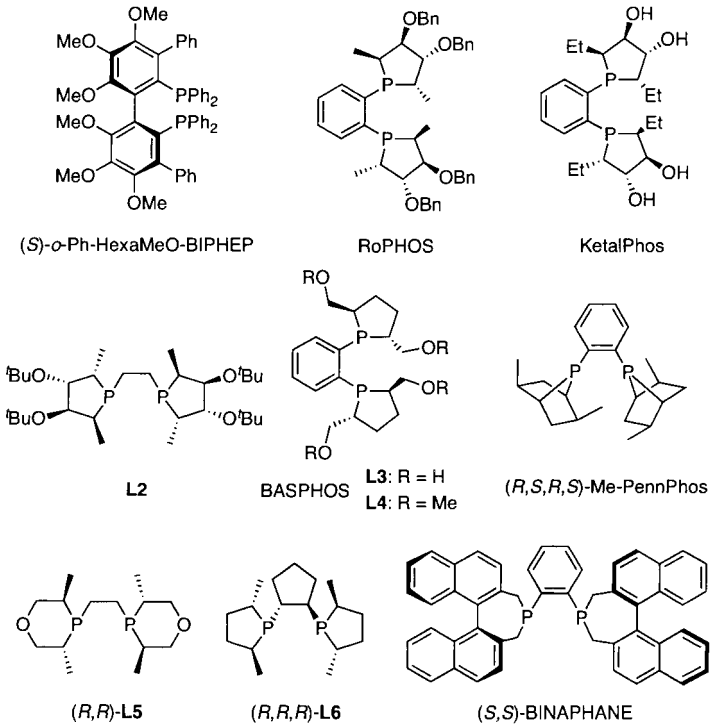

Scheme 1.2

1.2.2

Chiral Bisphosphane Ligands Based on the Modification of DuPhos and BPE

An array of bisphosphanes has emerged based on modification of the DuPhos and BPE ligands, which have proven so successful for the asymmetric hydrogenation of functionalized olefins and ketones (Scheme 1.2). Börner [32], Zhang [33], and Rajan-Babu [34] have independently reported a series of modified DuPhos and BPE ligands – RoPhos, KetalPhos, and **L2** – derived from readily available D-mannitol. The ligand with four hydroxy groups, KetalPhos, enabled the hydrogenation to be carried out in aqueous solution with high enantioselectivity. Another water-soluble ligand, BASPHOS (**L3**), developed by Holz and Börner, also exhibits high efficiency for asymmetric hydrogenation in aqueous solution [35].

Zhang *et al.* reported a sterically bulky and conformationally rigid bisphosphane, PennPhos, which shows excellent enantioselectivity for rhodium-catalyzed hydrogenation of aryl/alkyl methyl ketones [36], cyclic enamides, and cyclic enol acetates [37]. Helmchen's bisoxaphosphinane ligand **L5** [38] and Zhang's bisdinaphthophosphepine ligand BINAPHANE [39] provide excellent enantioselectivity (up to 99% *ee*) for hydrogenation of *E*/*Z*-isomeric mixtures of *β*-substituted arylenamides. The BPE analog (*R*,*R*,*R*)-1,2-bis(phospholano)cyclopentane, **L6**, provides improved enantioselectivity for the hydrogenation of dehydroamino acids [40].

1.2.3
Chiral Bisphosphane Ligands Based on the Modification of DIOP

Although the development of DIOP prompted significant advances in asymmetric hydrogenation, the enantioselectivity is often inferior to that of other chiral bisphosphines. A possible reason for the diminished selectivity may be the formation of a conformationally flexible seven-membered chelate of the DIOP ligand with the metal. In order to rigidify the conformational flexibility of the DIOP ligand, several rigidified DIOP-type ligands have been developed (Scheme 1.3). Zhang [41, 42] and RajanBabu [43] have independently reported the development of BICP and DIOP* ligands. Lee has developed a type of 1,4-diphosphane ligand BDPMI with an imidazolidin-2-one backbone [44], which has successfully been applied to the asymmetric rhodium-catalyzed hydrogenation of arylenamides, with up to 99% enantioselectivity. A series of 1,4-diphosphane ligands with a conformationally rigid 1,4-dioxane backbone, as exemplified by T-Phos and SK-Phos, developed by Zhang, have proven highly efficient and selective (up to 99% *ee*) for the asymmetric hydrogenation of arylenamides and MOM-protected *β*-hydroxyl enamides [45].

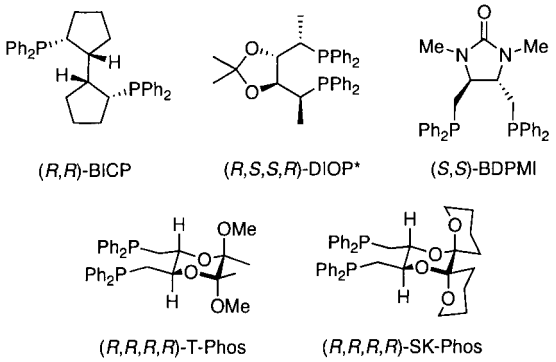

Scheme 1.3

1.2.4
Chiral Ferrocene-Based Bisphosphane Ligands

Recently, many effective chiral bisphosphane ligands with a ferrocene backbone have been developed (Scheme 1.4). Ito has successfully developed a series of *trans*-chelating bisphosphane ligands, TRAPs, which are highly selective for rhodium-catalyzed asymmetric hydrogenation [46].

Togni and Spindler introduced non-C_2-symmetric ferrocene-based Josiphos-type ligands [47], which are effective for rhodium-catalyzed hydrogenation of *α*-(acetamido)cinnamate, dimethyl itaconate, and *β*-keto esters. The Josiphos-type ligands have been applied as the stereodefining step in a number of industrial processes, as exemplified the use of PPF-^{t}Bu$_2$ for the commercial synthesis of (+)-biotin [48], and Xyli-Phos for the preparation of the herbicide (*S*)-metolachlor [49].

Two C_2-symmetric bisphosphane ligands, namely Kang's FerroPhos [50] and Knochel's FERRIPHOS (MandyPhos) [51], have provided excellent enantioselectivities in

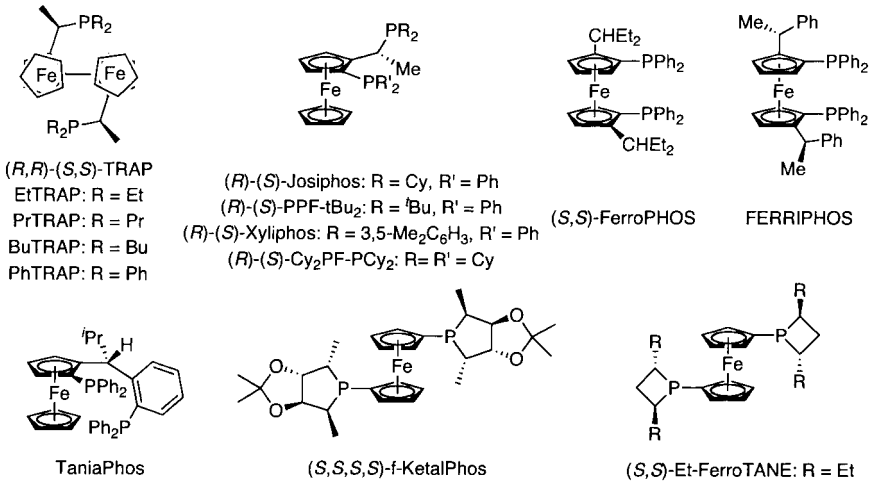

Scheme 1.4

asymmetric hydrogenation of α-dehydroamino acids. A non-C_2-symmetrical ferrocene-based 1,5-diphosphane ligand (TaniaPhos), has also been developed by Knochel [52] for asymmetric hydrogenation.

Marinetti [53] and Burk [54] reported the preparation of chiral 1,1′-bis(phosphetano)ferrocenes (FerroTANE) independently, in which Et-FerroTANE demonstrated excellent enantioselectivity in the rhodium-catalyzed hydrogenation of itaconates. Zhang has reported a 1,1′-bis(phospholanyl)ferrocene ligand (f-KetalPhos) with ketal substituents at 3,4-positions [55], which proved an excellent ligand for the enantioselective hydrogenation of α-dehydroamino acid derivatives [56].

1.2.5
P-Chiral Bisphosphane Ligands

Although development of the first *P*-chiral bisphosphane, DIPAMP, was achieved over 30 years ago, that of new *P*-chiral bisphosphanes has been comparatively slow due to difficulties associated with their synthesis. Imamoto [57] initiated their revival through the synthesis of a series of *P*-chiral ligands, BisP* (Scheme 1.5), which demonstrate excellent catalytic activity and enantioselectivity in the hydrogenation of α-dehydroamino acids, enamides [58], (*E*)–β(acylamino)acrylates [59], and α,β-unsaturated-α-acyloxyphosphonates [60]. In addition to BisP*, several other *P*-chiral bisphosphanes have been introduced by Imamoto, as exemplified by MiniPhos [61], 1,2-bis(isopropylmethylphosphino)-benzene (**L7**) [62], and the unsymmetrical *P*-chiral BisP* (**L8** and **L9**) [63]. Zhang has recently reported two rigid *P*-chiral bisphospholane ligands, TangPhos [64] and BINAPINE [65]. TangPhos provides an efficient ligand for the rhodium-catalyzed hydrogenation of a variety of functionalized olefins such as α-dehydroamino acids, α-arylenamides, β-(acylamino)acrylates [66], itaconic acids, and enol acetates [67]. The BINAPINE ligand, on the other hand, demonstrates excellent enantioselectivity and reactivity, with turnover numbers up to 10 000, for the asymmetric hydrogenation of *Z*-aryl(β-acylamino)acrylates. Mathey's bisphosphane ligand BIPNOR is also effective

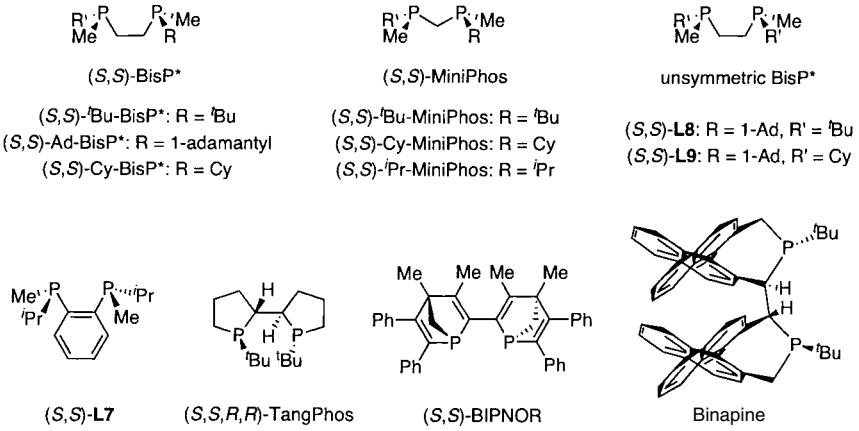

Scheme 1.5

in the enantioselective hydrogenation of α-(acetamido)cinnamic acids and itaconic acids [68].

1.2.6
Other Bisphosphane Ligands

Pye and Rossen have developed a planar chiral bisphosphine ligand, [2.2]PHANEPHOS, based on a paracyclophane backbone (Scheme 1.6) [69]. Moreover, the *ortho*-phenyl substituted NAPHOS ligand, Ph-*o*-NAPHOS, has been successfully applied for the rhodium-catalyzed hydrogenation of α-dehydroamino acid derivatives [70].

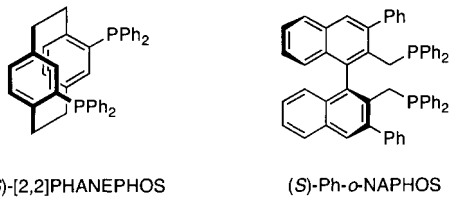

Scheme 1.6

1.2.7
Bisphosphinite, Bisphosphonite, and Bisphosphite Ligands

The development of bisphosphinites, bisphosphonites, and bisphosphites for asymmetric hydrogenation has lagged behind that of chiral bisphosphane ligands, due to the former groups' greater conformational flexibility and instability. Nevertheless, some efficient P–O ligands with rigid backbones have been discovered (Scheme 1.7). Rajan-Babu has developed a series of bisphosphinites (**L10**), based on a sugar backbone, that demonstrate excellent enantioselectivity in hydrogenation of α-dehydroamino acid derivatives [71]. Chan and Jiang's rigid spirocyclic bisphosphinite ligand (spirOP) has been

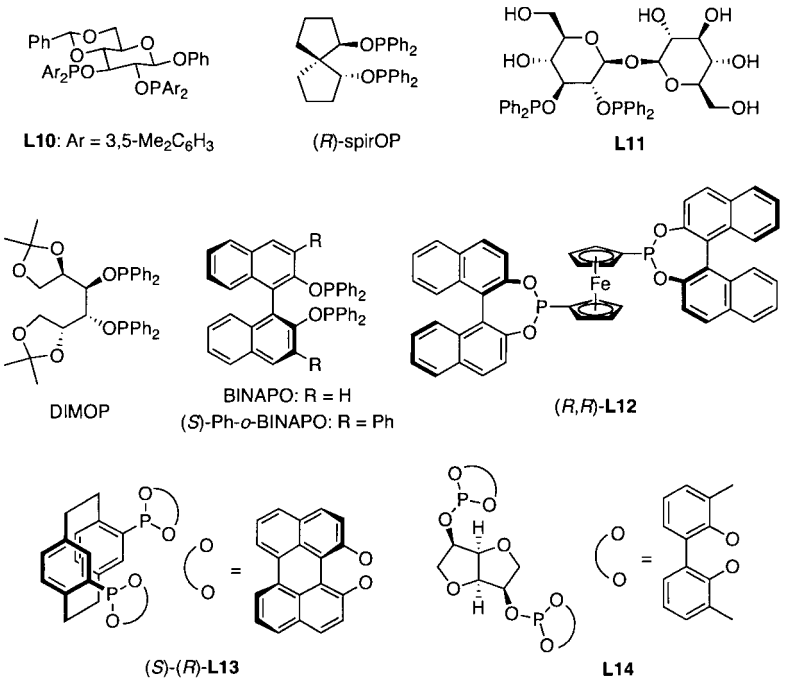

Scheme 1.7

applied in the hydrogenation of α-dehydroamino acid derivatives [72]. The D-manitol derived bisphosphinite ligand DIMOP, which was prepared by Chan, affords enantioselectivities of up to 97% *ee* for the hydrogenation of α-dehydroamino acids [73]. A water-soluble rhodium complex of the bisphosphinite ligand **L11**, which is derived from the β,β-trehalose backbone, provided an effective catalyst for the enantioselective hydrogenation of α-dehydroamino acid derivatives in water or an aqueous/organic biphasic medium (up to 99.9% *ee*) [74]. In order to rigidify the flexible structure of BINAPO, Zhang has recently reported a series of *o*-BINAPO ligands with substituents at the 3,3′-positions of the binaphthyl group [75]. The ligand Ph-*o*-BINAPO with phenyl groups at the 3,3′-positions provides an effective ligand for hydrogenation of α-dehydroamino acid derivatives [70].

Some excellent bisphosphonite ligands have also been developed. For example, Reetz's binaphthol-derived ferrocene-based bisphosphonite ligand **L12** has demonstrated to have excellent reactivity and enantioselectivity in the rhodium-catalyzed hydrogenation of itaconates and α-dehydroamino acid derivatives [76]. Zanotti-Gerosa's bisphosphonite ligand **L13** has also been successfully applied to the asymmetric hydrogenation of α-dehydroamino acid derivatives with up to 99% *ee* [77].

A few efficient bisphosphite ligands have been used for asymmetric hydrogenation of itaconates or α-dehydroamino acid derivatives. Reetz has developed a series of C_2-symmetric bisphosphite ligands such as **L14**, which are based on the structure of 1,4:3,6-dianhydro-D-mannite [78]. The ligands exhibit excellent reactivity and enantioselectivity for the asymmetric hydrogenation of itaconates.

1.2.8
Chelating Aminophosphine- and Amidophosphine-phosphoramidites

Several efficient amidophosphine- and aminophosphine-phosphinite ligands have been reported by Agbossou and Carpentier [79]. The amidophosphine-phosphinite ligands (*S*)-Cy,Cy-oxoProNOP, (*S*)-Cp,Cp-oxoProNOP, (*S*)-Cp,Cp-IndoNOP and (*S*,2*S*)-Cr(CO)-3-Cp,Cp-IndoNOP (Scheme 1.8) have been demonstrated to be effective for rhodium-catalyzed hydrogenation of dihydro-4,4-dimethyl-2,3-furandione. Another aminophosphine-phosphinite, DPAMPP, reported by Jiang and Mi [80] recently, has shown excellent enantioselectivity for hydrogenation of a series of α-dehydroamino acid derivatives. Some bisaminophosphine ligands such as H_8-BDPAB and BDPAB have been reported by Chan, and have been successfully applied for hydrogenation of arylenamides [81]. Xyl-BDPAB is also found to be an efficient ligand for asymmetric hydrogenation of α-dehydroamino acid derivatives [82]. Boaz has developed a family of ferrocene-based phosphine-aminophosphine ligands, BoPhoz [83], which are air-stable and exhibit excellent reactivity and selectivity for hydrogenation of α-dehydroamino acid derivatives and itaconic acids.

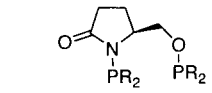

(*S*)-Cy,Cy-oxoProNOP: R = Cy
(*S*)-Cp,Cp-oxoProNOP: R = Cp

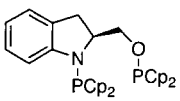

(*S*)-Cp,Cp-IndoNOP

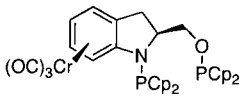

(*S,2S*)-Cr(CO)$_3$-Cp,Cp-IndoNOP

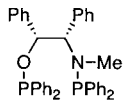

(*1R,2S*)-DPAMPP

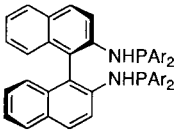

(*R*)-BDPAB: Ar = Ph
(*R*)-Xyl-BDPAB:
Ar = 3,5-Me$_2$C$_6$H$_3$

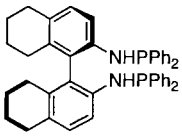

(*R*)-H$_8$-BDPAB

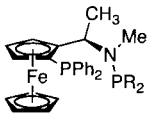

BoPhoz
L15: R = Ph
L16: R = Cy

Scheme 1.8

1.2.9
Chiral Monophosphorous Ligands

Compared to the rapid development of chelating bisphosphorous ligands, the discovery of effective monophosphorous ligands has been relatively slow [84]. Scheme 1.9 illustrates several monophosphorous ligands for rhodium-catalyzed asymmetric hydrogenation. Reetz has developed a series of monophosphite ligands which have shown excellent reactivity and enantioselectivity for asymmetric hydrogenation of dimethyl itaconate [85]. de Vries and Feringa have developed a phosphoramidite ligand, named MonoPhos, which has shown high enantioselectivity in asymmetric hydrogenation of dehydroamino acid derivatives [86] and arylenamides [87]. Zhou reported a monophosphoramidite ligand SIPHOS, based on a chiral 1,1′-spirobiindane-7,7′-diol, which affords enantio-

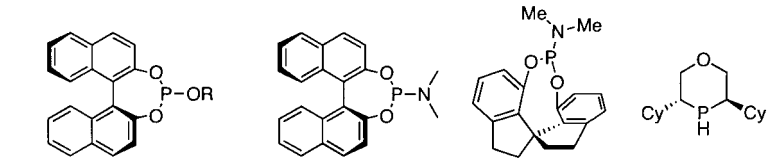

(*S*)-(*R*)-**L17**: R = (*R*)-CH(Me)Ph (*S*)-MonoPhos (*S*)-SIPHOS (*R*,*R*)-**L18**

Scheme 1.9

selectivities of up to 99% *ee* for the asymmetric hydrogenation of *α*-dehydroamino acids, arylenamides, and itaconates [88]. The secondary monodentate phosphane **L18** reported by Helmchen is also very effective for hydrogenation of itaconates [38].

1.3 Applications of Chiral Phosphorous Ligands in Rhodium-Catalyzed Asymmetric Hydrogenation

1.3.1 Hydrogenation of Olefins

1.3.1.1 Hydrogenation of Dehydroamino Acid Derivatives

Several chiral phosphorous ligands with great structural diversity are effective for the rhodium-catalyzed hydrogenation of *α*-dehydroamino acid derivatives. Tab. 1.1 summarizes the asymmetric hydrogenation of (*Z*)-2-(acetamido)cinnamic acid, 2-(acetamido)acrylic acid, and their methyl ester derivatives.

A number of chiral ligands have proven very efficient and selective for the hydrogenation of *α*-dehydroamino acid derivatives. Examples include PYRPHOS [26b], Et-DuPhos [89], f-KetalPhos [55], TangPhos [64], DPAMP [90], and BoPhoz (**L15**) [83], for which substrate-to-catalyst ratios as high as 50 000 : 1 have been observed. Indeed, asymmetric rhodium-catalyzed hydrogenation reactions using the Me-DuPhos and Et-DuPhos ligands are tolerant to *β*-alkyl and aryl substituents (≥95% *ee*), even in supercritical CO_2 [91].

In contrast to the high enantioselectivity achieved for the *Z*-isomeric substrates, hydrogenation of the *E*-isomers usually proceeds with lower rates and afford products with diminished enantioselectivities [92]. The rhodium-catalyzed hydrogenation of the *E*- and *Z*-isomers, with BINAP as a ligand in THF, affords products with opposite absolute configurations [16]. Remarkably, the DuPhos–Rh system provides excellent enantioselectivity for both isomeric substrates with the same absolute configuration, irrespective of the *E*/*Z*-geometry (Eqs. 1 and 2). This result is particularly important for the construction of alkyl dehydroamino acid derivatives, which are difficult to prepare in enantiomerically pure form.

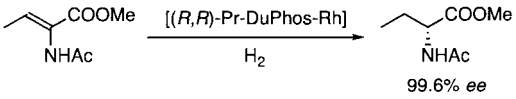

99.6% *ee* (1)

Tab. 1.1

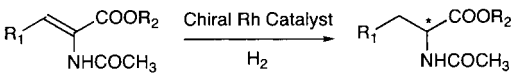

A: R_1 = H, R_2 = H B: R_1 = H, R_2 = CH_3
C: R_1 = Ph, R_2 = H D: R_1 = Ph, R_2 = CH_3

Ligand	*Substrate*	*S/C ratio*	*Reaction conditions*	*% ee (config.)*	*Ref.*
(*R*,*R*)-DIPAMP	D	900	MeOH, 50 °C, 3 atm. H_2	96 (*S*)	8a
(*R*,*R*)-NORPHOS	C	95	MeOH, RT, 1.1 atm. H_2	96 (*R*)	25
(*R*,*R*)-PYRPHOS	D	50000	MeOH, RT, 61 atm. H_2	96.5 (*S*)	26b
(*S*)-BINAP	D [a)]	100	EtOH, RT., 3 atm. H_2	100 (*S*)	15
(*R*)-BICHEP	D [b)]	1000	EtOH, RT, 1 atm. H_2	95 (*S*)	20c
(*S*,*S*)-Et-DuPhos	B	50440	MeOH, RT, 2 atm. H_2	>99 (*S*)	89
(*R*,*R*)-BICP	A	100	THF, Et_3N, RT, 1 atm. H_2	97.5 (*S*)	41a
ROPHOS	D	100	MeOH, RT, 1 atm. H_2	98.4 (*S*)	32a
KetalPhos	C	100	MeOH, RT, 3 atm. H_2	>99 (*S*)	33b
L3	A	100	H_2O, RT, 50 psi H_2	>99 (*S*)	35a
(*R*,*R*)-**L5**	A	1000	MeOH, 20 °C, 1.1 atm. H_2	97.4 (*R*)	38
(*R*,*R*,*R*)-**L6**	D	1000	MeOH, 25 °C, 2 atm. H_2	98 (*R*)	40
(*R*,*R*)-(*S*,*S*)-EtTRAP	B	100	CH_2Cl_2, 60 °C, 0.5 atm. H_2	96 (*R*)	46b
(*R*)-(*S*)-JosiPhos	D	100	MeOH, 35 °C, 1 atm. H_2	96 (*S*)	47
(*S*,*S*)-FerroPhos	C	100	EtOH, RT, 2 atm. H_2	98.9 (*R*)	50a
(*R*)-(*S*)-FERRIPHOS	D	100	MeOH, RT, 1 atm. H_2	98.0 (*S*)	51a
Taniaphos	D	100	MeOH/PhMe, 1 atm. H_2	96.6 (*R*)	52a
(*S*,*S*,*S*,*S*)-f-KetalPhos	B	10000	THF, RT, 3 atm. H_2	100 (*S*)	55
(*S*,*S*)-^{f}Bu-BisP*	D	500	MeOH, RT, 2 atm. H_2	99.9 (*R*)	57a
(*S*,*S*)-^{t}Bu-MiniPhos	B	500	MeOH, RT, 2 bar H_2	99.9 (*R*)	61
(*S*,*S*)-**L7**	B	500	0 °C, 2 bar H_2	97 (*S*)	62
(*S*,*S*)-**L8**	D	500	MeOH, RT, 2 atm. H_2	99.2 (*R*)	63a
(*S*,*S*,*R*,*R*)-TangPhos	D	10000	MeOH, RT, 20 psi H_2	99.8 (*S*)	64
(–)-BIPNOR	C	100	EtOH, RT, 3 atm. H_2	>98 (*S*)	68a
(*R*)-PHANEPHOS	B	100	MeOH, RT, 1 atm. H_2	99.6 (*R*)	69a
(*S*)-Ph-*o*-NAPHOS	B	100	MeOH, RT, 3 atm. H_2	98.7 (*S*)	70
L10	C	1000	THF, RT, 30 psi H_2	99.0 (*S*)	71a
(*R*)-spirOP	C	100	MeOH, RT, 1 atm. H_2	97.9 (*R*)	72a
DIMOP	A	500	Me_2CO, RT, 500 psi H_2	96.7 (*R*)	73
L11	D	100	H_2O, RT, 5 atm. H_2 [c)]	99.9 (*S*)	74
(*S*)-Ph-*o*-BINAPO	B	100	MeOH, RT, 3 atm. H_2	99.9 (*S*)	70
(*R*,*R*)-**L12**	B	1000	CH_2Cl_2, RT, 1.3 atm. H_2	99.5 (*S*)	76
(*S*)-(*R*)-**L13**	B	5000	MeOH, RT, 3.5 atm. H_2	98.5 (*S*)	77
(1*R*,2*S*)-DPAMPP	D	10000	MeOH, RT, 50 atm. H_2	97 (*R*)	80b
(*S*)-Xyl-BDPAB	D	500	MeOH, RT, 50 psi H_2	98 (*S*)	82
L15	D	10000	THF, RT, 10 psi H_2	99.4 (*S*)	83
(*S*)-MonoPhos	B	20	EtOAc, RT, 1 atm. H_2	99.6 (*R*)	86
(*S*)-SIPHOS	D	200	CH_2Cl_2, RT, 1 atm. H_2	96.4 (*S*)	88b

a) Benzoyl derivative.
b) Ethyl ester.
c) Sodium dodecyl sulfate (10 mol%) was added.

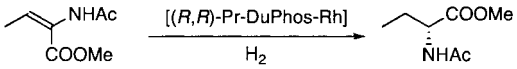

99.4% *ee* (2)

Hydrogenation of *β*,*β*-disubstituted *α*-dehydroamino acids remains a challenging problem. Remarkably, the less bulky DuPhos- or BPE-type ligands, such as Me-DuPhos and Me-BPE, provide excellent enantioselectivity for a variety of this type of substrate [93]. The rhodium complexes of chiral ligands such as BuTRAP [46 b], f-KetalPhos [55], Cy-BisP* [57a], MiniPhos [61], and unsymmetrical BisP* (**L9**) [63 b] have also shown high efficiencies for some *β*,*β*-disubstituted *α*-dehydroamino acid substrates, as outlined in Tab. 1.2.

Tab. 1.2

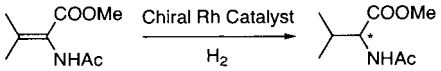

Ligand	*S/C ratio*	*Reaction conditions*	*% ee (config.)*	*Ref.*
(*R*,*R*)-(*S*,*S*)-BuTRAP	100	^{i}PrOH, 15 °C, 1 atm. H_2	88 (*S*)	46 b
(*S*,*S*)-Me-DuPhos	500	PhH, 25 °C, 90 psi H_2	96.0 (*S*)	93
(*R*,*R*)-Me-BPE	500	PhH, 25 °C, 90 psi H_2	98.2 (*R*)	93
(*S*,*S*,*S*,*S*)-f-KetalPhos	100	THF, RT, 15 psi H_2	87.3 (*S*)	55
(*S*,*S*)-Cy-BisP*	500	MeOH, RT, 6 atm. H_2	90.9 (*R*)	57 a
(*S*,*S*)-^{t}Bu-MiniPhos	500	MeOH, RT, 6 atm. H_2	87 (*R*)	61
(*S*,*S*)-**L7**	500	RT, 6 atm. H_2	87 (*S*)	62
(*S*,*S*)-**L9**	100	MeOH, RT, 20 atm. H_2	96.1 (*R*)	63b

The asymmetric hydrogenation of *β*,*β*-disubstituted *α*-dehydroamino acids, in which the *β*-substituents are nonequivalent, provides the opportunity to selectively construct two stereogenic centers. The Me-DuPhos or Me-BPE ligands facilitate the rhodium-catalyzed hydrogenation of the *E*- and *Z*-isomers of *β*,*β*-disubstituted *α*-dehydroamino acid

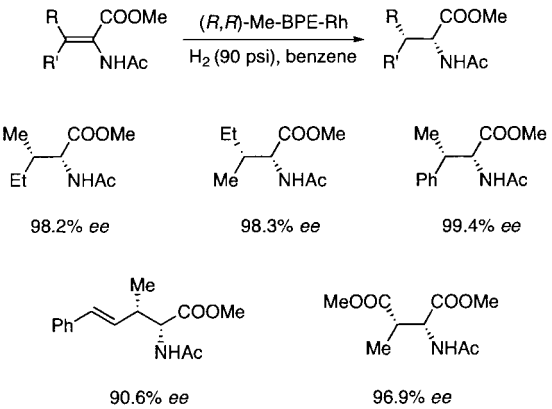

Scheme 1.10

derivatives with excellent enantioselectivity (Scheme 1.10). Moreover, excellent chemoselectivity is observed in hydrogenation of substrates that contain additional olefin functionality [94]. Thus hydrogenation of β-substituted α,β,γ,δ-unsaturated amino acids with the Me-DuPhos and Me-BPE ligands provides a series of β-substituted γ,δ-unsaturated amino acids with good enantioselectivity.

The asymmetric hydrogenation of the *E*- or *Z*-isomer of β-(acetylamino)-β-methyl-α-dehydroamino acids with Me-DuPhos–Rh catalyst provides either diastereomer of the *N,N*-protected 2,3-diaminobutanoic acid derivatives with excellent enantioselectivity (Eqs. 3 and 4) [95].

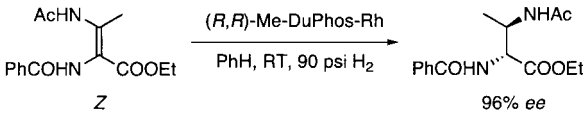

(3)

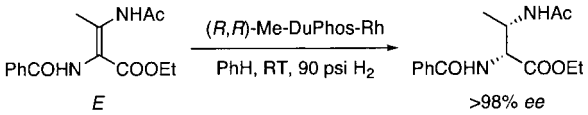

(4)

1.3.1.2 **Hydrogenation of Enamides**

Recently, high enantioselectivity was obtained in the rhodium-catalyzed hydrogenation of α-aryl enamides and *E*/*Z*-isomeric mixtures of β-substituted enamides. Tab. 1.3 lists some examples for the hydrogenation of α-phenylenamide and the *E*/*Z*-isomeric mixture of β-methyl-α-phenylenamide. A *P*-chiral ligand, TangPhos, proved to be particularly efficient for the rhodium-catalyzed hydrogenation of enamides, given the excellent enantioselectivity and reactivity, with up to 10 000 turnovers.

Some alkyl enamides, such as *tert*-butylenamide or 1-admantylenamide, can also be hydrogenated using a ^{t}Bu-BisP*–Rh catalyst [58] or a Me-DuPhos–Rh catalyst [97] with excellent enantioselectivity (≥99% *ee*; Eq. 5). Hydrogenation of *N*-acetyl-6,7-dimethoxy-1-methylene-1,2,3,4-tetrahydroquinoline can be catalyzed by an (*S,S,R,R*)-TangPhos–Rh complex to afford (*R*)-(–)-*N*-acetylsalsolidine in 97% *ee* (Eq. 6) [64]. PennPhos [37a], *o*-Ph-HexaMeO-BIPHEP [31], and Me-BPE [97] have also shown high efficiencies in the rhodium-catalyzed hydrogenation of cyclic enamides (Eq. 7). The racemic cyclic enecarbamate was hydrogenated with an *o*-Ph-HexaMeO-BIPHEP–Rh catalyst to furnish the *cis*-carbamate in 96% *ee* (Eq. 8) [31]. The enantiomerically enriched product was then directly employed for the synthesis of sertraline, an antidepressant agent. Interestingly, 2-substituted *N*-acetylindoles can also be effectively hydrogenated by the Ph-TRAP–Rh catalyst with excellent enantioselecitivities (Eq. 9) [46g]. Hydrogenation of some tetra-substituted enamides has also been reported. ^{t}Bu-BisP* and ^{t}Bu-MiniPhos have provided excellent enantioselectivity for the hydrogenation of β,β-dimethyl-α-phenyl enamide derivatives (Eq. 10). The PennPhos–Rh [37a] and *o*-Ph-BIPHEP–Rh catalysts [31] facilitate the hydrogenation of tetra-substituted enamides derived from 1-indanone and 1-tetralone with excellent enantioselectivity.

Tab. 1.3

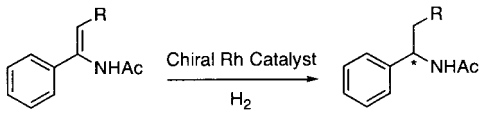

A: R = H
B: R = CH_3 (*Z*/*E*)

Ligand	*Substrate*	*S/C ratio*	*Reaction conditions*	*% ee (config.)*	*Ref.*
(*R*,*R*)-Me-BPE	A	500	MeOH, 22 °C, 6 psi H_2	95.2 (*R*)	96
	B	500	MeOH, 22 °C, 6 psi H_2	95.4 (*R*)	96
KetalPhos	A	100	MeOH, RT, 10 atm. H_2	96 (*S*)	33b
(*S*,*S*)-BINAPHANE	B	100	CH_2Cl_2, RT, 20 psi H_2	99.1 (*S*)	39a
(*R*,*R*)-BICP	B	100	PhMe, RT, 40 psi H_2	95.0 (*R*)	41b
(*R*,*S*,*S*,*R*)-DIOP*	A	50	MeOH, RT, 10 bar H_2	98.8 (*R*)	42
	B	50	MeOH, RT, 10 bar H_2	97.3 (*R*)	42
(*R*,*R*,*R*,*R*)-T-Phos	B	100	MeOH, RT, 45 psi H_2	98 (*S*)	45
(*R*,*R*,*R*,*R*)-SK-Phos	B	100	MeOH, RT, 45 psi H_2	97 (*S*)	45
(*S*,*S*)-BDPMI	A	100	CH_2Cl_2, RT, 1 atm. H_2	98.5 (*R*)	44a
	B	100	CH_2Cl_2, RT, 1 atm. H_2	>99 (*R*)	44a
(*S*,*S*)-^{t}Bu-BisP*	A	100	MeOH, RT, 3 atm. H_2	98 (*R*)	58
(*S*,*S*,*R*,*R*)-TangPhos	A	10^4	MeOH, RT, 20 psi H_2	99.3 (*R*)	64
	B	100	MeOH, RT, 20 psi H_2	98 (*R*)	64
(*R*)-H_8-BDPAB	A	200	THF, 5 °C, 1 atm. H_2	96.8 (*R*)	81a
(*S*)-MonoPhos	A	100	CH_2Cl_2, –20 °C, 300 psi H_2	95 (*S*)	87
(*S*)-SIPHOS	A	200	toluene, 5 °C, 10 atm. H_2	98.7 (*S*)	88a

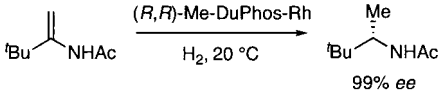

(5)

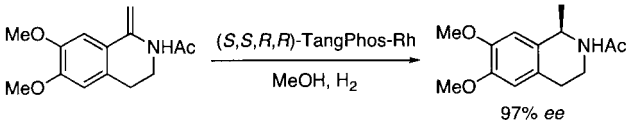

(6)

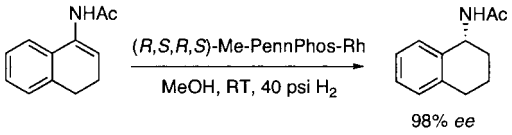

(7)

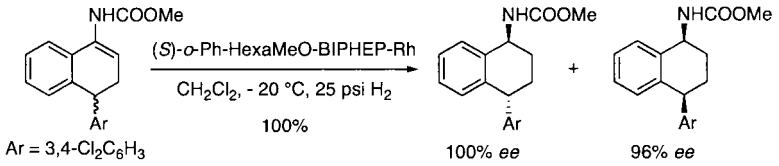

(8)

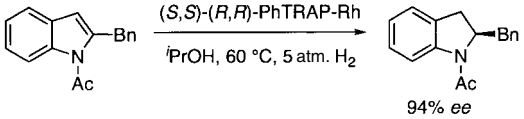

(9)

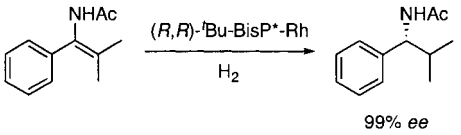

(10)

The hydrogenation of a series of *E*/*Z*-isomeric mixtures of *α*-arylenamides containing a MOM-protected *β*-hydroxyl group, using BICP–Rh and Me-DuPhos–Rh catalysts, affords the *β*-amino alcohol derivatives with excellent enantioselectivity [41c]. A 1,4-diphosphane, T-Phos, with a rigid 1,4-dioxane backbone is also a very effective ligand for this transformation (Eq. 11) [45].

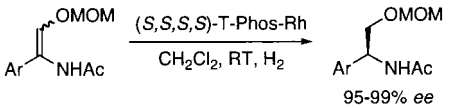

(11)

1.3.1.3 **Asymmetric Hydrogenation of *β*-(Acylamino)acrylates**

Owing to the significance of *β*-amino acid derivatives for pharmaceuticals, asymmetric hydrogenation of *β*-(acylamino)acrylates has gained significant attention in recent years [98]. The ability to utilize mixtures of *E*- and *Z*-isomers that furnish a single enantiomer is very important for the practical synthesis of *β*-amino acid derivatives, since it circumvents the necessity to prepare geometrically defined alkenes. Several rhodium complexes with chiral phosphorous ligands such as DuPhos [99], BICP [41e], BDPMI [44b], *o*-Ph-HexaMeO-BIPHEP [31], ^{t}Bu-BisP* [59], and TangPhos [66] are effective for the hydrogenation of (*E*)-alkyl(*β*-acylamino)acrylates. However, only a few chiral ligands, such as BDPMI and TangPhos, have been reported to effectively hydrogenate the corresponding (*Z*)-alkyl-*β*-(acylamino)acrylates (Tab. 1.4). Although the alkyl-*β*-(acylamino)acrylic acid derivatives have been extensively studied, there has been significantly less work on the aryl-*β*-(acylamino)acrylic acid derivatives. Since (*E*)-*β*-aryl-*β*-(acylamino)acrylic acid derivatives are difficult to obtain compared to the corresponding (*Z*)-*β*-aryl-*β*-(acylamino)acrylic acid derivatives, the *Z*-isomeric substrates represent important substrates for the practical synthesis of enantiomerically enriched *β*-aryl-*β*-amino acids via asymmetric hydrogenation. Few ligands have been reported for the selective hydrogenation of (*Z*)-*β*-aryl-(*β*-acylamino)acrylates. However, the Rh–BINAPINE complex has proven excellent, both

Tab. 1.4

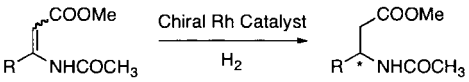

Ligand	*R*	*Geometry*	*S/C ratio*	*% ee (config.)*	*Ref.*
(*S*,*S*)-Me-DuPhos [a)]	CH_3	*E*		98.2 (*S*)	99
(*R*,*R*)-BICP [b)]	CH_3	*E*		96.1 (*R*)	41e
(*S*,*S*)-BDPMI [c)]	CH_3 [f)]	*E*		94.6 (*R*)	44b
(*S*,*S*)-^{t}Bu-BisP* [d)]	CH_3	*E*		98.7 (*R*)	59
(*S*,*S*)-MiniPhos [d)]	CH_3	*E*		96.4 (*R*)	59
(*S*,*S*,*S*,*S*)-TangPhos [e)]	CH_3	*E*		99.6 (*R*)	66
(*S*,*S*)-Me-DuPhos [a)]	CH_3	*Z*		87.8 (*S*)	99
(*S*,*S*)-BDPMI [c)]	CH_3 [f)]	*Z*		95 (*R*)	44b
(*S*,*S*,*R*,*R*)-TangPhos [e)]	CH_3	*Z*	200	98.5 (*R*)	66
(*S*,*S*,*S*,*S*)-TangPhos [e)]	Ph	*E*/*Z*	200	93.8 (*S*)	66
(*S*,*S*,*S*,*S*)-TangPhos [e)]	*p*-F-Ph	*E*/*Z*	200	95.0 (*S*)	66
(*S*,*S*,*S*,*S*)-TangPhos [e)]	*p*-MeO-Ph	*E*/*Z*	200	98.5 (*S*)	66
BINAPINE [e)]	Ph	*Z*	10000	99 (*S*)	65
BINAPINE [e)]	*p*-F-Ph	*Z*	10000	99 (*S*)	65
BINAPINE [e)]	*p*-Me-Ph	*Z*	10000	99 (*S*)	65
BINAPINE [e)]	*p*-MeO-Ph	*Z*	10000	99 (*S*)	65

Reaction conditions:
a) MeOH, 25 °C, 1 atm. H_2.
b) PhMe, RT, 40 psi H_2.
c) CH_2Cl_2, RT, 1 atm. H_2.
d) THF, RT, 3 atm. H_2.
e) THF, RT, 20 psi H_2.
f) Ethyl ester.

in terms of enantioselectivity (96 to ≥99% *ee*) and turnover (10000 turnovers), using a wide range of (*Z*)-*β*-aryl-*β*-(acylamino)acrylic acid derivatives (Tab. 1.4) [65].

1.3.1.4 **Asymmetric Hydrogenation of Enol Esters**

Although enol esters have a similar structure to enamides, they have proven more difficult substrates for asymmetric hydrogenation, which is evident from the significantly fewer number of examples. One possible explanation is the weaker coordinating ability of the enol ester to the metal center, as compared to the corresponding enamide. Some rhodium complexes associated with chiral phosphorous ligands such as DIPAMP [100, 101] and DuPhos [102] are effective for asymmetric hydrogenation of *α*-(acyloxy)acrylates.

For example, a wide range of *α*-(acyloxy)acrylates have been hydrogenated with excellent enantioselectivity using the Et-DuPhos–Rh catalyst. High selectivities are also obtained for the asymmetric hydrogenation of the *E*/*Z*-isomeric mixtures of *β*-substituted derivatives (Eq. 12). Asymmetric hydrogenation of enol phosphates with either DuPhos–Rh or BPE–Rh catalyst provides moderate to excellent enantioselectivity (Eq. 13)

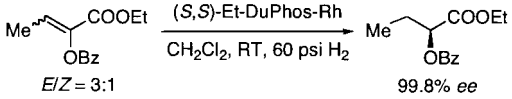

(12)

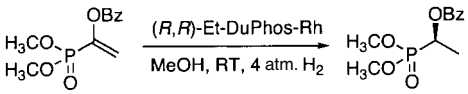

(13)

[103]. Indeed, several rhodium catalysts with chiral phosphorous ligands such as DuPhos [104], KetalPhos [33], and TangPhos [67] have been utilized for the asymmetric hydrogenation of aryl enol acetates lacking additional functionality. For example, aryl enol acetates are hydrogenated with enantioselectivities ranging from 92 to 99% *ee*, using the TangPhos–Rh catalyst (Eq. 14) [67]. The asymmetric hydrogenation of cyclic enol acetates is also a challenging problem. Me-PennPhos is an effective ligand in the rhodium-catalyzed hydrogenation of five- or six-membered cyclic enol acetates (Eq. 15) [37b]. Hydrogenation of acyclic enol acetates is also possible as vinylic, acetylenic [105] and trifluoromethyl [106] enol acetates have also been hydrogenated with both the DuPhos–Rh and BPE–Rh catalysts with excellent enantioselectivity (Eqs. 16 and 17).

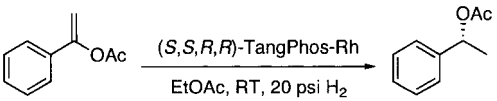

(14)

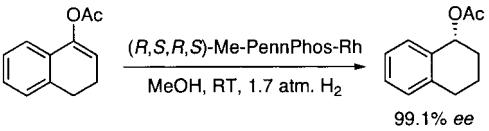

(15)

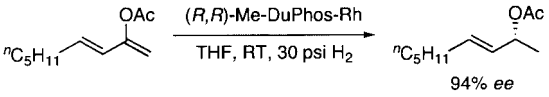

(16)

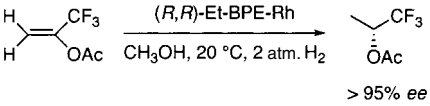

(17)

1.3.1.5 Asymmetric Hydrogenation of Unsaturated Acids and Esters

***α,β*-Unsaturated Carboxylic Acids** Although significant advances have been achieved in the asymmetric hydrogenation of *α,β*-unsaturated carboxylic acids with chiral ruthenium catalysts, there are relatively few systems that have been reported for the rhodium-catalyzed version of this reaction. For example, the (aminoalkyl)ferrocenylphosphine ligand **L1** provides excellent enantioselectivity and turnover for the rhodium-catalyzed hydrogenation of trisubstituted acrylic acids (Eq. 18). The (*R*)-(*S*)-

L1–Rh complex was employed for the enantioselective synthesis of (*S*)-2-(4-fluorophenyl)-3-methylbutanoic acid (98% *ee*) [107], while the ^{i}Pr-DuPhos–Rh complex was utilized for the enantioselective hydrogenation of *α,β*-unsaturated carboxylic acids, as exemplified by tiglic acid [29].

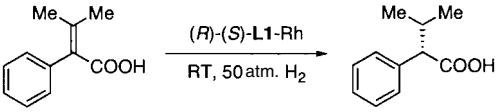

(18)

Itaconic Acids and Their Derivatives Tab. 1.5 outlines some of the chiral phosphorous ligands that provide excellent enantioselectivity and reactivity in the rhodium-catalyzed hydrogenation of itaconic acids or esters. Interestingly, both the electron-rich phosphane ligands (BICHEP [20c], Et-DuPhos [108], and TangPhos [67]) and electron-deficient phosphite or phosphonite ligands (**L12** [76] and **L14**) are effective for this type of transformation [78]. Some monophosphorous ligands, such as MonoPhos [87] and **L17** [85a], are as efficient as bisphosphorous bidentate ligands, as exemplified by the secondary phosphane **L18** [38]. Furthermore, the tetrahydroxy bisphospholane ligand allows the hydrogenation to proceed in aqueous media [33b].

In contrast to the many examples of asymmetric hydrogenation of the parent itaconic acid or its dimethyl ester, very few ligands have been reported for the enantioselec-

Tab. 1.5

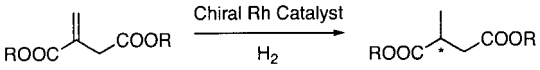

Ligand	*R*	*S/C*	*Reaction conditions*	*% ee (config.)*	*Ref.*
(*R*)-BICHEP-Rh	H	1000	EtOH, 25 °C, 1 atm. H_2	96 (*R*)	20c
(*R,R*)-Et-DuPhos	Me	10000	MeOH, 25 °C, 5 atm. H_2	98 (*R*)	108
KetalPhos	H	100	MeOH/H_2O (3:97), RT, 10 atm. H_2	>99 (*R*)	33b
L2	Me	100	MeOH, RT, 1 atm. H_2	99.1 (*R*)	32a
L4	Me	100	MeOH, RT, 1 atm. H_2	97.9 (*R*)	34b
(*R,R*)-(*S,S*)-Et-TRAP	Me	200	CH_2Cl_2, reflux, 1 atm. H_2	96 (*S*)	47c
Taniaphos	Me	100	MeOH, RT, 1 atm. H_2	98 (*S*)	52a
(*S,S*)-Et-FerroTANE	Me	200	MeOH, RT, 5.5 atm. H_2	98 (*R*)	54
(*S,S,S,S*)-f-KetalPhos	H	100	MeOH, RT, 80 psi H_2	99.5 (*R*)	55
(*S,S*)-Ad-BisP*	Me	500	MeOH, RT, 1.6 atm. H_2	99.6	57b
(*S,S,R,R*)-TangPhos	Me	5000	THF, RT, 20 psi H_2	99 (*S*)	67
(*R,R*)-**L12**	Me	5380	CH_2Cl_2, RT, 1.3 bar H_2	>99.5 (*R*)	76
L14	Me	1000	CH_2Cl_2, –10 °C, 0.3 bar H_2	98.7 (*R*)	78
L15	H	100	MeOH, RT, 300 psi H_2	97.4 (*R*)	83
(*S*)-MonoPhos	H	20	CH_2Cl_2, 25 °C, 1 atm. H_2	96.6 (*S*)	87
(*S*)-(*R*)-**L17**	Me	5000	CH_2Cl_2, 20 °C, 1.3 atm. H_2	97.4 (*S*)	85a
(*R,R*)-**L18**	H	100	^{i}PrOH, 20 °C, 1.1 atm. H_2	96.0 (*S*)	38

Tab. 1.6

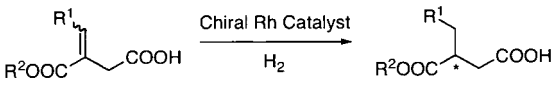

Ligand	R^1	R^2	*Geometry*	*S/C ratio*	*% ee (config.)*	*Ref.*
(*R,R*)-MOD-DIOP [a]	Ph	Me	*E*	500	96 (*S*)	23c
(*R,R*)-BPPM [a]	Ph	H	*E*	200	94 (*R*)	109
(*S,S*)-Et-DuPhos [b]	Ph	Me	*E/Z*	3000	97 (*S*)	108
(*S,S,R,R*)-TangPhos [c]	Ph	Me	*E/Z*	200	95 (*S*)	67
(*S,S*)-Et-DuPhos [b]	^{i}Pr	Me	*E/Z*	3000	99 (*R*)	108
(*S,S,R,R*)-TangPhos [c]	^{i}Pr	Me	*E/Z*	200	96 (*S*)	67

Reaction conditions:
a) MeOH, NEt_3, 25 °C, 1 atm. H_2.
b) MeOH, RT, 5.5 atm. H_2, 10 mol% NaOMe.
c) THF, RT, 20 psi H_2.

tive hydrogenation of β-substituted itaconic acid derivatives. Effective ligands for this class of substrates are MOD-DIOP [23], BPPM, Et-DuPhos, and TangPhos, as illustrated in Tab. 1.6.

Chiral 1,1′-diphosphetanylferrocene Et-FerroTANE serves as an effective ligand for the rhodium-catalyzed hydrogenation of β-aryl- and β-alkyl-substituted monoamido itaconates (Eqs. 19 and 20) [54]. The Et-DuPhos–Rh catalyst was utilized for the asymmetric hydrogenation of the trisubstituted olefin derivative in the preparation of an important intermediate for the drug candoxatril (≥99% *ee*) [110].

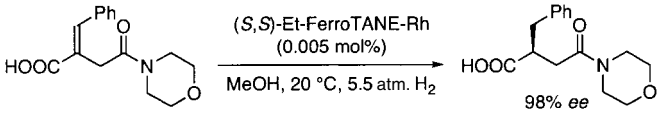

(19)

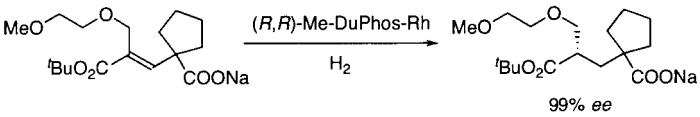

(20)

1.3.2 Hydrogenation of Ketones

1.3.2.1 Hydrogenation of Functionalized Ketones

***α*-Keto Esters** Asymmetric hydrogenation of α-keto esters has been studied with several rhodium catalysts. Some neutral rhodium catalysts with chiral ligands, such as MCCPM [24b, 111], Cy,Cy-oxoProNOP [79c,d,f], Cp,Cp-IndoNOP [79g], and $Cr(CO)_3$-Cp,Cp-IndoNOP [79g], demonstrate excellent enantioselectivity and reactivity in the hydrogenation of α-keto esters or amides (Tab. 1.7). The cyclic α-keto ester, such as dihydro-4,4-dimethyl-2,3-furandione, have also been selectively hydrogenated by a number of rhodium

Tab. 1.7

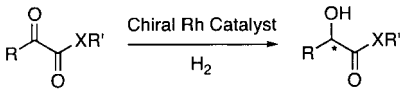

Catalyst	*R*	*XR'*	*S/C ratio*	*% ee (config.)*	*Ref.*
(*S*,*S*)-MCCPM-Rh [a)]	Me	OMe	2000	87 (*R*)	111
(*S*)-Cy,Cy-oxoProNOP- Rh [b)]	Me	OEt	200	95 (*R*)	79 f
L16-Rh [a)]	$Ph(CH_2)_2$	OEt	100	92.4 (*R*)	83
(*S*)-Cp,Cp-IndoNOP-Rh [c)]	Ph	NHBn	200	91 (*S*)	79 g
(*S*,2*S*)-$Cr(CO)_3$-Cp,Cp-IndoNOP-Rh [c)]	Ph	NHBn	200	97 (*S*)	79 g

Reaction conditions:
a) THF, 20 °C, 20 atm. H_2.
b) PhMe, 20 °C, 50 atm. H_2.
c) PhMe, 20 °C, 1 atm. H_2.

Tab. 1.8

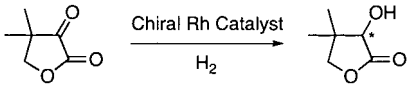

Ligand	*S/C ratio*	*% ee (config.)*	*Ref.*
(*S*,*S*)-BCPM-Rh [a)]	1000	90.5 (*R*)	112
(*S*,*S*)-*m*-MePOPPM [b)]	150000	95 (*R*)	113
(*S*)-Cp,Cp-oxoProNOP [c)]	70000	96 (*R*)	79 d
(*S*)-Cp,Cp-IndoNOP [d)]	200	>99 (*R*)	79 g
(*S*,2*S*)-$Cr(CO)_3$-Cp,Cp-In doNOP [d)]	200	>99 (*R*)	79 g
L16 [e)]	100	97.2 (*R*)	83

Reaction conditions:
a) THF, 50 °C, 50 atm. H_2.
b) Toluene, 40 °C, 12 atm. H_2.
c) Toluene, 40 °C, 40 atm. H_2.
d) Toluene, 20 °C, 1 atm. H_2.
e) THF, RT, 20 atm. H_2.

catalysts, with high turnover numbers (Tab. 1.8). For example, (*R*)-pantolactone, a key intermediate for the synthesis of vitamin B and co-enzyme A, has been readily prepared through the asymmetric hydrogenation of the corresponding *α*-keto ester.

***β*-Keto Esters** Asymmetric hydrogenation of *β*-keto esters has been extensively studied using chiral ruthenium catalysts. However, there are relatively few examples of the analogous rhodium-catalyzed reaction. Nonetheless, the Josiphos–Rh complex provides an effective catalyst for the asymmetric hydrogenation of ethyl 3-oxobutanoate (Eq. 21) [47].

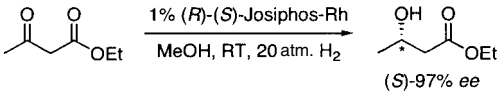

(21)

Amino Ketones Amino ketones and their hydrochloride salts can be effectively hydrogenated with chiral rhodium catalysts (Tab. 1.9). The rhodium precatalysts, combined with chiral phosphorous ligands such as BPPFOH [10b], MCCPM [24f–k], Cy,Cy-oxoProNOP [79c, e], Cp,Cp-oxoProNOP [79c, e], and IndoNOP [79g], have provided excellent enantioselectivity and reactivity for the asymmetric hydrogenation of α, β, and γ-alkyl amino ketone hydrochloride salts.

The enantioselective hydrogenation of amino ketones has been applied extensively to the synthesis of chiral drugs (Eq. 22). For example, the enantioselective hydrogenation of 3-aryloxy-2-oxo-1-propylamine derivatives directly leads to 1-amino-3-aryloxy-2-propanol derivatives, which serve as β-adrenergic blocking agents. (*S*)-Propranolol is obtained in 90.8% *ee* from the corresponding α-amino ketone, using 0.01 mol% of the neutral (*S*,*S*)-MCCPM–Rh complex [24f].

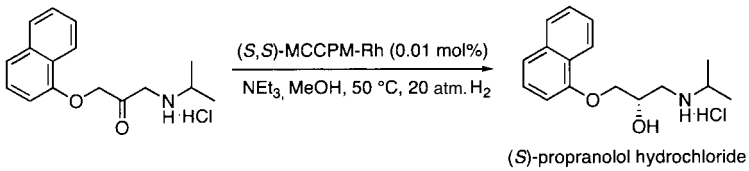

(22)

Tab. 1.9

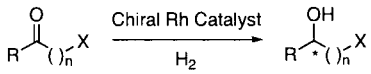

Catalyst	*R*	*n*	*X*	*S/C ratio*	*% ee (config.)*	*Ref.*
(*R*)-(*S*)-BPPFOH-Rh [a)]	(3,4)-$(OH)_2C_6H_3$	1	NHMe·HCl	100	95 (*R*)	10b
(2*S*,4*S*)-MCCPM-Rh [b)]	Ph	1	NEt_2·HCl	100 000	96 (*S*)	114
(*S*)-Cp,Cp-oxoProNOP-Rh [c)]	Ph	1	NMe_2·HCl	200	96 (*S*)	79e
(*S*)-Cp,Cp-oxoProNOP-Rh [c)]	Me	1	NMe_2·HCl	200	97 (*S*)	79e
(*S*)-Cp,Cp-IndoNOP-Rh [d)]	Ph	1	NMe_2·HCl	200	99 (*S*)	79g
(*S*)-Cy,Cy-oxoProNOP-Rh [d)]	Ph	2	NMe_2·HCl	200	93 (*R*)	79g
(2*S*,4*S*)-MCCPM-Rh [e)]	Ph	2	N(Me)Bn·HCl	1000	91 (*R*)	24g
(*S*)-Cy,Cy-oxoProNOP-Rh [f)]	Ph	3	NMe_2·HCl	200	92 (*R*)	79g

Reaction conditions:
a) NEt_3, MeOH, RT, 50 atm. H_2.
b) NEt_3, MeOH, 50 °C, 20 atm. H_2.
c) MeOH, 20 °C, 50 atm. H_2.
d) PhMe, 20 °C, 20 atm. H_2.
e) MeOH, 50 °C, 30 atm. H_2.
f) PhMe, 80 °C, 50 atm. H_2.

1.3.2.2 Hydrogenation of Unfunctionalized Ketones

The asymmetric hydrogenation of unfunctionalized ketones is a much more challenging task than that of functionalized ketones [3j, 115]. Many chiral catalysts which are effective for functionalized ketones do not provide useful levels of enantioselectivity for unfunctionalized ketones, due to a lack of secondary coordination to the metal center. Zhang demonstrated the enantioselective hydrogenation of simple aromatic and aliphatic ketones using the electron-donating diphosphane PennPhos, which has a bulky, rigid and well-defined chiral backbone, in the presence of 2,6-lutidine and potassium bromide [36].

Aromatic Ketones The DIOP–Rh [116] and DBPP–Rh [117] complexes, in conjunction with a tertiary amine, have been employed in the asymmetric hydrogenation of acetophenone, albeit with moderate enantioselectivity (80 and 82% respectively; Tab. 1.10). The asymmetric hydrogenation of aromatic ketones was significantly improved by using the Me-PennPhos–Rh complex, with which enantioselectivities of up to 96% *ee* were achieved [36]. Interestingly, the additives 2,6-lutidine and potassium bromide were again found to be crucial for optimum selectivity, although their specific role has not been determined.

Tab. 1.10

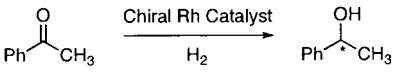

Catalyst	*S/C ratio*	*Yield [%]*	*% ee (config.)*	*Ref.*
$[RhCl(nbd)]_2$-(*S*,*S*)-DIOP+NEt_3 [a)]	200	64	80	116
$[RhCl(nbd)]_2$-(*S*,*S*)-BDPP+NEt_3 [a)]	100	72	82 (*S*)	117
$[RhCl(cod)]_2$-(*R*,*S*,*R*,*S*)-Me-PennPhos+2,6-lutidine [b)]	100	97	95 (*S*)	36

Reaction conditions:
a) MeOH, 50 °C, 69 atm. H_2, 6 h.
b) MeOH, RT, 30 atm. H_2, 24 h.

Aliphatic Ketones The asymmetric hydrogenation of simple aliphatic ketones remains a challenging problem. This may be attributed to the difficulty with which the chiral catalyst differentiates between the two-alkyl substituents of the ketone. Promising results have been obtained in asymmetric hydrogenation of aliphatic ketones using the PennPhos–Rh complex in combination with 2,6-lutidine and potassium bromide (Tab. 1.11) [36]. For example, the asymmetric hydrogenation of *tert*-butyl methyl ketone affords the requisite secondary alcohol in 94% *ee*. Similarly, isopropyl, ^{n}Butyl, and cyclohexyl methyl ketones have been reduced to the corresponding secondary alcohols with 85% *ee*, 75% *ee*, and 92% *ee* respectively.

Tab. 1.11

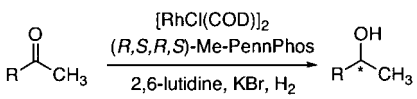

R	*S/C ratio*	*Time*[a] *[h]*	*Yield [h]*	*% ee (config.)*
^{n}Bu	100	48	96	75 (*S*)
^{i}Bu	100	75	66	85 (*S*)
^{i}Pr	100	94	99	84 (*S*)
Cyclohexyl	100	106	90	92 (*S*)
^{t}Bu	100	96	51	94 (*S*)

a) Other reaction conditions: MeOH, RT, 30 atm. H_2.

1.3.3 Asymmetric Hydrogenation of Imines

The paramount significance of chiral amines in pharmaceutical and agrochemical substances drives the development of efficient catalytic asymmetric methods for their formation. In contrast to the high enantioselectivities observed in asymmetric reduction of both alkenes and ketones, only limited success has been achieved in the enantioselective hydrogenation of imines [118]. Currently, there are few efficient chiral catalytic systems available for the asymmetric hydrogenation of imines.

1.3.3.1 Acyclic *N*-Alkylimines

Several chiral rhodium, iridium, titanium, and zirconium catalysts have been applied to the asymmetric hydrogenation of acyclic *N*-alkylimines, with limited success. While the chiral titanocene catalyst has a broad substrate scope for the reduction of *N*-alkylimines [119], affording the secondary amines with moderate to good enantioselectivity, the corresponding rhodium and iridium catalysts are limited to acetophenone *N*-benzylimine derivatives. The substrates are generally mixtures of *E*- and *Z*-isomers, of which several examples are outlined in Tab. 1.12. The asymmetric hydrogenation of acetophenone *N*-benzylimine derivatives using the neutral CycPhos–Rh complex in the presence of potassium iodide affords moderate to good enantioselectivity (up to 91% *ee*) [120]. (*S*,*S*)-BDPP is also an effective ligand for the reduction of acetophenone *N*-benzylimine, in which enantioselectivities of up to 83% *ee* have been observed at 0 °C, albeit with low conversion [117 b]. The selectivity in this transformation was improved (89% *ee*) through the addition of reversed aggregated micelles of sodium bis(2-ethylhexyl)sulfosuccinate (AOT) and 15-crown-5 [121]. The optimum enantioselectivity (94% *ee*) for hydrogenation of acetophenone *N*-benzylimine was obtained with a neutral monosulfonated (*S*,*S*)-BDPP–Rh complex in a mixed solvent system ($EtOAc/H_2O$) [122]. The *para*-chloro- and *para*-methoxy-substituted derivatives also provide good enantioselectivity (≥90% *ee*). Interestingly, the di-, tri-, and tetrasulfonated (*S*,*S*)-BDPP ligands are much less selective for this particular transformation [123].

Tab. 1.12

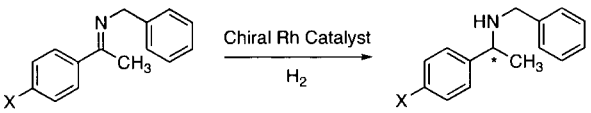

Catalyst	*X*	*Additive*	*Yield [%]*	*% ee (config.)*	*Ref.*
$[Rh(nbd)Cl]_2$+ (*R*)-CycPhos [a)]	H	KI	>99	79 (*S*)	120
$[Rh(nbd)Cl]_2$+ (*R*)-Cycphos [a)]	OMe	KI	>99	91 (*S*)	120
$[Rh(cod)Cl]_2$+ (*S,S*)-BDPP [b)]	H	NEt_3	55	83 (*R*)	117b
$[Rh(cod)Cl]_2$+ (*S,S*)-BDPP [b)]	H	–	96	84 (*R*)	122
$[Rh(cod)Cl]_2$+ monosulfonated (*S,S*)-BDPP [c)]	H	–	>98	94 (*R*)	122
$[Rh(cod)Cl]_2$+ monosulfonated (*S,S*)-BDPP [c)]	OMe	–	>98	92 (*R*)	122
$[Rh(cod)Cl]_2$+ monosulfonated (*S,S*)-BDPP [c)]	Cl	–	>98	92 (*R*)	122
[Rh(*S,S*)-BDPP(nbd)]ClO_4 [d)]	H	15-crown-5	98	89 (*R*)	121
[Rh(*S,S*)-BDPP(nbd)]ClO_4 [d)]	OMe	–	96	92 (*R*)	121

Reaction conditions:
a) PhH/MeOH (1:1), 1000 psi H_2.
b) MeOH, 70 atm. H_2.
c) EtOAc/H_2O, 20 °C, 70 atm. H_2.
d) AOT/PhH, 70 atm. H_2.

1.3.3.2 C=N–X Substrates

The presence of a heteroatom directly connected to the nitrogen atom of the imine activates it toward hydrogenation, while creating a second coordination site for the catalyst. Indeed, some successful results have been achieved for the hydrogenation of *N*-acylhydrazone, sulfonimide, and *N*-diphenylphosphinyl ketimines. The Et-DuPhos–Rh complex is an efficient catalyst for the asymmetric hydrogenation of a variety of *N*-acylhydrozone derivatives [124], as outlined in Tab. 1.13, with up to 97% *ee*.

Tab. 1.13

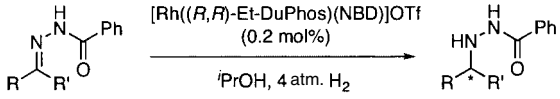

R	*R'*	*Temp (°C)*	*Time (h)*	*% ee (config.)*
Ph	Me	–10	24	95 (*S*)
4-MeOPh	Me	0	24	88 (*S*)
4-EtO_2CPh	Me	0	12	96 (*S*)
4-NO_2Ph	Me	0	12	97 (*S*)
Ph	Et	–10	24	85 (*S*)
2-NP	Me	0	12	95 (*S*)
COOEt	Et	0	24	91 (*S*)
$PO(OEt)_2$	Ph	–10		90

The asymmetric hydrogenation of *N*-diphenylphosphinyl ketimines was achieved using the (*R*)-(*S*)-Cy2PF-PCy2–Rh complex as the catalyst (Tab. 1.14) [125], in which *N*-diphenylphosphinyl acetophenone imine was reduced with up to 99% *ee* at 60 °C under 70 atm. of hydrogen. Interestingly, the reaction temperature is crucial for achieving high levels of enantioselectivity.

Tab. 1.14

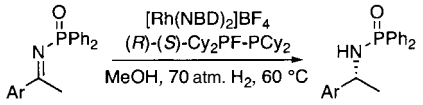

R	*S/C ratio*	*Time (h)*	*% ee (config.)*
H	500	1	99 (*R*)
OMe	100	19	62 (*R*)
Me	100	21	97 (*R*)
CF_3	100	18	93 (*R*)
Cl	100	53	30 (*R*)

1.4 Conclusion

Asymmetric catalytic hydrogenation is unquestionably one of the most significant transformations for academic and industrial-scale synthesis. The development of tunable chiral phosphorous ligands, and of their ability to control enantioselectivity and reactivity, has allowed asymmetric catalytic hydrogenation to become a reaction of unparalleled versatility and synthetic utility. This is exemplified in the ability to prepare enantiomerically enriched intermediates from prochiral olefins, ketones, and imines through asymmetric hydrogenation, which has been exploited in industry for the synthesis of enantiomerically enriched drugs and fine chemicals.

Despite the many advances there remain many unresolved challenges in the field of asymmetric hydrogenation, in which excellent enantioselectivity and high turnover numbers remain elusive with certain substrates. Asymmetric hydrogenation of imines and aromatic rings, for example, remain challenging. Hence, the development of new chiral phosphorous ligands and of their application to asymmetric hydrogenation reactions remains an important and significant area of endeavor.

1.5 References

1 (a) Y. Izumi, A. Tai *Stereo-Differentiating Reactions: The Nature of Asymmetric Reactions*; Academic Press: New York, **1977**. (b) B. Bosnich, Ed. *Asymmetric Catalysis*; Martinus Nijhoff: New York, **1986**. (c) I. Ojima, Ed. *Catalytic Asymmetric Synthesis*; VCH: New York, **1993**. (d) H. Brunner, W. Zettlmeier *Handbook of Enantioselective Catalysis*; VCH: Weinheim, **1993**. (e) R. Noyori *Asymmetric Catalysis in Organic Synthesis*; Wiley: New York, **1994**. (f) G. Jannes, V. Dubois, Eds. *Chiral Reactions in Heterogeneous Catalysis*; Plenum: New York, **1995**. (g) B. Cornils, W.A. Herrmann, Eds. *Applied Homogeneous Catalysis with Organometallic Compounds*; VCH: Weinheim, **1996**; Vol. 1, p. 2. (h) M. Beller, C. Bolm, Eds. *Transition Metals for Organic Synthesis*: *Building Blocks and Fine Chemicals*; Wiley-VCH: Weinheim, **1998**; Vol. 1, p. 2. (i) E.N. Jacobsen, A. Pfaltz, H. Yamamoto, Eds. *Comprehensive Asymmetric Catalysis*; Springer: Berlin, **1999**; Vols. 1–3. (j) I. Ojima, Ed. *Catalytic Asymmetric Synthesis*; Wiley-VCH: New York, **2000**.

2 (a) G.M.R. Tombo, D. Bellus *Angew. Chem. Int. Ed. Engl.* **1991**, *30*, 1193. (b) B. Cornils, W.A. Herrmann, M. Rasch *Angew. Chem. Int. Ed. Engl.* **1994**, *33*, 2144. (c) H.-U. Blaser, B. Pugin In *Chiral Reactions in Heterogeneous Catalysis*, G. Jannes, V. Dubois Eds.; Plenum: New York, **1995**; p. 33. (d) R. Noyori, S. Hashiguchi In *Applied Homogeneous Catalysis with Organometallic Compounds*, B. Cornils, W.A. Herrmann, Eds.; VCH: Weinheim, **1996**; Vol. 1, p. 552. (e) H.-U. Blaser, B. Pugin, F. Spindler In *Applied Homogeneous Catalysis with Organometallic Compounds*, B. Cornils, W.A. Herrmann, Eds.; VCH: Weinheim, **1996**; Vol. 2, p. 992. (f) W. A. Herrmann, B. Cornils *Angew. Chem. Int. Ed. Engl.* **1997**, *36*, 1048. (g) W. Keim In *Transition Metals for Organic Synthesis*: *Building Blocks and Fine Chemicals*, M. Beller, C. Bolm, Eds.; Wiley-VCH: Weinheim, **1998**; Vol. 1, p. 14. (h) H-U. Blaser, F. Spindler In *Comprehensive Asymmetric Catalysis*, E.N. Jacobsen, A. Pfaltz, H. Yamamoto, Eds.; Springer: Berlin, **1999**; Vol. 3, p. 1427. (i) R. Schmid, M. Scalone, In *Comprehensive Asymmetric Catalysis*, E.N. Jacobsen, A. Pfaltz, H. Yamamoto, Eds.; Springer: Berlin, **1999**; Vol. 3, p. 1440. (j) T. Aratani In *Comprehensive Asymmetric Catalysis*, E.N. Jacobsen, A. Pfaltz, H. Yamamoto, Eds.; Springer: Berlin, **1999**; Vol. 3, p. 1451. (k) S. Akutagawa In *Comprehensive Asymmetric Catalysis*, E.N. Jacobsen, A. Pfaltz, H. Yamamoto, Eds.; Springer: Berlin, **1999**; Vol. 3, p. 1461. (l) H.-U. Blaser, F. Spindler, M. Studer *Applied Catalysis A: General* **2001**, *221*, 119. (m) G. Beck *Synlett* **2002**, 837.

3 (a) R. Noyori, M. Kitamura In *Modern Synthetic Methods*, R. Scheffold Ed.; Springer: Berlin, **1989**; Vol. 5, p. 115. (b) H. Takaya, T. Ohta, R. Noyori In *Catalytic Asymmetric Synthesis*, I. Ojima, Ed.; VCH: New York, **1993**; p. 1. (c) R. Noyori *Asymmetric Catalysis in Organic Synthesis*; Wiley: New York, **1994**; Chap. 2. (d) T. Ohkuma, R. Noyori In *Transition Metals for Organic Synthesis*: *Building Blocks and Fine Chemicals*, M. Beller, C. Bolm, Eds.; Wiley-VCH: Weinheim, **1998**; Vol. 2, p. 25. (e) J.M. Brown In *Comprehensive Asymmetric Catalysis*, E.N. Jacobsen, A. Pfaltz, H. Yamamoto, Eds.: Springer: Berlin, **1999**; Vol. 1, p. 121. (f) R.L. Halterman In *Comprehensive Asymmetric Catalysis*, E.N. Jacobsen, A. Pfaltz, H. Yamamoto, Eds.; Springer: Berlin, **1999**; Vol. 1, p. 183. (g) T. Ohkuma, R. Noyori In *Comprehensive Asymmetric Catalysis*, E.N. Jacobsen, A. Pfaltz, H. Yamamoto, Eds.; Springer: Berlin, **1999**; Vol. 1, p. 199. (h) H.-U. Blaser, F. Spindler In *Comprehensive Asymmetric Catalysis*, E.N. Jacobsen, A. Pfaltz, H. Yamamoto, Eds.; Springer: Berlin, **1999**; Vol. 1, p. 247. (i) T. Ohkuma, M., Kitamura, R. Noyori *Catalytic Asymmetric Synthesis*, I. Ojima, Ed.; Wiley-VCH: New York, **2000**; p. 1. (j) R. Noyori, T. Ohkuma *Angew. Chem. Int. Ed.* **2001**, *40*, 40. (k) W.S. Knowles *Angew. Chem. Int. Ed.* **2002**, *41*, 1998. (l) R. Noyori *Angew. Chem. Int. Ed.* **2002**, *41*, 2008.

4 J.A. Osborn, F.H. Jardine, J.F. Young, G. Wilkinson *J. Chem. Soc. A* **1966**, 1711.

5 W. S. Knowles, M. J. Sabacky *Chem. Commun.* **1968**, 1445.

6 L. Horner, H. Siegel, H. Büthe *Angew. Chem. Int. Ed. Engl.* **1968**, *7*, 941.

7 (a) H. B. Kagan, T. P. Dang *Chem. Commun.* **1971**, 481. (b) H. B. Kagan, T. P. Dang *J. Am. Chem. Soc.* **1972**, *94*, 6429. (c) H. B. Kagan, N. Langlois, T. P. Dang *J. Organomet. Chem.* **1975**, *90*, 353.

8 (a) B. D. Vineyard, W. S. Knowles, M. J. Sabacky, G. L. Bachman, O. J. Weinkauff *J. Am. Chem. Soc.* **1977**, *99*, 5946. (b) W. S. Knowles *Acc. Chem. Res.* **1983**, 16, 106.

9 W. S. Knowles *J. Chem. Educ.* **1986**, *63*, 222.

10 (a) T. Hayashi, T. Mise, M. Kumada *Tetrahedron Lett.* **1976**, 4351. (b) T. Hayashi, A. Katsumura, M. Konishi, M. Kumada *Tetrahedron Lett.* **1979**, 425.

11 K. Achima *J. Am. Chem. Soc.* **1976**, *98*, 8265.

12 (a) J. Halpern, D. P. Riley, A. S. C. Chan, J. J. Pluth *J. Am. Chem. Soc.* **1977**, *99*, 8055. (b) A. S. C. Chan, J. Halpern *J. Am. Chem. Soc.* **1980**, *102*, 838. (c) A. S. C. Chan, J. J. Pluth, J. Halpern *J. Am. Chem. Soc.* **1980**, *102*, 5952. (d) J. Halpern, *Science* **1982**, *217*, 401. (e) C. R. Landis, J. Halpern *J. Am. Chem. Soc.* **1987**, *109*, 1746. (f) M. T. Ashby, J. Halpern *J. Am. Chem. Soc.* **1991**, *113*, 589.

13 (a) J. M. Brown, P. A. Chaloner *J. Chem. Soc., Chem. Commun.* **1978**, 321. (b) J. M. Brown, P. A. Chaloner *Tetrahedron Lett.* **1978**, *19*, 1877. (c) J. M. Brown, P. A. Chaloner *J. Chem. Soc., Chem. Commun.* **1979**, 613. (d) J. M. Brown, P. A. Chaloner *J. Chem. Soc., Chem. Commun.* **1980**, 344. (e) J. M. Brown, P. A. Chaloner, R. Glaser, S. Geresh *Tetrahedron* **1980**, *36*, 815. (f) N. W. Alcock, J. M. Brown, A. Derome, A. R. Lucy *J. Chem. Soc., Chem. Commun.* **1985**, 575. (g) J. M. Brown, P. A. Chaloner, G. A. Morris *J. Chem. Soc., Perkin Trans. 2*, **1987**, 1583. (h) J. M. Brown *Chem. Soc. Rev.* **1993**, *22*, 25.

14 (a) R. Noyori *Chem. Soc. Rev.* **1989**, *18*, 187. (b) R. Noyori, H. Takaya *Acc. Chem. Res.* **1990**, *23*, 345. (c) R. Noyori *Science*, **1990**, *248*, 1194. (d) R. Noyori *CHEMTECH* **1992**, 360. (e) R. Noyori *Tetrahedron* **1994**, *50*, 4259.

15 A. Miyashita, A. Yasuda, H. Takaya, K. Toriumi, T. Ito, T. Souchi, R. Noyori *J. Am. Chem. Soc.* **1980**, *102*, 7932.

16 A. Miyashita, H. Takaya, T. Souchi, R. Noyori *Tetrahedron* **1984**, *40*, 1245.

17 (a) R. Noyori, M. Ohta, Y. Hsiao, M. Kitamura, T. Ohta, H. Takaya *J. Am. Chem. Soc.* **1986**, *108*, 7117. (b) M. Hitamura, Y. Hsiao, R. Noyori, H. Takaya *Tetrahedron Lett.* **1987**, *28*, 4829. (c) H. Takaya, T. Ohta, N. Sayo, H. Kumobayashi, S. Akutagawa, S.-I. Inoue, I. Kasahara, R. Noyori *J. Am. Chem. Soc.* **1987**, *109*, 1596. (d) T. Ohta, H. Takaya, M. Kitamura, K. Nagai, R. Noyori *J. Org. Chem.* **1987**, *52*, 3174.

18 (a) R. Noyori, T. Ohkuma, M. Kitamura, H. Takaya, N. Sayo, H. Kumobayashi, S. Akutagawa *J. Am. Chem. Soc.* **1987**, *109*, 5856. (b) M. Kitamura, T. Ohkuma, S. Inoue, N. Sayo, H. Kumobayashi, S. Akutagawa, T. Ohta, H. Takaya, R. Noyori *J. Am. Chem. Soc.* **1988**, *110*, 629. (c) M. Kitamura, I. Kasahara, K. Manabe, R. Noyori, H. Takaya *J. Org. Chem.* **1988**, *53*, 708. (d) R. Noyori, T. Ikeda, T. Ohkuma, M. Widhalm, M. Kitamura, H. Takaya, S. Akutagawa, N. Sayo, T. Saito, T. Taketomi, H. Kumobayashi *J. Am. Chem. Soc.* **1989**, *111*, 9134.

19 T. Ohkuma, H. Ooka, S. Hashiguchi, T. Ikariya, R. Noyori *J. Am. Chem. Soc.* **1995**, *117*, 2675.

20 (a) A. Miyashita, H. Karino, J. Shimamura, T. Chiba, K. Nagano, H. Nohira, H. Takaya *Chem. Lett.* **1989**, 1007. (b) A. Miyashita, H. Karino, J. Shimamura, T. Chiba, K. Nagano, H. Nohira, H. Takaya *Chem. Lett.* **1989**, 1849. (c) T. Chiba, A. Miyashita, H. Nohira *Tetrahedron Lett.* **1991**, *32*, 4745. (d) T. Chiba, A. Miyashita, H. Nohira, H. Takaya *Tetrahedron Lett.* **1993**, *34*, 2351.

21 R. Schmid, M. Cereghetti, B. Heiser, P. Schönholzer, H.-J. Hansen *Helv. Chim. Acta* **1988**, *71*, 897.

22 R. Schmid, J. Foricher, M. Cereghetti, P. Schönholzer *Helv. Chim. Acta*. **1991**, *74*, 870.

23 (a) M. Chiba, H. Takahashi, T. Morimoto, K. Achiwa *Tetrahedron Lett.* **1987**, *28*, 3675. (b) T. Morimoto, M. Chiba, K. Achiwa *Tetrahedron Lett.* **1988**, *29*, 4755. (c) T. Morimoto, M. Chiba, K. Achiwa *Teterahedron Lett.* **1989**, *30*, 735.

(d) T. Morimoto, M. Chiba, K. Achiwa *Chem. Pharm. Bull.* **1989**, *37*, 3161. (e) T. Morimoto, M. Chiba, K. Achiwa *Heterocycles* **1990**, *30*, 363. (f) T. Morimoto, M. Chiba, K. Achiwa *Tetrahedron Lett.* **1990**, *31*, 261. (g) K. Yoshikawa, K. Inoguchi, T. Morimoto, K. Achiwa *Heterocycles*, **1990**, *31*, 261. (h) T. Morimoto, M. Chiba, K. Achiwa *Chem. Pharm. Bull.* **1993**, *41*, 1149.

24 (a) H. Takahashi, M. Hattori, M. Chiba, T. Morimoto, K. Achiwa *Tetrahedron Lett.* **1986**, *27*, 4477. (b) H. Takahashi, T. Morimoto, K. Achiwa *Chem. Lett.* **1987**, 855. (c) H. Takahashi, K. Achiwa *Chem. Lett.* **1987**, 1921. (d) K. Inoguchi, T. Morimoto, K. Achiwa *J. Organomet. Chem.* **1989**, *370*, C9. (e) H. Takahashi, N. Yamamoto, H. Takeda, K. Achiwa *Chem. Lett.* **1989**, 559. (f) H. Takahashi, S. Sakuraba, H. Takeda, K. Achiwa *J. Am. Chem. Soc.* **1990**, *112*, 5876. (g) H. Takeda, S. Hosokawa, M. Aburatani, K. Achiwa *Synlett* **1991**, 193. (h) S. Sakuraba, K. Achiwa *Synlett* **1991**, 689. (i) S. Sakuraba, N. Nakajima, K. Achiwa *Synlett* **1992**, 829. (j) S. Sakuraba, N. Nakajima, K. Achiwa *Tetrahedron: Asymmetry* **1993**, *7*, 1457. (k) S. Sakuraba, H. Takahashi, H. Takeda, K. Achiwa *Chem. Pharm. Bull.* **1995**, *43*, 738.

25 H. Brunner, W. Pieronczyk, B. Schönhammer, K. Streng, I. Bernal, J. Korp *Chem. Ber.* **1981**, *114*, 1137.

26 (a) U. Nagel *Angew. Chem. Int. Ed. Engl.* **1984**, *23*, 435. (b) U. Nagel, E. Kinzel, J. Andrade, G. Prescher *Chem. Ber.* **1986**, *119*, 3326. (c) K. Inoguchi, K. Achiwa *Chem. Pharm. Bull.* **1990**. *38*, 818.

27 (a) J. Bakos, I. Toth, L. Markó *J. Org. Chem.* **1981**, *46*, 5427. (b) P.A. NacNeil, N.K. Roberts, B. Bosnich *J. Am. Chem. Soc.* **1981**, *103*, 2273. (c) J. Bakos, I. Tóth, B. Heil, L. Markó *J. Organomet. Chem.* **1985**, *279*, 23.

28 T. Hayashi, N. Kawamura, Y. Ito *J. Am. Chem. Soc.* **1987**, *109*, 7876.

29 (a) W.A. Nugent, T.V. RajanBabu, M.J. Burk *Science* **1993**, *259*, 479. (b) M.J. Burk *Acc. Chem. Res.* **2000**, *33*, 363.

30 (a) M.J. Burk, J.E. Feaster, R.L. Harlow *Organometallics* **1990**, *9*, 2653. (b) M.J. Burk, R.L. Harlow *Angew. Chem. Int. Ed. Engl.* **1990**, *29*, 1462. (c) M.J. Burk, J.E. Feaster, R.L. Harlow *Organometallics* **1990**, *9*, 2653.

31 W. Tang, Y. Chi, X. Zhang *Org. Lett.* **2002**, *4*, 1695.

32 (a) J. Holz, M. Quirmbach, U. Schmidt, D. Heller, R. Stürmer, A. Börner *J. Org. Chem.* **1998**, *63*, 8031. (b) J. Holz, R. Stürmer, U. Schmidt, H.-J. Drexler, D. Heller, H.-P. Krimmer, A. Börner *Eur. J. Org. Chem.* **2000**, 4615.

33 (a) W. Li, Z. Zhang, D. Xiao, X. Zhang *Tetrahedron Lett.* **1999**, *40*, 6701. (b) W. Li, Z. Zhang, D. Xiao, X. Zhang *J. Org. Chem.* **2000**, *65*, 3489.

34 (a) Y.-Y. Yan, T. V. RajanBabu *J. Org. Chem.* **2000**, *65*, 900. (b) Y.-Y. Yan, T.V. RajanBabu *Org. Lett.* **2000**, *2*, 199. (c) T. V. RajanBabu, Y.-Y. Yan, S. Shin *J. Am. Chem. Soc.* **2001**, *123*, 10207.

35 (a) J. Holz, D. Heller, R. Stürmer, A. Börner *Tetrahedron Lett.* **1999**, *40*, 7059. (b) J. Holz, R. Stürmer, U. Schmidt, H.-J. Drexler, D. Heller, H.-P. Krimmer, A. Börner *Eur. J. Org. Chem.* **2000**, 4615.

36 Q. Jiang, Y. Jiang, D. Xiao, P. Cao, X. Zhang *Angew. Chem. Int. Ed.* **1998**, *37*, 1100.

37 (a) Z. Zhang, G. Zhu, Q. Jiang, D. Xiao, X. Zhang *J. Org. Chem.* **1999**, *64*, 1774. (b) Q. Jiang, D. Xiao, Z. Zhang, P. Cao, X. Zhang *Angew. Chem. Int. Ed.* **1999**, *38*, 516.

38 M. Ostermeier, J. Priess, G. Helmchen *Angew. Chem. Int. Ed.* **2002**, *41*, 612.

39 D. Xiao. Z. Zhang, X. Zhang *Org. Lett.* **1999**, *1*, 1679.

40 E. Fernandez, A. Gillon, K. Heslop, E. Horwood, D.J. Hyett, A.G. Orpen, P.G. Pringle *Chem. Commun.* **2000**, 1663.

41 (a) G. Zhu, P. Cao, Q. Jiang, X. Zhang *J. Am. Chem. Soc.* **1997**, *119*, 1799. (b) G. Zhu, X. Zhang *J. Org. Chem.* **1998**, *63*, 9590. (c) G. Zhu, A.L. Casalnuovo, X. Zhang *J. Org. Chem.* **1998**, *63*, 8100. (d) G. Zhu, X. Zhang *Tetrahedron: Asymmetry* **1998**, *9*, 2415. (e) G. Zhu, Z. Chen, X. Zhang *J. Org. Chem.* **1999**, *64*, 6907. (f) P. Cao, X. Zhang *J. Org. Chem.* **1999**, *64*, 2127.

42 W. Li, X. Zhang *J. Org. Chem.* **2000**, *65*, 5871.

43 (a) Y.-Y. Yan, T.V. RajanBabu *J. Org. Chem.* **2000**, *65*, 900. (b) Y.-Y. Yan, T.V. RajanBabu *Org. Lett.* **2000**, *2*, 199. (c) Y.-Y. Yan, T. V. RajanBabu *Org. Lett.* **2000**, *2*, 4137.

44 (a) S.-G. Lee, Y.J. Zhang, C.E. Song, J.K. Lee, J.H. Choi *Angew. Chem. Int. Ed.* **2002**, *41*, 847. (b) S.-G. Lee, Y.J. Zhang *Org. Lett.* **2002**, *4*, 2429. (c) S.-G. Lee, Y. J. Zhang *Tetrahedron: Asymmetry* **2002**, *13*, 1039.

45 W. Li, J.P. Waldkirch, X. Zhang *J. Org. Chem.* **2002**, 7618.

46 (a) M. Sawamura, H. Hamashima, M. Sugawara, N. Kuwano, Y. Ito *Organometallics* **1995**, *14*, 4549. (b) M. Sawamura, R. Kuwano, Y. Ito *J. Am. Chem. Soc.* **1995**, *117*, 9602. (c) R. Kuwano, M. Sawamura, Y. Ito *Tetrahedron: Asymmetry* **1995**, *6*, 2521. (d) R. Kuwano, S. Okuda, Y. Ito *Tetrahedron: Asymmetry* **1998**, *9*, 2773. (e) R. Kuwano, S. Okuda, Y. Ito *J. Org. Chem.* **1998**, *63*, 3499. (f) R. Kuwano, Y. Ito *J. Org. Chem.* 1999, 64, 1232. (g) R. Kuwano, K. Sato, T. Kurokawa, D. Karube, Y. Ito *J. Am. Chem. Soc.* **2000**, *122*, 7614.

47 A. Togni, C. Breutel, A. Schnyder, F. Spindler, H. Landert, A. Tijani *J. Am. Chem. Soc.* **1994**, *116*, 4062.

48 J. McGarrity, F. Spindler, R. Fuchs, M. Eyer (Lonza AG), EP-A 624587 A2, **1995**; *Chem. Abstr.* **1995**, *122*, P81369q.

49 (a) H.-U. Blaser *Adv. Synth. Catal.* **2002**, *344*, 17. (b) H.-U. Blaser, H.-P. Buser, K. Coers, R. Hanreich, H.-P. Jalett, E. Jelsch, B. Pugin, H.-D. Schneider, F. Spindler, A. Wegmann *Chimia* **1999**, *53*, 275.

50 (a) J. Kang, J.H. Lee, A.H. Ahn, J.S. Choi *Tetrahedron Lett.* **1998**, *39*, 5523. (b) J. Kang, J.H. Lee, J.B. Kim, G.J. Kim *Chirality* **2000**, *12*, 378.

51 (a) J.J. Almena Perea, A. Börner, P. Knochel *Tetrahedron Lett.* **1998**, *39*, 8073. (b) J.J. Almena Perea, M. Lotz, P. Knochel *Tetrahedron: Asymmetry* **1999**, *10*, 375. (c) M. Lotz, T. Ireland, J.J. Almena Perea, P. Knochel *Tetrahedron: Asymmetry* **1999**, *10*, 1839.

52 (a) T. Ireland, G. Grossheimann, C. Wieser-Jeunesse, P. Knochel *Angew. Chem. Int. Ed.* **1999**, *38*, 3212. (b) T. Ireland, K. Tappe, G. Grossheimann, P. Knochel *Chem. Eur. J.* **2002**, *8*, 843.

53 A. Marinetti, F. Labrue, J.-P. Gent *Synlett* **1999**, 1975.

54 U. Berens, M.J. Burk, A. Gerlach, W. Hems *Angew. Chem. Int. Ed.* **2000**, *39*, 1981.

55 D. Liu, W. Li, X. Zhang *Org. Lett.* **2002**, *4*, 4471.

56 M.J. Burk, M.F. Gross *Tetrahedron Lett.* **1994**, *35*, 9363.

57 (a) T. Imamoto, J. Watanabe, Y. Wada, H. Masuda, H. Yamada, H. Tsuruta, S. Matsukawa, K. Yamaguchi *J. Am. Chem. Soc.* **1998**, *120*, 1635. (b) I.D. Gridnev, Y. Yamanoi, N. Higashi, H. Tsuruta, M. Yasutake, T. Imamoto *Adv. Synth. Catal.* **2001**, *343*, 118.

58 I. D. Gridnev, M. Yasutake, N. Higashi, T. Imamoto *J. Am. Chem. Soc.* **2001**, *123*, 5268.

59 M.Yasutake, I.D.Gridnev, N. Higashi, T. Imamoto *Org. Lett.* **2001**, *3*, 1701.

60 I. D. Gridnev, N. Higashi, T. Imamoto *J. Am. Chem. Soc.* **2001**, *123*, 4631.

61 Y. Yamanoi, T. Imamoto *J. Org. Chem.* **1999**, *64*, 2988.

62 T. Miura, T. Imamoto *Tetrahedron Lett.* **1999**, *40*, 4833.

63 (a) A. Ohashi, T. Imamoto *Org. Lett.* **2001**, *3*, 373. (b) A. Ohashi, S.-i. Kikuchi, M. Yasutake, T. Imamoto *Eur. J. Org. Chem.* **2002**, 2535.

64 W. Tang, X. Zhang *Angew. Chem. Int. Ed.* **2002**, *41*, 1612.

65 W. Tang, W. Wang, Y. Chi, X. Zhang *Angew. Chem. Int. Ed.* **2003**, *42*, 3509.

66 W. Tang, X. Zhang *Org. Lett.* **2002**, *4*, 4159.

67 W. Tang, D. Liu, X. Zhang *Org. Lett.* **2003**, *5*, 205.

68 (a) F. Robin, F. Mercier, L. Ricard, F. Mathey, M. Spagnol *Chem. Eur. J.* **1997**, *3*, 1365. (b) F. Mathey, F. Mercier, F. Robin, L. Ricard *J. Organometallic Chem.* **1998**, *577*, 117.

69 (a) P.J. Pye, K. Rossen, R.A. Reamer, N.N. Tsou, R.P. Volante, P.J. Reider *J. Am. Chem. Soc.* **1997**, *119*, 6207. (b) P.J. Pye, K. Rossen, R.A. Reamer, R.P. Volante, P.J. Reider *Tetrahedron Lett.* **1998**, *39*, 4441. (c) M.J. Burk, W. Hems, D. Herzberg, C. Malan, A. Zanotti-Gerosa *Org. Lett.* **2000**, *2*, 4173.

70 Y.-G. Zhou, X. Zhang *Chem. Commun.* **2002**, 1124.

71 (a) T.V. RajanBabu, T.A. Ayers, A.L. Casalnuovo *J. Am. Chem. Soc.* **1994**, *116*, 4101. (b) T.V. RajanBabu, T.A. Ayers, G.A. Halliday, K.K. You, J.C. Calabrese *J. Org. Chem.* **1997**, *62*, 6012.

72 (a) A.S.C. Chan, W. Hu, C.-C. Pai, C.-P. Lau, Y. Jiang, A. Mi, M. Yan, J. Sun, R. Lou, J. Deng *J. Am. Chem. Soc.* **1997**,

119, 9570. (b) W. Hu, M. Yan, C.-P. Lau, S.M. Yang, A.S.C. Chan, Y. Jiang, A. Mi *Tetrahedron Lett.* **1999**, *40*, 973.

73 Y. Chen, X. Li, S.-K. Tong, M.C.K. Choi, A.S.C. Chan *Tetrahedron Lett.* **1999**, *40*, 957.

74 K. Yonehara, T. Hashizume, K. Mori, K. Ohe, S. Uemura *J. Org. Chem.* **1999**, *64*, 5593.

75 Y.-G. Zhou, W. Tang, W.-B. Wang, W. Li, X. Zhang *J. Am. Chem. Soc.* **2002**, *124*, 4952.

76 M.T. Reetz, A. Gosberg, R. Goddard, S.-H. Kyung *Chem. Commun.* **1998**, 2077.

77 A. Zanotti-Gerosa, C. Malan, D. Herzberg *Org. Lett.* **2001**, *3*, 3687.

78 M.T. Reetz, T. Neugebauer *Angew. Chem. Int. Ed.* **1999**, *38*, 179.

79 (a) A. Roucoux, F. Agbossou, A. Mortreux, F. Petit *Tetrahedron: Asymmetry* **1993**, *4*, 2279. (b) F. Agbossou, J.-F. Carpentier, C. Hatat, N. Kokel, A. Mortreux *Organometallics* **1995**, *14*, 2480. (c) A. Roucoux, M. Devocelle, J.-F. Carpentier, F. Agbossou, A. Mortreux *Synlett* **1995**, 358. (d) A. Roucoux, L. Thieffry, J.-F. Carpentier, M. Devocelle, C. Méliet, F. Agbossou, A. Mortreux *Organometallics* **1996**, *15*, 2440. (e) M. Devocelle, F. Agbossou, A. Mortreux, *Synlett* **1997**, 1306. (f) J.-F. Carpentier, A. Mortreux *Tetrahedron: Asymmetry* **1997**, *8*, 1083. (g) C. Pasquier, S. Naili, L. Pelinski, J. Brocard, A. Mortreux, F. Agbossou *Tetrahedron: Asymmetry* **1998**, *9*, 193. (h) F. Agbossou, J.-F. Carpentier, F. Hapiot, I. Suisse, A. Mortreux *Coord. Chem. Rev.* **1998**, *178–180*, 1615.

80 (a) Y. Xie, R. Lou, Z. Li, A. Mi, Y. Jiang *Tetrahedron: Asymmetry* **2000**, *11*, 1487. (b) R. Lou, A. Mi, Y. Jiang, Y. Qin, Z. Li, F. Fu, A.S.C. Chan *Tetrahedron* **2000**, *56*, 5857.

81 (a) F.-Y. Zhang, C.-C. Pai, A.S.C. Chan *J. Am. Chem. Soc.* **1998**, *120*, 5808. (b) F.-Y. Zhang, W.H. Kwok, A.S.C. Chan *Tetrahedron: Asymmetry* **2001**, *12*, 2337.

82 R. Guo, X. Li, J. Wu, W.H. Kwok, J. Chen, M.C.K. Choi, A.S.C. Chan *Tetrahedron Lett.* **2002**, *43*, 6803.

83 N.W. Boaz, S.D. Debenham, E.B. Mackenzie, S.E. Large *Org. Lett.* **2002**, *4*, 2421.

84 F. Lagasse, H.B. Kagan *Chem. Pharm. Bull.* **2000**, *48*, 315.

85 (a) M.T. Reetz, G. Mehler *Angew. Chem. Int. Ed.* **2000**, *39*, 3889. (b) M.T. Reetz, G. Mehler, A. Meiswinkel, T. Sell *Tetrahedron Lett.* **2002**, *43*, 7941.

86 M. van den Berg, A.J. Minnaard, E.P. Schudde, J. van Esch, A.H.M. de Vries, J. G. de Vries, B.L. Feringa *J. Am. Chem. Soc.* **2000**, *122*, 11539.

87 (a) X. Jia, R. Guo, X. Li, X. Yao, A.S.C. Chan *Tetrahedron Lett.* **2002**, *43*, 5541. (b) M. van den Berg, R.M. Haak, A.J. Minnaard, A.H.M. de Vries, J.G. de Vries, B.L. Feringa *Adv. Synth. Catal.* **2002**, *344*, 1003.

88 (a) A.-G. Hu, Y. Fu, J.-H. Xie, H. Zhou, L.-X. Wang, Q.-L. Zhou *Angew. Chem. Int. Ed.* **2002**, *41*, 2348. (b) Y. Fu, J.-H. Xie, A.-G. Hu, H. Zhou, L.-X. Wang, Q.-L. Zhou *Chem. Commun.* **2002**, 480.

89 M.J. Burk, J.E. Feaster, W.A. Nugent, R. L. Harlow *J. Am. Chem. Soc.* **1993**, *115*, 10125.

90 M. Diéguez, A. Ruiz, C. Claver *J. Org. Chem.* **2002**, *67*, 3796.

91 M.J. Burk, S. Feng, M.F. Gross, W. Tumas *J. Am. Chem. Soc.* **1995**, *117*, 8277.

92 (a) J.W. Scott, D.D. Kieth, G. Nix Jr., D.R. Parrish, S. Remington, G.P. Roth, J.M. Townsend, D. Valentine Jr., R. Yang *J. Org. Chem.* **1981**, *46*, 5086. (b) B.D. Vineyard, W.S. Knowles, M.J. Sabacky, G.L. Bachman, D.J. Weinkauff *J. Am. Chem. Soc.* **1977**, *99*, 5946.

93 M.J. Burk, M.F. Gross, J.P. Martinez *J. Am. Chem. Soc.* **1995**, *117*, 9375.

94 M.J. Burk, K.M. Bedingfield, W.F. Kiesman, J.G. Allen *Tetrahedron Lett.* **1999**, *40*, 3093.

95 A.J. Robinson, P. Stanislawski, D. Mulholland, L. He, H.-Y. Li *J. Org. Chem.* **2001**, *66*, 4148.

96 M.J. Burk, Y.M. Wang, J.R. Lee *J. Am. Chem. Soc.* **1996**, 118, 5142.

97 M.J. Burk, G. Casy, N.B. Johnson *J. Org. Chem.* **1998**, *63*, 6084.

98 (a) T. Tang, J.A. Ellman *J. Org. Chem.* **1999**, *64*, 12. (b) M.P. Sibi, H.J. Shay, M. Liu, C.P. Jasperse *J. Am. Chem. Soc.* **1998**, *120*, 6615. (c) S. Kobayashi, H. Ishitani, M. Ueno *J. Am. Chem. Soc.* **1998**, *120*, 431. (d) H. Boesch, S. Cesco-Cancian, L.R. Hecker, W.J. Hoekstra, M. Justus, C.A. Maryanoff, L. Scott, R.D. Shah,

G. Solms, K.L. Sorgi, S.M. Stefanick, U. Thurnheer, F.J., Jr. Villani, D.G. Walker *Org. Process Res. Dev.* **2001**, *5*, 23. (e) W.J. Hoekstra, B.E. Maryanoff, B.P. Damiano, P. Andrade-Gordon, J.H. Cohen, M.J. Costanzo, B.J. Haertlein, L.R. Hecker, B.L. Hulshizer, J.A. Kauffman, P. Keane, D.F. McComsey, J.A. Mitchell, L. Scott, R.D. Shah, S.C. Yabut *J. Med. Chem.* **1999**, *42*, 5254. (f) H.M. Zhong, J.H. Cohen, A.F. Abdel-Magid, B.D. Kenney, C.A. Maryanoff, R.D. Shah, F.J. Villani Jr., F. Zhang, X. Zhang *Tetrahedron Lett.* **1999**, *40*, 7721. (g) B.B. Shankar, M.P. Kirkup, S.W. McCombie, J.W. Clader, A.K. Ganguly *Tetrahedron Lett.* **1996**, *37*, 4095. (h) D.A. Burnett, M.A. Caplen, H.R. Davis Jr., R.E. Burrier, J.W. Clader *J. Med. Chem.* **1994**, *59*, 1733.

99 D. Heller, J. Holz, H.-J. Drexler, J. Lang, K. Drauz, H.-P. Krimmer, A. Börner *J. Org. Chem.* **2001**, *66*, 6816.

100 K.E. Koenig, G.L. Bachman, B.D. Vineyard *J. Org. Chem.* **1980**, *45*, 2362.

101 U. Schmidt, J. Langner, B. Kirschbaum, C. Braun *Synthesis* **1994**, 1138.

102 M.J. Burk, C.S. Kalberg, A. Pizzano *J. Am. Chem. Soc.* **1998**, *120*, 4345.

103 M.J. Burk, T.A. Stammers, J.A. Straub *Org. Lett.* **1999**, *1*, 387.

104 M.J. Burk *J. Am. Chem. Soc.* **1991**, *113*, 8518.

105 N.W. Boaz *Tetrahedron Lett.* 1998, 39, 5505.

106 (a) K. Iseki *Tetrahedron* **1998**, *54*, 13887. (b) Y. Kuroki, D. Asada, Y. Sakamaki, K. Iseki *Tetrahedron Lett.* **2000**, *41*, 4603.

107 Y. Crameri, J. Foricher, M. Scalone, R. Schmid *Tetrahedron: Asymmetry* **1997**, *8*, 3617.

108 M.J. Burk, F. Bienewald, M. Harris, A. Zanotti-Gerosa *Angew. Chem. Int. Ed.* **1998**, *37*, 1931.

109 H. Jendralla, R. Henning, B. Seuring, J. Herchen, B. Kulitzscher, J. Wunner *Synlett* **1993**, 155.

110 M.J. Burk, F. Bienewald, S. Challenger, A. Derrick, J. A. Ramsden *J. Org. Chem.* **1999**, *64*, 3290.

111 K. Inoguchi, S. Sakuraba, K. Achiwa *Synlett* **1992**, 169.

112 H. Takahashi, M. Hattori, M. Chiba, T. Morimoto, K. Achiwa *Tetrahedron Lett.* **1986**, 4477.

113 (a) E.A. Broger, Y. Crameri EP 0218970, 1987. (b) E.A. Broger, Y. Crameri US 5 142 063, **1992**. (c) R. Schmid *Chimia* **1996**, *50*, 110.

114 H. Takeda, T. Tachinami, M. Aburatani, H. Takahashi, T. Morimoto, K. Achiwa *Tetrahedron Lett.* **1989**, *30*, 363.

115 V. Fehring, R. Selke *Angew. Chem. Int. Ed.* **1998**, *37*, 1827.

116 S. Törös, B. Heil, L. Kollár, L. Markó *J. Organomet. Chem.* **1980**, *197*, 85.

117 (a) J. Bakos, I. Tóth, B. Heil, L. Markó *J. Organomet. Chem.* **1985**, *279*, 23. (b) J. Bakos, I. Tőth, B. Heil, G. Szalontai, L. Párkányi, V. Fülöp *J. Organomet. Chem.* **1989**, *370*, 263.

118 C. Bolm *Angew. Chem. Int. Ed. Engl.* **1993**, *32*, 232.

119 (a) C.A. Willoughby, S.L. Buchwald *J. Am. Chem. Soc.* **1992**, *114*, 7562. (b) C.A. Willoughby, S.L. Buchwald *J. Org. Chem.* **1993**, *58*, 7627. (c) C.A. Willoughby, S.L. Buchwald *J. Am. Soc. Chem.* **1994**, *116*, 8952. (d) A. Viso, N.E. Lee, S.L. Buchwald *J. Am. Chem. Soc.* **1994**, *116*, 9373.

120 G.-J. Kang, W.R. Cullen, M.D. Fryzuk, B.R. James, J.. Kutney *J. Chem. Soc., Chem. Commun.* **1988**, *1466*.

121 J.M. Buriak, J.A. Osborn *Organometallics* **1996**, *15*, 3161.

122 J. Bakos. A. Orosz, B. Heil, M. Laghmari, P. Lhoste, D. Sinou *J. Chem. Soc., Chem. Commun.* **1991**, 1684.

123 C. Lensink, E. Rijnberg, G. de Vries *J. Mol. Cat. A: Chem.* **1997**, *116*, 199.

124 M.J. Burk, J.E. Feaster *J. Am. Chem. Soc.* **1992**, *114*, 6266.

125 F. Spindler, H.-U. Blaser *Adv. Synth. Catal.* **2001**, *343*, 68.

2
Rhodium-Catalyzed Hydroborations and Related Reactions

John M. Brown

2.1
Introduction

The development of metal-catalyzed hydroboration was initiated in a single paper by Männig and Nöth in 1985 [1]. They demonstrated that catecholborane reacted with simple alkenes in the presence of transition-metal catalysts, the most effective being Wilkinson's catalyst, $RhCl(PPh_3)_3$. Since this reaction of catecholborane with alkenes is normally rather slow, even at elevated temperatures, this observation provided a real opportunity for catalysis. Prior to this work, the only precedent had been the addition of a secondary alkoxyborane to the same rhodium complex, giving a borylrhodium hydride analogous to known silylrhodium hydrides [2]. The synthetic potential of catalytic hydroboration was quickly realized and further extended through Burgess's demonstration of asymmetric catalysis [3], which was later refined and extended by Hayashi [4]. All this early work has been reported in a 1991 review [5], with a later and more extensive review by Beletʹskaya and Pelter in 1997 [6]. As these reviews are readily available, the present chapter is confined largely to developments that have taken place since the beginning of 1997. Fig. 2.1 summarizes some of these early milestones. Although metal catalysts other than rhodium have been examined, for example in the palladium-catalyzed hydroboration of allenes [7], the majority of the interesting developments have been made with rhodium.

In the interim period, results have accumulated steadily, in endeavors to address and extend the chemistry beyond the initial perceived limitations. These limitations include the following: (a) the effective catalytic syntheses are confined to the reactions utilizing catecholborane; (b) the scope of alkenes for which efficient rate, regio- and enantioselectivity can be achieved is limited, and (c) the "standard" transformation mandates the oxidation of the initially formed (secondary) boronate ester to a secondary alcohol, albeit with complete retention of configuration [8]. Nonetheless, for noncatalytic hydroboration reactions that lead to the formation of a trialkylborane, a wide range of stereospecific transformations may be carried out directly from the initial product, and thereby facilitate direct C–N and C–C bond formation [9].

A reaction pathway for catalytic hydroboration was suggested by Evans and co-workers [10], and amplified through computational studies [11]. This involves the rhodium acting through oxidative addition across the B–H bond, and the resulting borylrhodium hydride complexing to the alkene (reversibly). This is followed by a hydride migration, with a subsequent reductive elimination of the alkylboronate ester to complete

Modern Rhodium-Catalyzed Organic Reactions. Edited by P. Andrew Evans

ISBN: 3-527-30683-8

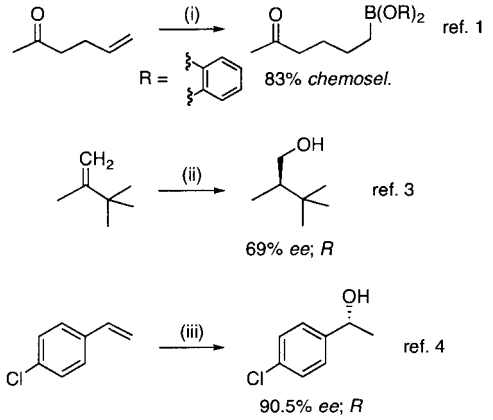

Fig. 2.1 Some initial developments in catalytic hydroboration: (i) 0.05 mol% $RhCl(PPh_3)_3$, 1 eq. catecholborane, 1 eq. alkene, C_6H_6, 20 °C; (ii) 2 mol% DIOP (unspecified hand), 1 mol% $[Rh(COD)Cl]_2$, alkene,1.2 eq. catecholborane, H_2O_2/NaOH workup; (iii) 1 mol% $Rh(COD)_2$ BF_4, 1.1 mol% *R*-BINAP, 1 eq. alkene, 1.1 eq. catecholborane, DME, –78 °C, 6 h, H_2O_2/NaOH workup.

the catalytic cycle. The observed regiochemistry in the formation of the α-substituted product argues for this mechanism over that involving an initial boryl migration. This is consistent with the expectation that the more stable rhodium alkyl species would predominate. This argument is further supported by the fact that benzylrhodium complexes are stabilized by η^3-interactions with π-systems [12]. A recent computational study examined the associative and dissociative reaction pathways for hydroboration employing the model system $[C_2H_4 + BH(OH)_2]$ catalyzed by the model complex $RhCl(PH_3)_2$, using DFT calculations at the BP86 level (Fig. 2.2) [13]. Their conclusions allow for either mechanism; in the associative mechanism, the initial hydride migration is only slightly favored over boron migration as both have similar energy profiles, whereas in the dissociative mechanism initial boryl migration is considerably uphill (19.5 kcal/mol) relative to that of initial hydride migration (8.5 kcal/mol). However, reductive C–B formation in the boryl migration pathway is energetically favored (6.5 kcal/mol) over that of C–H bond formation (15.8 kcal/mol) in the hydride migration pathway. They also conclude that in either mechanism a boryl migration would lead to greater amounts of side products, that is, vinylboranes and alkanes. All the energies in the associative pathways were computed for the *trans*-bisphosphine intermediates. The authors favor an associative pathway, in contrast to earlier computa-

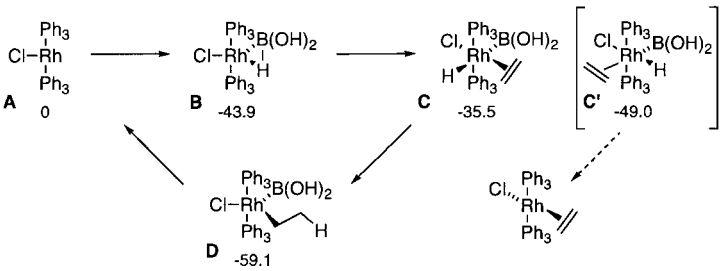

Fig. 2.2 Key features of the computational pathway for rhodium-catalyzed hydroboration, with energies in kcal/mol. Similar results were obtained for the related dioxaborolidine pathway. The isomeric intermediate **C′** does not have access to a low energy H-migration pathway but rather eliminates B-H.

tional studies [11], but allow the possibility of a dissociative pathway with bulky electron-withdrawing phosphine ligands. Since the best catalysts for asymmetric hydroboration are *cis*-chelating bidentate ligands, these calculations will require generalization before they can be applied to realistic systems with confidence. Experimental [14] and computational work [15] provides an interesting contrast to the pathway elucidated for the Cp_2Ti-catalyzed hydroboration, in which the alkene reacts with the fully characterized η^2-B–H titanium adduct by initial boryl transfer followed by reductive elimination from an alkyltitanium hydride. This is a two-step process, the first being conversion of a bridging B–H–Ti intermediate, with reductive elimination occurring from the open form.

It is a striking feature of metal-catalyzed hydroboration that alkoxyboranes are more effective than borane or its alkyl derivatives. Analysis of the electronic features of the two classical reagents, catecholborane and 9-BBN, reveal only modest differences in the B–H region (Fig. 2.3). This by itself does not explain the narrow convergence of

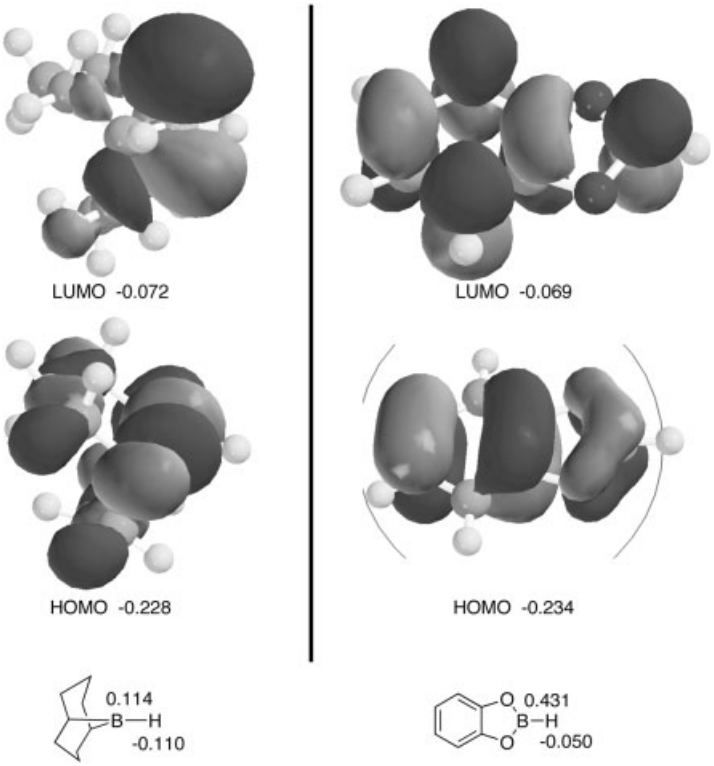

Fig. 2.3 The frontier orbitals of 9-BBN in comparison with those of catecholborane, arising from DFT calculations at the LSDA/pBP86/DN* level. Orbital energies are quoted in Hartree units; charges at the B and H atoms in the two reagents are inserted on the structural diagrams.

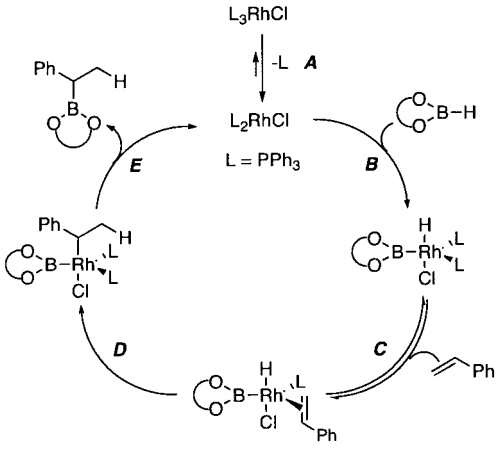

Fig. 2.4 A possible pathway for rhodium-catalyzed hydroboration by $RhCl(PPh_3)_3$, based on the mechanism of hydrogenation and the contributions of Evans and others [17]. This takes into account the theoretical support for an associative pathway [13] and the observed irreversibility of the H-transfer step with styrenes. ***A***, ligand dissociation; ***B***, H-B addition; ***C***, alkene addition; ***D***, H-migration; ***E***, reductive elimination and decomplexation.

the catalytic chemistry, where only catecholborane (and to a lesser extent other alkoxyboranes) are generally effective reagents [16]. The nature of the metal–boronate bond is distinct from that of the metal–boryl bond, and any additional stabilization in the former must be reflected at the transition-state for B–H transfer to rhodium. A further important factor is the planarity of the boronate ester that must facilitate the oxidative addition step by minimizing the steric hindrance of approach.

Overall, mechanistic aspects of catalytic hydroboration have been underemphasized in more recent work; the best source for this information remains a survey by Evans and co-workers in 1992 [17]. On the basis of labeling experiments coupled with substrate variation, the major pathway involves a set of steps in accord with that expected from precedent, theory, and intuition, as illustrated in Fig. 2.4, albeit with the qualification that the steps involving alkene addition and migration of hydride to alkene may be reversible, depending on the substrate. The rhodium–phosphine complex is the true catalyst, but there is a very rapid competing reaction when phosphine-free rhodium species are present. A consequence of this is that oxidized samples of Wilkinson's catalyst can give misleading results [18]. The lack of characterization of reactive intermediates is a hindrance to further progress on understanding the mechanism, although the recent report of the observation of a borylrhodium complex by NMR during catalytic turnover is a step in the right direction [19].

2.2
General Advances in Catalytic Hydroboration

For adoption by the synthetic-organic community, a new method must pass certain tests. If it is catalytic, then the turnover must be efficient so that the quantity of (presumably expensive) catalyst employed is small. The reaction needs to be selective in all the desirable ways, where appropriate including chemo-, regio-, and stereospecificity. Much of the work on hydroboration has been aimed at progress toward those goals. The rhodium-catalyzed reaction of catecholborane with a simple styrene frequently forms part of the standard catalytic screening procedures for a novel ligand.

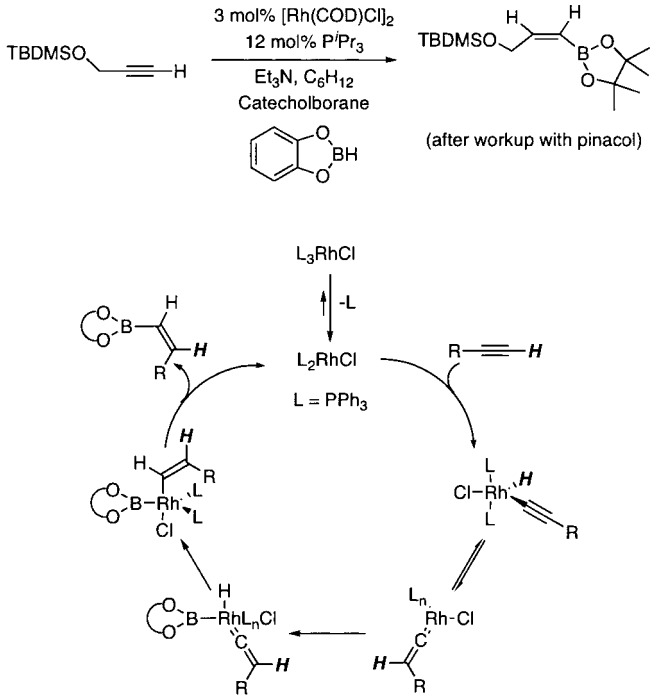

Fig. 2.5 The *trans*-addition of dialkoxyboranes to alkynes, in the presence of triethylamine that suppresses the "normal" addition pathway by capturing the rhodium B-H adduct. The bold hydrogen has been traced between reactant and product by deuterium labelling. Iridium catalysts also function but less effectively.

As would be expected, catalytic hydroboration is effective for alkynes as well as alkenes, and prior examples have been reviewed [6]. An interesting development has been the diversion of the normal *syn*- to the *anti*-addition pathway for a terminal alkyne, with 99% (catechoborane) and 91% (pinacolborane) respectively (Fig. 2.5) [20]. The new pathway arises when basic alkylphosphines are employed in combination with $[Rh(COD)Cl]_2$ as the catalyst in the presence of Et_3N. Current thinking implies that this is driven by the initial addition of the rhodium catalyst into the alkynyl C–H bond, followed by [1,3]-migration of hydride and formal 1,1-addition of B–H to the resulting alkylidene complex. The reaction is general for terminal alkynes.

In an analogous manner to homogeneous hydrogenation, a polar functionality remote from the reaction site can direct the stereochemical course of the reaction. The results, dating back to early work by Burgess [21] and with a set of definitive examples from Evans' work [22], demonstrate that an oxygen functionality, especially the carbonyl of a tertiary amide, is *cis*-directing in the hydroboration of a cyclic alkene. In subsequent work, the regio- and stereospecific hydroboration of 3-benzyloxycyclohexene has been employed as a test reaction. Indenylrhodium complexes give good results, the main component after oxidation being the *cis*-3-hydroxy compound, formed with 84% diastereoselectivity [23]. This was further improved to 98% by employing the corresponding iri-

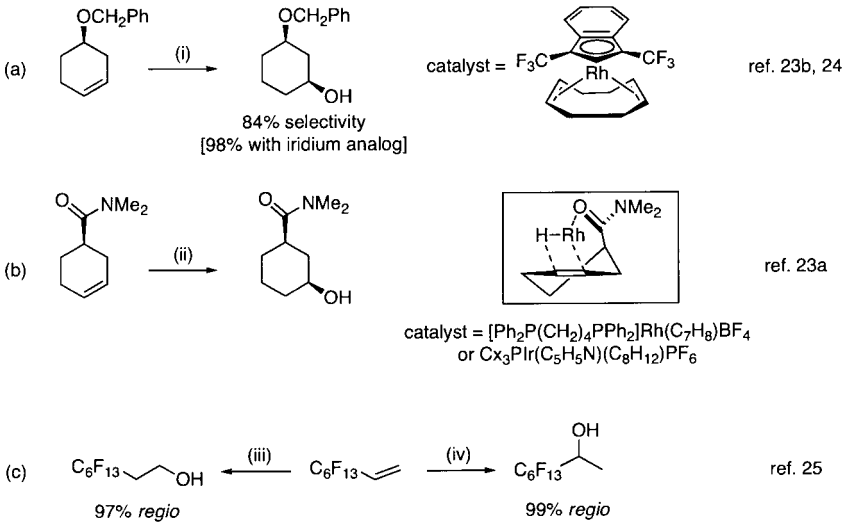

Fig. 2.6 Selectivity in catalytic hydroboration. Reaction conditions: (i) Catecholborane, 10 mol% catalyst, hexane, RT, 24 h; (ii) catecholborane, (iii) pinacolborane, 2 mol% $RhCl(PPh_3)_3$, THF, RT, 2.5 h; (iv) catecholborane, 1 mol% $(Ph_2P(CH_2)_4PPh_2)Rh(COD)BF_4$, 25 °C, 45 min.

dium complex of 1,3-bistrifluoromethylindenyl as the catalyst (Fig. 2.6) [24]. The regiochemistry is directed by the *exo*-metallic hydride transfer (see Fig. 2.6, inset) which requires that the C–B bond is formed at the atom nearer the directing group.

Catecholborane has been the primary reagent in rhodium-catalyzed hydroboration, as discussed earlier. With perfluoroalkylethylenes and the Rh-DPPB catalyst, the reaction course was temperature-dependent, with high regioselectivity toward formation of the internal borane (the secondary alcohol was isolated after oxidative workup) at –25°C. Equally selective formation of the primary borane was observed when the reaction was carried out at ambient temperature using pinacolborane as the reagent and $RhCl(PPh_3)_3$ as the catalyst [25]. Employing catalyst and reagent variation to control regioselectivity in catalytic hydroboration is an underdeveloped area; the use of bulky alkylphosphine catalysts can redirect styrene hydroboration to the primary product [26], and a steric argument can be employed to explain the outcome in the present case of perfluoroalkenes.

Much recent effort has been engaged in modifying the reaction medium for homogeneous catalysis, and hydroboration has received such scrutiny, including the hydroboration of alkynes in ionic liquids [27], and with a diphosphine–rhodium complex immobilized in the macroporous pore structure of an ethylene glycol bismethacrylate polymer [28]. Advantages over conventional solvents are claimed for hydroboration reactions in $scCO_2$ [29]. As is common in this field, partially fluorinated phosphine ligands proved to be optimal. Up to 100% α-regioselectivity was observed in the hydroboration of 4-methoxystyrene with catecholborane. A detailed study of catalytic hydroboration in fluorous biphasic media employing a fluoroalkyl analog of Wilkinson's catalyst was also carried out (Fig. 2.7). The intent of this study was to provide an efficient means of conducting hydroboration/oxidation in an experimentally convenient man-

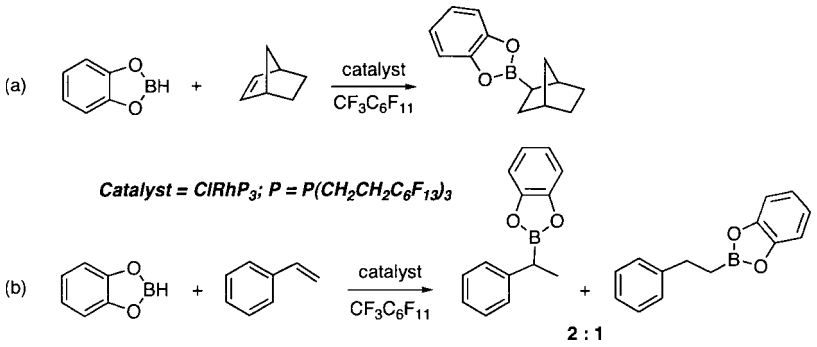

Fig. 2.7 Fluorous phase catalytic hydroboration. The procedure involves stirring the catalyst (0.1 mol%) in the fluorous phase with neat reactants at 40–45 °C, the cooling on completion of reaction and extracing with THF. The catalyst remains in the fluorous phase, whilst the product is completely extracted, and secondary alcohol can be prepared by H_2O_2 oxidation. The catalyst solution can be recycled several time without loss of activity.

ner. The catalyst was prepared in analytically pure form by mixing the ligand in $C_6F_{11}CF_3$ with $[Rh(COD)_2Cl]_2$ in toluene and evaporation of the solvents. The catalytic hydroboration was carried out in $C_6F_{11}CF_3$ at 40 °C, with between 500 and 10 000 equivalents of substrate and a slight excess of catecholborane. Extraction with THF or C_6D_6 on completion of the reaction and oxidation *in situ* of the organic phase with alkaline H_2O_2 gave the product essentially free from rhodium contaminants. The resulting fluorous catalyst solution may be recycled up to five times, without loss of activity. The products were achieved as expected, except that the reaction with three different styrenes led to a mixture of regioisomers in which the α:βratio varied from 39:61 (OMe) to 65:35 (Cl) [30].

When a phosphine-free catalyst is deliberately used, a complex reaction ensues that can be interpreted completely on the basis of a rhodium hydride catalytic cycle (Fig. 2.8). The product is partitioned between primary borane (β-addition to styrene), vinylborane, and alkane, with the last two in equal proportions. With ephedrine-derived boranes, only the last two products are formed, affording a simple route to vinylboranes [31]. More recently, this has been developed into a useful synthetic method; with pinacolborane and vinylarenes, phosphine-free rhodium catalysts give the corresponding *trans*-β-vinylboronate [32]. The facility of rhodium hydride driven alkene isomerization under the conditions of catalytic hydroboration has also been utilized. This does not apply to aliphatic alkenes, since *trans*-oct-4-ene can be converted into the saturated terminal pinacolboronate with pinacolborane and $RhCl(PPh_3)_3$ [33]. Further divergence in the catalytic chemistry of pinacolborane is revealed in its reaction with vinyl ethers catalyzed by Wilkinson's catalyst, where the corresponding β-boronate ester is the sole boron-containing product [34]. Employing terminal alkenes, with BH_3 as the reagent and $RhCl_3$ as the catalyst, gives rise to internal alcohols on oxidation, and hence isomerization of the alkene (or a derived rhodium alkyl) must occur faster than the irreversible borylation and reductive elimination steps [35].

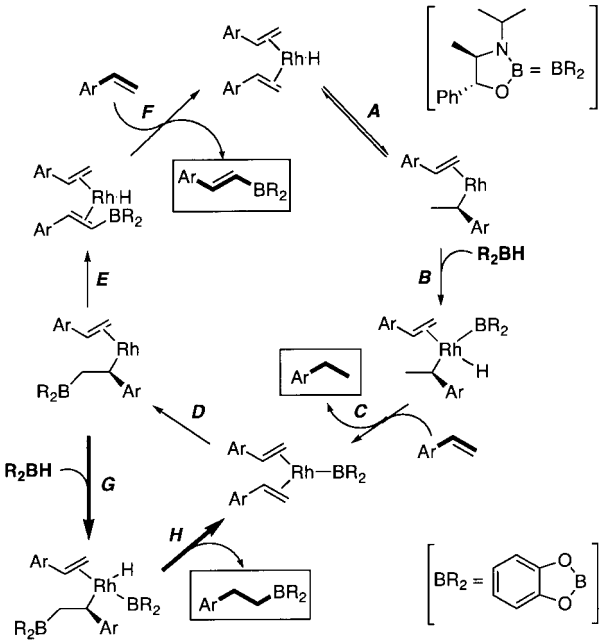

Fig. 2.8 A direct route to vinylboranes in rhodium-catalyzed hydroborations with phosphine-free catalysts (including oxidative degradation of a rhodium phosphine). The key intermediate is a rhodium hydride, capable of reversible insertion into the alkene (step ***A***), followed by addition of borane in step ***B***. This leads to reductive elimination of RH in step ***C*** followed by boryl migration in step ***D***. A further Rh-H β-elimination step in step ***E*** gives the vinylborane which then dissociates to generate the first intermediate. This cycle explains the production of equimolar quantities of alkane and *E*-vinylborane with unreactive R_2BH derived from ephedrines; with catecholborane there is an additional shunt pathway – step ***G*** in competition with step ***E*** leading to the *primary* regioisomer of alkylborane.

2.3
Advances in Asymmetric Hydroboration

Two early successes in catalytic asymmetric hydroboration involved the use of BINAP and QUINAP respectively [6]. In the absence of a reasonable model for the enantio-determining step of the reaction and knowledge of the structure of reactive intermediates, much of the progress has been achieved empirically. The configuration of the product is set at the hydride transfer stage [17], and the coordination sphere must contain C–H, C–B, alkene, and chelating diphosphine at that stage. Either the complex is cationic, or a further η^1-ligand is required to complete the 16e or 18e configuration. The stereochemistry of the five- or six-coordinate complex is unknown, thus creating further uncertainty in predictive analysis. As a speculative attempt, the structures shown in Fig. 2.9 reconcile the different outcomes for the two distinct ligand families. Further progress will require better information on the reactive intermediates in asymmetric hydroboration, either by experiment or by computational analysis of the complete molecular system, as has been attempted for asymmetric hydrogenation [36]. In

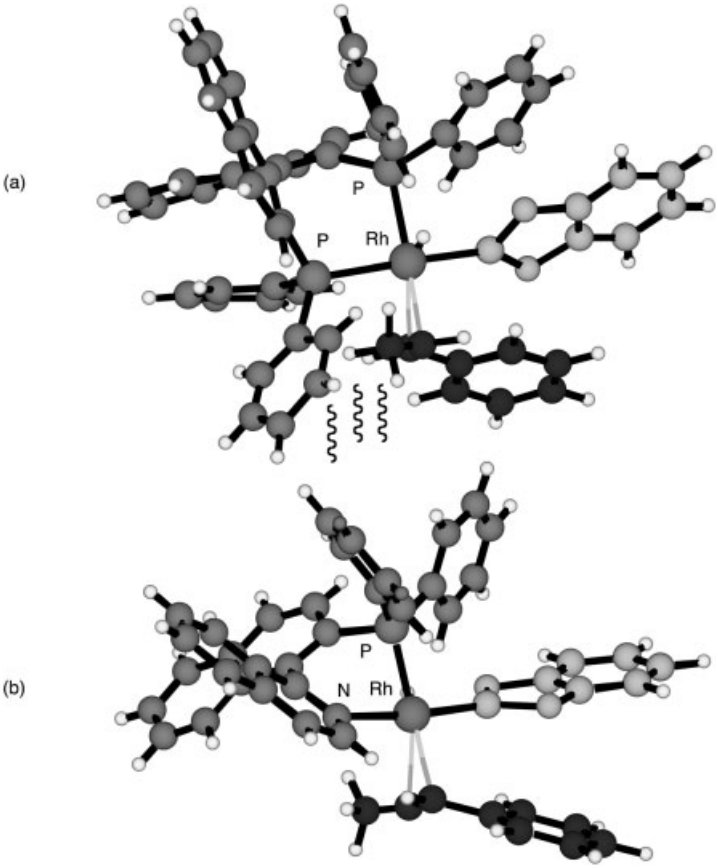

Fig. 2.9 Template structures for the intermediate in catalytic asymmetric hydroboration with alkene, ligand, catechoborane and hydride coordinated. (a) *R*-BINAP and (b) *R*-QUINAP. *E*-propenylbenzene is illustrated to show the increased steric hindrance to the alkene in the BINAP case.

any event, it is convenient to separate the two classes of catalyst in further analysis of the experimental results.

2.3.1 Diphosphine Ligands

Recent results in this area are summarized in Tab. 2.1 [37–41]. A majority of the experiments employ styrene or a simple derivative as the reactant, and for good reasons. Although this is the most general application of asymmetric hydroboration, *ortho*-substitution of the ring, and either α- or β-substitution of the double bond, generally lead to low enantioselectivities with this particular class of ligands. The new results obtained demonstrate that a variety of ligands give satisfactory results according to the defined constraints. The work cited in reference 37 is notable for the neat synthetic route to 1,2-bisphosphinocyclohexanes involving a double [2,3]-sigmatropic shift of a bi-

Tab. 2.1 Recent rhodium-catalyzed hydroborations with diphosphine ligands – work-up by H_2O_2 oxidation

Ligand	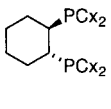	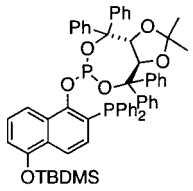	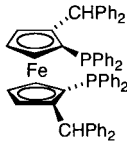	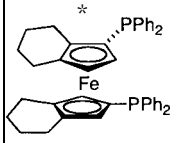	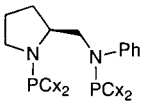
ee conditions	92% *ee*; *S* –35 °C, DME	88% *ee*; *R* –78 °C, DME	84.6% *ee*; *R* –78 °C, DME	84% *ee*; *S* –60 °C, C_7H_8	42% *ee*; *S*• THF, –78 °C
	ref. 37	ref. 38	ref. 39	ref. 40	ref. 41

* Absolute configuration undetermined.
• 77% *ee S* with norbornene.

sphosphinite followed by lipase resolution. The results taken from reference 38 represent part of a modular approach to ligand design; a family of 20 related phosphinophosphites (or close relatives) were prepared and tested for their effectiveness in this reaction.

It will be clear from the preceding discussion that genuinely novel reaction products arising from catalytic hydroboration are welcomed. The additional structural complexity that can be introduced in a single-step reaction is very attractive. This is nicely illustrated by the catalytic hydroboration of the cycloadducts derived from the Diels–Alder reaction of cyclopentadiene and azodicarboxylates. The hydroboration stage can be carried out with 84% enantiomeric excess using a Rh-BDPP complex as the catalyst and the product can be converted into a single stereoisomer of a protected 2,4-diaminocyclopentanol (Fig. 2.10a) [42]. Interestingly, iridium catalysts give the opposite enantiomer in the hydroboration step, albeit with lower efficiency [43]. Although they are readily synthesized, cyclopropenes are infrequently used in asymmetric catalysis. The successful demonstration of a highly enantioselective and diastereoselective addition of pinacolborane to cyclopropenes requires that one of the substituents at the 3-position is *cis*-directing (CO_2R or CH_2OMe). Enantioselectivities of 92–99% can be obtained for a variety of cases using BINAP or BPE ligands (Fig. 2.10b) [44].

As a final comment in this section, the target of asymmetric hydroboration is to introduce a stereochemically defined C–B bond. This can also be achieved by the hydrogenation of a prostereogenic vinylborane, as was successfully demonstrated by Miyaura and co-workers in 80% enantiomeric excess using a Rh-BINAP complex [45]. In a related approach, the hydrogenation over Pd/C of vinylboronates carrying a remote stereogenic center was shown to exhibit significant levels of diastereocontrol. (Fig. 2.11) [46].

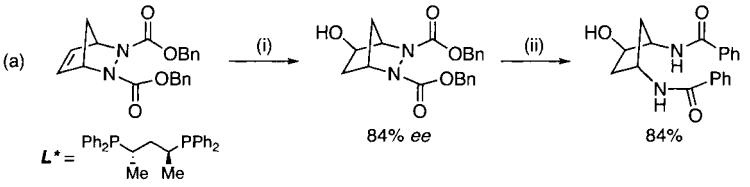

(i) Catecholborane, 1 mol% $[Rh(COD)Cl]_2$,***L****, –50 °C, 30 min; aq. NaOH, H_2O_2; (ii) Pt, H_2, AcOH; PhCOCl, pyridine

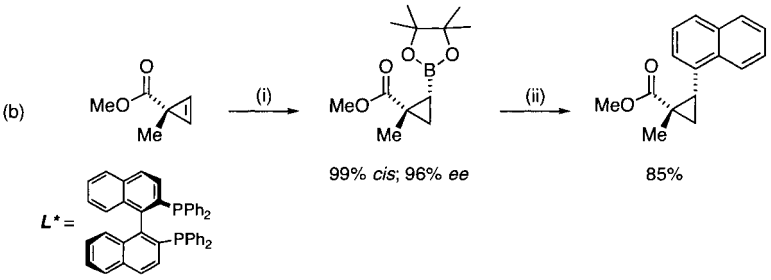

(i) Pinacolborane, 3 mol% $[Rh(COD)Cl]_2$,***L***,,THF, RT, 20 min; (ii) hydrolysis (*cf. JOC,* 2001, *66,* 7148) then 10 mol% $Pd[(P^tBu)_3]_2$, CsF, 1-naphthyl iodide, C_6H_6, 80 °C, 1h.

Fig. 2.10 Applications of asymmetric hydroboration with diphosphine catalysts to *meso*-symmetric alkenes. For 10(a), iridium complexes reverse the sense of enantioselectivity in up to 64% enantiomeric excess.

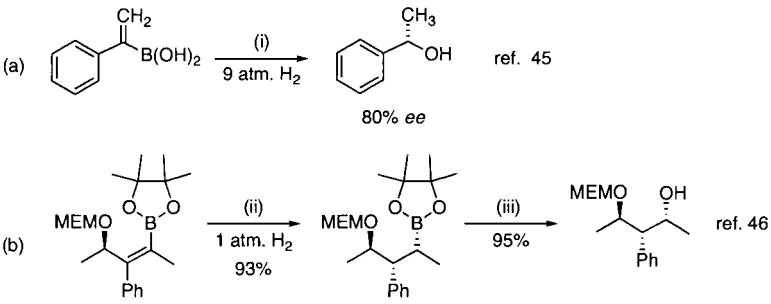

Fig. 2.11 Hydrogenation of vinylboronates. Conditions: (i) 3 mol%, *R*-BINAP, –20 °C, $ClCh_2CH_2Cl$, 65%, 7 days, then H_2O_2, NaOH; (ii) Pd/C, MeOH, 25 °C, 97%; (ii) H_2O_2 NaOH, 88%.

2.3.2
Phosphinamine and Related Ligands

Asymmetric hydroboration of styrenes employing diphosphine complexes provides a successful solution to the generation of chirality at a benzylic site, a potentially important route to many bioactive molecules. Since substitution on the double bond leads to severe loss of enantioselectivity, the applications are necessarily limited. It was adventitiously discovered that the *P,N*-ligand QUINAP [47], which is effective in asymmetric

hydroboration, lacks this limitation. A range of cyclic and acyclic *β*-substituted vinylarenes may be hydroborated in high enantiomeric excess [48]. The results obtained with simple styrenes are often no better than those obtained with Rh-BINAP, although there is greater tolerance of *ortho*-substitution, and reactions can be carried out at ambient temperature rather than –78°C. Interestingly, the difurylphosphine analog is a superior ligand for the enantioselective hydroboration of electron-deficient styrenes, albeit not in a general sense. Fig. 2.12 illustrates a part of the extended range of substrates that can be converted into secondary alcohols with these catalysts; it was demonstrated in several cases that the catecholboronate ester may be isolated by distillation without compromising its enantiomeric purity [49]. A speculative explanation for the ability to tolerate *β*-substitution on the double bond is the difference in steric hindrance around the isoquinoline nitrogen, as compared to *ArC*PPh_2; if the substituent is forced to reside in that region of space during the hydride transfer step it would account for the contrasting outcomes (see Fig. 2.9). The catalytic chemistry can be effectively transferred to a supported-phase environment by adsorbing the cationic Rh(COD) complex on clay [50]. Of the various ones tested, Montmorillonite K10 heated to 100°C for 24 hours proved superior, and in it QUINAP proved to be the most effective ligand. The catalyst was stable through several cycles, in contrast to the corresponding homogeneous catalyst. The reactivity and stereoselectivity are comparable to those of the solution-phase reaction, although there is an interesting equivalent of an induction period. In the first cycle (normally of four) the regio- and enantioselectivities are markedly lower than those obtained subsequently, as if the clay needs to be conditioned by the borane reagent, thereby to give the optimal performance. In the specific case of racemic 4-methyl- and 4-aryl-1,2-dihydronaphthalene derivatives, an efficient kinetic resolution is observed for the QUINAP-directed asymmetric hydroboration; the reactive hand is converted into the corresponding *trans*-alcohol on oxidation [51]. In the simpler case of divinylbenzene, the first hydroboration step proceeds in 96% enantiomeric excess. The stereogenic center so-formed has little effect on the second hydroboration step, and with Rh-QUINAP high enantioselectivity and *dl*:*meso* discrimination is observed in the diol product. There is very little evidence of double stereodifferentiation with achiral catalysts, and *dl*:*meso* ≤ 2:1 [52].

Although commercially available in both enantiomers [53], the QUINAP ligands and related members of this family require a multi-step synthesis and resolution [54]. Hence, alternatives with comparable characteristics are clearly warranted; several new examples are listed in Tab. 2.2. A planar chiral (*ortho*-formylphenyl)diphenylphosphine chromium tricarbonyl complex, synthesised in turn from a simple glucose derivative, reacted with 2-pyridyllithium, albeit in low enantiomer excess. The derived benzyl ether was an effective catalyst for the enantioselective hydroboration of styrenes in up to 86% enantiomeric excess [55]. In the conceptually similar ferrocenyl ligands introduced by Knochel and co-workers [56], the steregenic center is introduced by an oxazaborolidine reduction of a ferrocenyl aryl ketone, whereby the ensuing oxygen functionality serves to control a directed lithiation step in which the heterocyclic ring is introduced. As observed earlier by Togni with a different family of ferrocene-based *P,N*-ligands [57], the high enantioselectivity in styrene hydroboration is accompanied by lower regioselectivity. A simple atropisomerically chiral *P,N*-ligand based on 2-(2′-diphenylphosphinophenyl)pyridine has been prepared and resolved, and its rhodium complex is at least as effective as the corresponding QUINAP complex for the asymmetric hydroboration of simple styrenes

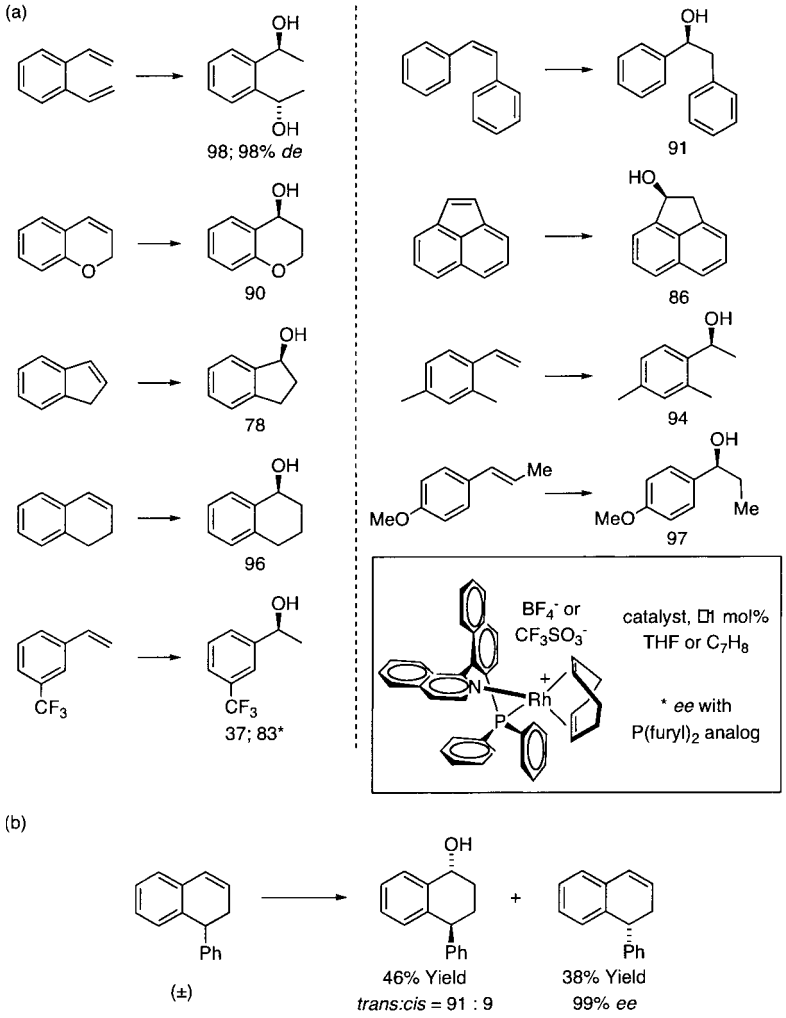

Fig. 2.12 (a) Hydroboration/oxidation with (*S*)-QUINAP-Rh complexes at ambient temperature. The numbers refer to the *ee* of the *S*-enantiomer of product. (b) Kinetic resolution with (*R*)-QUINAP-Rh; conditions 0.6 equiv. catecholborane, 1 mol% catalyst, toluene, 2 h; H_2O_2/NaOH.

[58]. Perhaps the most useful development in this area has been the introduction of quinazoline analogs of the ligand framework, where the 3-substituent can be systematically varied [59]. That variation has a significant effect on the catalytic chemistry, and permits the highest enantiomeric excesses to be obtained for several members of the *β-R*-vinylarene class, as indicated in Fig. 2.12 [60].

Tab. 2.2 Recent rhodium-catalysed hydroborations with *P,N*-ligands; products of H_2O_2 oxidazition

Ligand	*Reaction*	*Ref.*
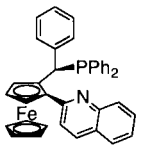	 92% *ee* 68:32 *regio*	56
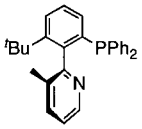	 92% *ee* 98:2 *regio*	58
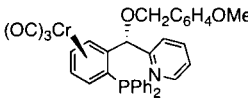	 96% *ee* 93:7 *regio*	55
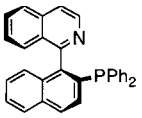	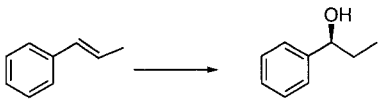 *4th cycle with clay-based catalyst* 85% *ee* 99:1 *regio*	50
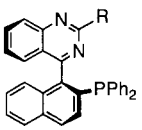	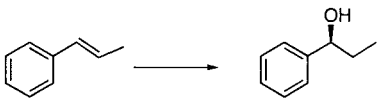 R = Me 97% *ee* 99% *regio* R = ^{i}Pr 96% *ee* 96% *regio*	59–60; 74

2.3.3
Transformations of the Initial Boronate Ester

The direct synthetic utility of boronate esters like those derived from catalytic addition of catecholborane to alkenes is well recognized as being limited [9]. Given the utility of enantiomerically pure α-substituted benzylamines in pharmacology, extension of catalytic asymmetric hydroboration to amine synthesis is a worthwhile synthetic goal. Initial attempts to carry this out by direct reaction with the aminating agent $ClMgN(Me)OSiMe_3$ were only partially successful, since the alcohol was always formed in comparable yield to the desired secondary amine [61]. A better solution proved to be conversion of the initial catecholboronate ester into a trialkylborane by reaction with one equivalent of diethyl zinc [62] or two equivalents of methylmagnesium chloride.

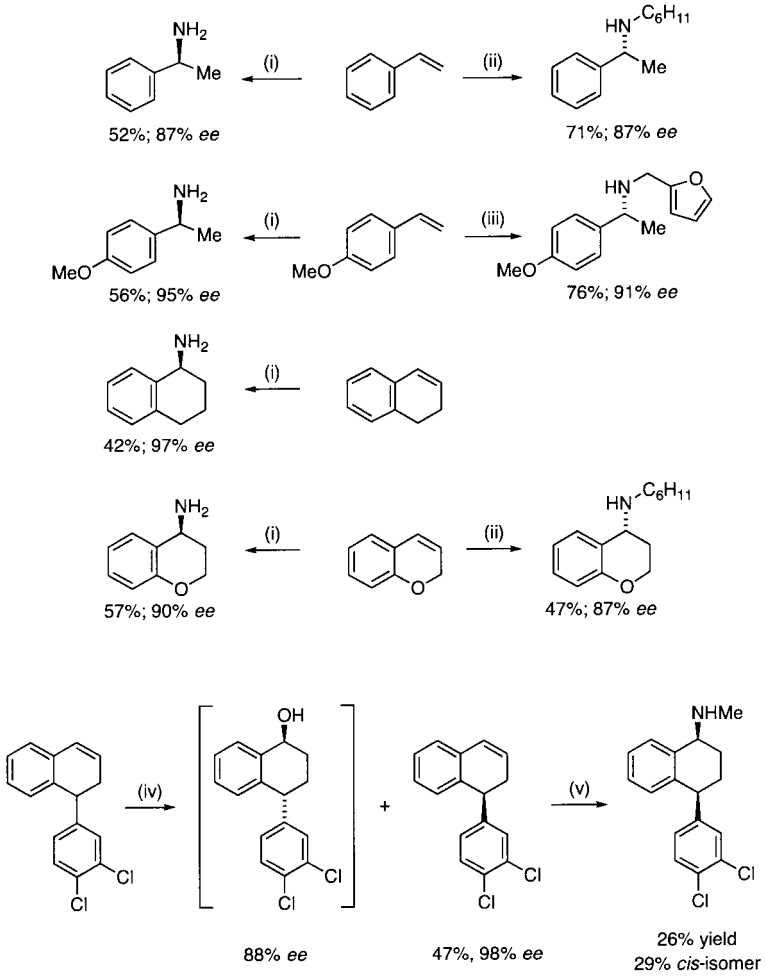

Fig. 2.13 Examples of hydroboration/amination using Rh-QUINAP complexes and electrophilic aminating agents. (i) Catecholborane, 1 mol% (*S*)-QUINAP-Rh catalyst, THF, RT, 1 h; 2 equiv. MeMgCl in THF, 30 min; solid H_2NOSO_3H, 1.5 equiv., 12 h; (ii) As (i) with (*R*)-QUINAP-Rh catalyst, then 1 equiv. $ZnEt_2$, C_7H_8; slow addition then stir 2 h; add at 0 °C to mixture of amine and aq. NaOCl also at 0 °C; (iii) as (ii), but with isolation of the catecholboronate ester by pentane addition, filtraton and solvent removal after the hydroboration step; (iv) 0.6 equiv. catecholborane, 1 mol% (*S*)-QUINAP-Rh catalyst, toluene, 2 h, then H_2O_2/NaOH; (v) 5 equiv. catecholborane, 10 mol% (*S*)-QUINAP-Rh catalyst, toluene, 12 h, then styrene, 5 equiv. 2 h; $ZnEt_2$, 5,5 equiv., 2 h, then MeNHCl, 6 equiv., 0 °C to RT, 1 h.

Methyl and ethyl are known to be poor migrating groups in the amination of boranes [63], permitting a selective and general route to primary benzylamines through reaction of the trialkylborane with hydroxylamine-*O*-sulfonic acid, maintaining the configurational integrity of the boronate ester [64]. The chemistry can be extended to synthesis of a variety of secondary, but not tertiary, amines through the synthesis *in situ* of *N*-chloramines that can be employed as *N*-electrophiles (Fig. 2.13) [65]. In combination

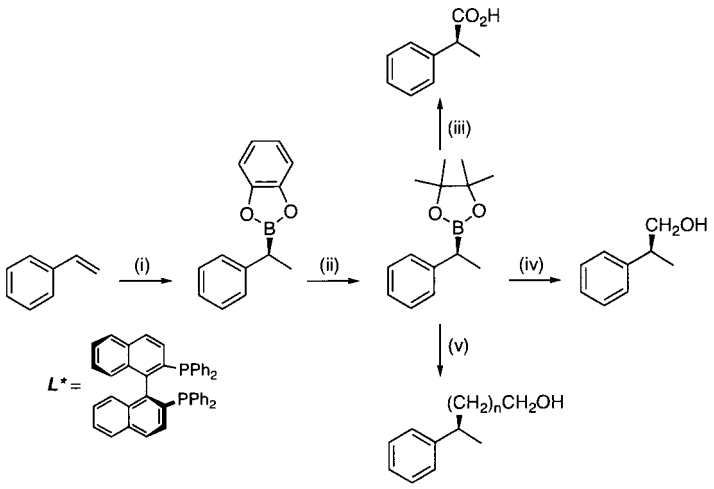

Fig. 2.14 Carbon-carbon bond formation from the initital adduct of asymmetric hydroboration of styrene. (i) 2 mol% $Rh(COD)_2BF_4$, ***L****, 12 equiv. catecholborane, –66 °C, DME; (ii) pinalcol, 2 equiv., –66 °C – RT, 12 h; flash chromatography; (iii) $LiCHCl_2$, 1.5 equiv., $ZnCl_2$, THF, –100 °C; (iv) $LiCH_2Cl$, THF, –78 °C; (v) $LiCH_2Br$ *xs*., THF, –78 °C.

with the kinetic resolution of alkenes described earlier, the amination sequence can be directed to a formal synthesis of the antidepressant sertraline [52].

The formation of carbon–carbon bonds through catalytic asymmetric hydroboration is an important advance. A key to the initial success by Crudden and co-workers was the conversion of the initially formed catecholboronate ester into the corresponding pinacolboronate ester. This product can then be made to react with the carbenoid MeOCHLiSPh, or better with Cl_2CHLi. After treatment with sodium perborate to give the homologated aldehyde, either the carboxylic acid or the alcohol may be formed by further functional-group interconversion, albeit with reduced enantioselectivity. The optimum procedure consists of the direct reaction of the pinacolboronate with Cl_2CHLi, followed by workup with $NaClO_2$ to give the carboxylic acid directly without compromising enantioselectivity (Fig. 2.14) [66]. In contrast, the reaction with $ClCH_2Li$ followed by H_2O_2 workup gave the alcohol directly [67]. A further development of this chemistry was provided by the observation of multiple insertion reactions when the reagent was $BrCH_2Li$, as up to 40% of the double insertion product (reaction of the initial product with further carbenoid reagent) was observed, along with some triple insertion product [68]. There is clearly still considerable scope for additional synthetic outlets based on the initial catalyzed addition of catecholborane to alkenes.

2.4
Catalytic Diboration of Alkenes

This area has been dominated by platinum catalysts, and studied extensively by Ishiyama, and by Marder [69]. The initial observation in organorhodium chemistry of the catalytic addition of dicatecholdiborane, catalyzed by (optimally) Rh-DPPB, still gave only 44% of the diborated product accompanied by 22% of vinylborane and 22% of "conventional" α-hydroboration product [70]. The work was extended by using the zwitterionic Rh-DPPM complex as the catalyst, where good yields of 1,2-diaddition products were obtained from a range of mono- and disubstituted alkenes [71]. By a relatively minor variation of the reaction conditions, employing $RhCl(CO)(PPh_3)_2$ as the catalyst, either the vinylboronate ester and/or the vinyl bisboronate ester become the main reaction product [72]. The promise of this result has been further developed by its extension to an effective asymmetric synthesis, applicable to a variety of disubstituted (and even trisubstituted) alkenes. This simple protocol, applicable to simple *trans*-disubsti-

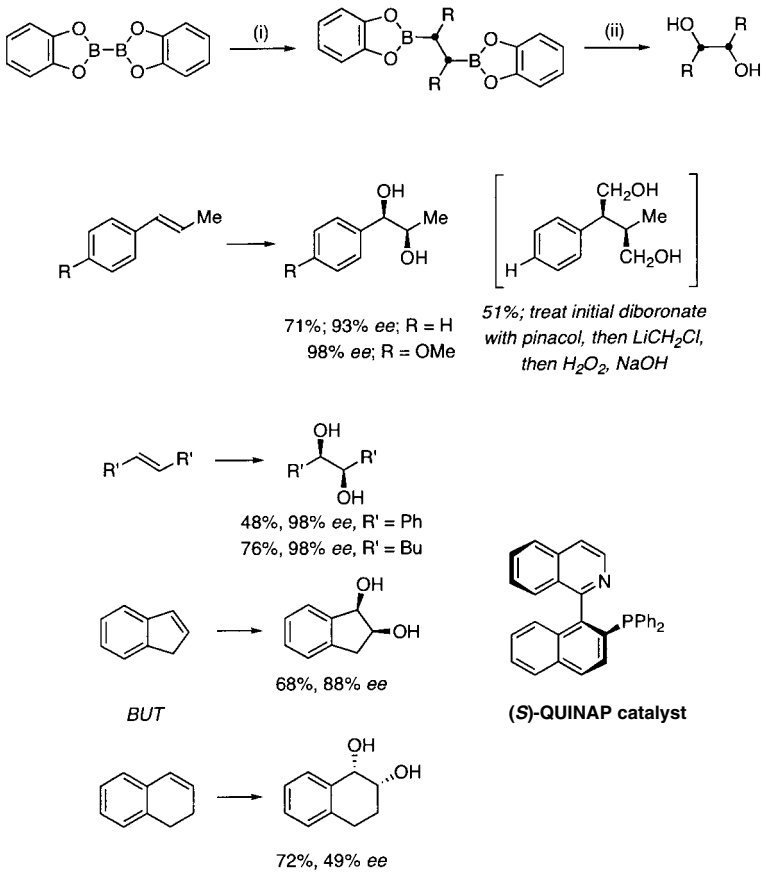

Fig. 2.15 Catalytic diboration with dicatecholdiborane and Rh-QUINAP; General Conditions: (i) 5 mol% (*S*)-QUINAP, 5 mol% acacRh(C_7H_8), 1.1 equiv. reagent, THF, RT, 24 h. (ii) H_2O_2/ NaOH workup.

tuted alkenes, complements the Sharpless asymmetric dihydroxylation reaction, but with a wider scope as the intermediate diboronate ester can be converted into related products, including that of bishydroxymethylation (Fig. 2.15) [73].

2.5 Summary and Conclusions

Catalytic hydroboration is now an established procedure for asymmetric synthesis. The major strength is that it permits the regiospecific functionalization of a vinylarene adjacent to an aromatic or heterocyclic ring. At the present time the C–B bond can be replaced by oxygen, nitrogen, or carbon substituents with complete retention of configuration. The range of reactants continues to be systematically extended, as exemplified by recent successes in the cyclopropene and diazabicyclo[2.2.1]heptane series. Extending the range of post-catalytic reactions remains an ongoing challenge, and application of the initial adducts in Pd-catalyzed couplings should be expected. Despite these highly positive attributes several problems remain before the reaction can be regarded in a similar fashion to some of the most generally utilized methodologies. The solutions required for these problems include: (a) an improved synthesis of, or a replacement for, catecholborane, since this reagent is expensive, and needs purification before use, which raises the barrier for the occasional nonexpert user; (b) catalysts that can overcome the present substrate limitations, as even with the *P,N*-ligand Quinap that is tolerant of alkene bulk, *ortho*-disubstitution of the arene in addition to α- and β,β-disubstitution of the double bond renders the catalytic reaction ineffective; (c) a range of transformations of the initial weakly electrophilic benzylic catecholboronate that rivals the noncatalyzed version. All of these are goals that provide a focus for ensuing work in this important area of catalysis [75].

Acknowledgments

Thanks go especially to the students who have contributed over the past several years to the Oxford publications on catalytic asymmetric hydroboration, most recently Antonia Black, Christophe Pichon, and Kenji Maeda.

2.6 References

1 D. Maennig, H. Nöth, *Angew. Chem., Int. Ed. Engl.* **1985**, *97*, 854.
2 H. Kono, K. Ito, Y. Nagai, *Chem. Lett.* **1975**, 1095.
3 K. Burgess, M.J. Ohlmeyer, *J. Org. Chem.* **1988**, *53*, 5178.
4 T. Hayashi, Y. Matsumoto, Y. Ito, *Tetrahedron: Asymmetry* **1991**, *2*, 601.
5 K. Burgess, M.J. Ohlmeyer, *Chem. Rev.* **1991**, *91*, 1179.
6 I. Beletskaya, A. Pelter, *Tetrahedron* **1997**, *53*, 4957.
7 Y. Matsumoto, M. Naito, Y. Uozumi, T. Hayashi, *J. Chem. Soc., Chem. Commun.* **1993**, 1468. Y. Matsumoto, M. Naito, T. Hayashi, *Organometallics* **1992**, *11*, 2732.
8 H.C. Brown, G. Zweifel, *J. Am. Chem. Soc.* **1961**, *83*, 486.
9 H.C. Brown, B. Singaram, *Acc. Chem. Res.* **1988**, *21*, 287.
10 D.A. Evans, G.C. Fu, *J. Org. Chem.* **1990**, *55*, 2280.
11 A.E. Dorigo, P.V. Schleyer, *Angew. Chem., Int. Ed. Engl.* **1995**, *34*, 115; D.G. Musaev, A.M. Mebel, K. Morokuma, *J. Am. Chem. Soc.* **1994**, *106*, 10693.
12 M.D. Fryzuk, D.H. McConville, S.J. Rettig, *J. Organometal. Chem.* **1993**, *445*, 245; H. Werner, M. Schafer, O. Nurnberg, J. Wolf, *Chem. Ber.* **1994**, *127*, 27.
13 C. Widauer, H. Grutzmacher, T. Ziegler, *Organometallics* **2000**, *19*, 2097.
14 X.M. He, J.F. Hartwig, *J. Am. Chem. Soc.* **1996**, *118*, 1696; J.F. Hartwig, C.N. Muhoro, *Organometallics* **2000**, *19*, 30; M.J. Pender, P.J. Carroll, L.G. Sneddon, *J. Am. Chem. Soc.* **2001**, *123*, 12222.
15 D. Liu, Z.Y. Lin, *Organometallics* **2002**, *21*, 4750.
16 A. Lang, H. Noeth, A.M. Thomann, *Chem. Ber./Recl.* **1997**, *130*, 363.
17 D.A. Evans, G.C. Fu, B.A. Anderson, *J. Am. Chem. Soc.* **1992**, *114*, 6679.
18 K. Burgess, W.A. Vanderdonk, S.A. Westcott, T.B. Marder, R.T. Baker, J.C. Calabrese, *J. Am. Chem. Soc.* **1992**, *114*, 9350.
19 A. Korostylev, I.D. Gridnev and J.M. Brown, *J. Organometal. Chem.* **2003**, *680*, 329.
20 T. Ohmura, Y. Yamamoto, N. Miyaura, *J. Am. Chem. Soc.* **2000**, *122*, 4990.
21 K. Burgess, M.J. Ohlmeyer, *Tetrahedron Lett.* 1989, *30*, 395; K. Burgess, M.J. Ohlmeyer, *J. Org. Chem.* **1991**, *56*, 1027.
22 D.A. Evans, G.C. Fu, *J. Am. Chem. Soc.* **1991**, *113*, 4042.
23 C.E. Garrett, G.C. Fu, *J. Org. Chem.* **1998**, *63*, 1370.
24 J.A. Brinkman, T.T. Nguyen, J.R. Sowa, *Org. Lett.* **2000**, *2*, 981.
25 P.V. Ramachandran, M.P. Jennings, H.C. Brown, *Organic Lett.* **1999**, *1*, 1399.
26 S.A. Westcott, H.P. Blom, T.B. Marder, R.T. Baker, *J. Am. Chem. Soc.* **1992**, *114*, 8863.
27 S. Aubin, F. Le Floch, D. Carrie, J.P. Guegan, M. Vaultier, *ACS Symposium Series* **2002**, *818*, 334.
28 R.A. Taylor, B.P. Santora, M.R. Gagne, *Org. Lett.* **2000**, *2*, 1781.
29 C.A.G. Carter, R.T. Baker, S.P. Nolan, W. Tumas, *Chem. Commun.* **2000**, 347.
30 J.J. J. Juliette, I.T. Horvath, J.A. Gladysz, *Angew. Chem., Int. Ed Engl.* **1997**, *36*, 1610; J.J. J. Juliette, D. Rutherford, I.T. Horvath, J.A. Gladysz, *J. Am. Chem. Soc.* **1999**, *121*, 2696. Generally speaking, rhodium catalysts are not reemployed in hydroboration reactions because they deteriorate after the first cycle. For an exception, see: J. Liedtke, H. Ruegger, S. Loss, H. Grutzmacher, *Angew. Chem., Int. Ed. Engl.* **2000**, *39*, 2478.
31 J.M. Brown, G.C. Lloyd-Jones, *J. Am. Chem. Soc.* **1994**, *116*, 866.
32 M. Murata, K. Kawakita, T. Asana, S. Watanabe, Y. Masuda, *Bull. Chem. Soc. Jpn.* **2002**, *75*, 825.
33 T.C. Morrill, C.A. D'Souza, *Organometallics* **2003**, *22*, 1626.
34 C.M. Vogels, P.E. O'Connor, T.E. Phillips, K.J. Watson, M.P. Shaver, P.G. Hayes, S.A. Westcott, *Can. J. Chem,* **2001**, *79*, 1898.

35 T.C. Morrill, C.A. D'Souza, L. Yang, A.J. Sampognaro, *J. Org. Chem.* **2002**, *67*, 2481.

36 S. Feldgus, C.R. Landis, *Organometallics* **2001**, *20*, 2374; C.R. Landis, S. Feldgus, *Angew. Chem., Int. Ed.* **2000**, *39*, 2863; S. Feldgus, C.R. Landis, *J. Am. Chem. Soc.* **2000**, *122*, 12714.

37 S. Demay, F. Volant, P. Knochel, *Angew. Chem., Int. Ed.* **2001**, *40*, 1235.

38 F. Blume, S. Zemolka, T. Fey, R. Kranich, H.G. Schmalz, *Adv. Synth. Catal.* **2002**, *344*, 868.

39 J. Kang, J.H. Lee, J.B. Kim, G.J. Kim, *Chirality* **2000**, *12*, 378.

40 M.T. Reetz, E.W. Beuttenmuller, R. Goddard, M. Pasto, *Tetrahedron Lett.* **1999**, *40*, 4977.

41 J.-M. Brunel, G. Buono, *Tetrahedron Lett.* **1999**, *40*, 3561.

42 A.P. Luna, M.A. Ceschi, M. Bonin, L. Micouin, H.P. Husson, S. Gougeon, G. Estenne-Bouhtou, B. Marabout, M. Sevrin, P. George, *J. Org. Chem.* **2002**, *67*, 3522.

43 A.P. Luna, M. Bonin, L. Micouin, H.P. Husson, *J. Am. Chem. Soc.* **2002**, *124*, 12098.

44 M. Rubina, M. Rubin, V. Gevorgyan, *J. Am. Chem. Soc.* **2003**, *125*, 7198.

45 M. Ueda, A. Saitoh, N. Miyaura, *J. Organomet. Chem.* **2002**, *642*, 145.

46 E. Hupe, I. Marek, P. Knochel, *Org. Lett.* **2002**, *4*, 2861.

47 N.W. Alcock, J.M. Brown, D.I. Hulmes, *Tetrahedron: Asymmetry* **1993**, *4*, 743; J.M. Brown, D.I. Hulmes, P.J. Guiry, *Tetrahedron* **1994**, *50*, 4493.

48 J.M. Brown, D.I. Hulmes, T.P. Layzell, *Chem. Commun.* **1993**, 1673.

49 H. Doucet, E. Fernandez, T.P. Layzell, J.M. Brown, *Chem. Eur. J.* **1999**, *5*, 1320.

50 A.M. Segarra, R. Guerrero, C. Claver, E. Fernandez, *Chem. Commun.* **2001**, 1808–1809; A.M. Segarra, R. Guerrero, C. Claver, E. Fernandez, *Chem. Eur. J.* **2003**, *9*, 191.

51 K. Maeda, J.M. Brown, *Chem. Commun.* **2002**, 310.

52 D. Connolly, P.J. Guiry, J.M. Brown, (unpublished).

53 Strem Chemicals, Inc., Newburyport, MA 01950. Catalogue numbers 15–1778; 15–1777.

54 C.W. Lim, O. Tissot, A. Mattison, M.W. Hooper, J.M. Brown, A.R. Cowley, D.I. Hulmes, A.J. Blacker, *Org. Process Res. Dev.* **2003**, *7*, 379.

55 S.U. Son, H.Y. Jang, J.W. Han, I.S. Lee, Y.K. Chung, *Tetrahedron: Asymmetry* **1999**, *10*, 347.

56 R.J. Kloetzing, M. Lotz, P. Knochel, *Tetrahedron: Asymmetry* **2003**, *14*, 255.

57 A. Schnyder, L. Hintermann, A. Togni, *Angew. Chem., Int. Ed. Engl.* **1995**, *34*, 931; A. Schnyder, A. Togni, U. Wiesli, *Organometallics* **1997**, *16*, 255.

58 F.Y. Kwong, Q.C. Yang, T.C.W. Mak, A.S.C. Chan, K.S. Chan, *J. Org. Chem.* **2002**, *67*, 2769.

59 M. McCarthy, M.W. Hooper, P.J. Guiry, *Chem. Commun.* **2000**, 1333.

60 M. McCarthy, P.J. Guiry, *Tetrahedron* **2001**, *57*, 3809; P.J. Guiry, private communication of unpublished work by D. Connolly.

61 F.I. Knight, J.M. Brown, D. Lazzari, A. Ricci, A.J. Blacker, *Tetrahedron* **1997**, *53*, 11 411.

62 The initial displacement of catecholzincate is rapid. With excess zinc reagent transmetallation has been shown to occur: F. Langer, L. Schwink, A. Devasagayaraj, P.Y. Chavant, P. Knochel, *J. Org. Chem.* **1996**, *61*, 8229.

63 B. Carboni, M. Vaultier, *Bull. Soc. Chim. Fr.* **1995**, *132*, 1003.

64 E. Fernandez, M.W. Hooper, F.I. Knight, J.M. Brown, *Chem. Commun.* **1997**, 173.

65 E. Fernandez, K. Maeda, M.W. Hooper, J.M. Brown, *Chem. Eur. J.* **2000**, *6*, 1840.

66 A.C. Chen, L. Ren, C.M. Crudden, *Chem. Commun.* **1999**, 611.

67 A. Chen, L. Ren, C.M. Crudden, *J. Org. Chem.* **1999**, *64*, 9704.

68 L. Ren, C.M. Crudden, *Chem. Commun.* **2000**, 721.

69 Leading experimental references: T. Ishiyama, N. Matsuda, N. Miyaura, A. Suzuki, *J. Am. Chem. Soc.* **1993**, *115*, 11018; T. Ishiyama, N. Matsuda, M. Murata, F. Ozawa, A. Suzuki, N. Miyaura, *Organometallics* **1996**, *15*, 713; G. Lesley, P. Nguyen, N.J. Taylor, T.B. Marder, A.J. Scott, W. Clegg, N.C. Norman, *Organometallics* **1996**, *15*, 5137; T. Ishiyama, M. Yamamoto, N. Miyaura, *Chem. Commun.* **1997**, 689;

C. N. Iverson, M. R. Smith, *Organometallics* **1997**, *16*, 2757; Y. G. Lawson, M. Lesley, T. B. Marder, N. C. Norman, C. R. Rice, *Chem. Commun.* **1997**, 2051; W. Clegg, T. Johann, T. B. Marder, N. C. Norman, A. G. Orpen, T. M. Peakman, M. J. Quayle, C. R. Rice, A. J. Scott, *J. Chem. Soc., Dalton Trans.* **1998**, 1431; T. Ishiyama, T. Kitano, N. Miyaura, *Tetrahedron Lett.* **1998**, *39*, 2357; T. B. Marder, N. C. Norman, *Topics Catal.* **1998**, *5*, 63; T. B. Marder, N. C. Norman, C. R. Rice, *Tetrahedron Lett.* **1998**, *39*, 155. K. M. Anderson, M. Lesley, N. C. Norman, A. G. Orpen, J. Starbuck, *New J. Chem.* **1999**, *23*, 1053; T. Ishiyama, S. Momota, N. Miyaura, *Synlett* **1999**, 1790; R. L. Thomas, F. E. S. Souza, T. B. Marder, *J. Chem. Soc., Dalton Trans.* **2001**, 1650.

70 R. T. Baker, P. Nguyen, T. B. Marder, S. A. Westcott, *Angew. Chem., Int. Ed. Engl.* **1995**, *34*, 1336.

71 C. Y. Dai, E. G. Robins, A. J. Scott, W. Clegg, D. S. Yufit, J. Howard, T. B. Marder, *Chem. Commun.* **1998**, 1983.

72 R. B. Coapes, F. E. S. Souza, R. Ll. Thomas, J. J. Hall, T. B. Marder, *Chem. Commun.* **2003**, 614.

73 J. B. Morgan, S. P. Miller, J. P. Morken, *J. Am. Chem. Soc.* **2003**, *125*, 8702; S. P. Miller, J. B. Morgan, F. J. Nepeux, J. P. Morken, *Org. Lett.* **2004**, *6*, 131.

74 D. J. Connolly, P. M. Lacey, M. McCarthy, C. P. Saunders, A.-M. Carroll, R. Goddard, P. J. Guiry, *J. Org. Chem.* **2004**, *69*, 6572.

75 C. M. Crudden, D. Edwards, *Eur. J. Org. Chem.* **2003**, 4695.

3
Rhodium(I)-Catalyzed Asymmetric Addition of Organometallic Reagents to Electron-Deficient Olefins

Kazuhiro Yoshida and Tamio Hayashi

3.1
Introduction

Conjugate addition of organometallic reagents to electron-deficient olefins is one of the most useful processes in organic synthesis [1]. The organometallic reagents often used for these reactions – organolithiums, -magnesiums, and -zincs in the presence of copper or nickel catalysts – usually give rise to the desired conjugate addition products in high yields. The major problems are incompatibility with some functional groups, and the noncatalyzed 1,2-addition as a competitive reaction. The use of an active catalyst in combination with a less reactive organometallic reagent would solve these problems. Since the 1980s, considerable efforts have been focused on catalytic asymmetric conjugate addition [2]. The most successful example is the addition of organozincs, catalyzed by copper (I) complexes having chiral phosphorous ligands [3]. In these copper-catalyzed reactions, high enantioselectivity has been achieved (>90% *ee*) for several types of *α,β*-unsaturated ketones. However, the organic groups introduced are unfortunately limited to primary alkyl groups and there have been no successful examples of introduction of sp^2 carbons with high enantioselectivity. Recently, there have appeared reports on highly enantioselective rhodium-catalyzed asymmetric conjugate addition. The reaction has the advantage of permitting the introduction of sp^2 carbons to a wide range of electron-deficient olefins under mild reaction conditions. This chapter reviews the recent development of rhodium-catalyzed conjugate addition [4].

3.2
Addition of Organoboron Reagents to *α,β*-Unsaturated Ketones

In 1997, Miyaura reported important work describing conjugate addition of aryl- and alkenylboronic acids to *α,β*-unsaturated ketones [5], using the rhodium catalyst generated from Rh(acac)$(CO)_2$ and 1,4-bis(diphenylphosphino)butane (dppb) in aqueous solvents (Scheme 3.1). The conjugate addition takes place not only for *β*-unsubstituted enones such as methyl vinyl ketone, but also for *β*-substituted enones such as 2-cyclohexenone, although the yields are low. It is noteworthy that even enals undergo chemoselective conjugate addition in high yields, indicating the great potential of this reaction. Organoboronic acids are not reactive toward enones in the absence of a rhodium catalyst, and their stability to oxygen and moisture allows them to be handled

Modern Rhodium-Catalyzed Organic Reactions. Edited by P. Andrew Evans

ISBN: 3-527-30683-8

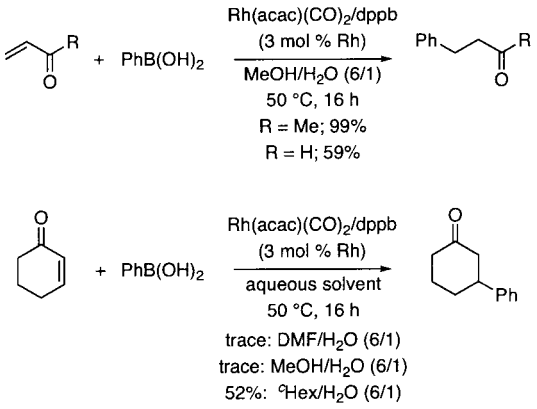

Scheme 3.1 Rhodium-catalyzed conjugate addition of phenylboronic acid to α,β-unsaturated ketones [5].

without special precautions. In this rhodium-catalyzed reaction the use of an aqueous solvent is essential; the role of the solvent will be discussed in Section 3.3.

In 1998, Hayashi and Miyaura reported the first example of rhodium-catalyzed asymmetric conjugate addition [6]. After optimization of the reaction conditions, high enantioselectivities were achieved using (*S*)-BINAP as a chiral bisphosphine ligand (Tab. 3.1). On this occasion, the rhodium precursor was changed from $Rh(acac)(CO)_2$ to $Rh(acac)(C_2H_4)_2$, the temperature was increased to 100 °C, the solvent was changed to a 10 : 1 mixture of dioxane and water, and the reaction time was shorten to 5 h. The scope of the reaction is very broad. Under the reaction conditions, addition of phenylboronic acid **2m** to 2-cyclohexenone **1a** gave a 99% yield of (*S*)-3-phenylcyclohexanone **3am** with 97% enantiomeric excess (entry 1). Aryl groups substituted with either electron-donating or -withdrawing groups, such as 4-MeC_6H_4, 4-$CF_3C_6H_4$, 3-$MeOC_6H_4$, and 3-ClC_6H_4, were introduced into 2-cyclohexenone **1a** with similar enantioselectivity by reaction with the corresponding boronic acids **2n–q** (entries 2–5). Asymmetric addition of 1-alkenylboronic acids was also highly successful, as (*E*)-1-heptenylboronic acid **4m** and (*E*)-3,3-dimethyl-1-butenylboronic acid **4n** afforded the corresponding alkenylation products **5am** and **5an** with over 90% enantiomeric excess (entries 10–12).

Cyclopentenone **1b** underwent asymmetric addition of phenyl- and 1-heptenylboronic acids with high enantioselectivity under the same reaction conditions to give 3-substituted cyclopentanones, **3bm** (97% *ee*) (entry 6) and **5bm** (96% *ee*) (entry 12), in high yields. High enantioselectivity was also observed in the reaction of linear enones **1d** and **1e**, which have *trans*-olefin geometry (entries 8–9). Thus, rhodium-catalyzed asymmetric conjugate addition proceeds with high enantioselectivity for both cyclic and linear α,β-unsaturated ketones with a variety of aryl- and alkenylboronic acids.

A change in the rhodium precursor from $Rh(acac)(CO)_2$ to $Rh(acac)(C_2H_4)_2$ is of crucial importance for obtaining a high yield and excellent enantioselectivity. The use of $Rh(acac)(CO)_2$ in place of $Rh(acac)(C_2H_4)_2$ under the same conditions for the reaction of 2-cyclohexenone **1a** with phenylboronic acid **2m** resulted in much lower yield and only 43% enantioselectivity. This is explained by incomplete formation of catalytically active species, namely Rh(acac)((*S*)-BINAP), because of the stronger coordination ability of carbon monoxide to rhodium than that of ethylene. In this reaction, a major problem is rhodium-catalyzed hydrolysis of organoboronic acid as a competing side re-

Tab. 3.1 Asymmetric conjugate addition of organoboronic acids to α,β-unsaturated ketones catalyzed by Rh(acac)$(C_2H_4)_2$/(*S*)-BINAP [6].

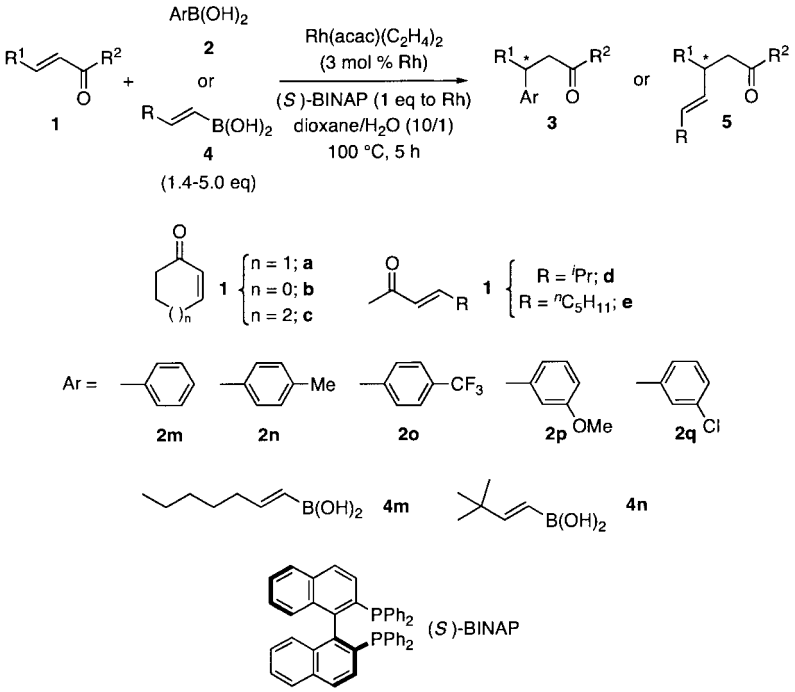

Entry	*Enone 1*	*Boronic acid 2 or 4 (equiv. to 1)*	*Ketone 3 or 5*			
				Yield (%)	*% ee*	
1	**1a**	**2m** (5.0)	**3am**	>99	97	(*S*)
2	**1a**	**2n** (5.0)	**3an**	>99	97	
3 [a)]	**1a**	**2o** (2.5)	**3ao**	70	99	
4	**1a**	**2p** (5.0)	**3ap**	97	96	
5	**1a**	**2q** (5.0)	**3aq**	94	96	
6	**1b**	**2m** (1.4)	**3bm**	93	97	(*S*)
7	**1c**	**2m** (1.4)	**3cm**	51	93	
8	**1d**	**2m** (5.0)	**3dm**	82	97	
9	**1e**	**2m** (2.5)	**3em**	88	92	
10	**1a**	**4m** (2.5)	**5am**	88	94	
11	**1a**	**4n** (5.0)	**5an**	76	91	
12	**1b**	**4m** (2.5)	**5bm**	64	96	

a) In 1-propanol/H_2O (10:1).

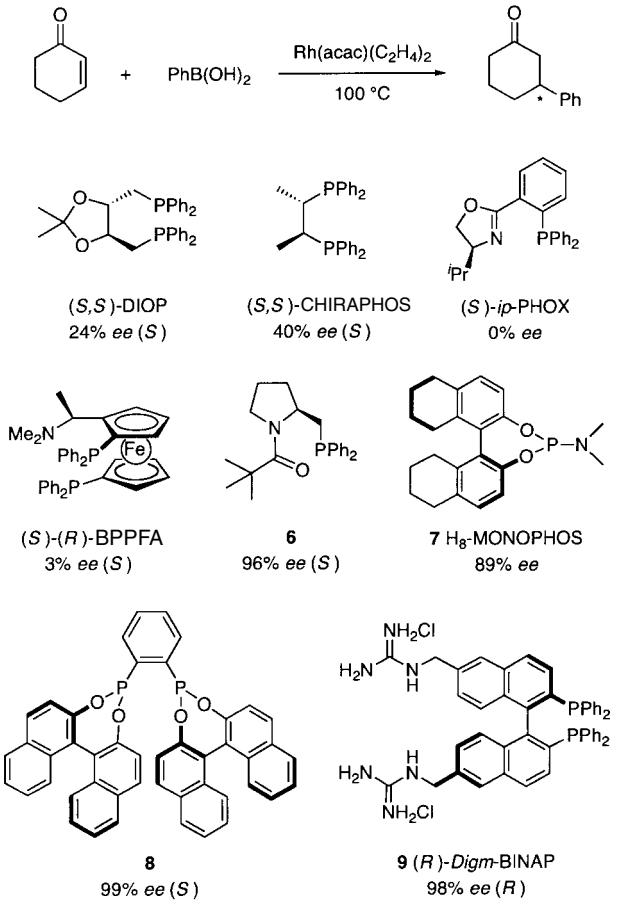

Scheme 3.2 Asymmetric conjugate addition catalyzed by chiral phosphine–rhodium complexes [7–11].

action. As a result, large excesses of organoboronic acids (1.4–5.0 equiv. relative to the enone) were used to achieve high yields.

After the report by Hayashi and Miyaura [6], several other chiral ligands have been examined for enantioselectivity in asymmetric conjugate addition under similar reaction conditions (Scheme 3.2). For example, DIOP, CHIRAPHOS, *ip*-PHOX, and BPPFA gave much lower enantioselectivity and the reactions were much less efficient [7]. Enantioselectivities as high as that with BINAP were observed by use of L-proline-based amidomonophosphine **6** [8], H_8-MONOPHOS **7** [9], binaphthol-based diphosphonite **8** [10], or (*R*)-*Digm*-BINAP **9** [11]. In these cases, high yields were also achieved. It is especially noteworthy that 13 200 turnovers were achieved in the reaction with the (*R*)-*Digm*-BINAP **9** ligand. This result shows the possibility of industrial-scale application of this asymmetric reaction.

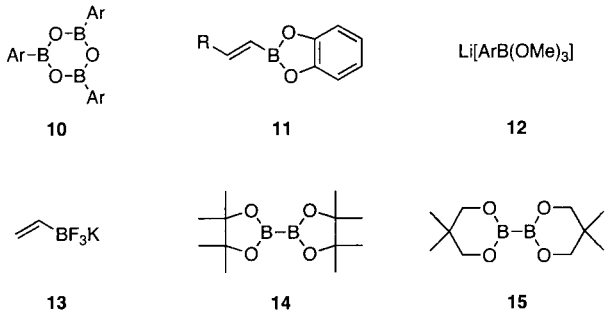

Scheme 3.3 Organoboron compounds used for rhodium-catalyzed conjugate addition [12–15].

In place of organoboronic acid, several other organoboron compounds can also be used for the asymmetric conjugate addition (Scheme 3.3); this has some advantages:

- Due to the tendency of organoboronic acids to undergo cyclic trimerization with loss of water to form organoboroxines, the determination of the exact stoichiometry of the organoboronic acids is usually difficult. Use of more stable organoboroxines **10**, which have similar reactivity to organoboronic acid, can avoid this problem.
- Alkenylcatecholborane **11** is a good reagent for the conjugate addition and is easily obtained by the hydroboration of an alkyne with catecholborane. One-pot asymmetric synthesis of the conjugate addition product, β-alkenyl ketone, is possible starting from an alkyne and catecholborane without isolation of the alkenylcatecholborane [12].
- Lithium trimethyl arylborate **12** is also a good reagent for the asymmetric conjugate addition. It is readily generated in situ by treatment of an aryl bromide with butyllithium and trimethoxyborane, and it has higher activity than the corresponding organoboronic acid in some cases [13].
- Potassium organotrifluoroborate **13** is generally more stable than the corresponding organoboronic acid. As a typical example, an unsubstituted vinyl group can be introduced with high enantioselectivity in high yield by use of vinyltrifluoroborate. The corresponding boronic acid cannot be used because of its instability under the reaction conditions [14].
- Bis(pinacolato)diboron **14** and bis(neopentyl glycolate)diboron **15** have been used for rhodium-catalyzed conjugate addition to α,β-unsaturated ketones giving β-boryl ketones, though the asymmetric version has not been reported [15].

3.3 Mechanism

Hayashi and co-workers established the catalytic cycle of the asymmetric conjugate addition in 2002 [16]. An example is outlined in Scheme 3.4 for the reaction of phenylboronic acid **2m** with 2-cyclohexenone **1a**. The reaction has three main intermediates: hydroxorhodium (**A**), phenylrhodium (**B**), and oxa-π-allylrhodium (**C**) complexes. They are related in the catalytic cycle by: (1) transmetallation of a phenyl group from boron to hydroxo-

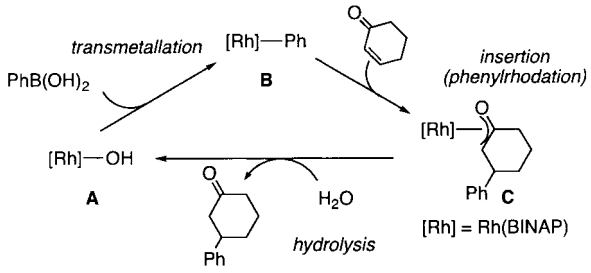

Scheme 3.4 Catalytic cycle for the rhodium-catalyzed conjugate addition [16].

rhodium **A** giving phenylrhodium **B**; (2) insertion of 2-cyclohexenone into the phenyl–rhodium bond of phenylrhodium **B** forming oxa-π-allylrhodium **C**; and (3) its hydrolysis giving the conjugate addition product and regenerating hydroxo-rhodium **A**.

Hayashi proved the validity of this catalytic cycle by the observation of all three intermediates and their respective transformations using NMR experiments (Scheme 3.5) [16]. Transmetallation of a phenyl group from boron to rhodium takes place by addition of phenylboronic acid **2m** to hydroxo-rhodium complex **16** in the presence of triphenylphosphine to generate the phenylrhodium complex **17**. The reaction of **17** with 2-cyclohexenone **1a** gives oxa-π-allylrhodium **18**, which is converted immediately into hydroxo-rhodium complex **16** upon addition of water, liberating the phenylation product **3am**. In this NMR study, triphenylphosphine was used to stabilize the phenylrhodium(I) complex. In the absence of triphenylphosphine, the characterization of the phenyl–rhodium species was unsuccessful.

These NMR experiments provided great insight into the catalytic reaction. Whereas the catalytic reaction requires a high reaction temperature of 100 °C, all three transformations in Scheme 3.5 proceed at 25 °C. In the same paper [16], Hayashi answered the question of why the catalytic reaction does not take place at the lower temperature. An outline of the reason is illustrated in Scheme 3.6. In the catalytic reaction, Rh(acac)(BINAP) is involved as a significant intermediate, because Rh(acac)$(C_2H_4)_2$ is used as the rhodium precursor. It was confirmed that the hydroxo-rhodium complex is immediately converted into Rh(acac)(BINAP) by the reaction with 1 equiv. acetylacetone at 25 °C, in which the transmetallation from boron to rhodium is very slow at the same temperature. Thus, the acetylacetonato ligand inhibits the catalytic reaction (Scheme 3.6, path a).

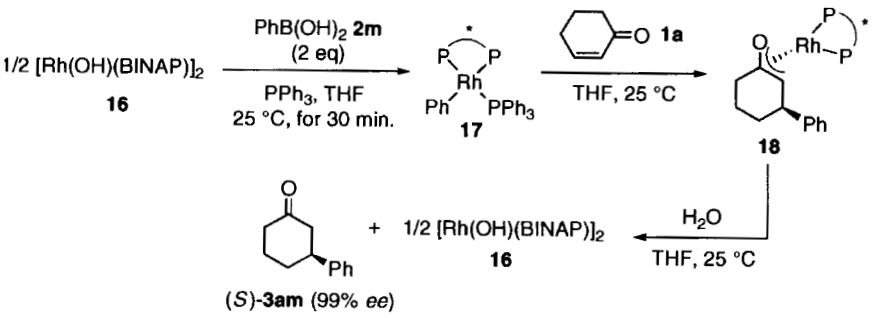

Scheme 3.5 Reactions of the rhodium–BINAP complex **16** [16].

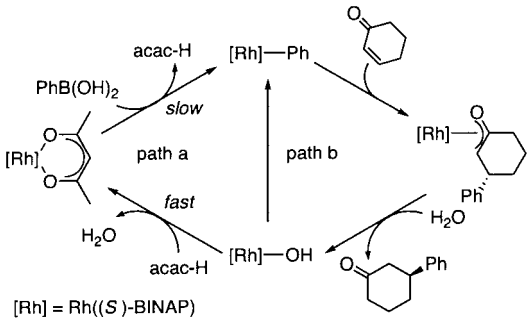

Scheme 3.6 Catalytic cycle for the conjugate addition catalyzed by a rhodium–acetylacetonato complex [16].

On the basis of this finding, $[Rh(OH)(BINAP)]_2$, which is an acetylacetonato-free rhodium complex, was used as a catalyst for the reaction (Scheme 3.6, path b). As expected, the conjugate addition took place at a lower temperature (Tab. 3.2). For example, the addition of phenylboronic acid **2m** or phenylboroxine **10m** to 2-cyclohexenone **1a**, catalyzed by $[Rh(OH)(BINAP)]_2$ at 35 °C, affords a quantitative yield of **3am** with 99.3% enantiomeric purity. This catalytic system is also applicable to the reaction of other enones and organoboron reagents. Because the reaction temperature is lower, the enantioselectivity is always higher than that in the reaction catalyzed by the rhodium–acac complex at 100 °C. The chemical yields are higher using a lower amount of the boron reagents because the hydrolysis of the boronic acids, which is the main side reaction, is suppressed at the lower temperature. The higher efficiency of the $[Rh(OH)(BINAP)]_2$ catalyst was also observed in the asymmetric addition of 3-thiopheneboronic acid **2z** to enones [17].

Scheme 3.7 shows the stereochemical pathway in the reaction catalyzed by the rhodium complex coordinated with (*S*)-BINAP. According to the highly skewed structure known for transition metal complexes coordinated with a BINAP ligand [18], (*S*)-BINAP–rhodium intermediate **D** should have an open space at the lower part of the vacant coordination site, the upper part being blocked by one of the phenyl rings of the BINAP ligand. The olefinic double bond of 2-cyclohexenone **1a** coordinates to rhodium with its *α,si*-face forming **E** rather than with its *α,re*-face, which undergoes migratory insertion to form a stereogenic carbon center in **F** whose absolute configuration is *S*. The absolute configuration of all the conjugate addition products can be predicted by this type of stereochemical model, in which the (*S*)-BINAP–rhodium complex attacks the *α,si*-face of cyclic and linear *α,β*-unsaturated ketones. Moreover, this model is also applicable to other electron-deficient olefins, including *α,β*-unsaturated esters and alkenylphosphonates (*vide infra*).

Miyaura reported that a rhodium complex coordinated with 1,5-cyclooctadiene (COD) is a highly active catalyst for rhodium-catalyzed conjugate addition [19]. The addition of *p*-tolylboronic acid to methyl vinyl ketone was carried out in the presence of $[RhCl(COD)]_2$ in water at 100 °C. The corresponding conjugate addition product was obtained with turnover numbers (TON) of 46 000. Additionally, the phosphine-free conditions gave a TON of 24 000 for the addition of *p*-tolylboronic acid to 2-cyclohexenone. These results indicate that the generation of a chiral phosphine–rhodium catalyst by mixing a rhodium–COD precursor with a chiral phosphine ligand may afford lower enantioselectivity if the ligand exchange is incomplete. Therefore, the asymmetric reac-

Tab. 3.2 Asymmetric conjugate addition catalyzed by [Rh(OH)((*S*)-BINAP)]$_2$ [16].

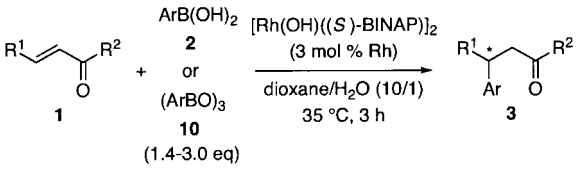

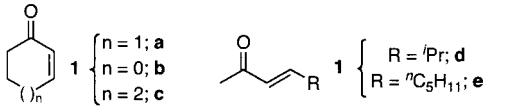

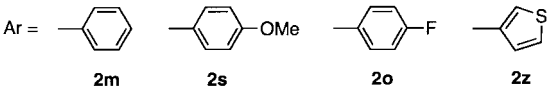

Entry	*Enone 1*	*2 or 10 (equiv. to 1)*	*Ketone 3*			
				Yield [%]	*% ee*	
1	**1a**	**2m** (2.5)	**3am**	96	99	(*S*)
2	**1a**	**10m** (2.5)	**3am**	98	99.3	(*S*)
3	**1a**	**10m** (1.4)	**3am**	94	99.2	(*S*)
4	**1a**	**10s** (2.5)	**3as**	96	99.1	
5	**1a**	**10x** (2.5)	**3ax**	96	99.1	
6	**1b**	**10m** (2.5)	**3bm**	95	98	(*S*)
7	**1c**	**10m** (2.5)	**3cm**	94	96	(*S*)
8	**1d**	**10m** (2.5)	**3dm**	89	98	(*S*)
9	**1e**	**10m** (2.5)	**3em**	92	98	(*R*)
10[a)]	**1a**	**2z** (3.0)	**3az**	67	99	(*S*)
11[a)]	**1b**	**2z** (3.0)	**3bz**	78	97	(*S*)
12[a)]	**1c**	**2z** (3.0)	**3cz**	81	99	(*S*)
13[a)]	**1d**	**2z** (3.0)	**3dz**	75	99	(*S*)

a) At 40 °C for 24 h.

tions are usually carried out by use of an isolated chiral phosphine–rhodium catalyst or combination of a chiral phosphine and the more labile bis(ethylene)rhodium precursor. Alternatively, a solution of a chiral phosphine and a rhodium–COD precursor is heated before addition of the starting materials.

3.4
Addition of Organoboron Reagents to Other Electron-Deficient Olefins

The rhodium-catalyzed asymmetric conjugate addition is applicable to *α,β*-unsaturated esters (Scheme 3.8). Hayashi reported [20] that the reaction of 5,6-dihydro-2*H*-pyran-2-one **19a** with phenylboronic acid gave a 94% yield of phenylated lactone (*S*)-**20am** with 98% enantiomeric excess. For the linear enoates, organoboronic acids did not give

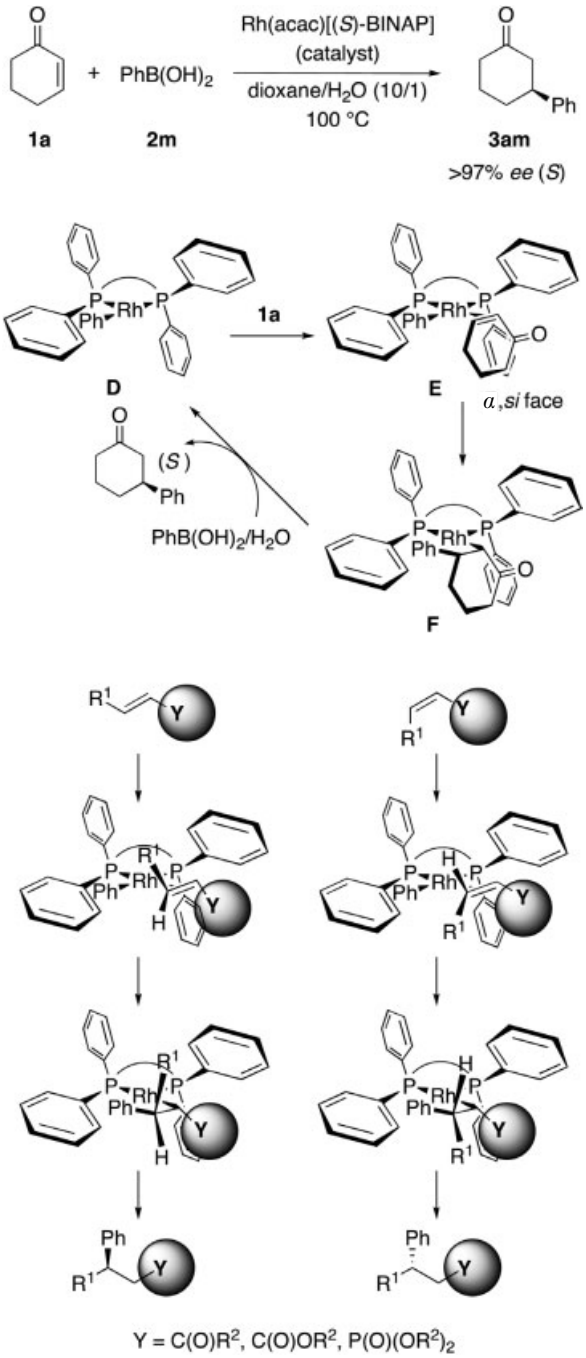

Scheme 3.7 Stereochemical pathway in the conjugate addition catalyzed by the rhodium–(*S*)-BINAP complex [6, 20, 25].

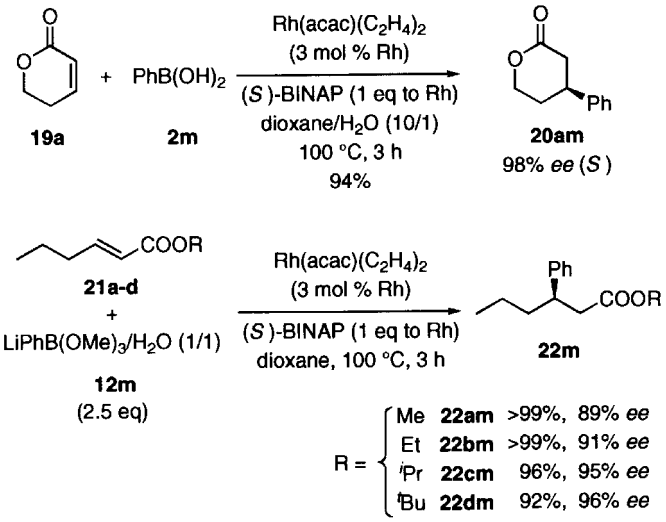

Scheme 3.8 Asymmetric conjugate addition of organoboron reagents to α,β-unsaturated esters [20].

Tab. 3.3 Asymmetric conjugate addition of organoboronic acids to α,β-unsaturated amides [22].

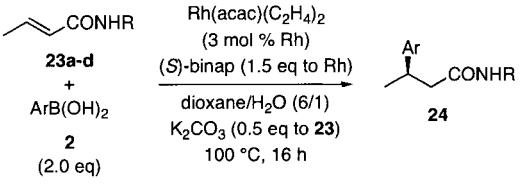

R = CH_2Ph **23a**, ^cHex **23b**, H **23c**, Ph **23d**
Ar = Ph **2m**, 4-MeC_6H_4 **2n**, 4-$CF_3C_6H_4$ **2o**, 4-$MeOC_6H_4$ **2s**

Entry	*Amide 23*	*Boronic acid 2*	*Amide 24*			
				Yield [%]	*% ee*	
1 [a)]	**23a**	**2m**	**24am**	67	93	(*R*)
2	**23a**	**2m**	**24am**	85	93	(*R*)
3	**23b**	**2m**	**24bm**	89	93	
4	**23c**	**2m**	**24cm**	62	89	
5	**23d**	**2m**	**24dm**	88	90	
6	**23a**	**2n**	**24an**	74	87	
7	**23a**	**2o**	**24ao**	82	92	
8	**23a**	**2s**	**24as**	50	77	

a) Without K_2CO_3.

high yields of the addition products. Much better results were obtained with the lithium arylborates **12**. The enantioselectivity is higher with the sterically bulkier ester group, though the yields decrease as the steric bulk increases. The molecular recognition model outlined in Scheme 3.7 nicely explains these results: the (*S*)-BINAP/rhodium catalyst recognizes the enantioface of *α,β*-unsaturated esters by the steric bulk of the ester moiety. Similar results for asymmetric conjugate addition to *α,β*-unsaturated esters have been reported independently by Miyaura [21].

α,β-Unsaturated amides **23** were less reactive than the enones or enoates under the standard conditions (Tab. 3.3, entry 1). Miyaura found [22] that the conjugate addition is accelerated by the addition of potassium carbonate, which is considered to cause the conversion of a rhodium–acetylacetonato complex into a more reactive rhodium–hydroxide species (see Section 3.3). The enantioselectivity is comparable to that in addition to the corresponding esters.

Asymmetric addition to cyclic *α,β*-unsaturated amides gave optically active 4-(4-fluorophenyl)-2-piperidinone **26x**, which is a key intermediate of biologically active compounds such as paroxetine [23]. Since the hydrolysis of the boronic acids **10x** was the serious side reaction in this case, slightly modified conditions were required (Scheme 3.9). Thus, the reaction of lactam **25** with 4-fluorophenylboroxine **10x** and water (1 equiv. relative to boron) in the presence of $Rh(acac)(C_2H_4)_2$/(*R*)-BINAP catalyst in dioxane at 40 °C gave a 63% yield of (*R*)-**26x** with 97% enantiomeric excess. The use of boroxine **10x** and 1 equiv. water is a key factor for successful conjugate addition. This is much better than the reaction carried out with the corresponding boronic acid under the usual reaction conditions. Thus, in the presence of a large excess of water as a cosolvent, the yield of **26** in the reaction at 100 °C is only 17%. The use of a modified BINAP ligand containing 3,5-dimethyl-4-methoxyphenyl group on the phosphorus atoms (BINAP*, **27**) gave a higher yield.

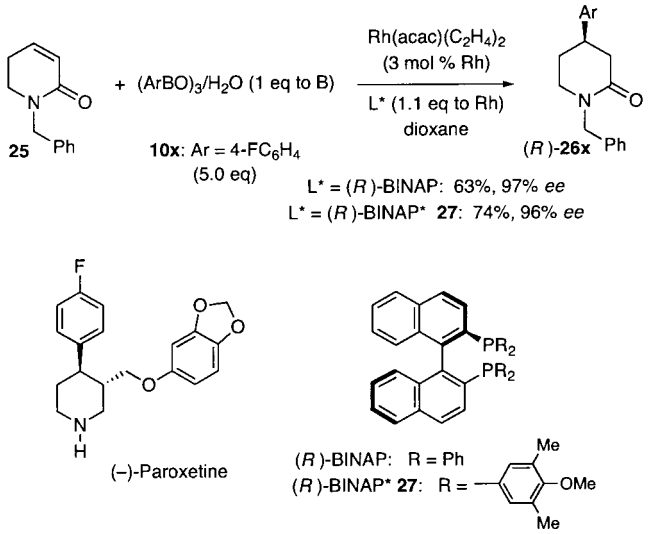

Scheme 3.9 Asymmetric conjugate addition to cyclic *α,β*-unsaturated amides [23].

Maddaford reported the diastereoselective synthesis of *C*-glycosides **29** using conjugate addition catalyzed by cationic rhodium catalysts such as $[Rh(COD)_2]BF_4$ (Eq. 1) [24]. Addition of phosphine ligands to the reaction system inhibited the conjugate addition. It is likely that the enone **28** derived from the pyranose is less reactive toward the conjugate addition.

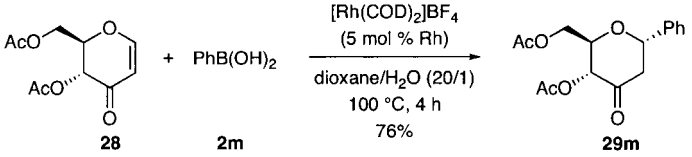

(1)

An interesting asymmetric transformation is the asymmetric conjugate addition to *α*-acetamidoacrylic ester **30** giving phenylalanine derivative **31**, which has been reported by Reetz (Scheme 3.10) [10]. The addition of phenylboronic acid **2m** in the presence of a rhodium complex of 1,1′-binaphthol-based diphosphinite ligand **32** gave a quantitative yield of **31** with up to 77% enantiomeric excess. In this asymmetric reaction the stereochemical outcome is determined at the hydrolysis step of an oxa-*π*-allylrhodium intermediate, not at the insertion step (compare Scheme 3.7).

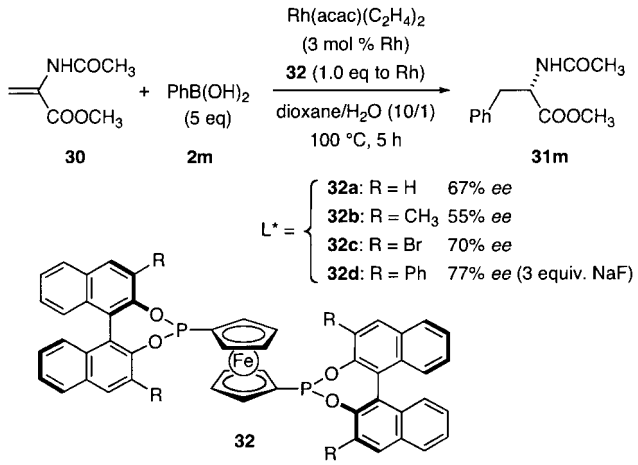

Scheme 3.10 Rhodium-catalyzed asymmetric conjugate addition forming phenylalanine [10].

In the asymmetric addition to alkenylphosphonate **33** (Eq. 2) [25], the yield is dependent on the amount of water present. The combination of boroxine and water (1 equiv. relative to boron) gave a high yield of the desired product **34**, with 96% enantiomeric excess. The alkylphosphonate **34** can be used as a chiral building block for the synthesis of optically active alkenes, using a Horner–Emmons type of reaction.

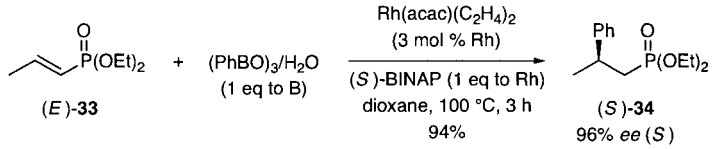

(2)

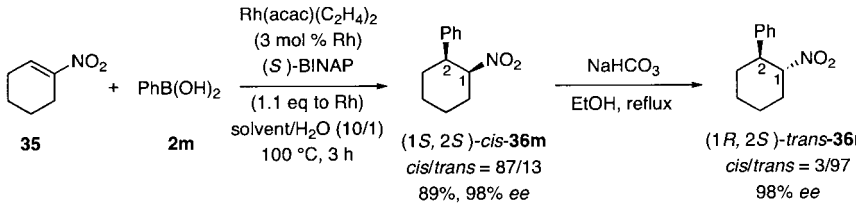

Scheme 3.11 Catalytic asymmetric conjugate addition to nitrocyclohexene **35** [26].

A nitroalkene is another good substrate for the rhodium-catalyzed asymmetric conjugate addition of organoboronic acids [26]. Hayashi reported that the reaction of 1-nitrocyclohexene **35** with phenylboronic acid **2m** in the presence of the rhodium–(*S*)–BINAP catalyst at 100 °C for 3 h gave an 89% yield of 2-phenyl-1-nitrocyclohexane **36m** (Scheme 3.11). The main phenylation product **36m** is a *cis*-isomer (*cis*/*trans*=87:13) and both of the *cis*- and *trans*-isomers are produced with 98% enantiomeric purity. Equilibration of the *cis*-isomer to the thermodynamically more stable *trans*-isomer (*trans*/*cis* = 97:3) was achieved with sodium bicarbonate in refluxing ethanol. The optically active nitroalkanes obtained by this method are useful chiral building blocks, which can be readily converted into a wide variety of optically active compounds by taking advantage of the versatile reactivity of nitro compounds.

Murakami [27] and Lautens [28] independently reported the rhodium-catalyzed addition of arylboronic acids to oxanorbornenes (Scheme 3.12). Murakami reported that the reaction of oxabenzonorbornadiene **37a** with phenylboronic acid **2m**, in the presence of a rhodium–$P(OEt)_3$ catalyst in MeOH at reflux, gave an 86% yield of the ring-opened alcohol **38am**. Lautens reported the asymmetric version of the reaction, where high enantioselectivity was observed with chiral ferrocenylbisphosphine ligand **39** in a

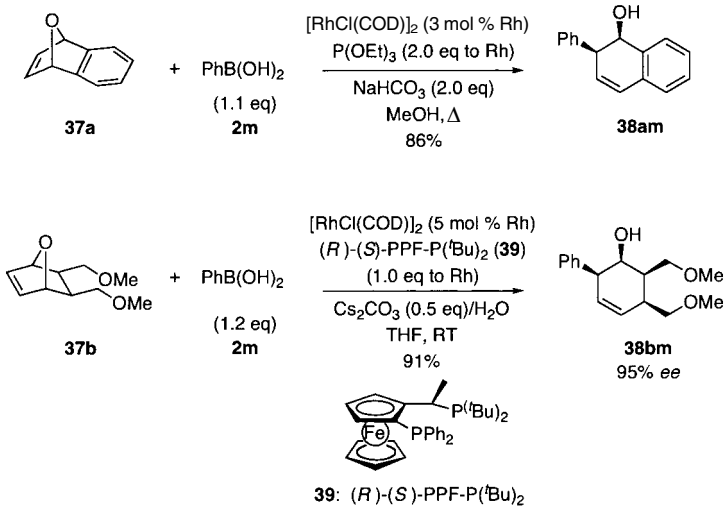

Scheme 3.12 Rhodium-catalyzed asymmetric addition of phenylboronic acid to oxanorbornenes [27, 28].

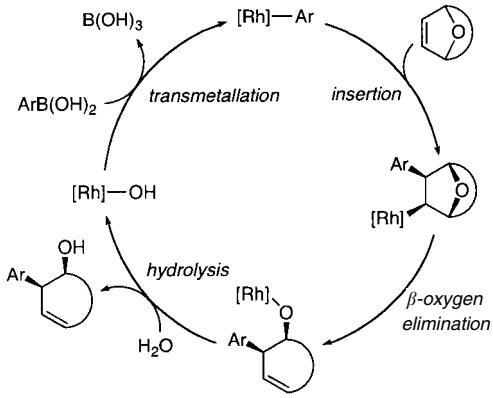

Scheme 3.13 Catalytic cycle for the rhodium-catalyzed addition of organoboronic acids to oxanorbornenes [27, 28].

THF solution containing aqueous cesium carbonate. The reaction of [2.2.1]oxabicycle **37b** with phenylboronic acid **2m** gave the ring-opened alcohol **38bm**, with 95% enantiomeric excess.

The catalytic cycle was proposed to involve *β*-oxygen elimination as a key step (Scheme 3.13). Thus, insertion of the double bond of oxanorbornene into the aryl–rhodium bond forms an alkylrhodium intermediate, which undergoes *β*-oxygen elimination to give an alkoxyrhodium intermediate. Subsequent hydrolysis and transmetallation regenerates the arylrhodium intermediate. The stereochemical outcome for the asymmetric reaction is determined during the enantioposition-selective carborhodation of the *meso*-type alkene.

3.5 Addition of Organotin and -silicon Reagents

In 1998, the rhodium-catalyzed conjugate addition of organostannanes to *α,β*-unsaturated ketones and esters was reported by Oi [29]. In the reaction, which was carried out in the presence of $[Rh(COD)(MeCN)_2]BF_4$ in THF at 60 °C, a variety of *α,β*-unsaturated ketones and esters were transformed into the corresponding conjugate addition products. It is noted that the yield was highly dependent on the substitution pattern of the substrates. For example, *β*-substituted enone **40** afforded an 86% yield of **41**, whereas methyl vinyl ketone **42** gave only an 18% yield of **43** (Scheme 3.14). The addition of water to the reaction mixture improved the reactivity for the formation of **41** (98%) and **43** (80%) [30].

The reaction mechanism proposed for the addition of organostannanes [29] is similar to that for organoboronic acids. An example of the reaction of methyl vinyl ketone **42** is outlined in Scheme 3.15. The catalytic cycle involves a cationic rhodium complex **G**, phenylrhodium **H**, and oxa-*π*-allylrhodium **I**. Stannyl enol ether **44** is formed by the reaction of oxa-*π*-allylrhodium **I** with Me_3SnBF_4, which upon hydrolysis gives the ketone **43**. The lower yields in the absence of water were explained by the further reaction of **44** with methyl vinyl ketone **42**. The rapid hydrolysis with water may prevent such oligomerization.

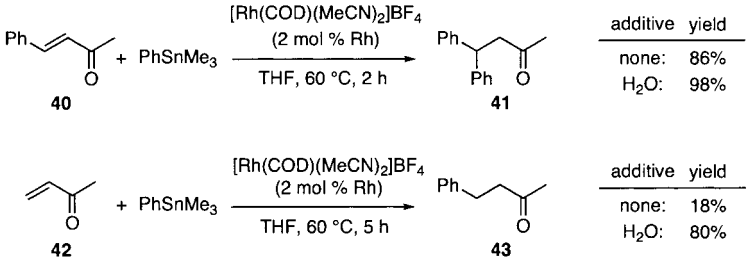

Scheme 3.14 Rhodium-catalyzed conjugate addition of phenyltrimethylstannane [29, 30].

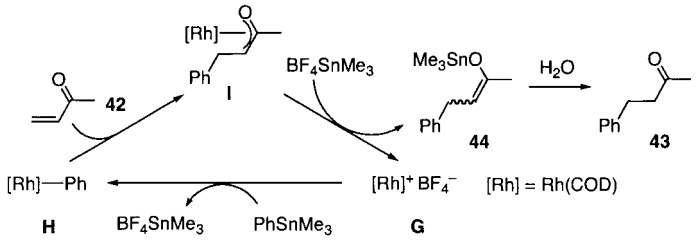

Scheme 3.15 Catalytic cycle for rhodium-catalyzed conjugate addition of organostannanes [29].

Li has reported a similar rhodium-catalyzed conjugate addition of organostannanes in water [31], where the electronic nature of the substituents on tin was demonstrated to have a significant impact on the reactivity (Scheme 3.16) [32]. Alkyl and hydroxy groups on tin, which effectively donate electrons to the metal, proved to be good substituents for the reaction, while electron-withdrawing substituents, as exemplified by chloride, lowered the overall reactivity. An *in-situ* halogen-hydroxy exchange by the addition of KOH brought about a high yield of the conjugate addition product.

The rhodium-catalyzed conjugate addition of organostannanes has not been applied to asymmetric synthesis. The active rhodium catalyst used for this reaction is $[Rh(COD)(MeCN)_2]BF_4$, in which the addition of phosphine ligands has been reported to inhibit the catalytic activity [30]. Hence, the low catalytic activity of the phosphine–rhodium complexes makes this approach difficult for asymmetric synthesis applications.

The use of organosilanes for rhodium-catalyzed conjugate addition is also feasible. In 2001, Mori reported that the catalytic conjugate addition of aryl(ethyl)silanediols to *α,β*-unsaturated carbonyl compounds takes place in the presence of $[Rh(OH)(COD)]_2$ in a

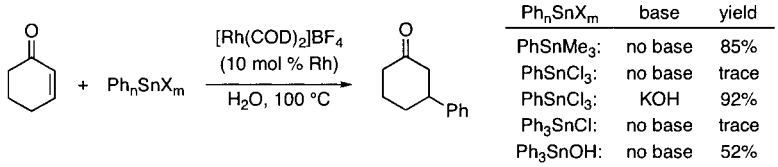

Scheme 3.16 Rhodium-catalyzed conjugate addition of phenylstannanes [31, 32].

2:1 mixture of THF and water at 60 °C (Scheme 3.17) [33]. The reaction of butyl acrylate **45** with (4-methylphenyl)(ethyl)silanediol **46** gave the conjugate addition product **47** in a good yield. In the absence of water, the Mizoroki–Heck type of product **48** is formed selectively.

For rhodium-catalyzed conjugate addition using organosilanes, several other conditions have been reported [34]. Cationic rhodium catalysts such as $[Rh(COD)_2]BF_4$ and $[Rh(COD)(MeCN)_2]BF_4$ are more active than neutral rhodium catalysts such as $[Rh(OH)(COD)]_2$.

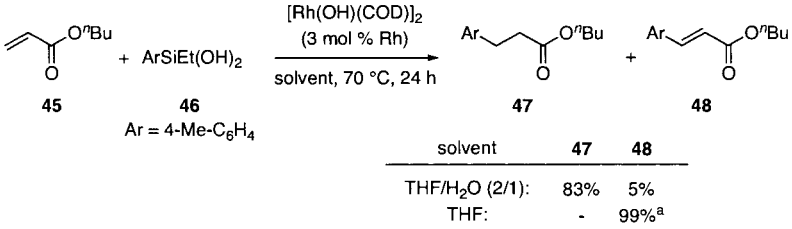

Scheme 3.17 Rhodium-catalyzed reaction of arylsilane **46** with acrylate **45** [33].

Oi and Inoue recently described the asymmetric rhodium-catalyzed addition of organosilanes [35]. The addition of aryl- and alkenyltrialkoxysilanes to α,β-unsaturated ketones takes place, in the presence of 4 mol% of a cationic rhodium catalyst generated from $[Rh(COD)(MeCN)_2]BF_4$ and (*S*)-BINAP in dioxane/H_2O (10:1) at 90 °C, to give the corresponding conjugate addition products (Eq. 3). The enantioselectivity is comparable to that observed with the boronic acids, as the same stereochemical pathway is applicable to these reactions (compare Scheme 3.7).

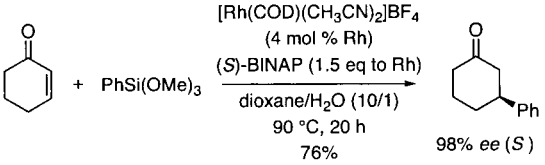

(3)

Recently, triphenylbismuth has been used for rhodium-catalyzed conjugate addition (Eq. 4) [36]. The reaction carried out in the presence of $[RhCl(COD)]_2$ or $[Rh(COD)_2]BF_4$ as a catalyst under an atmosphere of air gave high yields of the products. No asymmetric version has yet been reported.

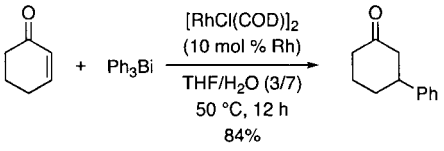

(4)

3.6
New Aspects of Addition of Organoboron and -titanium Reagents

The rhodium-catalyzed conjugate addition of organoboron, -tin, and -silicon reagents has been carried out in solvents containing water to give the addition products as hydrolyzed compounds (Sections 3.2 to 3.5). Although the reactions in protic solvents have some advantages over those in aprotic solvents, it would be more useful if the products were isolated as metal enolates, thereby providing an opportunity to carry out further transformations. In 2003, Hayashi reported a catalytic asymmetric conjugate addition that formed chiral boron enolates using a new reaction system in which no protic solvent was employed (Scheme 3.18) [37]. As a typical example, the reaction of 2-cyclohexenone **1a** with 1.1 equiv. *B*-Ph-9BBN **50m** in the presence of 3 mol% of a rhodium catalyst generated from $[Rh(OMe)(COD)]_2$ and (*S*)-BINAP in toluene at 80 °C for 1 h furnished the boron enolate **51** in high yield with 98% enantiomeric excess having the (*S*)-configuration. Boron enolate formation was not observed in the reaction with phenylboronate esters, phenylboroxine, or tetraphenylborate. The boron enolate **51** was treated with propanal to give the aldol product without loss of enantiomeric purity.

Investigation using ^{31}P NMR revealed that a direct transmetallation of the phenyl group from boron to rhodium of the (oxa-π-allyl)rhodium complex is involved in the reaction of *B*-Ph-9BBN. The catalytic cycle consists of two steps: 1) insertion of the enone into the aryl–rhodium bond and 2) transmetallation to the (oxa-π-allyl)rhodium complex forming an arylrhodium species and the boron enolate (Scheme 3.19). Unfor-

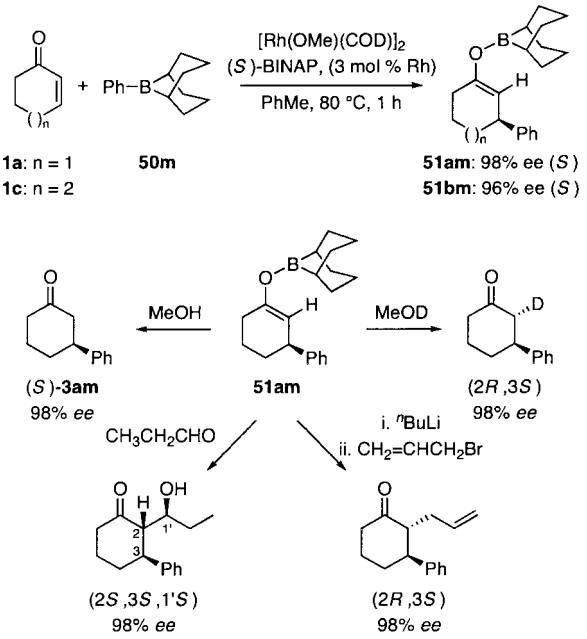

Scheme 3.18 Rhodium-catalyzed asymmetric conjugate addition of *B*-Ph-9BBN forming boron enolate [37].

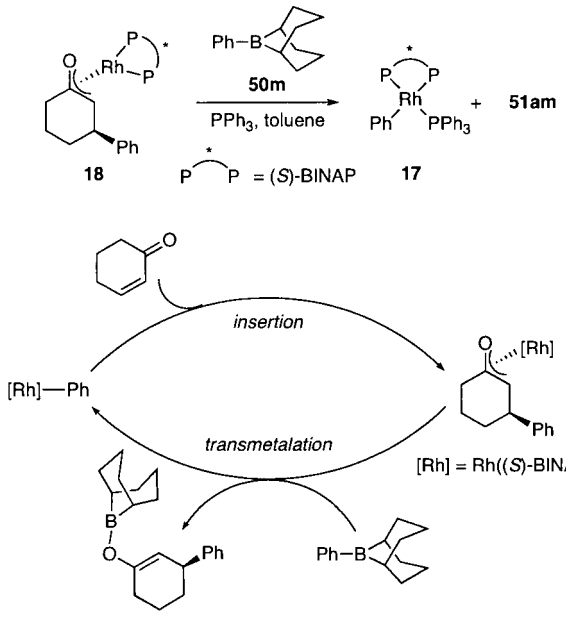

Scheme 3.19 Catalytic cycle for the conjugate addition of *B*-Ph-9BBN [37].

tunately, the formation of the chiral boron enolate is only observed with 2-cyclohexenone and 2-cycloheptenone.

It was found that aryltitanium triisopropoxides **52** ($ArTi(O^iPr)_3$) also participate in asymmetric conjugate addition to *α,β*-unsaturated ketones in an aprotic solvent [38] (Scheme 3.20). The addition of **52** to 2-cyclohexenone **1a** was complete within 1 h in the presence of 3 mol% of $[Rh(OH)((S)\text{-BINAP})]_2$ in THF at 20 °C to give high yields of the titanium enolates **53** as conjugate addition products. The enantioselectivity is very high, 99.5, 99.0, and 99.8% enantiomeric excess, for Ar = Ph, 4-FC_6H_4, and

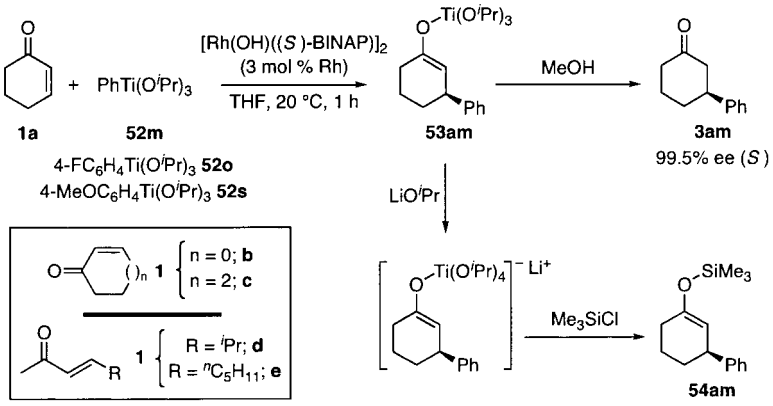

Scheme 3.20 Rhodium-catalyzed asymmetric conjugate addition of organotitanium reagents forming titanium enolates [38].

4-$MeOC_6H_4$, respectively. The titanium enolates were converted into silyl enol ethers **54** by treatment with chlorotrimethylsilane and lithium isopropoxide. Additionally, cyclic enones **1b** and **1c**, and linear enones **1d** and **1e**, are also good substrates for the asymmetric conjugate addition of phenyltitanium triisopropoxide, giving the corresponding arylation products with over 97% enantioselectivity.

In an aprotic solvent using *B*-Ar-9BBN **50** as an arylating reagent, Hayashi found a new type of catalytic tandem conjugate addition–aldol reaction [39]. Thus, the reaction of *B*-Ar-9BBN **50**, vinyl ketone **55**, and aldehyde **56** catalyzed by 3 mol% of $[Rh(OMe)(COD)]_2$ proceeded in toluene at 20 °C to give high yields of the aldol-type product **57** with high *syn*-selectivity (Scheme 3.21). The asymmetric reaction using $[Rh(OH)((S)\text{-BINAP})]_2$ as a catalyst gave *syn*-(4*S*,5*R*)-**57** and *anti*-(4*R*,5*R*)-**57** in 41 and 94% enantiomeric excess respectively. The formation of the enantiomerically enriched products demonstrates that the reaction proceeds through the (oxa-π-allyl)rhodium complex **P** coordinated with the (*S*)-BINAP ligand, which is formed by the carborhodation of the vinyl ketone and undergoes an aldol-type reaction with an aldehyde to form the rhodium aldolate **Q**. The boron enolate is ruled out as an intermediate, which would lead to a racemic aldol product.

Krische reported an intramolecular version of the tandem conjugate addition–aldol reaction. The reaction of enone-ketone **58** with phenylboronic acid **2m** occurs in diox-

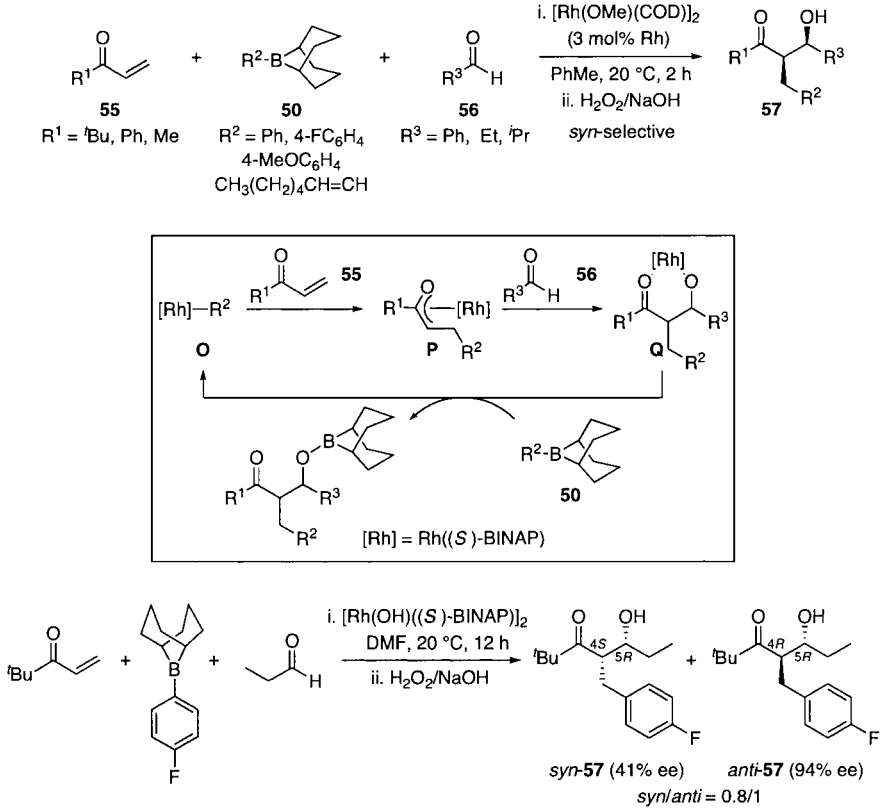

Scheme 3.21 Rhodium-catalyzed tandem conjugate addition–aldol reaction [39].

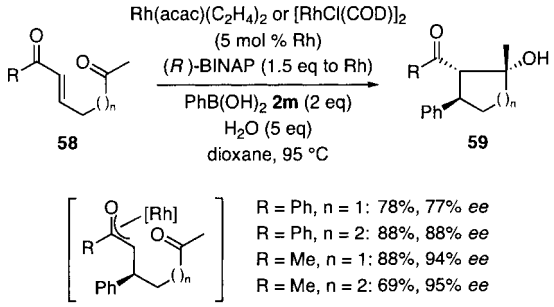

Scheme 3.22 Rhodium-catalyzed asymmetric intramolecular conjugate addition–aldol reaction [40].

ane containing water (5 equiv. relative to **58**) (Scheme 3.22) [40]. This cyclization probably proceeds through the (oxa-π-allyl)rhodium intermediate. Because the intramolecular reaction of the intermediate with the ketone moiety is faster than protonolysis with water, the aldol product is obtained in high yield. BINAP is again the ligand of choice, which gave the conjugate addition–aldol product with up to 95% enantiomeric excess.

Very recently, Hayashi found an interesting new *cine*-substitution by use of alkenyl sulfones **60** for the rhodium-catalyzed addition of aryltitanium reagents **52** ($ArTi(O^iPr)_3$) (Scheme 3.23) [41]. The addition to linear alkenyl sulfones **60a** and **60b** gave the corresponding *cine* substitution products, where the sulfonyl group is substituted with the phenyl group on the next carbon of the double bond. The catalytic cycle was established by deuterium labeling studies to proceed through *anti*-elimination of rhodium and the sulfonyl group from the alkyl–rhodium intermediate. In the addition reaction to cyclic alkenyl sulfone **60c**, the asymmetric carbon center created at the carborhodation step is retained in the substitution product. Thus, the reaction of **60c** with the aryltitanium triisopropoxides **52**, in the presence of 3 mol% of [Rh(OH)((*S*)-BINAP)]$_2$ in THF at 40 °C, gave a quantitative yield of 1-arylcyclohexenes **61c** with over 99% enantioselectivity. The reaction of the sulfone **60d**, which has an internal alkene, also proceeded with high enantioselectivity to afford the allylarene **61ds** with 99.2% enantiomeric excess.

3.7 Outlook

Rhodium-catalyzed asymmetric conjugate addition has enjoyed uninterrupted prosperity since the first report by Hayashi and Miyaura [6]. Its high enantioselectivity and wide applicability are truly remarkable. However, some problems still remain, since the carbon atoms that can be successfully introduced by this rhodium-catalyzed reaction have been limited to sp^2 carbons and the substrates employed have been limited mostly to the electron-deficient olefins free from sterically bulky substituents at α- and β-positions. These issues will be the subject of increasing attention in the future.

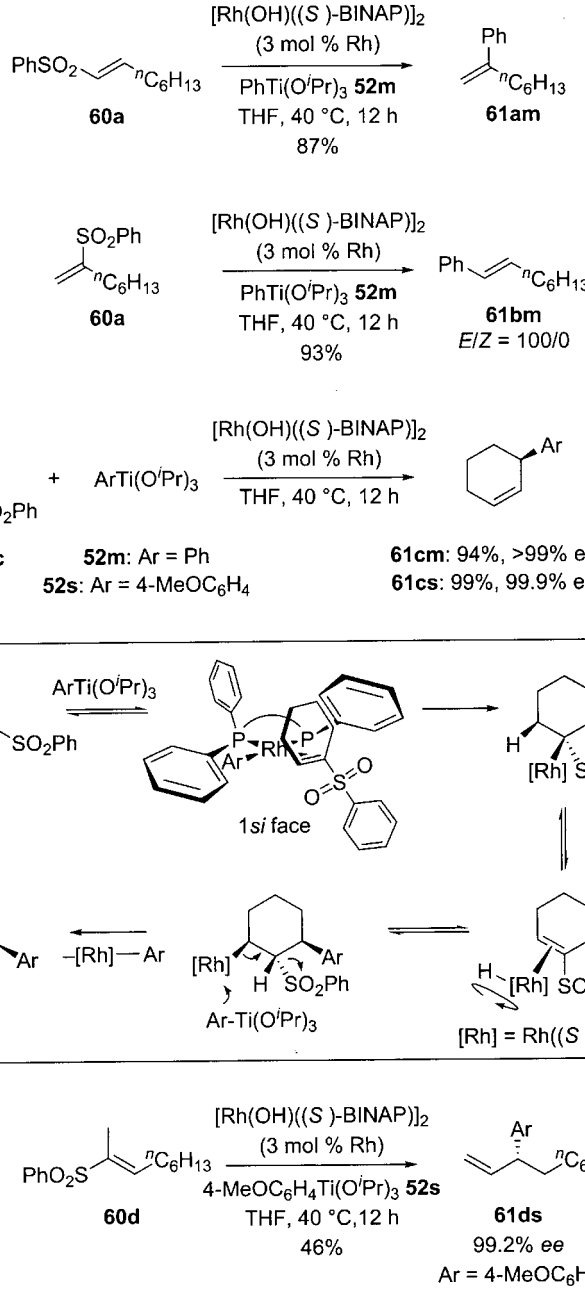

Scheme 3.23 Rhodium-catalyzed *cine*-substitution of alkenyl sulfones with aryltitanium reagents [41].

3.8 References

1 For reviews on conjugate addition: (a) Perlmutter, P. *Conjugate Addition Reactions in Organic Synthesis*, Pergamon Press: Oxford, **1992**. (b) Schmalz, H.-G. In *Comprehensive Organic Synthesis*; Trost, B.M.; Fleming, I., Eds.; Pergamon: Oxford, **1991**; Vol. 4, Chapter 1.5. (c) Rossiter, B.E.; Swingle, N.M. *Chem. Rev.* **1992**, *92*, 771.

2 For recent reviews on catalytic asymmetric conjugate addition: (a) Krause, N.; Hoffmann-Röder, A. *Synthesis* **2001**, 171. (b) Sibi, M.P.; Manyem, S. *Tetrahedron* **2000**, *56*, 8033. (c) Tomioka, K.; Nagaoka, Y. In *Comprehensive Asymmetric Catalysis*; Jacobsen, E.N.; Pfaltz, A.; Yamamoto, H., Eds.; Springer: Berlin, **1999**; Vol. 3, Chapter 31.1. (d) Kanai, M.; Shibasaki, M. In *Catalytic Asymmetric Synthesis, 2nd Ed.*; Ojima, I., Ed.; Wiley: New York, **2000**; pp. 569–592.

3 As recent examples of copper-catalyzed asymmetric conjugate addition of organozinc reagents: (a) Mizutani, H.; Degrado, S.J.; Hoveyda, A.H. *J. Am. Chem. Soc.* **2002**, *124*, 779. (b) Alexakis, A.; Benhaim, C.; Rosset, S.; Humam, M. *J. Am. Chem. Soc.* **2002**, *124*, 5262. (c) Arnold, L.A.; Naasz, R.; Minnaard, A.J.; Feringa, B.L. *J. Am. Chem. Soc.* **2001**, *123*, 5841. (d) Alexakis, A.; Trevitt, G.P.; Bernardinelli, G. *J. Am. Chem. Soc.* **2001**, *123*, 4358. (e) Degrado, S.J.; Mizutani, H.; Hoveyda, A.H. *J. Am. Chem. Soc.* **2001**, *123*, 755. (f) Escher, I.H.; Pfaltz, A. *Tetrahedron* **2000**, *56*, 2879. (g) Yan, M.; Chan, A.S.C. *Tetrahedron Lett.* **1999**, *40*, 6645.

4 For reviews on rhodium-catalyzed addition: (a) Hayashi, T. *Synlett* **2001**, 879. (b) Fagnou, K.; Lautens, M. *Chem. Rev.* **2003**, *103*, 169. (c) Hayashi, T.; Yamasaki, K. *Chem. Rev.* **2003**, *103*, 2829.

5 Sakai, M.; Hayashi, H.; Miyaura, N. *Organometallics* **1997**, *16*, 4229.

6 Takaya, Y.; Ogasawara, M.; Hayashi, T.; Sakai, M.; Miyaura, N. *J. Am. Chem. Soc.* **1998**, *120*, 5579.

7 Takaya, Y.; Ogasawara, M.; Hayashi, T. *Chirality* **2000**, *12*, 469.

8 (a) Kuriyama, M.; Tomioka, K. *Tetrahedron Lett.* **2001**, *42*, 921. (b) Kuriyama, M.; Nagai, K.; Yamada, K.-I.; Miwa, Y.; Taga, T.; Tomioka, K. *J. Am. Chem. Soc.* **2002**, *124*, 8932.

9 Boíteau, J.-G.; Imbos, R.; Minnaard, A.J.; Feringa, B.L. *Org. Lett.* **2003**, *5*, 681.

10 Reetz, M.T.; Moulin, D.; Gosberg, A. *Org. Lett.* **2001**, *3*, 4083.

11 Amengual, R.; Michelet, V.; Genêt, J.-P. *Synlett* **2002**, 1791.

12 Takaya, Y.; Ogasawara, M.; Hayashi, T. *Tetrahedron Lett.* **1998**, *39*, 8479.

13 Takaya, Y.; Ogasawara, M.; Hayashi, T. *Tetrahedron Lett.* **1999**, *40*, 6957.

14 (a) Batey, R.A.; Thadani, A.N.; Smil, D.V. *Org. Lett.* **1999**, *1*, 1683. (b) Pucheault, M.; Darses, S.; Genet, J.-P. *Tetrahedron Lett.* **2002**, *43*, 6155. (c) Pucheault, M.; Darses, S.; Genet, J.-P. *Eur. J. Org. Chem.* **2002**, 3552.

15 Kabalka, G.W.; Das, B.C.; Das, S. *Tetrahedron Lett.* **2002**, *43*, 2323.

16 Hayashi, T.; Takahashi, M.; Takaya, Y.; Ogasawara, M. *J. Am. Chem. Soc.* **2002**, *124*, 5052.

17 Yoshida, K.; Hayashi, T. *Heterocycles* **2003**, *59*, 605.

18 Ozawa, F.; Kubo, A.; Matsumoto, Y.; Hayashi, T. *Organometallics* **1993**, *12*, 4188, and references cited therein.

19 Itooka, R.; Iguchi, Y.; Miyaura, N. *Chem. Lett.* **2001**, 722.

20 Takaya, Y.; Senda, T.; Kurushima, H.; Ogasawara, M.; Hayashi, T. *Tetrahedron: Asymmetry* **1999**, *10*, 4047.

21 Sakuma, S.; Sakai, M.; Itooka, R.; Miyaura, N. *J. Org. Chem.* **2000**, *65*, 5951.

22 Sakuma, S.; Miyaura, N. *J. Org. Chem.* **2001**, *66*, 8944.

23 Senda, T.; Ogasawara, M.; Hayashi, T. *J. Org. Chem.* **2001**, *66*, 6852.

24 Ramnauth, J.; Poulin, O.; Bratovanov, S.S.; Rakhit, S.; Maddaford, S.P. *Org. Lett.* **2001**, *3*, 2571.

25 Hayashi, T.; Senda, T.; Takaya, Y.; Ogasawara, M. *J. Am. Chem. Soc.* **1999**, *121*, 11591.

26 Hayashi, T.; Senda, T.; Ogasawara, M. *J. Am. Chem. Soc.* **2000**, *122*, 10716.

27 Murakami, M.; Igawa, H. *Chem. Commun.* **2002**, 390.

28 (a) Lautens, M.; Dockendorff, C.; Fagnou, K.; Malicki, A. *Org. Lett.* **2002**, *4*, 1311. (b) Lautens, M.; Fagnou, K.; Hiebert, S. *Acc. Chem. Res.* **2003**, *36*, 48.

29 Oi, S.; Moro, M.; Ono, S.; Inoue, Y. *Chem. Lett.* **1998**, 83.

30 Oi, S.; Moro, M.; Ito, H.; Honma, Y.; Miyano, S.; Inoue, Y. *Tetrahedron* **2002**, *58*, 91.

31 (a) Huang, T.-S.; Li, C.-J. *Org. Lett.* **2001**, *3*, 2037. (b) Venkatraman, S.; Meng, Y.; Li, C.-J. *Tetrahedron Lett.* **2001**, *42*, 4459.

32 Huang, T.; Meng, Y.; Venkatraman, S.; Wang, D.; Li, C.-J. *J. Am. Chem. Soc.* **2001**, *123*, 7451.

33 Mori, A.; Danda, Y.; Fujii, T.; Hirabayashi, K.; Osakada, K. *J. Am. Chem. Soc.* **2001**, *123*, 10774.

34 (a) Huang, T.-S.; Li, C.-J. J. *Chem. Commun.* **2001**, 2348. (b) Koike, T.; Du, X.; Mori, A.; Osakada, K. *Synlett* **2002**, 301. (c) Oi, S.; Honma, Y.; Inoue, Y. *Org. Lett.* **2002**, *4*, 667. (d) Murata, M.; Shimazaki, R.; Ishikura, M.; Watanabe, S.; Masuda, Y. *Synthesis* **2002**, 717.

35 Oi, S.; Taira, A.; Honma, Y.; Inoue, Y. *Org. Lett.* **2003**, *5*, 97.

36 Venkatraman, S.; Li, C.-J. *Tetrahedron Lett.* **2001**, *42*, 781.

37 Yoshida, K.; Ogasawara, M.; Hayashi, T. *J. Org. Chem.* **2003**, *68*, 1901.

38 Hayashi, T.; Tokunaga, N.; Yoshida, K.; Han, J.W. *J. Am. Chem. Soc.* **2002**, *124*, 12102.

39 Yoshida, K.; Ogasawara, M.; Hayashi, T. *J. Am. Chem. Soc.* **2002**, *124*, 10984.

40 Cauble, D.F.; Gipson, J.D.; Krische, M.J. *J. Am. Chem. Soc.* **2003**, *125*, 1110.

41 Yoshida, K.; Hayashi, T. *J. Am. Chem. Soc.* **2003**, *125*, 2872.

4
Recent Advances in Rhodium(I)-Catalyzed Asymmetric Olefin Isomerization and Hydroacylation Reactions

Gregory C. Fu

4.1
Rhodium(I)-Catalyzed Asymmetric Isomerization of Olefins

In light of the fact that this topic was reviewed in 1999 [1], in this chapter I shall simply highlight a few of the particularly noteworthy early achievements, and then describe recent progress, including efforts from our laboratory at MIT.

4.1.1
Allylic Amines

The commercialization in 1983 of the process illustrated in Eq. (1) is undoubtedly one of the most significant triumphs of asymmetric catalysis to date [2]. Takasago Chemical Company produced more than 22 000 tons of menthol by this route during the period 1983–1996, consuming only 125 kg of the chiral ligand in the process. Rh(I)/Tol-BINAP-catalyzed isomerizations of allylic amines are believed to proceed through the pathway outlined in Eq. (2) [3].

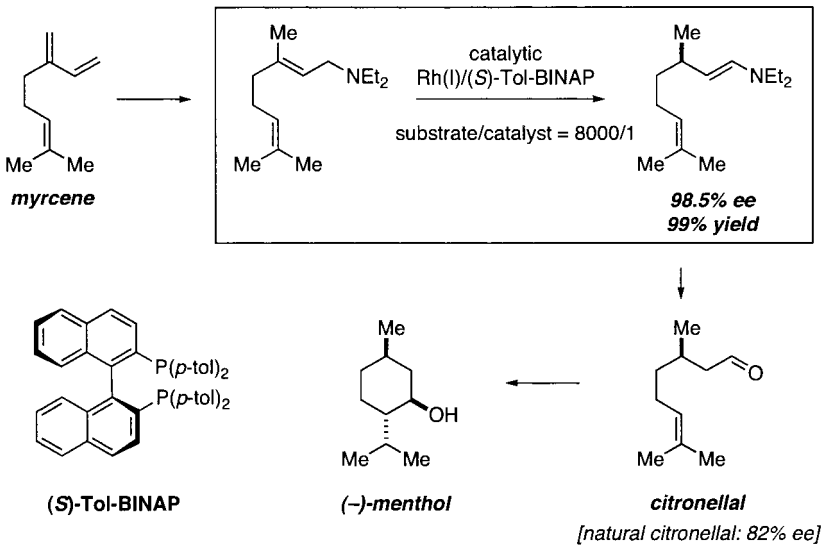

(1)

Modern Rhodium-Catalyzed Organic Reactions. Edited by P. Andrew Evans

ISBN: 3-527-30683-8

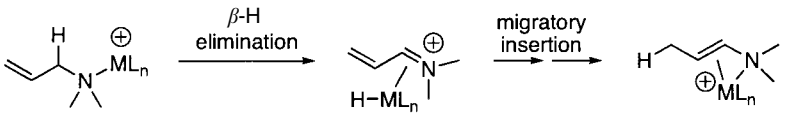

(2)

4.1.2
Allylic Ethers

The same level of success has not yet been achieved for isomerization reactions of allylic ethers. Nevertheless, several promising results (≥80% *ee*) have been described, all involving the desymmetrization of conformationally restricted cyclic compounds. For example, in 1995 Ogasawara reported that Rh(I)/BINAP catalyzes the isomerization of several tricyclic *meso*-1,4-enediol ethers (Eq. 3) with very good enantiomeric excess [4]. Lower stereoselectivity (<50% *ee*, favoring the *other* enantiomer) is observed for the isomerization of the corresponding diol (R=H). Through a labeling study, Ogasawara established that the reaction involves a net suprafacial 1,3-migration of hydrogen.

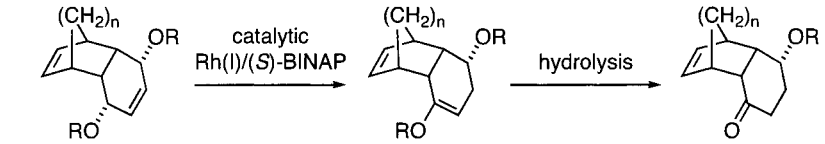

(3)

In 2000, Mathey described the use of the interesting bidentate phosphine BIPNOR in the rhodium-catalyzed asymmetric isomerization of the *meso*-diene illustrated in Eq. (4) [5]. Interestingly, the reaction proceeds with much lower enantioselectivity when BINAP is employed as the ligand (<40% *ee*).

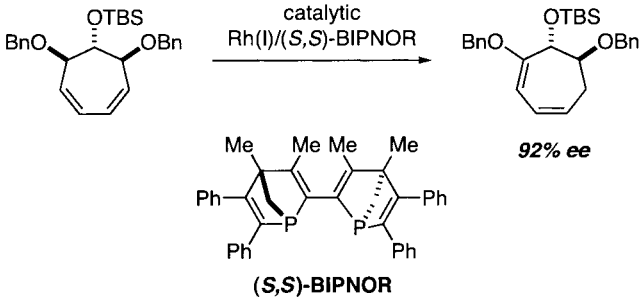

(4)

4.1.3 Allylic Alcohols

As for allylic ethers, there are relatively few reports of highly enantioselective rhodium-catalyzed isomerizations of allylic alcohols (for example, ≥80% *ee*). Relative to the other processes described above, reactions of allylic alcohols are more "atom economical" [6] since they obviate the need for a separate hydrolysis step (Eq. 5).

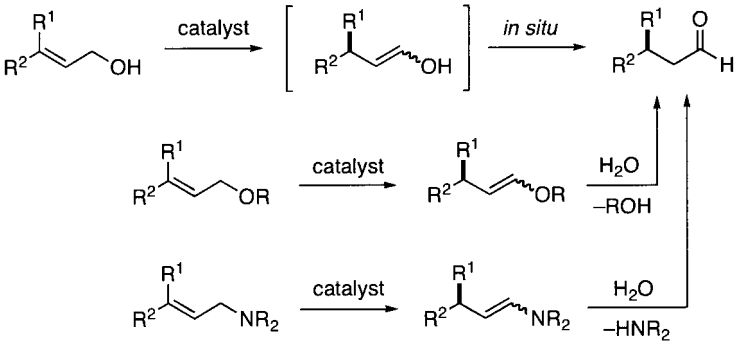

(5)

In 2000, we demonstrated that the planar-chiral phosphaferrocene PF–PPh_2 is a useful ligand for rhodium-catalyzed asymmetric isomerizations of several allylic alcohols, providing the first catalyst system that furnishes the target aldehyde in >60% *ee* (Eq. 6) [7]. It appears that, in order to obtain high enantiomeric excess (≥0% *ee*), the olefin should bear a relatively bulky substituent (for example, ^{i}Pr; Eq. 6).

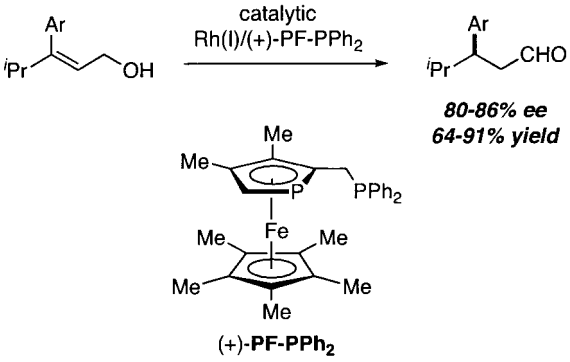

(6)

With Rh(I)/PF–PPh_2, reactions of *Z*-allylic alcohols generally afford higher enantioselectivity than the corresponding *E*-isomers. We applied this process to formal total syntheses of (–)-7-hydroxycalamenene and (–)-7-hydroxycalamenenal [8], two naturally occurring sesquiterpenes in the cadinene family (Eq. 7).

An X-ray crystal structure of [Rh(PF–PPh_2)(COD)]PF_6 reveals a distorted square-planar geometry around rhodium (Fig. 4.1). The Rh-phosphaferrocene bond length (2.25 Å) is shorter than the Rh-(tertiary phosphine) bond length (2.30 Å). We postulated that the strong π-accepting capacity of the phosphaferrocene [9] may lead to effective Rh → P back-bonding that decreases the conformational flexibility of the metal–

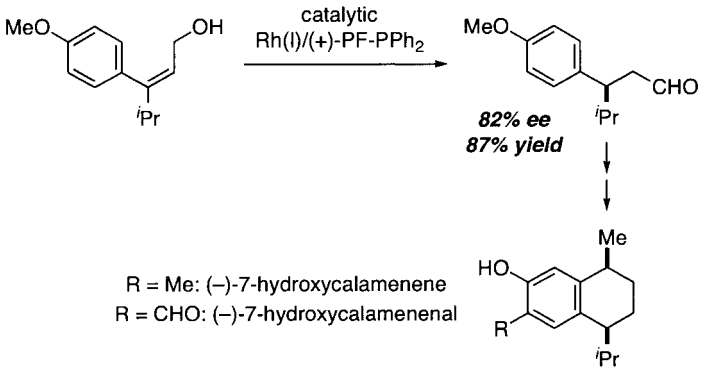

(7)

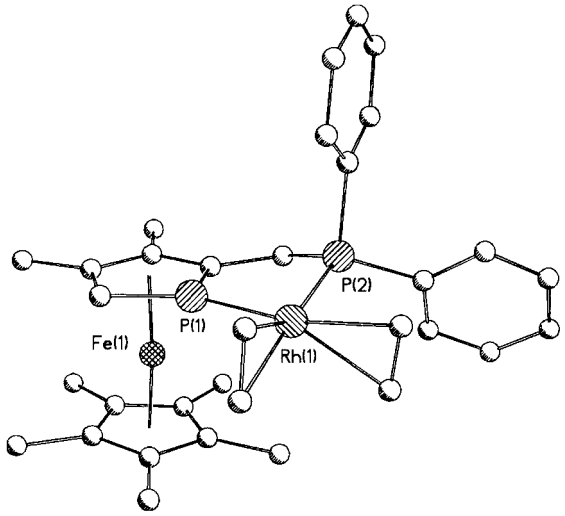

Fig. 4.1 X-ray crystal structure of $Rh(PF–PPh_2)(COD)PF_6$. The methylene groups of the COD, as well as the PF_6 counter-ion, have been omitted for clarity.

ligand complex. Furthermore, on the basis of the crystal structure, we speculated that the orientation of the phenyl groups may be important in defining the asymmetric environment of the catalyst.

We subsequently reported that altering the structure of the aryl groups of the tertiary phosphine can indeed produce a more effective catalyst [10]. Thus, replacement of Ph with *o*-Tol ($PF–PPh_2 \rightarrow PF–P(o\text{-Tol})_2$) furnishes a ligand that provides improved enantioselectivity and yield for the rhodium-catalyzed isomerization of *E*-allylic alcohols (Tab. 4.1).

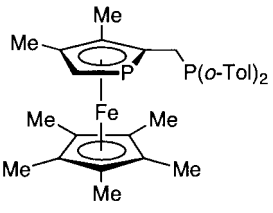

(+)-PF-P(*o*-Tol)$_2$

Tab. 4.1 Rh(I)/PF–P(*o*-Tol)$_2$-catalyzed isomerization of *E*-allylic alcohols.

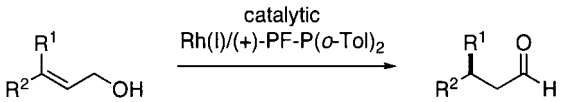

Entry	*Allylic alcohol*	*Yield (%)* [a]	*ee (%)* [a]
1	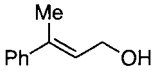	91 (82)	75 (56)
2	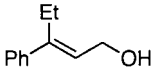	96	76
3	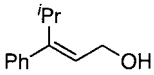	98 (81)	92 (78)
4	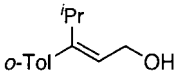	86 (8)	92 (87)
5	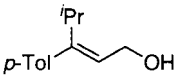	90 (85)	91 (64)
6	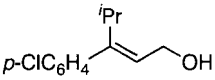	86 (79)	92 (73)

a) The values in parentheses are for Rh(I)/(+)-PF-PPh$_2$.

A range of allylic alcohols are isomerized with good enantioselection by Rh(I)/PF–P(*o*-Tol)$_2$ (Tab. 4.1). As the steric demand of the alkyl group on the olefin increases, the enantioselectivity increases (entries 1–3). In contrast, the stereoselectivity does not appear to be particularly sensitive to either steric or electronic variations in the aryl substituent (entries 3–6).

Interestingly, whereas rhodium-catalyzed isomerizations of *Z*-allylic alcohols generally afford higher enantioselectivities than the corresponding *E*-isomers when PF–PPh$_2$ is employed as the ligand, the opposite trend is observed for PF–P(*o*-Tol)$_2$. Thus, Rh(I)/PF–P(*o*-Tol)$_2$ furnishes relatively modest enantioselectivities for isomerizations of *Z*-allylic alcohols (compare Tab. 4.2 with Tab. 4.1).

Olefins that lack an aromatic substituent can also be isomerized by Rh(I)/PF–P(*o*-Tol)$_2$ with good enantioselectivity (Eq. 8). Interestingly, for this class of substrates the reactions of *E*- and *Z*-allylic alcohols proceed with similar enantioselection.

Tab. 4.2 Rh(I)/PF–P(*o*-Tol)$_2$-catalyzed isomerization of *Z*-allylic alcohols.

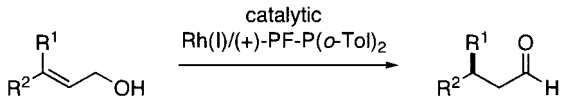

Entry	*Allylic alcohol*	*Yield (%)*	*ee (%)*
1	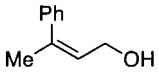	80	59
2	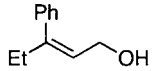	78	57
3	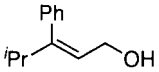	82	82
4	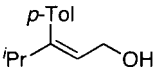	83	77
5	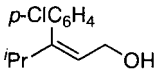	83	85
6	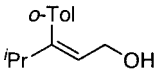	60	81
7	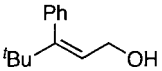	90	90

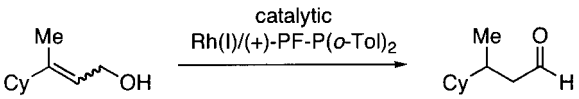

(8)

Z-isomer: ***80% ee*** *(87% yield)* ⇨ *R*-product
E-isomer: ***74% ee*** *(94% yield)* ⇨ *S*-product

For Rh(I)/BINAP-catalyzed isomerizations of allylic amines, the mechanistic scheme outlined in Eq. (2) has been proposed. The available data are consistent with the notion that Rh(I)/PF–P(*o*-Tol)$_2$-catalyzed isomerizations of allylic alcohols follow a related pathway [11]. For example, the only deuterium-containing product of the reaction depicted in Eq. (9) is the 1,3-dideuterated aldehyde, which establishes that the isomerization involves a clean intramolecular 1,3-migration. The data illustrated in Eqs. (10) and (11) reveal that the catalyst selectively abstracts one of the "enantiotopic" hydrogens/deuteriums alpha to the hydroxyl group.

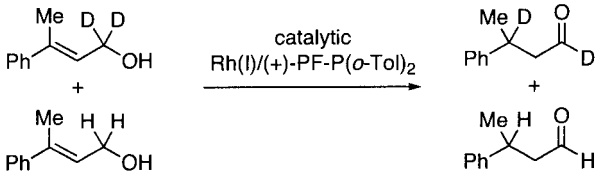

(9)

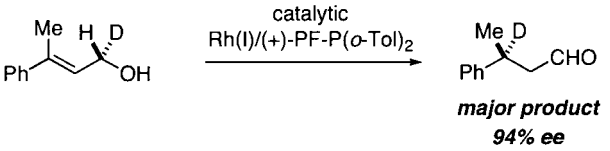

(10)

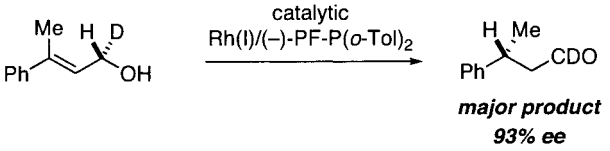

(11)

4.1.4 Summary

One of the landmark achievements in the area of enantioselective catalysis has been the development of a large-scale commercial application of the Rh(I)/BINAP-catalyzed asymmetric isomerization of allylic amines to enamines. Unfortunately, methods for the isomerization of other families of olefins have not yet reached a comparable level of sophistication. However, since the early 1990s promising catalyst systems have been described for enantioselective isomerizations of allylic alcohols and allylic ethers. In view of the utility of catalytic asymmetric olefin isomerization reactions, I have no doubt that the coming years will witness additional exciting progress in the development of highly effective catalysts for these and related substrates.

4.2 Rhodium(I)-Catalyzed Asymmetric Hydroacylation of Olefins and Alkynes with Aldehydes

The most significant progress that has been described to date in the area of rhodium-catalyzed asymmetric hydroacylation of olefins/alkynes with aldehydes has involved intramolecular processes that generate either cyclopentanones or cyclopentenones. Fig. 4.2 illustrates two of the more likely mechanisms for these ring-forming reactions [12, 13].

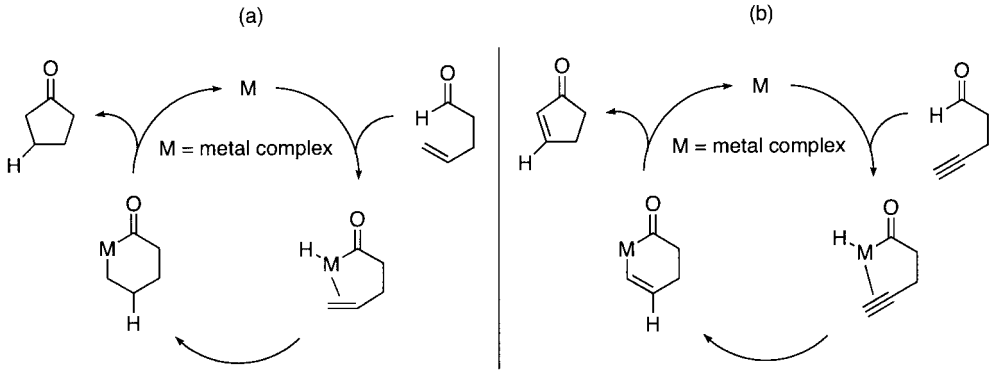

Fig. 4.2 Possible mechanisms for the formation of: (a) cyclopentanones from 4-alkenals; (b) cyclopentenones from 4-alkynals.

4.2.1 Cyclopentanones

In 1992, Sakai provided the first examples of highly enantioselective (≥80% *ee*) hydroacylations of olefins with aldehydes, the Rh(I)/BINAP-catalyzed cyclization of 4-alkenals (Eq. 12) [14]. Additional work from the same laboratory established that certain 4-aryl-substituted substrates also undergo ring formation with good enantioselectivity [15].

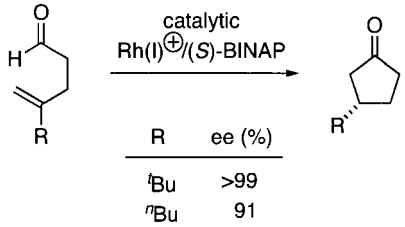

(12)

Two years later, Bosnich described an extensive study of asymmetric rhodium-catalyzed intramolecular hydroacylation reactions [16]. Like Sakai, Bosnich found that Rh(I)/BINAP is an unusually effective catalyst for this process, furnishing excellent enantioselectivity for a range of substrates (Eq. 13). Bosnich also reported that, if the R substituent is a relatively unhindered alkyl (for example, Me) or an aromatic group, lower (<80% *ee*) enantioselectivity is observed.

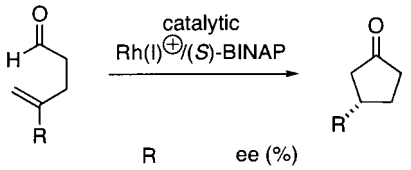

R	ee (%)
^{t}Bu	>99
TMS	>99
CO_2Et	>99
COPh	94
cyclopentyl	81
Me	78

(13)

In 1997, Bosnich discovered that Me-DUPHOS serves as a highly effective ligand for rhodium-catalyzed hydroacylations, particularly when R is a medium or small alkyl substituent (Eq. 14) [17]. Interestingly, in contrast to BINAP (Eq. 13), Me-DUPHOS furnishes lower stereoselection when the R group is a *tert*-butyl or TMS group (44 and 64% *ee* respectively).

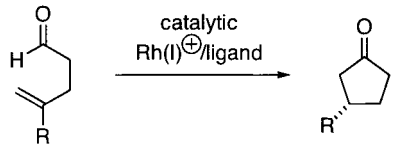

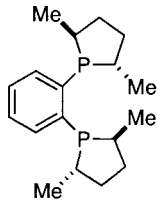

(*S*,*S*)-Me-DUPHOS

	ee (%)	
R	(*S*)-BINAP	(*S*,*S*)-Me-DUPHOS
^{i}Pr	60	94
cyclopentyl	81	94
Me	78	94
Bn	–	94

(14)

In addition to the asymmetric hydroacylations described above, highly efficient desymmetrizations of 4-alkenals have been achieved. For example, in 1993 Sakai reported that Rh(I)/BINAP very capably differentiates between the enantiotopic olefins of the diene illustrated in Eq. (15), furnishing the target cyclopentanone with excellent enantioselectivity (>99%) [18]. Intriguingly, a neutral Rh(I)/BINAP complex, RhCl(BINAP), preferentially generates the *cis*-3,4-disubstituted cyclopentanone, whereas a cationic Rh(I)/BINAP complex, [Rh(BINAP)]ClO_4, produces the *trans*-isomer with excellent stereoselection. Thus, by appropriate choice of neutral or cationic rhodium complex and (*S*)- or (*R*)-BINAP, each of the four possible isomers can be generated with high diastereo- and enantioselectivity.

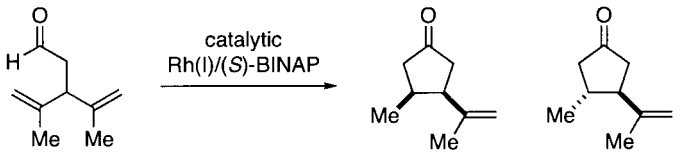

neutral Rh(I) catalyst	97 ***(>99% ee)***	:	3
cationic Rh(I) catalyst	4	:	96 ***(>99% ee)***

(15)

In 2000, Tanaka, Sakai, and Suemune expanded the scope of these desymmetrization reactions to more highly substituted substrates (Eq. 16) [19]. The high selectivity of Rh(I)/BINAP for addition to one of the enantiotopic olefins leads to the generation of adjacent quaternary and tertiary stereocenters with excellent stereoselection. Unfortunately, for these more sterically demanding substrates, neutral Rh(I)/BINAP complexes furnish a poor yield of the desired cyclopentanone.

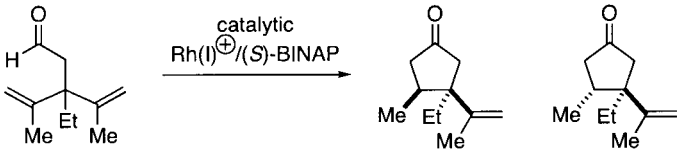

3 : 97 ***(92% ee)***

(16)

Finally, in 2001 Tanaka and Suemune described kinetic resolutions and parallel kinetic resolutions of dienals through the use of cationic and neutral Rh(I)/BINAP complexes, respectively (Eqs. 17 and 18) [20–22].

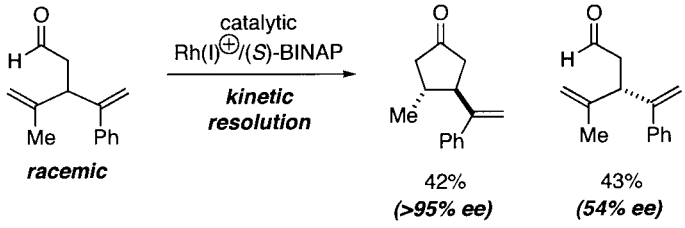

42% ***(>95% ee)*** 43% ***(54% ee)***

(17)

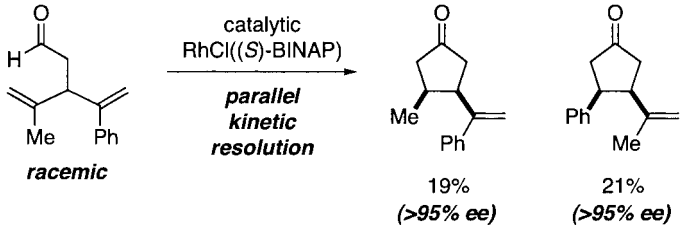

19% ***(>95% ee)*** 21% ***(>95% ee)***

(18)

4.2.2
Cyclopentenones

In 2002, we reported that Rh(I)/^{i}Pr-DUPHOS catalyzes the kinetic resolution of 3-methoxy-4-alkynals with good selectivity factors (selectivity factor, s=[rate of fast-reacting enantiomer]/[rate of slow-reacting enantiomer]) (Eq. 19) [23]. Interestingly, the presence of the methoxy group is essential for achieving effective resolution – presumably, it organizes the metal–substrate complex by serving as a ligand for rhodium.

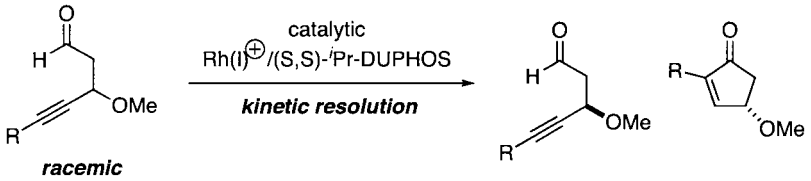

(19)

R	% ee of unreacted aldehyde (% conversion)	s
Ph	93 (56)	22
o-Tol	90 (56)	19
Me_2C=CH	93 (53)	41

If the 3-position is a quaternary stereocenter, then Rh(I)/Tol-BINAP is the catalyst of choice for the hydroacylation process. With this catalyst, both kinetic resolutions (Eq. 20) and desymmetrization reactions (Eq. 21) may be accomplished.

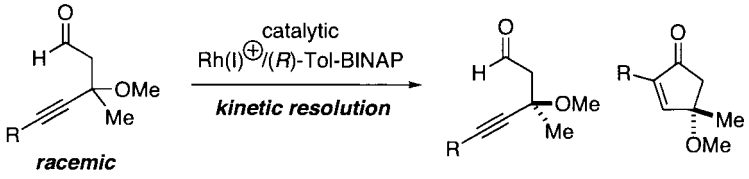

(20)

R	% ee of unreacted aldehyde (% conversion)	s
Ph	99 (60)	22
1-cyclohexenyl	99 (63)	18

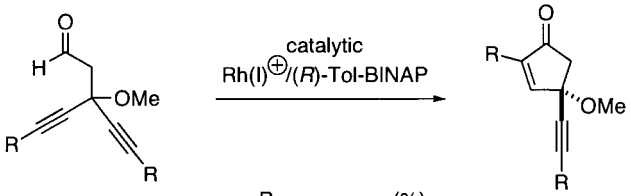

R	ee (%)
$^{n}C_5H_{11}$	92
Cy	95
$(CH_2)_3Cl$	91
CH_2OMe	82

(21)

If the 3-position is a tertiary, rather than a quaternary, stereocenter, Rh(I)/Tol-BINAP effects an intriguing parallel kinetic resolution – thus, one enantiomer of the substrate selectively undergoes hydroacylation to generate a cyclobutanone, while the other enantiomer is transformed into a cyclopentanone (Eq. 22) [24]. This observation is quite interesting, given the limited number of examples of parallel kinetic resolutions, particularly catalytic processes that involve carbon–carbon bond formation, and catalytic methods for the construction of cyclobutanones.

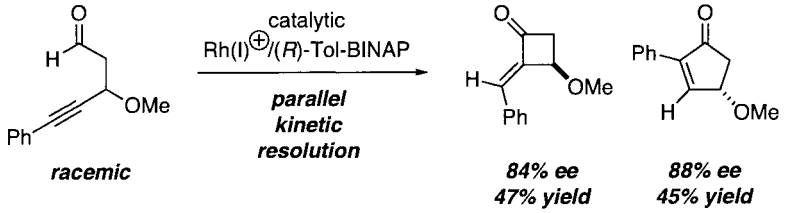

(22)

4.2.3
Summary

Since the early 1990s, considerable progress has been achieved in the development of catalytic enantioselective intramolecular hydroacylation reactions of alkenes/alkynes that generate five-membered rings. Nonetheless, the vast majority of interesting hydroacylation reactions has not yet proven susceptible to effective asymmetric catalysis. This deficiency represents an exciting opportunity for future investigations in this area.

4.3 References

1 Akutagawa, S. In *Comprehensive Asymmetric Catalysis*; Jacobsen, E.N., Pfaltz, A., Yamamoto, H., Eds.; Springer: New York, **1999**; Chap. 23.

2 Akutagawa, S. In *Comprehensive Asymmetric Catalysis*; Jacobsen, E.N., Pfaltz, A., Yamamoto, H., Eds.; Springer: New York, **1999**; Chap. 41.4.

3 Inoue, S.-I.; Takaya, H.; Tani, K.; Otsuka, S.; Sato, T.; Noyori, R. *J. Am. Chem. Soc.* **1990**, *112*, 4897; see also Reference 1.

4 Hiroya, K.; Kurihara, Y.; Ogasawara, K. *Angew. Chem. Int. Ed. Engl.* **1995**, *34*, 2287.

5 Faitg, T.; Souli, J.; Lallemand, J.-Y.; Mercier, F.; Mathey, F. *Tetrahedron* **2000**, *56*, 101.

6 For a review, see: Trost, B.M. *Angew. Chem. Int. Ed. Engl.* **1995**, *34*, 259.

7 Tanaka, K.; Qiao, S.; Tobisu, M.; Lo, M.M.-C.; Fu, G.C. *J. Am. Chem. Soc.* **2000**, *122*, 9870.

8 The previously reported nonracemic syntheses are based on chiral-pool starting materials and are not stereoselective: (a) Takaki, K.; Ohsugi, M.; Okada, M.; Yasumura, M.; Negoro, K. *J. Chem. Soc., Perkin Trans. I* **1984**, 741. (b) Takaki, K.; Okada, M.; Yamada, M.; Negoro, K. *J. Org. Chem.* **1982**, *47*, 1200.

9 For leading references, see: Deschamps, B.; Ricard, L.; Mathey, F. *J. Organomet. Chem.* **1997**, *548*, 17.

10 Tanaka, K.; Fu, G. C. *J. Org. Chem.* **2001**, *66*, 8177.

11 For a study of rhodium-catalyzed isomerizations of allylic alcohols to enols, see: Bergens, S.H.; Bosnich, B. *J. Am. Chem. Soc.* **1991**, *113*, 958.

12 For mechanistic studies of the rhodium-catalyzed cyclization of 4-alkenals to cyclopentanones, see: (a) Campbell, R.E., Jr.; Miller, R.G. *J. Organomet. Chem.* **1980**, *186*, C27. Campbell, R.E., Jr.; Lochow, C.F.; Vora, K.P.; Miller, R. G. *J. Am. Chem. Soc.* **1980**, *102*, 5824. (b) Fairlie, D.P.; Bosnich, B. *Organometallics* **1988**, *7*, 946.

13 For preliminary mechanistic studies of the rhodium-catalyzed cyclization of 4-alkynals to cyclopentenones, see: Tanaka, K.; Fu, G.C. *J. Am. Chem. Soc.* **2001**, *123*, 11492.

14 Wu, X.-M.; Funakoshi, K.; Sakai, K. *Tetrahedron Lett.* **1992**, *33*, 6331.

15 Fujio, M.; Tanaka, M.; Wu, X.-M.; Funakoshi, K.; Sakai, K.; Suemune, H. *Chem. Lett.* **1998**, 881.

16 Barnhart, R.W.; Wang, X.; Noheda, P.; Bergens, S.H.; Whelan, J.; Bosnich, B. *J. Am. Chem. Soc.* **1994**, *116*, 1821.

17 (a) Barnhart, R.W.; McMorran, D.A.; Bosnich, B. *Inorg. Chim. Acta.* **1997**, *263*, 1. (b) Barnhart, R.W.; McMorran, D.A.; Bosnich, B. *Chem. Commun.* **1997**, 589.

18 Wu, X.-M.; Funakoshi, K.; Sakai, K. *Tetrahedron Lett.* **1993**, *34*, 5927.

19 Tanaka, M.; Imai, M.; Fujio, M.; Sakamoto, E.; Takahashi, M.; Eto-Kato, Y.; Wu, X.M.; Funakoshi, K.; Sakai, K.; Suemune, H. *J. Org. Chem.* **2000**, *65*, 5806. See also: Takahashi, M.; Tanaka, M.; Sakamoto, E.; Imai, M.; Matsui, A.; Funakoshi, K.; Sakai, K.; Suemune, H. *Tetrahedron Lett.* **2000**, *41*, 7879. Tanaka, M.; Takahashi, M.; Sakamoto, E.; Imai, M.; Matsui, A.; Fujio, M.; Funakoshi, K.; Sakai, K.; Suemune, H. *Tetrahedron* **2001**, *57*, 1197. Takahashi, M.; Tanaka, M.; Sakamoto, E.; Imai, M.; Funakoshi, K.; Sakai, K.; Suemune, H. *Chem. Pharm. Bull.* **2000**, *48*, 1822.

20 Imai, M.; Tanaka, M.; Suemune, H. *Tetrahedron* **2001**, *57*, 1205.

21 For reviews of kinetic resolution, see: (a) Kagan, H.B.; Fiaud, J.C. *Top. Stereochem.* **1988**, *18*, 249. (b) Hoveyda, A.H.; Didiuk, M.T. *Curr. Org. Chem.* **1998**, *2*, 489. (c) Keith, J.M.; Larrow, J.F.; Jacobsen, E.N. *Adv. Synth. Catal.* **2001**, *1*, 5.

22 For reviews of parallel kinetic resolution, see: (a) Dehli, J.R.; Gotor, V. *Chem. Soc. Rev.* **2002**, *31*, 365. (b) Eames, J. *Angew. Chem. Int. Ed. Engl.* **2000**, *39*, 885.

23 Tanaka, K.; Fu, G.C. *J. Am. Chem. Soc.* **2002**, *124*, 10296.

24 Tanaka, K.; Fu, G.C. *J. Am. Chem. Soc.* **2003**, *125*, 8078.

5
Stereoselective Rhodium(I)-Catalyzed Hydroformylation and Silylformylation Reactions and their Application to Organic Synthesis

James L. Leighton

5.1
Introduction

This chapter will address the development of selected stereoselective rhodium-catalyzed carbonylation reactions and their application to problems in organic synthesis. It is in no way intended to serve as a comprehensive review of rhodium-catalyzed carbonylation chemistry. The focus, rather, is on the development of stereoselective rhodium-catalyzed carbonylation reactions for use in the synthesis of stereochemically complex natural products, particularly polyketides.

Polyketides are a large and diverse family of natural products characterized by a wide array of biological activities, stereochemical complexity, and often by one or more (1,3,5 . . .)-polyol chains derived from the biosynthetic coupling of acetate and propionate units. Without question, various aldol reactions and related processes have played, and continue to play, a dominant role in the development of methods for the synthesis of such structures. An alternative approach may be envisioned wherein the key disconnection is between the carbonyl carbon and the carbon alpha to the carbonyl group (Scheme 5.1). This simple disconnection can be regarded as a hydroformylation of enol ether-type substrates or, alternatively, as an oxidative carbonylation of simple alkenes. In principle, an important advantage that accrues from this approach is that the products are protected β-hydroxyalkanals, ready for further chain extension without the need for either protecting-group manipulations or oxidation-state adjustments.

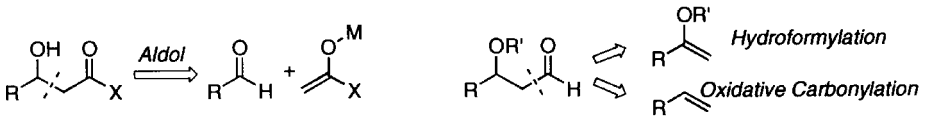

Scheme 5.1

5.2
Hydroformylation

Rhodium(I)-catalyzed hydroformylation is a powerful reaction that combines three simple reactants – an alkene, H_2, and CO – to form a carbon–carbon bond and provide valuable aldehyde products. Depending on the substitution pattern of the alkene sub-

Modern Rhodium-Catalyzed Organic Reactions. Edited by P. Andrew Evans

ISBN: 3-527-30683-8

strate, one or two stereocenters may be created in the hydroformylation reaction. All aspects of this venerable reaction have been extensively reviewed; including stereoselective variants [1]. This section will thus focus primarily on the development of strategies and methods to control diastereoselectivity in hydroformylation reactions of chiral alkene substrates with relevance to natural product synthesis.

5.2.1 Diastereoselective Hydroformylation of Chiral Alkene Substrates

Rhodium(I)-catalyzed hydroformylation of cyclic enol acetals **1** leads to acetal-protected *syn*-3,5-dihydroxyalkanals **2** with extraordinarily high levels (>50:1) of diastereoselectivity (Scheme 5.2) [2]. The diastereoselectivity cannot be ascribed to any obvious steric bias, and serves as a powerful demonstration that the hydroformylation reaction may be subject to exquisite stereoelectronic control. Indeed, while the addition of a *pseudo*-axial methyl group to the acetal carbon (as in acetonide **3**) has a deleterious effect on the rate of the reaction, the *syn*-diastereomer **4** is still produced selectively, in what is surely a *contra-steric* hydroformylation reaction.

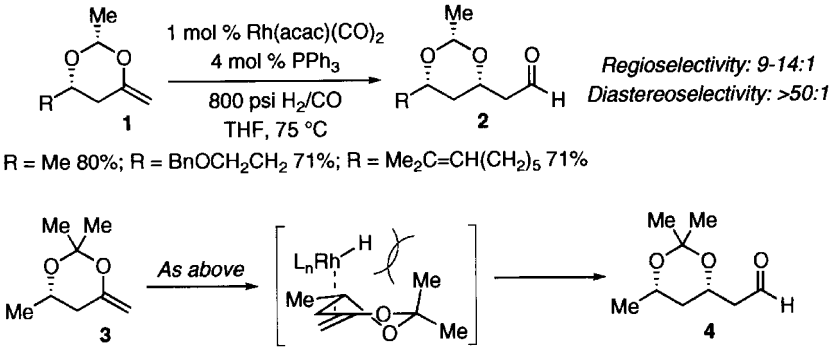

Scheme 5.2

Stereochemical diversity may be accessed in these reactions by careful control over the conformation of the substrate enol acetals. Thus, alkene **5** is converted to aldehyde **6** (along with ~20% of isomerization product **5a**), and **7** to **8**, both with moderate to good diatereoselectivity (Scheme 5.3) [3]. In both cases, the *tert*-butyl group controls the conformation of the substrate and thereby the diastereoselectivity. Conversely, alkene **9** undergoes isomerization to **9a** exclusively. Evidence that the isomerization proceeds by way of reversed regioselectivity in the rhodium-hydride alkene insertion step followed by *β*-hydride elimination was provided. This fact, combined with reasonable conformational predictions with respect to substrates **5** (mostly half-chair, some twist-boat), **7** (exclusively half-chair), and **9** (exclusively twist-boat), led to the conclusion that the regiochemistry in this enol acetal substrate family is controlled completely by the equilibrium between the half-chair (selective for aldehyde product) and twist-boat (selective for alkene isomerization) conformations. That such a subtle change in the steric and electronic properties of the alkene can completely reverse the regioselectivity of rhodium-hydride alkene insertion again belies the unusual control elements that could

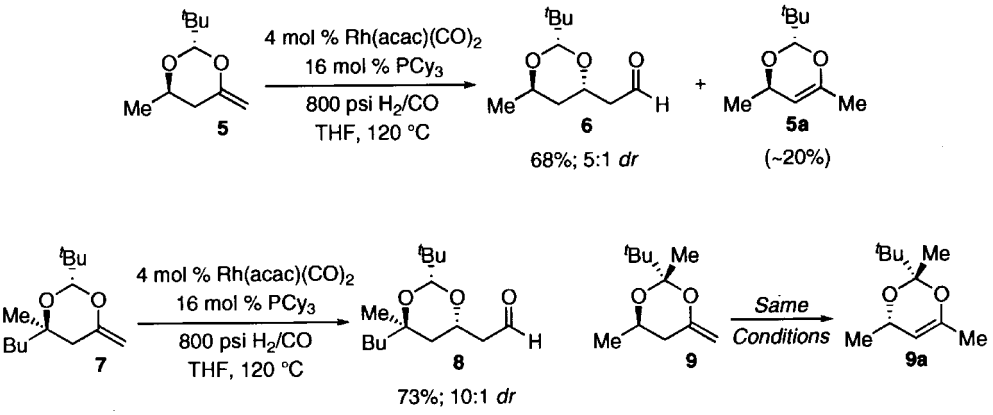

Scheme 5.3

in principle be harnessed in the development of new regio- and stereoselective hydroformylation reactions.

Recently, and for the first time, it has been shown that high levels of diastereocontrol may be realized in the rhodium(I)-catalyzed hydroformylation of acyclic alkenes. In one example, acetals **10** afford aldehydes **11** with superior diastereoselectivity (Scheme 5.4) [4]. This result was attributed to a strong conformational bias in the substrate, as shown. Evidence for this conformational bias was secured by 2D-NOESY NMR experiments and MM3 force field calculations. When the experiment was repeated with R = H, the diastereoselectivity was lost, lending further support to the model.

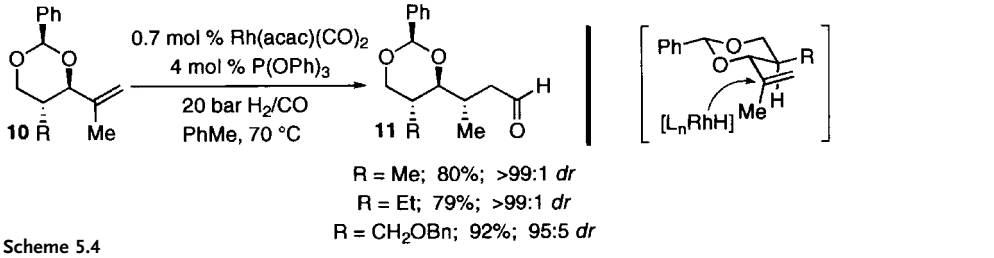

Scheme 5.4

An equally intriguing report concerned the rhodium(I)-catalyzed hydroformylation of *C*-glycoside alkenes **12** (Scheme 5.5) [5]. As depicted, aldehydes **13** were formed with excellent diastereoselectivity. It was proposed that the diastereoselectivity is due to a strong conformational bias favoring the depicted alkene conformation.

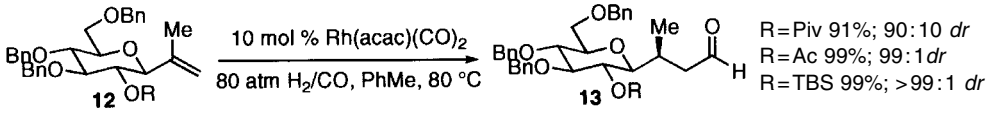

Scheme 5.5

5.2.2
Hydroformylation of Organomercurials

The approach to polyketide synthesis described in Scheme 5.2 requires the relatively nontrivial synthesis of acid-sensitive enol acetals **1**. An alternative can be envisioned wherein hemiacetals derived from homoallylic alcohols and aldehydes undergo diastereoselective oxymercuration. Transmetallation to rhodium could then intercept the hydroformylation pathway and lead to formylation to produce aldehydes **2**. This proposal has been reduced to practice as shown in Scheme 5.6. For example, $Yb(OTf)_3$-catalyzed oxymercuration of the illustrated homoallylic alcohol provided organomercurial **14** [6]. Rhodium(I)-catalyzed hydroformylation of **14** proved successful, giving aldehyde **15**, but was highly dependent on the use of exactly 0.5 equiv of DABCO as an additive [7]. Several other amines and diamines were examined with variation of the stoichiometry and none proved nearly as effective in promoting the reaction. This remarkable effect has been ascribed to the facilitation of transmetallation by formation of a 2:1 R–HgCl:DABCO complex and the unique properties of DABCO when both amines are complexed/protonated.

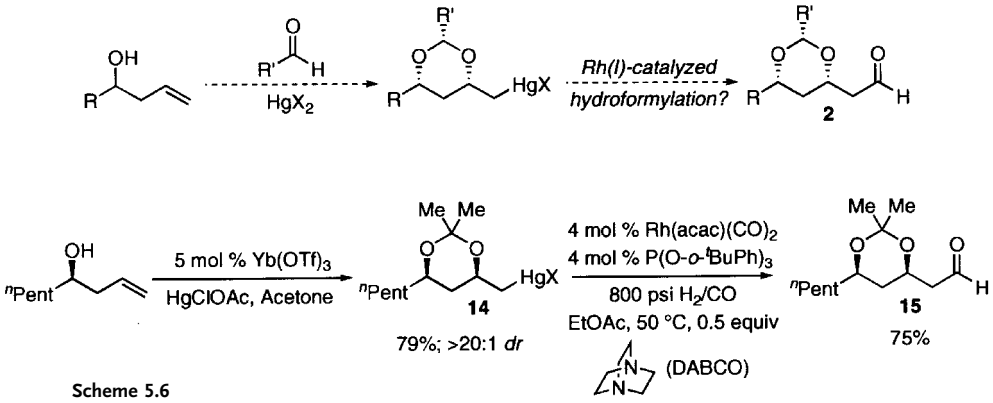

Scheme 5.6

5.2.3
Directed Diastereo- and Regioselective Hydroformylation

Substrate-directed reactions have for many years served as an excellent strategy for regio- and stereochemical control [8]. Many examples of directed rhodium(I)-catalyzed hydroformylation are now known that typically involve attachment of a removable phosphine/phosphite directing group to the substrate. Pioneering work by Burke and Jackson established the validity of this approach, and these studies have been recently reviewed [1]. More recently, Breit and co-workers have systematically developed a new strategy for acyclic diastereoselection in the rhodium(I)-catalyzed hydroformylation of methallylic alcohols. Commercially available 2-(diphenylphosphino)benzoic acid is used to esterify methallylic alcohols to give substrates **16**. Hydroformylation of esters **16** proceeds with good to excellent diastereoselectivity, giving aldehydes **17** (Scheme 5.7) [9].

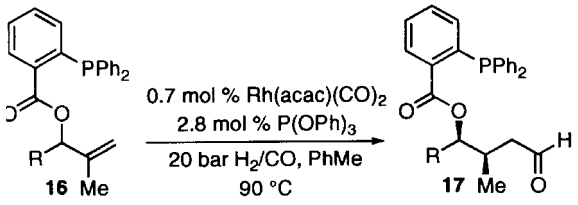

R	yield	*dr*
Ph	99	92:8
^{i}Pr	98	96:4
Cy	81	95:5
CO_2Me	80	90:10
(*E*)-EtCH=C(Me)	55	92:8

Scheme 5.7

A control experiment wherein the phosphorous was replaced with a CH group proceeded with no diastereoselectivity and at a significantly reduced rate, thus providing convincing support for the proposed catalyst-directing role of the triarylphosphine group.

Homomethallylic alcohols have also been established to be viable substrates. Thus, a series of esters **18** were prepared and subjected to rhodium(I)-catalyzed hydroformylation. As illustrated, aldehydes **19** were isolated with very good levels of diastereoselectivity (Scheme 5.8) [10].

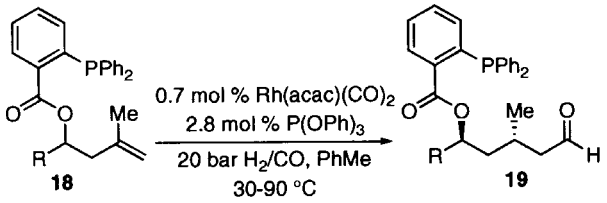

R	yield	*dr*
Ph	72	90:10
^{i}Pr	99	87:13
Cy	90	91:9
Hex	81	90:10
(*E*)-EtCH=C(Me)	85	90:10

Scheme 5.8

Directing groups may be used to reverse intrinsic regioselectivity in addition to controlling diastereoselectivity. In this vein it will be noted that regioselective hydroformylation of allylic alcohols favoring the normally disfavored *branched* aldehyde product

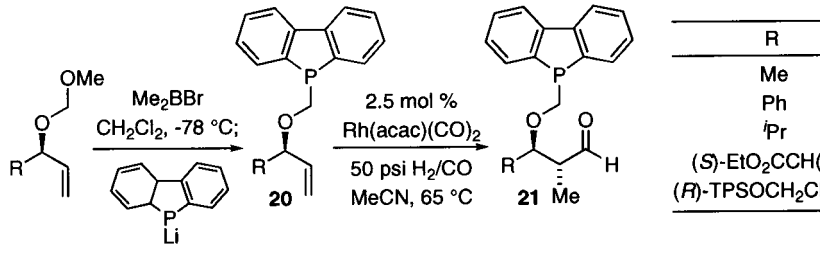

R	*dr*	yield(%)
Me	81:19	92
Ph	86:14	96
^{i}Pr	94:6	94
(*S*)-$EtO_2CCH(Me)$	90:10	98
(*R*)-$TPSOCH_2CH(Me)$	93:7	87

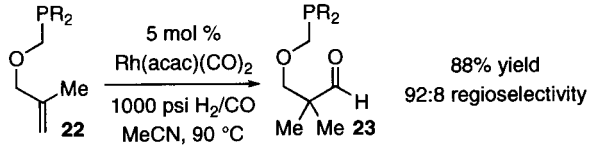

Scheme 5.9

would amount to a new approach to catalytic propionate aldol synthesis. This has recently been reduced to practice through the use of a new phosphine-directing group. MOM ethers of allylic alcohols are transformed into dibenzophosphol-5-ylmethyl ethers **20**. Rhodium(I)-catalyzed hydroformylation is carried out under very mild conditions, with no added phosphine or phosphite ligands, to provide aldehydes **21** both regiospecifically and with good to excellent diastereoselectivity (Scheme 5.9) [11]. Remarkably, the regiochemical control is maintained with 1,1-dialkylsubstituted alkene **22**, providing quaternary aldehyde **23** with 92:8 regioselectivity.

5.2.4 Applications in Natural Product Synthesis

In one remarkable example, Burke and Cobb employed a directed hydroformylation to functionalize regio- and diastereoselectively alkene **24** to provide aldehyde **25** as the major product of a 7.7:0.3:1:1 mixture in 69% yield (Scheme 5.10) [12]. When the ester-directing group was replaced with a *tert*-butyldimethylsilyl group, a nonselective and inefficient reaction resulted. Aldehyde **25** was converted to the target (+)-phyllanthocin in just a few additional steps.

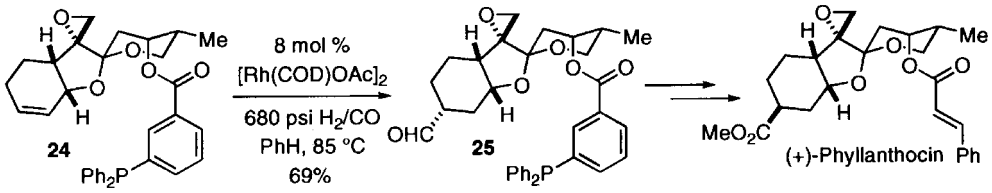

Scheme 5.10

Common substructural motifs in polyketide natural products are six-membered ring lactones, lactols, and tetrahydropyrans. It was recognized by Wuts and co-workers that hydroformylation of readily available homoallylic alcohols would provide a direct and efficient entry into these ring systems. Such an approach was employed in a synthesis of Prelog–Djerassi lactone (Scheme 5.11) [13].

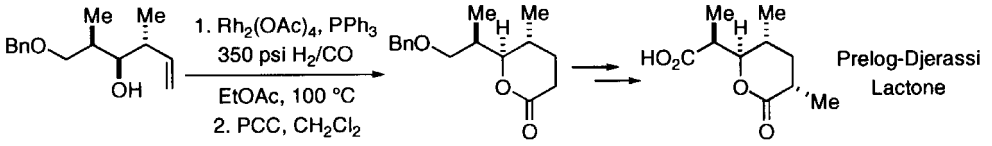

Scheme 5.11

Buchwald has employed hydroformylation as a key step in formal syntheses of indolizidine and pyrrolizidine natural products (Scheme 5.12) [14]. Highly regioselective hydroformylation of **26** to aldehyde **27** using the BIPHEPHOS ligand proceeded in 83% yield. One-pot deprotection and Strecker reaction then delivered aminonitrile **28**, which is a known intermediate in a synthesis of indolizidine alkaloid 209D [15]. In a related approach to the ant venom pyrrolizidine alkaloid 3-heptyl-5-methylpyrrolizidine, **29** was converted to

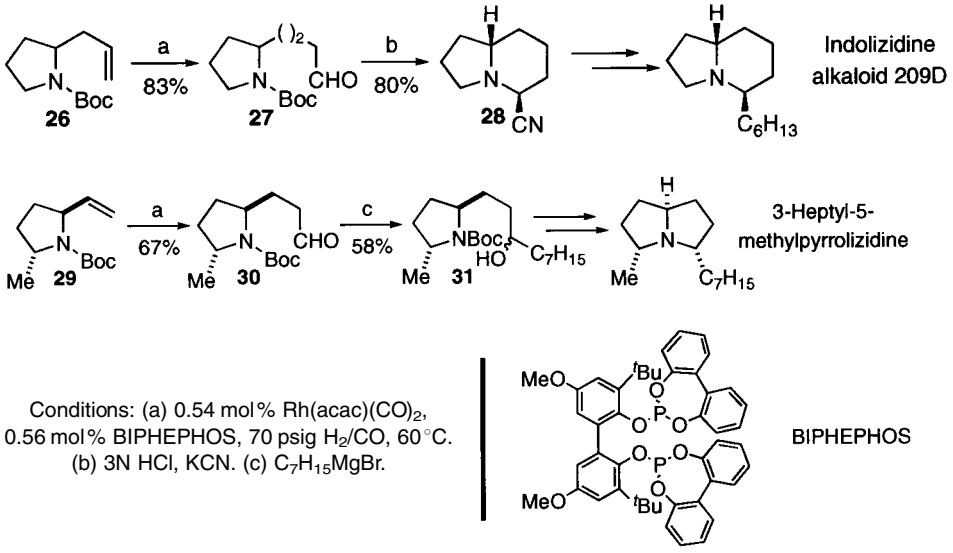

Scheme 5.12

aldehyde **30** by hydroformylation, and subsequent Grignard addition provided alcohols **31**. A switch in protecting groups, from the *tert*-butyloxy (BOC) to the benzyloxycarbamate (Cbz), provided a known intermediate from a previous synthesis [16].

Ojima and coworkers have developed a similar approach to the synthesis of piperidine and related ring systems, which they describe as cyclohydrocarbonylation. In this approach, carbamate-protected allylglycines (for example, **32**) are subjected to rhodium(I)-catalyzed hydroformylation in an alcohol solvent (Scheme 5.13) [17]. 6-Alkoxypipecolates **33** are isolated in good yield and were shown to be amenable to further stereoselective transformations. This methodology has recently been expanded to include fully intramolecular variants that can form two rings in a single reaction. Thus, alkenes **34** are subjected to the cyclohydrocarbonylation conditions to provide azabicyclo[4.4.0]alkane amino acids **35** which can serve as conformationally restricted dipeptide surrogates and β-turn mimetics [18].

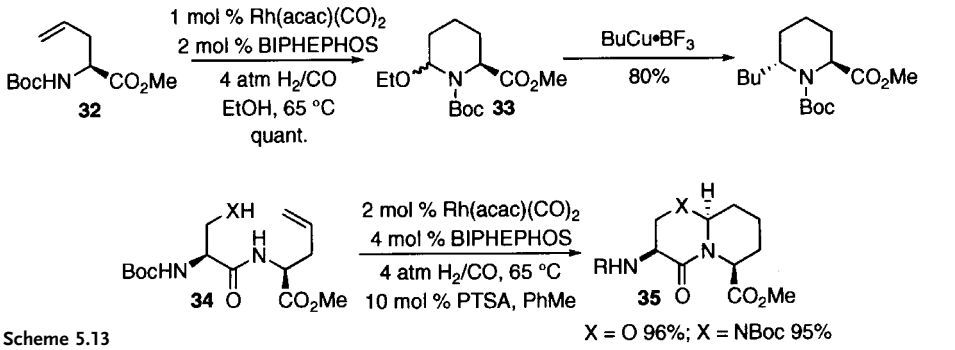

Scheme 5.13

Hydroformylation reactions have been shown to be amenable to use in tandem or domino reaction sequences. In one elegant example, alkene **36** was subjected to rhodium(I)-catalyzed hydroformylation, and the resulting aldehyde underwent smooth intramolecular allylboration (Scheme 5.14) [19]. This produced a new terminal alkene which underwent a second hydroformylation to provide, after workup,lactols **37** in 80% yield and with excellent diastereoselectivity.

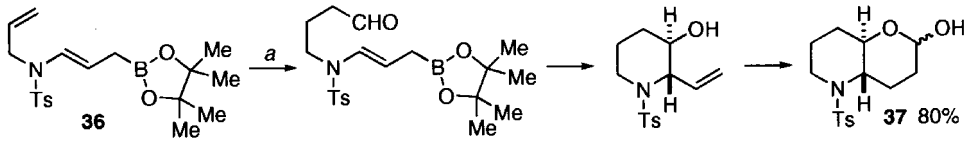

Conditions: (a) 1 mol % Rh(acac)(CO_2), 2 mol % BIPHEPHOS, 5 bar H_2/CO, 60 °C

Scheme 5.14

Wittig ylides have been shown to be compatible with hydroformylation conditions, and may thus be used in a domino reaction sequence such as from **16a** to **38** (Scheme 5.15) [20]. When an α-unsubstituted ylide is employed, the resulting alkene undergoes *in-situ* rhodium-catalyzed hydrogenation in a triple tandem reaction to convert **10a** to **39**. Several other examples were reported establishing the generality of this domino reaction sequence.

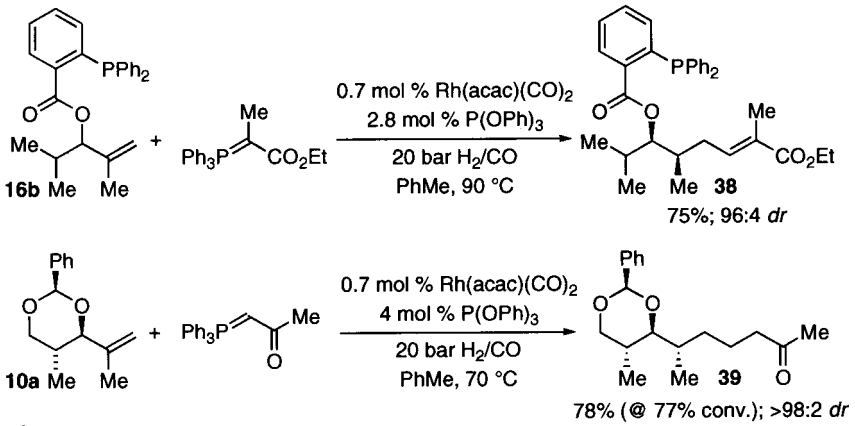

Scheme 5.15

Aldehyde **11a**, produced by diastereoselective hydroformylation (R = Me; Scheme 5.4), has been employed in the synthesis of polyketide fragment **40**, a key building block for the synthesis of bafilomycin A_1 (Scheme 5.16) [21].

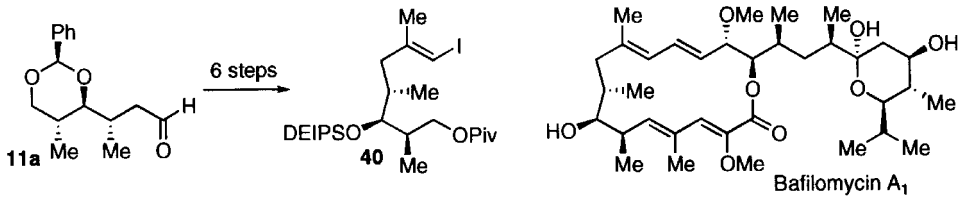

Scheme 5.16

The $Yb(OTf)_3$-catalyzed oxymercuration and hydroformylation of the resulting organomercurials, described in Scheme 5.6, may be effectively combined in a one-pot procedure leading to a highly efficient polyol synthesis. This methodology has been employed in a six-step synthesis of *Tolypothrix* pentaether, employing asymmetric allylboration technology between iterations of the carbonylation methodology (Scheme 5.17) [22].

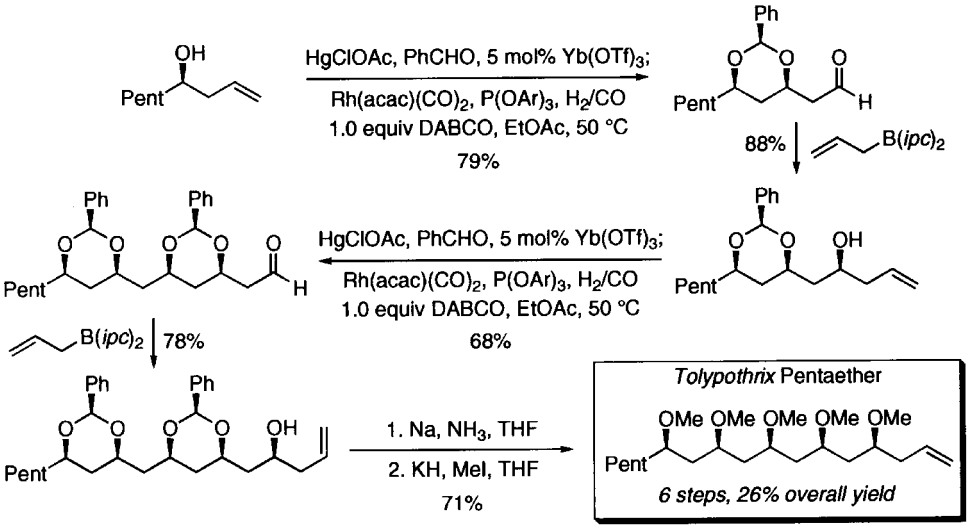

Scheme 5.17

This methodology also figured prominently in a formal synthesis of the oxopolyene macrolide mycoticin A. Homoallylic alcohol **41** was subjected to the $Yb(OTf)_3$-catalyzed oxymercuration and hydroformylation sequence described above, and after transformation of the resulting aldehyde into a methyl ketone, **42** was isolated in good overall yield (Scheme 5.18) [23]. Likewise, homoallylic alcohol **43** was transformed into aldehyde **44** in just two steps. Fragments **42** and **44** were combined to produce completed polyol fragment **45** in just four additional steps. This constitutes a formal synthesis, as **45** has been converted into mycoticin A [24].

The first total synthesis of the marine macrolide leucascandrolide A relied upon the use of two key hydroformylation reactions [25]. $Yb(OTf)_3$-catalyzed oxymercuration of homoallylic alcohol **46** provided organomercurial **47**, which was hydroformylated to give

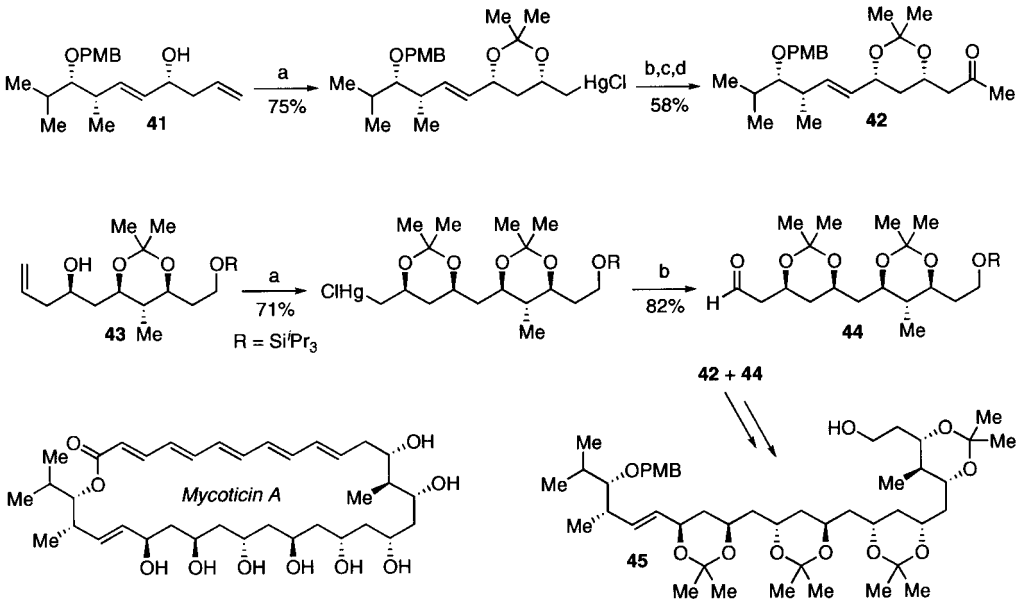

Conditions: (a) 10 mol % $Yb(OTf)_3$, HgClOAc, acetone. (b) 6 mol % $Rh(acac)(CO)_2$, 6 mol % $P(OAr)_3$, 0.5 equiv DABCO, 800 psi H_2/CO, EtOAc, 50 °C. (c) MeMgBr, Et_2O. (d) Dess-Martin periodinane, CH_2Cl_2.

Scheme 5.18

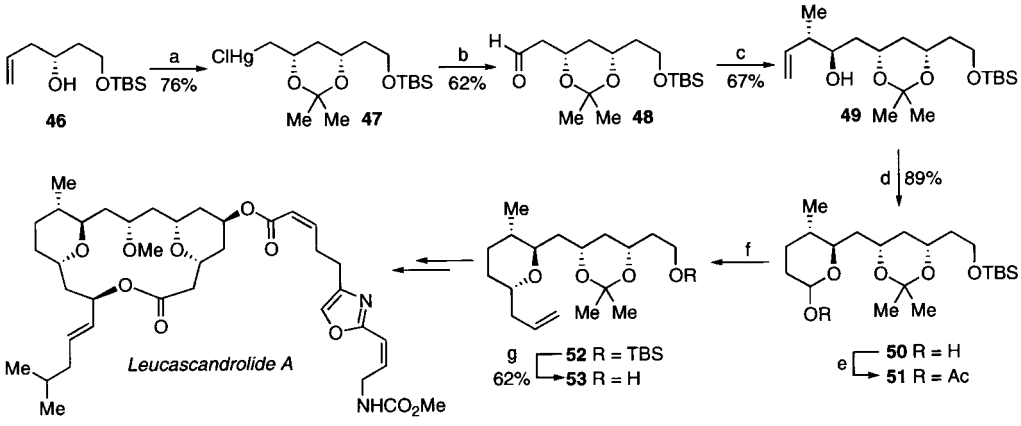

Conditions: (a) HgClOAc, acetone, 5 mol % $Yb(OTf)_3$, 0 °C to RT; (b) 4 mol % $Rh(acac)(CO)_2$, 4 mol % P(O-*o*-^{t}BuPh)$_3$, 0.5 equiv DABCO, 800 psi 1:1 CO/H_2, EtOAc, 50 °C; (c) (*E*)-crotyl-(-)-diisopinocampheylborane, BF_3•OEt_2, THF, -78 °C; NaOH, H_2O_2; (d) 2 mol % $Rh(acac)(CO)_2$, 8 mol % PPh_3, 400 psi 1:1 CO/H_2, THF, 50 °C; (e) Ac_2O, DMAP, pyridine, CH_2Cl_2; (f) $H_2C{=}CHCH_2SiMe_3$, $Ti(O^iPr)_2Cl_2$, CH_2Cl_2, -78 °C; (g) ^{n}Bu$_4$NF, THF.

Scheme 5.19

aldehyde **48** (Scheme 5.19). Following asymmetric crotylboration, homoallylic alcohol **49** was subjected to regioselective hydroformylation to produce lactol **50** in 89% yield. Following acetylation to give **51**, diastereoselective allylation produced tetrahydropyran **52**, which upon deprotection gave alcohol **53** in 62% overall yield from **50**. This hydroformylation–crotylation–hydroformylation–allylation sequence allows the efficient synthesis of a significant fragment used in the first total synthesis of leucascandrolide A.

5.3 Silylformylation

Silylformylation, defined as the addition of R_3Si– and –CHO across various types of bonds using a silane R_3SiH, CO, and a transition metal catalyst, was discovered by Murai and co-workers, who developed the $Co_2(CO)_8$-catalyzed silylformylation of aldehydes, epoxides, and cyclic ethers [26]. More recently, as described in detail in Section 5.3.1, below, alkynes and alkenes have been successfully developed as silylformylation substrates. These reactions represent a powerful variation on hydroformylation, in that a C–Si bond is produced instead of a C–H bond. Given that C–Si groups are subject to, among other reactions, oxidation to C–OH groups, silylformylation could represent an oxidative carbonylation of the type described in Scheme 5.1.

5.3.1 Silylformylation of Alkynes and Alkenes

The development of the first alkyne silylformylation reaction was reported in 1989 by Matsuda [27]. Alkynes were treated with Me_2PhSiH and Et_3N with 1 mol% $Rh_4(CO)_{12}$ under CO pressure to produce *β*-silyl-*α*,*β*-unsaturated aldehydes (Scheme 5.20). A second report from Ojima detailed the development of rhodium–cobalt mixed metal clusters as effective catalysts for alkyne silylformylation [28]. Shortly thereafter, Doyle reported that rhodium(II) perfluorobutyrate was a highly efficient and selective catalyst for alkyne silylformylation under remarkably mild reaction conditions (0 °C, 1 atm CO) [29]. In all these reports, terminal alkynes react regiospecifically with attachment of the silane to the unsubstituted end of the alkyne. The reaction is often (but not always) stereospecific, producing the *cis*-product preferentially.

In an effort to access the normally disfavored regioisomer and thereby expand the scope of the reaction, two groups developed intramolecular versions of the reaction nearly simultaneously [30, 31]. In one study, the hydrosilane was tethered to the alkyne by way of an alkyl chain, and in the other a silyl ether attachment strategy was employed (Scheme 5.21). In both cases, the result was regio- and stereospecific generation of the illustrated *β*-silyl-*α*,*β*-unsaturated aldehyde products even when internal alkynes were employed. It has recently been demonstrated as well that 1,6-heptadiynes can be desymmetrized by way of an intramolecular silylformylation (**56** to **57**) [32]. Intramolecular alkyne silylformylation has also been demonstrated by tethering the hydrosilane to aminoalkynes (**58** to **59**) [33]. As with the other intramolecular reactions, the products are generated regio- and stereospecifically.

Alkenes had been identified as potentially important substrates for silylformylation, but initial attempts using $Co_2(CO)_8$ as the catalyst produced instead the silyl enol ether

Matsuda:

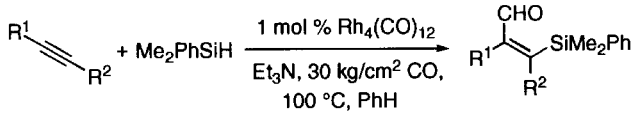

R^1	R^2	*Z:E*	yield(%)
Me	H	80:20	99
Cy	H	100:0	96
Ph	H	88:12	89
Me	Me	100:0	93
Ph	Ph	95:5	90
Me	CO_2Me	100:0	67

Ojima:

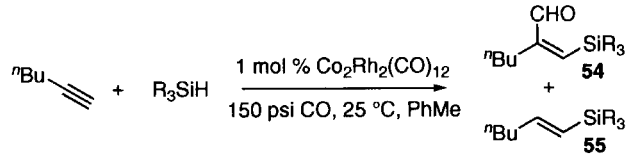

R_3SiH	**54:55**	yield(%)[a]
$PhMe_2SiH$	100:0	92
$EtMe_2SiH$	100:0	84
Me_3SiH	93:7	80
$(MeO)_3SiH$	38:62	95

[a]Yield determined by GLC analysis based on 1-hexyne consumed.

Doyle:

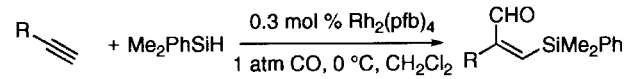

R	*Z:E*	yield(%)
p-Tol	38:1	84
6-MeO-2-Npth	11:1	95
^{n}Hex	14:1	81
$MeOCH_2$	14:1	87[a]

[a]Et_3SiH used instead of Me_2PhSiH.

Scheme 5.20

of the hydroformylated alkene [34]. In rendering the reaction intramolecular by tethering the hydrosilane to homoallylic alcohols, Leighton and Chapman developed the first examples of alkene silylformylation (Scheme 5.22) [35]. The aldehyde products proved unstable to chromatography, so for the purposes of purification and characterization, they were reduced and acetylated. In all cases the *cis*-diastereomer was the major product formed, with moderate to good selectivity.

5.3.2
Tandem Silylformylation/Allylsilylation

One of the important advantages of the intramolecular alkene silylformylation reaction as an aldol equivalent is that the products are masked 3,5-dihydroxyalkanals, and therefore that no manipulations are required prior to iteration of the process by aldehyde allylation to set up the next intramolecular silylformylation. Given that allylsilanes are well-known aldehyde allylation reagents, intramolecular silylformylation employing a diallylhydrosilane would, in principle, allow for the possibility of a tandem silylformylation/allylsilylation reaction. This has been reduced to practice: the diallylsilyl ethers **60** were subjected to the previously developed silylformylation conditions and the unpurified reaction mixtures were subjected to the Tamao oxidation [36] to provide triols **61**

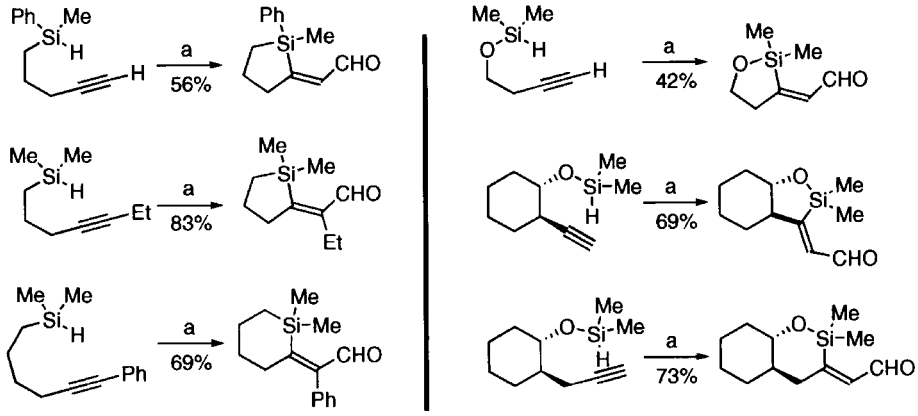

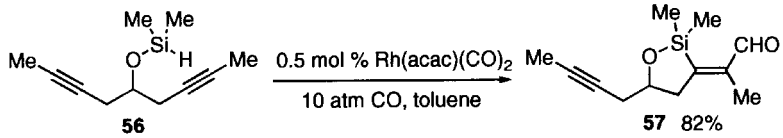

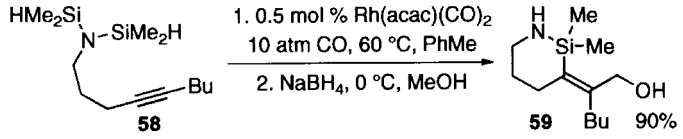

Scheme 5.21

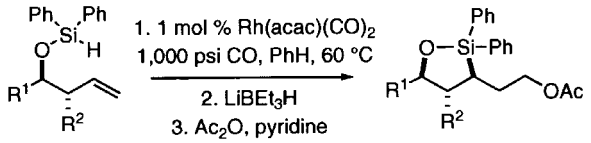

R^1	R^2	*dr*	yield (%)
Me	H	4.5 : 1	67
$H_2C{=}CHCH_2$	H	4 : 1	64
*i*Pr	H	6 : 1	79
*i*Pr	Me	10 : 1	71

Scheme 5.22

(Scheme 5.23) [37]. This unusual spontaneous aldehyde allylsilylation in the absence of a Lewis acid promoter/catalyst was attributed to strain-release Lewis acidity.

Alkynes are viable substrates for the tandem intramolecular silylformylation/allylsilylation reaction. The 1,5-diastereoselectivity is reversed from that observed with alkene substrates, as the 1,5-*anti* product predominates (Scheme 5.24) [38]. Synthetic flexibility was demonstrated in that either of two carbon–silicon cleavage procedures may be employed. Protodesilylation with tetra-*n*-butylammonium fluoride followed by acetylation (determi-

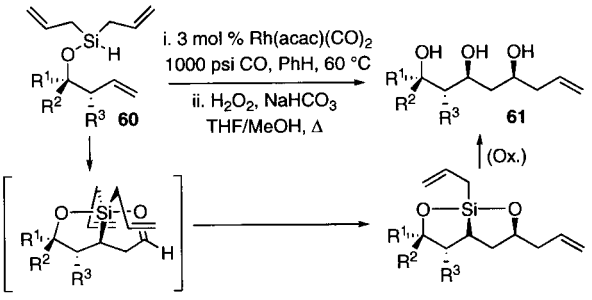

R^1	R^2	R^3	dr^a	yield(%)^b
H	^{i}Pr	H	77:23	59
H	$TBSO(CH_2)_2$	H	71:29	45
H	$H_2C{=}CHCH_2$	H	69:31	50
H	^{i}Pr	Me	92:8	59
Me	Me	H	93:7	65

[a] *Syn,Syn* triol:Σ all other diastereomers.
[b] Isolated yield of purified major product.

Scheme 5.23

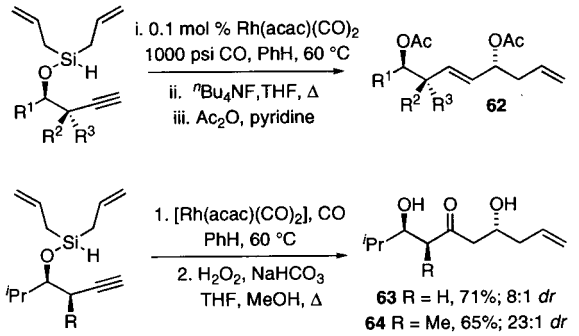

R^1	R^2	R^3	dr^a	yield(%)^b
^{i}Pr	H	H	8:1	83
Ph	H	H	7:1	83
^{t}Bu	H	H	10:1	66
^{i}Pr	Me	H	23:1	70
^{i}Pr	H	Me	7:1	70

[a] 1,5-*anti*:1,5-*syn*. [b] Isolated yield of the purified mixture of diastereomers.

Scheme 5.24

nation of diastereoselectivity was best carried out on the derived diacetates) gives diacetates **62** and the oxidative procedure gives ketodiols **63** and **64**. Evidence was secured that the diastereoselectivity is the result of preferential transfer of one of the two diastereotopic allyl groups, and that the minor diastereomer arises by transfer of the other allyl group.

The use of crotylsilanes instead of allylsilanes in both the alkene and alkyne tandem reactions allows the creation of a third and a second stereocenter respectively (Scheme 5.25) [39]. These reactions allow extremely rapid and efficient access to stereochemically complex polyketide chains, as demonstrated by the five-step conversion of alcohol **65** to triol **66** in 31% overall yield. The conversion of **67** to both **68** and **69** establishes the scope of this chemistry to allow access to different structural and stereochemical motifs.

5.3.3
Applications in Natural Product Synthesis

Silylformylation and hydroformylation reactions figured prominently in Ojima's approach to isoretronecanol and trachelanthamidine [40]. Thus, silylformylation of alkyne **70** proceeded smoothly to produce aldehyde **71** (Scheme 5.26). Reduction and protodesilylation provided allylic alcohol **72**, which was protected to give **73**. Hydroformylation in the presence of $HC(OEt)_3$ led to a 2:1 mixture of **74** and **75**. Deprotection and amide and amidal reduction then provided the target compounds.

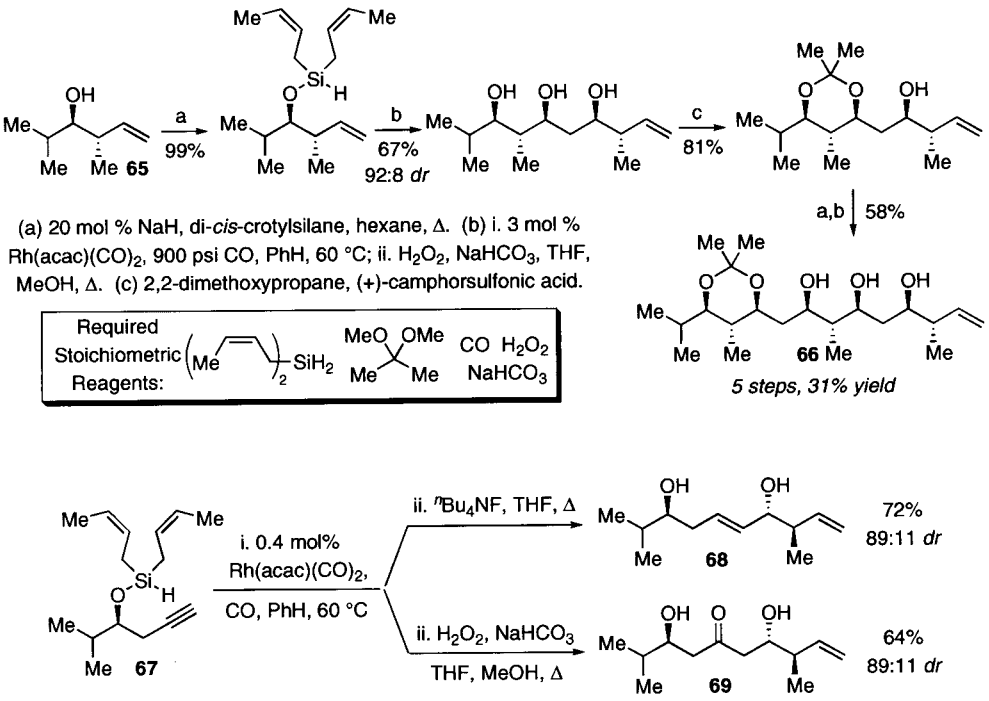

Scheme 5.25

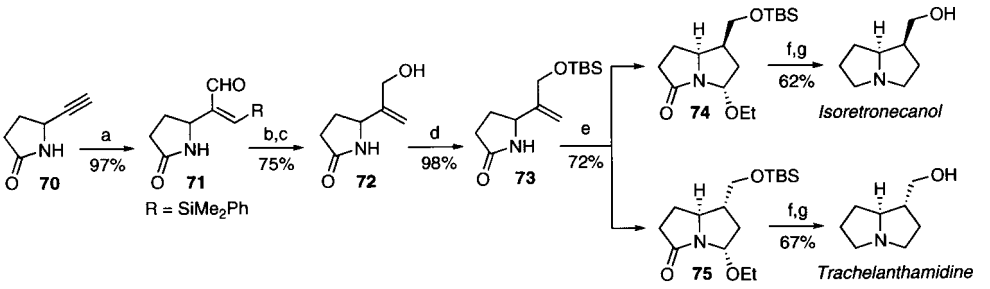

Conditions: (a) 0.8 mol% $Rh(acac)(CO)_2$, $HSiMe_2Ph$, 300 psi CO, toluene. (b) $NaBH_4$, $EtOH/H_2O$. (c) TsOH, MeCN, H_2O, Δ. (d) TBSCl, imidazole, DMF, 40 °C. (e) 1 mol% $HRh(CO)(PPh_3)_3$, 1/1 CCO/H_2, $HC(OEt)_3$ 100 °C. (f) $^nBU_4NF$, THF. (g) $LiAlH_4$, THF, Δ.

Scheme 5.26

The tandem silylformylation/allylsilylation reaction is particularly well suited to the synthesis of skipped polyol motifs such as are found in the oxopolyene macrolides. The synthesis of protected triol **43** (an intermediate in the mycoticin A formal synthesis described above; see Scheme 5.18) relied on an application of this methodology. Thus, homoallylic alcohol **76** was transformed into triol **77** in 55% overall yield and >10:1 diastereoselectivity (Scheme 5.27) [23]. Selective protection of the triol to give **43**

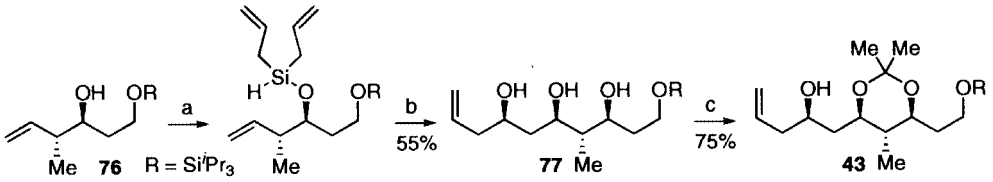

Conditions: (a) ^{n}BuLi, $HSiCl_3$, allylMgBr, THF, -78 °C. (b) i. 3 mol % $Rh(acac)(CO)_2$, 1000 psi CO, PhH, 60 °C; ii. H_2O_2, $NaHCO_3$, THF, MeOH, Δ. (c) 10 mol % (+)-Camphorsulfonic acid, acetone.

Scheme 5.27

was accomplished under equilibrating conditions to give a 7:1 mixture of acetonides from which **43** could be isolated in 75% yield.

A fragment of the marine macrolide dolabelide A has been synthesized employing the tandem silylformylation/allylsilylation of alkynes as a key step (Scheme 5.28) [41]. The transformation of **67** to **68** (see Scheme 5.25) is clearly reminiscent of the highlighted portion of dolabelide A with two important distinctions: (1) the methodology provides 1,5-*anti*-diols, whereas 1,5-*syn* selectivity was required for dolabelide A; and (2) modification of the methodology to allow for the synthesis of the trisubstituted alkene was required. To address the first problem, a catalytic asymmetric silane alcoholysis reaction was developed [42]. Thus, monocrotylsilane **78** was synthesized with 4:1 diastereoselectivity. Stereospecific transfer of chirality from silicon to carbon occurred in the tandem silylformylation/crotylsilylation reaction and, upon quenching with

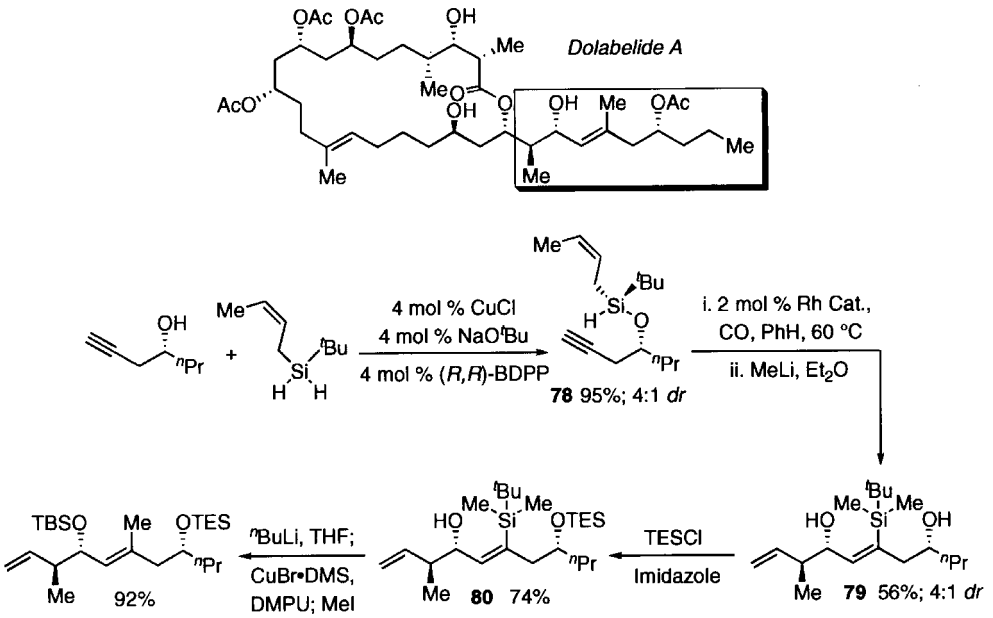

Scheme 5.28

methyllithium, 1,5-*syn*-diol **79** was obtained as a 4:1 mixture of diastereomers in 56% yield. Selective protection of the less hindered alcohol as a triethylsilyl (TES) ether led to alcohol **80** in 74% yield as a single diastereomer following separation by chromatography. A Brook-like 1,4-carbon (sp^2) to oxygen silyl migration using the protocol reported by Takeda then delivered the target fragment in 92% yield.

5.4 Conclusion

The vast majority of the work described in this chapter was reported since 1995. Rhodium(I)-catalyzed hydroformylation and silylformylation reactions have only very recently been adapted and developed for use in the efficient synthesis of stereochemically complex natural products. In addition, the recent development of tandem reactions that take advantage of the direct production of aldehydes in these carbonylation reactions have only begun to demonstrate the versatility of this chemistry. Rhodium(I)-catalyzed hydroformylation and silylformylation, venerable reactions that have primarily been associated with organometallic chemistry, must now be considered important tools for natural product synthesis. The continued development of these methodologies for that purpose may be expected.

5.5 References

1 Breit, B.; Seiche, W. *Synthesis* **2001**, 1. A comprehensive list of reviews on other aspects of hydroformylation (refs. 4–35) is provided therein.

2 Leighton, J.L.; O'Neil, D.N. *J. Am. Chem. Soc.* **1997**, *119*, 11118.

3 Sarraf, S.T.; Leighton, J.L. *Tetrahedron Lett.* **1998**, *39*, 6423.

4 Breit, B.; Zahn, S.K. *Tetrahedron Lett.* **1998**, *39*, 1901.

5 Takahashi, T.; Ebata, S.; Yamada, H. *Synlett* **1998**, 381.

6 Dreher, S.D.; Hornberger, K.R.; Sarraf, S.T.; Leighton, J.L. *Org. Lett.* **2000**, *2*, 3197.

7 Sarraf, S.T.; Leighton, J.L. *Org. Lett.* **2000**, *2*, 3205.

8 Hoveyda, A.H.; Evans, D.A.; Fu, G.C. *Chem. Rev.* **1993**, *93*, 1307.

9 (a) Breit, B. *Angew. Chem. Int. Ed. Engl.* **1996**, *35*, 2835. (b) Breit, B. *Liebigs Ann./Recueil* **1997**, 1841.

10 (a) Breit, B. *Chem. Commun.* **1997**, 591. (b) Breit, B. *Eur. J. Org. Chem.* **1998**, *3*, 1123.

11 Krauss, I.J.; Wang, C.C.-Y.; Leighton, J.L. *J. Am. Chem. Soc.* **2001**, *123*, 11514.

12 Burke, S.D.; Cobb, J.E. *Tetrahedron Lett.* **1986**, *27*, 4237.

13 Wuts, P.G.M.; Obrzut, M.L.; Thompson, P.A. *Tetrahedron Lett.* **1984**, *25*, 4051.

14 Cuny, G.D.; Buchwald, S.L. *Synlett* **1995**, 519.

15 Polniaszek, R.P.; Belmont, S.E. *J. Org. Chem.* **1990**, *55*, 4688.

16 Provot, O.; Celerier, J.P.; Petit, H.; Lhommet, G. *J. Org. Chem.* **1992**, *57*, 2163.

17 (a) Ojima, I.; Tzamarioudaki, M.; Eguchi, M. *J. Org. Chem.* **1995**, *60*, 7078. (b) Ojima, I.; Iula, D.M.; Tzamarioudaki, M. *Tetrahedron Lett.* **1998**, *39*, 4599.

18 Mizutani, N.; Chiou, W.-H.; Ojima, I. *Org. Lett.* **2002**, *4*, 4575.

19 (a) Hoffmann, R.W.; Brückner, D.; Gerusz, V.J. *Heterocycles* **2000**, *52*, 121. (b) Hoffmann, R.W.; Brückner, D. *New J. Chem.* **2001**, *25*, 369.

20 Breit, B.; Zahn, S.K. *Angew. Chem. Int. Ed.* **1999**, *38*, 969.

21 Breit, B.; Zahn, S.K. *J. Org. Chem.* **2001**, *66*, 4870.

22 Sarraf, S.T. Ph.D. Thesis, Columbia University, **2001**.

23 Dreher, S.D.; Leighton, J.L. *J. Am. Chem. Soc.* **2001**, *123*, 341.

24 Poss, C.S.; Rychnovsky, S.D.; Schreiber, S.L. *J. Am. Chem. Soc.* **1993**, *115*, 3360.

25 Hornberger, K.R.; Hamblett, C.L.; Leighton, J.L. *J. Am. Chem. Soc.* **2000**, *122*, 12894.

26 (a) Murai, S.; Sonoda, N. *Angew. Chem., Int. Ed. Engl.* **1979**, *18*, 837. (b) Fukumoto, Y.; Chatani, N.; Murai, S. *J. Org. Chem.* **1993**, *58*, 4187. (c) Chatani, N.; Murai, S. *Synlett* **1996**, 414.

27 (a) Matsuda, I.; Ogiso, A.; Sato, S.; Izumi, Y. *J. Am. Chem. Soc.* **1989**, *111*, 2332. (b) Matsuda, I.; Fukuta, Y.; Tsuchihashi, T.; Nagashima, H.; Itoh, K. *Organometallics* **1997**, *16*, 4327.

28 Ojima, I.; Ingallina, P.; Donovan, R.J.; Clos, N. *Organometallics* **1991**, *10*, 38.

29 (a) Doyle, M.P.; Shanklin, M.S. *Organometallics* **1993**, *12*, 11. (b) Doyle, M.P.; Shanklin, M.S. *Organometallics* **1994**, *13*, 1081.

30 Monteil, F.; Matsuda, I.; Alper, H. *J. Am. Chem. Soc.* **1995**, *117*, 4419.

31 Ojima, I.; Vidal, E.; Tzamarioudaki, M.; Matsuda, I. *J. Am. Chem. Soc.* **1995**, *117*, 6797.

32 Bonafoux, D.; Ojima, I. *Org. Lett.* **2001**, *3*, 1303.

33 Ojima, I.; Vidal, E.S. *Organometallics* **1999**, *18*, 5103.

34 (a) Seki, Y.; Hidaka, A.; Makino, S.; Murai, S.; Sonada, N. *J. Organomet. Chem.* **1977**, *140*, 361. (b) Seki, Y.; Hidaka, A.; Murai, S.; Sonada, N. *Angew. Chem., Int. Ed. Engl.* **1977**, *16*, 174. (c) Seki, Y.; Murai, S.; Hidaka, A.; Sonada, N. *Angew. Chem., Int. Ed. Engl.* **1977**, *16*, 881. (d) Chatani, N.; Ikeda, S.; Ohe, K.; Murai, S. *J. Am. Chem. Soc.* **1992**, *114*, 9710.

35 Leighton, J.L.; Chapman, E. *J. Am. Chem. Soc.* **1997**, *119*, 12416.

36 Jones, G.R.; Landais, Y. *Tetrahedron* **1996**, *52*, 7599.

37 Zacuto, M.J.; Leighton, J.L. *J. Am. Chem. Soc.* **2000**, *122*, 8587.

38 O'Malley, S.J.; Leighton, J.L. *Angew. Chem. Int. Ed.* **2001**, *40*, 2915.

39 Zacuto, M.J.; O'Malley, S.J.; Leighton, J.L. *J. Am. Chem. Soc.* **2002**, *124*, 7890.

40 Ojima, I.; Donovan, R.J.; Eguchi, M.; Shay, W.R.; Ingallina, P.; Korda, A.; Zeng, Q. *Tetrahedron* **1993**, *49*, 5431.

41 Schmidt, D.R.; Park, P.K.; Leighton, J.L. *Org. Lett.* **2003**, *5*, 3535.

42 Schmidt, D.R.; O'Malley, S.J.; Leighton, J.L. *J. Am. Chem. Soc.* **2003**, *125*, 1190.

6
Carbon–Carbon Bond–Forming Reactions Starting from Rh–H or Rh–Si Species

Isamu Matsuda

6.1
Introduction

Hydrosilanes are known to undergo oxidative addition with a transition metal complex to afford an H–M–Si species [1]. The resulting complexes are considered key intermediates in the catalytic cycle of the hydrosilylation of carbon–carbon and carbon–heteroatom unsaturated bonds [2]. The importance of hydrosilanes in synthetic organic chemistry would be greatly enhanced if the two σ-bonds, M–H and M–Si, in the species derived from oxidative addition could be differentiated in the subsequent insertion into an unsaturated bond (Scheme 6.1). Although a conventional way to differentiate clearly between path A and path B has not yet been identified, cascade type reactions may provide some insight into the controlling factors. To address these issues, we have focused on the development of new reactions for carbon–carbon bond formation catalyzed by low-valence rhodium complexes. This chapter summarizes the development of novel multi-component coupling reactions that begin with the oxidative addition of a hydrosilane to a rhodium complex.

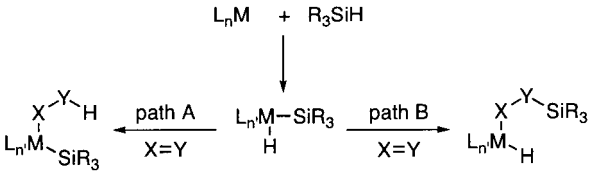

Scheme 6.1 Two paths for the insertion of X=Y into H–M–Si.

6.2
Background

The strict differentiation of two α-positions in unsymmetric aliphatic ketones was a difficult problem in enolate formation until the mid 1980s (Scheme 6.2). For example, ketone **1** gives a mixture of **2** and **3** according to a conventional procedure. It is well known that while α-silylketones **4** and **5** are the immediate precursors of the corresponding enoxysilanes **2** and **3**, there have been few reports on reliable routes for the selective synthesis of **4** or **5** [3].

Modern Rhodium-Catalyzed Organic Reactions. Edited by P. Andrew Evans

ISBN: 3-527-30683-8

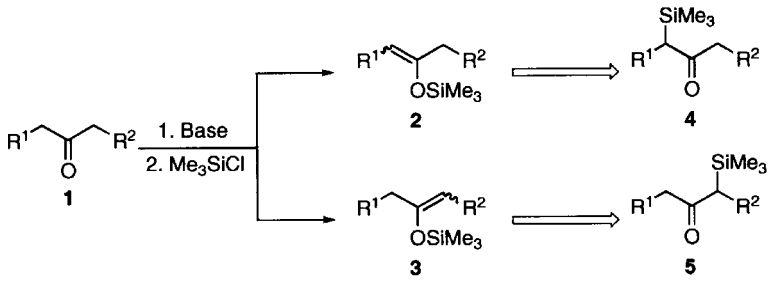

Scheme 6.2 Enoxysilanes derived from unsymmetrical ketones.

At this stage, we focused on the synthesis of α-silylketones **7** utilizing a rhodium-catalyzed isomerization of **6** to provide a new route to **4** and **5** (Scheme 6.3). As a result, neither **7** nor **8** was obtained from **6** in the presence of a catalytic amount of $RhH(PPh_3)_4$. However, when **9a** (R = Ph) was present in **6a** (R = Ph) as an impurity, **6a** was isomerized in the presence of the rhodium catalyst, to afford the ketone **7a** (R = Ph), thus providing the breakthrough for the studies outlined herein [4].

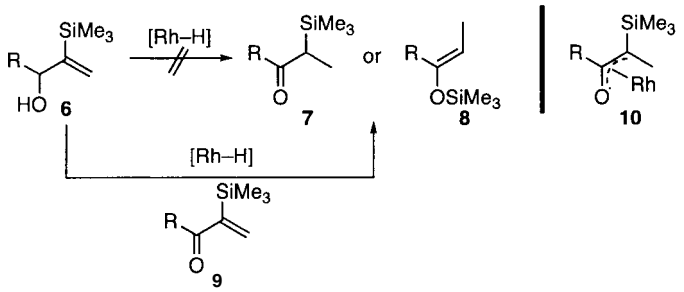

Scheme 6.3 Rhodium-catalyzed isomerization of **6**.

Thus, the transformation of **6** to **7** was established as a general route by using the co-catalysis of $RhH(PPh_3)_4$ and an α,β-unsaturated ketone. These results strongly suggest the intervention of rhodium–enolate complex **10**, which would be formed by the insertion of **9** into a Rh–H bond. This intuitive conclusion is supported by the coupling reaction of a vinyl ketone with an aldehyde in the presence of $RhH(PPh_3)_4$ or $RuH_2(PPh_3)_4$ without solvent (Eq. 1) [5].

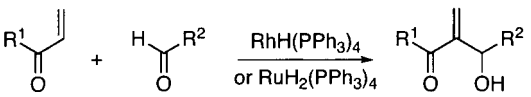

(1)

Although the pattern of this reaction is identical to that of the Morita–Baylis–Hillman reaction [6], we concluded on the basis of control experiments that the presence of a rhodium or ruthenium complex is crucial for smooth coupling. The possible intermediacy of the enolate complex in the above examples suggests a transition metal-cata-

lyzed Mukaiyama-type aldol coupling. Cationic complexes $[Rh(COD)(PPh_3)_2]X$ ($X = PF_6$ or ClO_4), in addition to the neutral $Rh_4(CO)_{12}$, worked well as catalysts in the reaction of an enoxysilane with an aldehyde or a ketone under neutral conditions (Eq. 2) [7]. These results further support the intermediacy of a rhodium–enolate formed by the oxidative addition of an enoxysilane to a low-valence rhodium complex. Since there is no evidence for the presence of an enolate complex at this stage, we cannot offer any persuasive arguments to counter the claim that the rhodium complex simply plays a role as a Lewis acid. Thus, the purpose of our new project was to acquire unambiguous evidence for the intermediacy of a rhodium–enolate in this catalytic reaction.

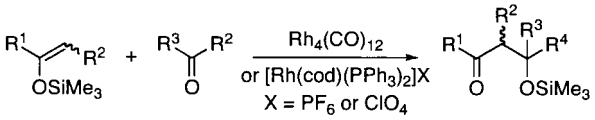

(2)

6.3
Design of Reactions Starting from Insertion into a Rh–H Bond

6.3.1
Aldol-Type Coupling under Neutral Conditions

Analysis of the Mukaiyama-type aldol coupling (Eq. 2) and the well-known hydrosilylation of *α,β*-unsaturated carbonyl compounds **11** in the presence of a rhodium catalyst, indicate that both can be explained by the intervention of the rhodium enolate **13**. This line of reasoning provided the impetus to develop a new crossed aldol coupling using a hydrosilane, an *α,β*-unsaturated ketone **11**, and an aldehyde to form **15** (Scheme 6.4).

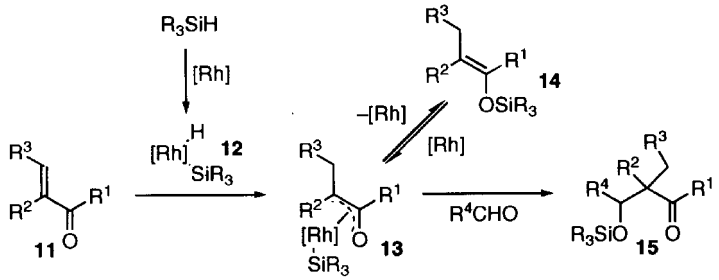

Scheme 6.4 Aldol-type three-component coupling of **11**.

However, since both *α,β*-unsaturated ketone **11** and an aldehyde are readily hydrosilylated in the presence of a rhodium complex, the interaction of these substrates with the metal complex must be controlled. Experimental studies demonstrated that Et_2MeSiH and $Rh_4(CO)_{12}$, *modified* by $MePh_2P$, provided the requisite combination to furnish **15a** in acceptable yield, as demonstrated in the reaction of 3-buten-2-one **11a** ($R^1 = CH_3$, $R^2 = R^3 = H$) with benzaldehyde (Eq. 3; Tab. 6.1) [8].

Tab. 6.1 Rhodium-catalyzed aldol-type coupling of **11** with Et_2MeSiH and PhCHO.

α,β-unsaturated carbonyl 11		*Product 15*		*α,β-unsaturated carbonyl 11*		*Product 15*	
		Yield (%)	*syn/anti*			*Yield (%)*	*syn/anti*
a	3-Buten-2-one	99	83:17	**g**	Methyl propenoate	96	37:63
b	1-Penten-3-one	100	84:16	**h**	Methyl 2-methyl-propenoate	99	—
c	4-Phenyl-3-buten-2-one	88	55:46	**i**	Methyl 2-butenoate	71	40:60
d	4-Methyl-3-penten-2-one	86	80:20	**j**	Ethyl 3-methyl-2-butenoate	7	9:91
e	1-Acetylcyclohexene	69	–	**k**	2(5*H*)-Furanone	75	54:46
f	2-Cyclohexenone	75	73:27	**l**	*α*-Methylene-*γ*-butyrolactone	26	57:43

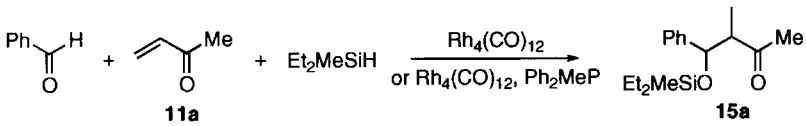

(3)

The present coupling was extended to other *α,β*-unsaturated carbonyl compounds and aldehydes. Although enoxysilane **14** was inevitably formed in the reactions using *α,β*-enones as a component, the aldehyde was completely converted to **15** with sufficient selectivity by using two molar equivalents of both **11** and Et_2MeSiH at low temperature (below 20 °C). Since the ratio of aldol coupling to the formation of ketene silylacetal in the reaction of *α,β*-enoates was higher than that in the reaction of *α,β*-enones, the use of 1.3 equivalents of Et_2MeSiH was sufficient for the complete conversion of benzaldehyde, to give **15** in high yield (Tab. 6.1). In addition to $Rh_4(CO)_{12}$ *modified* by $MePh_2P$, other rhodium complexes, such as $Et_2MeSiRh(CO)_4$, $[Rh(COD)(P(OPh)_3)_2]OTf$, and [Rh(COD)(*R*-BINAP)]OTf, also demonstrated high catalytic activity for this type of coupling with an *α,β*-enoate. In addition to aromatic aldehydes, aliphatic and alicyclic aldehydes could be used in the present reactions, albeit with somewhat reduced reactivity.

Morken and co-workers have reported the highly enantioselective version of this reaction, albeit with low efficacy in the aldol-type coupling [8d,e]. Unfortunately, we obtain low enantioselectivity (*ee* ~2–4%) using chiral rhodium complexes under our reaction conditions. An intramolecular adaptation has led to new opportunities in cobalt-catalyzed carbocyclizations, wherein the use of $PhSiH_3$ was essential for smooth ring formation (Eq. 4) [9]. The identical products were also formed by a combination of $[Rh(COD)_2]OTf/(p\text{-}CF_3Ph)_3P$ and molecular hydrogen [10].

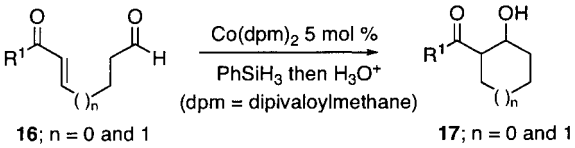

16; n = 0 and 1 **17**; n = 0 and 1

(4)

6.3.2
Apparent Hydrocarbamoylation to α,β-Enoates and Mannich-Type Coupling

Leaving precise mechanistic arguments aside, it should be stressed that an α,β-unsaturated carbonyl compound can behave as a latent nucleophile with the assistance of a hydrosilane and a low-valence rhodium complex. With this simplification, isocyanates **18** and aldimines **20** were used as electrophiles for a similar protocol. Both were successfully incorporated with the aid of $[Rh(COD)(P(OPh)_3)_2]OTf$ to afford **19** and **21**, respectively (Scheme 6.5) in a reaction that was similar to the aldol-type coupling [11].

Due to their high electrophilicity, isocyanates are useful starting materials for the synthesis of heterocycles and C–C bond formation using carbon nucleophiles. A key feature of these reactions is the requirement for more than one equivalent of base. Additionally, a few examples of transition metal-catalyzed homologation of the central carbon of the heterocumulene moiety have been reported.

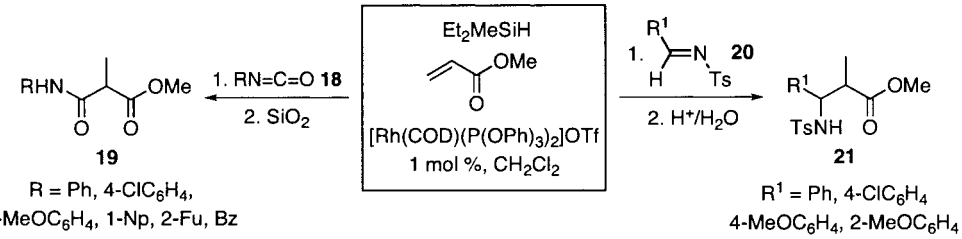

Scheme 6.5 Three-component coupling of **18** and **20** catalyzed by a rhodium complex.

6.3.3
Apparent Hydroallylation toward α,β-Unsaturated Carbonyl Compounds

Palladium-catalyzed allylic alkylation is a widely accepted procedure for carbon–carbon bond formation in synthetic organic chemistry. Although many improved versions have been reported with regard to regiochemistry and stereochemistry [12], some important issues have not yet been resolved. Remaining challenges include expanding the pool of carbon nucleophiles and developing a system that can be carried out under neutral reaction conditions.

The previous findings on reductive aldol coupling prompted the examination of the possibility of easily access to a designated enolate under almost neutral conditions. In the first stage of this project, coupling between an isolated enoxysilane and an allylic ester was used as a model system to obtain preliminary information on a catalyst precursor and optimize the reaction conditions. The cationic complex $[Rh(COD)(PMePh_2)_2]OTf$ demonstrated modest catalytic activity, affording a mixture of **23** and **24** for the coupling of an enoxysilane with an allylic carbonate in CH_2Cl_2 at 80 °C (Eq. 5) [13a]. This result clearly demonstrated that a cationic rhodium(I) complex is suitable for the activation of an allylic carbonate **22**. This cationic complex was effective in the one-pot reaction between Et_2MeSiH, **11h**, and **22a** ($R^4 = Ph$, $R^5 = CH_3$) to give the expected products **23a** and **24a** (Eq. 6) [13b].

The reaction rate and product yield were dramatically affected by the nature of the phosphorus ligands in the catalyst precursor. $[Rh(COD)(PMePh_2)_2]OTf$ gave a mixture

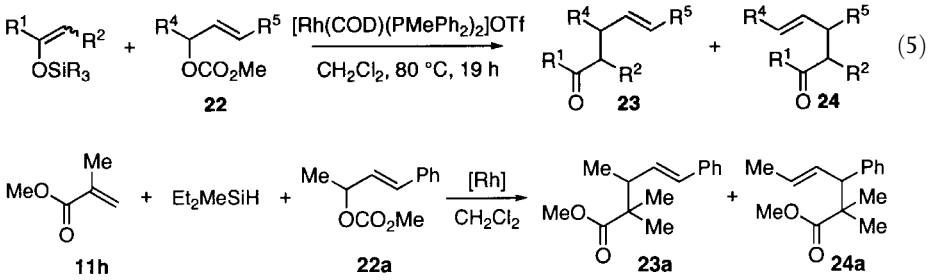

(5)

(6)

of coupling products in 90% yield under mild conditions (25 °C, 42 h), whereas [Rh(COD)(P(OPh)$_3$)$_2$]OTf demonstrated the highest activity for the consumption of **11h**, albeit affording the desired product in only 38% yield with the concomitant formation of a mixture of 1-phenyl-1-butene and 1-phenyl-2-butene. The latter byproducts are formed by the direct interaction of Et_2MeSiH with **22a**.

Thus, the efficiency of [Rh(COD)(P(OPh)$_3$)$_2$]OTf in hydroallylation could be enhanced by the suppression of the hydrosilylation of the allylic carbonate **22a**. The yield of **23a** and **24a** increased to 93% when a solution of **22a** was slowly added to a mixture of the *α,β*-unsaturated ester **11h**, Et_2MeSiH, and [Rh(COD)(P(OPh)$_3$)$_2$]OTf (1 mol% based on **22a**) over one hour. A similar procedure was effective for the reactions of other *α,β*-unsaturated carbonyl compounds (Tab. 6.2), as the reactions proceeded smoothly with a variety of allylic carbonates **22**.

The regiochemistry of the reaction of unsymmetrical allylic esters was addressed by the introduction of a silyl group, equivalent to H, on the carbon of the allylic terminus. For example, **25** bearing a $^tBuMe_2Si$ group afforded **26** as the sole product in the three-component coupling. Since the subsequent protodesilylation of **26** selectively formed **27** (Scheme 6.6), this sequential procedure provides a practical method to control the regiochemistry in the substitution of unsymmetrical allylic substrates [13c].

Tab. 6.2 Hydroallylation of **11** with **22a** and Et_2MeSiH catalyzed by [Rh(COD)(P(OPh)$_3$)$_2$]OTf.

α,β-unsaturated carbonyl 11	*Product (23+24)*		*α,β-unsaturated carbonyl 11*	*Product (23+24)*	
	Yield (%)	*Ratio (23+24)*		*Yield (%)*	*Ratio (23+24)*
h	93	35:65	**l**	38	52:48
h	83 [a]	32:68	**a**	96	48:52
h	83 [b]	35:65	**m** [c]	99	48:52
g	90	33:67	**f**	90	46:54
i	76	51:49			

a) Me_2PhSiH was used as R_3SiH.
b) $EtMe_2SiH$ was used as R_3SiH.
c) 2-Cyclopentenone.

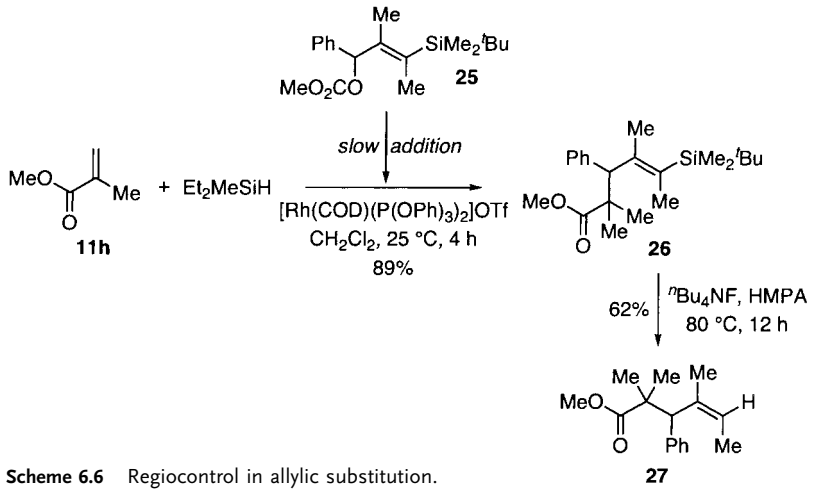

Scheme 6.6 Regiocontrol in allylic substitution.

6.4
Design of Reactions Starting from Insertion into a Rh–Si Bond

6.4.1
Silylformylation toward Acetylenic Triple Bonds

The aldol-type coupling described in the previous section was completely suppressed under CO (20 atm.). However, Murai and co-workers have reported a new approach to enoxysilanes based on the coupling of an alkene, a hydrosilane, and CO in the presence of $Co_2(CO)_8$ [14]. This conspicuous difference in catalytic ability between rhodium and cobalt stimulated us to examine the incorporation of CO and a hydrosilane in the presence of rhodium.

Silylformylation of acetylenic C–C triple bonds was investigated in the first stage of the project. The reaction proceeded smoothly to selectively form *β*-silylalkenals by a one-pot operation utilizing a molar equivalent each of an alkyne and hydrosilane with a catalytic amount (0.1–1 mol%) of $Rh_4(CO)_{12}$ under CO (> 5 atm.) (Eq. 7). This type of CO incorporation is suitable for a variety of hydrosilanes and alkynes, including both terminal and internal types. Some examples are summarized in Tab. 6.3 [15 a, b].

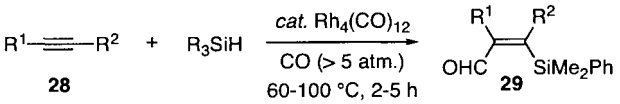

(7)

A moderate pressure (> 5 atm.) of CO in the reaction system leads to the selective formation of **29**, while alkynes undergo rhodium-catalyzed hydrosilylation with a hydrosilane to afford vinylsilanes in the absence of CO. The presence of the rhodium complex is crucial for the smooth progression of silylformylation, regardless of the presence of mononuclear or polynuclear complexes. This generalization is supported by the studies of many others [15]. The most important feature of this reaction is the excellent regioselectivity, which favors the formylation of the internal *sp*-carbon of the acetylenic bond of terminal

Tab. 6.3 $Rh_4(CO)_{12}$-catalyzed silylformylation of **28** in the presence of Me_2PhSiH and CO.

	Alkyne 28		*Product 29*			*Alkyne 28*		*Product 29*	
	R^1	R^2	*Yield (%)*	*Z:E*		R^1	R^2	*Yield (%)*	*Z:E*
a	Ph	H	90	98:2	**l**	$Cl(CH_2)_3$	H	78	88:12
b	H	H	73	0:100	**m**	$HOCH_2$	H	78	77:23
c	Me	H	99	80:20	**n**	$HOCH(CH_3)$	H	76	65:35
d	Et	H	91	94:6	**o**	$HOC(CH_3)_2$	H	94	97:3
e	$^nC_3H_7$	H	93	95:5	**p**	*p*-$TsNHCH_2$	H	60	67:33
f	$^nC_4H_9$	H	86	85:15	**q**	MeO_2CNHCH_2	H	61	50:50
g	$^nC_5H_{11}$	H	71	87:13	**r**	CH_3	CH_3	94	100:0
h	$cycloC_6H_{11}$	H	96	100:0	**s**	$^nC_3H_7$	CH_3	85 [a]	70:30 [b]
i	$CH_2{=}CHCH_2$	H	90	73:27	**t**	Ph	Me	95 [a]	89:11 [b]
j	Me_3SiCH_2	H	94	91:9	**u**	CH_3	CO_2Me	67	100:0
k	Me_3Si	H	55	100:0	**v**	Ph	Ph	90	95:5

a) Yield containing the regioisomer.
b) The ratio of **29** to the corresponding regioisomer.

alkynes. The silylformylation of internal alkynes gives rise to lower regioselectivity. An *sp*-carbon bearing a bulkier substituent seems to be preferred to an *sp*-carbon bearing a less bulky substituent as the formylation site in the reactions of **28s** and **28t**. Strict control of the formylation site was achieved by the application of an intramolecular version that involves substrates that contain both an acetylenic bond and a hydrosilyl moiety (Scheme 6.7) [16]. Hydrosilane **30** ($n=1$ or 2) selectively affords **31** according to an *exo-dig* mode of cyclization under conditions identical to those described for the intermolecular version. Products based on the *endo-dig* mode of cyclization or intermolecular coupling of **30** were not formed under these reaction conditions.

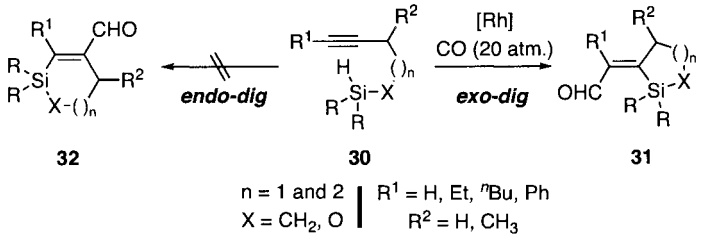

Scheme 6.7 Intramolecular version of silylformylation.

$Rh_4(CO)_{12}$ reacts with four molar equivalents of R_3SiH under CO (>5 atm.) to afford $Rh(CO)_4SiR_3$ (**33**). This new species was too unstable to be isolated, but provides an excellent catalyst for the silylformylation of **28** with efficiency comparable to that of $Rh_4(CO)_{12}$. Reaction of **33** with a mixture containing a molar equivalent of both **28** and a hydrosilane bearing the same substituents as the silyl group in **33**, under carbon monoxide, produced **29** and unchanged **33**. However, in the absence of hydrosilane, **33**

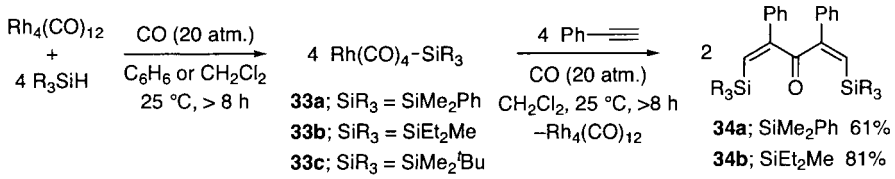

Scheme 6.8 Formation of a Rh–Si species and its reaction with phenylacetylene.

reacted with one molar equivalent of **28a** to afford the divinyl ketone **34** as the sole organic product with the regeneration of $Rh_4(CO)_{12}$ under carbon monoxide (Scheme 6.8) [15b].

Interestingly, the complete conversion of **33** to **34** was observed when the reaction was carried out in the presence of carbon monoxide at atmospheric pressure. The possible interaction of **33** with a hydrosilane at room temperature was supported by the appreciable line broadening of the corresponding silylmethyl groups in the ^{1}H NMR spectrum of a mixture of **33a** and Me_2PhSiH, and by the fact that an identical mixture (**33a**/**33b** ~88:12) was obtained from a solution of either **33a** and ^{t}BuMe$_2$SiH or **33c** and Me_2PhSiH. This equilibration is rationalized by assuming intervention of the disilylrhodium(III) species **35** (Scheme 6.9) [15b]. A similar exchange process for silyl groups has been well documented with cobalt complexes.

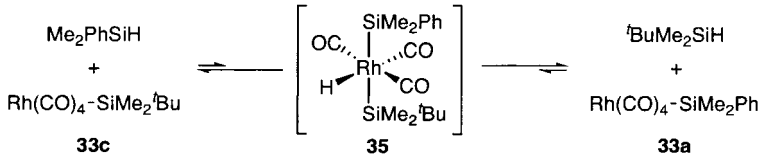

Scheme 6.9 Exchange of the silyl group of **33**.

A further piece of evidence to elucidate the catalytic pathway of silylformylation was provided by a pair of deuterium-labeled reactions. The results revealed that the scrambling of hydrogen atoms between a hydrosilane and a terminal acetylene is minimal during the reaction and that the hydrogen atom of the formyl group and the vinylic hydrogen are derived from the hydrosilane and the acetylenic proton, respectively (Eq. 8) [15b].

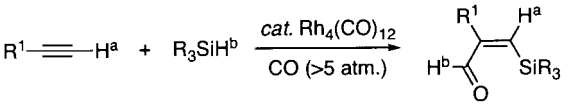

(8)

Based on the previous information, catalytic cycles A and B are proposed as a possible mechanism (Scheme 6.10), in which the rhodium catalyst plays a crucial role in the smooth progression of the reaction, irrespective of the catalyst precursors.

Generally the functional groups in **28** do not interfere in the silylformylation to afford **29** (Tab. 6.3), for example, **28** having hydroxy, *p*-tosylamino and carbomate

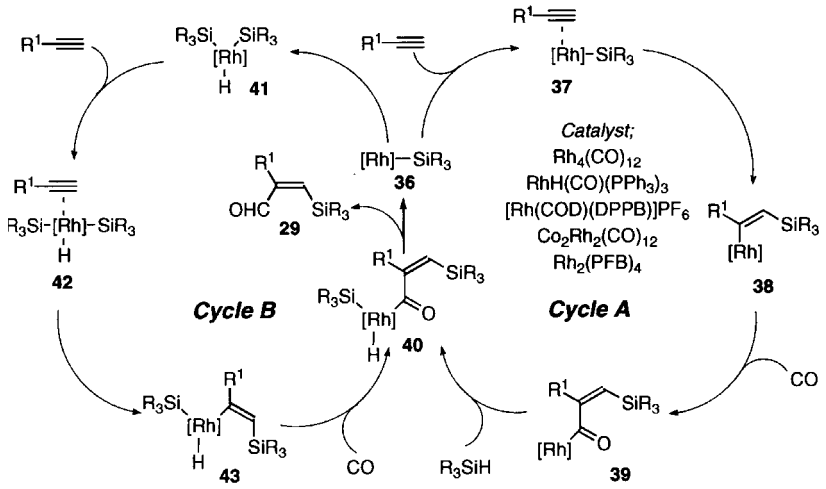

Scheme 6.10 Proposed mechanism for silylformylation.

groups afforded **29** under standard conditions. The utility of this reaction has been demonstrated by its successful incorporation into a number of synthetic sequences. However, under these conditions, propargylic amines proved inferior substrates, with about 20% of the starting acetylenes being recovered (compare Eq. 7). Nonetheless, it was demonstrated that an alternative silylformylation was possible by carrying out the reaction with two molar equivalents of Me_2PhSiH in the presence of CO. Hence, the 2-silylmethyl-2-alkenal **45** was formed selectively with the concomitant formation of **46** in the reaction of **44** under these reaction conditions (Eq. 9) [17a].

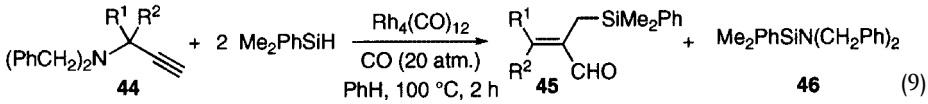

(9)

The present transformation seems to be accelerated by the presence of electron-donating substituents on the amino nitrogen of **44** (Tab. 6.4), while the *p*-toluenesulfonyl group and methoxycarbonyl groups suppress the formation of **45** under similar conditions.

Tab. 6.4 One-pot formation of *α*-silylmethylalkenals **45**.

	Propargylic amine 44				*Product 45*		*Propargylic amine 44*				*Product 45*
	R¹	*R²*	*R³*	*R⁴*	*Yield (%)*		*R¹*	*R²*	*R³*	*R⁴*	*Yield (%)*
a	H	H	CH_2Ph	CH_2Ph	94	**e**	$^nC_5H_{11}$	H		$-(CH_2)_5-$	93
b	H	H	CH_3	CH_2Ph	83	**f**	CH_3	CH_3		$-(CH_2)_5-$	65
c	CH_3	H	CH_2Ph	CH_2Ph	90	**g**	$-(CH_2)_5-$			$-(CH_2)_5-$	80
d	CH_3	H	^{n}Bu	^{n}Bu	72	**h**	$-(CH_2)_5-$		H	CH_2Ph	88

Interestingly, **47**, **48**, and **49** were isolated in 49%, 33%, and 4% yield respectively after chromatographic purification of the crude product derived from the reaction of the propargylic amine **44b** with two molar equivalents of $^{t}BuMe_2SiH$, and CO (Eq. 10) [17b].

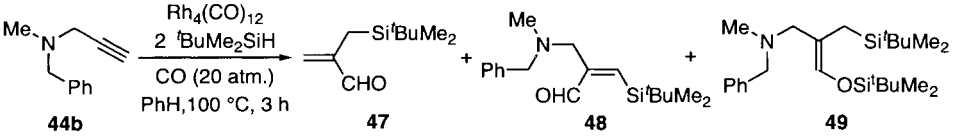

44b **47** **48** **49**

(10)

Increasing the amount of the $^{t}BuMe_2SiH$ (four molar equivalents) furnished the enoxy–silane **49** as the sole product in 94% isolated yield after distillation; this was converted to **47** upon treatment with a benzene or hexane suspension of silica gel. These results suggest that **47** is the indirect product formed by the sequence **44b** → **48** → **49** → **47**. Thus, the reaction to form **45** (Eq. 9) can be considered to occur according to similar consecutive reactions. If the rate of incorporation of the second Me_2PhSiH into the initially formed silylformylation product, such as **48**, is faster than the rate of silylformylation of the acetylenic triple bond, then **45a** is isolated as the sole product due to the instability of **46** on silica gel. The formation of **45** can be explained by the intervention of a silylformylation product similar to **48**, which suggests that the same compound **45** can be constructed by a similar sequential reaction starting from the propargylic alcohol **50a** (Scheme 6.11). Since silylformylation of **50a** is known to give **51a** in high yield under standard conditions in the first stage, isolated **51a** was treated with a molar equivalent of Me_2PhSiH under CO in the presence of a catalytic amount of $Rh_4(CO)_{12}$ to afford **45** in high yield (route 1, Scheme 6.11). The identical transformation was attained by a one-pot reaction of **50a** with more than two molar equivalents of Me_2PhSiH under CO (route 2, Scheme 6.11) [22c]. Propargylic esters **50b** and propargylic carbonates **50c** were also suitable for a similar one-pot procedure. The transformation of **51** to **45** is equivalent to a formal S_N2' reaction employing hydride anion as a nucleophile. If this is the case, molecular hydrogen could play the role of Me_2PhSiH in this step. In fact, the reaction of **50** with Me_2PhSiH, CO, and H_2 was designed for the conversion of **50** to **45** (route 3, Scheme 6.11) [17d].

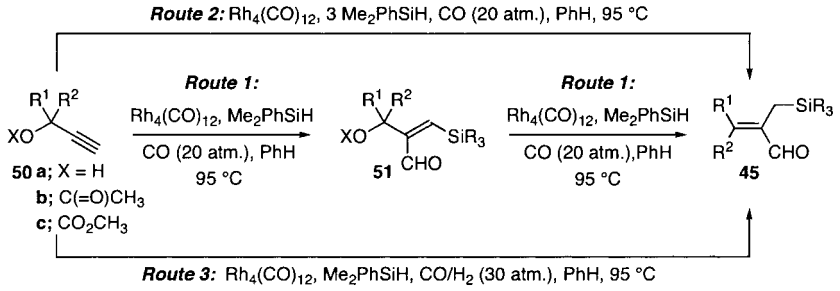

Scheme 6.11 Variations for the synthesis of **45**.

Despite the rich chemistry of **45** [18], the only method for accessing this compound is the oxidation of the corresponding alcohol derived from 2-methyl-2-propen-1-ol or other sources, which can be obtained through multi-step operations. In contrast to the known methods, **45** can be readily derived from **44** and **50** by a simple one-pot operation. Since the propargylic alcohol **50a** is readily accessed from a ketone or aldehyde, realization of the transformation of **50** to **45** through a one-pot procedure provides a novel method for carbonyl olefination of ketones or aldehydes.

6.4.2
Dehydrogenative Cyclization Forming Lactones and Lactams

γ-Lactone **53** was obtained in 89% yield as the sole product in the reaction of **52** with a molar equivalent each of Me_2PhSiH and Et_3N under CO, while conventional silylformylation to give **54** was a major pathway in the absence of Et_3N under similar conditions (Scheme 6.12). β-Lactones and δ-lactones were selectively formed from the corresponding propargylic alcohols and bis-homopropargylic alcohols respectively, in which ^{t}BuMe$_2$SiH with a catalytic amount of DBU (1,8-diazabicyclo[5.4.0]undec-7-ene) was required (Tab. 6.5) [19a].

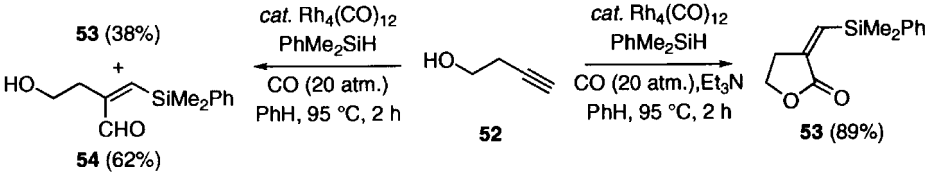

Scheme 6.12 Remarkable effect of Et_3N in the reaction of **52**.

Tab. 6.5 $Rh_4(CO)_{12}$-catalyzed construction of lactone frameworks.

Alkynol	*Lactone*	*Yield (%)*	*Alkynol*	*Lactone*	*Yield (%)*
	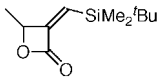	79	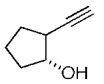	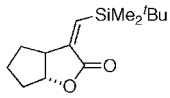	84
	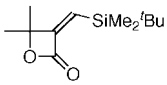	86	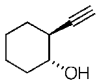	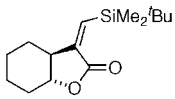	83
	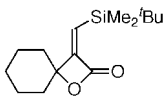	85	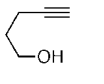	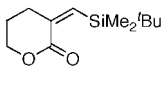	84
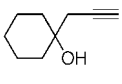	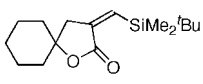	82	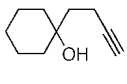	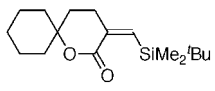	84

Mass spectroscopic analysis of the gas phase revealed that **53** is formed with the concomitant generation of H_2. Based on the proposed catalytic cycle for silylformylation (Scheme 6.12), the formation of **53** and **54** can be explained by the intervention of **55** ($n=2$), which plays a pivotal role in the differentiation between intramolecular nucleophilic attack of the hydroxy group and reductive elimination of **54**. Thus, the addition of base is believed to accelerate the conversion of **55** to the rhodate anion **56**. This notation is supported by the fact that the introduction of a strong base such as DBU is advantageous for the selective formation of a lactone framework.

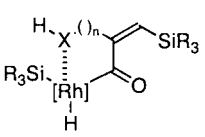

55 (X = O)
57 (X = NR^1)

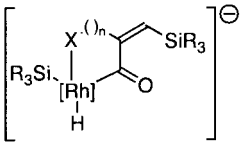

56 (X = O)
58 (X = NR^1)

A similar protocol can be extended to a wider range of lactams than lactones (Tab. 6.6), although an electron-withdrawing substituent on the amino nitrogen is required for selective formation of a β-lactam from sterically less-constrained propargylic

Tab. 6.6 $Rh_4(CO)_{12}$-catalyzed construction of lactam frameworks.

Alkynylamine	*Lactam*	*Yield (%)*	*Alkynylamine*	*Lactam*	*Yield (%)*
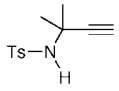	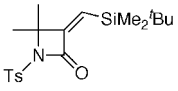	80	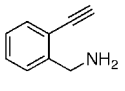	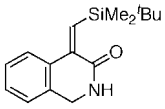	73
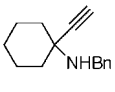	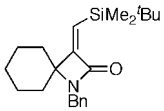	98		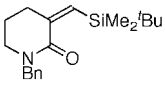	68
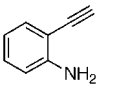	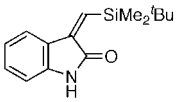	93	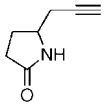	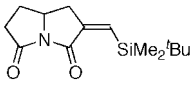	97
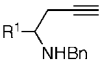	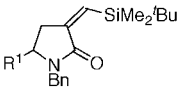	R^1 = H 93 R^1 = Ph 84	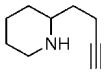	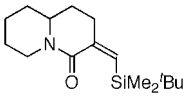	66
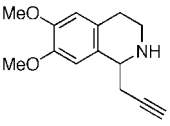	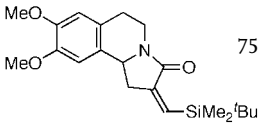	75	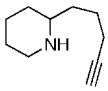	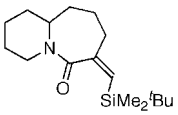	55

amines, due to a competitive pathway yielding **45**. Interestingly, the intermediacy of **57** and **58** is also suggested in the formation of lactams [19b].

A novel route was examined for the synthesis of the *α,β*-unsaturated amide **59** *via* the intermolecular coupling of four components; an alkyne, a hydrosilane, an amine, and CO (Eq. 11). All of these components are assembled in an ordered manner with the assistance of a rhodium complex. The use of pyrrolidine as the nucleophile gave the optimum results, whereas alcohols were not reactive nucleophiles under similar reaction conditions [19e].

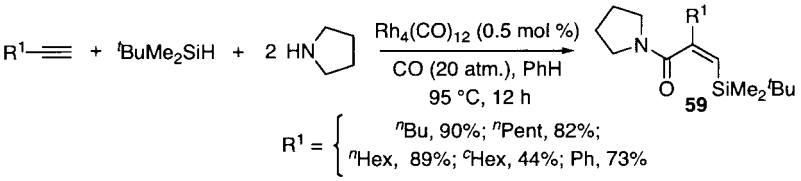

(11)

6.4.3

Silylative Cyclocarbonylation of 1,6-Diynes and 1,6-Enynes

An appreciable decrease in the reaction rate was observed in the silylformylation of **28a** with $^{t}BuMe_2SiH$. Forcing conditions (100 °C, 16 h) did not accelerate the reaction, but rather resulted in the competitive formation of **60** (49%), **61** (23%), and **62** (3%). The yields of cyclopentenones **61** and **62** were increased to 38% and 6% respectively, with a slight decrease in **60**, by using two molar equivalents of **28a** under CO (Eq. 12) [15b]. Thus, 1,6-diyne **63** can be considered as a model for the possible consecutive intramolecular insertion of two acetylenic bonds into a Rh–Si bond. Bicyclic ketones **64** and **65** were isolated in the one-pot reaction of **63** with a molar equivalent of $^{t}BuMe_2SiH$ under CO (Scheme 6.13, mode 1) [20a–d]. Although fluctuation in the product ratio was observed (Tab. 6.7), the results for **63a** and **63b** suggest that the initially formed ketone **64** isomerizes to **65** during either the reaction or isolation.

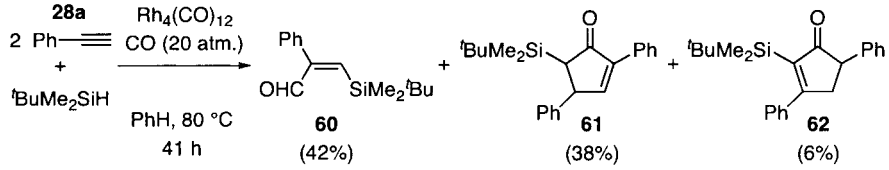

(12)

However, linear **68a** was a major product (59%) with the concomitant formation of **65a** (20%) in the reaction of **63a** with two molar equivalents of $^{t}BuMe_2SiH$ at 25 °C (Scheme 6.13, mode 2) [20a]. Based on these results, the formation of **64** and **65** is thought to involve the intermediacy of **70** and **71**. This idea is supported by the fact that catalyst **72**, prepared *in situ* by the interaction of $RhCl(PPh_3)_3$ with a molar equivalent of R_3SiH, selectively formed **69** as the major product in the reaction of **63** with R_3SiH under a nitrogen atmosphere (Scheme 6.13, mode 3) [21]. When $Rh_4(CO)_{12}$ was used as a catalyst instead of **72**, **69** was obtained as a minor component along with

Tab. 6.7 Silylative cyclocarbonylation of **63** catalyzed by $Rh_4(CO)_{12}$.

	1,6-Diyne 63	*Solvent*	*Yield (%) of products*			
	X		*64*	*65*	*66*	*67*
a	H_2C	C_6H_6	14	63	0	0
		CH_3CN	0	60	0	0
b	$(MeO_2C)_2C$	C_6H_6	58	6	0	0
		CH_3CN	70	14	0	0
c	*p*-TsN	C_6H_6	18	51	5	0
d	$PhCH_2N$	C_6H_6	0	9	31	0
		CH_3CN	0	8	72	0
e	O	C_6H_6	0	3	0	6
		CH_3CN	0	35	0	2
f	(HO)(H)C	C_6H_6	20[a)]	49[a)]	0	0

a) A mixture of diastereomers.

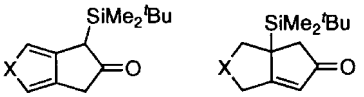

66 **67**

other products involving two molecules of **63**. Although the present silylative cyclocarbonylation is not fully refined, it is notable that this rhodium-catalyzed method may offer a unique route to **64** and **65**. The building block **75**, utilized in the synthesis of hirstene, was readily constructed by this rhodium-catalyzed carbonylation of **73** (Scheme 6.14) [20e].

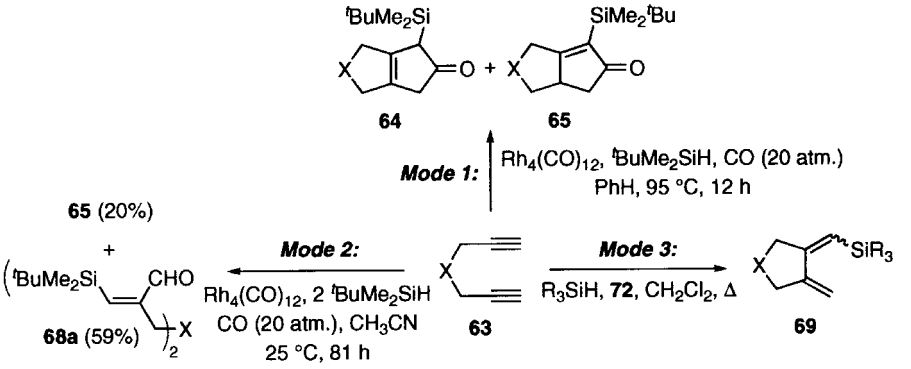

Scheme 6.13 Reaction modes of 1,6-diyne **63.**

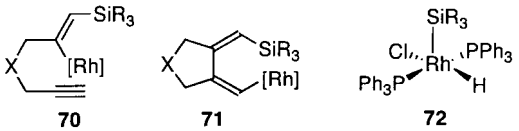

70 **71** **72**

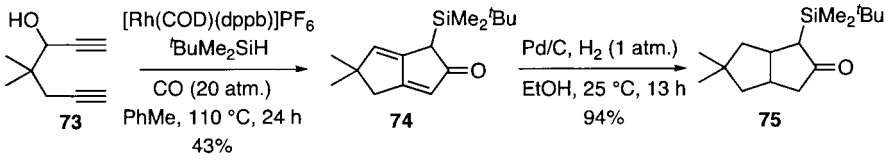

Scheme 6.14 Facile synthesis of **75** from **73.**

In sharp contrast to the unique pattern for the incorporation of carbon monoxide into the 1,6-diyne **63**, aldehyde **77** was obtained as the sole product in the rhodium-catalyzed reaction of 1,6-enyne **76** with a molar equivalent of Me_2PhSiH under CO (Scheme 6.15, mode 1) [22]. This result can be explained by the stepwise insertion of the acetylenic and vinylic moieties into the Rh–Si bond, the formyl group being generated by the reductive elimination to afford **77**. The fact that a formyl group can be introduced to the olefinic moiety of **76** under mild conditions should be stressed, since enoxysilanes are isolated in the rhodium-catalyzed silylformylation of simple alkenes under forcing conditions. The 1,6-enyne **76** is used as a typical model for Pauson–Khand reactions (Scheme 6.15, mode 2) [23], whereas formation of the corresponding product was completely suppressed in the presence of a hydrosilane. The selective formation of **79** in the absence of CO (Scheme 6.15, mode 3) supports the stepwise insertion of the acetylenic and olefinic moieties in the same molecules into the Rh–Si bond.

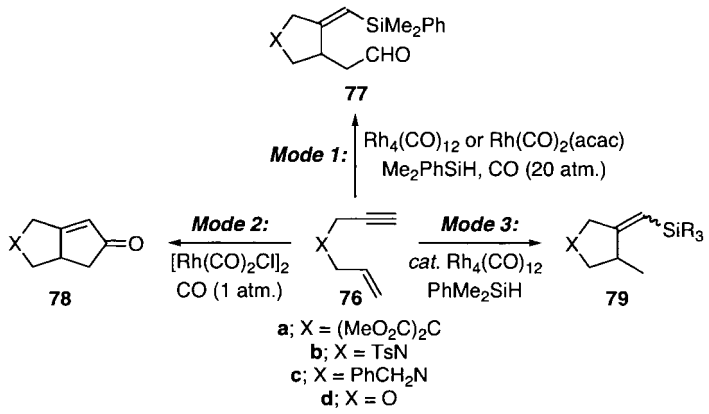

Scheme 6.15 Reaction modes of 1,6-enynes **76.**

6.5 Conclusion

We have explored two types of carbon–carbon bond forming reactions operated under almost neutral conditions. Both reactions are initiated by the formation of an H–Rh–Si species through oxidative addition of a hydrosilane to a low-valence rhodium complex. Aldol-type three-component couplings are followed by the insertion of an α,β-unsaturated carbonyl compound into a Rh–H bond, whereas silylformylation is accomplished by the insertion of an acetylenic moiety into a Rh–Si bond.

Acknowledgement

The author acknowledges the late Professor Yoshio Ishii and Professor Kenji Itoh (Nagoya University) for their valuable suggestions and encouragement to pursue this project. This work was financially supported by a Grant-in-Aid for Scientific Research and the 21st Century COE Program "Nature-Guided Materials Processing" of the Ministry of Education, Culture, Sports, Science, and Technology (Japan).

6.6 References

1 (a) Chalk, A.J.; Hallod, J.F. *J. Am. Chem. Soc.* **1965**, *87*, 16; (b) Muir, K.W.; Ibers, J.A. *Inorg. Chem.* **1970**, *9*, 440; (c) Aiszenberg, M.; Milstein, D. *J. Am. Chem. Soc.* **1995**, *117*, 6456; (d) Osakada, K.; Koizumi, T.; Yamamoto, T. *Organometallics* **1997**, *16*, 2063.

2 (a) Speier, J.L. In *Adv. Organomet. Chem.* **1979**, *17*, 407; (b) Ojima, I. In *The Chemistry of Organic Silicon Compounds*, Part 2; Patai, S.; Rappoport, Z. Eds.; John Wiley and Sons; Chichester, **1989**, p 1479; (c) Hiyama, T.; Kusumoto, T. In *Comprehensive Organic Synthesis*; Trost, B.M.; Fleming, I. Eds.; Pergamon Press; Oxford, **1991**, Vol. 8, p 763; (d) Marciniec, B. *Comprehensive Handbook on Hydrosilylation*; Pergamon Press; Oxford, **1992**.

3 (a) Obayashi, M.; Utimoto, K.; Nozaki, H. *Tetrahedron Lett.* **1977**, 1807; (b) Obayashi, M.; Utimoto, K.; Nozaki, H. *Bull. Chem. Soc. Jpn.* **1979**, *52*, 2646.

4 (a) Matsuda, I.; Sato, S.; Izumi, Y. *Tetrahedron Lett.* **1983**, *24*, 2787; (b) Sato, S.; Matsuda, I.; Izumi, Y. *Tetrahedron Lett.* **1983**, *24*, 3855; (c) Sato, S.; Matsuda, I.; Izumi, Y. *Tetrahedron Lett.* **1985**, *26*, 4229; (d) Sato, S.; Matsuda, I.; Izumi, Y. *J. Organomet. Chem.* **1988**, *344*, 71.

5 (a) Sato, S.; Matsuda, I.; Izumi, Y. *Chem. Lett.* **1985**, 1875; (b) Matsuda, I.; Shibata, M.; Sato, S. *J. Organomet. Chem.* **1988**, *340*, C5; (c) Sato, S.; Matsuda, I.; Shibata, M. *J. Organomet. Chem.* **1989**, *377*, 347: This finding stimulated Bergman and Heathcock to isolate Rh–enolate complexes; (d) Slough, G.A.; Bergman, R.G.; Heathcock, C.H. *J. Am. Chem. Soc.* **1989**, *111*, 938.

6 Ciganek, E. *Org. React.* **1996**, *51*, 201.

7 (a) Sato, S.; Matsuda, I.; Izumi, Y. *Tetrahedron Lett.* **1986**, *27*, 5517; (b) Sato, S.; Matsuda, I.; Izumi, Y. *Tetrahedron Lett.* **1987**, *28*, 6657; (c) Sato, S.; Matsuda, I.; Izumi, Y. *J. Organomet. Chem.* **1988**, *352*, 223; (d) Reetz, M.T.; Vougioukas, A.E. *Tetrahedron Lett.* **1987**, *28*, 793.

8 (a) Matsuda, I.; Takahashi, K.; Sato, S. *Tetrahedron Lett.* **1990**, *31*, 5331; $RhCl_3 \cdot 3H_2O$ and $Co(dpm)_2$ are used for the similar coupling of *α,β*-enoates, however, neither is effective for the reaction of *α,β*-enones; (b) Revis, A.; Hilty, T.K. *Tetrahedron Lett.* **1987**, *28*, 4809; (c) Isayama, S.; Mukaiyama, T. *Chem. Lett.* **1989**, 2005; (d) Taylor, S.J.; Morken, J.P. *J. Am. Chem. Soc.* **1999**, *121*, 12202; (e) Taylor, S.J.; Duffey, M.O.; Morken, J.P. *J. Am. Chem. Soc.* **2000**, *122*, 4528.

9 Wang, L.; Jang, H.; Roh, Y.; Lynch, V.; Schultz, A.J.; Wang, X.; Kirsche, M.J. *J. Am. Chem. Soc.* **2002**, *124*, 9448.

10 Jang, H.; Huddleton, R.R.; Kirsche, M.J. *J. Am. Chem. Soc.* **2002**, *124*, 15156.

11 (a) Muraoka, T.; Matsuda, I.; Itoh, K. *Organometallics* **2001**, *20*, 4676; (b) Muraoka, T.; Kamiya, S.; Matsuda, I.; Itoh, K. *Chem. Commun.* **2002**, 1284.

12 (a) Takeuchi, R.; Kashio, M. *J. Am. Chem. Soc.* **1998**, *120*, 8647; (b) Evans, P. A.; Nelson, J.D. *J. Am. Chem. Soc.* **1998**, *120*, 5581; (c) Evans, P.A; Kennedy, L.J. *Org. Lett.* **2000**, *2*, 2213.

13 (a) Muraoka, T.; Matsuda, I.; Itoh, K. *Tetrahedron Lett.* **2000**, *41*, 8807; (b) Muraoka, T.; Matsuda, I.; Itoh, K. *J. Am. Chem. Soc.* **2000**, *122*, 9552; (c) Muraoka, T.; Matsuda, I.; Itoh, K. unpublished results.

14 (a) Seki, Y.; Hidaka, A.; Murai, S.; Sonoda, N. *Angew. Chem., Int. Ed. Engl.* **1977**, *16*, 174; (b) Seki, Y.; Hidaka, A.; Makino, S.; Murai, S.; Sonoda, N. *J. Organomet. Chem.* **1977**, *140*, 361;

(c) Seki, Y.; Kawamoto, K.; Chatani, N.; Hidaka, A.; Sonoda, N.; Ohe, K.; Kawasaki, Y.; Murai, S.; *J. Organomet. Chem.* **1991**, *403*, 73.

15 (a) Matsuda, I.; Ogiso, A.; Sato, S.; Izumi, Y. *J. Am. Chem. Soc.* **1989**, *111*, 2332; (b) Matsuda, I.; Fukuta, Y.; Tsuchihashi, T.; Nagashima, H.; Itoh, K. *Organometallics* **1997**, *16*, 4327; (c) Ojima, I.; Ingallina, P.; Donovan, R.J.; Clos, N. *Organometallics* **1991**, *10*, 38; (d) Doyle, M.P.; Shanklin, M.S. *Organometallics* **1994**, *13*, 1081; (e) Zhou, J.; Alper, H. *Organometallics* **1994**, *13*, 1586; (f) Alonso, M.A.; Casares, J.A.; Espinet, P.; Vallés, E.; Soulantica, K. *Tetrahedron Lett.* **2001**, *42*, 5697.

16 (a) Monteil, F.; Matsuda, I.; Alper, H. *J. Am. Chem. Soc.* **1995**, *117*, 4419; (b) Ojima, I.; Vidal, E.; Tzamarioudaki, M.; Matsuda, I. *J. Am. Chem. Soc.* **1995**, *117*, 6797.

17 (a) Matsuda, I.; Sakakibara, J.; Inoue, H.; Nagashima, H. *Tetrahedron Lett.* **1992**, *33*, 5799; (b) Matsuda, I.; Fukuta, Y.; Itoh, K. *Inorg. Chim. Acta* **1999**, *296*, 72; (c) Matsuda, I.; Niikawa, N.; Kuwabara, R.; Inoue, H.; Nagashima, H. Itoh, K. *J. Organomet. Chem.* **1999**, *574*, 133; (d) Matsuda, I.; Sobue, H., unpublished results.

18 (a) Carter, M. J.; Fleming, I.; Percival, A. *J. Chem. Soc., Perkin Trans. I* **1981**, 2415; (b) Denmark, S.E. In *Comprehensive Organic Synthesis*; Trost, B.M.; Fleming, I.; Paquette, L.A. Eds.; Pergamon Press; Oxford, **1991**, Vol. 5, pp. 751–784; (c) Trost, B.M.; Mignani, S.M.; Nanninga, T.N. *J. Am. Chem. Soc.* **1988**, *110*, 1602.

19 (a) Matsuda, I.; Ogiso, A.; Sato, S. *J. Am. Chem. Soc.* **1990**, *112*, 6120; (b) Matsuda, I.; Niikawa, N. unpublished results; (c) Matsuda, I.; Sakakibara, J.; Nagashima, H. *Tetrahedron Lett.* **1991**, *32*, 7431; (d) Matsuda, I.; Tsuchihashi, T.; Takeuchi, K.; Sobue, H. unpublished results; (e) Matsuda, I.; Takeuchi, K.; Itoh, K. *Tetrahedron Lett.* **1999**, *40*, 2553.

20 (a) Matsuda, I.; Ishibashi, H.; Ii, N. *Tetrahedron Lett.* **1995**, *36*, 241; (b) Ojima, I.; Fracchiolla, D.A.; Donovan, R.J.; Banerji, P. *J. Org. Chem.* **1994**, *59*, 7594; (c) Ojima, I.; Fracchiolla Kass, D.; Zhu, J. *Organometallics* **1996**, *15*, 5191; (d) Ojima, I.; Zhu, J.; Vidal, E.S.; Fracchiolla Kass, D. *J. Am. Chem. Soc.* **1998**, *120*, 6690; (e) Matsuda, I.; Fukuta, Y.; Itoh, K. unpublished results.

21 (a) Muraoka, T.; Matsuda, I.; Itoh, K. *Tetrahedron Lett.* **1998**, *39*, 7325; (b) Muraoka, T.; Matsuda, I.; Itoh, K. *Organometallics* **2002**, *21*, 3650.

22 (a) Fukuta, Y.; Matsuda, I.; Itoh, K. *Tetrahedron Lett.* **1999**, *40*, 4703; (b) Ojima, I.; Vu, A.T.; Lee, S.; McCullagh, J. V.; Moralee, A.C.; Fujiwara, M.; Hoang, T.H. *J. Am. Chem. Soc.* **2002**, *124*, 9164.

23 Kobayashi, T.; Koga, Y.; Narasaka, K. *J. Organomet. Chem.* **2001**, *624*, 73.

7
Rhodium(I)-Catalyzed Cycloisomerization and Cyclotrimerization Reactions

Masaki Fujiwara and Iwao Ojima

7.1
Introduction

Highly efficient catalytic processes for the synthesis of natural and unnatural compounds of medicinal interest or functional materials play a central role in modern organic synthesis. The transformation of simple starting materials into monocyclic, bicyclic, and polycyclic scaffolds using transition metal-catalyzed cyclization reactions is one of the most powerful approaches to such methodology. Among the transition metal catalysts used in these reactions, rhodium complexes are particularly important because of their high efficiency and broad functional group tolerance.

The carbocyclizations of enynes, ynals, dienes, and diynes, as well as enediynes, dienynes, diynals, and triynes, are extremely important and useful reactions for the syntheses of a variety of carbocyclic compounds. Cascade carbocyclization is a powerful method, providing a rapid access to polycyclic skeletons in a single step. The term "carbocyclization" has been used to describe an annulation process involving carbon–carbon bond formation *via* carbometallation, which distinguishes it from radical cyclization as well as from thermal and photochemical cycloadditions. When the carbocyclization process incorporates carbon monoxide, this process is categorized as carbonylative carbocyclization, which provides efficient routes to cyclic and fused cyclic ketones. Excellent reviews have been published on transition metal-mediated carbocyclizations [1] and cycloadditions [2] covering the major advances in this field up to 1996. Metal-assisted cycloaddition reactions [3] and their applications to polysubstituted benzene derivatives [4] as well as to medium-sized ring syntheses [5], have also been reviewed. A review on the reactions involving hydrosilane, carbon monoxide, and unsaturated substrates promoted by transition-metal catalysts was published in 1996 [6]. This chapter describes recent advances in the rhodium-catalyzed carbocyclization processes, including various cascade- and carbonylative carbocyclizations.

Modern Rhodium-Catalyzed Organic Reactions. Edited by P. Andrew Evans

ISBN: 3-527-30683-8

7.2 Carbocyclization

7.2.1 Cycloisomerization of Enynes

7.2.1.1 Cycloisomerization

Transition metal-catalyzed intramolecular cycloisomerization of enynes represents one of the most useful carbocyclization reactions; specifically, the rhodium-catalyzed cycloisomerization of 1,6-enynes that provide 1,3- and 1,4-dienes with high degrees of regio- and stereoselectivity has been extensively studied. Cyclization of 1,6-enyne **1** catalyzed by $RhCl(PPh_3)_3$ gives 1-*exo*-methylene-2-cyclohexene **2** regioselectively, *via* a 6-*exo-trig* mode in 83% yield (Eq. 1) [7]. Substitution in the alkene moiety suppresses the cyclization significantly, while substitution of the terminal triple bond shuts down the reaction.

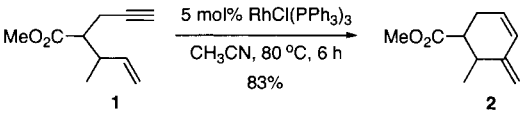

(1)

Cycloisomerization of enynes is also affected by cationic rhodium complexes generated *in situ* from $[RhL_2Cl]_2$ (L_2 = bidentate phosphorus ligand) and $AgSbF_6$. The 1,4-diphosphite ligand BICPO and the diphosphine ligands 1,4-diphenylphosphinobutane (dppb) and 1,2-diphenylphosphinoethane (dppe) have been demonstrated to promote this transformation. For example, the reaction of 1,6-enyne **3** affords the *exo*-3-ethylene-4-ethenylcyclopentane **4** in 90% yield using $[Rh(BICPO)Cl]_2$ as the catalyst precursor (Scheme 7.1) [8].

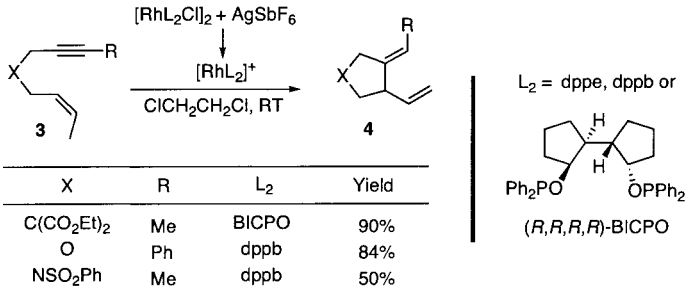

X	R	L_2	Yield
$C(CO_2Et)_2$	Me	BICPO	90%
O	Ph	dppb	84%
NSO_2Ph	Me	dppb	50%

Scheme 7.1

When (*R,R*)-Me-Duphos, (*R,R,R,R*)-BICPO [9] or BINAP [10] is used, the rhodium-catalyzed asymmetric cycloisomerization of **3** affords **4** with up to >99.5% enantiomeric excess (Scheme 7.2). This methodology was applied to the synthesis of functionalized α-methylene-γ-butyrolactone derivatives **6** such as (+)-pilocarpine **7** (Scheme 7.3) [11].

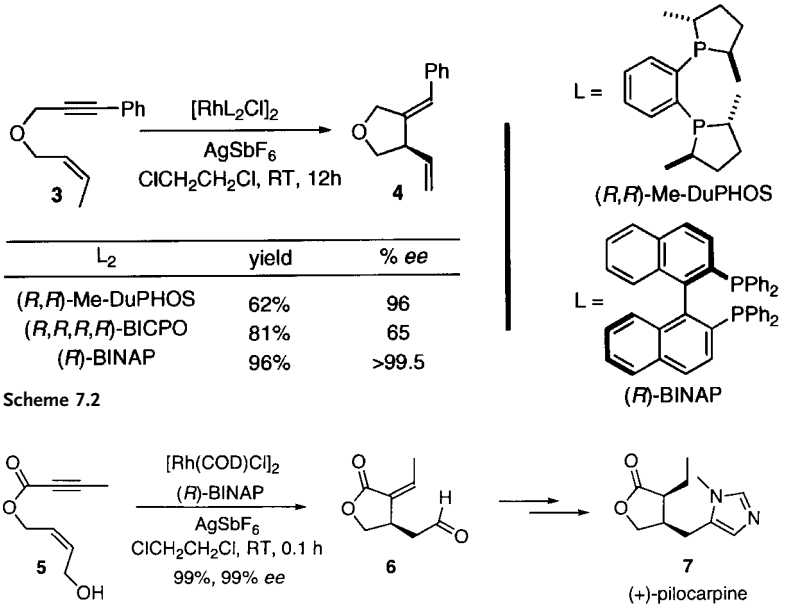

Scheme 7.2

Scheme 7.3

7.2.1.2 **Silylcarbocyclization (SiCaC and CO–SiCaC)**

In the first rhodium-catalyzed carbonylative silylcarbocyclization (CO–SiCaC), which was reported in 1992 [12, 13], silylcyclopentenone **9** was isolated as a minor product in the silylformylation of 1-hexyne **8** (Scheme 7.4). Under optimized conditions using Et_3SiH and $(^tBuNC)_4RhCo(CO)_4$ as the catalyst at 60 °C, **9** is formed in 54% yield [13]. A possible mechanism proposed for this intermolecular CO–SiCaC is shown in Scheme 7.4 [13]. In this mechanism, the formation of **9** is proposed to proceed *via* in-

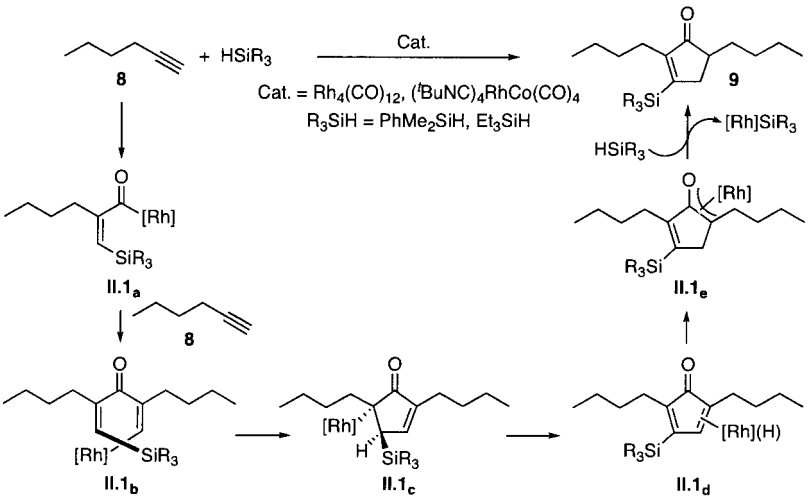

Scheme 7.4

termolecular trapping of the β-silylacryloyl–[Rh] complex **II.1$_a$** by another molecule of 1-hexyne to give intermediate **II.1$_b$**. Subsequent carbocyclization gives intermediate **II.1$_c$**, which undergoes β-hydride elimination to form cyclopentadienone–[Rh]H complex **II.1$_d$**. Highly regioselective hydrometallation of the olefin moiety at the sterically less congested site forms intermediate **II.1$_e$** and subsequent reductive elimination affords **9**.

A similar but different mechanism has also been proposed for the intermolecular CO–SiCaC reaction of phenylacetylene catalyzed by $Rh_4(CO)_{12}$, which gives silylcyclopentenone **9a** and **9b** (Scheme 7.5) [14]. In this mechanism β-silylethenyl–[Rh] intermediate **II.1$_g$**, arising from insertion of the alkyne moiety into the Si–[Rh] bond, reacts sequentially with a second molecule of phenylacetylene and CO, to afford δ-silylpentadienoyl–[Rh] complex **II.1$_h$**. Finally, carbocyclization followed by double-bond migration gives **9a** and **9b**.

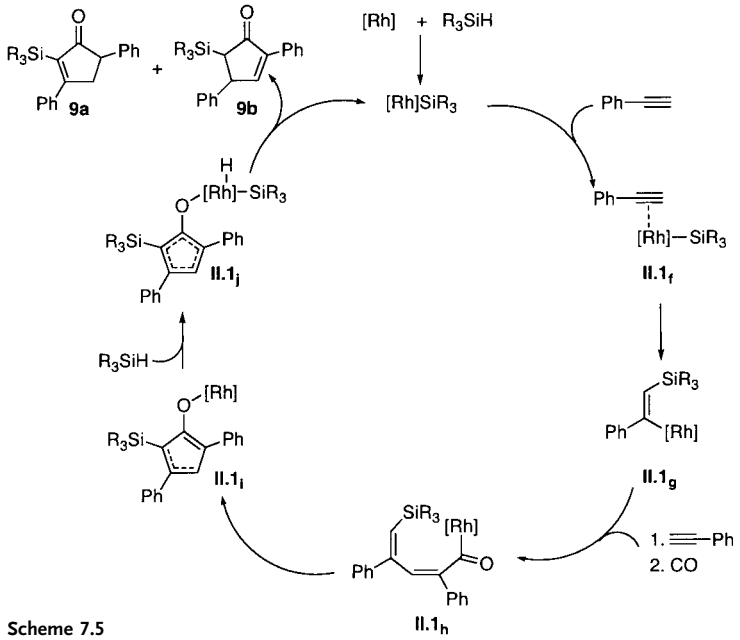

Scheme 7.5

Immediately after the discovery of the intermolecular CO–SiCaC reaction of 1-alkynes, the intramolecular version of the SiCaC reaction was investigated using 1,6-enynes [12]. For example, the reaction of allyl propargyl ether **10** with $PhMe_2SiH$, catalyzed by $Rh_2Co_2(CO)_{12}$, gave 3-(silylmethylene)-4-methylhydrofuran **11** in 62% yield. The result clearly indicates that the β-silylethenyl–[Rh] species can efficiently be trapped by the olefin moiety of a 1,6-enyne (Scheme 7.7) [12]. When the reaction of **10** was carried out under 10 atm CO using Et_3SiH, the CO–SiCaC reaction took place to give the corresponding aldehyde **12** as a minor product (10–15%) together with the silylformylation product **13** (70–75%) (Scheme 7.6) [12].

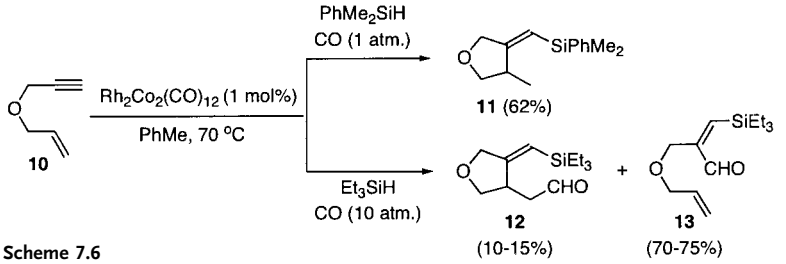

Scheme 7.6

The SiCaC reaction of enynes has been investigated in detail and applied to a wide range of substrates. Rhodium carbonyl clusters, such as $Rh_4(CO)_{12}$ and $Rh_2Co_2(CO)_{12}$, are very effective catalysts to promote this transformation. For example, the reaction of 1,6-enyne **14** (X=C($CO_2Et)_2$) with $PhMe_2SiH$ catalyzed by $Rh_4(CO)_{12}$ is complete within 1 minute at room temperature, giving the corresponding silylmethylene-2-methylcyclopentane **15** (X=C($CO_2Et)_2$) in 99% yield (Scheme 7.7) [15]. When the reaction of **14** is catalyzed by $Rh_4(CO)_{12}$ [16] or $Rh_4(CO)_{12}/P(OEt)_3$ [15] under 20 atm. CO, the CO–SiCaC reaction takes place to afford **16** almost exclusively (Schemes 7.8 and 7.9). The rhodium-catalyzed SiCaC and CO–SiCaC reactions show good functional group tolerance, and thus provide efficient methods for the construction of synthetically useful substituted cyclopentane, tetrahydrofuran, and pyrrolidine skeletons.

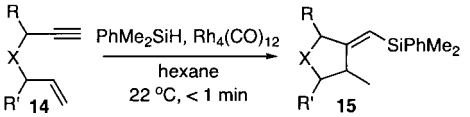

X	yield
$C(CO_2Et)_2$	99%
$C(CH_2OH)_2$	52%
$C(CH_2OAc)_2$	90%
N-Ts	86%
N-Bn	83%

Scheme 7.7

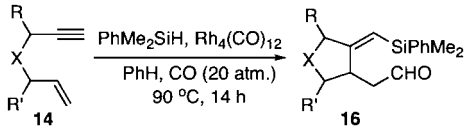

X	R	R'	yield
CMe_2	$OSiMe_3$	H	69%
CMe_2	H	$OSiMe_3$	66%

Scheme 7.8

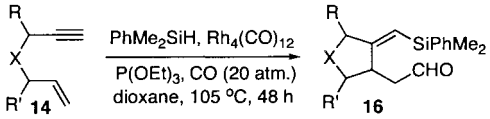

X	yield
$C(CO_2Et)_2$	91%
$C(CH_2OMe)_2$	83%
$C(CH_2OAc)_2$	91%
N-Ts	85%

Scheme 7.9

A proposed mechanism for the SiCaC and CO–SiCaC reactions of 1,6-enynes is illustrated in Scheme 7.10 [15, 17]. First, the acetylene moiety of enyne **14** regioselectively inserts into the Si–metal bond of the catalytically active R_3Si-[M_n](H) species **II.1$_k$** to form *β*-silylalkenyl–[M_n] intermediate **II.1$_l$**, which is followed by carbocyclization to give intermediate **II.1$_m$**. At this point the pathways leading to the formation of SiCaC **15** and CO–SiCaC product **16** diverge. The SiCaC product **15** is formed through reductive elimination of **II.1$_m$** promoted by another molecule of hydrosilane to regenerate the R_3Si–[M_n](H) species **II.1$_k$**. When CO insertion into the carbon–metal bond of **II.1$_m$** is faster than reductive elimination, acyl–[Rh] intermediate **II.1$_n$** is formed. Subsequent reductive elimination gives CO–SiCaC product **16** and regenerates **II.1k**.

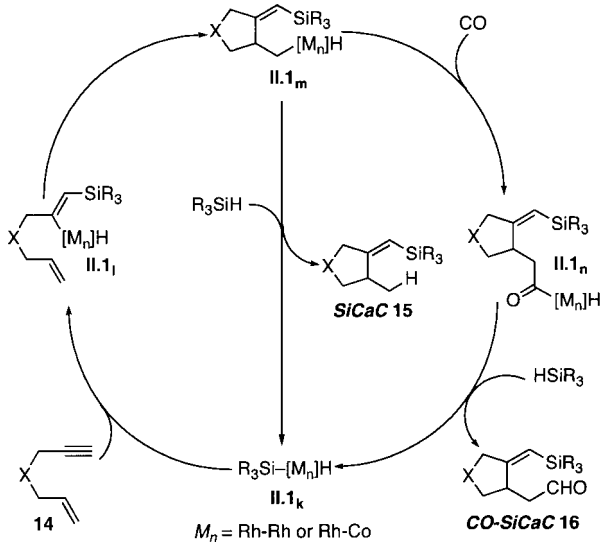

Scheme 7.10

The SiCaC reaction is applicable to the construction of bicyclic skeletons. For example, the reaction of the cyclohexenyl(propargyl)malonate **17** affords the corresponding bicyclo[4.3.0] ring system **18** (Eq. 2) [15]. In this case, this reaction proceeds by the proposed mechanism for the rhodium-catalyzed SiCaC reaction, but is terminated through *β*-hydride elimination rather than reductive elimination. This methodology can be generalized by using 1,6-enyne **19** as the substrate, to give 1-*exo*-methylene-5-ethenylcyclopentane **20** (Eq. 3) [18]. When (*R*)-BIPHEMP is used, the rhodium-catalyzed asymmetric silylcarbocyclization of 1,6-enyne **21** affords 1-*exo*-methylene-5-methylcyclopentane **22** with up to 92% enantiomeric excess (Eq. 4) [19].

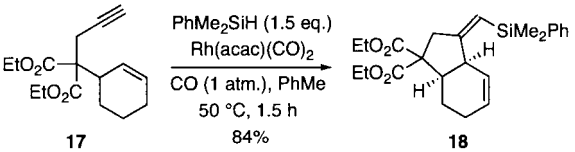

(2)

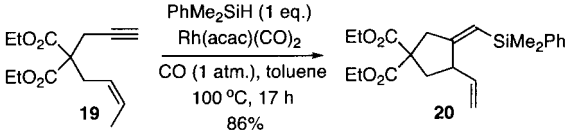

(3)

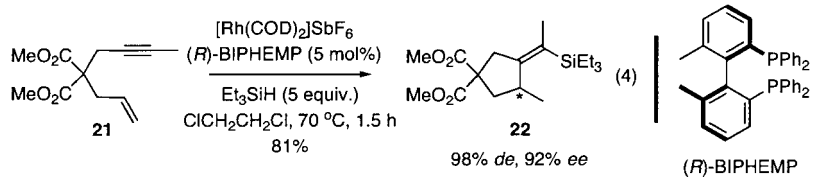

(4)

7.2.2
Silylcarbocyclization of Ynals

The SiCaC reaction of 5-hexyn-1-al **23** gives the corresponding 2-(*exo*-silymethylene)-1-cyclopentanol **24** in high yield (Scheme 7.11) [20]. The reaction is accelerated by *gem*-disubstitution; for example, the reaction of 3,3-*gem*-disubstituted 5-hexyn-1-al **23** (X = $C(CO_2Et)_2$, $C(CH_2OMe)_2$) is substantially faster and cleaner than the unsubstituted derivative ($X=CH_2$), which is accompanied by a small amount of silylformylation product [21]. It should also be noted that the formation of 1-siloxy-2-methylenecyclopentane is not observed, in sharp contrast with the nickel-catalyzed version of this reaction [20].

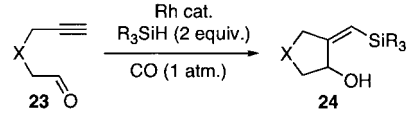

X	time	yield
$C(CO_2Et)_2$	24 h	86%
$C(CH_2OMe)_2$	24 h	80%
CH_2	72 h	80%

Scheme 7.11

7.2.3
Cycloisomerization of Dienes

Cycloisomerization of 1,6-diene **25** is effected by a number of transition metal catalysts. For example, both rhodium trichloride [22, 23] and Wilkinson's catalyst [24, 25] promote this reaction efficiently to give methylenecyclopentane **26** (Scheme 7.12). In the latter case, the active catalyst species is believed to be $[Rh(PPh_3)_2HCl_2]$. A mechanism proposed for this cycloisomerization is shown in Scheme 7.13. Coordination of a diene to $[Rh(PPh_3)_2HCl_2]$ and insertion of one of the olefin moieties of the diene into the [Rh]–H bond gives complex $\mathbf{II.3_a}$. Carbocyclization affords alkyl–[Rh] intermediate $\mathbf{II.3_b}$. Subsequent reductive elimination of the methylenecyclopentane regenerates the active catalyst species.

X	[Rh]	yield
NCO^nPr	$RhCl_3$	83%
$C(CO_2Et)_2$	$Rh(PPh_3)_3Cl$	90%

Scheme 7.12

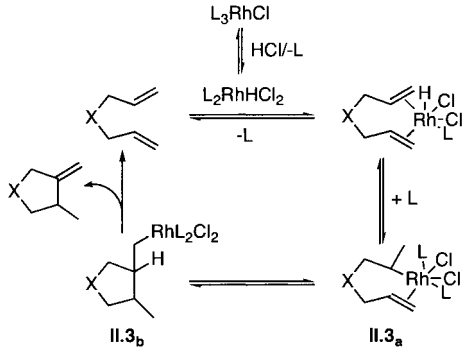

Scheme 7.13

Rhodium(I) complexes have also been shown to promote metallo-ene type reactions efficiently (Scheme 7.14) [26]. Typically, the reaction of 2,7-octadienyl-1-carbonate **27** is carried out using the $RhH(PPh_3)_4$-*tris*(2,4,6-trimethoxyphenyl)phosphine system as the catalyst in acetic acid at 80 °C for 1–1.5 h, to give the corresponding 1-*exo*-methylene-2-ethenylcyclopentane **28** in high yield.

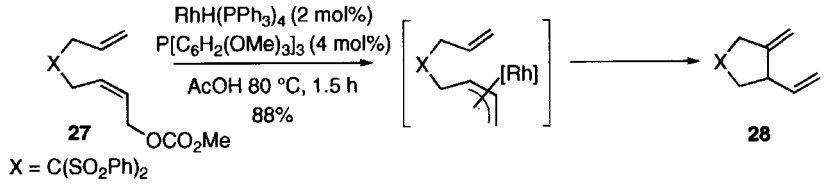

Scheme 7.14

The reaction of 5-aza-2,7-nonadienyl-1-carbonate **29** gives 3,4-diethenylpyrrolidine **30** with reasonable *cis*-selectivity (Eq. 5), whereas 1-(*trans*-4-acetoxycyclohexenyl)allylmalonate **31** affords *cis*-fused *exo*-methylenebicyclo[4.3.0]nonene **32** exclusively (Eq. 6).

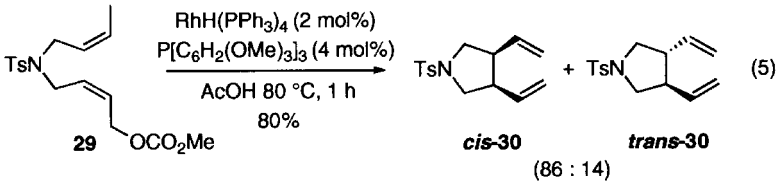

(5)

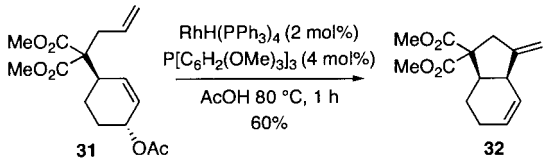

(6)

7.2.4

Silylcarbocyclization of Diynes

Silylcarbocyclization of diyne **33** catalyzed by $Rh_4(CO)_{12}$ gives silylated bis-*exo*-methylidenecyclopentane **34**, as well as dimer **35** and trimer **36** (Eq. 7) [27a] The product selectivity was improved by using $Rh(H)(SiR_3)(PPh_3)_2Cl$ (Eq. 8) [27b] or a cationic Rh–BINAP complex (Eq. 9) [28] to yield 1,2-bis-*exo*-dialkylidenecyclopentane **38** or **40**. This silicon-initiated diyne carbocyclization is applicable to a variety of functionalized diynes possessing terminal and internal alkynes to afford the corresponding 1,2-bis-*exo*-alkylidenecyclopentanes in moderate to good yield with high stereoselectivity [27b, 28].

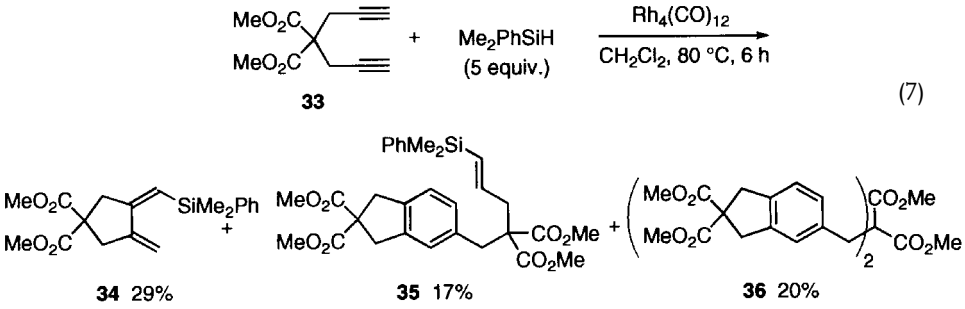

(7)

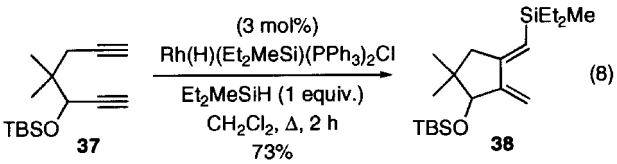

(8)

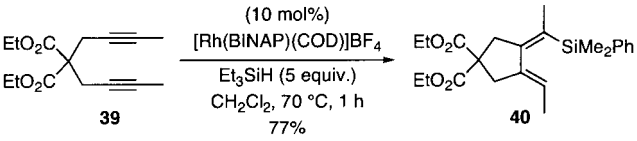

(9)

Rhodium-catalyzed three-component domino coupling of 1,6-diyne **41**, hydrosilane, and C_{60} proceeds to give fullerene adduct **42** in good yield (Eq. 10) [29]. In this case, dienophile C_{60} does not interfere with the silylcarbocyclization process and traps the 1,2-bis-*exo*-methylidenecyclopentane intermediates to furnish the corresponding C_{60}-linked carbo- or heterocycle **42**.

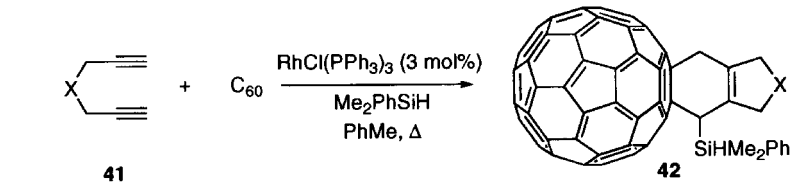

41
X = $C(CO_2Me)_2$, O, NTs

42 (10)

7.3
Cascade Carbocyclization

7.3.1
Cyclotrimerization of Triynes or Dienynes

Transition metal-catalyzed intermolecular [2+2+2] cyclotrimerization of alkynes to benzene derivatives has been extensively studied. In this section, the focus is on the cyclotrimerizations of the substrates bearing three independent unsaturated bond components. The key issue with this type of process usually involves the challenge of controlling regioselectivity [1–4]. However, 1,3,5-trisubstituted benzene **44** can be obtained as the sole product in good yield when 3-butyn-2-one **43** is used as the substrate for the cyclotrimerization catalyzed by $Rh_2(pfb)_4$ (pfb = perfluorobutyrate) in the presence of Et_3SiH under a CO atmosphere (Eq. 11) [30].

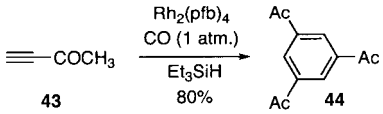

43 44 (11)

A cationic rhodium complex-catalyzed codimerization of 1,3-dienes with alkynes gives the corresponding cyclohexadienes in good yields with high regioselectively, as exemplified in the reaction of 2-methyl-1,3-butadiene with phenylacetylene (Eq. 12) [31].

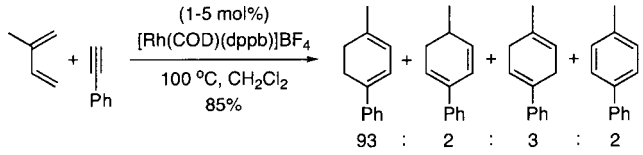

(12)

A bimetallic rhodium complex has also been employed for the cyclotrimerization of (trifluoromethyl)acetylene **45** at room temperature to afford 1,3,5-trifluoromethylbenzene **46** in good yield (Eq. 13) [32].

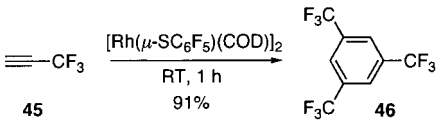

(13)

It is possible to carry out the [2+2+2] cyclotrimerization reaction in a regioselective manner by using a partially or completely intramolecular approach. Rhodium-catalyzed intramolecular cyclotrimerization of 1,6,11-triynes, which construct fused 5–6–5 ring-systems, has been studied extensively [33–36]. Cyclization of 1,6,11-triyne **47** catalyzed by $RhCl(PPh_3)_3$, gives the tricyclic benzene **48** in good yield (Eq. 14) [33a].

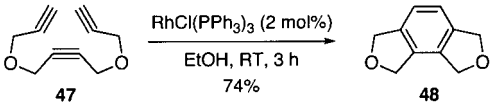

(14)

This rhodium-catalyzed intramolecular cyclotrimerization method has been utilized as the key step for the synthesis of the marine illudalane sesquiterpenoid, alcyopterosin E, **51**, which has a fused 5–6–5 ring system as illustrated in Scheme 7.15 [37].

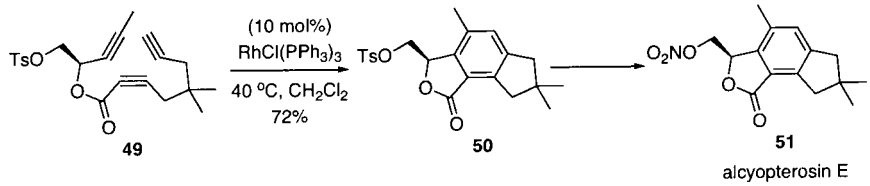

Scheme 7.15

An interesting application of the rhodium-catalyzed cyclotrimerization of diynes with alkynes to the synthesis of *C*-acyl glycosides has been reported, wherein ethynylglycal **52** (Eq. 15), as well as diethynylglucose derivative **54** (Eq. 16), are employed to give the corresponding adducts **53** and **55**, respectively [38].

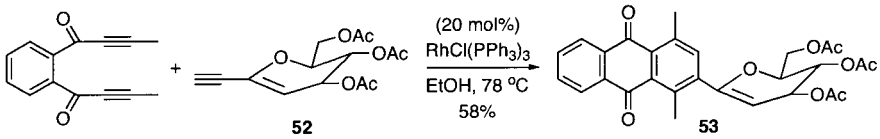

(15)

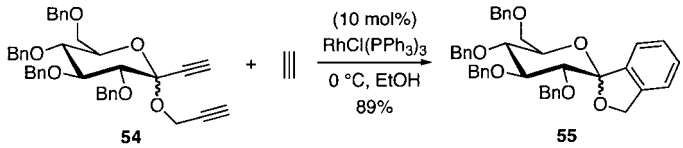

(16)

Inter- and intramolecular alkyne cyclotrimerizations of **57** catalyzed by $RhCl(PPh_3)_3$ afford substituted carbazoles that are relevant to natural product and drug-related synthe-

ses (Scheme 7.16) [39]. Thus, the A to ABC ring or A to ABCD ring-construction, starting from readily available 2-iodoaniline **56**, provides a highly efficient approach to the synthesis of a variety of substituted carbazoles **58** in good to excellent yield.

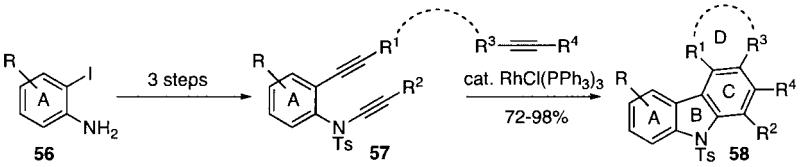

Scheme 7.16

Rhodium-catalyzed alkyne cyclotrimerization is also applicable to the synthesis of a polyalkyne substrate bearing ether-linked 1,6-diyne moieties **59**, which is easily prepared by Pd–Cu-catalyzed Sonogashira coupling reactions. These reactions provide a novel and efficient synthetic route to oligophenylene **60**, which bears benzodihydrofuran moieties (Scheme 7.17) [40].

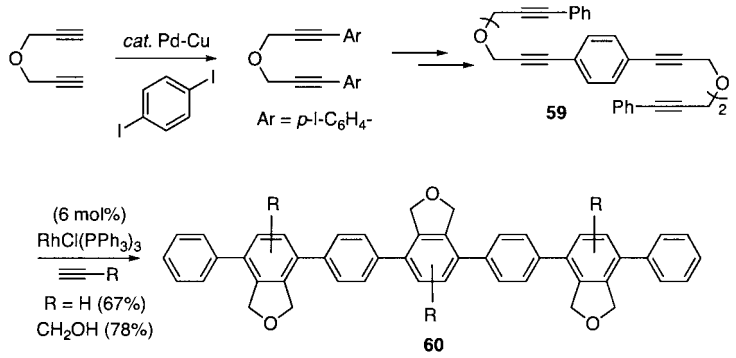

Scheme 7.17

A combination of the alkyne cyclotrimerization catalyzed by $RhCl(PPh_3)_3$ with a 1,3-dipolar cycloaddition provides rapid access to 3-dihydroindenylmethyl-3,7-diaza[3.3.0]-octane **61** in excellent yield; thus five new bonds, four stereocenters, and three rings are created in a one-pot operation (Scheme 7.18) [41].

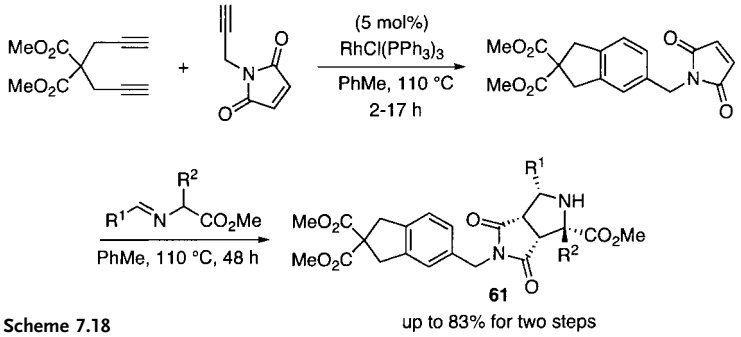

Scheme 7.18

Metal-catalyzed [4+2+2] cyclotrimerizations of either heteroatom-containing enyne **62** with 1,3-butadiene (Eq. 17) [42] or heteroatom-containing dienyne **64** with an alkyne (Eq. 18) [43] are effected by cationic rhodium complexes generated *in situ* from a chlororhodium complex modified with silver salts. These processes afford eight-membered ring products **63** and **65**, respectively. In both processes, the nature and amount of the silver salt profoundly affect the outcomes.

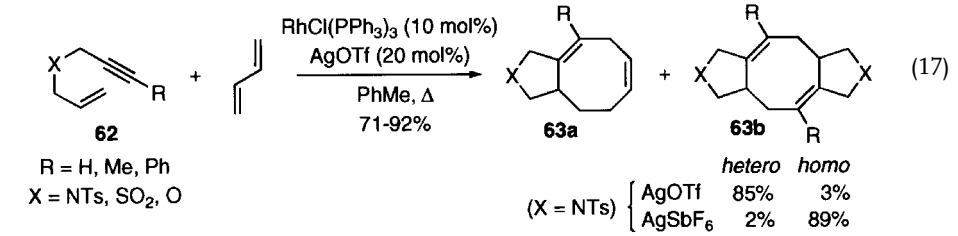

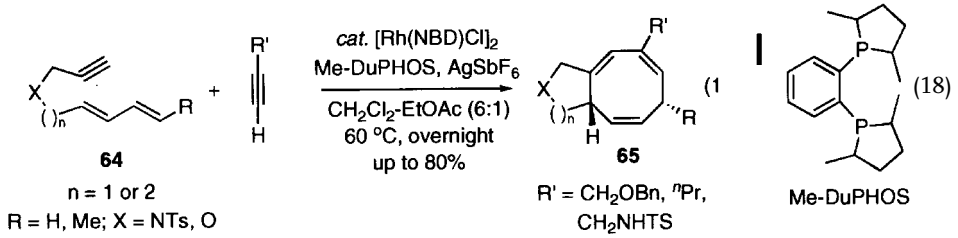

A novel, one-step entry to an unprecedented polycyclic ring system from a 1,6,11-dienyne is illustrated in Scheme 7.19 [36]. The $[Rh(OCOCF_3)_2]_2$-catalyzed cascade cycloisomerization of dienyne **66** proceeds through isomerization of the metallabiscyclooctane **III.1**$_a$ to the bicyclic carbene intermediate **III.1**$_b$, which then gives the fused tetracyclic product **67** as single diastereomer. Other transition metal complexes such as $[RuCl_2(CO)_3]_2$ and $PtCl_2$ also demonstrate catalytic activity for this complex transformation.

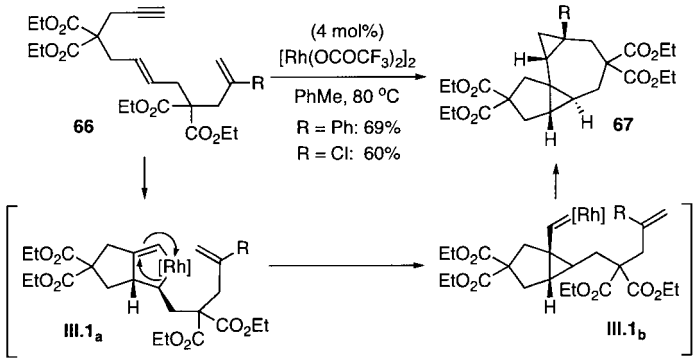

Scheme 7.19

7.3.2

Cascade Silylcarbocyclization of Enediynes, Triynes (SiCaT), and Diynals

Cascade silylcarbocyclization reactions have been developed based on the fact that it is possible to realize successive intramolecular carbocyclizations, as long as the competing reductive elimination is slower than the carbometallation. For example, the reaction of dodec-6-ene-1,11-diyne **67** with $PhMe_2SiH$ catalyzed by $Rh(acac)(CO)_2$ at 50 °C under 1 atm CO gives bis(*exo*-methylenecyclopentyl) **68** in 55% yield [44]. The reaction is stereospecific: that is, (6*E*)- and (6*Z*)-dodec-6-ene-1,11-diynes, (*E*)-**67** and (*Z*)-**67**, afford (*R**,*R**)-**68** and (*S**,*R**)-**68** respectively. A possible mechanism for this reaction is outlined in Scheme 7.20. It should be noted that none of the tricyclic product is formed even though a third carbocyclization in the intermediate $\mathbf{III.2_c}$ is conceptually possible.

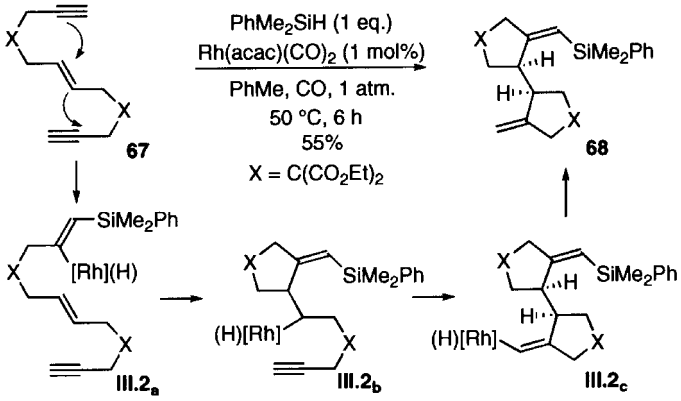

Scheme 7.20

Replacement of the carbon–carbon double bond in **67** with a triple bond connecting the two other alkyne moieties allows the third cyclization to occur in a cascade SiCaC process. Thus, the silylcarbotricyclization (SiCaT) of a variety of triynes **69** is effectively catalyzed by rhodium-complexes such as $Rh(acac)(CO)_2$, $[Rh(COD)Cl]_2$, $[Rh(NBD)Cl]_2$, $Rh_4(CO)_{12}$, and $Rh_2Co_2(CO)_{12}$ to give the corresponding fused tricyclic benzene derivatives **70** and **71** in good to excellent yield (Eq. 19) [45]. The reactions, catalyzed by rhodium carbonyl clusters $Rh_4(CO)_{12}$ and $Rh_2Co_2(CO)_{12}$, proceed smoothly at room temperature with high selectivity for the formation of **70**. It is worth mentioning that the SiCaT reaction is applicable to 1,7,12- and 1,7,13-triynes to afford 6–6–5 and 6–6–6 fused tricyclic benzene derivatives, respectively [45].

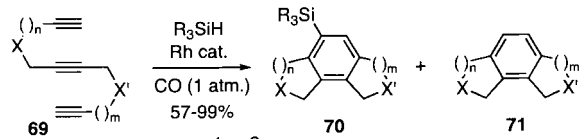

(19)

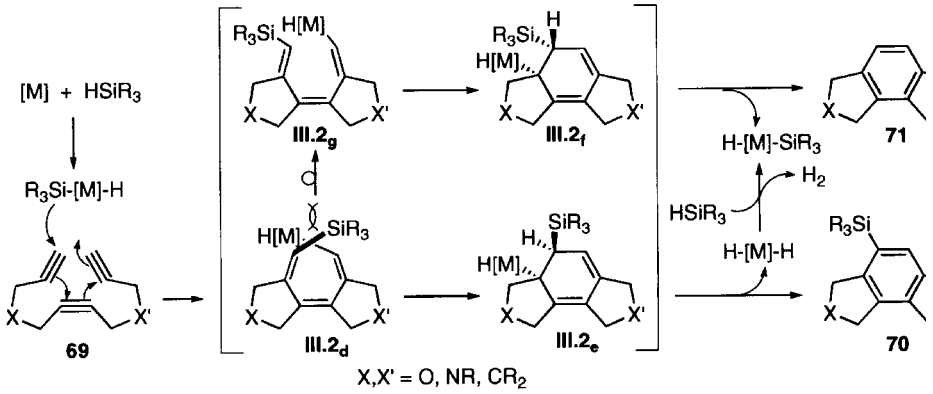

Scheme 7.21

A proposed mechanism for the SiCaT reaction using the 1,6,11-triyne system as an example is illustrated in Scheme 7.21. The reaction proceeds through insertion of one of the terminal alkynes into the Si–[Rh] bond of the hydrosilane–[Rh] oxidative adduct, generating an ethenyl–[Rh] intermediate, which undergoes addition to the second and third alkyne moieties to form intermediate **III.2$_d$**. Subsequent carbocyclization followed by β-hydride elimination gives the tricyclic silylbenzene derivative **70**. Alternatively, ethenyl–[Rh] intermediate **III.2$_d$** can be isomerized to the thermodynamically more favorable intermediate **III.2$_g$** *via* a zwitterionic carbene species, that is, by the "Ojima–Crabtree mechanism" [46, 47]. Subsequent carbocyclization gives **III.2$_f$**, which undergoes β-silyl elimination to afford nonsilylated product **71**.

The cascade silylcarbocyclization is applicable to diynals. For example, the reaction of undec-1,6-diyn-11-al **72** with $PhMe_2SiH$, catalyzed by $Rh(acac)(CO)_2$ affords the corresponding silylated *exo*-silylmethylene(hydroxy)bis(cyclopentylidene) **73** (Eq. 20) [48].

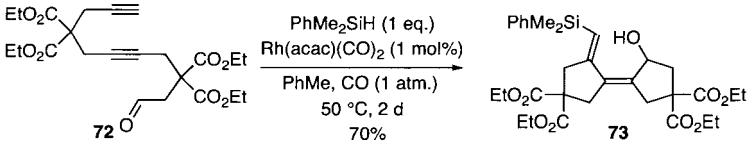

(20)

The reaction of enediyne **74** in which the olefin moiety is located as a part of the cyclohexenyl ring proceeds through a cascade SiCaC bicyclization process, followed by β-hydride elimination, to give tricyclic *exo*-silylmethylene-bis(cyclopentylidene) **75** in good yield (Eq. 21) [48].

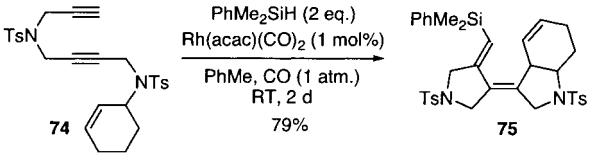

(21)

7.4
Carbonylative Carbocyclization

7.4.1
Silylcyclocarbonylation (SiCCa) of Aminoalkynes

The reaction of 1-propargyltetrahydroisoquinoline **76** with $PhMe_2SiH$, catalyzed by $Rh(acac)(CO)_2$ at 60 °C and 50 atm. CO furnished the silylcyclocarbonylation (SiCCa) product **77** in 65% yield (Eq. 22) [49]. The SiCCa reaction has been applied to the syntheses of enantiopure indolizidine skeletons, where the aminolysis of the acyl–[Rh] bond took place instead of reductive elimination after silylmetallation of the alkyne moiety [49].

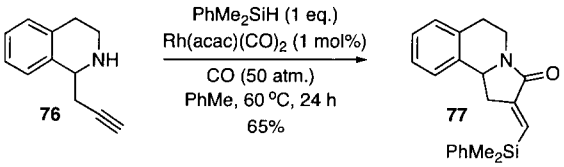

(22)

7.4.2
Silylcarbobicyclization (SiCaB) of 1,6-Diynes

The reaction of 4,4-*gem*-bis(carbethoxy)hepta-1,6-diyne **78a** ($X=C(CO_2Et)_2$) with $^tBuMe_2SiH$ at 50 °C and 15 atm. CO affords 2-silylbicyclo[3.3.0]oct-$\Delta^{1,5}$-en-3-one **79** in 98% yield (Scheme 7.22) [50, 51]. Compound **79a** can be quantitatively isomerized to the more stable 2-silylbicyclo[3.3.0]oct-1-en-3-one **80a** using a catalytic amount of $RhCl_3 \cdot 3H_2O$.

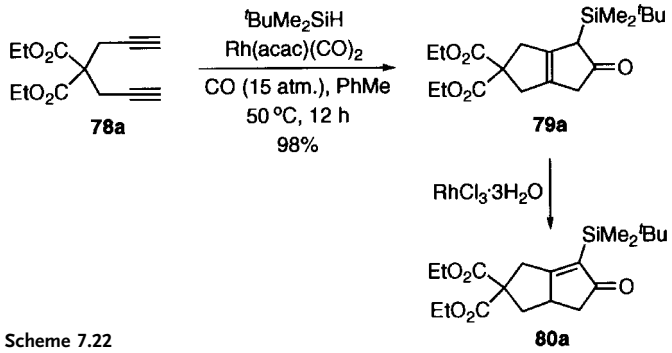

Scheme 7.22

Another type of SiCaB reaction takes place when the 4-position is a basic amine moiety. For example, the reaction of *N*-benzyl-, *N*-^{n}hexyl- or *N*-allyldipropargylamine **78b** with Et_3SiH catalyzed by $Rh(acac)(CO)_2$ at 65 °C and 50 atm. CO affords the corresponding 2-silyl-7-azabicyclo[3.3.0]octa-5,8-dien-3-one **80b** as the predominant or sole product (Scheme 7.23).

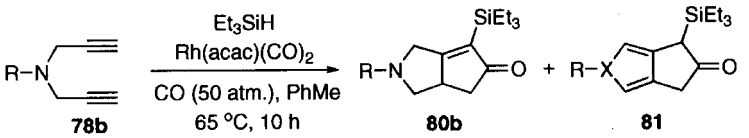

R	yield (%)	80b/81
Bn	66	97/3
^{n}hexyl	58	100/0
allyl	62	100/0

Scheme 7.23

7.4.3 Carbonylative Carbotricyclizations (CO–SiCaT and CO–CaT) of Enediynes

In the contrast to the SiCaT reaction of triynes (*vide supra*), when an enediyne has an olefin at the terminal position a novel silicon-initiated carbonylative carbotricyclization (CO–SiCaT) reaction takes place, incorporating CO into the product [52]. As Scheme 7.24 indicates, the reaction of dodec-11-ene-1,6-diynes **82** catalyzed by $Rh(acac)(CO)_2$ under 1 atm. CO affords the corresponding cyclopenta[*e*]azulenes **83** in good to excellent yield.

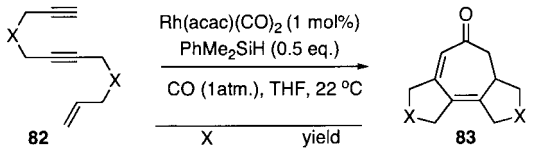

X	yield
$C(CO_2Et)_2$	92%
$C(CH_2OH)_2$	62%
N-Ts	85%
O	50%

Scheme 7.24

A proposed mechanism for the CO–SiCaT reaction is illustrated in Scheme 7.25. The reaction begins with the extremely regioselective insertion of the terminal alkyne moiety into the Si–[Rh] bond of the hydrosilane–[Rh] oxidative adduct, $H[Rh]SiR_3$. The second carbocyclization leads to the formation of bis(cyclopentylidene)methyl–[Rh] complex **IV.3**$_c$ arising from the *Z*- to *E*-isomerization of the ethenyl–Si bond *via* the "Ojima-Crabtree mechanism" (see Scheme 7.21) [46, 47]. The CO insertion into the [Rh]–C bond of **IV.3**$_c$ gives acyl–[Rh] intermediate **IV.3**$_d$, which undergoes carbocyclization to form the tricyclic intermediate **IV.3**$_e$. Subsequent β-silyl elimination affords the fused 5–7–5 tricyclic product **83** and regenerates the active catalyst, $H[Rh]SiR_3$. When one equivalent or more of hydrosilane is used, reductive elimination (that is, hydride shift) is accelerated so that products **84** and **85** are obtained in addition to **83** [52]. It is noteworthy that cyclopenta[*e*]azulene **85** is the exclusive product under optimized conditions that employ a catalytic amount of the hydrosilane.

When the carbotricyclization reaction of **82** is carried out in the absence of hydrosilane using $[Rh(COD)Cl]_2$ as the specific catalyst, a novel [2+2+2+1] reaction (CO–CaT) takes place to give the same cyclopenta[*e*]azulene **83** accompanied by a small amount of 5–6–5 fused tricyclic product **86** (Scheme 7.26) [53]. It is noteworthy that an attempted CO–

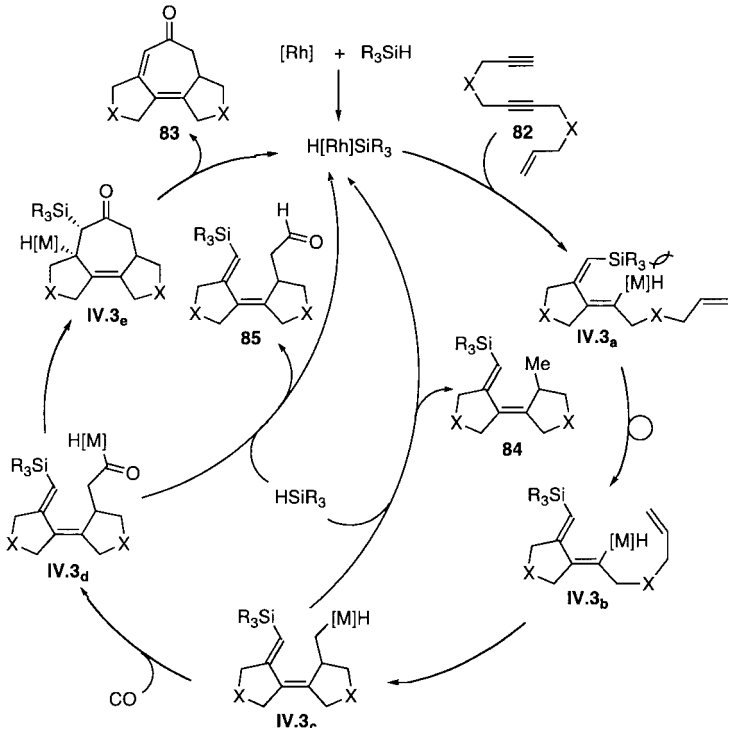

Scheme 7.25

SiCaT reaction of **82** (R = H, X = Y = $C(CO_2Et)_2$) with $PhMe_2SiH$, in the presence of this rhodium catalyst, afforded **86** (R = H, X = Y = $C(CO_2Et)_2$) as the exclusive product. Interestingly, none of the CO–SiCaT/CO–CaT product **83** was formed in this reaction. Thus, it is clearly indicated that the CO–CaT reaction involves metallacycle intermediates, which makes a sharp contrast to the mechanism of CO–SiCaT reaction.

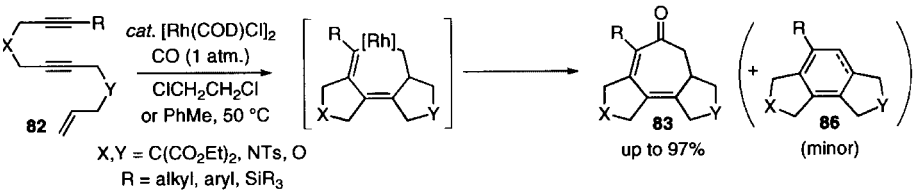

Scheme 7.26

7.4.4
Carbonylative Silylcarbobicyclization of Diallenes

Diallenes undergo rhodium-catalyzed cascade carbobicyclization similar to the SiCaB reaction (see Section 4.2) [21]. For example, the reaction of diallene **87** with $PhMe_2SiH$ catalyzed by $Rh(acac)(CO)_2$ at ambient temperature and pressure of CO gives *cis*-2-

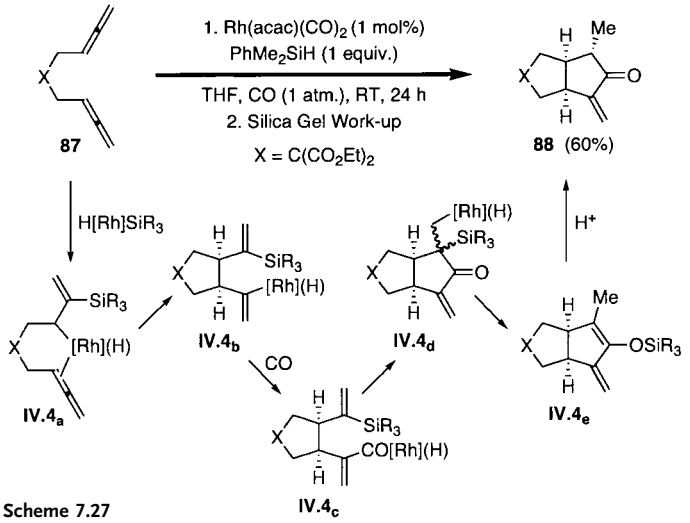

Scheme 7.27

methyl-4-methylenebicyclo[3.3.0]octan-3-one **88** (X=C(CO_2Et)$_2$) in 60% yield (Scheme 7.27). The reaction starts with the insertion of one of the allene moieties of **87** into the Si–[Rh] bond of the active catalyst species to give σ-alkyl–[Rh] intermediate **IV.4$_a$**. Insertion of the second allene moiety (giving **IV.4$_b$**) and CO (yielding **IV.4$_c$**), followed by carbocyclization, leads to the bicyclo[3.3.0]octanonylmethyl–[Rh] **IV.4$_d$**. Subsequent reductive elimination and 1,3-Si shift affords enoxysilane **IV.4$_e$**, which is hydrolyzed to give **88** on silica gel.

7.5 Conclusion

Recent advances in the carbocyclizations catalyzed by rhodium complexes are described in the context of cycloisomerization, silylcarbocyclizations (SiCaC and others), carbonylative silylcarbocyclization (CO–SiCaC, SiCaB), cyclotrimerization, cascade silylcarbocyclizations (bicyclizations, SiCaT), and carbonylative carbocyclizations (CO–SiCaT, CO–CaT). These reactions serve as efficient and useful methods for the syntheses of a variety of heterocycles and carbocycles that have importance in both medicinal and materials chemistry. In most cases, the reactions proceed under catalytic conditions to afford products with a high degree of regio-, diastereo-, and/or enantioselectivity, which gives additional value to such methods for organic synthesis.

7.6 References

1 Ojima, I.; Tzamarioudaki, M.; Li, Z.; Donovan, R.J. *Chem. Rev.* **1996**, *96*, 635.
2 Lautens, M.; Klute, W.; Tam, W. *Chem. Rev.* **1996**, *96*, 49.
3 Frühauf, H.-W. *Chem. Rev.* **1997**, *97*, 523.
4 Saito, S.; Yamamoto, Y. *Chem. Rev.* **2000**, *100*, 2901.
5 Yet, L. *Chem. Rev.* **2000**, *100*, 2963.
6 Chatani, N.; Murai, S. *Synlett* **1996**, *5*, 414.
7 Grigg, R.; Stevenson, P.; Worakun, T. *Tetrahedron* **1988**, *44*, 4967.
8 Cao, P.; Wang, B.; Zhang, X. *J. Am. Chem. Soc.* **2000**, *122*, 6490.
9 Cao, P.; Zhang, X. *Angew. Chem., Int. Ed. Engl.* **2000**, *39*, 4104.
10 Lei, A.; He, M.; Wu, S.; Zhang, X. *Angew. Chem. Int. Ed. Engl.* **2002**, *41*, 3457.
11 Lei, A.; He, M.; Zhang, X. *J. Am. Chem. Soc.* **2002**, *124*, 8198.
12 Ojima, I.; Donovan, R.J.; Shay, W.R. *J. Am. Chem. Soc.* **1992**, *114*, 6580.
13 Ojima, I.; Donovan, R.J.; Eguchi, M.; Shay, W.R.; Ingallina, P.; Korda, A.; Zeng, Q.P. *Tetrahedron* **1993**, *49*, 5431.
14 Matsuda, I.; Fukuta, Y.; Tsuchihashi, T.; Nagashima, H.; Itoh, K. *Organometallics* **1997**, *16*, 4327.
15 Ojima, I.; Vu, A.T.; Lee, S.-Y.; McCullagh, J.V.; Moralee, A.C.; Fujiwara, M.; Hoang, T.H. *J. Am. Chem. Soc.* **2002**, *124*, 9164.
16 Fukuta, Y.; Matsuda, I.; Itoh, K. *Tetrahedron Lett.* **1999**, *40*, 4703.
17 Ojima, I.; Li, Z. In *Catalysis by Di- and Polynuclear Metal Complexes*; Adams, R.A.; Cotton, F.A., Eds.; John Wiley & Sons: Chichester, **1998**, pp. 307–343.
18 Ojima, I.; Fujiwara, M. **2002**, unpublished results.
19 Chakrapani, H.; Liu, C.; Widenhoefer, R.A. *Org. Lett.* **2003**, *5*, 157.
20 Ojima, I.; Tzamarioudaki, M.; Tsai, C.Y. *J. Am. Chem. Soc.* **1994**, *116*, 3643.
21 Lee, S.-Y. Ph.D. Thesis, State University of New York at Stony Brook, **2000**.
22 Schmitz, E.; Heuck, U.; Habisch, D. *J. Prakt. Chem.* **1976**, 471.
23 Schmitz, E.; Urban, R.; Heuck, U.; Zimmermann, G.; Gründemann, E. *J. Prakt. Chem.* **1976**, 185.
24 Grigg, R.; Mitchell, T.R.B.; Ramasubbu, A. *J. Chem. Soc., Chem. Commun.* **1980**, 27.
25 Grigg, R.; Malone, J.F.; Mitchell, T.R.B.; Ramasubbu, A.; Scott, R.M. *J. Chem. Soc., Perkin Trans. 1* **1984**, 1745.
26 Oppolzer, W.; Fürstner, A. *Helv. Chim. Acta* **1993**, *76*, 2329.
27 (a) Muraoka, T.; Matsuda, I.; Itoh, K. *Tetrahedron Lett.* **1998**, *39*, 7325. (b) Muraoka, T.; Matsuda, I.; Itoh, K. *Organometallics* **2002**, *21*, 3650.
28 Liu, C.; Widenhoefer, R.A. *Organometallics* **2002**, *21*, 5666.
29 Muraoka, T.; Asaji, H.; Yamamoto, Y.; Matsuda, I.; Itoh, K. *Chem. Commun.* **2000**, 199.
30 Doyle, M.P.; Shanklin, M.S. *Organometallics* **1994**, *13*, 1081.
31 Matsuda, I.; Shibata, M.; Sato, S.; Izumi, Y. *Tetrahedron Lett.* **1987**, *28*, 3361.
32 Garcia, J.J.; Sierra, C.; Torrens, H. *Tetrahedron Lett.* **1996**, *37*, 6097.
33 For rhodium-catalyzed [2+2+2] acetylene cyclotrimerizations, see: (a) Grigg, R.; Scott, R.; Stevenson, P. *Tetrahedron Lett.* **1982**, *23*, 2691. (b) Grigg, R.; Scott, R.; Stevenson, P. *J. Chem. Soc., Perkin Trans. 1* **1988**, 1357. (c) Neeson, S.J.; Stevenson, P.J. *Tetrahedron Lett.* **1988**, *29*, 813. (d) Neeson, S.J.; Stevenson, P.J. *Tetrahedron* **1989**, *45*, 6239. (e) Neidlein, R.; Kux, U. *Helv. Chim. Acta* **1994**, *77*, 1051; see also: ref. 34.
34 For rhodium-catalyzed hetero-[2+2+2] with nitriles: (a) Diversi, P.; Ermini, L.; Ingrosso, G.; Lucherrini, A. *J. Organomet. Chem.* **1993**, *447*, 291 and references cited therein. (b) Ingrosso, G.; Ronca, P.; Cioni, P. Italian Patent 1 164 249, May 27, **1983**. (c) Cioni, P.; Diversi, P.; Ingrosso, G.; Lucherrini, A.; Ronca, P. *J. Mol. Catal.* **1987**, *40*, 337.
35 For Rh-catalyzed [2+2+2] cycloadditions of acetylenes with olefins, see: (a) Singleton, D.M. *Tetrahedron Lett.* **1973**, 1245. (b) Grigg, R.; Scott, R.; Stevenson, P. *J. Chem. Soc., Perkin Trans. 1* **1988**, 1365.
36 Chatani, N.; Kataoka, K.; Murai, S.; Furukawa, N.; Seki, Y. *J. Am. Chem. Soc.* **1998**, *120*, 9104.

37 Witulski, B.; Zimmermann, A.; Gowans, N.D. *Chem. Commun.* **2002**, 2984.

38 McDonald, F.E.; Zhu, H.Y.H.; Holmquist, C.R. *J. Am. Chem. Soc.* **1995**, *117*, 6605.

39 Witulski, B.; Alayrac, C. *Angew. Chem. Int. Ed.* **2002**, *41*, 3281; see also: Witulski, B.; Stengel, T. *Angew. Chem. Int. Ed.* **1999**, *38*, 2426.

40 McDonald, F.E.; Smolentsev, V. *Org. Lett.* **2002**, *4*, 745.

41 Grigg, R.; Sridharan, V.; Wang, J.; Xu, J. *Tetrahedron* **2000**, *56*, 8967.

42 Evans, P.A.; Robinson, J.E.; Baum, E.W.; Fazal, A.N. *J. Am. Chem. Soc.* **2002**, *124*, 8782.

43 Gilbertson, S.R.; DeBoef, B. *J. Am. Chem. Soc.* **2002**, *124*, 8784.

44 Ojima, I.; McCullagh, J.V.; Shay, W.R. *J. Organomet. Chem.* **1996**, *521*, 421.

45 Ojima, I.; Vu, A.T.; McCullagh, J.V.; Kinoshita, A. *J. Am. Chem. Soc.* **1999**, *121*, 3230.

46 Ojima, I.; Clos, N.; Donovan, R.J.; Ingallina, P. *Organometallics* **1990**, *9*, 3127.

47 Tanke, R.S.; Crabtree, R.H. *J. Am. Chem. Soc.* **1990**, *112*, 7984.

48 Ojima, I.; Lee, S.-Y.; Fujiwara, M., unpublished results.

49 Ojima, I.; Machnick, D.; Donovan, R.J.; Mneimne, O. *Inorg. Chim. Acta* **1996**, *251*, 299.

50 Ojima, I.; Fracchiolla, D.A.; Donovan, R.J.; Banerji, P. *J. Org. Chem.* **1994**, *59*, 7594.

51 Ojima, I.; Zhu, J.W.; Vidal, E.S.; Kass, D.F. *J. Am. Chem. Soc.* **1998**, *120*, 6690.

52 Ojima, I.; Lee, S.-Y. *J. Am. Chem. Soc.* **2000**, *122*, 2385.

53 Bennacer, B.; Fujiwara, M.; Ojima, I. *Org. Lett.* **2004**, *6*, 3589.

8
The Rhodium(I)-Catalyzed Alder-Ene Reaction

Kay M. Brummond and Jamie M. McCabe

8.1
Introduction

The bond reorganization process shown in Eq. (1) is formally known as an Alder-ene reaction, where X = H. The classic example involving the thermal reaction of an alkene having allylic hydrogen(s) (an ene) with an electron-deficient unsaturated compound (an enophile) was first reported by Alder in 1943 [1].

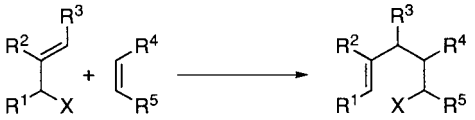

(1)

Very high temperatures (>450 °C) are typically required to effect this reaction thermally. A few years after the demonstration of the thermal ene reaction, it was shown that it could be accelerated by main group metals, which involved transfer of a metal atom instead of a hydrogen atom, and consequently was classified as a metallo–ene reaction, where X = metal [2]. More recently, Cohen has shown the lithium–ene cyclization to be much more facile than the widely used magnesium analog [3]. In addition, the zinc–ene reaction has been effected [4]. Some limitations to the metallo–ene reaction still existed though, such as moderate reaction temperatures (80 °C) and homocoupling byproducts. Although these two limitations were eventually overcome by using activated magnesium and other main group metals, stoichiometric amounts of metal are still required for complete conversion, and functional group compatibility is nearly always a complicating factor when *main group* metals are used.

Analogously to many other carbon–carbon bond forming processes, transition metals have also been used to effect the Alder-ene reaction. Notably, as in many transition metal-mediated processes, the reactions are performed using less than stoichiometric amounts of the metal, and lower reaction temperatures. Furthermore, transition metals typically show higher functional group compatibility than do main group metals. Trost and Lautens reported the first transition metal-catalyzed Alder-ene reaction involving carbon–hydrogen activation [5]. Enynes were subjected to palladium(II) acetate and shown to provide good yields of the intramolecular carbocyclization product. Subsequently to this initial report, a variety of catalysts, such as a Ni-Cr catalyst combination [6], dicobalt octacarbonyl [7], and dicyclopentadienyl titanium biscarbonyl [8], have

Modern Rhodium-Catalyzed Organic Reactions. Edited by P. Andrew Evans

ISBN: 3-527-30683-8

been used to effect this transformation. Excellent reviews have been published that describe the various catalysts and substrates that afford Alder-ene products, with the most common conditions employing a palladium catalyst [9]. Moreover, the corresponding *inter*molecular Alder-ene reaction, between an alkyne and an alkene and using cyclopentadienyl cyclooctadiene ruthenium chloride catalyst, has been reported [10].

Substrates possessing an allene that participate in the Alder-ene reaction are less common, but a few examples are known. Malacria [11] and Livinghouse [12] have independently used cobalt to effect intramolecular allenic Alder-ene reactions; but the scope of these reactions was not investigated. Sato has performed an allenic Alder-ene reaction to form five-membered rings, using stoichiometric amounts of titanium [13], and Trost has shown that 1,3-dienes can be prepared *via* an intermolecular Alder-ene reaction between allenes and enones using a ruthenium(II) catalyst [14].

As evidenced by the plethora of reviews cited in the preceding paragraphs, certain substrates and transition metals that affect the intra- and intermolecular Alder-ene reaction have been extensively studied. However, new ways to attain this synthetically useful reaction are valuable since some of these processes are completely substrate-dependent and involve metal catalysts with low functional group compatibility. This chapter details the role of rhodium(I) catalysts in achieving the formal Alder-ene reaction.

8.2
Diene Alder-Ene Reactions

8.2.1
Alkene Formation

The first example involving a rhodium catalyst in an ene reaction was reported by Schmitz in 1976. An intramolecular cyclization of a diene occurred to give a pyrrole when exposed to rhodium trichloride in isobutanol (Eq. 2) [15]. Subsequently to this work, Grigg utilized Wilkinson's catalyst to effect a similar cycloisomerization reaction (Eq. 3) [16]. Opplozer and Furstner showed that a π-allyl–rhodium species could be formed from an allyl carbonate or acetate and intercepted intramolecularly by an alkene to afford 1,4-dienes (Eq. 4). Hydridotetrakis(triphenylphosphine)rhodium(I) proved to be the most efficient catalyst for this particular transformation. A direct comparison was made between this catalyst and palladium bis(dibenzylidene) acetone, in which it was determined that rhodium might offer an additional stereochemical perspective. In the latter case, this type of reaction is typically referred to as a metallo–ene reaction [17].

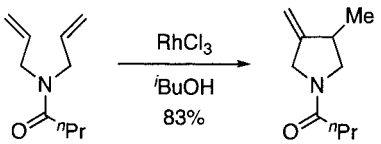

(2)

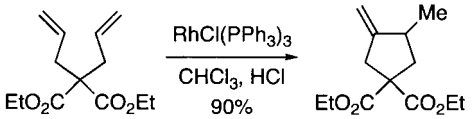

(3)

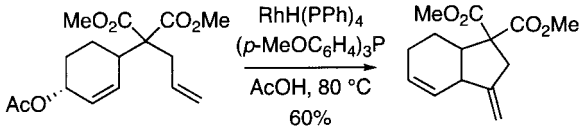

(4)

8.3
Enyne Alder-Ene Reactions

8.3.1
1,4-Diene Formation

Zhang was the first to successfully perform a rhodium(I)-catalyzed Alder-ene reaction of 1,6-enynes **1** to afford 1,4-dienes **2** (Eq. 5) [18]. The use of rhodium for this transformation was beneficial because the reactions could be performed at room temperature and the ligands on the metal could be easily tuned to accommodate steric or electronic factors in the substrates. Initially, 1,4-diphosphinite (BICPO), a ligand developed in Zhang's group [19], and 1,4-bis(diphenylphos-phino)butane (dppb) were the most active ligands for the Alder-ene reaction. Optimum yields were obtained when the catalyst was prepared by the addition of $AgSbF_6$ to $[Rh(BICPO)Cl]_2$ in the presence of the substrate. Other catalyst systems such as $[Rh(NBD)_2]SbF_6$ also gave the Alder-ene products, but the stereochemistry of the exocyclic double bond was obtained as a mixture of isomers, suggesting that an alternative mechanism to the one proposed might be operating [20]. Catalysts such as [Rh(I)(dppb)] afforded only the simple isomerization products and none of the desired cycloisomerization product.

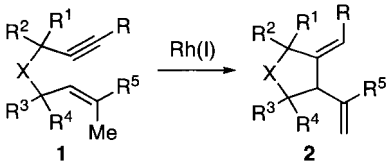

(5)

Tab. 8.1 summarizes the various substrates that were subjected to the rhodium-catalyzed reaction using a Rh–dppb catalyst system. Only *cis*-alkenes were cycloisomerized under these conditions, because the *trans*-alkenes simply did not react. Moreover, the formation of the γ-butyrolactone (Tab. 8.1, entry 8) is significant, because the corresponding palladium-, ruthenium-, and titanium-catalyzed Alder-ene versions of this reaction have not been reported. In each of the precursors shown in Tab. 8.1 (excluding entry 7), a methyl group is attached to the alkene. This leads to cycloisomerization products possessing a terminal alkene, thus avoiding any stereochemical issues. Also,

Tab. 8.1 Rhodium-catalyzed cycloisomerization of 1,6-enynes [a)]

Entry	*Substrate*	*Product*	*Temp.*	*Time (h)*	*Yield (%)* [b)]
	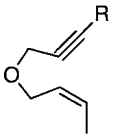	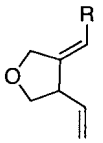			
1	R = Ph		RT	2	84%
2	R = (p-Me)-C_6H_4		RT	12	50%
3	R = (p-Cl)-C_6H_4		RT	2	91%
4	R = (p-CF_3)-C_6H_4		RT	1	80%
5	R = CH_2Ph		RT	6	83%
6	R = CO_2Me		RT	12	85%
7	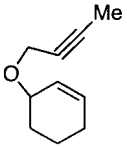	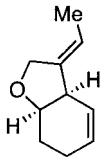	RT	2	85%
8	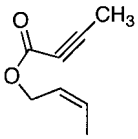	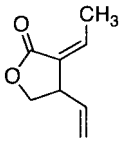	50 °C	24	50%
9	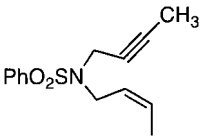	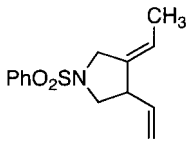	40 °C	12	50% [c)]

a) All reactions were carried out in DCE with substrate (0.2 mmol, 0.1 M)/[Rh(dppb)Cl_2/$AgSbF_6$ = 1 : 0.05 : 0.1. The catalyst [Rh(dppb)]$^+$ was prepared by adding $AgSbF_6$ to the [Rh(dppb)Cl]$_2$ in the presence of substrate.

b) The stereochemistry is relative.

c) Conversion determined by ^{1}H NMR (360 MHz), ene products cannot be separated from the substrate.

the sulfonamide functionality (entry 9) was not particularly tolerant of the reaction conditions. Some of these limitations led to a search for a more general catalyst system.

The Rh–BICPO catalyst proved to be quite general for this reaction, since the nitrogen-, oxygen-, or carbon-tethered substrates gave excellent yields of the cycloisomerized products (Tab. 8.2, entries 1–8). Moreover, this catalyst facilitated the Alder-ene reaction with an *E*-olefin, which afforded a mixture of 1,3- and 1,4-dienes (entry 6). Finally, the geometry of the appending olefin in the final product appears to give only the *E*-stereochemistry where relevant (entries 4, 6, and 8).

Tab. 8.2 Rhodium-catalysed cycloisomerizaton of 1,6-enynes with phosphinite ligands [a)]

Entry	*Substrate*	*Product*	*Cat. (mol)%*	*T (h)*	*Yield (%)* [b)]
1	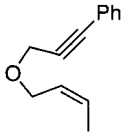	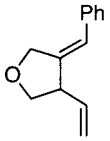	10	1.5	81
	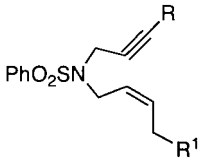	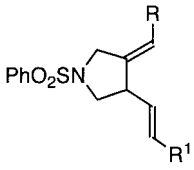			
2	R = CH_3, R^1 = H		3	13	98
3	R = CH_2CH_3, R^1 = H		3	13	100
4	R = CH_3, R^1 = CH_3		3	16	99
5	R = Ph, R^1 = H		10	4	96
6	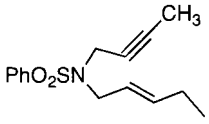	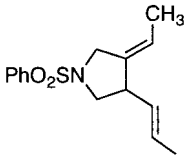	10	5	98 [b)]
		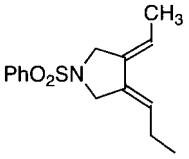			
7	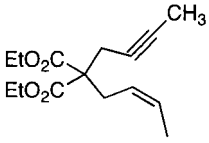	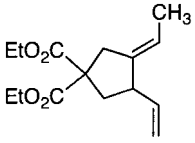	3	16	90
8	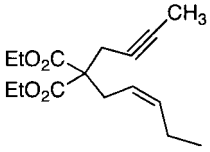	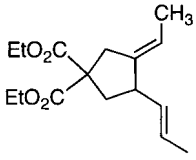	3	16	89

a) All reactions were carried out in DCE with substrate (0.2 mmol, 0.1 M). The catalyst $[Rh(BICPO)]^+$ was prepared by adding $AgSbF_6$ to the $[Rh(BICPO)Cl]_2$ after substrated were introduced.

b) 66 : 34.

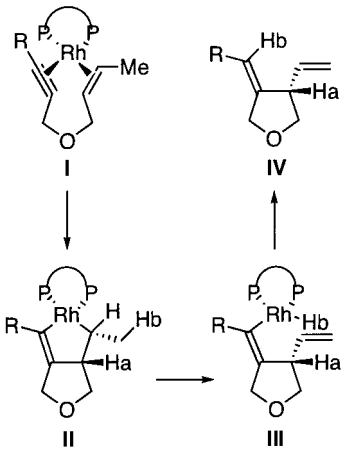

Scheme 8.1 Proposed mechanism of rhodium(I) Alder-ene reaction.

Zhang has proposed a mechanism for the rhodium-catalyzed Alder-ene reaction based on rhodium-catalyzed [4+2], [5+2], and Pauson–Khand reactions, which invoke the initial formation of a metallacyclopentene as the key intermediate (Scheme 8.1) [21]. Initially, the rhodium(I) species coordinates to the alkyne and olefin moieties forming intermediate **I**. This intermediate then undergoes an oxidative cyclization forming the metallacyclopentene **II**, followed by a β-hydride elimination to give the appending olefin shown in intermediate **III**. Finally, intermediate **III** undergoes reductive elimination to afford the 1,4-diene **IV**.

8.3.2
Asymmetric 1,4-Diene Formation

One of the major advantages of the rhodium(I)-catalyzed Alder-ene reaction is that mild conditions are used to effect the cycloisomerization process; thus increasing the likelihood of being able to facilitate an asymmetric reaction. In fact, Zhang has demonstrated convincingly that the Alder-ene reaction of enynes can indeed be performed with *excellent* enantioselectivity and with similar efficiency. These examples are highlighted below in chronological order.

Initial studies, performed by Zhang, demonstrated that the substrate structure and chiral ligand were both important factors in controlling the enantioselectivity and turnover (Eq. 6) [22]. For enynes possessing an oxygen tether, (*R,R*)-Me-DuPhos (DuPhos=1,2-bis(phospholano)benzene) was the ligand of choice, affording the corresponding furans in high yields and with high enantioselectivity. Unfortunately, this ligand proved to be very substrate-dependent, since minor changes in the substrate had a substantial effect on enantioselectivity and reaction times. Furthermore, catalyst preparation was an important factor in the reaction outcome. For example, the highest enantioselectivity was obtained when the rhodium(I) catalyst was generated *in situ* by the addition of $AgSbF_6$ after the substrate had been added. These reactions also needed to be monitored closely, since isomerization of 1,4-dienes to the corresponding 1,3-dienes proved problematic. Later studies established that $[Rh(COD)Cl]_2$/BINAP functioned as the optimal catalyst, furnishing the tetrahydrofurans in high yield with >99% enantio-

selectivity [23]. This report contrasts with the initial one where the use of $[Rh(BINAP)Cl]_2$ (BINAP = 2,2′-bis(diphenylphosphanyl)-1,1′-binaphthyl) resulted in no product formation. Moreover, BINAP turned out to be a superior ligand for the majority of substrates, which is advantageous since both enantiomers are commercially available.

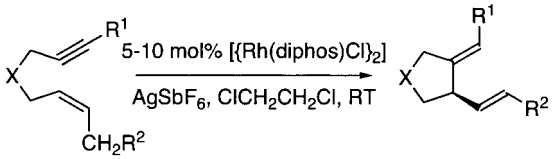

(6)

Highly functionalized tetrahydrofuran substrates were also prepared using the Rh(I)–BINAP conditions, producing products with enantioselectivities greater than 99%. The terminus of the alkyne was varied to afford ketones, esters, ethers, and even free alcohols under these conditions (Tab. 8.3 and Eq. 7).

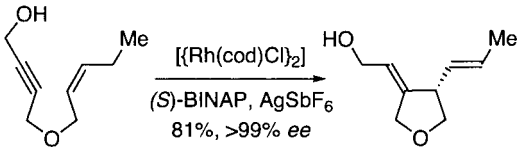

(7)

Functional groups were also placed on the allylic terminus; these included a propargyl ether (Eq. 8), acetate, and ether (Eq. 9) that afforded unique products. With a free alcohol on the allylic terminus, the alkyne underwent the Alder-ene reaction, followed by tautomerization of the corresponding enol to give the aldehyde in a 98% yield and with 99% enantiomeric excess (Eq. 10).

Tab. 8.3 Rhodium(I)-catalyzed enantioselective Alder-ene reactions of **3** [a)]

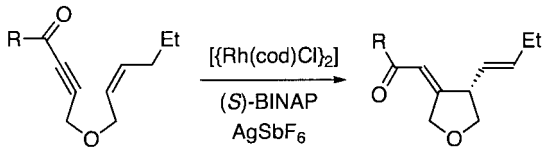

3 **4**

Entry	*Enyne*	*R*	*Furan*	*Yield (%)* [b)]	*ee [5]* [c)]
1	**3a**	Me	(+)-**4a**	86	99.5
2	**3b**	Ph	(+)-**4b**	99	>99.9
3	**3c**	EtO	(+)-**4c**	82	>99.9

a) All reaction were performed using 10 mol% Rh(I) and 12 mol% BINAP on 0.2 mmol scale.
b) Yield of isolated product.
c) Determined by GC.

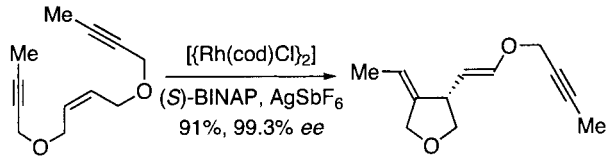

(8)

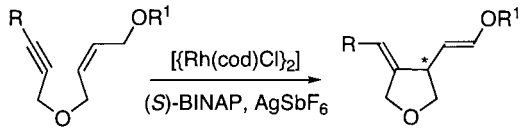

(9)

(+)-**5a**, R = Ph, R^1 = Ac, 96%, 99.7% *ee*
(+)-**5b**, R = Me, R^1 = Ac, 92%, >99.9% *ee*
(+)-**5c**, R = Ph, R^1 = Me, 92%, >99% *ee*
(+)-**5d**, R = COPh, R^1 = Et, 93%, >99% *ee*

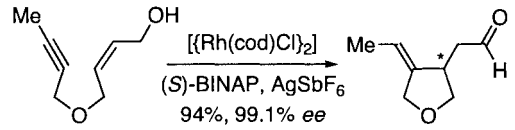

(10)

Ester-tethered enyne systems cycloisomerized to give lactone products (Eq. 11) [24]. For example, enyne **6** reacted under the Alder-ene conditions of $[Rh(COD)Cl]_2$/BINAP/$AgSbF_6$ to give the corresponding lactone (Eq. 11). Once again free hydroxyl groups on the allylic terminus were incorporated into the cyclization precursors and subjected to the Alder-ene conditions, which led to the exclusive formation of the tautomerized products in good yields and enantioselectivities (Eq. 12).

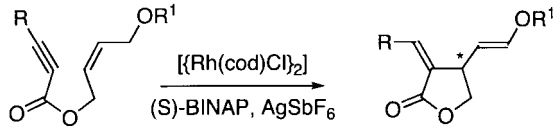

6 **7**

(11)

(*S*)-(+)-**7a**, R = Ph, R^1 = Bn, 92%, >99% *ee*
(*S*)-(+)-**7b**, R = Me, R^1 = Ac, 98%, >99% *ee*
(*S*)-(-)-**7c**, R = Me, R^1 = Me, 95%, >99% *ee*
(*S*)-(+)-**7d**, R = Me, R^1 = Bn, 91%, >99% *ee*

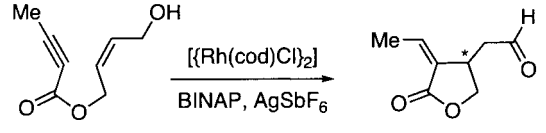

8 **9**

(12)

(*R*)-(+)-**9a**, R = Me, (*R*)-BINAP, 99%, >99% *ee*
(*S*)-(-)-**9a**, R = Me, (*S*)-BINAP, 98%, >99% *ee*
(*S*)-(-)-**9b**, R = $^nC_5H_{11}$, (*S*)-BINAP, 95%, >99% *ee*
(*R*)-(+)-**9c**, R = Ph, (*R*)-BINAP, 92%, >99% *ee*

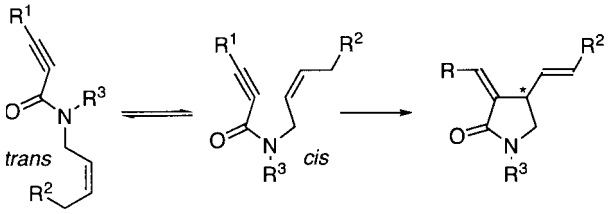

Scheme 8.2 Effect of *trans*/*cis*-isomers on the rhodium-catalyzed Alder-ene reaction.

Lactams are another interesting class of compounds that have been thoroughly explored by Zhang [25]. Methods that are typically used in the synthesis of nonracemic lactams involve C–N bond formation of substrates with preset chiral centers. The Alder-ene carbon–carbon bond forming strategy allows for chiral centers to be set without the use of other pre-existing chirality in the substrate. Initially, enynes with secondary amide tethers were studied but no cyclization was observed. Zhang reasoned that the favored *transoid* conformation of the secondary amide prevents the necessary conformation required for cyclization (Scheme 8.2).

Protecting the amide prior to the Alder-ene reaction leads to the formation of a variety of lactams, presumably by allowing for the formation of the *cisoid* conformation. Analogously to furan formation, lactam formation showed high functional group tolerability. For example, amides possessing allylic acetates and ethers were subjected to the rhodium(I)/BINAP/$AgSbF_6$ conditions to afford the differentially functionalized lactams in high yield and with excellent enantioselectivities (Tab. 8.4).

Tab. 8.4 Asymmetric lactams

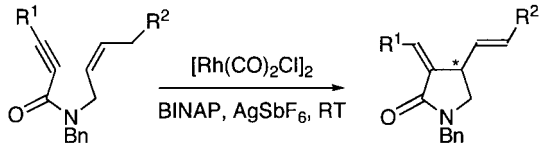

Entry	*Substrate*			*Product*	
	R^1	R^2	*BINAP*	*%Yield*	*%ee*
1	Ph	Et	(*S*)	95	>99
2	Ph	Et	(*R*)	96	>99
3	Ph	H	(*S*)	90	>99
4	Me	H	(*R*)	91	>99
5	Me	H	(*S*)	92	>99
6	Ph	OMe	(*S*)	87	>99
7	Ph	OMe	(*R*)	88	>99
8	Ph	OBn	(*S*)	89	>99
9	$^nC_5H_{11}$	OMe	(*S*)	92	>99
10	Ph	OAc	(*S*)	89	>99

8.3.3
Diversification of Alder-Ene Cyclization Products

Zhang has applied the cyclization of esters to the formation of α-methylene-γ-butyrolactones, providing a novel and enantioselective entry to these substructures. The importance of this type of unsaturated lactone is evident by its ubiquitous presence in nearly one-third of all naturally occurring secondary metabolites. The Alder-ene reaction has been applied to a formal total synthesis of (+)-pilocarpine [26], a leading therapeutic reagent for the treatment of narrow and wide glaucoma. Zhang intersected Büchi's synthetic intermediate (*R*)-**10a** **[27]** in only two steps with 99% enantiomeric excess in 91% overall yield (Eq. 13). In comparison, Büchi synthesized (*R*)-**10a** in five steps with 92% enantiomeric excess and 20% overall yield.

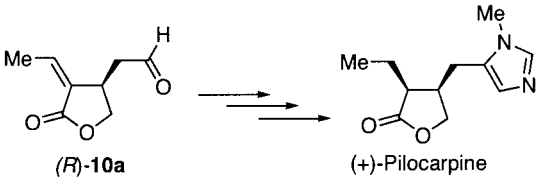

(13)

8.4
Allenyne Alder-Ene Reactions

8.4.1
Cross-Conjugated Triene Formation

Brummond [28] was the first to illustrate that cross-conjugated trienes could be obtained *via* an allenic Alder-ene reaction catalyzed by $[Rh(CO)_2Cl]_2$ (Eq. 14). Selective formation of the cross-conjugated triene was enabled by a selective cycloisomerization reaction occurring with the distal double bond of the allene. Typically directing groups on the allene, differential substitution of the allene termini, or intramolecularization are required for constitutional group selectivity. However, rhodium(I), unlike other transition metals examined, facilitated selective cyclization with the distal double bond of the allene in nearly all the cases examined.

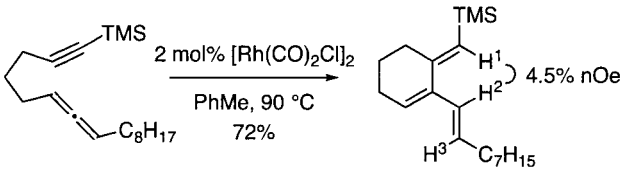

(14)

The mechanism proposed for this allenic Alder-ene reaction is shown in Scheme 8.3. The rhodium(I) catalyst coordinates with the allenyne **V** forming intermediate **VI**, which undergoes an oxidative addition to form the metallocycle **VII**. The metallocycle then undergoes a β-hydride elimination producing triene intermediate **VIII**, which

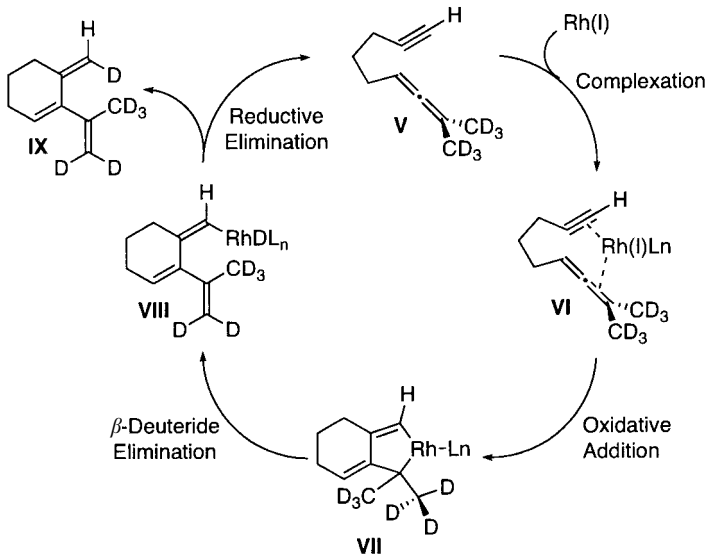

Scheme 8.3 Postulated mechanism of the allenic Alder-ene reaction.

after reductive elimination affords the cross-conjugated triene **IX** in very high yield along with the regenerated rhodium(I) catalyst.

Evidence for this mechanism includes: (1) an experiment showing a 4.5% nOe between H^1 and H^2 of the triene in Eq. (14), validating the *E*-stereochemistry of the exocyclic olefin; and (2) preparation of a hexadeuterated allenyne that was subjected to the reaction conditions which gave complete transfer of a deuterium atom to the exocyclic double bond of the triene (Eq. 15).

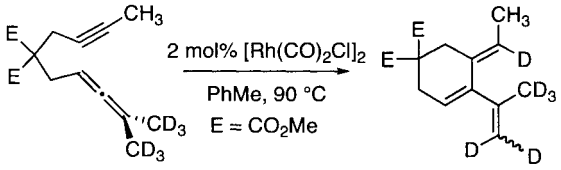

(15)

Synthesis of these highly unsaturated, cross-conjugated triene ring systems from readily available starting materials is a method that has been largely overlooked; despite their vast synthetic potential, very few examples have been reported [29]. Following their brief mechanistic study, the Brummond group explored the scope of the formal allenic Alder-ene reaction using rhodium biscarbonyl chloride dimer $[Rh(CO)_2Cl]_2$ which proved to be a general catalyst for this reaction. For example, placement of a methyl substituent on the terminus of the allene gave a 71% yield of triene **12** (Tab. 8.5, entry 1). Replacement of this group with a longer alkyl chain also gave a high yield of the corresponding triene (entry 2). However, in this case a mixture of *E*- and *Z*-isomers were obtained. Interestingly, rhodium cyclooctadiene chloride dimer ($[Rh(COD)Cl]_2$ (entry 3), afforded almost identical results to those in entry 1, with the exception that the rate of reaction was substantially increased. Modification of the sub-

Tab. 8.5

Entry	*Allenyne*	*Triene*	*Temp. (°C)*	*Time*	*E:Z*	*Yield (%)*
	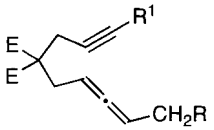	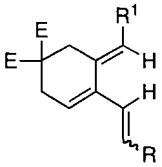				
1	**11** R=H, R^1=H	**12**	90	1 h	–	71
2	**13** R=C_5H_{11}, R^1=H	**14**	90	1 h	3:1	80
3[a]	**11**	**12**	RT	15 min	–	74
4	**15** R=C_5H_{11}, R^1=TMS	**16**	RT	3 h	3:1	60
5	**17** R=H, R^1=TMS	**18**	RT	3 h	–	45
	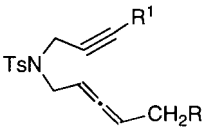	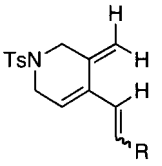				
6	**19** R=C_5H_{11}, R^1=H	**20**	90	1 h	4:1	64
7	**19**	**20**	RT	6 h	6:1	90
8	**21** R=H, R^1=H	**22**	RT	3 h	–	93
9	**23** R=C_5H_{11}, R^1=TMS	**24**	RT	5 h	5:1	85
10	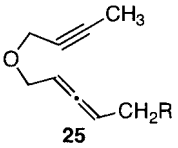 **25**	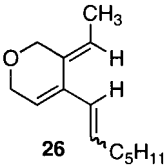 **26**	90	1 h	6:1	74
	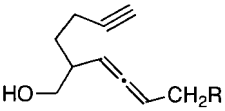	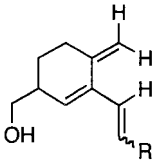				
11	**27** R=C_5H_{11}	**28**	RT	6 h	2:1	80[b]
12	**29** R=H	**30**	RT	3 h	–	80[b]
13	**31** R=C_5H_{11}, R^1=TMS	**32**	RT	6 h	3:1	69[b]

Conditions: 2 mol% $[Rh(CO)_2Cl]_2$, toluene, N_2.

a) 5 mol% $[Rh(COD)Cl]_2$, 10 mol% $AgSbF_6$.

b) Reactions were run in CH_2Cl_2 or DCE, toluene gave on average, yields that were 15% lower.

stituent on the terminus of the alkyne from hydrogen to a silane led to lower reaction rates and yields (compare entries 2 and 6 with 1 and 5). The results observed for the tethered tosyl amides were similar to those observed for the carbon tethers (entries 6–9). One major difference is that products were obtained in higher yields if the reaction was carried out at room temperature and for longer reaction times. Allenyne **25**, possessing an oxygen tether, cyclized to afford the triene **26** in 74% yield (entry 10). Finally, the successful cyclization of allenynes **27**, **29**, and **31** possessing a free hydroxyl group on the tether is another example demonstrating the high functional group compatability of the rhodium(I) catalyst (entries 11, 12, and 13). For these examples, the optimum solvent proved to be CH_2Cl_2 or dichloroethane (DCE). The yields of the Alder-ene reaction were on average 15% lower when performed in toluene. The results described above show the scope of this method to be general, the stereoselectivity of *exocyclic* olefin excellent, and the reaction conditions mild and tolerant of a wide range of functionality. Thus far, the major limitation of this process is the low *E/Z*-selectivities obtained for the *appending* olefin. Efforts to increase this selectivity are being addressed and are discussed below. Interestingly, Shibata [30] demonstrated that Wilkinson's catalyst ($RhCl(PPh_3)_3$) can also be used to afford a variety of conjugated trienes.

During investigations to explore alternative catalyst systems to effect the allenic Alder-ene reaction, an increase in *E/Z*-selectivity was observed with the cationic rhodium species ($[Rh(COD)Cl]_2/AgSbF_6$) (compare entries 1 and 2, Tab. 8.6). Other cationic rhodium species were examined, but none gave as high a selectivity. Iridium(I) complexes have been used to catalyze a variety of cycloisomerization reactions [31], and it is known the higher oxidation states of these complexes cycloisomerize more slowly than the corresponding rhodium(III) complexes. This information led to the idea that an iridium(I)-catalyzed Alder-ene reaction may afford the appending double bond with higher *E/Z*-selectivities. Indeed, treatment of a variety of allenynes with $[Ir(COD)_2Cl]_2/AgBF_4$ furnished the trienes as predominantly one stereoisomer (Tab. 8.6, entries 4–7). Whereas the observed *E/Z*-selectivities are excellent, the quantity of catalyst needed to effect the cycloisomerization reaction is relatively high (10 mol%) and the presence of a trimethylsilyl group on the terminus of the alkyne is required. Additional efforts will be necessary to further optimize the iridium(I)-catalyzed reaction conditions.

Tab. 8.6 Stereochemistry of olefinic side-chain

Entry	*Allenyne*	*Triene*	*Conditions*	*E:Z*	*Yield (%)*
1	**15**	**16**	A	5:1	72
2	**15**	**16**	B [b)]	13:1	67
3	**15**	**16**	C [b)]	4:1	46
4	**15**	**16**	D	>20:1	57
5	**15**	**16**	D	180:1 [a)]	67
6	**23**	**24**	D	>20:1	62
7	**31**	**32**	D	>99:1 [a)]	74

Conditions: A: 2 mol% $[Rh(CO)_2Cl]_2$, toluene, N_2, 90 °C, 1 h. B: 5 mol $[Rh(COD)Cl]_2$, 10 mol% $AgSbF_6$, DCE, RT, 15 min. C: 5 mol% $[Rh(CH_2CH_2)_2Cl]_2$, 10 mol% $AgSbF_6$, DCE, RT, 15 min. D: 10 mol% $[Ir(COD)Cl]_2$, 20 mol% $AgBF_4$, DCE, 60 °C, 5 min.

a) *E/Z* ratio determined by GC analysis.

b) Under these conditions the silyl group was completely removed from the exocyclic olefin.

Soon after the discovery of the allenic Alder-ene reaction efforts were underway to explore the synthetic potential of this cycloisomerization process. Allenynes possessing amino acids as part of the tether were subjected to the allenic Alder-ene reaction conditions to afford high yields of the unnaturally occurring amino acids (Tab. 8.7) [32]. A variety of amine protecting groups (Cbz, Bz, and Boc), substituents on the alkyne terminus (H, TMS, Ph, Me), and functionality on the amino acid (Me, Bn, CH_2OTBS) all afforded excellent yields of triene products. The 1,1,3-trisubstituted allenes gave uniquely substituted trienes (Tab. 8.7, entries 10 and 11), and the isopropyl-substituted allenes also gave excellent yields of the trienes (entries 9 and 10). The trienes of entries 9 and 10 contain only one hydrogen that can undergo β-hydride elimination, but this does not appear to be problematic. The rate of cycloisomerization of these amino acid-containing substrates was particularly noteworthy (Tab. 8.7, entries 1–11), in that the reactions were complete in less than 10 minutes at room temperature. This procedure not only saves on time, but also allows one to carry out these reactions open to the atmosphere!

Lactams are ubiquitous in a variety of natural and unnatural products, making them desirable targets for synthesis. The amide-tethered allenynes underwent the catalyzed allenic Alder-ene reaction to give the desired lactams in good yields (Scheme 8.4). Both the amide-protected and -unprotected allenynes afforded the desired cross-conjugated trienes. However, the unprotected substrates were more recalcitrant to cycloisomerization, requiring higher reaction temperatures (60 °C). The rhodium(I)-catalyzed Alder-ene reaction of an amide has been reported by Zhang, but this is the first example of an Alder-ene reaction of an amide-tethered substrate to form a six-membered lactam.

Tab. 8.7 Unnaturally occurring amino acids

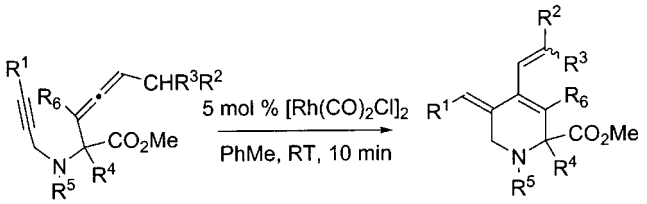

Entry	R^1	R^2	R^3	R^4	R^5	R^6	*Yield (%)*
1	H	H	H	Me	Cbz	H	87
2	TMS	H	H	Me	Cbz	H	89
3	Ph	H	H	Me	Cbz	H	95
4	Me	H	H	Me	Cbz	H	95
5	H	H	H	Bn	Bz	H	75
6	TMS	H	H	Bn	Bz	H	91
7	Ph	H	H	Bn	Bz	H	81
8	Me	H	H	CH_2OTBS	Bz	H	95
9	Me	Me	Me	Me	Cbz	H	80
10	Me	Me	Me	Me	Cbz	C_4H_9	86
11	Me	H	C_5H_{11}	Bn	Boc	Me	80

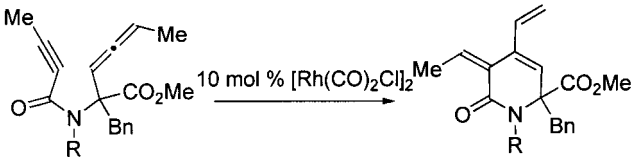

Scheme 8.4 Synthesis of lactams from amide-tethered allenynes.

Moreover, in Zhang's systems cycloisomerization of an unprotected secondary amide in the enyne Alder-ene reaction was not possible.

The allylic sulfonyl allene **35**, possessing unsymmetrical substitution at the distal double bond of the allene, was examined. Since there are two possible sites for *β*-hydride elimination, a variety of isomers are possible. Treatment of allene **35** with $[Rh(CO)_2Cl]_2$ gave a 3:5:1 ratio of the three possible products **36**, **37**, and **38**, which translates into an 8:1 constitutional group selectivity in the *β*-hydride elimination step ((**36**+**37**):**38**) and an *E*/*Z*-selectivity of 1:2 (Tab. 8.8, entry 1).

The ratio of the isomeric trienes (**36**, **37**, and **38**) is governed by the nature of the rhodium catalyst. For example, when the catalyst was changed to a cationic rhodium(I) species ($[Rh(COD)Cl]_2/AgBF_4$), the *E*/*Z*-selectivity reversed and gave exclusively the *E*-isomer, while the constitutional group selectivity was dramatically decreased to a 1:1 ratio (entry 3). Furthermore, lower reaction temperatures and changing the catalyst to a cationic iridium(I) species furnished the *E*-isomer **36** selectively (entries 4–6). Clearly, additional work is required to increase and understand the selectivity issues [33].

Tab. 8.8 Selectivity of isomeric trienes **36**, **37**, and **38**.

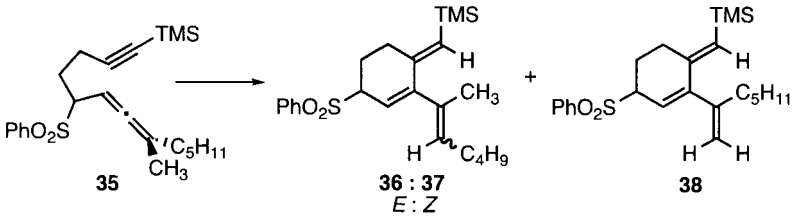

Entry	*Catalyst*	*Additive*	*Temp. (°C)*	*36:37:38*	*36+37:38*	*36:37*
1	5 mol% $[Rh(CO)_2Cl]_2$	–	50	3:5:1	8:1	1:2
2	3 mol% $[Rh(CO)_2Cl]_2$	–	RT	2:4:1	6:1	1:2
3	5 mol% $[Rh(COD)_2Cl]_2$	$AgBF_4$	RT	1:0:1	1:1	1:0
4	10 mol% $[Ir(COD)_2Cl]_2$	$AgBF_4$	0	4:1:1	5:1	4:1
5	10 mol% $[Ir(COD)_2Cl]_2$	$AgBF_4$	–10	5:1:2	3:1	5:1
6	10 mol% $[Ir(COD)_2Cl]_2$	$AgBF_4$	–30	6:1:1	7:1	6:1

Reactions using $[Rh(CO)_2Cl]_2$ were run in toluene. Reactions using $[Ir(COD)Cl]_2$ or $[Rh(COD)Cl]_2$ were run in DCE. Amount of additive used was twice the molar amount of catalyst. 75–90% yields for all entries were obtained. Ratios determined by ^1H NMR.

8.4.2

Diversification of Alder-Ene Products

The cross-conjugated trienes have potential in many different types of diversification strategies. For example, the triene clearly lends itself to inter- and intramolecular Diels–Alder reactions. Incorporation of the hydroxymethyl group on the tether allows attachment of functionality suitable for reactions subsequent to the Alder-ene reactions. As depicted in Scheme 8.5, propargyl tosylamides **A**, alkynyl silanes **B**, acrylate esters **C**, and propargyl ethers **D** can all be readily prepared from **39**

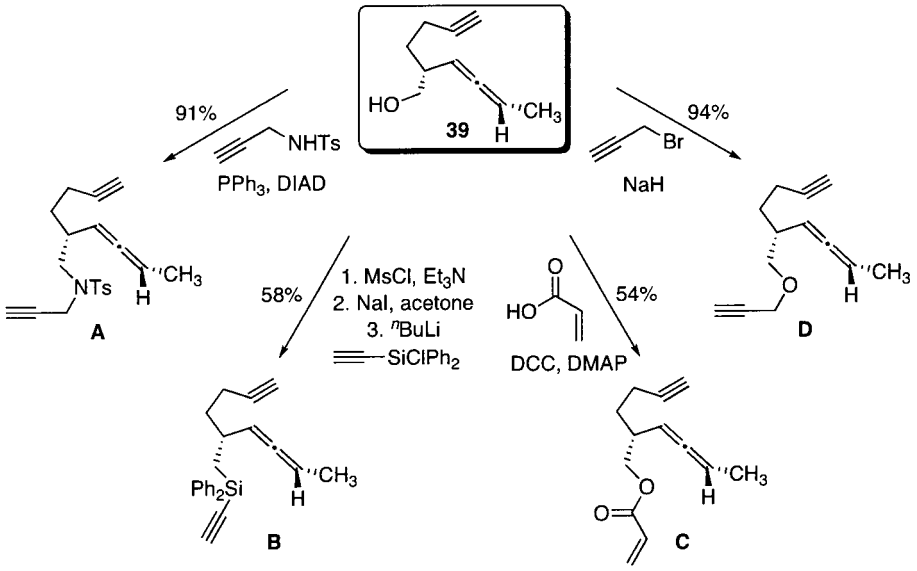

Scheme 8.5 Tethering dienophiles to the allenyne.

The Alder-ene reaction of these substrates occurs with little or no interference from the additional unsaturated functionality appended to the tether, based on the excellent yields and fast reaction times (Scheme 8.6).

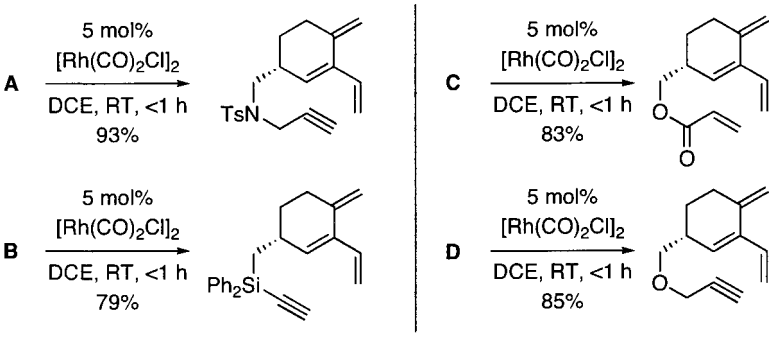

Scheme 8.6 Rhodium-catalyzed Alder-ene reaction of substrates **A**–**D** from Scheme 8.5.

The trienes were then subjected to a formal Diels–Alder reaction using conditions developed by Gilbertson and others (Scheme 8.7) [34]. The propargyl tosylamide **40** and the propargyl ether **43** have both afforded the formal intramolecular Diels–Alder adducts **44** and **45** in high yield. To date, the formal cycloaddition of the silicon-tethered alkyne **41** has not been affected and heating triene **42** led to a thermal Diels–Alder reaction to furnish cycloadduct **46**, albeit in lower yield than the corresponding rhodium-catalyzed examples.

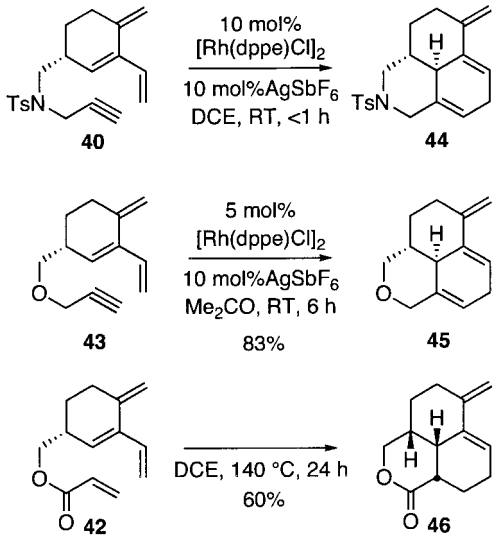

Scheme 8.7 Intramolecular Diels–Alder reactions.

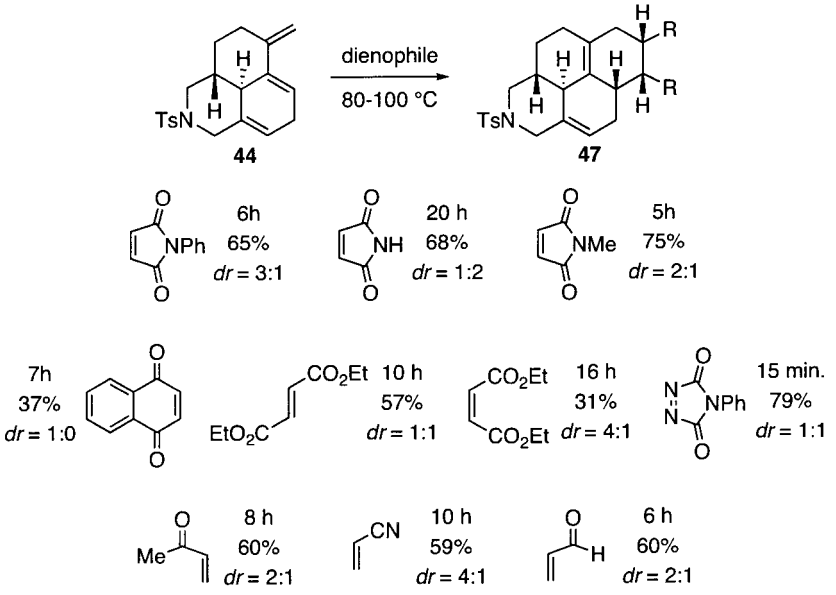

Scheme 8.8 Thermal intermolecular Diels–Alder reactions.

Subsequently to the intermolecular Diels–Alder reaction, a new diene is produced which can then be utilized in a second cycloaddition process. The feasibility of the second Diels–Alder process was demonstrated by the thermal cycloaddition of **44** with a variety of dienophiles to afford the cycloadducts **47** in high yields, albeit with moderate diastereoselectivity (Scheme 8.8). Additional investigations will be necessary to delineate further the scope and limitations of this rapid increase in molecular complexity.

8.5 Kinetic Resolution

The power of the rhodium(I)-catalyzed Alder-ene reaction is shown by a highly enantioselective kinetic resolution process [35]. The key result stems from an observation that a racemic mixture of **48**, when treated with $[Rh(COD)Cl]_2$ and (±)-BINAP, afforded *rac*-49 (2*R*,3*S* and 2*S*,3*R*, and not 2*R*,3*R* and 2*S*,3*S*; Eq. (16).

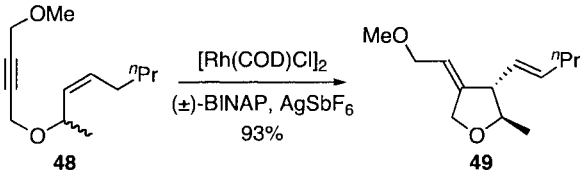

(16)

The kinetic resolution was systematically studied by using diastereomerically pure enynes and an enantiomerically pure rhodium(I) catalyst (Scheme 8.9). Each product was obtained in high yield (~100% for the reacted **51** + unreacted **50**) and high enantiomeric purity. Furthermore, these results were validated by subjecting each enantiomer

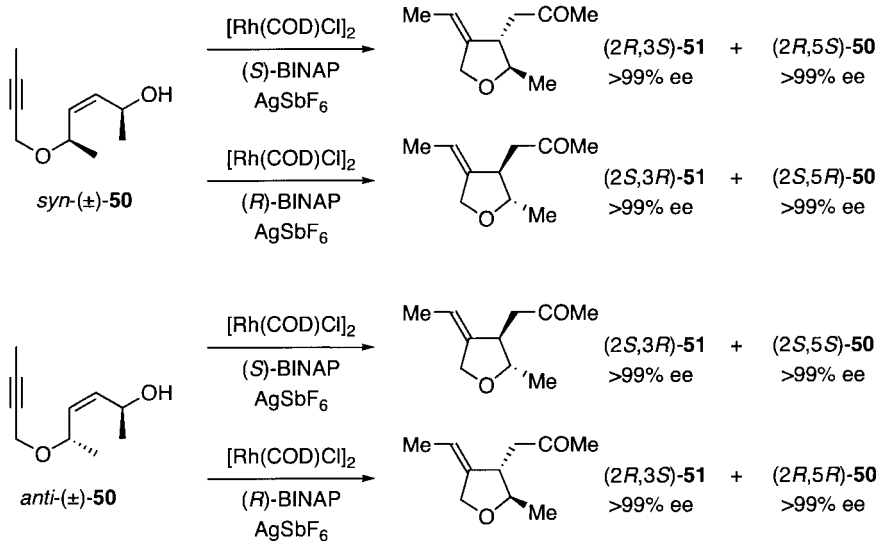

Scheme 8.9 Kinetic resolution of **50** and **51**.

of **50** independently to both enantiomers of the catalyst. In all the cases examined, either 100% or 0% conversion was observed. It was determined that the allylic substituents were needed in order to obtain the high enantioselectivity.

8.6
Other Rhodium-Catalyzed Ene-Type Reactions

8.6.1
Intramolecular Halogen Shift

In the course of exploring the scope of the ester-tethered enyne substrates, Zhang discovered that the placement of a halogen on the allylic terminus gave a surprising result. These substrates yielded another type of rhodium(I)-catalyzed ene reaction [36], in which the enyne substrates containing an allylic halogen underwent a halogen shift (Eq. 17).

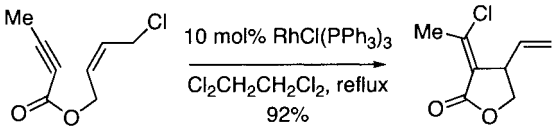

(17)

Substantial evidence from investigation of the formation of this product suggests that the mechanism is different from that of the typical Alder-ene reaction. It is thought to involve the formation of a π-allyl–rhodium complex species rather than a metallocyclopentene intermediate (Scheme 8.10).

Subsequently to rhodium coordination with the enyne to form **X**, oxidative addition with the allyl chloride affords a rhodium–π-allyl complex. Then η^3–η^1 isomerization of this complex **XI** gives intermediate **XII**, which undergoes a halometallation of the

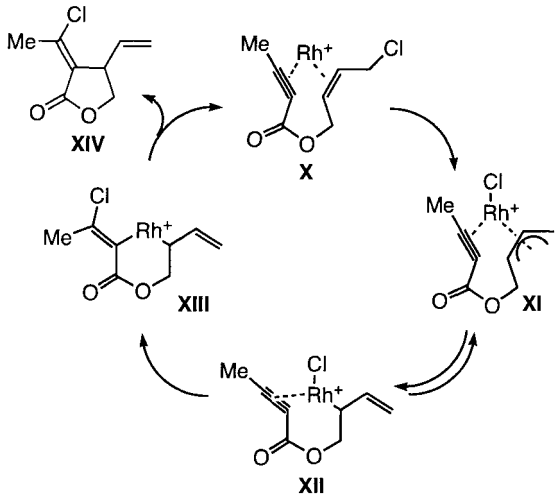

Scheme 8.10 Proposed mechanism of rhodium(I)-catalyzed halogen shift.

Tab. 8.9 Scope of halogen shift reaction

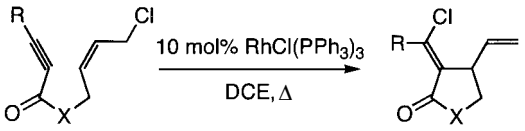

Entry	*Sub*	*R*	*X*	*Time (h)*	*Yield (%)*
1	**Z-54a**	CH_3	O	1	92
2	**E-54a**	CH_3	O	1	90
3	**54b**	Ph	O	2	87
4	**54c**	C_4H_9	O	2	90
5	**54d**	CH_2OMe	O	2	72 [a]
6	**54e**	CH_3	NBn	3	89
7	**54f**	Ph	NBn	6	85
8	**54g**	CH_3	NTs	4	83
9	**54h**	CH_3	O	24	85 [b]
10	**54e**	CH_3	NBn	24	81 [b]

a) With an unidentified by-product.
b) 10 equiv. of $BnN(CH_3)_3Cl$ was added.

alkyne to afford the metallocycle **XIII**, followed by reductive cyclization to furnish the observed product **XIV**. This mechanistic proposal was supported the analogous cyclization of enyne **52** to afford the lactone **53** (Eq. 18).

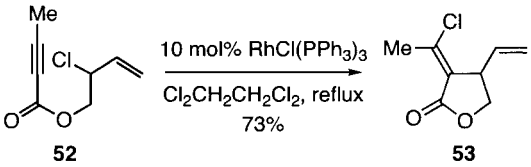

(18)

Moreover, both the *cis*- and *trans*-alkenes react at the same rate and yield the same product (Tab. 8.9, entries 1 and 2). As demonstrated above, this was not the case with the *N*-tethered enynes (Tab. 8.2, entry 6) which gave a mixture of products. Nitrogen- and oxygen-tethered enynes were subjected to the rhodium(I) conditions affording high yields of the halogen shift product (Tab. 8.9, entries 1–10).

8.7 Conclusion

The rhodium catalyzed Alder-ene reaction represents just one exciting cycloisomerization process that is still in its infancy. The synthetic potential of this reaction is currently being investigated, and new findings will undoubtedly be made.

8.8 References

1 For a review on the Alder-ene reaction, see: Snider, B. B. "Ene Reactions with Alkenes as Enophiles," in *Comprehensive Organic Synthesis*; Trost, B. M., Ed.; Pergamon Press: Oxford, UK, **1991**; Vol. 5, pp. 1–27.

2 For a review of the metallo–ene reactions, see: Oppolzer, W. *Angew. Chem. Int. Ed. Engl.* **1989**, *28*, 38. Oppolzer, W. "Metallo–ene Reactions," in *Comprehensive Organic Synthesis*; Trost, B. M., Ed.; Pergamon Press: Oxford, UK, **1991**; Vol. 5, pp. 29–61.

3 Cheng, D.; Xiaojun, L.; Norton, S. H.; Cohen, T. "The Lithium–Ene Cyclization and the Purported Carbanion-Induced Ene Cyclization," *J. Am. Chem. Soc.* **1999**, *121*, 10 241.

4 Nakamura, E.; Kubota, K. *J. Org. Chem.* **1997**, *62*, 792; Lorthiois, E.; Marek, I.; Normant, J.-F. *J. Org. Chem.* **1998**, *63*, 2442.

5 Trost, B. M.; Lautens, M. *J. Am. Chem. Soc.* **1985**, *107*, 1781. Trost, B. M.; Lautens, S. M.; Chan, C.; Jebaratnam, D. J.; Mueller, T. *J. Am. Chem. Soc.* **1991**, *113*, 636.

6 Trost, B. M.; Tour, J. M. *J. Am. Chem. Soc.* **1987**, *109*, 5268.

7 Krafft, M. E.; Wilson, A. M.; Dasse, O. A.; Bonaga, V. R.; Cheung, Y. Y.; Fu, Z.; Shao, B.; Scott, I. L. *Tetrahedron Lett. 1998*, *39*, 5911.

8 Sturla, S. J.; Kablaoui, N. M.; Buchwald, S. L. *J. Am. Chem. Soc.* **1999**, *121*, 1976.

9 Aubert, C.; Buisine, O.; Malacria, M. *Chem. Rev.* **2002**, *102*, 813. Trost, B. M.; Krische, M. J. *Synlett*, **1998**, 1.

10 Trost, B. M.; Indolese, A. *J. Am. Chem. Soc.* **1993**, *115*, 4361.

11 Llerena, D.; Aubert, C.; Malacria, M. *Tetrahedron Lett.* **1996**, *37*, 7027.

12 Pagenkopf, B. L.; Belanger, D. B.; O'Mahony, D. J. R.; Livinghouse, T. *Synthesis* **2000**, 1009.

13 Yamazaki, T.; Urabe, H.; Sato, F. *Tetrahedron Lett.* **1998**, *39*, 7333.

14 Trost, B. M.; Pinkerton, A. B. *J. Am. Chem. Soc.* **1999**, *121*, 4068; Trost, B. M.; Pinkerton, A. B.; Seidel, M. *J. Am. Chem. Soc.* **2001**, *123*, 12 466.

15 Schmitz, E.; Heuck, U.; Habisch, D. *J. Prakt. Chem.* **1976**, *318*, 471. Schmitz, E.; Urban, R.; Heuck, U.; Zimmerman, G.; Grundermann, E. *J. Prakt. Chem.* **1976**, *318*, 185.

16 Grigg, R.; Malone, J. F.; Mitchell, T. R. B.; Ramasubbu, A.; Scott, R. M. *J. Chem. Soc., Perkin Trans. I* **1984**, 1746. Grigg, R.; Mitchell, T. R. B.; Ramasubbu, A. *J. Chem. Soc., Chem. Commun.* **1980**, *27*.

17 Oppolzer, W.; Furstner, A. *Helv. Chim. Acta*. **1993**, *76*, 2329.

18 Cao, P.; Wang, B.; Zhang, X. *J. Am. Chem. Soc.* **2000**, *122*, 6490.

19 Zhu, G.; Zhang, X. *J. Org. Chem.* **1998**, *63*, 9590.

20 Zhu, G.; Zhang, X. *J. Org. Chem.* **1998**, *63*, 9590.

21 Lei, A; Waldkirch, J. P.; He, M.; Zhang, X. *Angew. Chem. Int. Ed. Engl.* **2002**, *41*, 4526.

22 Cao, P.; Zhang, Z. *Angew. Chem. Int. Ed. Engl.* **2000**, *39*, 4104.

23 Lei, A.; He, M.; Wu, S.; Zhang, X. *Angew. Chem. Int. Ed. Engl.* **2002**, *41*, 3457.

24 Lei, A.; He, M.; Zhang, X. *J. Am. Chem. Soc.* **2002**, *124*, 8198.

25 Lei, A; Waldkirch, J. P.; He, M.; Zhang, X. *Angew. Chem. Int. Ed. Engl.* **2002**, *41*, 4526.

26 Lei, A.; He, M.; Zhang, X. *J. Am. Chem. Soc.* **2002**, *124*, 8198.

27 Horne, D. A.; Fugmann, B.; Yakushijin, K.; Büchi, G. *J. Org. Chem.* **1993**, *58*, 62.

28 Brummond, K. M.; Chen, H.; Sill, P.; You, L. *J. Am. Chem. Soc.* **2002**, *124*, 15 186.

29 Tsuge, O.; Wada, E.; Kanemasa, *Chem. Lett.* **1983**, 239. Tsuge, O.; Wada, E.; Kanemasa, *Chem. Lett.* **1983**, 1525; Woo, S.; Squires, N.; Fallis, A.G. *Org. Lett.* **1999**, *1*, 573. Woo, S.; Legoupy, S.; Parra, S.; Fallis, A. G.*Org. Lett.* **1999**, *1*, 1013; Spino, C.; Tu, N. *Tetrahedron Lett.* **1994**, *35*, 3683. Spino, C.; Liu, G.; Tu, N.; Girard, S. *J. Org. Chem.* **1994**, *59*, 5596.

30 Shibata, T.; Takesue, Y.; Kadowaki, S.; Takagi, K. *Synlett* **2003**, *2*, 268.

31 Shibata, T.; Takagi, K. *J. Am. Chem. Soc.* **2000**, *122*, 9852. Chatani, N.; Inoue, H.; Morimoto, T.; Muto, T.; Murai, S. *J. Org. Chem.* **2001**, *66*, 4433. Shibata, T.; Takagi, K. *J. Am. Chem. Soc.* **2000**, *122*, 9852. Chatani, N.; Inoue, H.; Morimoto, T.; Muto, T.; Murai, S. *J. Org. Chem.* **2001**, *66*, 4433.

32 Brummond, K.M.; Mitasev, B. *Org. Lett.* **2004**, *6*, 2245.
33 Brummond group, unpublished results.
34 Gilbertson, S.R.; Hoge, G.S.; Genov, D.G. *J. Org. Chem.* **1998**, *63*, 10077. Jolly, R.S.; Leudtke, G.; Sheehan, D.; Livinghouse, T. *J. Am. Chem. Soc.* **1990**, *112*, 4965. Wang, B.; Cao, P.; Zhang, X. *Tetrahedron Lett.* **2000**, *41*, 8041. Paik, S.-J.; Son, S.U.; Chung, Y.K.. *Org. Lett.* **1999**, *1*, 2045. Matsudo, I.; Shibata, M.; Sato, S.; Izumi, Y. *Tetrahedron Lett.* **1987**, *28*, 3361. McKinstry, L.; Livinghouse, T. *Tetrahedron* **1994**, *50*, 6145.
35 Lei, A.; He, M.; Zhang, X. *J. Am. Chem. Soc.* **2003**, *125*, 11472.
36 Tong, X.; Zhang, Z.; Zhang, X. *J. Am. Chem. Soc.* **2003**, *125*, 6370.

9
Rhodium-Catalyzed Nucleophilic Ring Cleaving Reactions of Allylic Ethers and Amines

Keith Fagnou

9.1
Introduction

Since the first report in 1973, there has been significant growth in the use of rhodium catalysis to cleave strained ethers and amines, particularly in the preparation of enantiomerically enriched decalins, cyclohexenes, amino alcohols, and diamino compounds. This chapter describes the major advances in synthetic capabilities and outlines the mechanistic evidence pointing to a working model for the reaction pathway in these processes.

9.2
Seminal Work

In 1973 Hogeveen and Middelkoop reported the first examples of rhodium-catalyzed ring opening reactions of oxabicyclic compounds. They discovered that $[Rh(CO)_2Cl]_2$ catalyzed the ring opening of **1a/b** in the presence of methanol to give **2a/b** (Eq. 1) [1]. The stereochemistry of the methoxyl and hydroxyl substituents was later determined to be *cis*, indicating that nucleophilic attack had occurred from the more sterically accessible *exo* face [2]. Although no mechanistic information was obtained, acid catalysis was deemed unlikely since only aromatic ring-opened products were obtained under analogous conditions with protic catalysts [1].

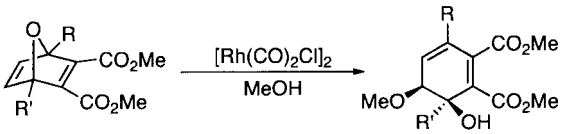

R = R' = Me **1a**
R = R' = H **1b**

R = R' = Me **2a**
R = R' = H **2b**

(1)

Modern Rhodium-Catalyzed Organic Reactions. Edited by P. Andrew Evans

ISBN: 3-527-30683-8

9.3
Asymmetric Reactions with Oxabicyclic Alkenes

Since the early 1990s, Lautens and co-workers have been engaged in the development of new ring cleaving reactions of strained substrates such as oxabicyclic alkenes [3]. Recently, rhodium catalysis has been employed to achieve enantioselective ring opening reactions of oxabicyclic alkenes with a wide range of nucleophiles, for example, alcohols, phenols, anilines, simple amines, malonates, and carboxylates. Depending on the nature of the nucleophile, different catalysts and reaction conditions are required to achieve optimal results. These different catalyst systems can be grouped into first, second, and third generations, and their applications are presented below.

9.3.1
First-Generation Catalyst: $[Rh(COD)Cl]_2$/PPF-P^{t}Bu$_2$

In 2000, Lautens reported that a catalyst generated from $[Rh(COD)Cl]_2$ and the chiral ligand PPF-P^{t}Bu$_2$ [4] could be used with alcohol and most phenol nucleophiles to achieve the enantioselective ring opening of oxabenzonorbornadienes **3** [5]. These reactions are typically carried out under neutral conditions in refluxing THF, and provide the ring-opened product **4** in typically greater than 90% isolated yield, and with 93 to ≥99% enantiomeric excess (Scheme 9.1). Interestingly, the relative stereochemistry of the alkoxy and hydroxyl substituents was determined to be *trans*, opposite to that obtained in the Hogeveen and Middelkoop reaction.

In contrast to the high reactivity of *meta*- and *para*-substituted halophenols, *ortho*-halophenols give low yields, even after prolonged reaction times with the $[Rh(COD)Cl]_2$/

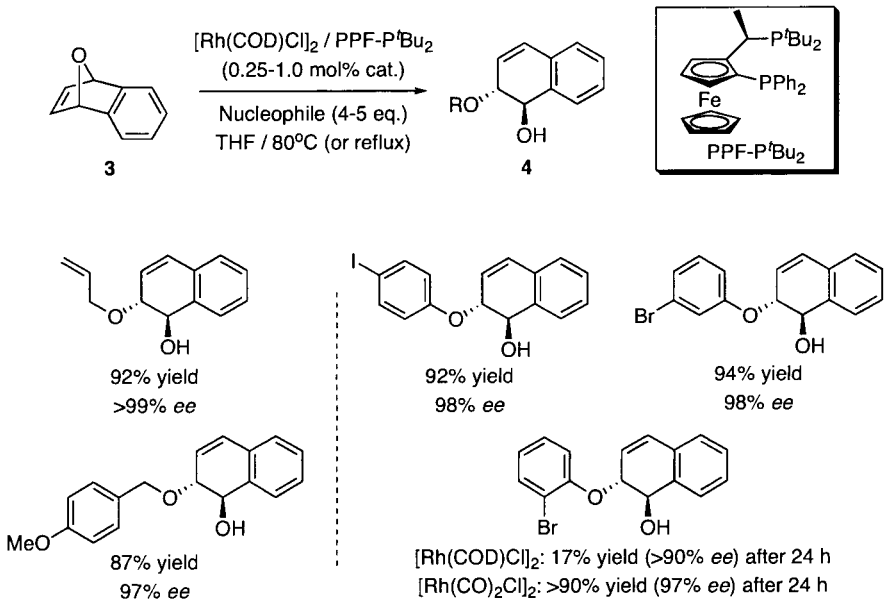

Scheme 9.1

PPF-P^{t}Bu$_2$ catalyst. In these cases, substitution of [Rh(COD)Cl]$_2$ with [Rh(CO)$_2$Cl]$_2$ gave better results, providing complete conversion after 24 h with 5 mol% catalyst. A plausible rationale for the diminished catalyst activity in the presence of 2-halophenols may be the ability of these compounds to form a chelate with the metal center through the halide and hydroxyl groups. This mode of binding has been proposed in hydrogenation reactions with similar catalysts [6]. Hence, by changing the rhodium source to [Rh(CO)$_2$Cl]$_2$, the occupation of an open coordination site with a carbonyl ligand may disfavor this mode of binding.

9.3.2
Second-Generation Catalyst: [Rh(PPF-P^{t}Bu$_2$)I] Generated *in situ*

Despite the high enantioselectivity obtained with alcohol and phenol nucleophiles, the application of the first-generation catalyst to other types of nucleophiles gave inferior results. For example, reaction of **3** with 5 equivalents of *N*-methylaniline and [Rh(COD)Cl]$_2$/PPF-P^{t}Bu$_2$ affords **5** in greater than 90% yield, but with only 70% enantiomeric excess. This diminished enantioselectivity is also observed with other aromatic amines. Furthermore, reactions with the first-generation catalyst and malonates or carboxylic acids/carboxylates give less than 50% conversion, even after prolonged reaction, and afford products with low enantiomeric excess. The poor reactivity and selectivity with these nucleophile classes were ultimately resolved through the development of a more highly active and robust rhodium–iodide catalyst.

In 2001, Lautens reported that the outcome of the rhodium-catalyzed asymmetric ring opening reactions is highly dependent on the nature of the anionic ligand (Scheme 9.2) [7]. Halide–ligand exchange on the rhodium metal is performed by first dissolving the [Rh(COD)Cl]$_2$ and PPF-P^{t}Bu$_2$ in THF, followed by transfer to another flask containing 1.5 equivalents of silver triflate per chloride atom. The resulting heterogeneous mixture is than transferred to a flask containing 2 equivalents of Bu$_4$NX

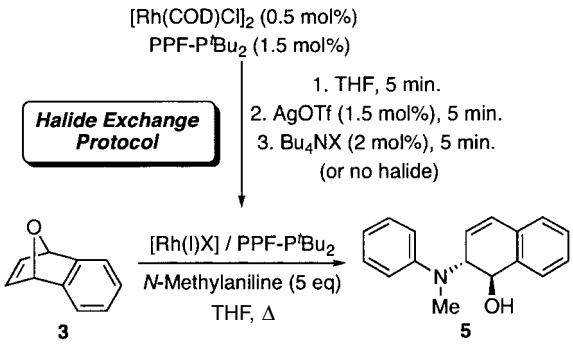

Scheme 9.2

relative to the rhodium monomer, and after a few minutes the solution becomes dark red/brown and is ready to be used. A comparison of the reaction outcome with fluoride, chloride, bromide, iodide, and triflate ligands revealed that optimal results with *N*-methylaniline are obtained with the triflate, fluoride, and iodide catalysts.

Despite the excellent results using *N*-methylaniline and the rhodium–triflate catalyst, with many other nucleophile classes this catalyst gave only substrate decomposition. The rhodium–fluoride is more generally applicable than the triflate complex; its preparation, however, requires the handling of very hygroscopic fluoride salts and must be used under a strictly inert atmosphere, making its general use somewhat limited. On the other hand, the iodide catalyst is robust, generally applicable to a wide range of nucleophiles, and easily prepared from air-stable catalyst precursors. The halide exchange protocol can be easily executed on a wide range of reaction scales. However, care must be taken to not expose the cationic rhodium complex (after step 2 in the halide exchange protocol, Scheme 9.2) to air, as significant catalyst poisoning can occur at this stage. Once the iodide ligand has been added, the reaction can be exposed briefly to the open atmosphere without loss in reactivity or enantioselectivity.

Application of the second-generation [Rh(PPF-P^{t}Bu$_2$)I] catalyst with other activated nitrogen nucleophiles furnished the ring-opened products in high yield and greater than 90% enantiomeric excess (Fig. 9.1) [8]. In some cases, improvements in enantioselectivity of up to 50% can be obtained by changing the halide ligand from chloride to iodide. The problems with reactivity and enantioselectivity associated with malonate nucleophiles are also overcome by making use of the second-generation [Rh(PPF-P^{t}Bu$_2$)I] catalyst [8]. The *trans* relative stereochemistry of the newly formed carbon–carbon bond and the hydroxyl functionality makes this methodology complementary to the palladium-catalyzed addition of dialkyl zinc nucleophiles, which gives the *cis*-products [9]. In order to overcome the lack of reactivity observed with carboxylic acid nu-

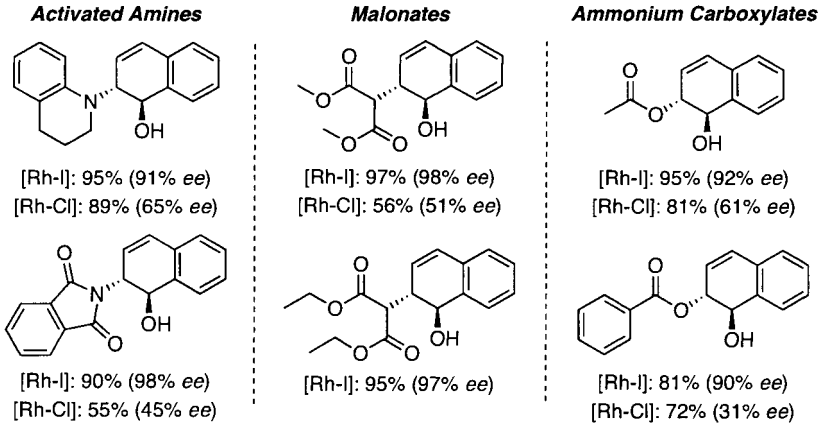

Fig. 9.1 Yields and *ee* values for ring-opened products prepared using [Rh(PPF-P^{t}Bu$_2$)I] catalyst in the presence of activated amines, malonates, or ammonium carboxylates.

cleophiles, ammonium carboxylates are employed, which both retain the necessary proton source and exhibit enhanced nucleophilicity compared to the free acid. For example, the [Rh(PPF-P^{t}Bu$_2$)I] catalyst, with ammonium acetate, furnished the desired product in 95% yield and with 92% enantiomeric excess [10].

The robust nature of the rhodium–iodide catalyst is also revealed in reactions with *ortho*-halo phenols that proved to be problematic with the first-generation catalyst system (Section 9.3.1). By employing the [Rh(PPF-P^{t}Bu$_2$)I] catalyst, complete conversion is obtained with 2-bromophenol to give **6** in 94% yield, and with 95% enantiomeric excess after only 1.5 h of reaction time at 1 mol% catalyst loading (Scheme 9.3) [11]. The ready availability of these ring-opened compounds has been utilized to prepare enantiomerically enriched benzofurans **7**.

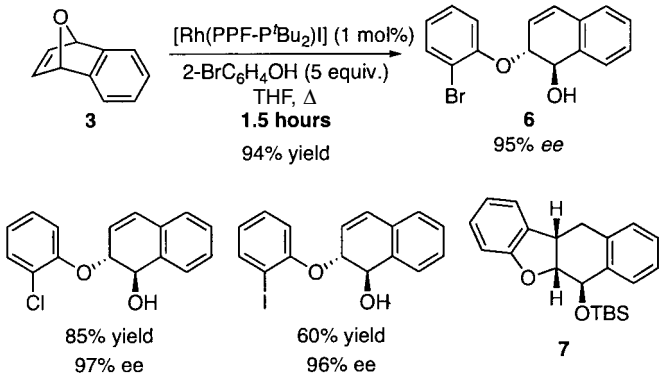

Scheme 9.3

9.3.3
Third-Generation Catalyst: [Rh(PPF-P^{t}Bu$_2$)I] with Excess NH_4I

Simple aliphatic amines proved to be the most challenging class of nucleophiles for the asymmetric rhodium-catalyzed ring opening reaction. Neither the first nor the second-generation catalysts gave any product formation when treated with amines such as pyrrolidine. The poisoning nature of these amines can be illustrated by the addition of 5 equivalents of pyrrolidine to a reaction with *N*-methylaniline. Interestingly, neither amine undergoes reaction, indicating that the aliphatic amine is presumably poisoning the rhodium catalyst and preventing reaction with *N*-methylaniline, which otherwise adds in quantitative yield (Eq. 2). Since it is known that amines are good ligands for rhodium complexes, tight binding of the aliphatic amine to the metal is a likely explanation of the observed behavior.

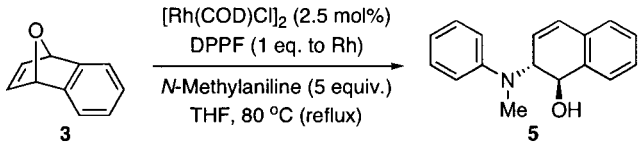

Additive	Time	Yield (%)
none	30 min	98
pyrrolidine (5 equiv.)	6 h	no reaction

(2)

Employing protic and halide additives can effectively reverse the deleterious effect with aliphatic amines [8, 11]. The optimum results are obtained when ammonium iodide is employed as the additive in combination with the second-generation rhodium–iodide catalyst. Under these conditions, a variety of aliphatic amines can be used to generate the aminotetralin products in high yields and with excellent enantiomeric excess (Scheme 9.4). From a technical perspective, ammonium iodide benefits from being a combined proton and iodide source that is air-stable and nonhygroscopic.

Distinct trends in reactivity and enantioselectivity exist in the halide group. With PPF-P^{t}Bu$_2$ as the chiral ligand, the optimal reactivity is obtained with iodide additives. Inferior results are obtained as one moves up the halide group to fluoride, which fails to overcome the catalyst poisoning and affords no reaction (I > Br > Cl >>> F). Optimum enantioselectivity is also observed with iodide additives, with the trend mirroring that for reactivity (I > Br > Cl). Significantly, these trends depend not only on the halide, but also on the nature of the chiral ligand. When BPPFA is employed instead of PPF-P^{t}Bu$_2$, the enantioselectivity trend for the halides is reversed, with optimal results being obtained with chloride additives (Cl > Br > I) [8, 11]. The reversal in the halide

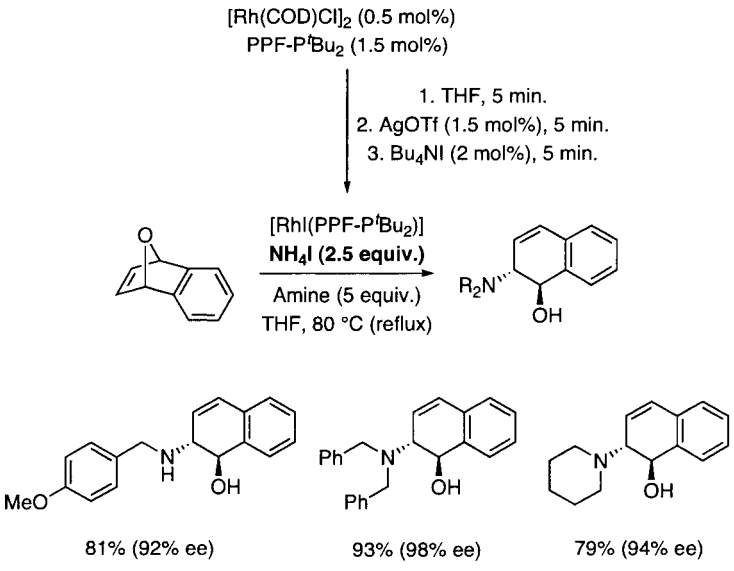

Scheme 9.4

trend in enantioselectivity with these two chiral ligands underlines the complex nature of the halide effect and its influence on enantioselectivity [7].

9.3.4 Catalyst Efficiency

The rhodium-catalyzed ring opening reactions are typically carried out using 0.5–1 mol% catalyst, which can be considered practical and reasonably cost-effective for the reaction scales used in research laboratories. However, for a reaction to be considered synthetically useful on larger scales, turnover numbers should be greater than 10 000 for high-value products and greater than 50 000 for large-scale or less expensive products [12]. The second-generation rhodium–iodide catalyst and modification of the reaction conditions provide the ability to obtain a high level of catalyst efficiency in the ring opening reactions. For example, the addition of the rhodium–iodide catalyst to a melt of the substrate **3** and 1.1 equivalents of nucleophile at 100 °C in the absence of solvent allows catalyst loadings of 0.01 mol% (TON 10 000) to be used to obtain complete conversion within hours (Scheme 9.5) [11]. In some cases the ring-opened product can be isolated in pure form by recrystallization of the crude reaction mixture, thereby obviating the need for chromatography.

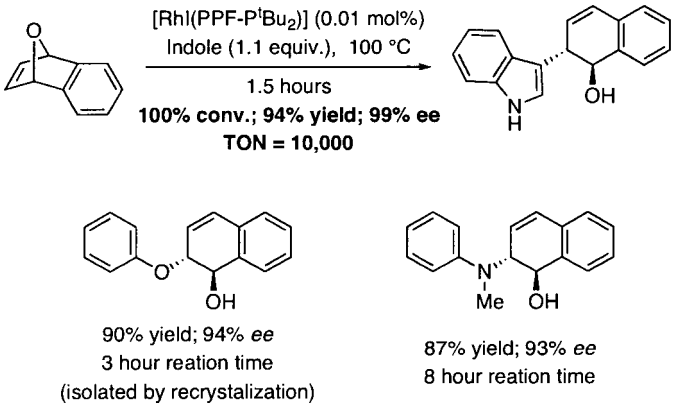

Scheme 9.5

The solventless reaction conditions also enable the reaction to be performed with less reactive substrates such as oxabicyclic alkene **8**, which does not react under the standard conditions. For example, treatment of **8** with catalytic [RhI(PPF-P^{t}Bu$_2$)] and various nucleophiles at 110 °C furnished the cyclohexenol products **9** in good yield and with >90% enantiomeric excess (Scheme 9.6) [11]. The formation of the *trans*-1,2-cyclohexenols from **8** is of mechanistic significance, since the regio- and stereochemical outcomes are the same whether **3** or **8** is employed. Therefore, it appears that the regiochemical outcome is not governed by the developing conjugation, since this would only be present in the 1,2-dihydronaphthalene products.

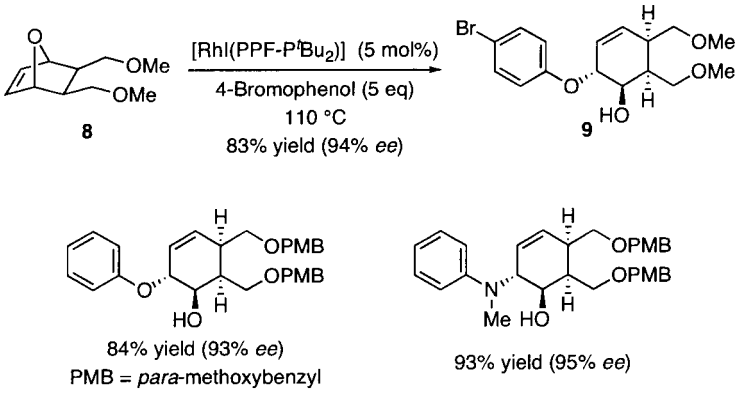

Scheme 9.6

9.4
Azabicyclic Alkenes

Despite the many similarities between oxa- and azabicyclic alkenes, the development of nucleophilic ring opening reactions of azabicycles was hindered by two factors. Firstly, nitrogen functionalities are often poorer leaving groups than those based on oxygen, and as a result azabicycles are far less reactive than the corresponding oxabicycles. This diminished reactivity is mirrored in aziridines and epoxides. Secondly, a nucleophilic nitrogen anion is generated during the ring opening process which can compete with the desired nucleophile and lead to the formation of oligomerization byproducts. These challenges probably explain the relative paucity of reports dealing with aziridines in π-allyl metal chemistry compared to vinyl epoxides. The successful application of rhodium to these systems may indicate that rhodium catalysis could be of more general synthetic utility with these types of challenging substrates.

9.4.1
Nitrogen-Activating Group Effects

The rhodium-catalyzed asymmetric ring opening reaction of azabicyclic alkenes **10** has been examined with aliphatic amine nucleophiles (Fig. 9.2) [13]. The nature of the nitrogen-activating group of the azabicyclic alkene is a key factor in obtaining good reactivity. For example, *N*-methyl and *N*-benzyl azabicycles do not react under the standard conditions used for the oxabicyclic alkenes, and the *N*-Boc azabicycle affords only trace amounts of the product after prolonged reaction times. Increasing the reaction temperature to 100 °C using tetrahydropyran (THP) improves the reactivity with the *N*-Boc substrate, leading to complete conversion overnight. On the other hand, *N*-4-toluenesulfonyl (tosyl) and *N*-4-nitrobenzenesulfonyl (nosyl) substrates both exhibit enhanced reactivity in refluxing THF, giving complete reaction in hours. As with oxabicyclic substrates, protic and halide additives play an important role in the ring opening with aliphatic amines. Optimal catalyst activity is obtained with most aliphatic amine nucleophiles when NH_4I is employed as the protic and halide additive.

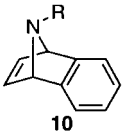

R = Me, Bn	No reaction
R = Boc	No reaction in refluxing THF Good reactivity at 100 °C in THP
R = Ts, Nos	Good reactivity in refluxing THF

Bn = benzyl, Boc = *tert*-butyloxycarbonyl, Ts = 4-toluenesulfonyl, Ns = *tert*-nitrobenzenesulfonyl

Fig. 9.2 Reactivity of azabicyclic alkenes **10**.

9.4.2
Enantioselective Ring Opening Reactions

In contrast to reactions with oxabicyclic alkenes, a single set of reaction conditions fails to provide optimal yield and enantioselectivity with all nucleophiles. Importantly, by varying the reaction conditions, good to excellent results can be obtained in all cases [13]. Optimum results in asymmetric ring opening reactions are obtained with the *N*-Boc-protected azabicycle (Scheme 9.7). For example, when pyrrolidine was used as the nucleophile, the catalyst generated from $[Rh(COD)Cl]_2$ and C_2-Ferriphos, combined with Et_3NHCl as a chloride and protic additive in THP at 100 °C, afforded **11** in 77% yield and with 86% enantiomeric excess. In contrast, amines possessing a neighboring heteroatom such as *N*-phenylpiperazine and morpholine react best in the absence of additive. The more sterically hindered dibenzylamine also reacts well in the absence of additive.

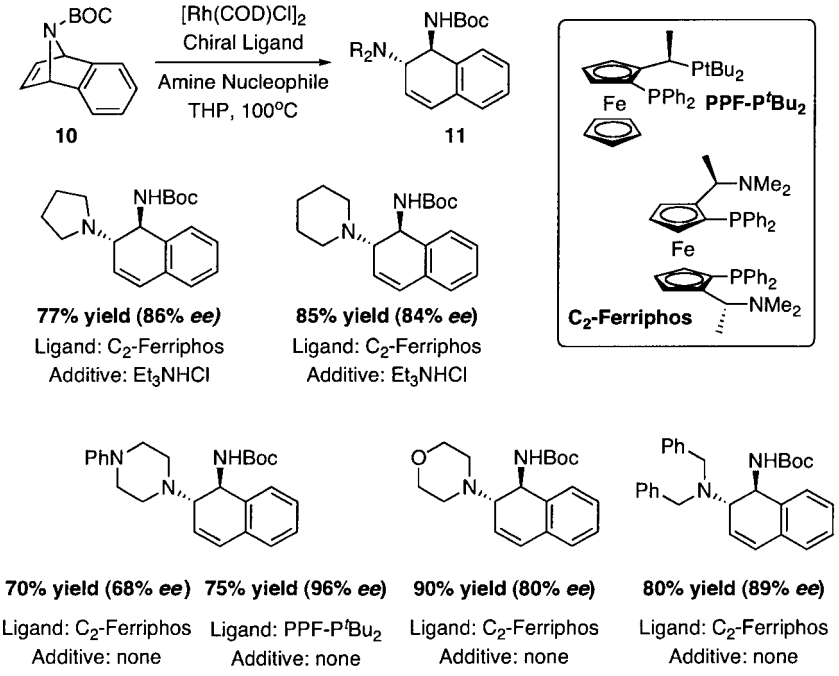

Scheme 9.7

Interestingly, the sense of induction is reversed compared to the enantioselective ring opening of oxabicyclic alkenes. The reversal in stereochemical induction and the lower selectivities with azabicyclic alkene substrates may be due to the availability of different binding modes with the *N*-activating group on the substrate. The synthetic utility of this methodology has been demonstrated in the preparation of a κ-opioid analgesic compound **12** (Eq. 3) [13].

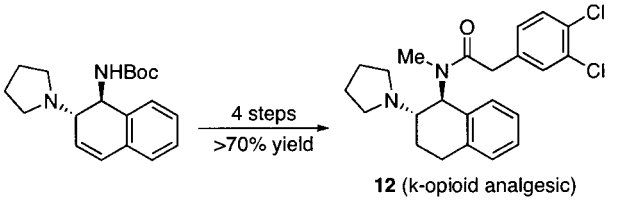

12 (k-opioid analgesic) (3)

9.5 Properties of the PPF-P^{t}Bu$_2$ Ligand

Recent studies have delineated the important properties of the PPF-P^{t}Bu$_2$ ligand that contribute to its successful application in asymmetric ring opening reactions (Scheme 9.8) [14]. For example, increasing the steric bulk of the benzylic phosphane from Cy_2P (ligand **13**) to $^tBu_2P$ (ligand **14**) increases the enantioselectivity from 88 to 96% enantiomeric excess. This increase in enantioselectivity comes at the expense of reactivity, since the $^tBu_2P$ ligand **14** produces a catalyst that is roughly half as active as that gen-

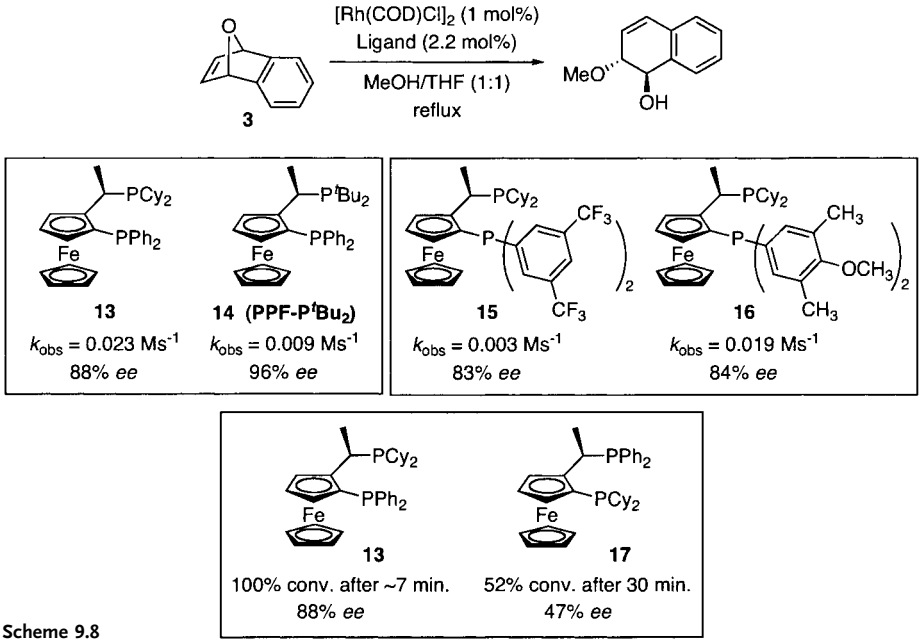

Scheme 9.8

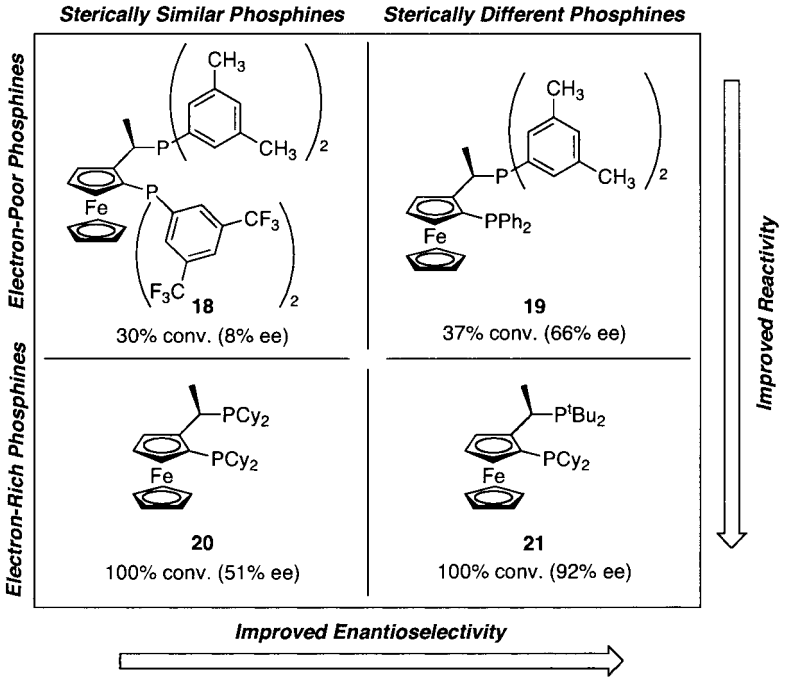

Fig. 9.3 Relative reactivity and enantioselectivity of various [Rh(PPF-P^{t}Bu$_2$)I] ligands.

erated from the Cy_2P ligand **13** (k_{obs} 0.023 versus 0.009 M s^{-1}). Furthermore, the larger phosphane must be situated at the benzylic position, as illustrated by the different outcomes with ligands **13** and **17**. This demonstrates that when the large phosphane is located on the ferrocenyl ring, poor reactivity and enantioselectivity are obtained (ligand **17**). Ligand electronics are also important; this is demonstrated by reactions with electron-deficient **15** and electron-rich **16**. These ligands provide similar enantioselectivity (83% *ee* with **15** versus 84% *ee* with **16**), but the more electron-rich ligand **16** produces a catalyst that is 6.8 times more reactive than one generated from ligand **15**.

Ligands **18**, **19**, **20**, and **21** also shed light on some important ligand parameters (Fig. 9.3). Ligand **18**, which is electron-deficient and has two phosphanes of similar size, gives only 30% conversion and 8% enantiomeric excess after 30 min. The best result is obtained with electron-rich ligand **21** bearing a large benzylic phosphine and a smaller ferrocenyl phosphine. With ligand **21**, 100% conversion and 92% enantiomeric excess were obtained. Intermediary results are obtained with ligands **19** and **20**, supporting the notion that electron-rich ligands produce more reactive catalysts (ligands **20** and **21** versus ligands **18** and **19**) and that sterically larger phosphines at the benzylic position give improved enantiomeric excess (ligands **19** and **21** versus ligands **18** and **20**).

The relative importance of the planar and central elements of chirality within the Josiphos skeleton has also been established. Diastereomeric ligands **13** and **22** bear the same (*R*) central chirality but have the opposite planar chirality (Fig. 9.4). Under standard reaction conditions with methanol as the nucleophile, the (*R*),(*S*)-ligand **13** gives 100% conversion after approximately 7 min. Conversely, the (*R*),(*R*)-diastereomer **22** gives incom-

13
(*R*),(*S*)-PPF-PCy_2
100% conv. after ~7 min.
87.6% *ee*

22
(*R*),(*R*)-PPF-PCy_2
67% conv. after 30 min.
-33.4% *ee*

Fig. 9.4 Importance of planar chirality for diastereomeric ligands **13** and **22**.

plete conversion (67%) after 30 min. The enantioselectivity is also influenced by both elements of chirality. By changing only the planar chirality, the sense of induction is reversed giving the opposite enantiomer in 33.4% enantiomeric excess. This indicates that the planar chirality plays the largest role in determining the absolute sense of induction, and that the highest enantioselectivity is obtained with the (*R*),(*S*)-diastereomer. Conveniently, this diastereomer also provides the highest reactivity.

9.6 Mechanistic Working Model

9.6.1 Proposed Catalytic Cycle

The proposed catalytic cycle is outlined in Scheme 9.9 [14]. Dimeric complex **23** is cleaved to give the monomeric complex **24** by solvation, substrate binding, or reaction with the nucleophile. Reversible *exo*-coordination of the substrate is followed by oxidative insertion with retention into a bridgehead C–O bond to give the π-allyl or σ-rhodium alkoxide complexes **26** or **27**. It is likely that the formation of these rhodium(III) alkoxide complexes is irreversible due to the release of the ring strain present in the oxabicyclic alkene substrate. The oxidative cleavage of the C–O bond is proposed to be the enantiodiscriminating step in the catalytic cycle.

Regardless of the precise mode of binding to the allyl moiety, the rhodium metal will probably be situated closer to the benzylic carbon atom, due to the directing influence of the alkoxide ligand. This is illustrated by the two σ-complexes **27** and **28**. Since there will be a significant degree of ring strain associated with the [4.2.0] structure **28**, this complex will be disfavored compared to the more stable [2.2.2]-**27**. This argument can also be applied to the π-allyl rhodium complex **26**. By shifting the rhodium metal on the π-allyl moiety to the distal position relative to the alkoxide, ring strain will be minimized.

Once **26** or **27** has been formed, the rhodium–alkoxide complex is protonated by a nucleophile molecule, generating the cationic rhodium complex **29** and an alkoxide or phenoxide nucleophile. This proton transfer step is supported by kinetics experiments and has two effects [14]. Firstly, the organorhodium species is made more electrophilic as a result of the positive charge, and secondly, the nucleophile is rendered more nucleophilic by becoming deprotonated.

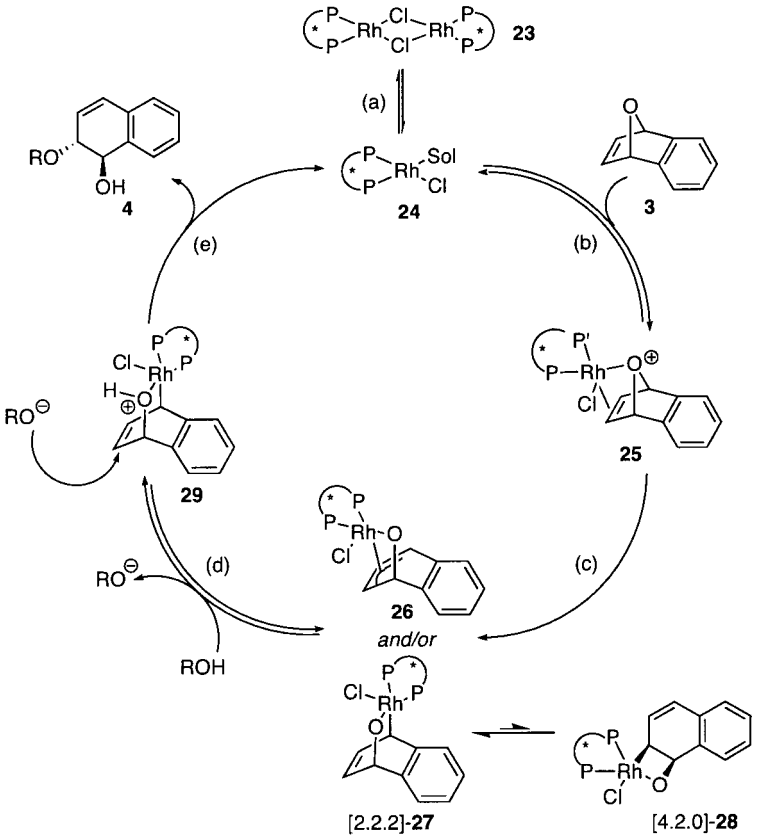

Scheme 9.9 (a) Cleavage of the dimeric rhodium complex; (b) *exo*-coordination of the oxabicyclic alkene; (c) oxidative insertion into the bridgehead C-O bond with retention; (d) protonation of the rhodium-alkoxide by the nucleophile; (e) nucleophilic attack with inversion and product liberation

The positioning of the rhodium metal on the π-allyl moiety will influence the regioselectivity of nucleophilic attack. Nucleophilic attack with inversion is proposed to occur adjacent to the alkoxy group in an S_N2' fashion relative to the rhodium metal. The product is subsequently liberated and the regenerated rhodium monomer will either reform the dimer (if another rhodium monomer is encountered) or continue the catalytic cycle.

9.6.2
Proposed Role of Protic/Halide Additives

The current working model for the beneficial role of protic and halide additives in reactions with aliphatic amines is outlined in Scheme 9.10 [11]. In these reactions, the rhodium dihalide dimer **30** is proposed to enter two different catalytic cycles. In the productive catalytic cycle, the dimer is cleaved by solvation or binding with the substrate to give **31**. Oxidative insertion followed by protonation of the rhodium alkoxide

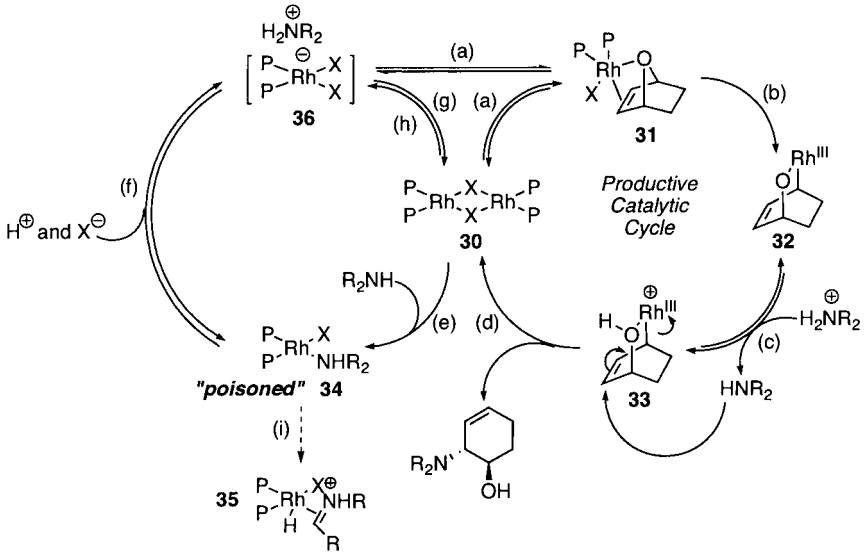

Scheme 9.10 (a) Substrate binding on the *exo*-face (displacement of a halide ligand or dimer bridge cleavage); (b) oxidative insertion; (c) protonation of the rhodium alkoxide; (d) nucleophilic attack and product liberation; (e) irreversible amine binding; (f) amine ligand protonation and nucelophilic displacement by a halide nucleophile; (g) dimer formation with loss of a halide ligand; (h) dimer cleavage by nucleophilic displacement with a halide; (i) α-oxidation of the amine ligand.

32 by an ammonium salt will give the cationic complex **33**. Intermediate **33** will react with the nucleophile to give the ring-opened product and regenerate the catalyst.

Alternatively, the rhodium dimer **30** may be cleaved by an amine nucleophile to give **34**. Since amine–rhodium complexes are known to be stable, this interaction may sequester the catalyst from the productive catalytic cycle. Amine–rhodium complexes are also known to undergo α-oxidation to give hydridorhodium imine complexes **35**, which may also be a source of catalyst poisoning. However, in the presence of protic and halide additives, the amine–rhodium complex **34** could react to give the dihalorhodate complex **36**. This could occur by associative nucleophilic displacement of the amine by a halide anion. Dihalorhodate **36** could then reform the dimeric complex **30** by reaction with another rhodium monomer, or go on to react directly with another substrate molecule with loss of one of the halide ligands. It is important to note that the dihalorhodate **36** may become a new resting state for the catalyst under these conditions, in addition to or in place of the dimeric complex.

9.7
Vinyl Epoxides

The epoxide functionality has tremendous versatility in the preparation of complex molecules, since its treatment with a nucleophile affords an alcohol, two contiguous stereocenters, and a new carbon–carbon or carbon–heteroatom bond in a single step.

Furthermore, epoxides are stable to prolonged storage, yet "spring-loaded" due to their inherent ring strain. In recent years, significant effort has been devoted to both enantioselective desymmetrizations [15] and kinetic resolutions of these substrates [16, 17]. Vinyl epoxides represent an important subset of this class of compound [18]. Not only does the presence of the vinyl functionality activate the epoxide to certain types of reactions but the vinyl acts as a directing group to influence the regiochemical outcome. Recently, rhodium complexes have been demonstrated to catalyze the diastereoselective ring opening of vinyl epoxides.

9.7.1
Current Capabilities

A variety of rhodium complexes, including $[Rh(CO)_2Cl]_2$ and $[Rh(COD)Cl]_2$ when used in combination with a variety of bisphosphine ligands, will catalyze the ring opening of vinyl epoxides in the presence of aniline nucleophiles [19, 20]. These reactions occur under very mild and neutral conditions (at room temperature or with mild heating) and are highly regio- and stereoselective. In all cases, nucleophilic attack occurs at the allylic epoxide carbon atom and proceeds with inversion of stereochemistry (Scheme 9.11).

In contrast to reactions with vinyl epoxides and palladium catalysts, the reactions with rhodium retain the stereochemistry of the alkene fragment during the reaction [20]. This is illustrated by the reactions of ***trans*-37 a/b** and ***cis*-37 a/b**, which give only one product possessing the same olefin geometry as the starting epoxides (Eqs. 4 and 5). The retention of olefin stereochemisty has also been documented in allylic functionalizations with iridium catalysts, indicating that similar modes of action may be present [21, 22].

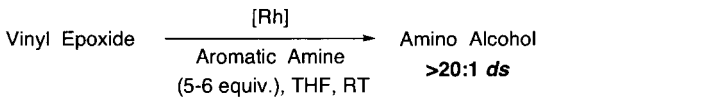

[Rh] = $[Rh(CO)_2Cl]_2$, or $[Rh(COD)Cl]_2$ / ligand (dppf, dppm, dppe, dppp, dppb, PPF-P^{t}Bu$_2$)

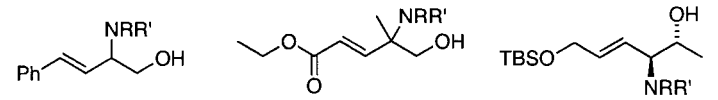

N-Methylaniline: 93%

Aniline: 91%
p-Bromoaniline: 89%
1-aminonaphthalene: 86%

N-Methylaniline: 94%

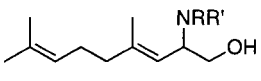

N-Methylaniline: 94%

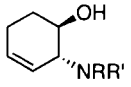

N-Methylaniline: 91%

Scheme 9.11

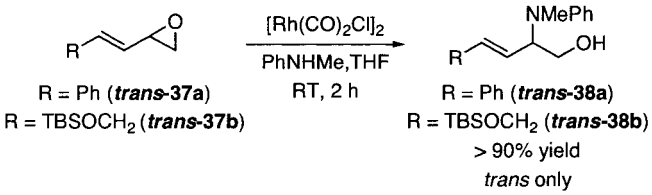

(4)

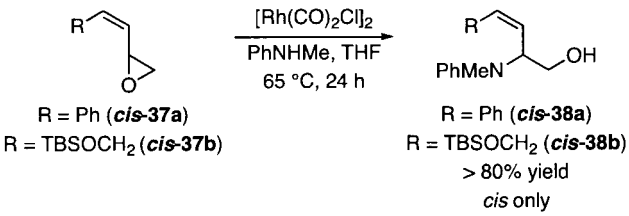

(5)

9.7.2 Mechanistic Working Model

The proposed catalytic cycle is described in Scheme 9.12. Coordination of the rhodium catalyst to the vinyl epoxide via the olefin and the oxygen atom gives complex **39**. Subsequent oxidative insertion with retention gives the [4.2.0]bicyclic rhodium species **40**, which will rearrange to its complementary σ-form **41**. By virtue of the larger ring sizes within the [2.2.2] core, **41** will be more stable and should be the major organorhodium intermediate in solution. Since nucleophilic attack can theoretically occur with both **40** and **41**, attack at **40** must be slower than the isomerization to **41** (that is, $k_1 \gg k_2$). In addition to the two σ-intermediates, the π-allyl–rhodium complex **42** may also be invoked. Since the same strain associated with ring strain will be present in **42**, it can be expected that the rhodium lies at the distal allylic carbon relative to the alkoxide.

Based on this model, the regiochemical outcome of *both* oxabicyclic alkenes and vinyl epoxides can be explained by the relative stability of the two σ-intermediates. With oxabicyclic alkenes intermediate **41** is generated directly and then goes on to give product, whereas with the vinyl epoxides a more highly strained intermediate **40** is first produced which must first isomerize to **41** prior to product formation. The regiochemical outcome with each substrate may therefore arise from the commonality of a σ–intermediate **41** to both reaction pathways (Scheme 9.13).

9.8 Conclusion

Rhodium catalysis has proven to be an efficient means of selectively cleaving strained ethers and amines. These reactions occur under mild conditions and generate products in high yield and enantiomeric excess. Three different catalyst "generations" have been developed that enable a wide range of substrate and nucleophile compatibility. A catalytic cycle has been proposed that involves a new mode of action for rhodium complexes and rationalizes the similar regioselectivities observed in reactions between oxabicyclic alkenes and vinyl epoxides. Given the ease with which these reactions can be carried out and the synthetic utility of the products, these new rhodium-catalyzed transformations should find significant synthetic utility and provide a framework upon which new transformations may be developed.

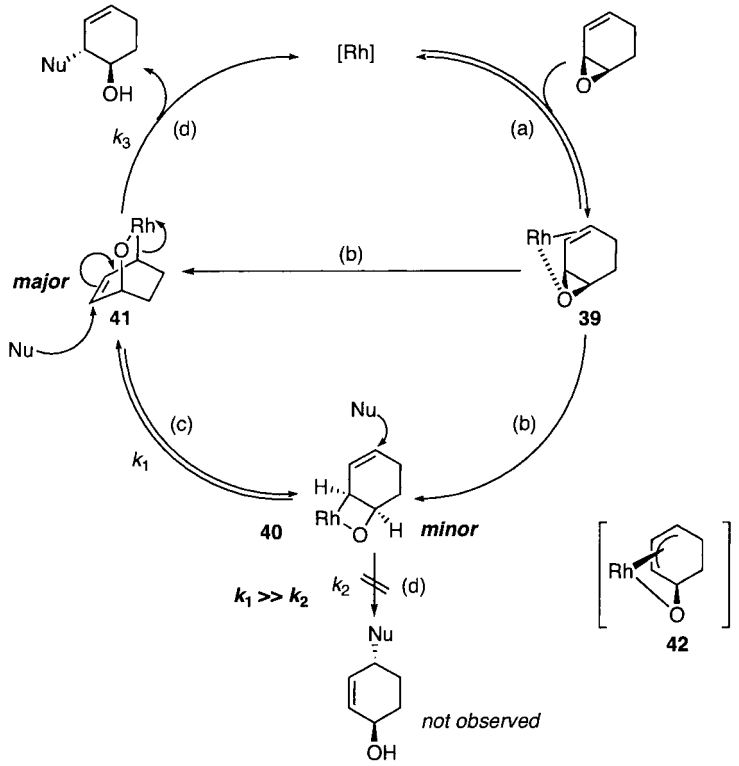

Scheme 9.12 (a) *exo*-coordination of the oxabicyclic alkene; (b) oxidative insertion into the allylic C-O bond with retention; (c) isomerization of the organorhodium intermediate; (d) nucleophilic attack with inversion and product liberation.

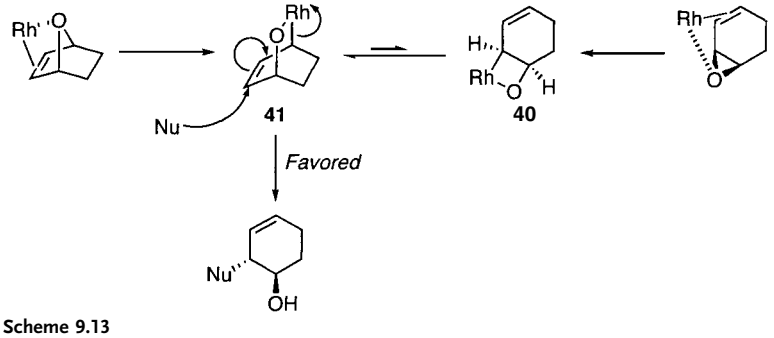

Scheme 9.13

Acknowledgement

The bulk of the work reported in this review was carried out in the Lautens Laboratories at the University of Toronto [23]. Professor Mark Lautens (University of Toronto) is gratefully acknowledged for his supervision, guidance, and mentorship during my graduate studies in his research group and for helpful comments during the writing of this review. Professor Tomislav Rovis (Colorado State University), Mark Taylor, Jasmine Almas, Valentin Zunic, and Professor Dingqiao Yang (South China Normal University) are also acknowledged for their intellectual and experimental contributions to the rhodium-catalyzed ring opening chemistry.

9.9 References

1 Hogeveen, H.; Middelkoop, T.B. *Tetrahedron Lett.* **1973**, 3671.
2 Ashworth, R.W.; Berchtold, G.A. *Tetrahedron Lett.* **1977**, 339.
3 (a) Lautens, M. *Synlett* **1993**,177. (b) Chiu, P.; Lautens, M. *Top.Curr.Chem.* **1997**, *190*, 1. (c) Lautens, M.; Fagnou, K.; Hiebert, S. *Acc. Chem. Res.* **2003**, *36*, 48.
4 (a) Togni, A.; Breutel, C.; Schnyder, A.; Spindler, F.; Landert, H.; Tijani, A. *J. Am. Chem. Soc.* **1994**, *116*, 4062. (b) Hayashi, T.; Mise, T.; Fukushima, M.; Kagotani, M.; Nagashima, N.; Hamada, Y.; Matsumoto, A.; Kawakami, S.; Konishi, M.; Yamamoto, K.; Kumada, M. *Chem. Bull. Soc. Jpn.* **1980**, *53*, 1138.
5 (a) Lautens, M.; Fagnou, K.; Rovis, T. *J. Am. Chem. Soc.* **2000**, *122*, 5650. (b) Lautens, M.; Fagnou, K.; Taylor, M. *Org. Lett.* **2000**, *2*, 1677. (c) Lautens, M.; Fagnou, K.; Taylor, M.; Rovis, T. *J. Organomet. Chem.* **2001**, *624*, 259.
6 Brenchley, G.; Fedouloff, M.; Merifield, E.; Wills, M. *Tetrahedron: Asymmetry* **1996**, 2809. See also: Kitamura, M.; Ohkuma, T.; Inoue, S.; Sayo, N.; Kumobayashi, H.; Kkutagawa, S.; Ohta, T.; Takaya, H.; Noyori, R. *J. Am. Chem. Soc.* **1988**, *110*, 629.
7 For a review, see: Fagnou, K.; Lautens, M. *Angew. Chem. Int. Ed.* **2002**, *41*, 26.
8 Lautens, M.; Fagnou, K. *J. Am. Chem. Soc.* **2001**, *123*, 1770.
9 Lautens, M.; Renaud, J.-L.; Hiebert, S. *J. Am. Chem. Soc.* **2000**, *122*, 1804.
10 Lautens, M.; Fagnou, K. *Tetrahedron* **2001**, *57*, 5067.
11 Lautens, M.; Fagnou, K.; Yang, D. *J. Am. Chem. Soc.* **2003**, *125*, 14884.
12 Blasser, H.U. *Chem. Commun.* **2003**, 293.
13 Lautens, M.; Fagnou, K.; Zunic, V. *Org. Lett.* **2002**, *4*, 3465.
14 Lautens, M.; Fagnou, K. *Proc. Nat. Acad. Sci. USA* **2004**, *101*, 5455.
15 For example, see: Matsunaga, S.; Das, J.; Roels, J.; Vogl, E.M.; Yamamoto, N.; Iida, T.; Yamaguchi, K.; Shibasaki, M. *J. Am. Chem. Soc.* **2000**, *122*, 2252; and references therein.
16 For example, see: Tokunaga, M.; Larrow, J.F.; Kakiuchi, F.; Jacobsen, E.N. *Science* **1997**, *277*, 936.
17 For reviews, see: (a) Hodgson, D.M.; Gibbs, A.R.; Lee, G.P. *Tetrahedron* **1996**, *52*, 14361. (b) Willis, M.C. *J. Chem. Soc., Perkin Trans. 1* **1999**, 1765.
18 *Comprehensive Organic Synthesis, Vol. 6*, Trost, B.M.; Flemming, I. (Eds.), Pergamon Press, New York, **1991**.
19 Fagnou, K.; Lautens, M. *Org. Lett.* **2000**, *2*, 2319.
20 Almas, J.M.Sc. Thesis, University of Toronto, **2004**.
21 Takeuchi, R.; Shiga, N. *Org. Lett.* **1999**, *1*, 265.
22 Takeuchi, R.; Ue, N.; Tanabe, K.; Yamashita, K.; Shiga, N. *J. Am. Chem. Soc.* **2001**, *123*, 9525.
23 Fagnou, K. Ph.D Thesis, University of Toronto, **2003**.

10
Rhodium(I)-Catalyzed Allylic Substitution Reactions and their Applications to Target Directed Synthesis

David K. Leahy and P. Andrew Evans

10.1
Introduction

The drive for the development of more cost-effective, expeditious, and environmentally benign synthetic transformations for the production of fine chemicals, pharmaceuticals, and agrochemicals provides the impetus for the development of new catalytic processes. The allylic substitution reaction represents a powerful synthetic transformation that has been extensively studied using a wide range of transition metal complexes [1–3]. The enantioselective metal-catalyzed reaction manifold is particularly pertinent; however, the major limitation with this transformation is the necessity to employ substrates that furnish symmetrical π-allyl intermediates, to circumvent problems associated with regiochemical infidelity. Although there are reports of regio- and enantioselective allylic alkylation with acyclic 3-substituted propenyl derivatives, useful selectivity is, for the most part, limited to electronically biased cinnamyl derivatives [4]. Furthermore, the alkylation of unsymmetrical chiral nonracemic allylic alcohols generally leads to considerable racemization through π–σ–π isomerization due to the fluxional or rapidly equilibrating nature of π-allyl intermediates [5]. Hence, although these reactions were previously unselective with other transition metal catalysts, they may be accomplished with unparalleled selectivity using rhodium catalysts. This chapter outlines some of the most recent advances in the area of rhodium-catalyzed allylic substitution reactions.

10.2
Regioselective Rhodium-Catalyzed Allylic Alkylation

By 1984, the palladium-catalyzed allylic alkylation reaction had been extensively studied as a method for carbon–carbon bond formation, whereas the synthetic utility of other metal catalysts was largely unexplored [1, 2]. Hence, prior to this period rhodium's ability to catalyze this transformation was cited in only a single reference, which described it as being poor by comparison with the analogous palladium-catalyzed version [6]. Nonetheless, Yamamoto and Tsuji independently described the first rhodium-catalyzed decarboxylation of allylic phenyl carbonates and the intramolecular decarboxylative allylation of allyl β-keto carboxylates respectively [7, 8]. These findings undoubtedly laid the groundwork for Tsuji's seminal work on the regiospecific rho-

Modern Rhodium-Catalyzed Organic Reactions. Edited by P. Andrew Evans

ISBN: 3-527-30683-8

dium-catalyzed allylation of carbonucleophiles with unsymmetrical acyclic allylic carbonates under neutral conditions [9]. Interestingly, the rhodium(I) and (II) oxidation states proved catalytically active, and $RhH(PPh_3)_4$ modified *in situ* with tri-(*n*-butyl) phosphine proved to be the most efficient catalyst for this transformation (Eq. 1).

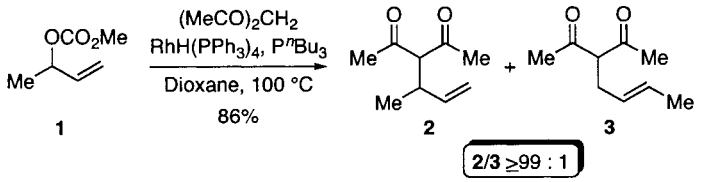

(1)

A key feature of this reaction was the unusual regiospecificity: isomeric allylic carbonates furnish the analogous isomeric alkylation products with modest to excellent regioselectivity. This prompted additional studies to compare these results to the analogous palladium-catalyzed version of the reaction (Scheme 10.1) [10]. Interestingly, rhodium-catalyzed allylic alkylation with the branched allylic carbonate **1** leads to predominant formation of the branched product **5**, while the isomeric linear allylic carbonate **4** favors the linear products **6**/**7**. These results are in sharp contrast to the palladium-catalyzed version of the reaction, in which the same ratio branched to of linear products **6**/**7** is obtained irrespective of which allylic carbonate is employed. These results suggest that rhodium-catalyzed allylic alkylation does not proceed through a fluxional π-allyl organorhodium intermediate. Tsuji proposed that the rhodium-catalyzed version may proceed via a σ-allyl organorhodium complex, but this hypothesis was not corroborated with additional experimental studies. Despite the unique and exciting possibilities for controlling regioselectivity in unsymmetrical acyclic allylic alcohol derivatives, this reaction lay dormant for 14 years.

Evans and Nelson reexamined the rhodium-catalyzed allylic substitution reaction, in which they demonstrated that a triorganophosphite-modified Wilkinson's catalyst facilitates the allylic alkylation of secondary and tertiary allylic carbonates with excellent regioselectivity (Eq. 2). This work provided a convenient method for the construction of ternary and quaternary allylic products [11]. Additionally, they demonstrated that the modification of Wilkinson's catalyst with triorganophosphites serves to increase the re-

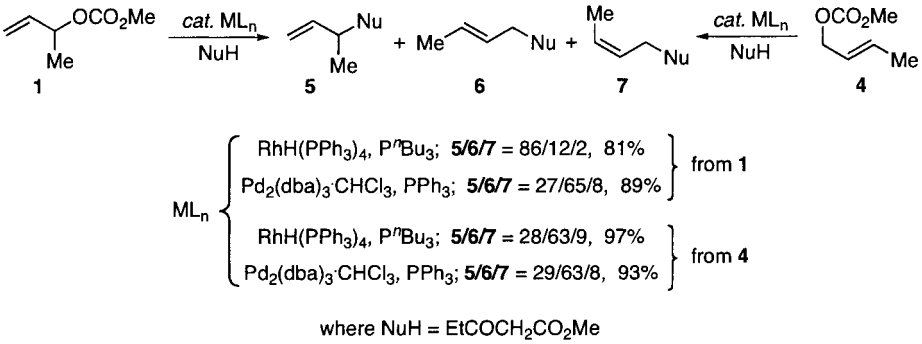

Scheme 10.1 The effect of the metal on regiospecificity in the allylic substitution.

action rate in addition to enhancing regiospecificity. This was attributed to the increased π-accepting nature of the triorganophosphite additive, which promotes alkylation at the more substituted terminus. Subsequently, Takeuchi and Kitamura published a similar approach, wherein they demonstrated that the triphenylphosphite-modified $[Rh(COD)Cl]_2$ complex also catalyzes the allylic alkylation of secondary allylic acetates, with modest to excellent selectivity [12].

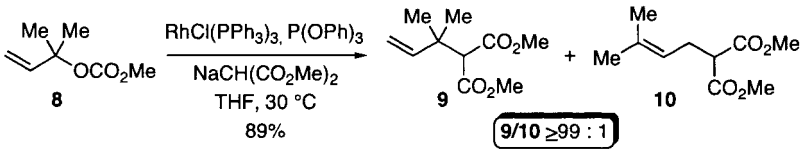

(2)

Evans and Kennedy later combined the regioselective rhodium-catalyzed allylic alkylation, using α-substituted malonates, with ring-closing metathesis for the construction of five-, six-, and seven-membered carbocycles (Scheme 10.2) [13]. The combination of these methodologies allowed for the rapid and flexible assembly of carbocycles possessing vicinal ternary–quaternary or quaternary–quaternary stereogenic centers.

This study demonstrated that the allylic alkylation of secondary carbonates with α-branched malonates using the trifluoroethyl phosphite-modified Wilkinson's catalyst proceeds with excellent selectivity. Although the trifluoroethyl phosphite catalyst proved optimal for secondary carbonates, modification with triphenylphosphite proved superior for the tertiary carbonates, affording the vicinal quaternary–quaternary alkylation products in excellent yield and with good regioselectivity. The dienes were then subjected to either Grubbs' catalyst or the more reactive second-generation Grubbs' *N*-heterocyclic carbene catalyst to afford the desired carbocycles [14, 15].

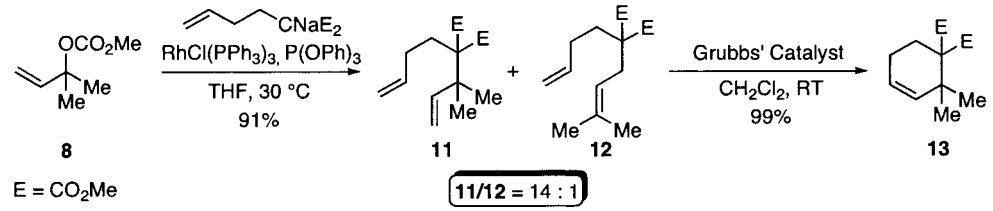

Scheme 10.2 The allylic alkylation/ring-closing metathesis approach to vicinally substituted carbocycles.

10.3
Enantiospecific Rhodium-Catalyzed Allylic Alkylation

Evans and Nelson examined the stereospecificity of the rhodium-catalyzed allylic alkylation, with the expectation that it would provide additional insight into the mechanism for this particular reaction [16]. They reasoned that the enantiomerically enriched allylic alcohol derivative **i** would furnish the enantioenriched product **iv**, provided the initial enyl intermediate **ii** does not isomerize to the achiral σ-organorhodium intermediate **iii** prior to alkylation ($k_2 \gg k_1$; Scheme 10.3). Alternatively, the product of re-

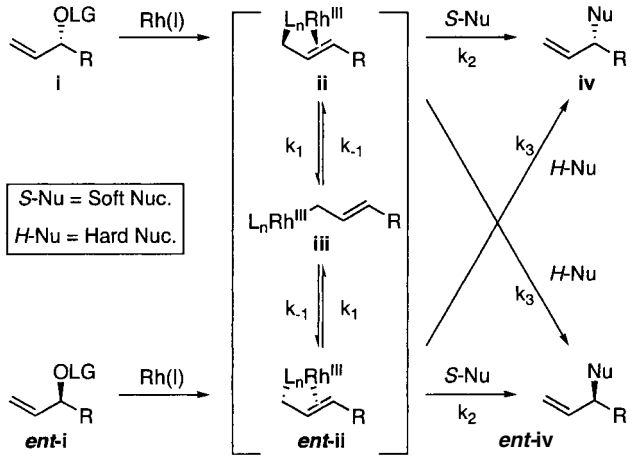

Scheme 10.3 The origin of stereospecificity in rhodium-catalyzed allylic substitution.

tention, ***ent*-iv**, would be derived from direct attack of the metal center in **ii** followed by reductive elimination ($k_3 \gg k_2$). These mechanistic pathways are generally discriminated by whether the nucleophile is stabilized or unstabilized, and usually are accompanied by significant stereochemical leakage.

Treatment of the enantiomerically enriched acyclic allylic carbonate **(*S*)-1** (97% *ee*) under the standard reaction conditions furnished the allylic alkylation product **(*S*)-14** (95% *ee*) in 86% yield, with net retention of absolute configuration (Eq. 3). This result implies that the displacement occurs *via* a classical double inversion process, albeit through a configurationally stable distorted π-allyl or enyl ($\sigma+\pi$) organorhodium intermediate. This is supported by the fact that the achiral σ-species **iii** would undoubtedly have afforded the racemate of **14** (Scheme 10.3). Additionally, the enyl ($\sigma+\pi$) organometallic intermediate provides a model for the regio- and enantiospecificity observed in the reaction.

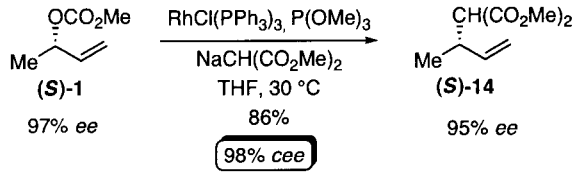

(3)

10.3.1

Rhodium-Catalyzed Allylic Alkylation Reaction with Stabilized Carbon Nucleophiles

Rhodium-catalyzed allylic alkylation provides an expeditious entry into a variety of useful synthons for asymmetric synthesis. For example, the application of this reaction to a range of enantiomerically enriched allylic carbonates with the sodium salt of methyl phenylsulfonylacetate provides products that represent important synthons for target-directed synthesis (Tab. 10.1) [17].

Tab. 10.1 Regioselective and enantiospecific rhodium-catalyzed allylic alkylation of enantiomerically enriched allylic carbonates.

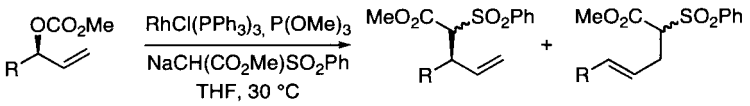

Entry	*R*	*Ratio (2°:1°)*	*cee (%)*	*Yield (%)*
1	Me	36:1	98	86
2	CH_2=$CH(CH_2)_3$	26:1	98	91
3	$PhCH_2$	9:1	98	86
4	$Ph(CH_2)_2$	22:1	97	87
5	$BnOCH_2$	≥99:1	98	86
6	$TBSOCH_2$	18:1	100	86
7	$TPSOCH_2$	3:1	100	78
8	Ph	61:1	98	97

Tab. 10.1 summarizes the results of this study, in which the allylic alkylation is tolerant to a wide range of substituents, as demonstrated by the excellent regio- and enantiospecificities obtained in the reaction. Useful substituents include the alkyl, aryl, alkenyl, and protected hydroxymethyl groups. Interestingly, excellent enantiospecificity is obtained with substrates that exhibit reduced regioselectivity (entry 7). This observation implies that the organorhodium intermediate is indeed configurationally stable, and not subject to π–σ–π isomerization or metal–metal displacement as a means of *facial* exchange. These results also suggest that the regio- and enantiospecificity of the reaction are independent of one another.

The allylic alkylation products represent useful synthons, as exemplified by the reaction sequence outlined in Scheme 10.4. For example, reductive ozonolysis of the allylic alkylation product **15** afforded the γ-lactone **16** as a single diastereoisomer. Sequential alkylation with methyl iodide, and reductive alkylation using lithium naphthalenide with allyl iodide furnished the ternary–quaternary substituted γ-lactones **17a/17b** in 72% overall yield, as a 10:1 mixture of diastereomers favoring **17a** [18]. This method provides a versatile approach to the construction of a variety of α-quaternary-β-ternary stereogenic centers.

The stereospecific construction of acyclic *anti*-1,3-carbon stereogenic centers and C_2-symmetrical fragments was also accomplished via the sequential allylic alkylation

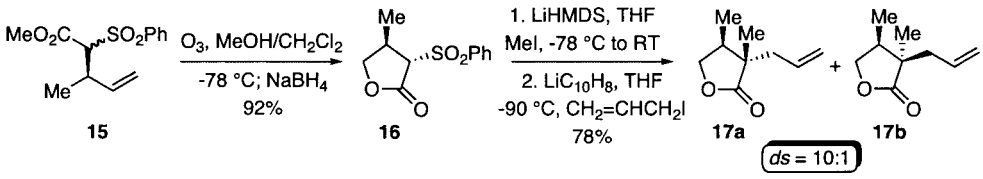

Scheme 10.4 The diastereoselective approach to quaternary carbon stereogenic centers.

Tab. 10.2 The scope of rhodium-catalyzed allylic alkylation with enantiomerically enriched α-branched malonates.

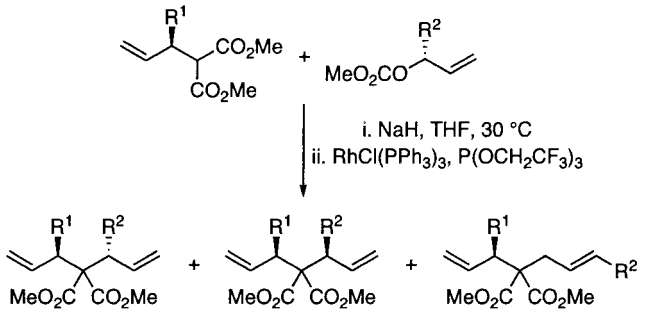

Entry	R^1	R^2	*Ratio* (2°:1°)	*ds*	*Yield (%)*
1	Me	Me	21:1	16:1	91
2	Me	Ph	8:1	7:1	86
3	Me	$BnOCH_2$	≤1:99	–	81
4	Ph	Me	35:1	30:1	91
5	Ph	Ph	8:1	39:1	88
6	Ph	$BnOCH_2$	≤1:99	–	79
7	$BnOCH_2$	Me	47:1	10:1	90
8	$BnOCH_2$	Ph	6:1	3:1	83
9	$BnOCH_2$	$BnOCH_2$	≤1:99	–	82

using dimethyl malonate as a linchpin to couple two enantiomerically enriched allylic carbonates [19]. Tab. 10.2 highlights the examination of the scope of this rhodium-catalyzed allylic alkylation reaction using an enantiomerically enriched α-branched malonate.

Interestingly, this study demonstrated that the relative size of the α-branched malonate had only a marginal influence on regioselectivity (entries 1, 4, and 7), whereas the nature of the secondary allylic carbonate imparted significant control on this parameter (entries 1–3). For example, allylic alkylations with the phenyl and benzyloxymethyl allylic carbonates afforded diminished (entries 2, 5, and 8) or complete reversal in regioselectivity (entries 3, 6, and 9), while the methyl derivative is universally selective. The ability to completely reverse the regiochemistry for the benzyloxymethyl substituent was attributed to a proximal ligation with the more electrophilic metal–allyl intermediate, as a result of the increased π-acidity of the fluorophosphites. The diastereospecificity follows a similar trend to regioselectivity, with the exception of the phenyl-substituted α-branched malonate (entries 4 and 5). Overall, this study provided a predictive model for achieving the optimum selectivity in a specific cross-coupling reaction.

The stereospecific rhodium-catalyzed allylic linchpin cross-coupling reaction provides an expeditious route to stereotetrads (Scheme 10.5). This study demonstrated that improved stereospecificity could be obtained at lower temperature for the formation of the alkylation product **18** (2^o:1^o = 24:1; *ds* = 26:1; compare Tab. 10.2, entry 1). Krapcho

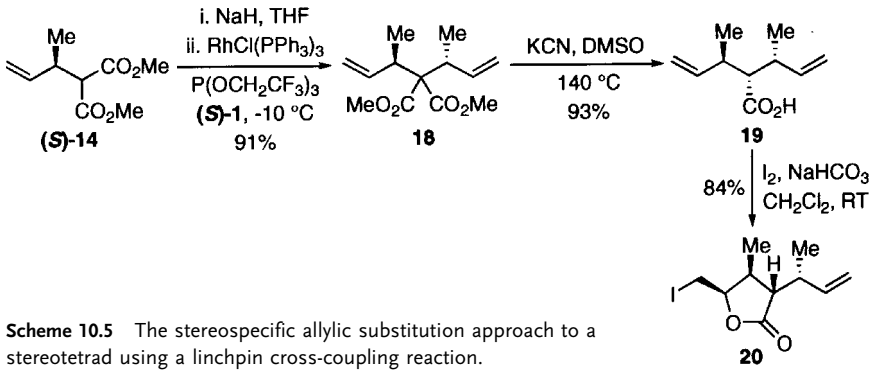

Scheme 10.5 The stereospecific allylic substitution approach to a stereotetrad using a linchpin cross-coupling reaction.

decarboxylation/saponification of the diester **18** furnished the pseudo-C_2-symmetrical carboxylic acid **19**, which was then desymmetrized through iodolactonization to afford **20** in 84% yield ($ds \geq 30:1$), thereby providing a useful synthon for target-directed synthesis [20, 21].

10.3.2
Ketones and Esters as Nucleophiles for Rhodium-Catalyzed Allylic Alkylation

Ketone and ester enolates have historically proven problematic as nucleophiles for the transition metal-catalyzed allylic alkylation reaction, which can be attributed, at least in part, to their less stabilized and more basic nature. In light of these limitations, Tsuji demonstrated the first rhodium-catalyzed allylic alkylation reaction using the trimethylsilyl enol ether derived from cyclohexanone, albeit in modest yield (Eq. 4) [9]. Matsuda and co-workers also examined rhodium-catalyzed allylic alkylation, using trimethylsilyl enol ethers with a wide range of allylic carbonates [22]. However, this study was problematic as exemplified by the poor regio- and diastereocontrol, which clearly delineates the limitations in terms of the synthetic utility of this particular reaction.

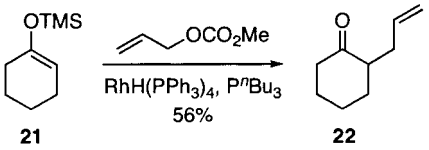

(4)

In light of these significant challenges, Evans and Leahy reexamined the rhodium-catalyzed allylic alkylation using copper(I) enolates, which should be softer and less basic nucleophiles [23]. The copper(I) enolates were expected to circumvent the problems typically associated with enolate nucleophiles in metal–allyl chemistry, namely elimination of the metal–allyl intermediate and polyalkylation as well as poor regio- and stereocontrol. Hence, the transmetallation of the lithium enolate derived from acetophenone with a copper(I) halide salt affords the requisite copper(I) enolate, which permits the efficient regio- and enantiospecific rhodium-catalyzed allylic alkylation reaction of a variety of unsymmetrical acyclic alcohol derivatives (Tab. 10.3).

Tab. 10.3 summarizes the application of the optimized reaction conditions to a variety of racemic secondary allylic carbonates, using the copper(I) enolate derived from

Tab. 10.3 The scope of the regioselective rhodium-catalyzed allylic alkylation with copper(I) enolates.

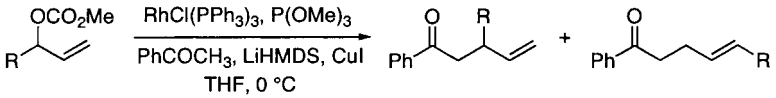

Entry	*R*	*Ratio (2°:1°)*	*Yield (%)*
1	Me	≥99:1	85
2	^{n}Pr	≥99:1	74
3	$Ph(CH_2)_2$	≥99:1	83
4	$CH_2{=}CH(CH_2)_3$	≥99:1	80
5	^{c}Hex	≥99:1	83
6	^{i}Pr	≥99:1	76
7	^{i}Bu	19:1	75
8	$(CH_3)_2CH(CH_2)_2$	≥99:1	82
9	Ph	≥99:1	84
10	Npth	≥99:1	73
11	Bn	76:1	80
12	$CH_2{=}CH$	28:1	66
13	$TBSOCH_2$	50:1	75 [a]
14	$BnO(CH_2)_2$	83:1	78

a) Reaction run at –10°C.

acetophenone (vide supra). The alkylation is tolerant of linear and branched alkyl substituents (entries 1–8), in which regiocontrol for the branched derivatives is particularly impressive, owing to the steric requirements for these alkylations (compare entries 5 and 6). The allylic alkylation also proved feasible for aryl, benzyl, and vinyl substituents (entries 9–12). However, a benzyl-protected hydroxymethyl substituent proved unsatisfactory due to low chemical yield and extensive side products. Nonetheless, the *tert*-butyldimethylsilyl-protected hydroxymethyl-and benzyl-protected hydroxyethyl substituents undergo alkylation without event (entries 13 and 14). The high degree of substrate tolerance coupled with the extensive synthetic utility of ketone enolates provides an important method for the stereocontrolled allylic alkylation. Additional studies were focused on reducing the catalyst load, in an effort to make the reaction more cost effective for large-scale synthesis. Interestingly, the catalyst loading was readily reduced to 0.5 mol% without significantly compromising selectivity or efficiency, albeit with slightly more dialkylation [24].

Extension of the rhodium-catalyzed allylic alkylation to α-substituted enolates was found to facilitate the introduction of an additional stereogenic center (Eq. 5).

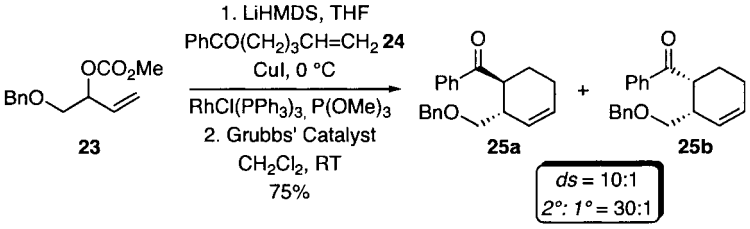

(5)

Interestingly, treatment of the allylic carbonate **23**, which had proven problematic in the previous study, under analogous reaction conditions with the copper enolate derived from **24** furnished the α,β-disubstituted ketone. Subsequent ring-closing metathesis furnished the 1,2-cyclohexenes **25a/25b** in 75% overall yield favoring the *trans*-diastereomer **25a** ($2^o{:}1^o = 30:1$, $ds = 10:1$) [14]. Overall, this reaction provides an alternative approach to an *exo*-selective Diels–Alder cycloaddition, and indicates that α-substituted enolates are even more tolerant nucleophiles than the unsubstituted derivatives.

The synthetic utility of this transformation was highlighted in the total synthesis of (–)-sugiresinol dimethyl ether **29**, in which the rhodium-catalyzed allylic alkylation served as the key tertiary carbon–carbon bond forming reaction (Scheme 10.6) [25, 26]. Interestingly, the required allylic carbonate derived from **(*R*)-26** was not isolable, due to facile ionization. Hence, it was prepared in situ and used directly, resulting in the ketone **(*R*)-27** in 80% yield as the only detectable regioisomer (100% *cee*) (*cee*, conservation of enantiomeric excess). Sharpless asymmetric dihydroxylation followed by a one-pot differential protection led to the cyclization precursor **28**, albeit as a 4:1 mixture of diastereomers [27]. The diastereomers were separated and the desired isomer was subjected to a one-pot bismuth-promoted reductive cyclization/deprotection producing (–)-sugiresinol dimethyl ether **29** in 99% yield as a single diastereomer [28], to furnish the most expeditious and efficient synthesis of (–)-sugiresinol dimethyl ether **29** developed to date.

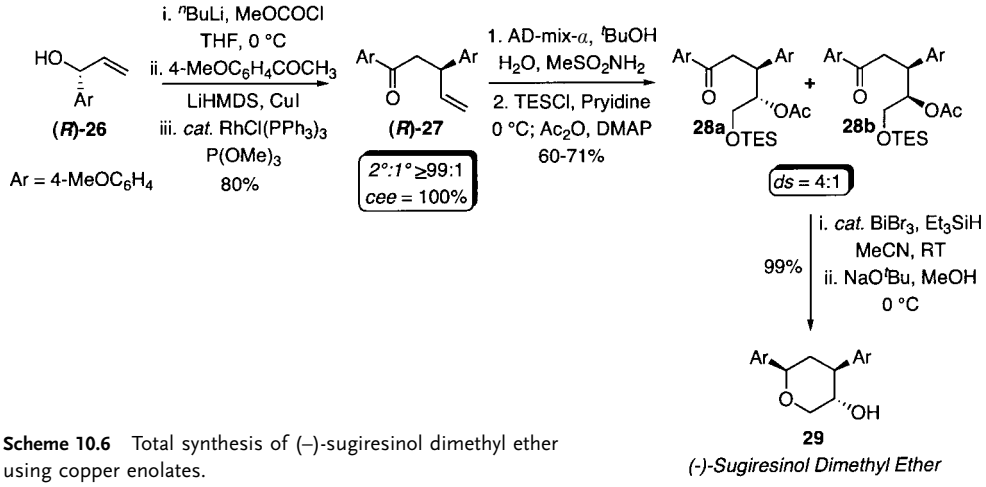

Scheme 10.6 Total synthesis of (–)-sugiresinol dimethyl ether using copper enolates.

10.3.3
Hard Nucleophiles in the Rhodium-Catalyzed Allylic Alkylation Reaction

The transition metal-catalyzed allylic substitution using hard or unstabilized nucleophiles has not been extensively studied, particularly with unsymmetrical allylic alcohol derivatives. This may be attributed to the highly reactive and basic nature of these nucleophiles and the inability to circumvent regiochemical infidelity in unsymmetrical systems. Hard nucleophiles may be characterized as those that undergo substitution with net inversion of stereochemistry [29], due to their propensity to add directly to the

transition metal catalyst, and thereby undergo alkylation *via* reductive elimination (compare Scheme 10.3).

Kabalka and co-workers reported the direct cross-coupling of cinnamyl alcohols with aryl- and vinylboronic acids using simple rhodium salts in an environmentally benign ionic liquid medium (Eq. 6) [30]. The ability to utilize allylic alcohols, without activation, is significant from the viewpoint of atom economy, yet challenging due to the poor leaving group ability of hydroxide.

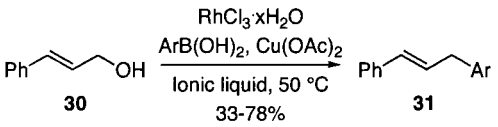

(6)

The allylic alkylation of aryl- and vinylboronic acids in the ionic medium 1-butyl-3-methylimidazolium hexafluorophosphate, catalyzed by hydrated rhodium (III) chloride, afforded the allylic alkylation products in moderate to very good yields. Although the presence of catalytic copper(II) acetate is not essential, higher product yields were obtained when using this additive. This transformation proved tolerant of a wide range of electron-rich and electron-deficient substituted arylboronic acids, in which the *para*-substituted electron-rich nucleophiles proved optimal. Although this work provided the first example of a rhodium-catalyzed allylic alkylation using an unstabilized nucleophile, the regio- and stereochemical consequences were not examined.

Evans and Uraguchi also examined the rhodium-catalyzed allylic alkylation with hard nucleophiles [31]. Aryl organozinc halides proved optimal nucleophiles for the regio- and stereospecific allylic alkylation of enantiomerically enriched unsymmetrical allylic alcohol derivatives (Tab. 10.4). The reaction occurs with net inversion of absolute

Tab. 10.4 The scope of the regiospecific $TpRh(C_2H_2)_2$-catalyzed allylic arylation reaction.

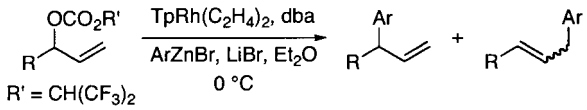

Entry	*R*	*Ar*	*Ratio (2°:1°)*	*Yield (%)*
1	$Ph(CH_2)_2$	Ph	15:1	87
2	$Ph(CH_2)_2$	*p*-MeO–C_6H_4	12:1	83
3	$Ph(CH_2)_2$	*p*-Me–C_6H_4	12:1	93
4	$Ph(CH_2)_2$	*p*-F–C_6H_4	18:1	82
5	$PhCH_2$	Ph	12:1	96
6	Me	Ph	12:1	76
7	$Me(CH_2)_8$	Ph	12:1	91
8	^{i}Bu	Ph	8:1	82
9	^{i}Pr	Ph	≥19:1	71
10	^{c}Hex	Ph	≥19:1	73
11	$TBSO(CH_2)_5$	Ph	12:1	97
12	$AcO(CH_2)_5$	Ph	≥19:1	99

configuration, which is consistent with direct addition to the metal center followed by reductive elimination (compare Scheme 10.3).

Surprisingly, the well-established triorganophosphite-modified Wilkinson's catalyst system, that had proven so general for the allylic alkylation using stabilized carbon and heteroatom nucleophiles, was not an effective catalyst for organozinc reagents. Instead, the hydrotris(pyrazolyl)borate–rhodium complex, which had not previously been utilized in any type of allylic alkylation reaction, proved optimal for this transformation. Interestingly, while traditional leaving groups favored the formation of the primary alkylation adducts, fluorinated leaving groups demonstrated a dramatic preference for the formation of the branched product (2^o:1^o = $(CF_3)_2CHOCO$ > CF_3CO > MeOCO > MeCO). The addition of lithium bromide to the catalyst proved to be a crucial component in terms of regioselectivity, which was further improved by the addition of catalytic dibenzylideneacetone. The former presumably serves as a surrogate ligand, given the volatility of the ethylene ligands present in the starting metal complex.

Tab. 10.4 summarizes the application of the optimized reaction conditions to a variety of racemic secondary allylic carbonates, in which both electron-withdrawing and -donating substituents within the organozinc reagent are readily tolerated (entries 1–4). Additional studies demonstrated that linear and branched allylic carbonates serve as suitable substrates (entries 5–12), with the α-branched derivatives affording the secondary alkylation products with optimum selectivity (entries 9 and 10). The allylic alkylation also proved feasible for the benzyl and acetate derivatives (entries 5 and 12), illustrating excellent substrate tolerance to the organozinc reagent. Hence, the regiospecific rhodium-catalyzed allylic alkylation with aryl zinc halides provides an important method for the construction of ternary carbon stereocenters.

The synthesis of (*S*)-ibuprofen **(*S*)-34** utilizing allylic alkylation was undertaken to determine the stereochemical course of this process. The reaction of the enantiomerically enriched allylic carbonate **(*S*)-32** (95% *ee*) with the requisite aryl zinc bromide (Scheme 10.7) [32], under optimized reaction conditions, furnished the 3-aryl propenyl derivative **(*R*)-33** in 90% yield (2^o:1^o = 10:1) with inversion of configuration (100% *cee*). The synthesis of (*S*)-ibuprofen **(*S*)-34** was then completed through the oxidative cleavage of the alkene **(*R*)-33** in 74% yield [33].

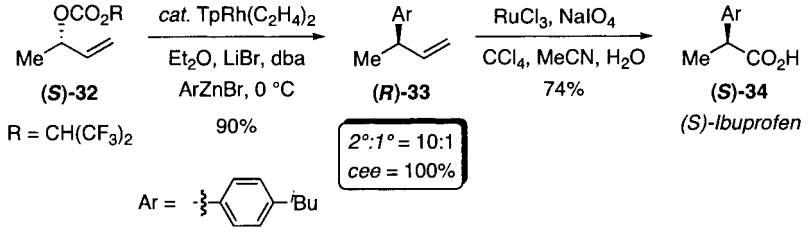

Scheme 10.7 Total synthesis of (*S*)-ibuprofen using aryl zinc halides.

10.3.4
Rhodium-Catalyzed Allylic Aminations

The transition metal-catalyzed allylic amination is particularly pertinent, because of the synthetic utility of allylic amines in the construction of biologically important natural and unnatural products [34]. The allylic amination of cyclic and acyclic substrates,

which proceeds through symmetrical η^3-intermediates, has been extensively studied with an array of transition metal catalysts. However, the use of unsymmetrical substrates has proven significantly more challenging owing to problems associated with regiochemical infidelity.

Evans and co-workers demonstrated that rhodium-catalyzed allylic amination of enantiomerically enriched acyclic unsymmetrical allylic carbonates occurs with excellent regio- and enantiospecificity (Tab. 10.5) [35]. Interestingly, while the classical nitrogen nucleophiles furnished allylic amination products in poor yield and with modest regioselectivity, the lithium anion of *N*-toluenesulfonyl-*N*-alkylamines proved optimal, in terms of nucleophilicity and basicity.

Tab. 10.5 summarizes the application of this transformation to a variety of enantiomerically enriched carbonates. The reaction is tolerant of a variety of substituents in terms of the regio- and enantiospecificity. Moreover, the *cee*, from the carbonate to the product, is independent of the regioselectivity (entries 1–3). The amination reaction proceeds with net overall retention of absolute configuration, which is consistent with a double inversion process proceeding through an enyl ($\sigma+\pi$) organorhodium intermediate, analogous to the stabilized carbon nucleophiles. Overall, this method represents a unique solution to the metal-catalyzed allylic amination, given the excellent stereospecificity and reaction rates.

Scheme 10.8 outlines the application of rhodium-catalyzed allylic amination to the preparation of (*R*)-homophenylalanine **(*R*)-38**, a component of numerous biologically active agents [36]. The enantiospecific rhodium-catalyzed allylic amination of **(*R*)-35** with the lithium anion of *N*-benzyl-2-nitrobenzenesulfonamide furnished allylamine **(*R*)-36** in 87% yield (2^o:1^o = 55 : 1; ≥99% *cee*) [37]. The *N*-2-nitrobenzenesulfonamide was employed to facilitate its removal under mild reaction conditions. Hence, oxidative cleavage of the alkene **(*R*)-36** followed by deprotection furnished the amino ester **(*R*)-37** [37, 38]. Hydrogenation of the hydrochloride salt of **(*R*)-37** followed by acid-catalyzed hydrolysis of the ester afforded (*R*)-homophenylalanine **(*R*)-38** in 97% overall yield.

Tab. 10.5 Enantiospecific rhodium-catalyzed allylic amination of enantiomerically enriched allylic carbonates.

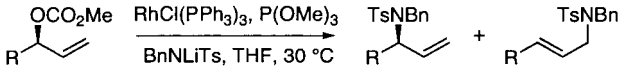

Entry	*R=*	*Ratio (2°:1°)*	*cee (%)*	*Yield (%)*
1	Me	≥99:1	100	86
2	CH_2=$CH(CH_2)_3$	19:1	100	87
3	^{c}Hex	9:1	100	92
4	$PhCH_2$	10:1	100	94
5	$Ph(CH_2)_2$	20:1	100	89
6	$TBSOCH_2$	9:1	100	91
7	$BnOCH_2$	≥99:1	100	84
8	Ph	19:1	100	87
9	Npth	≥99:1	100	90

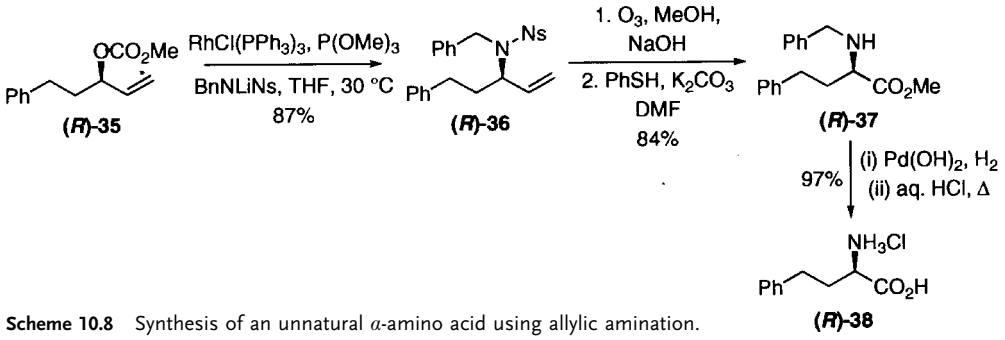

Scheme 10.8 Synthesis of an unnatural α-amino acid using allylic amination.

The stereoselective construction of nitrogen heterocycles remains a topic of intense synthetic interest [39]. Evans and Robinson described the combination of the stereospecific allylic amination with ring-closing metathesis as a strategy for the construction of mono- and disubstituted azacycles, which they demonstrated with the stereospecific construction of *cis*- and *trans*-2,5-disubstituted pyrrolines [40]. Furthermore, this approach provided an ideal system for the determination of whether the enantiospecific rhodium-catalyzed allylic amination with an enantiomerically enriched nucleophile experiences a matched and a mismatched reaction manifold.

The allylamine **(*S*)-39**, prepared *via* rhodium-catalyzed allylic amination with concomitant deprotection, was again subjected to allylic amination (Scheme 10.9). Stereospecific rhodium-catalyzed allylic amination with the enantiomerically enriched allylic carbonates **(*R*)-40** and **(*S*)-40**, using the lithium anion of **(*S*)-39**, furnished the dienes **41a** and **41b** as 31:1 and 42:1 mixtures of regioisomers, respectively. Interestingly, the matched alkylation with **(*R*)-40** proceeds with excellent stereospecificity (*ds* ≥99:1), while the analogous alkylation with the mismatched carbonate **(*S*)-40** proceeds with lower, but synthetically useful, stereospecificity (*ds*=22:1). Treatment of the dienes **41a** and **41b** with Grubbs' catalyst in refluxing benzene furnished the *cis*- and *trans*-2,5-disubstituted pyrrolines **42a** and **42b** [14]. This strategy represents one of the most expeditious routes to *cis*- and *trans*-disubstituted azacycles developed to date.

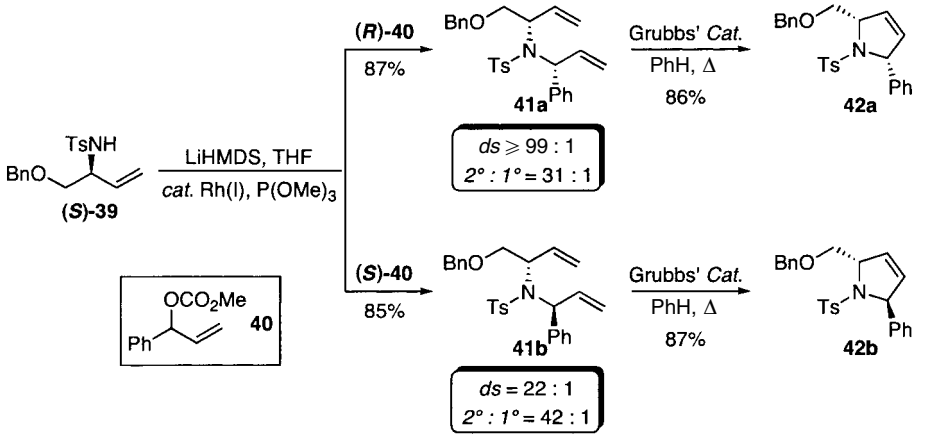

Scheme 10.9 Stereospecific approach to *cis*- and *trans*-disubstituted pyrrolines.

Tab. 10.6 The scope of regioselective rhodium-catalyzed allylic amination of carbonates with TolN(Li)Mbs.

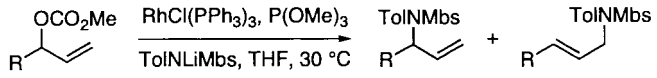

Entry	*R*	*Ratio (2°:1°)*	*Yield (%)*
1	Me	≥99:1	96
2	CH_2=$CH(CH_2)_3$	46:1	91
3	$(CH_3)_2CHCH_2$	12:1	94
4	$(CH_3)_2CH(CH_2)_2$	27:1	89
5	$PhCH_2$	20:1	86
6	$Ph(CH_2)_2$	90:1	93
7	$TBSOCH_2$	23:1	83
8	$BnOCH_2$	8:1	85
9	Ph	47:1	94
10	Npth	41:1	96

The relative importance of *N*-substituted arylamines for the construction of biologically significant molecules, particularly pharmaceuticals and agrochemicals, prompted the extension of rhodium-catalyzed allylic amination to aniline nucleophiles (Tab. 10.6) [41, 42]. The *N*-arylsulfonyl-protected anilines were again optimal for high selectivity, analogous to that observed with the *N*-toluenesulfonyl-*N*-alkylamines.

Tab. 10.6 summarizes the application of this transformation to a variety of racemic secondary allylic carbonates using the lithium anion of 4-methoxy-*N*-(*p*-toluidine)-benzene sulfonamide. The excellent regioselectivity obtained for this type of substitution provided an important advance in the synthesis of *N*-(arylsulfonyl)anilines using the metal-catalyzed allylic amination reaction. The allylic alcohol derivatives examined

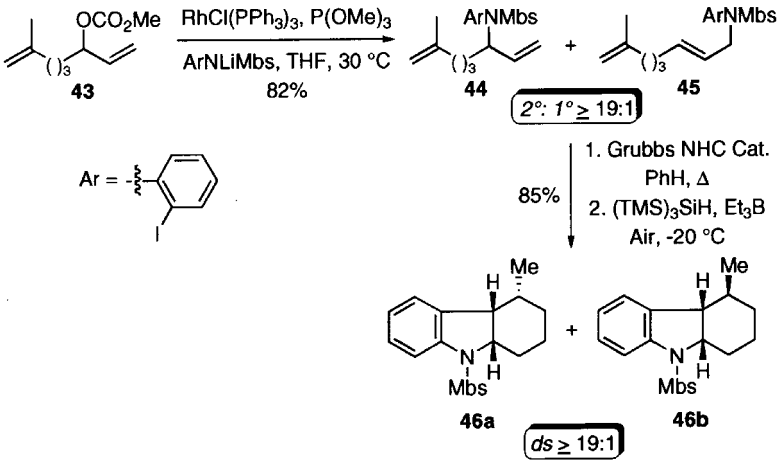

Scheme 10.10 Stereoselective construction of dihydrobenzo[*b*]indolines using allylic amination with anilines.

demonstrate a high degree of tolerance for linear and branched alkyl substituents, provided the branching is not at the *α*-position with respect to the leaving group (entries 1–6). The allylic amination also tolerates protected hydroxymethyl groups, where the silicon protecting group is presumably able to reduce proximal ligation of the ether oxygen to the metal center (entry 7 versus 8). Furthermore, aryl substituents furnish the allylic anilines with excellent regioselectivity (entries 9 and 10).

The combination of allylic amination, ring-closing metathesis, and a free radical cyclization provides a convenient approach to the dihydrobenzo[*b*]indoline skeleton, as illustrated in Scheme 10.10. The rhodium-catalyzed allylic amination of **43** with the lithium anion of 2-iodo-(*N*-4-methoxybenzenesulfonyl)aniline furnished the corresponding *N*-(arylsulfonyl)aniline **44**. The diene **44** was then subjected to ring-closing metathesis and subsequently treated with tris(trimethylsilyl)silane and triethylborane to afford the dihydrobenzo[*b*]indole derivative **46a** in 85% yield [14, 43].

10.3.5
Rhodium-Catalyzed Allylic Etherifications with Phenols and Alcohols

Transition metal-catalyzed allylic substitution with phenols and alcohols represents a fundamentally important cross-coupling reaction for the construction of allylic ethers, which are ubiquitous in a variety of biologically important molecules [44, 45]. While phenols have proven efficient nucleophiles for a variety of intermolecular allylic etherification reactions, alcohols have proven much more challenging nucleophiles, primarily due to their hard, more basic character. This is exemplified with secondary and tertiary alcohols, and has undoubtedly limited the synthetic utility of this transformation.

Evans and Leahy described the first rhodium-catalyzed allylic etherification using *ortho*-substituted phenols to determine the influence of the stereoelectronic environment of the phenol on regioselectivity (Tab. 10.7) [46]. Contrary to earlier studies with carbon and nitrogen nucleophiles, which demonstrated that a temperature of 30°C was crucial for obtaining good selectivity and turnover rates, rhodium-catalyzed allylic etherification proceeds smoothly at lower temperatures, affording the aryl allyl ether with significantly improved regioselectivity.

Tab. 10.7 summarizes the results of the application of rhodium-catalyzed allylic etherification to a series of *ortho*-substituted phenols. The etherification tolerates alkyls, including branched alkanes (entries 1 and 2), aryl substituents (entry 3), heteroatoms (entries 4 and 5), and halogens (entry 6). These results prompted the examination of *ortho*-disubstituted phenols, which were expected to be more challenging substrates for this type of reaction. Remarkably, the *ortho*-disubstituted phenols furnished the secondary aryl allyl ethers with similar selectivity (entries 7–12). The ability to employ halogen-bearing *ortho*-disubstituted phenols should facilitate substitutions that would have proven extremely challenging with conventional cross-coupling protocols.

This methodology was applied to a two-step sequence for the preparation of enantiomerically enriched dihydrobenzo[*b*]furans (Scheme 10.11) [46]. Rhodium-catalyzed allylic etherification of **(*S*)-47** (≥99% *ee*), with the sodium anion of 2-iodo-6-methylphenol, furnished the corresponding aryl allyl ethers **(*S*)-48/49** as a 28 : 1 mixture of regioisomers favoring **(*S*)-48** (92% *cee*). Treatment of the aryl iodide **(*S*)-48** with tris(trimethylsilyl)silane and triethylborane furnished the dihydrobenzo[*b*]furan derivatives **50a/50b** as a 29 : 1 mixture of diastereomers [43].

Tab. 10.7 Regioselective rhodium-catalyzed allylic etherification with *ortho*-substituted phenols.

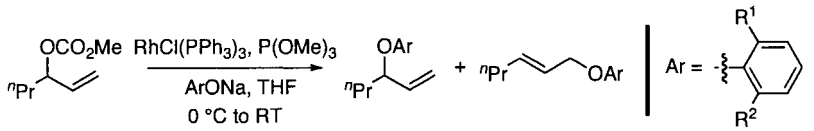

Entry	R^1	R^2	*Ratio (2°:1°)*	*Yield (%)*
1	Me	H	39:1	94
2	^{i}Pr	H	56:1	95
3	Ph	H	44:1	90
4	NHAc	H	≥99:1	95
5	OMe	H	11:1	82
6	Br	H	25:1	88
7	Me	Br	36:1	94
8	^{i}Pr	Br	57:1	90
9	Ph	Br	36:1	90
10	Me	Me	36:1	94
11	^{i}Pr	^{i}Pr	14:1	80
12	Ph	Ph	25:1	80

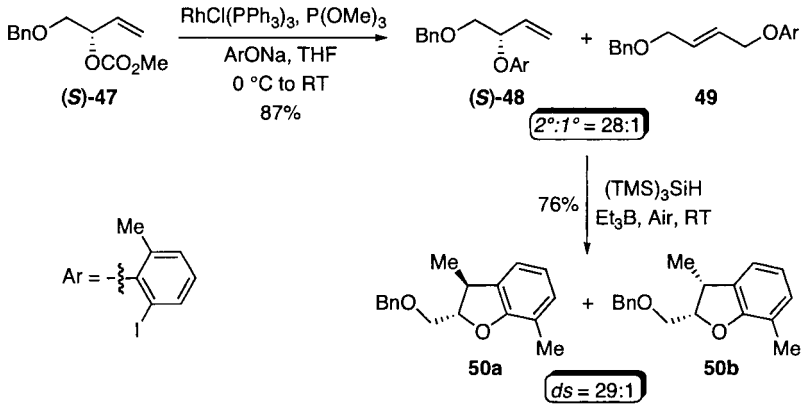

Scheme 10.11 Stereoselective construction of benzo[*b*]furans using allylic etherification with phenols.

Although the transition metal-catalyzed allylic etherification has been extensively studied, the ability to utilize secondary and tertiary alcohols, particularly with unsymmetrical allylic alcohol derivatives, remained elusive prior to the studies of Evans and Leahy. Although rhodium-catalyzed allylic etherification failed with hard alkali metal alkoxides, this problem was circumvented through the transmetallation of the alkali metal alkoxide with a copper(I) halide salt, which presumably softens the basic character of the metal alkoxide (Tab. 10.8) [47, 48]. Additional improvement in the chemical yield was obtained through the use of the *tert*-butyloxycarbonate leaving group, which appears to suppress competitive transacylation of the leaving group by the nucleophile.

Tab. 10.8 The scope of the regioselective rhodium-catalyzed allylic etherification reaction.

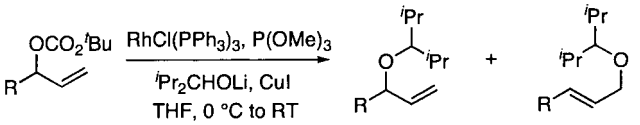

Entry	*R*	*Ratio (2°:1°)*	*Yield (%)*
1	$Ph(CH_2)_2$	≥99:1	73
2	Me	≥99:1	65
3	^{n}Pr	≥99:1	67
4	$CH_2{=}CH(CH_2)_3$	≥99:1	70
5	$(CH_3)_2CH(CH_2)_2$	≥99:1	71
6	$BnOCH_2$	18:1	50
7	$CH_2{=}CH$	13:1	46
8	Ph	22:1	70
9	Npth	28:1	73

Tab. 10.8 summarizes the application of rhodium-catalyzed allylic etherification to a variety of racemic secondary allylic carbonates, using the copper(I) alkoxide derived from 2,4-dimethyl-3-pentanol (*vide intra*). Although the allylic etherification is tolerant of linear alkyl substituents (entries 1–4), branched derivatives proved more challenging in terms of selectivity and turnover, the γ-position being the first point at which branching does not appear to interfere with the substitution (entry 5). The allylic etherification also proved feasible for hydroxymethyl, alkene, and aryl substituents, albeit with lower selectivity (entries 6–9). This transformation is remarkably tolerant, given that the classical alkylation of a hindered metal alkoxide with a secondary alkyl halide would undoubtedly lead to elimination. Hence, regioselective rhodium-catalyzed allylic etherification with a secondary copper(I) alkoxide provides an important method for the synthesis of allylic ethers.

Rhodium-catalyzed allylic etherification could also be extended to the more challenging tertiary alcohols (Eq. 7). Although preliminary attempts revealed that the alkylation of the allylic carbonate **51** was feasible, the reaction required increased catalyst loading (20 mol%), affording the allylic ether **52** in 67% yield ($2^o{:}1^o = 47:1$).

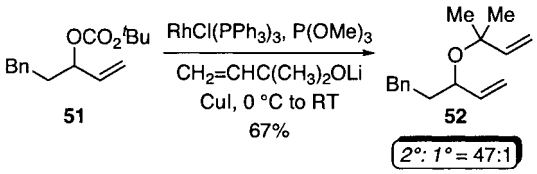

(7)

Examination of the stereospecificity of the etherification indicated that the reaction was subject to a dramatic halide effect (Tab. 10.9). Treatment of enantiomerically enriched allylic carbonate **(*R*)-53** (94% *ee*) under optimized conditions furnished the allyl ether **(*R*)-54** in 84% yield ($2^o{:}1^o \geq 99:1$), although with poor enantiospecificity (41% *cee*;

Tab. 10.9 Exploring the influence of the copper(I) halide salt on enantiospecificity.

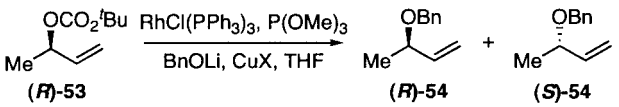

Entry	*CuX*	*Temperature*	*Ratio (2°:1°)*	*cee (%)*	*Yield (%)*
1	CuI	0 °C to RT	≥99:1	41	84
2	CuBr	0 °C to RT	91:1	85	86
3	CuCl	0 °C to RT	≥99:1	88	81
4	CuCl	–10 °C	≥99:1	96	81

entry 1). This result represented a significant departure from earlier studies and thus prompted the examination of other copper(I) halide salts. Interestingly, transmetallation with copper(I) chloride or bromide furnished the allylic ether **(*R*)-54** with significantly improved chirality transfer (entries 2, 3). Additional work demonstrated that the optimal stereospecificity was obtained at lower temperature (entry 4).

Although a possible explanation for the stereochemical erosion is the ability of the halide on the metal center's ability to influence the rate of nucleophilic trapping is, it was instead attributed to the halide's influence on the rate of π–σ–π isomerization. This phenomenon was supported by the fact that the amount of racemization caused by the various rhodium-halide catalysts parallels the strength of the *trans*-effect attributed to each halide ligand (I > Br > Cl) [49, 50]. Thus if the π-component of the enyl ligand is *trans* to the halide in the rhodium–allyl intermediate, then dissociation of the π-component of the enyl intermediate, leading to a σ-allyl, will be most facile when the halide ligand is iodide. Although speculative, this *trans* effect concept adequately explains the observed trend in enantiospecificity for the etherification reaction.

In light of the halide effects, the role of the copper alkoxide and the lithium halide, derived from the transmetallation, was probed by preparing the copper alkoxide under salt-free conditions (Tab. 10.10) [24, 51, 52]. Initially, mesityl copper, from which the metal halide salts are removed during preparation [53], was chosen to provide the copper(I) alkoxide. Interestingly, only a trace of product was observed in the absence of lithium

Tab. 10.10 Probing the role of lithium iodide and the copper(I) alkoxide in allylic etherification.

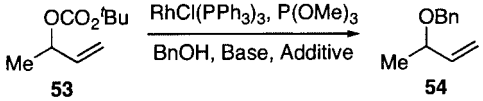

Entry	*Base*	*Additive*	*Ratio (2°:1°)*	*Yield (%)*
1	LiHMDS	CuI	≥99:1	84
2	mesityl copper	–	7:1	3
3	LiHMDS	LiI	86:1	4
4	mesityl copper	LiI	≥99:1	76

iodide (entry 2). Moreover, the addition of lithium iodide to the lithium alkoxide also furnished only a trace amount of the allylic ether **54**, indicating the necessity for copper (entry 3). Thus, when lithium iodide is added to the copper alkoxide derived from the alcohol treated with mesityl copper, analogous turnover and regioselectivity are obtained (entry 4). This clearly indicates that the copper alkoxide and lithium iodide are both required for optimal catalytic activity. Although the exact role of lithium iodide was unclear, it was tentatively attributed to an ability to reconstitute a catalytically inactive rhodium–alkoxide complex into a catalytically active rhodium–halide catalyst.

10.4
Enantioselective Rhodium-Catalyzed Allylic Alkylations

Enantioselective transition metal-catalyzed allylic alkylation has stimulated immense interest due to its potential synthetic utility [1 b]. Although excellent enantioselectivities have been obtained for a wide variety of cyclic and acyclic allylic alcohol derivatives, using a wide range of chiral transition metal complexes, the ability to also control regioselectivity has proven challenging. In light of the excellent selectivities observed for rhodium-catalyzed allylic substitution, it would seem reasonable to assume that the enantioselective rhodium-catalyzed version may provide the definitive solution to this problem.

In 1989, Consiglio, Scalone, and Rama published the enantioselective rhodium-catalyzed carbon dioxide extrusion from allyl phenyl carbonates using the (*S,S*)-CHIRAPHOS ligand (Eq. 8) [54]. Although the reaction was highly regioselective for the secondary allylic ether, the enantioselectivity was poor (23% *ee*), illustrating some of the challenges associated with this transformation.

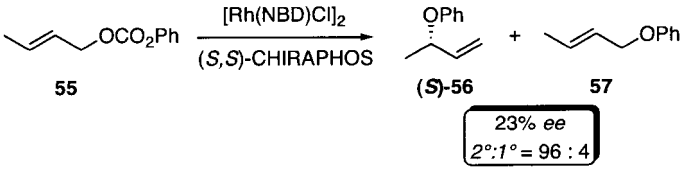

(8)

The first example of an intermolecular enantioselective rhodium-catalyzed allylic alkylation, relying on the phosphito-thioether ligands **58** and **59** and the *P,N*-ligand **60** (Scheme 10.12), was reported by Pregosin and co-workers in 1999 [55]. The *in-situ*

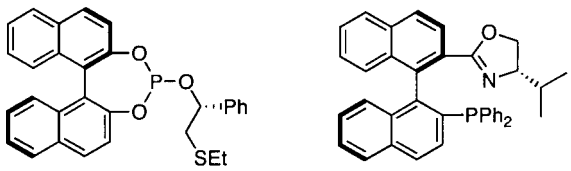

58 = (*R,R*)
59 = (*R,S*)

60

Scheme 10.12 Chiral ligands utilized for enantioselective rhodium-catalyzed allylic substitution.

Tab. 10.11 Regio- and enantioselective rhodium-catalyzed allylic substitution.

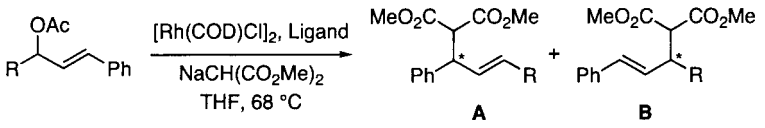

Entry	*R =*	*Ligand*	*A (% ee)* [a]	*B (% ee)* [a]	*Yield (%)*
1	H	58	49 (14)	51	95
2	H	59	39 (24)	61	95
3	H	58 + PPh_3 [b]	24 (42)	76	95
4	H	60	2	98	95
5	Me	58	19 (6)	81 (17)	80
6	Me	60	10 (80)	90 (13)	75
7	Et	58	16 (81)	84 (45)	70
8	Et	60	14 (82)	86 (26)	70

a) Numbers in parenthesis refer to % *ee*.
b) One equivalent.

modification of $[Rh(COD)Cl]_2$ with these ligands (**58**, **59**, or **60)** furnished a catalyst that facilitated the allylic alkylation with encouraging enantioselectivities.

Tab. 10.11 summarizes the results of this study. In the case of the primary allylic acetate (R = H), modest selectivity for the branched product could be achieved, in which the enantioselectivity and regioselectivity displayed an inverse relationship (entries 1–3). For the secondary allylic acetate (R = Et), high enantioselectivity was observed for the minor regioisomer **A**, while the major regioisomer **B** was formed with poor enantioselectivity (entries 5–8). This study again highlights some of the challenges associated with enantioselective transition metal-catalyzed allylic alkylations of unsymmetrical acyclic allylic alcohol derivatives, namely, simultaneous control of both regio- and enantioselectivity.

Hayashi and co-workers have recently reexamined the enantioselective rhodium-catalyzed allylic alkylation of unsymmetrical substrates, also using the *P,N*-ligand **60** (Tab. 10.12) [56]. They reasoned that in order to obtain high enantioselectivity when starting from a racemic secondary allylic acetate, the rhodium–allyl intermediate must have a longer lifetime, to allow equilibration between the isomeric intermediates. This concept contrasts with enantiospecific allylic alkylation, where the rhodium–allyl intermediate must have a short lifetime in order to avoid equilibration and thus racemization, as described by Evans and co-workers [16]. Thus, high enantioselectivities were observed using either high dilution or slow addition of the nucleophile. However, these reaction conditions are impractical due to long reaction times and low chemical yields. Fortunately, the use of cesium carbonate rather than sodium hydride leads to high enantioselectivities, due to its weaker basicity, which presumably achieves a low concentration of nucleophile and thus increases the lifetime of the rhodium–allyl intermediate

Tab. 10.12 summarizes the application of the optimized reaction conditions to a series of racemic secondary allylic acetates, wherein the reaction demonstrates remarkable enantioselectivity for an array of substrates. However, the regioselectivity of this

Tab. 10.12 Enantioselective rhodium-catalyzed allylic alkylations with dimethyl malonate.

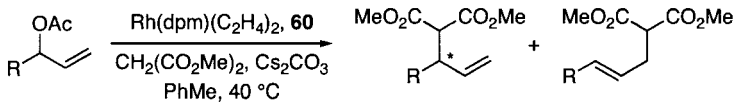

Entry	*R*	*Ratio (2°:1°)*	*ee (%)*	*Yield (%)*
1	Ph	98:2	97 (*S*)	94
2	4-MeC_6H_4	88:12	94	97
3	4-$CF_3C_6H_4$	99:1	97	97
4	4-ClC_6H_4	97:3	95	93
5	1-naphthyl	60:40	95	94
6	$Ph(CH_2)_2$	86:14	90	81

reaction is somewhat variable, with electron-deficient cinnamyl derivatives appearing to be optimum in terms of both regio- and enantioselectivity. These results are somewhat analogous to the array of other metals that have been examined for this type of transformation thus far. Hence, this study provides valuable insight that will be necessary for the development of a general regio- and enantioselective rhodium-catalyzed allylic substitution reaction.

10.5 Conclusion

The rhodium-catalyzed allylic substitution reaction provides one of the most versatile and general methods that has been developed for the cross-coupling of various stabilized carbon and heteroatom nucleophiles with unsymmetrical allylic alcohol derivatives. The stereospecific reaction manifold is particularly important, since it provides a complement to the enantioselective allylic substitution reaction. The ability to modify a commercially available catalyst *in situ*, and thus avoid the handling of air- and moisture-sensitive catalysts, makes this an ideal protocol for academic and industrial environments. Future challenges in this area will include the further development of unstabilized nucleophiles and diastereoselective variants of this important transformation. Finally, although the enantioselective reaction manifold has now been described, the problem of simultaneously controlling regio- and enantioselectivity in unbiased allylic systems remains a synthetic challenge.

Acknowledgments

We would like to acknowledge the experimental and intellectual contributions of our co-workers in the catalysis subgroup. In particular, we would like to highlight the seminal contributions of our former colleagues Lawrence J. Kennedy, Kristofer K. Moffett, Jade D. Nelson, John E. Robinson, and Daisuke Uraguchi. We sincerely

thank the National Institutes of Health (GM58877) and the Donors of The Petroleum Research Fund, administered by the American Chemical Society, for generous financial support. We also thank the numerous pharmaceutical companies for unrestricted funds (PAE), and the Department of Chemistry at Indiana University for an E.M. Kratz Fellowship (DKL).

10.6 References

1 For book chapters on metal-catalyzed allylic substitution, see: (a) Tsuji, J. in *Palladium Reagents and Catalysts: Innovations in Organic Synthesis*; Wiley: New York, **1996**, Ch. 4, pp. 290–404. (b) Trost, B.M.; Lee, C. in *Catalytic Asymmetric Synthesis*, 2nd ed.; Ojima, I., Ed.; Wiley-VCH: New York, **2000**, Ch. 8, pp. 593–649.

2 For review articles on metal-catalyzed allylic substitution, see: (a) Frost, C.G.; Howarth, J.; Williams, J.M.J. *Tetrahedron: Asymmetry* **1992**, *3*, 1089. (b) Trost, B.M.; Van Vranken, D.L. *Chem. Rev.* **1996**, *96*, 395 and pertinent references cited therein.

3 For lead references on other transition metal-catalyzed allylic substitution reactions, see: (a) *Cobalt*: Bhatia, B.; Reddy, M.M.; Iqbal, J. *Tetrahedron Lett.* **1993**, *34*, 6301. (b) *Iron*: Xu, Y.; Zhou, B. *J. Org. Chem.* **1987**, *52*, 974. (c) *Iridium*: Takeuchi, R.; Kashio, M. *Angew. Chem., Int. Ed.* **1997**, *36*, 263. (d) *Molybdenum*: Ward, Y.D.; Villanueva, L.A.; Allred, G.D.; Liebeskind, L.S. *J. Am. Chem. Soc.* **1996**, *118*, 897. (e) *Nickel*: Bricout, H.; Carpentier, J.-F.; Mortreux, A. *J. Chem. Soc., Chem. Commun.* **1995**, 1863. (f) *Platinum*: Brown, J.M.; McIntyre, J.E. *J. Chem. Soc., Perkin Trans. 2* **1985**, 961. (g) *Ruthenium*: Trost, B.M.; Fraisse, P.L.; Ball, Z.T. *Angew. Chem., Int. Ed.* **2002**, *41*, 1059. (h) *Tungsten*: Lloyd-Jones, G.C.; Pfalz, A. *Angew. Chem., Int. Ed. Engl.* **1995**, *34*, 462 and pertinent references cited therein.

4 (a) Trost, B.M.; Hachiya, I. *J. Am. Chem. Soc.* **1998**, *120*, 1104. (b) Bartels, B.; Helmchen, G. *Chem. Commun.* **1999**, 741. (c) You, S.-L.; Zhu, X.-Z.; Luo, Y.-M.; Hou, X.-L.; Dai, L.-X. *J. Am. Chem. Soc.* **2001**, *123*, 7471. (d) Lopez, F.; Ohmura, T.; Hartwig, J.F. *J. Am. Chem. Soc.* **2003**, *125*, 3426. (e) Hayashi, T.; Okada, A.; Suzuka, T.; Kawatsura, M. *Org. Lett.* **2003**, *5*, 1713 and pertinent references cited therein.

5 Hayashi, T.; Yamamoto, A.; Hagihara, T. *J. Org. Chem.* **1986**, *51*, 723.

6 Onoue, H.; Moritani, I.; Murahashi, S. *Tetrahedron Lett.* **1973**, *14*, 121.

7 Tsuji, J.; Minami, I.; Shimizu, I. *Chem. Lett.* **1984**, 1721.

8 Hayashi, Y.; Komiya, S.; Yamamoto, T.; Yamamoto, A. *Chem. Lett.* **1984**, 977.

9 Tsuji, J.; Minami, I.; Shimizu, I. *Tetrahedron Lett.* **1984**, *25*, 5157.

10 Minami, I.; Shimizu, I.; Tsuji, J. *J. Organomet. Chem.* **1985**, *296*, 269.

11 Evans, P.A.; Nelson, J.D. *Tetrahedron Lett.* **1998**, *39*, 1725.

12 Takeuchi, R.; Kitamura, N. *New J. Chem.* **1998**, *22*, 659.

13 Evans, P.A.; Kennedy, L.J. *Tetrahedron Lett.* **2001**, *42*, 7015.

14 Grubbs, R.H.; Chang, S. *Tetrahedron* **1998**, *54*, 4413.

15 Trnka, T.M.; Morgan, J.P.; Sanford, M.S.; Wilhelm, T.E.; Scholl, M.; Choi, T.; Ding, S.; Day, M.W.; Grubbs, R.H. *J. Am. Chem. Soc.* **2003**, *125*, 2546.

16 Evans, P.A.; Nelson, J.D. *J. Am. Chem. Soc.* **1998**, *120*, 5581.

17 Evans, P.A.; Kennedy, L.J. *Org. Lett.* **2000**, *2*, 2213.

18 For a related example of a reductive alkylation from an α-cyano ketone, see: Liu, H.J.; Zhu, J.L.; Shia, K.S. *Tetrahedron Lett.* **1998**, *39*, 4183 and pertinent references therein.

19 Evans, P.A.; Kennedy, L.J. *J. Am. Chem. Soc.* **2001**, *123*, 1234.

20 Krapcho, A.P. *Synthesis* **1982**, 805.

21 Kurth, M.J.; Brown, E.G. *J. Am. Chem. Soc.* **1987**, *109*, 6844.

22 Muraoka, T.; Matsuda, I.; Itoh, K. *Tetrahedron Lett.* **2000**, *41*, 8807. (b) Muraoka, T.; Matsuda, I.; Itoh, K. *J. Am. Chem. Soc.* **2000**, *122*, 9552.

23 Evans, P.A.; Leahy, D.K. *J. Am. Chem. Soc.* **2003**, *125*, 8974.

24 Evans, P.A.; Leahy, D.K.; Slieker, L.M. *Tetrahedron: Asymmetry* **2003**, *14*, 3613.

25 (a) Funaoka, K.; Kuroda, Y.; Kai, Y.; Kondo, T. *Nippon Mokuzai Gakkaishi* **1963**, *9*, 139. (b) Enzell, C.R.; Hirose, Y.; Thomas, B.R. *Tetrahedron Lett.* **1967**, 793.

26 (a) Beracierta, A.P.; Whiting, D.A. *Tetrahedron Lett.* **1967**, 2367. (b) Beracierta, A.P.; Whiting, D.A. *J. Chem. Soc., Perkin Trans. 1* **1978**, 1257. (c) Horii, Z.; Iwata, C.; Tanaka, T.; Momose, T. *Heterocycles* **1977**, *6*, 697. (d) Hashimoto, S.; Yamada, S.; Koga, K. *J. Am. Chem. Soc.* **1976**, *98*, 7450. (e) Muraoka, O.; Fujiwara, N.; Tanabe, G.; Momose, T. *Tetrahedron: Asymmetry* **1991**, *2*, 357. (f) Muraoka, O.; Zheng, B.-Z.; Fujiwara, N.; Tanabe, G. *J. Chem. Soc., Perkin Trans. 1* **1996**, 405. (g) Dujardin, G.; Maudet, M.; Brown, E. *Tetrahedron Lett.* **1997**, *38*, 1555. (h) Brown, E.; Dujardin, G.; Maudet, M. *Tetrahedron* **1997**, *53*, 9679. (i) Matsuo, K.; Sugimura, W.; Shimizu, Y.; Nishiwaki, K.; Kuwajima, H. *Heterocycles* **2000**, *53*, 1505. (j) Matsuo, K.; Ono, Y.; Seki, A.; Kuwajima, H.; Nishiwaki, K. *Heterocycles* **2000**, *53*, 2553.

27 Kolb, H.C.; Van Nieuwenhze, M.S.; Sharpless, K.B. *Chem. Rev.* **1994**, *94*, 2483.

28 (a) Evans, P.A.; Cui, J.; Gharpure, S.J.; Hinkle, R.J. *J. Am. Chem. Soc.* **2003**, *125*, 11456. (b) Evans, P.A.; Cui, J.; Gharpure, S.J. *Org. Lett.* **2003**, *5*, 3883. (c) Komatsu, N.; Ishida, J.-y.; Suzuki, H. *Tetrahedron Lett.* **1997**, *38*, 7219.

29 Consiglio, G.; Waymouth, R.M. *Chem. Rev.* **1989**, *89*, 257.

30 Kabalka, G.W.; Dong, G.; Venkataiah, B. *Org. Lett.* **2003**, *5*, 893.

31 Evans, P.A.; Uraguchi, D. *J. Am. Chem. Soc.* **2003**, *125*, 7158.

32 For recent enantioselective approaches to ibuprofen, see: (a) Park, H.; RajanBabu, T.V. *J. Am. Chem. Soc.* **2002**, *124*, 734. (b) Ishihara, K.; Nakashima, D.; Hiraiwa, Y.; Yamamoto, H. *J. Am. Chem. Soc.* **2003**, *125*, 24 and pertinent references therein.

33 Carlsen, P.H.; Katsuki, T.; Martin, V.S.; Sharpless, K.B. *J. Org. Chem.* **1981**, *46*, 3936.

34 For a recent review on allylic amination, see: Johannsen, M.; Jorgensen, K.A. *Chem. Rev.* **1998**, *98*, 1689.

35 Evans, P.A.; Robinson, J.E.; Nelson, J.D. *J. Am. Chem. Soc.* **1999**, *121*, 6761.

36 For a recent review on the asymmetric synthesis of -amino acids, see: Davis, F.A.; Zhou, P.; Chen, B.C. *Chem. Soc. Rev.* **1998**, *27*, 13.

37 Fukuyama, T.; Jow, C.K.; Cheung, M. *Tetrahedron Lett.* **1995**, *36*, 6373.

38 Marshall, J.A.; Garofalo, A.W. *J. Org. Chem.* **1993**, *58*, 3675.

39 For a recent review of methods for constructing saturated nitrogen heterocycles, see: Nadin, A. *J. Chem. Soc., Perkin Trans. 1* **1998**, 3493.

40 Evans, P.A.; Robinson, J.E. *Org. Lett.* **1999**, *1*, 1929.

41 For recent reviews on transition metal-catalyzed aryl amine formation, see: (a) Hartwig, J.F. *Angew. Chem., Int. Ed.* **1998**, *37*, 2046. (b) Belfield, A.J.; Brown, G.R.; Foubister, A.J.; *Tetrahedron* **1999**, *55*, 11399 and pertinent references therein.

42 Evans, P.A.; Robinson, J.E.; Moffett, K.K. *Org. Lett.* **2001**, *3*, 3269.

43 For a recent review on tris(trimethylsilyl)-silane, see: Chatgilialoglu, C. *Chem. Rev.* **1995**, *95*, 1229.

44 For recent approaches to the transition metal-catalyzed allylic etherification using phenols, see: (a) Goux, C.; Massacret, M.; Lhoste, P.; Sinou, D. *Organometallics* **1995**, *14*, 4585. (b) Trost, B.M.; Toste, F.D. *J. Am. Chem. Soc.* **1998**, *120*, 815. (c) Trost, B.M.; Fraisse, P.L.; Ball, Z.T. *Angew. Chem., Int. Ed.*. **2002**, *41*, 1059. (d) Lopez, F.; Ohmura, T.; Hartwig, J.F. *J. Am. Chem. Soc.* **2003**, *125*, 3426 and pertinent references therein.

45 For recent approaches to transition metal-catalyzed allylic etherification using alcohols, see: (a) Trost, B.M.; McEachern, E.J.; Toste, F.D. *J. Am. Chem. Soc.* **1998**, *120*, 12702. (b) Kim, H.; Lee, C. *Org. Lett.* **2002**, *4*, 4369. (c) Comely, A.C.; Eelkema, R.; Minnaard, M.J.; Feringa, B.L. *J. Am. Chem. Soc.* **2003**, *125*, 8714. (d) Haight, A.R.; Stoner, E.J.; Peterson, M.J.; Grover, V.K. *J. Org. Chem.* **2003**, *68*, 8092 and pertinent references therein.

46 Evans, P.A.; Leahy, D.K. *J. Am. Chem. Soc.* **2000**, *122*, 5012.

47 Evans, P.A.; Leahy, D.K. *J. Am. Chem. Soc.* **2002**, *124*, 7882.

48 For first report of copper(I) alkoxides, see: Whitesides, G.M.; Sadowski, J.S.; Lilburn, J. *J. Am. Chem. Soc.* **1974**, *96*, 2829.

49 The *trans*-effect has been defined as: the effect of a coordinated group on the rate of substitution reactions of ligands *trans* to itself. See: Basolo, F.; Pearson, R.G. *Prog. Inorg. Chem.* **1962**, *4*, 381.

50 For a recent review on *trans*-effects in octahedral transition metal complexes, see: Coe, B.J.; Glenwright, S.J. *Coord. Chem. Rev.* **2000**, *203*, 5.

51 For a recent review on halide effects in transition-metal catalysis, see: Fagnou, K.; Lautens, M. *Angew. Chem., Int. Ed.* **2002**, *41*, 26.

52 For recent examples of halide effects on enantioselectivity in transition metal-catalyzed allylic substitutions, see: (a) Bartels, B.; Helmchen, G. *Chem. Commun.* **1999**, 741. (b) Burckhardt, U.; Baumann, M.; Togni, A. *Tetrahedron: Asymmetry* **1997**, *8*, 155.

53 For preparation of mesityl copper, see: Tsuda, T.; Yazawa, T.; Watanabe, K.; Fujii, T.; Saegusa, T. *J. Org. Chem.* **1981**, *46*, 192.

54 Consiglio, G.; Scalone, M.; Rama, F. *J. Mol. Catal.* **1989**, *50*, L11.

55 Selvakumar, K.; Valentini, M.; Pregosin, P.K. *Organometallics* **1999**, *18*, 4591.

56 Hayashi, T.; Okada, A.; Suzuka, T.; Kawatsura, M. *Org. Lett.* **2003**, *5*, 1713.

11
Rhodium(I)-Catalyzed [2+2+1] and [4+1] Carbocyclization Reactions

Nakcheol Jeong

11.1
General Introduction to Rhodium-Mediated Carbocyclizations

Transition metal-mediated carbocyclizations have emerged as major tools for the construction of highly functionalized polycyclic systems. The major advantage of this type of approach is that it allows for carbon–carbon bond forming reactions that would otherwise be exceedingly difficult or even impossible with conventional organic reagents. Furthermore, the ability of metal-catalyzed reactions to facilitate the formation of multiple stereogenic centers in a single step provides opportunities for asymmetric catalysis, by use of the appropriate chiral catalyst, to generate optically active compounds. Significant progress has been made in the category of metal-catalyzed carbocyclizations of unactivated (more precisely, less polarized) olefins, dienes, acetylenes, and so forth [1].

Rhodium catalysis has played a critical role in the development of this type of reaction. The rhodium-mediated [4+2] carbocyclization between dienes and unactivated olefins or alkynes is a notable early example of this concept [2]. Further investigations demonstrated the extension of this methodology to the reaction between a diene and an allene [3]. Expansion of the scope of this strategy, to both the intra- and intermolecular [5+2] homologs of the Diels–Alder reaction, was accomplished with a vinylcyclopropane and either an alkyne or an olefin to afford the carbocyclization adducts (Scheme 11.1) [4, 5].

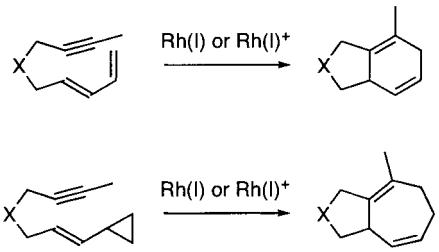

Scheme 11.1 Rhodium-mediated carbocyclization reactions.

The formation of a metallacyclopentene, which is presumed to be the key intermediate in the preceding examples, prompted the question of whether a C_1 unit, such as CO or an isocyanide, could be inserted into this intermediate and thereby allow for an $[m+n+1]$ carbocyclization reaction (Scheme 11.2). These types of reactions will be discussed in detail in this chapter.

Modern Rhodium-Catalyzed Organic Reactions. Edited by P. Andrew Evans

ISBN: 3-527-30683-8

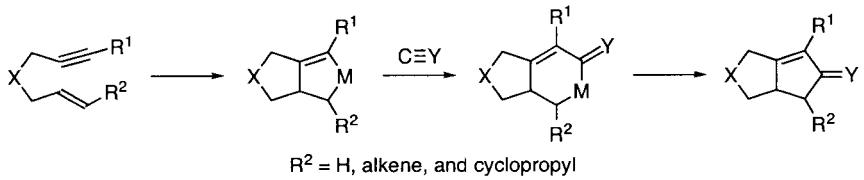

Scheme 11.2 General scheme for [*m*+*n*+1]carbocyclization reactions.

11.2 [2+2+1] Carbocyclization

11.2.1 Coupling of an Alkyne, an Olefin, and CO (Pauson–Khand Type Reactions)

The preparation of five-membered rings has been the subject of extensive studies, which may be attributed to the ubiquity of this motif in biologically relevant natural products. The three-component transition metal-mediated [2+2+1] carbocyclization of an alkyne, alkene, and carbon monoxide is one of the most convergent methods developed to date. Since the very first report of a metal-mediated [2+2+1] using stoichiometric dicobalt octacarbonyl [$Co_2(CO)_8$] by Pauson and Khand in 1973 (hereafter, PK or PK-type reaction) [6], numerous improvements to the original transformation have been reported. Key issues that have been addressed include the use of other metals, reduction of the reaction temperature, and the ability to accomplish a catalytic adaptation of this reaction [7]. Early investigations detailed the examination of promoters, such as trialkylamine *N*-oxides and sulfoxides, to enable the reaction to be accomplished at ambient or substantially lower temperature than the original reaction conditions [8]. Many metal carbonyl complexes other than cobalt; for example, iron, tungsten, and molybdenum, were also demonstrated to promote the PK-type reaction [9].

It should be noted that the catalytic version of the PK reaction was envisioned from the time of discovery, yet it was not until 1990 that the first example was reported using cobalt [10]. Since that report other variations of catalytic PK reactions employing cobalt, as well as titanium [11] and ruthenium [12], complexes have been reported. In addition to these examples, rhodium has been shown to catalyze the PK reaction, in which it was clear from the outset that this metal had a number of unique features [13]. A proposed mechanism for the generalized PK-type reaction is illustrated in Scheme 11.3.

Interestingly, the two key steps in this reaction, complexation of the metal with the enyne and the subsequent isomerization to the metallacyclopentene, have contradicting catalyst requirements. For the initiation of the reaction, the metal center of the catalyst should possess some degree of Lewis acidity to bind the enyne efficiently. This may account for the fact that all the metals used, except the intrinsically electron-deficient early transition metal titanium(II), require strong π-accepter ligands such as CO on the metal center. However, the oxidative isomerization to the metallacyclopentene, which appears to be the rate-determining step, should be expedited by the presence of electron-donating ligands. The ability to balance these two opposing requirements is vital to the success of the reaction (Scheme 11.3).

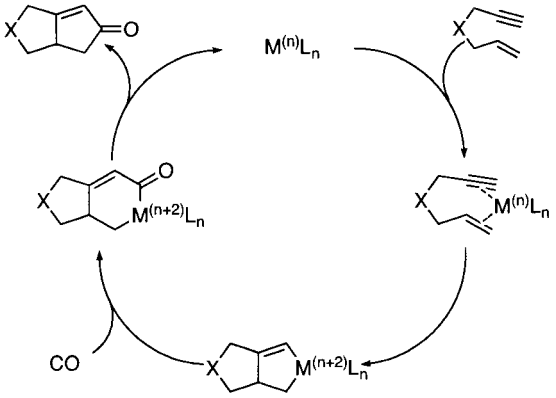

Scheme 11.3 A proposed catalytic cycle for the Pauson–Khand-type reaction.

Catalysts that are generally used for the rhodium(I)-mediated [4+2] and [5+2] carbocyclizations, specifically $[RhCl(CO)_2]_2$ or cationic rhodium complexes prepared by modification of Wilkinson catalyst $[RhCl(PPh_3)_3]$ with silver(I) salts, are also applicable to PK-type reactions [13]. Results from the systematic screening of various rhodium catalysts lend support to the aforementioned mechanistic considerations (Tab. 11.1) [13b]. While rhodium catalysts **3** and **4** bearing a π-accepter ligand (CO or a ligand replaceable by CO *in situ*) can promote the reaction with the enyne **1a** to afford the bicyclopentenone **2a** in refluxing xylene under an atmosphere of CO (1 atm.), other rhodium catalysts **6** and **7** with electron-donating ligands are inferior. The rhodium carbonyl cluster **5** is also less effective, presumably due to difficulty in the formation of the more reactive di- or monorhodium species. After extensive optimization, which included solvent screening, $[RhCl(CO)_2]_2$ in refluxing dibutyl ether under an atmosphere of CO (1 atm.) emerged as the optimal reaction conditions.

In a concurrent study, a variety of rhodium-complexes with phosphine ligands were also examined for their suitability in the catalytic PK reaction [13c]. A key aspect of this work

Tab. 11.1 Screening of rhodium catalysts for the Pauson–Khand-type reaction.

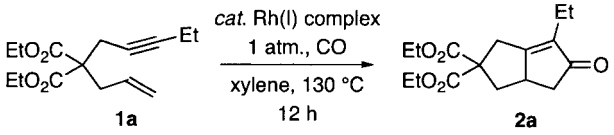

Catalyst (mol %)	*Yield (%)*
$[RhCl(CO)_2]_2$ **3** (2)	90
$[RhCl(COD)_2]_2$ **4** (2)	84
$Rh_4(CO)_{12}$ **5** (1)	18
$Rh(CO)_2(acac)$ **6** (4)	22
$[RhCl(CO)_2]_2$ (2)/PPh_3 (4) **7**	20

Tab. 11.2 Screening of rhodium catalysts bearing phosphine ligands for the Pauson–Khand-type reaction.

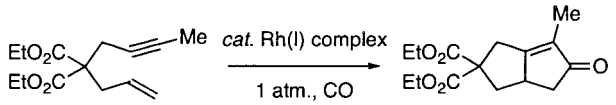

1b **2b**

Catalyst [a]	*Additive (mol %)*	*Reaction time (h)*	*Yield (%)*
8	none	12	0
6	AgOTf (10)	18	89
9	none	12	0
9	AgOTf (10)	18	90
10	none	18	58
10	AgOTf (10)	24	82
11	none	24	96
12	none	24	90

a) 5 mol%.

was the ability to modify the catalyst through variation of the phosphine ligands, which was expected to facilitate the development of the enantioselective version of this reaction. For example, $RhCl(PPh_3)_3$ **8**, *trans*-$RhCl(CO)(PPh_3)_2$ **9**, RhCl(CO)(dppe) **10**, *trans*-$[RhCl(CO)(dppp)]_2$ **11**, and $((\eta^6\text{-Ph})BPh_3)Rh(COD)$ **12** [13c,d] were effective for the PK-type transformation under the optimized reaction conditions (Tab. 11.2).

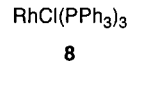

8

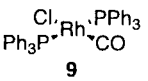

9

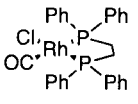

10

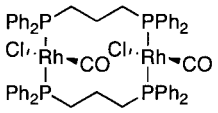

11

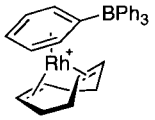

12

As indicated, the mononuclear neutral rhodium catalyst must be transformed into the cationic rhodium(I) species using AgOTf, in order to display effective catalytic activity (Tab. 11.2). Treatment of the 1,6-enyne **1b** with AgOTf-modified **8** or **9** in refluxing toluene under an atmosphere of CO (1 atm.) furnished the bicyclopentenone **2b** in 89 or 90% yield, respectively. It should be noted that rhodium-complex **10**, with the bidentate 1,2-bis(diphenylphosphino)ethane (dppe) ligand, is also an effective catalyst, albeit with the distinction that although the presence of AgOTf accelerates the reaction, it is not essential. This type of complex will be discussed later in the chapter in the context of chiral ligands that enable the enantioselective reaction. Interestingly, the zwitterionic rhodium(I) complex **12** is also an effective catalyst for this transformation (Tab. 11.2) [13d].

The optimum reaction condition, in terms of operational simplicity and chemical yield, involves the use of the dinuclear rhodium catalyst *trans*-$[RhCl(CO)(dppp)]_2$ **11**

(dppp = 1,2-bis(diphenylphosphino)propane), which affords the product in 96% yield, even in the absence of additive. Based on a preliminary study, the relative reactivity of mononuclear rhodium catalysts can be summarized qualitatively as:

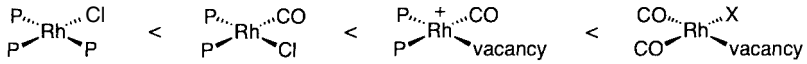

Rhodium complexes are able to transform various enynes **1** into the corresponding bicyclopentenones **2** with equal efficiency to that found with cobalt, and facilitate previously formidable PK reactions. The scope of the substituents on the alkyne for the intramolecular reaction is broad; alkyl **1a**/**b** and aryl-substituted substrates **1c** provide the desired products in excellent yield with both $[RhCl(CO)_2]_2$ and $[RhCl(CO)dppp]_2$ (Tab. 11.3).

Terminal alkyne **1d** affords **2d**, albeit with somewhat lower chemical yield, irrespective of which catalyst was employed. A distinct difference between the two catalysts is observed with the trialkylsilyl-substituted alkyne **1e**. An excellent chemical yield is obtained when $[RhCl(CO)_2]_2$ is employed, but the substrate is unreactive with $[RhCl(CO)dppp]_2$. Moreover, Wilkinson catalyst activated by AgOTf is unable to catalyze the PK reaction with this substrate effectively.

The heteroatom-tethered enynes, **1f–i**, were converted to the corresponding bicyclic heterocycles **2f–i** without event, thereby further illustrating the scope of this transformation. The $[RhCl(CO)_2]_2$-catalyzed PK reaction with the 1,6-enynes **1j** and **1j′**, which have a methyl group at a terminal position of the olefin moiety, furnishes the corresponding bicyclopentenone **2j** and **2j′** in good to excellent yield. Interestingly, treatment of **1j** with a phosphine ligand-bound catalyst, such as **10**, affords a mixture of the desired cyclopentenone **2j** with the cycloisomerization product **2j** (Eq. 1).

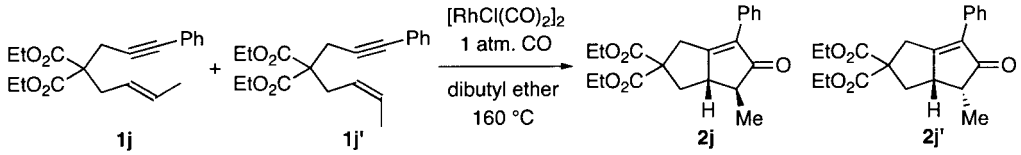

1j/1j′ { 91:9 (1 mol%, 6h) / 29:71 (1 mol%, 12h) } **2j/2j′** { 95:5 (96%) / 31:69 (90%) } (1)

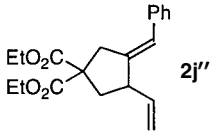

The 1,6-enyne **1k**, which has a methyl group at the internal position of the olefin moiety, furnished the corresponding bicyclopentenone **2k** in good yield under identical reaction conditions (Eq. 2). This can be attributed to the inability of the metallacyclopentene intermediate to undergo β-hydride elimination.

Tab. 11.3 Representative examples of neutral rhodium(I) catalysts.

1,6-Enyne 1	*Bicyclopentenone 2*	*Conditions*	*Reaction time*	*Yield (%)*
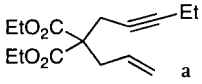 **a**	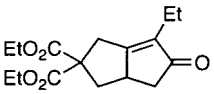	B	18	91
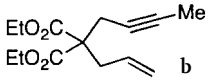 **b**	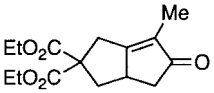	A	24	96
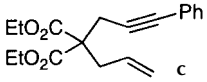 **c**	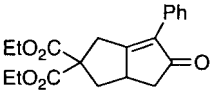	A B	24 18	99 94
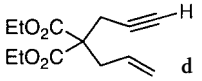 **d**	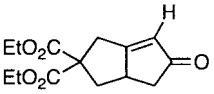	A B	24 18	55 55
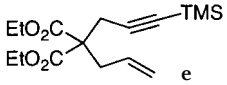 **e**	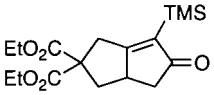	A A′ B	24 24 18	0 20 76
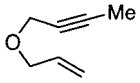 **f**	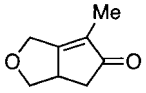	A	12	60
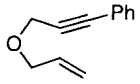 **g**	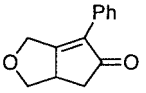	A B	12 18	82 89
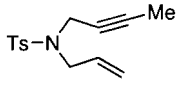 **h**	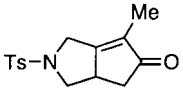	A	12	94
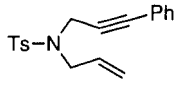 **i**	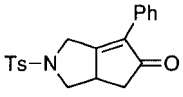	A B	12 18	97 92

a) Reaction conditions: A: $[RhCl(CO)dppp]_2$, CO (1 atm.), PhMe, 110 °C;[13c] A′: $[RhCl(PPh_3)_3]$, AgOTF, CO (1 atm.), PhMe, 110 °C;[13c] B; $[RhCl(CO)_2]_2$, CO (1 atm.), dibutyl ether, 130 °C–150 °C[13a,b].

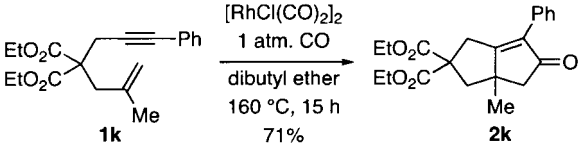

(2)

Electron-deficient alkenes, as exemplified by **1l**, are generally not suitable substrates for the cobalt-mediated PK reaction, since they often furnish dienes rather than cyclopentenones, although a few exceptions have been reported. However, since the inherently electron-rich rhodium(I) is able to donate electrons from the metal center to the electron-deficient multiple bonds, it initiates the reaction to furnish products in a highly facile and efficient manner. For example, **1l** undergoes the $[RhCl(CO)_2]_2$-catalyzed PK reaction smoothly; however, owing to the prolonged reaction times, a mixture of the initially formed product **2l** in addition to the decarboxylated product **2l′** is formed to varying degrees (Eq. 3).

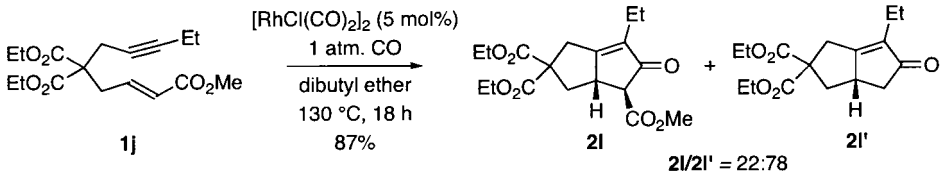

(3)

Since the PK reaction with electron-deficient alkynes was also problematic, even when stoichiometric $Co_2(CO)_8$ was employed, promoters such as trialkylamine *N*-oxide were required for the reaction to proceed [14]. Alternatively, $W(CO)_5 \cdot THF$ may be employed semi-catalytically for this class of substrates [9c]. The rhodium catalyst $[RhCl(CO)_2]_2$, has shown great versatility for electron-deficient alkynes (Scheme 11.4); the reaction times are much shorter (1–3 h) than those of the usual examples (Tab. 11.3). This rhodium-catalyzed PK reaction may be extended to the synthesis of 6,5-fused ring analogs, as exemplified in the synthesis of bicyclo[4.3.0]nonenone **2o** from the 1,7-enyne **1o** (Eq. 4) [13b].

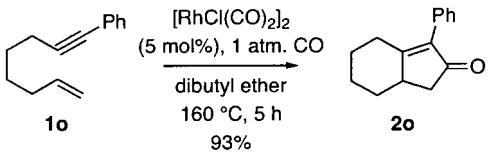

(4)

Due to the plethora of bicyclo[5.3.0]ring systems in natural products and the limited number of efficient methods that facilitate the construction of seven-membered rings; the synthesis of bicyclo[5.3.0]compounds based on a PK reaction has recently been a subject of intense interest. Generally, the preparation of larger ring systems [*n*.3.0] ($n>4$) has proven challenging with traditional PK reaction catalysts. One of the few examples reported is the $Co_2(CO)_8$ catalyzed formation of the azabicyclo[5.3.0]-decenonone derivative **15** (X=OTBS) from the conformationally restricted substrate **14**

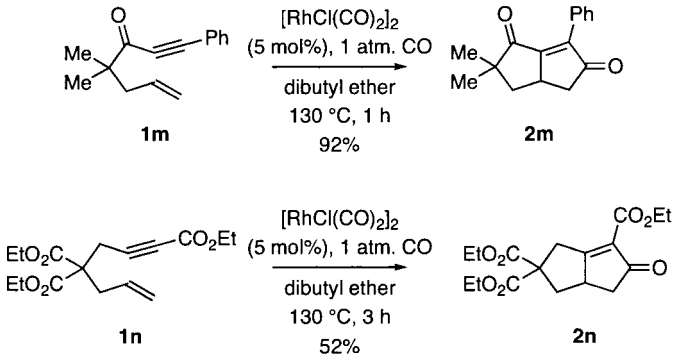

Scheme 11.4 PK reaction with electron-deficient alkynes.

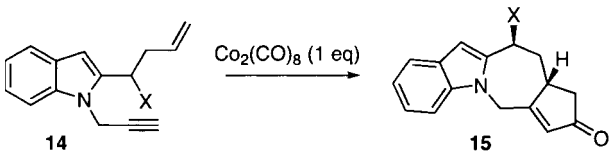

		X = OH	X = OTBS	X = NPhth
Reaction Conditions	Et_3N-*N*-oxide, 4Å MS	20	65	10
	PhMe, Δ, 4Å MS	10	75	30
	PhMe, Δ	-	40	-

Scheme 11.5 Synthesis of bicyclo[5.3.0]decenones using the PK reaction

(Scheme 11.5) [15]. More recently it has been demonstrated that bicyclo[5.3.0]-decenones may be prepared using rhodium catalysis, provided the requisite substrate is employed.

The intra- or intermolecular PK reaction of allenes with alkynes catalyzed by dicobalt octacarbonyl and *N*-methylmorpholine *N*-oxide (NMO) [16], as well as by other metals [17], has been thoroughly investigated. Annulation of allenyne **16** provides a versatile route to either the 5,5- or 5,6-ring systems, depending upon which transition metal catalyst is employed. Stoichiometric molybdenum hexacarbonyl with dimethyl sulfoxide selectively converts the allenyne **16** to the [2+2+1] carbocyclization *exo*-olefin product **17** in an efficient manner, which is a result of the internal olefin of the allene participating in the reaction (Scheme 11.6) [18]. The efficiency of the operation was demonstrated by the preparation of highly functionalized bicyclopentenes, which were used for the total synthesis of the antitumor agent (±)-hydroxymethylacylfulvene, an analog of the illudin family of natural products [19].

The rhodium-catalyzed transformation of allenyne **16** provides complementary regioselectivity to that obtained with molybdenum. For example, whereas the internal olefin of the allene is engaged in the molybdenum-catalyzed reaction, it is the allene's

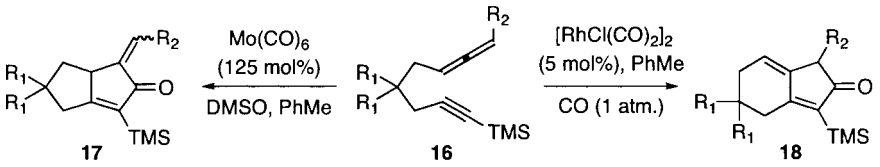

		17	18
$R_1 = CO_2Me$	$R_2 = C_6H_{13}$	95% (Z:E = 1.5:1)	62%
$R_1 = H$	$R_2 = H$	68%	45%

Scheme 11.6 Regiochemical reversal with allenes in the PK reaction.

terminal olefin that reacts when a rhodium catalyst is employed (Scheme 11.6) [20]. This selectivity is the opposite of that observed in the intramolecular [4+2]-diene allene carbocyclization, in which rhodium generally prefers to react with the internal olefin of the allene (Scheme 11.7) [3a]. This unique regioselectivity prompted others to examine the possibility of preparing bicyclo[5.3.0]derivatives using rhodium catalysis.

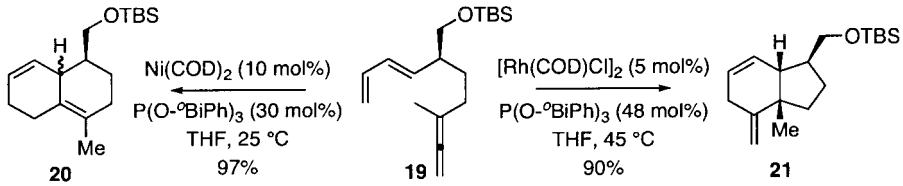

Scheme 11.7 Intramolecular rhodium-catalyzed [4+2]-diene allene carbocyclization.

Other transition metals were also examined, but with marginal success; for example, **23** was obtained in poor yield from **22**, and a mixture of **25** and **26** from **24**, using $Co_2(CO)_8$/*N*-methylmorpholine *N*-oxide (Eq. 5) [21]. When the $Fe(CO)_4(NMe_3)$ catalyst was examined for the PK reaction of an allenyne, the requisite bicyclo[5.3.0]dec-1,7-dien-9-one derivative was formed, albeit in low yield [22].

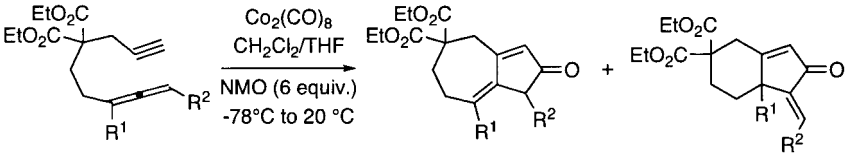

(5)

A major breakthrough in this type of transformation was accomplished using rhodium catalysis, which enabled the conversion of **27** and **29** with $[RhCl(CO)_2]_2$ or [RhCl(CO)-dppp]$_2$ in toluene under an atmosphere of CO (1 atm.), to afford the corresponding bicyclo[5.3.0]compounds **28** and **30** in 60–77% yield (Scheme 11.8) [20].

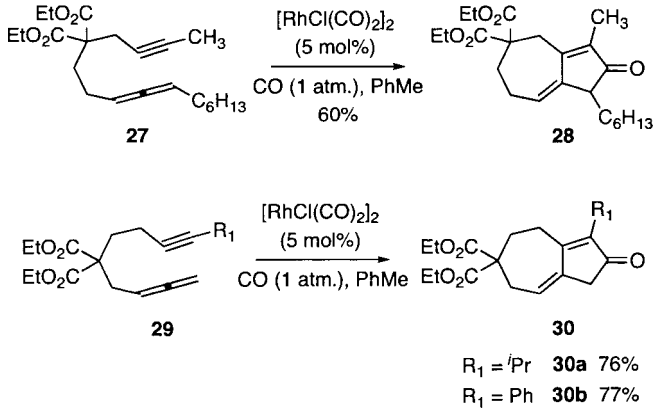

Scheme 11.8 Rhodium-catalyzed PK reaction for the synthesis of bicyclo[5.3.0]derivatives.

The 1-phenylsulfonylallenes **31**, possessing a hexynyl side chain, undergo a regioselective formal [2+2+1] cycloaddition to produce the corresponding bicyclo[5.3.0]dec-1,7-dien-9-one derivatives **32** in good yield, using catalytic $[RhCl(CO)_2]_2$ or $[RhCl(CO)dppp]_2$ under an atmosphere of CO (1 atm.) in refluxing toluene (Scheme 11.9) [20b].

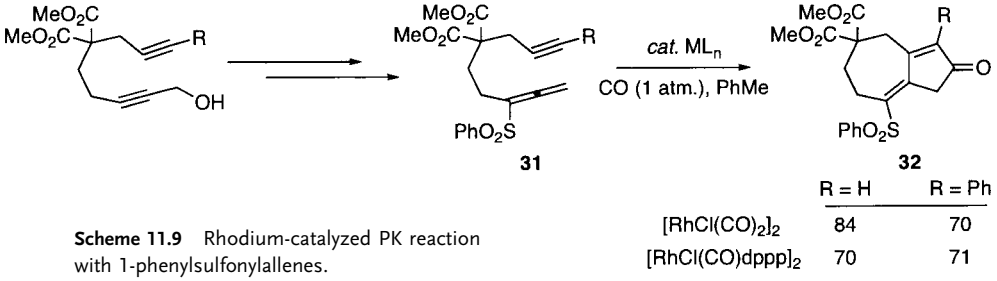

	R = H	R = Ph
$[RhCl(CO)_2]_2$	84	70
$[RhCl(CO)dppp]_2$	70	71

Scheme 11.9 Rhodium-catalyzed PK reaction with 1-phenylsulfonylallenes.

The beneficial effect of an allene functionality for the construction of bicyclo[5.3.0]decadienones is evident from the failure of the 1,8-enyne **33** to undergo conversion to **34**, to thereby produce the same skeleton (Eq. 6) [20b].

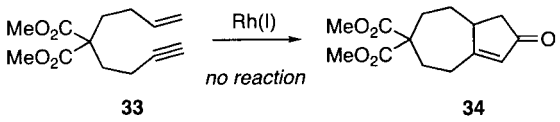

(6)

The intermolecular carbocyclization with a strained olefin, such as norbornene **35**, has been frequently used for proof-of-principle in challenging metal-catalyzed transformations. The use of rhodium catalysts facilitates the intermolecular reaction, albeit in modest yield and with poor regioselectivity (Scheme 11.10). Ethylene **39** can also be utilized to this end, but generally affords the carbocyclization products in low yield, as

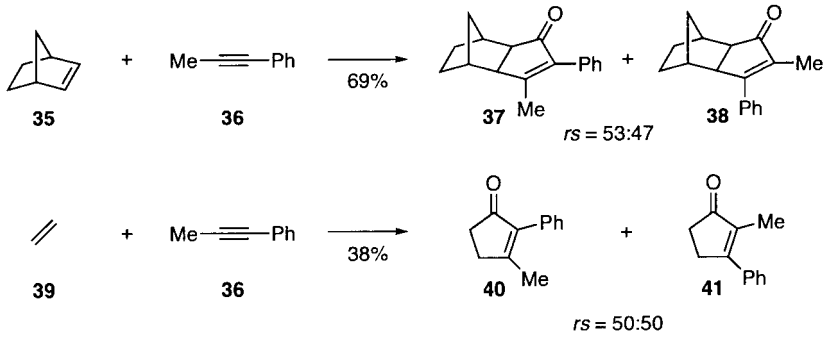

Scheme 11.10 Intermolecular PK reactions with strained olefins and ethylene.

exemplified by the formation of the cyclopentenones **40** and **41** in 38% yield, as a 1:1 mixture of regioisomers. However, one of the most notorious substrates for the PK reaction, styrene, is unsuitable for use in this particular reaction [13 b].

In addition to the [2+2+1] carbocyclization, an analogous [3+2+1] version has been reported [23]. The high π-character of the σ-bond of the cyclopropane provides reactivity similar to that of an olefin; thus when the 4-pentynyl cyclopropanes **42** were subjected to the PK reaction conditions, the bicyclo[4.3.0]nonenone **43**, in addition to a small amount of the oxidized product **44**, was afforded in modest yield (Eq. 7). The analogous transformation with the vicinally disubstituted cyclopropane **45** furnished regioisomers **46** and **47**, in which cleavage at the less substituted bond is favored (Eq. 8).

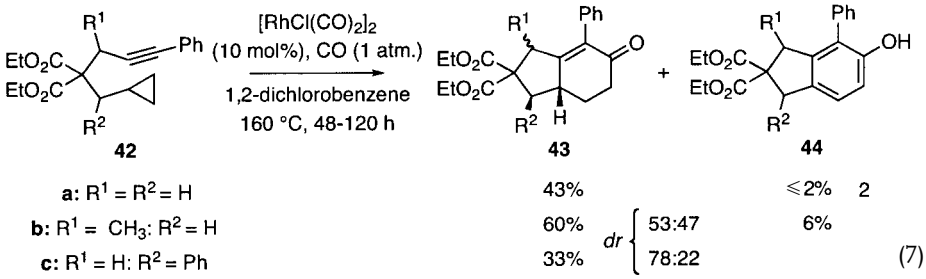

(7)

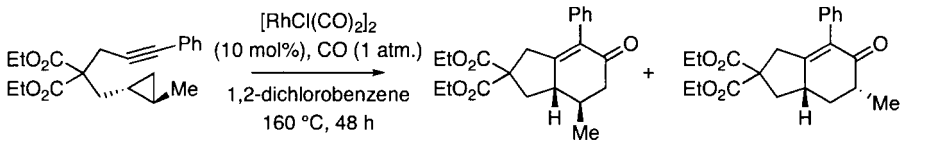

(8)

11.2.2
Reactions Under Reduced CO Pressure

The rhodium-catalyzed PK reaction has many unique features as compared to the original cobalt-mediated version. For example, most of the rhodium-catalyzed reactions could be carried out under only 1 atm CO. Initially, these reactions were expected to proceed more effectively under higher CO pressures. However, experimental results demonstrated that the reaction was retarded by elevated CO pressure (>1 atm.), while the reaction at a lower CO pressure (0.1 atm.) proved to be superior [13b]. For example, the reaction of **1a** with $[RhCl(CO)_2]_2$ under a high pressure of CO (3 atm.) afforded **2a** in 70% yield, but was not complete after 36 h. The analogous reaction under a mixed CO/Ar atmosphere (1 atm.; CO/Ar=1:9) was complete within an hour to afford **2a** in 90% yield.

The advantage of these reaction conditions became more obvious with the enyne **1l**, in which the reacting olefin is attached to an electron-withdrawing substituent. As mentioned earlier, the decarboxylation product **2l′** of the initially formed keto ester **21** was the major product, due to the prolonged reaction time (Eq. 3). Gratifyingly, when the reaction was carried out under a reduced pressure of CO, the reaction time was significantly reduced to facilitate the isolation of the keto ester **21** as the major product (Eq. 9).

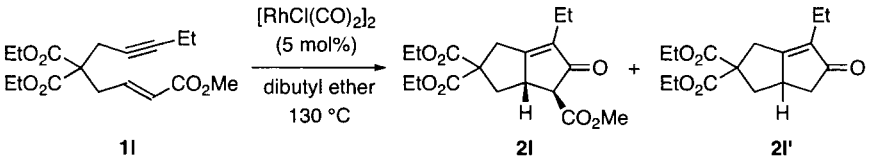

(9)

11.2.3
Alternative CO Sources

The facile formation of metal carbonyl complexes makes rhodium a very useful catalyst for both the hydroformylation of multiple bonds and the decarbonylation of the aldehydes. Two groups have independently utilized the metal carbonyl complex obtained from decarbonylation of aldehydes in the PK reaction (Scheme 11.11) [24].

After extensive screening of various aldehydes to optimize the reaction conditions, it was found that aromatic aldehydes were able to serve as a carbon monoxide source, in which the electronic nature of the aldehydes is responsible for their ability to transfer CO efficiently [24]. Consequently, aldehydes bearing electron-withdrawing substituents are more effective than those bearing electron-donating substituents, with pentafluorobenzaldehyde providing optimal reactivity. Interestingly, for all substrates tested the reaction is void of any complications from hydroacylation of either the alkene or alkyne of the enyne. Iridium and ruthenium complexes, which are known to decarboxylate aldehydes and catalyze the PK reaction, demonstrated inferior efficiency as compared to

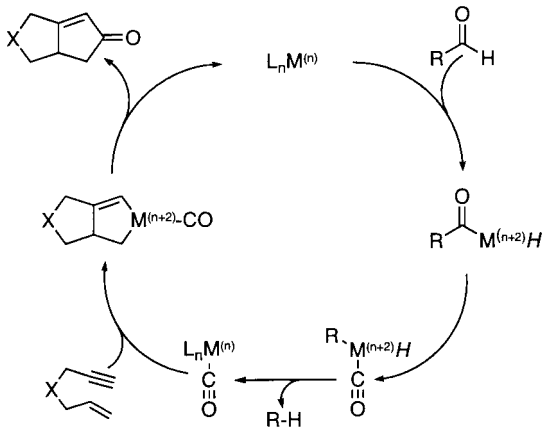

Scheme 11.11 PK reaction by metal carbonyls formed from aldehydes.

rhodium. A stoichiometric amount of aldehyde in refluxing xylene is generally enough to perform this transformation.

In a subsequent study, cinnamaldehyde was employed as the CO source in the absence of solvent [24b]. The enynes **1** were heated at reflux in excess cinnamaldehyde (20 equiv.) with 5 mol% $Rh(dppp)_2Cl$ (prepared *in situ* by mixing $[Rh(COD)Cl]_2$ and 2 equiv. dppp) under an atmosphere of argon, to furnish the corresponding bicyclopentenones **2** in almost quantitative yield. The reaction with only 1 equiv. cinnamaldehyde was also examined, although the chemical yield was slightly diminished. Nonetheless, the advantage of the reaction utilizing cinnamaldehyde under solvent-free conditions is that it allows for substantially shorter reaction times than the transformation using pentafluorobenzaldehyde in xylene (Tab. 11.4).

Tab. 11.4 The PK reaction using aldehydes as a source of carbon monoxide.

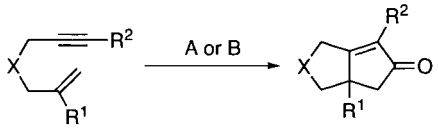

A: $[RhCl(COD)]_2$ (5 mol%), dppp (11 mol%), C_6F_5CHO (1 equiv.), xylene, 130 °C, 54 h, under N_2

B: $Rh(dppp)_2Cl$ (5 mol%), dppp (11 mol%), cinnamaldeyde (20 equiv.), 120 °C, 2-24 h, under Ar

X	*R¹*	*R²*	*Conditions*	*Yield (%)*
$(EtO_2C)_2C$	H	Ph	A	97
			B	56
TsN	H	Ph	A	95
			B	98
TsN	H	Bu	A	84
		Me	B	90
O	H	Ph	A	91
		p-$MeOC_6H_4$	B	88
		Bu	A	74
O	Me	Ph	A	92
			B	75

The origination of CO from the aldehyde was confirmed by mechanistic studies, in which labeling experiments demonstrated that the majority of the CO was derived from the aldehyde. For example, when the reaction was carried out with 1.2 equiv of aldehyde under a partial pressure of ^{13}CO instead of argon, only about 10% of the isotopically labeled product was formed. This indicated that the source of the CO incorporated into the PK product was derived primarily from the aldehyde (Eq. 10) [24c]. An additional experiment with 2-naphthylaldehyde **49** (2 equiv.) demonstrated that only 1 equiv. of aldehyde was consumed (Eq. 11) [24a].

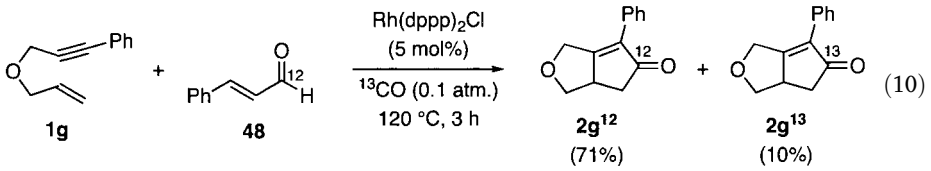

(10)

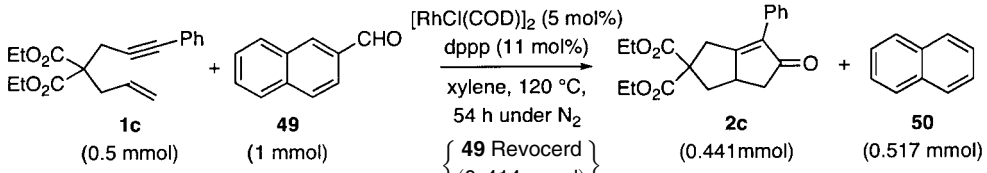

(11)

11.2.4 Enantioselective Pauson–Khand-Type Reaction

Despite impressive advances in the catalytic PK reaction, the development of an enantioselective version did not have the same degree of early success. However, the titanium catalyst (*S,S*)-(EBTHI)Ti(CO)$_2$ was efficient for the formation of the enantiomerically enriched carbocyclization adducts [25]. Unfortunately, the attempted utilization of late transition metals, such as cobalt, in analogous enantioselective variants proved disappointing [26]. This was attributed to these catalysts requiring strong π-accepting ligands, such as carbon monoxide, due to the intrinsic high electron density of the metal. This constraint has made it difficult to introduce chiral ligands on such catalysts, and is further complicated in that the replacement of CO with a tunable phosphine ligand causes a substantial decrease in the rate of reaction. Analysis reveals that under the PK reaction conditions the chiral phosphine-based catalyst is present along with the phosphine-free carbonyl complex, which presumably arises from an equilibrium between the phosphine-bound catalyst and CO. Thus, a competition arises that ultimately leads to diminished enantioselectivity, due to the superior catalytic ability of the achiral complex. Nonetheless, [IrCl(COD)]$_2$ coupled with (*S*)-TolBINAP was recently reported to afford high enantioselectivity in this transformation [27].

The application of a rhodium(I) catalyst bearing tunable bidentate phosphine ligands, such as **10**, opened the possibility for the development of a new catalytic enantioselective reaction [13c]. In a control experiment, it was noted that the reaction with a catalyst containing a bidentate phosphine ligand, specifically RhCl(CO)(dppe), was significantly decelerated as compared to the reaction with [RhCl(CO)$_2$]$_2$ (Scheme 11.12).

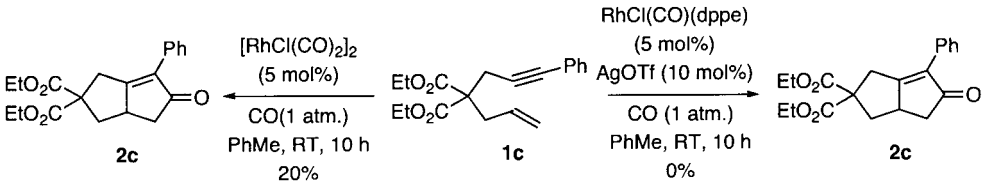

Scheme 11.12 Comparison of the reaction rates in the PK reactions using CO and phosphine-containing rhodium complexes.

As previously mentioned, this might be attributed to the diminished Lewis acidity of the phosphine-bound catalyst, and implies that a catalyst with strongly bound phosphine ligands is required to suppress the reaction occurring with a phosphine-free catalyst.

Efforts have been focused on the identification of the requisite combination of metal and ligand in addition to other parameters [28]. Results of this work have delineated the following features in this transformation: (1) catalysts prepared *in situ* by mixing of a slight excess of chiral bisphosphine ligands and $[RhCl(CO)_2]_2$ are effective; (2) solvent choice is important, since although the reaction proceeds more efficiently in toluene than in a coordinating solvent such as THF, it must be carried out in THF to achieve high enantioselectivity; (3) a silver salt, such as AgOTf, is often required for initiation in a coordinating solvent; (4) (*S*)- and (*R*)-BINAP are among the best ligands screened for enantioselectivity; and (5) balancing the CO pressure is critical to obtaining high enantioselectivity and high chemical yields, since there is a trade-off between the two in most PK reactions utilizing phosphine-based catalysts. Therefore, while a higher yield of PK products are afforded under higher CO pressure, better enantioselectivities are generally obtained under lower CO pressure due to suppression of the unfavorable equilibrium between potential catalysts. Based on these preliminary results, the optimal experimental protocol was determined to consist of 3 mol% $[RhCl(CO)_2]_2$, 9 mol% (*S*)-BINAP, 12 mol% AgOTf, 1 atm. CO, and 1 equiv. 1,6-enyne **1** in THF at the appropriate reaction temperature (Tab. 11.5).

Asymmetric catalytic reactions under solvent-free conditions have also been reported. Contrary to the previous result, a neutral rhodium(I) complex provided comparable enantioselectivity with high chemical yield [24c]. For certain cases, benzaldehyde gave improved enantioselectivity over cinnamaldehyde (Tab. 11.6), although the rationale behind choosing this particular CO source is not entirely clear. Additionally it should be noted that when the reaction was carried out using a stoichiometric amount of an aldehyde as the CO source in xylene, the reaction takes much longer and the enantioselectivity decreases substantially.

11.2.5 Domino Reactions

Domino reactions attract significant attention due to their ability to allow for multistep operations in one pot. Two classes of domino transformations are known for the PK reaction. The first involves the use of a dual-catalyst system, while the second uses a single catalyst with modification of the reaction parameters to control reactivity.

Tab. 11.5 Enantioselective Pauson–Khand-type reaction with a cationic rhodium(I) complex.

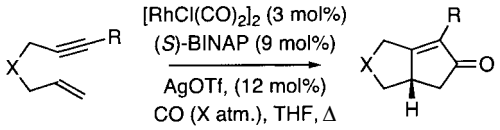

X	*R*	*CO (atm.)*	*Yield (%)*	*ee (%)*	*Abs. config.*
$(MeO_2C)_2C$	Me	2	91	62	
$(EtO_2C)_2C$	Me	3	93	71	*S*
$(^iPrO_2C)_2C$	Me	1	40	90	
$(EtO_2C)_2C$	Ph	1	70	61	
TsN	Me	1	80	84	
TsN	Ph	1	93	74	*S*
O	Me	2	85	86	
O	Me	1	40	96	*S*
O	Ph	1	88	81	*S*

Tab. 11.6 Solvent-free enantioselective Pauson–Khand-type reaction with a neutral rhodium(I) complex.

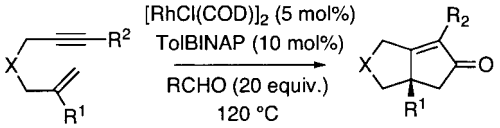

X	*R_1*	*R_2*	*CO source*	*Reaction time*	*Yield (%)*	*ee (%)*
$(EtO_2C)_2C$	Ph	H	(*E*)-PhCh=CHCHO	4	79	45
TsN	Ph	H	”	4	99	56
TsN	Ph	H	PhCHO	12	82	69
O	*p*-$MeOC_6H_4$	H	(*E*)-PhCH=CHCHO	6	86	81
O	*p*-ClC_6H_4	H	”	9	82	79
O	$Ph(CH_2)_3$	H	”	2	72	90
O	Ph	Me	”	18	41	82
O	Ph	Me	PhCHO	36	59	81

The following two-step operation was chosen as an example of the former case. The first step involves an allylation to generate the 1,6-enyne intermediate **1**, *via* the reaction between a metal π-allyl complex derived from **52** and propargyl anion **51**, followed by the PK-type reaction to furnish the bicyclopentenone **2** (Scheme 11.13). Since these two specific reactions have opposing electronic requirements (the first prefers Lewis basic character, while the second can be facilitated by Lewis acidic catalysts), finding the right combination of catalysts was the key to success.

The combination of $Pd_2(dba)_3 \cdot CHCl_3$ and dppb with $[RhCl(CO)dppp]_2$ provides the optimal balance of reactivity for the one-pot two-step allylic alkylation followed by PK

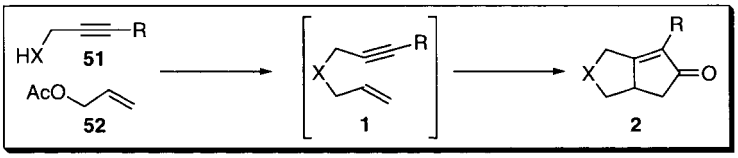

Scheme 11.13 Tandem π-allyl alkylation and PK reaction.

transformation at a normalized temperature [29]. In other words, it can be done by mixing all the ingredients and heating the mixture in toluene at 110°C (Tab. 11.7).

The regio- and diastereoselective rhodium-catalyzed sequential process, involving allylic alkylation of a stabilized carbon or heteroatom nucleophile **51**, followed by a PK reaction, utilizing a single catalyst was also described (Scheme 11.14). Alkylation of an allylic carbonate **53** was accomplished in a regioselective manner at 30°C using a π-acidic rhodium(I) catalyst under 1 atm CO. The resulting product **54** was then subjected *in situ* to an elevated reaction temperature to facilitate the PK transformation.

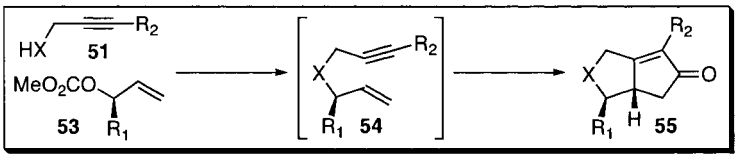

Scheme 11.14 Domino regio-and diastereoselective π-allyl alkylation and PK reaction.

Disappointingly, the trimethylphosphite-modified Wilkinson catalyst, which had proven effective for the allylic substitution reaction [30], furnished only a trace amount of the PK product. By screening various rhodium catalysts for both reactions, it was determined that $[RhCl(CO)dppp]_2$ was the optimum complex for the sequential pro-

Tab. 11.7 Representative examples of the domino π-allyl alkylation and PK reaction.

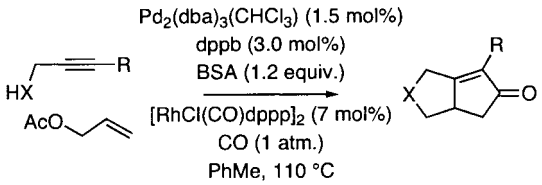

X	*R*	*Reaction time (h)*	*Yield (%)*
$(EtO_2C)_2C$	Ph	25	92
$(EtO_2C)_2C$	Me	25	73
$(EtO_2C)_2C$	H	25	0
TsN	Ph	10	90
TsN	Me	10	91
TsN	H	6	92

Tab. 11.8 Representative examples of the regio- and stereoselective tandem π-allyl alkylation and PK reaction.

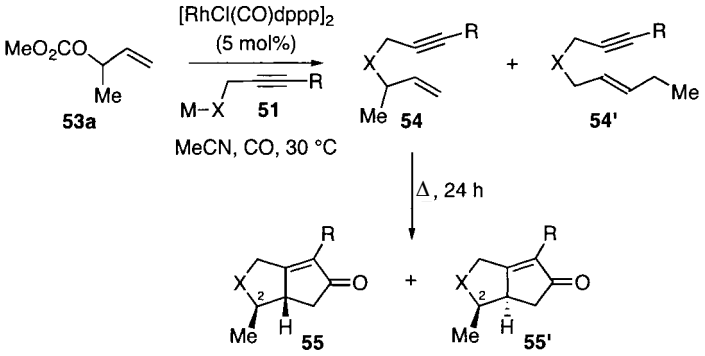

X	R	M	54/54′	55/55′	Yield (%)
$(EtO_2C)_2C$	Ph	Na	27:1	5:1	82
$(EtO_2C)_2C$	Me	Na	19:1	6:1	80
$(EtO_2C)_2C$	H	Na	11:1	9:1	78
TsN	Ph	Li	20:1	3:1	79
TsN	Me	Li	32:1	6:1	84
TsN	H	Li	57:1	7:1	81
O	Ph	Li	5:1	≥19:1	63
O	Me	Li	7:1	≥19:1	73
O	H	Li	8:1	≥19:1	81

cess. The allylic alkylation of **53a** with the sodium salt of the α-branched malonate **51** (X=C(CO_2Me)$_2$; R=H) provided the alkylated product **54** in acetonitrile at 30°C (**54**/**54′**=27:1). The reaction mixture was then heated at reflux for 24 h to result in the formation of the bicyclic cyclopentenones **55**/**55′** as a 5:1 mixture of diastereoisomers favoring **55** in 82% combined yield (Tab. 11.8) [31]. The moderate diastereoselectivity obtained in the PK reaction can be substantially increased by the introduction of a bulky substituent at C2 (Eq. 12).

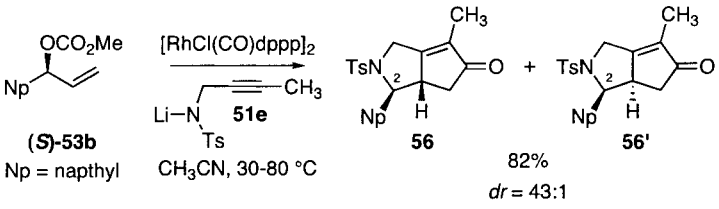

(12)

11.2.6
Coupling of Two Alkynes, and CO or Isocyanides

The metal-catalyzed [2+2+1] carbocyclization of two alkyne moieties with CO leading to cyclopentadienones can be mediated by various transition metals, including $CpCo(PPh_3)_2$, $CpCo(CO)_2$ [32], $Fe(CO)_5$ [33], and $RhCl(PPh_3)_3$ [34]. In the early studies, preparation of cyclopentadienones required a stepwise process using a stoichiometric amount of metal because of the intrinsic instability of the products. The reaction occurs by initially forming a metal-complexed cyclopentadienone, which then oxidatively demetallates to afford the thermodynamically more stable congeners (Scheme 11.15).

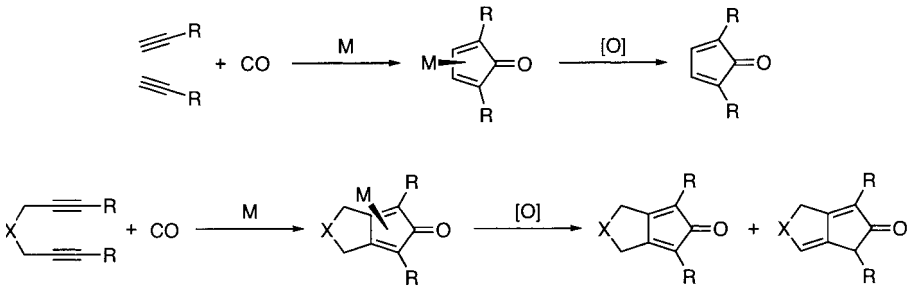

Scheme 11.15 [2+2+1] carbocyclization between two alkynes and CO.

The rhodium-entrapped cage compound which is formed using a stoichiometric amount of $[RhCl(CO)_2]_2$ is a notable paradigm of the rhodium-catalyzed [2+2+1] alkyne–alkyne and CO coupling [35]. Heating **57** in acetone at 50 °C for 8 h or irradiation by a tungsten or mercury lamp provided the cage compound in 50% yield based on NMR spectroscopy. However, due to mechanical losses it was isolated in only 16% yield from the reaction mixture, by crystallization as the hexafluorophosphate salt **58** (Eq. 13).

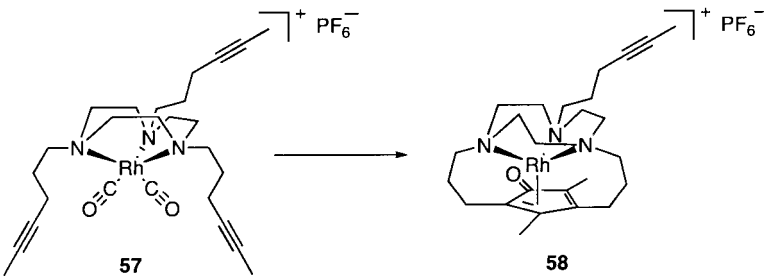

(13)

The $Co_2(CO)_8$- and $[Ir(COD)Cl]_2$-catalyzed processes may be carried out in the presence of the appropriate ligand under a CO atmosphere. These conditions, as well as the direct use of Vaska's complex $[IrCl(CO)(PPh_3)_2]$, are applicable to alkynes bearing bulky substituents, such as **59**, for synthesis of the parent products **60**. However, it should be noted that, in many cases, the thermodynamically more stable products **60′**

are obtained *via* isomerization of the olefin (Eq. 14) [36]. Rhodium complexes are generally less effective that iridium ones under these reaction conditions, given that the reaction of **59** (R = Ph) with $[Rh(COD)Cl]_2$ and $[Rh(COD)Cl]_2 + 4PPh_3$ afforded **60** in only 29% and 9% yield respectively [36a].

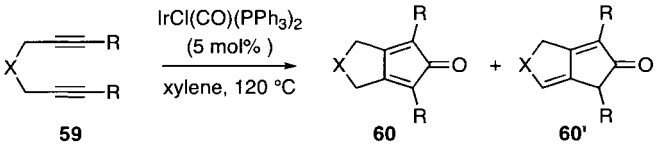

(14)

Alternatively, rhodium catalysts have been revealed to be effective for the coupling of two alkynes with an isocyanide to afford the iminocyclopentadienes **62** and **62′** in high yield (Tab. 11.9) [36b]. The coordinating solvent dibutyl ether, in combination with portionwise addition of the isocyanides, is key to the success of this transformation.

Tab. 11.9 Rhodium complex-catalyzed coupling of various diynes with isocyanide.

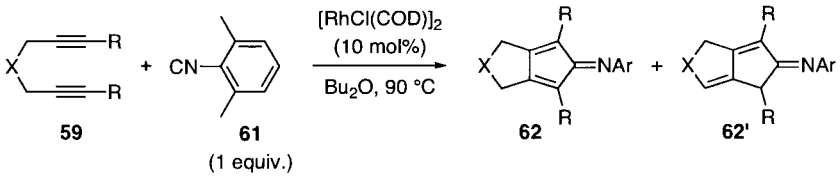

	R	*Z*	*Time (h)*	*Yield (%)*	*62/62′*
a	Ph	$(^tBuO_2C)_2C$	1.5	89	
b	TMS	$(BnO_2C)_2C$	1.5	74	
c	Me	$(BnO_2C)_2C$	1.5	73	2:1
d	Ph	O	0.5	92	
e	Ph	CH_2	3.5	80	3:1

11.3 [4+1] Carbocyclization

11.3.1 Coupling of Vinylallene and CO

In addition to the [3+2] and [2+2+1] carbocyclizations that facilitate the formation of five-membered rings, the [4+1] carbocyclization also has merit. Several transition metals have been engaged in this transformation [37], wherein it was found that vinylallene **63a** reacts with 1 equiv of Wilkinson catalyst to afford the planar σ_2-bonded (vinylallene)rhodium complex **64a** upon simple ligand displacement (Scheme 11.16). The structure of **64a** was confirmed unambiguously by X-ray crystallography, and represents the first structural characterization of a metallacycle intermediate [38a].

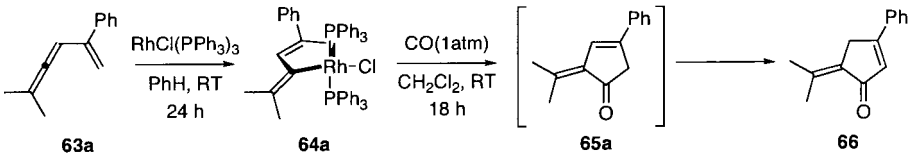

Scheme 11.16 Rhodium-catalyzed [4+1] reaction with a vinylallene.

Tab. 11.10 Representative examples of rhodium(I)-catalyzed [4+1] carbocyclization.

	Vinylallene 63	*Cyclopentenone 65*	*Conditions*	*Yield (%)*	*Isomer ratio*
c	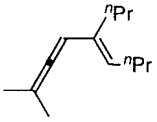	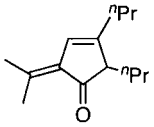	60 °C, 15 h	85	91:9
d	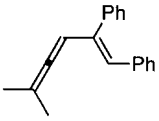	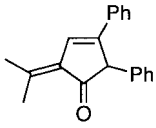	40 °C, 16 h	93	>99:1
e	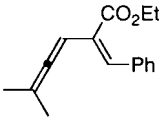	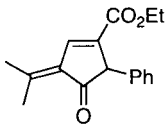	20 °C, 16 h	94	>99:1
f	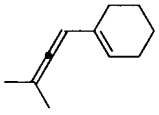	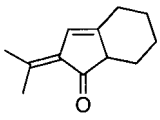	60 °C, 14 h	92	96:4
g	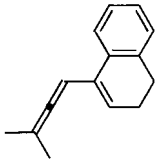	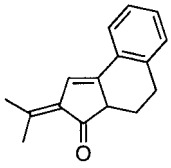	60 °C, 14 h	85	93:7
h	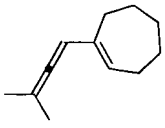	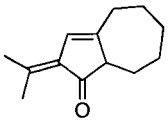	60 °C, 14 h	95	99:1

a) [Rh(COD)(dppbe)]OTf (5 mol%), CO (10 atm.) in DME.

Carbonylative [4+1] carbocyclization of **64a** was effected by simply stirring a solution of the complex in dichloromethane under an atmosphere of CO (1 atm.). The conjugated cyclopentenone **66** was formed in 96% yield, presumably by isomerization of the initially formed cyclopentenone **65a**.

Initial attempts to extend this methodology to the catalytic manifold using Wilkinson's catalyst furnished only a trace amount of the cyclopentenone [38]. This is possibly due to an irreversible reaction between the nascent catalytic species and CO to exclude **63b** from the coordination sphere (Scheme 11.17) [38d]. However, use of a catalytic amount of the cationic rhodium species $[Rh(COD)(MeCN)_2]BF_4$ efficiently led to the formation of the [4+1] cycloadducts.

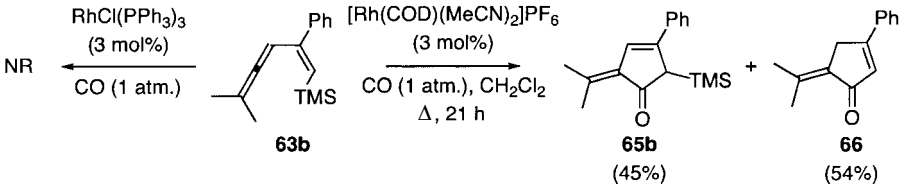

Scheme 11.17 Catalytic [4+1] reaction using a cationic rhodium complex.

Extensive experimentation delineated the crucial features for the catalytic process to be: (1) a cationic complex is necessary to promote the reaction efficiently; (2) the use of 1,2-bis(diphenylphosphino)benzene (dppbe) as the phosphine ligand and triflate as the counterion generates the product in high yield and suppresses isomerization; and (3) employment of 10 atm. CO in 1,2-dimethoxyethane (DME) provides the optimum results, which are summarized in Tab. 11.10.

11.3.2
Asymmetric [4+1] Carbocyclization

The asymmetric catalytic [4+1] reaction was attempted with a cationic rhodium complex, $[Rh(COD)_2]PF_6$ (5 mol%) and the chiral diphosphine ligand (*R,R*)-Me-DuPHOS (6 mol%) (Scheme 11.18) [38b,c,d].

A higher pressure of CO (5 atm.) was required to suppress the formation of a conjugated triene **68c**, which is probably formed through *β*-hydride elimination of the metallacyclopentene intermediate **70c** followed by reductive elimination (Scheme 11.19).

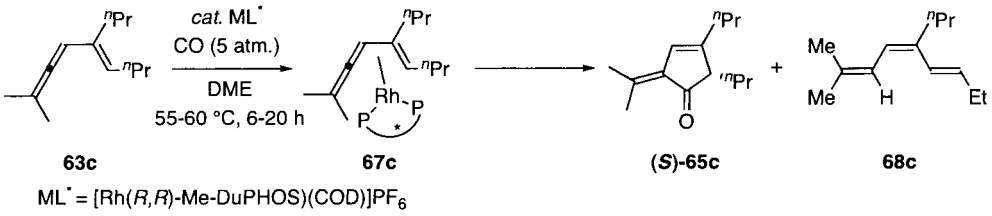

Scheme 11.18 Asymmetric rhodium-catalyzed [4+1] reaction.

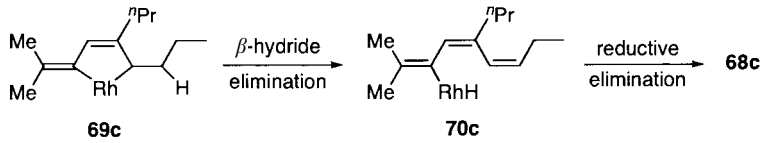

Scheme 11.19 β-Hydride elimination of a metallacyclopent-3-ene to afford a conjugated triene.

Tab. 11.11 Representative examples of rhodium(I)-catalyzed enantioselective [4+1] carbocyclization.

Vinylallene 63[a)]	*Cyclopentenone 65*	*Yield (%)*	*% ee*
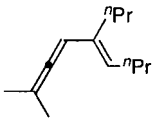	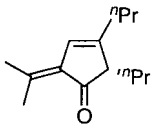	87	64.5 (S)
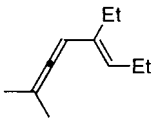	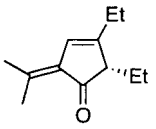	72	41.9 (S)
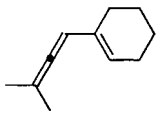	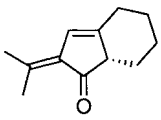	99	78.0 (S)
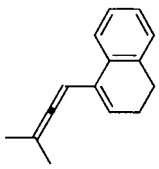	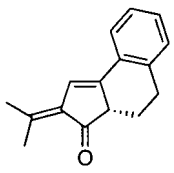	97	74.8 (S)
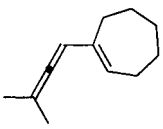	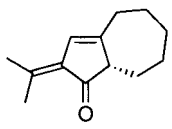	98	10.6 (S)

a) [Rh(*R,R*)-Me-DuPHOS)(COD)]PF_6, Co (5 atm), DME, 55–60 °C, 6–20 h..

The level of enantioselectivity was highly substrate-dependent, since even slight changes in the substrate led to decreased enantioselectivity (Tab. 11.11).

The optimum result in terms of enantioselectivity was obtained with the vinylallene bearing an ester group, **63e**, wherein the carbocyclization proceeds at lower temperature to afford remarkably improved selectivity (Scheme 11.20).

It is worth mentioning that, in a related study, a chiral platinum complex prepared from bis(cyclooctadiene) platinum [$Pt(COD)_2$] (5 mol %) and (*R,R*)-Me-DuPhos (6 mol%), also catalyzed the reaction of **63c** efficiently to provide the product **(*R*)-65c**

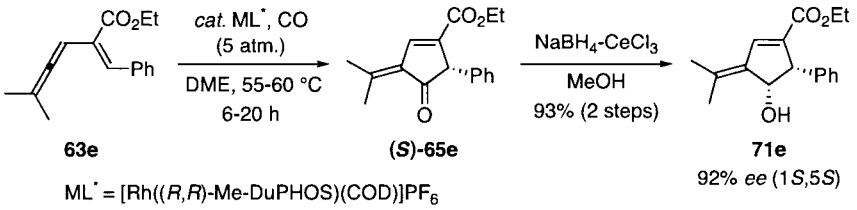

Scheme 11.20 Asymmetric rhodium-catalyzed [4+1] reaction with the ester-bearing vinylallene **63e**.

in 76% yield with 75% enantiomeric excess [38c]. Fascinatingly, the absolute configuration was the opposite of that obtained in the rhodium-catalyzed reaction.

11.4 Conclusion

The rhodium-catalyzed [$m+n+1$] reactions, as exemplified by the [2+2+1] may be accomplished with an array of substrates that have proven challenging for other metal complexes. Moreover, the ability to undertake the domino reactions significantly increases the molecular complexity and ultimately the synthetic utility of this venerable reaction. Although the [3+2+1] and [4+1] reactions have not been as extensively studied, they will undoubtedly be the subjects of future synthetic efforts.

11.5 References

1 Aubert, C.; Busine, O.; Malacria, M. *Chem. Rev.* **2002**, *102*, 813.

2 (a) Matsuda, I.; Shibata, M.; Sato, S.; Izumi, Y. *Tetrahedron Lett.* **1987**, *28*, 3361. (b) Jolly, R.S.; Luedtke, G.; Sheehan, D.; Livinghouse, T. *J. Am. Chem. Soc.* **1990**, *112*, 4965. (c) McKinstry, L.; Livinghouse, T. *Tetrahedron* **1994**, *50*, 6145. (d) O'Mahony, D.J.R.; Belanger, D.B.; Livinghouse, T. *Synlett* **1988**, 443. (e) Wender, P.A.; Jenkins, T.E. *J. Am. Chem. Soc.* **1989**, *111*, 6432.

3 (a) Wender, P.A.; Jenkins, T.E.; Suzuki, S. *J. Am. Chem. Soc.* **1995**, *117*, 1843. (b) Wender, P.A.; Smith, T.E. *J. Org. Chem.* **1996**, *61*, 824.

4 (a) Wender, P.A.; Takahashi, H.; Witulski, B. *J. Am. Chem. Soc.* **1995**, *117*, 4720. (b) Wender, P.A.; Husfeld, C.O.; Langkopf, E.; Love, J.A. *J. Am. Chem. Soc.* **1998**, *120*, 1940.

5 Wender, P.A.; Rieck, H.; Fuji, M. *J. Am. Chem. Soc.* **1998**, *120*, 10976.

6 (a) Khand, I.U.; Knox, G.R.; Pauson, P.L.; Watts, W.E.; Foreman, M.I. *J. Chem. Soc., Perkin Trans. 1* **1973**, 977. (b) Pauson, P.L.; Khand, I.U. *Ann.N.Y. Acad. Sci.* **1977**, *295*, 2. (c) Pauson, P.L. *Tetrahedron* **1985**, *41*, 5855.

7 (a) Brummond, K.M.; Kent, J.L. *Tetrahedron* **2000**, *56*, 3263. (b) Jeong, N. In *Transition Metals for Organic Synthesis;* Bellar, M.; Bolm, C. Eds.; Wiley-VCH: Weinheim, **1998**; Vol. 1, pp. 560–577. (c) Geis, O.; Schmalz, H.G. *Angew. Chem., Int. Ed.* **1998**, *37*, 911. (d) Chung, Y.K. *Coord. Chem. Rev.* **1999**, *188*, 297 and leading references therein.

8 (a) Shambayati, S.; Crowe, W.E.; Schreiber, S.L. *Tetrahedron Lett.* **1990**, *31*, 5289. (b) Jeong, N.; Chung, Y.K.; Lee, B.Y.; Lee, S.H.; Yoo, S.-e. *Synlett* **1991**, 204. (c) Sugihara, T.; Yamada, M.; Yamaguchi, M.; Nishizawa, M. *Synlett* **1999**, 771. (d) Sugihara, T.; Yamada, M.;

Ban, H.; Yamaguchi, M.; Kaneko, C. *Angew. Chem., Int. Ed. Engl.* **1997**, *36*, 2801.

9 (a) Iron: Pearson, A.J.; Dubbert, R.A. *J. Chem. Soc., Chem. Commun.* **1991**, 202. (b) Pearson, A.J.; Dubbert, R.A. *Organometallics* **1994**, *13*, 124. (c) Tungsten: Hoye, T.R.; Suriano, J.A. *Organometallics* **1992**, *11*, 2044. (d) Hoye, T.R.; Suriano, J.A. *J. Am. Chem. Soc.* **1993**, *115*, 1154. (e) Molybdenum: Jeong, N.; Lee, S.J.; Lee, B.Y.; Chung, Y.K. *Tetrahedron Lett.* **1993**, *34*, 4027.

10 (a) Rautenstrauch, V.; Megard, P.; Conesa, J.; Kuester, W. *Angew. Chem. Int., Ed. Engl.* **1990**, *29*, 1413. (b) Sugihara, T.; Yamaguchi, M. *Synlett* **1998**, 1384. (c) Lee, N.Y.; Chung, Y.K. *Tetrahedron Lett.* **1996**, *37*, 3145. (d) Rajesh, T.; Periasamy, M. *Tetrahedron Lett.* **1998**, *39*, 117. (e) Jeong, N.; Hwang, S.H.; Lee, Y.; Chung, Y.K. *J. Am. Chem. Soc.* **1994**, *116*, 3159. (f) Lee, B.Y.; Chung, Y.K.; Jeong, N.; Lee, Y.; Hwang, S.H. *J. Am. Chem. Soc.* **1994**, *116*, 8793. (g) Pagenkopf, B.; Livinghouse, T. *J. Am. Chem. Soc.* **1996**, *118*, 2285. (h) Jeong, N.; Hwang, S.H.; Lee, Y. W; Lim, J.S. *J. Am. Chem. Soc.* **1997**, *119*, 10549. (i) Kim, J.W.; Chung, Y.K. *Synthesis* **1998**, 142.

11 With isocyanides: (a) Berk, S.C.; Grossman, R.B.; Buchwald, S.L. *J. Am. Chem. Soc.* **1993**, *115*, 4912. (b) Berk, S.C.; Grossman, R.B.; Buchwald, S.L. *J. Am. Chem. Soc.* **1994**, *116*, 8593. With CO: (c) Hicks, F.A.; Berk, S.C.; Buchwald, S.L. *J. Org. Chem.* **1996**, *61*, 2713. (d) Hicks, F.A.; Kablaoui, N.M.; Buchwald, S.L. *J. Am. Chem Soc.* **1996**, *118*, 9450.

12 (a) Morimoto, T.; Chatani, N.; Fukumoto, Y.; Murai, S. *J. Org. Chem.* **1997**, *62*, 3762. (b) Kondo, T.; Suzuki, N.; Okada, T.; Mitsudo, T. *J. Am. Chem. Soc.* **1997**, *119*, 6187.

13 (a) Koga, Y.; Kobayashi, T.; Narasaka, K. *Chem. Lett.* **1998**, 249. (b) Kobayashi, T.; Koga, Y.; Narasaka, K. *J. Organomet. Chem.* **2001**, *624*, 73. (c) Jeong, N.; Lee, S.; Sung, B.K. *Organometallics* **1998**, *17*, 3642. (d) Jeong, N.; Kim, J.; Kim, M. unpublished results.

14 Krafft, M.E.; Romero, R.H.; Scott, I.L. *J. Org. Chem.* **1992**, *57*, 5277.

15 Perez-Serrano, L.; Casarrubios, L.; Dominguez, G.; Perez-Castells, J. *Chem. Commun.* **2001**, 2602.

16 (a) Ahmar, M.; Chabanis, O.; Gauthier, J.; Cazes, B. *Tetrahedron Lett.* **1997**, *38*, 5277. (b) Ahmar, M.; Antras, F.; Cazes, B. *Tetrahedron Lett.* **1995**, *36*, 4417.

17 (a) Iron: Aumann, R.; Weidenhaupt, H.J. *Chem. Ber.* **1987**, *120*, 23. (b) Titanium: Hicks, F.A.; Kablaoui, N.M.; Buchwald, S.L. *J. Am. Chem. Soc.* **1996**, *118*, 9450. (c) Urabe, H.; Takeda, T.; Hideura, D.; Sato, F. *J. Am. Chem. Soc.* **1997**, *119*, 11295.

18 (a) Kent, J.L.; Wan, H.; Brummond, K.M. *Tetrahedron Lett.* **1995**, *36*, 2407. (b) Brummond, K.M.; Wan, H. *Tetrahedron Lett.* **1998**, *39*, 931. (c) Brummond, K.M.; Wan, H.; Kent, J.L. *J. Org. Chem.* **1998**, *63*, 6535.

19 (a) Brummond, K.M.; Lu, J. *J. Am. Chem. Soc.* **1999**, *121*, 5087. (b) Brummond, K.M.; Lu, J.; Petersen, J.L. *J. Am. Chem. Soc.* **2000**, *122*, 4915.

20 (a) Brummond, K.M.; Chen, H.; Fisher, K.D.; Kerekes, A.D.; Rickards, B.; Sill, P.C.; Geib, S. J. *Org. Lett.* **2002**, *4*, 1931. (b) Mukai, C.; Nomura, I.; Yamanishi, K.; Hanaoka, M. *Org. Lett.* **2002**, *4*, 1755.

21 Ahmar, M.; Locatelli, J.; Colombier, D.; Cazes, B. *Tetrahedron Lett.* **1997**, *38*, 5281.

22 Shibata, T.; Koga, Y.; Narasaka, K. *Bull. Chem. Soc. Jpn.* **1995**, *68*, 911.

23 Koga, Y.; Narasaka, K. *Chem. Lett.* **1999**, 705.

24 (a) Morimoto, T.; Fuji, K.; Tsutsumi, K.; Kakiuchi, K. *J. Am. Chem. Soc.* **2002**, *124*, 3806. (b) Shibata, T.; Toshida, N.; Takagi, K. *Org. Lett.* **2002**, *4*, 1619. (c) Shibata, T.; Toshida, N.; Takagi, K. *J. Org. Chem.* **2002**, *67*, 7446.

25 (a) Hicks, F.A.; Buchwald, S.L. *J. Am. Chem. Soc.* **1996**, *118*, 11688. (b) Hicks, F.A.; Buchwald, S.L. *J. Am. Chem. Soc.* **1999**, *121*, 7026.

26 (a) Hiroi, K.; Watanabe, T.; Kawagishi, R.; Abe, I. *Tetrahedron Lett.* **2000**, *41*, 891. (b) Hiroi, K.; Watanabe, T.; Kawagishi, R.; Abe, I. *Tetrahedron: Asymmetry* **2000**, *11*, 797. (c) Sturla, S.J.; Buchwald, S.L. *J. Org. Chem.* **2002**, *67*, 3398.

27 Shibata, T.; Takagi, K. *J. Am. Chem. Soc.* **2000**, *122*, 9852.

28 Jeong, N.; Sung, B.K.; Choi, Y.K. *J. Am. Chem. Soc.* **2000**, *122*, 6771.

29 Jeong, N.; Seo, S.D.; Shin, J.Y. *J. Am. Chem. Soc.* **2000**, *122*, 10220.

30 (a) Evans, P.A.; Nelson, J.D. *J. Am. Chem. Soc.* **1998**, *120*, 5581. (b) Evans, P.A.; Robinson, J.E.; Nelson, J.D. *J. Am. Chem. Soc.* **1999**, *121*, 6761. (c) Evans, P.A.; Leahy, D.K. *J. Am. Chem. Soc.* **2000**, *122*, 5012. (d) Evans, P.A.; Kennedy, L.J. *Am. Chem. Soc.* **2001**, *123*, 1234.

31 Evans, P.A.; Robinson, J.E. *J. Am. Chem. Soc.* **2001**, *123*, 4609.

32 (a) Yamazaki, H.; Hagihara, N. *J. Organomet. Chem.* **1967**, *7*, C21. (b) Gesing, E.R.F.; Tane, J.–P.; Volhardt, K.P.C. *Angew. Chem., Int. Ed. Engl.* **1980**, *19*, 1023. (c) Halterman, R.L.; Vollhardt, K.P.C. *Organometallics* **1988**, *7*, 883.

33 (a) Pearson, A.J.; Dubbert, R.A. *J. Chem. Soc., Chem. Commun.* **1991**, 202. (b) Pearson, A.J. Jr.; Shively, R.J.; Dubbert, R.A. *Organometallics* **1992**, *11*, 4096. (c) Pearson, A.J. Jr.; Shively, R.J. *Organometallics* **1994**, *13*, 578. (d) Pearson, A.J.; Perosa, A. *Organometallics* **1995**, *14*, 5178. (e) Pearson, A.J.; Yao, X. *Synlett* **1997**, 1281. (f) Knoelker, H.-J.; Heber, J.; Mahler, C.H. *Synlett* **1992**, 1002. (g) Knoelker, H.-J.; Heber, J. *Synlett* **1993**, 924.

34 Mueller, E. *Synthesis* **1974**, 761–774.

35 Baker, M.V.; Brown, D.H.; Skelton, B.W.; White, A.H. *J. Chem. Soc., Dalton Trans.* **2002**, 2595

36 (a) Shibata, T.; Yamashita, K.; Ishida, H.; Takagi, K. *Org. Lett.* **2001**, *3*, 1217. (b) Shibata,T.; Yamashita, K.; Katayama, E.; Takagi, K. *Tetrahedron* **2002**, *58*, 8661.

37 (a) Eaton, B.E.; Rollman, B. *J. Am. Chem. Soc.* **1992**, 114, 6245. (b) Mandai, T.; Tsuji, J.; Tsujiguchi, Y.; Saito, S. *J. Am. Chem. Soc.* **1993**, *115*, 5865. (c) Sigman, M.S.; Eaton, B.E. *J. Am. Chem. Soc.* **1996**, *118*, 11783.

38 (a) Murakami, M.; Itami, K.; Ito, Y. *J. Am. Chem. Soc.* **1996**, *118*, 11672. (b) Murakami, M.; Itami, K.; Ito, Y. *J. Am. Chem. Soc.* **1997**, *119*, 2950. (c) Murakami, M.; Itami, K.; Ito, Y. *J. Am. Chem. Soc.* **1999**, *121*, 4130. (d) Murakami, M.; Itami, K.; Ito Y. *Organometallics* **1999**, *18*, 1326.

12
Rhodium(I)-Catalyzed [4+2] and [4+2+2] Carbocyclizations

John E. Robinson

12.1
Introduction

Transition metal-catalyzed carbocyclization reactions of tethered diene, enyne, diyne, and vinylallene derivatives represent an important class of transformations in synthetic organic chemistry. This may be attributed to the ability to significantly increase molecular complexity through the highly selective combination of acyclic components, thereby facilitating the synthesis of complex polycyclic products. Recently, rhodium-catalyzed carbocyclization reactions have attracted significant attention due to their immense synthetic versatility and the unique selectivities observed over a range of different transformations. This chapter provides an account of recent developments in rhodium-catalyzed [4 + 2] and [4 + 2 + 2] carbocyclization reactions.

12.2
Rhodium(I)-Catalyzed [4 + 2] Carbocyclization Reactions

The ability to construct substituted six-membered rings in a highly selective fashion has made the Diels–Alder reaction one of the most widely studied transformations in organic chemistry [1]. Moreover, the use of Lewis and Brönsted acids, sonication, and transition metal catalysis circumvents "forcing" reaction conditions and minimizes substrate incompatibility issues common to the thermally promoted [4 + 2] annulations, thereby dramatically expanding the synthetic repertoire [1]. The transition metal-catalyzed [4 + 2] reactions generally function by one of two modes: (1) Lewis acid complexation of polarizable groups; (2) direct complexation and activation of the π-bonds of the diene and/or dieneophile [1–3]. Since its inception, a wide range of transition metal complexes have been identified as catalysts for the [4 + 2] reaction; for example, complexes of nickel, titanium, iron, iridium, palladium, and rhodium have been demonstrated [1, 4].

12.2.1
Rhodium(I)-Catalyzed Intermolecular [4 + 2] Carbocyclizations

Matsuda and co-workers described the first intermolecular rhodium-catalyzed [4 + 2] reaction in 1987 [5]. Consistently with the other transition metal catalysts that had been developed for similar systems, the rhodium-catalyzed version was also limited to

Modern Rhodium-Catalyzed Organic Reactions. Edited by P. Andrew Evans

ISBN: 3-527-30683-8

Tab. 12.1 Cyclodimerization of 1,3-dienes and terminal acetylenes [5].

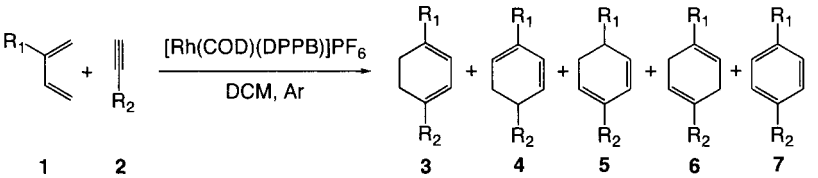

Ratio 1/2	*R_1*	*R_2*	*Time (h)*	*Temp. (°C)*	*Yield (%)*	*Selectivity 3:4:5:6:7*
1.3	Me	Ph	144	41	85	93:0:2:3:2
1	Me	^{n}Pr	43	43	65	94:1:1:3:1
1.4	Me	$^n C_5H_{11}$	145	25	74	88:2:1:4:4
6	Me	$TMSCH_2$	120	25	44	100:0:0:0:0
1.4	CH_2=C(CH_3)(CH_2)$_3$	Ph	168	25	75	78:3:4:7:8
1.3	CH_2=C(CH_3)(CH_2)$_3$	^{n}Pr	72	25	83	89:3:2:4:2
10	H	Ph	144	25	69	40:0:8:42:10
6	H	$^n C_5H_{11}$	144	25	58	8:0:2:78:12

monosubstituted alkynes [4a, 6]. As shown in Tab. 12.1, the cationic rhodium catalyst [Rh(COD)(DPPB)]PF_6 provides the desired product with a high degree of regiocontrol, in good to excellent yield, over a range of substrates.

Chung and co-workers have examined similar systems and have successfully employed a variety of trisubstituted dienes (Eq. 1) [7]. These represent the first examples using both di- and trisubstituted olefins. The addition of three substituents at R_1, R_3, and R_4 (compare Tab. 12.1) allows for the installation of up to five substituents; this had not been previously examined using a rhodium catalyst. This system is also applicable to the corresponding intramolecular reaction, which is discussed later in this chapter (Section 12.2.2).

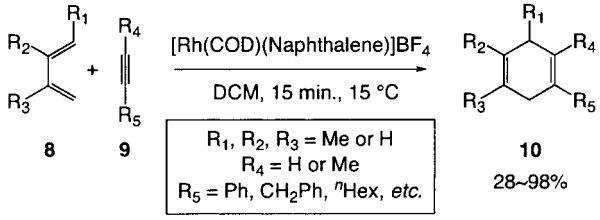

(1)

More recently, Murakami and co-workers have developed a highly regioselective method for the synthesis of substituted benzenes, which employs vinylallene derivatives and monosubstituted alkynes (Eq. 2) [8]. Simple olefins, such as ethylene, are also applicable as dieneophile components, albeit with decreased efficiency (Eq. 3). A mechanistic rationale was presented for the proposed catalytic cycle, which nicely explains the observed regioselectivity (Scheme 12.1). The regiochemical outcome was attributed to steric repulsion between the highly hindered metal center and the alkynyl substituent (**20** versus **18**).

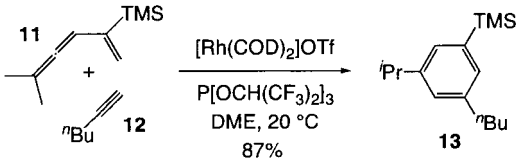

(2)

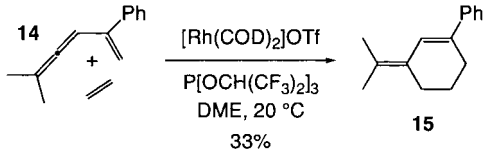

(3)

These catalysts are among the first to exhibit the ability to catalyze the intermolecular [4+2] annulation over a broad range of substrates, requiring neither strongly electron-withdrawing nor donating functionality.

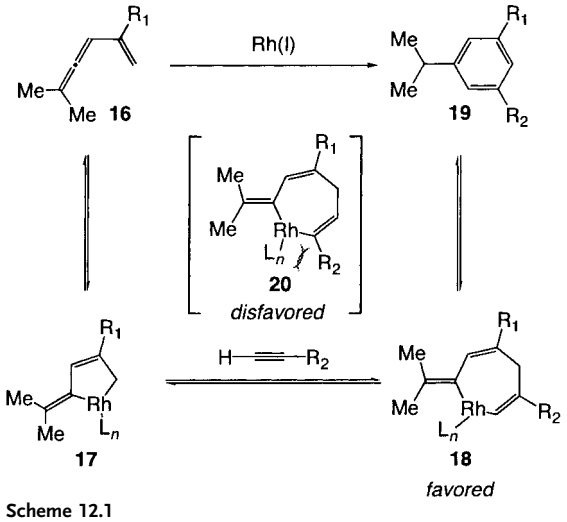

Scheme 12.1

12.2.2

Rhodium(I)-Catalyzed Intramolecular [4+2] Carbocyclizations [9]

The first examples of the intramolecular rhodium-catalyzed [4+2] reactions were developed to address the low reactivity associated with unactivated dienes and dienophiles [10]. Through multiple studies that examined solvent and ligands, Livinghouse and coworkers developed the first set of general conditions (Scheme 12.2). Treatment of the tethered diene **21** with Wilkinson's catalyst furnished the cycloadduct **24** in a highly efficient fashion and as a single diastereoisomer [11]. This reaction is proposed to proceed through initial complexation of the 1,6-dienyne **21**, presumably to afford rhodium complex **I** *en route* to the metallacycle **22** [12], which can then undergo insertion to **23**, followed by reductive elimination to afford the desired product **24**.

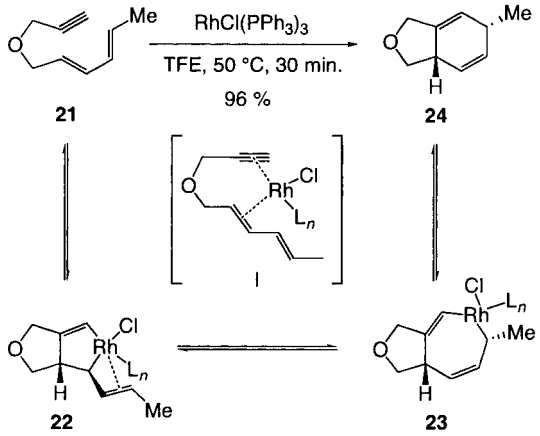

Scheme 12.2

Based on the precedent of Van Leeuwen and Roobeek, Livinghouse and co-workers screened a variety of electron-deficient phosphine/phosphite ligands for the rhodium-catalyzed [4+2] reaction, which provided an alternative catalyst system for the formation of 5,6- and 6,6-ring systems [13]. The most notable of these was the tris-(hexafluoro-2-propyl) phosphite-modified rhodium complex, which was applicable to both carbon- and oxygen-tethered substrates, and also provided the first example of a *facial*-directed diastereoselective intramolecular rhodium-catalyzed [4+2] reaction (Eq. 4).

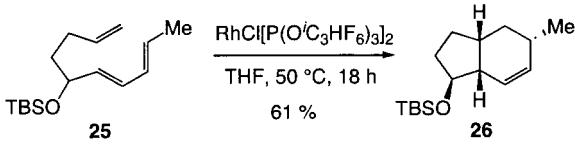

(4)

This catalyst system was the first to utilize both terminal alkynes and olefins in the intramolecular reaction. Although a mechanistic rationale for the observed stereoselectivity was not offered, the formation of the single stereoisomer **26** may be rationalized through the diastereotopic binding of the rhodium complex to the diene moiety (Scheme 12.3). This *facial* selective binding of the initial ene–diene would then lead to the formation the metallacycle **III**, which ultimately isomerizes and reductively eliminates to afford the product [14].

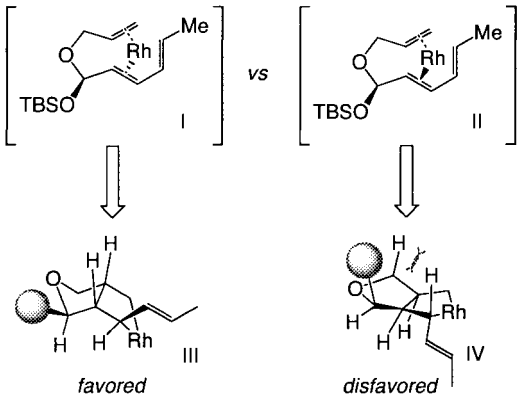

Scheme 12.3

12.2.2.1 **Rhodium(I)-Catalyzed Intramolecular [4+2]: Nonclassical Substrates**

In the ensuing years, the development of the rhodium-catalyzed [4+2] reaction has been directed toward nonclassical substrates, in addition to the problems associated with other transition metal catalyst systems. Wender and co-workers developed one of the first rhodium-catalyzed [4+2] reactions with nonclassical substrates using tethered allene derivatives (Scheme 12.4) [15]. Treatment of **27** (R=CH_2OTBS, X=Me) with catalytic $[Rh(COD)Cl]_2$ and P(O–^{o}BiPh)$_3$ in tetrahydrofuran furnished the 5,6-fused bicycle **30** as a single diastereoisomer, in 90% yield. The high degree of stereoselectivity can again be accounted for through facially selective binding of the initial ene–allene complex **I**, producing a single metallacycle **28**, in which the metal binding of the complex is proposed to occur in the least sterically hindered fashion (away from the face of the bulky R substituent). The olefin can then rotate, whereupon positional isomerization affords **29**, which upon reductive elimination gives **30**. This pathway is mechanistically similar to those proposed for the rhodium-catalyzed enyne cycloisomerization,

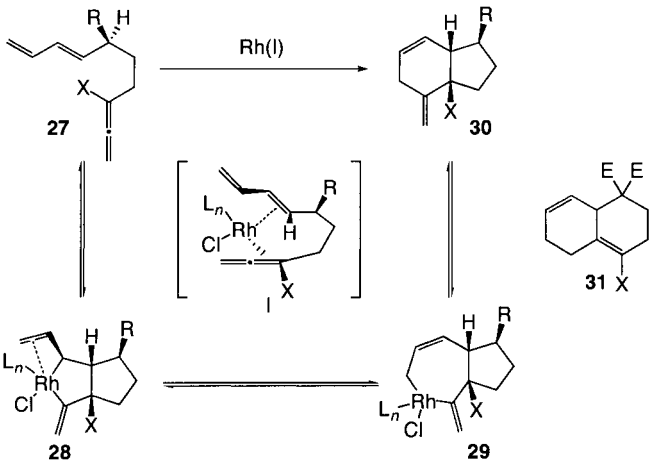

Scheme 12.4

[2+2+1], [2+2+2], [4+1], [5+2], [5+2+1], [6+2], and [4+2+2] methodologies, with similar sterically driven transition states. Moreover, it is consistent with the Magnus/Buchwald model for stereocontrol (first proposed for the Pauson–Khand reaction), as outlined Scheme 12.5 [14]. As the steric bulk of the R substituent is increased, the formation of the observed *cis*-diastereoisomer **30** is enhanced, as a direct result of increased $A^{1,3}$ strain as well as increased steric interactions between the allenic-type protons and the C9 proton in the disfavored transition-state [16]. Additionally, nonbonding and gearing interactions often play a role in this type of diastereocontrol, which is discussed throughout this chapter.

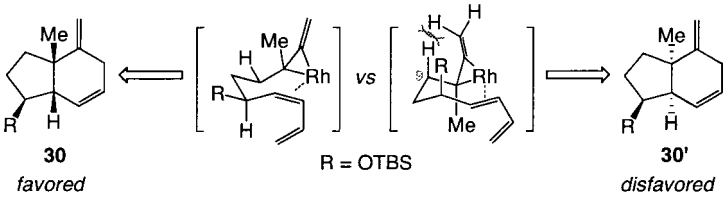

Scheme 12.5 Magnus/Buchwald model for sterically based stereocontrol.

The stereoselective rhodium-catalyzed diene allene [4+2] reaction exhibits chemoselective binding to the internal bond of the allene, which is opposite to that observed in the corresponding nickel-catalyzed [4+2] process [17]. The authors demonstrated that by altering the electronics of the catalyst system, employing tris(hexafluoro-2-propyl) phosphite, selective reaction of the terminal π-system may be achieved to furnish the decalin product **31** in excellent yield, analogous to the nickel-catalyzed version. These are also the first examples of rhodium-catalyzed [4+2] annulations that allow for installation of the quaternary bridgehead methyl substituents. Further, examination of the ability to control ring-fusion stereoselectivity in decalin systems proved that either stereoisomer (**33** versus **33′**) could be formed selectively through judicious choice of catalyst (Scheme 12.6). Again, the opposite chemoselectivity was obtained by changing the catalyst (Eq. 5), thus providing access to 6,7-bicyclic systems, which are uncommon in transition metal-catalyzed carbocyclizations.

These examples of rhodium-catalyzed [4+2] reactions provide the first chemo- and stereoselective carbocyclizations of tethered diene–allenes, through the facial differentiation of the rhodium-complex. This presumably results in the kinetic formation of a preferred metallacycle intermediate, which subsequently undergoes alkene insertion

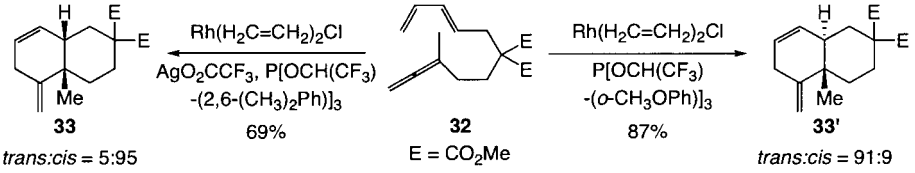

Scheme 12.6 Controlling ring-fusion stereochemistry.

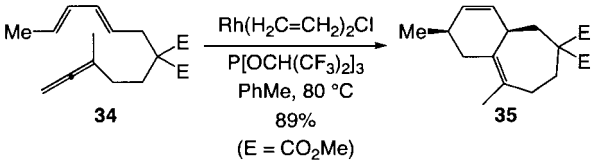

(5)

and reductive elimination in a highly efficient fashion. Additionally, the use of a coordinatively unsaturated rhodium species was implemented for the first time, thereby enabling a complete reversal in ring-fusion stereoselectivity.

12.2.3
Diastereoselective Rhodium(I)-Catalyzed Intramolecular [4+2]: Counter-Ion Effect

Livinghouse and co-workers undertook a more in-depth investigation into the counterion dependence of facially directed stereocontrol [18]. As summarized in Tab. 12.2, the standard reaction conditions using $[Rh(COE)_2Cl]_2$ and tris(hexafluoro-2-propyl) phosphite produced a highly selective transformation (*ds*=18.9:1). Nonetheless, optimum selectivity was obtained using the $SnCl_3$ anion, albeit requiring increased reaction time. In additional experiments other coordinatively unsaturated species were also examined, but they were less selective. A marked difference in the rate of reaction as well as in stereocontrol was noted between the triflate and hexafluoroantimonate examples, which is somewhat contrary to previous reports of the relative unimportance of the counterion in other cationic rhodium-catalyzed reactions [19, 20]. A second substitution pattern was also examined (Scheme 12.7), for which the catalyst produced a 2:1 mixture of the desired (**41**) and undesired product (**40**). This is in sharp contrast to the coordinatively unsaturated catalyst, which proceeded efficiently to the exclusive formation of **41**. The formation of **40**, though undesired, has significant mechanistic implications. It is proposed that initial coordination of the rhodium complex to the triene moiety produces the five-membered metallacycle intermediate **I**, which may either re-

Tab. 12.2 Effects of counterions on diastereoselectivity.

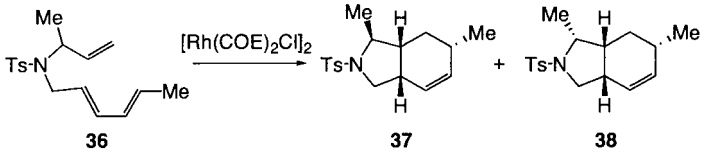

36 **37** **38**

Anion (X)	*Ligand (Ln)*	*Solvent*	*Temp. (°C)*	*Time (h)*	*Yield (%)*	*ds (37:38)*
Cl	$((F_3C)_2CHO)_3P)_2$	THF	55	6.5	90	18.9:1
Br	$((F_3C)_2CHO)_3P)_2$	THF	55	5	96	23.5:1
I	$((F_3C)_2CHO)_3P)_2$	THF	55	4.5	96	16.8:1
$SnCl_3$	$((F_3C)_2CHO)_3P)_2$	THF	55	24	93	31.2:1
OTf	$(PPh_3)_3$	PhMe	80	7	86	7.2:1
SbF_6	$(PPh_3)_3$	PhMe	80	2.5	80	4.3:1

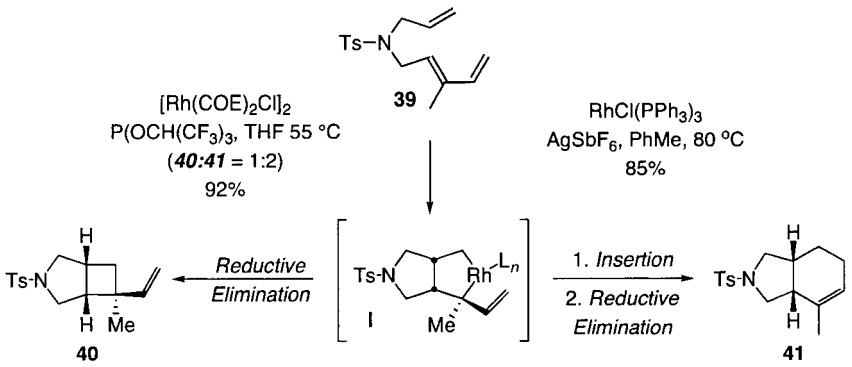

Scheme 12.7 Catalyst control of product distributions/mechanistic implications.

ductively eliminate to afford **40**, or undergo a subsequent insertion followed by reductive elimination to produce **41**. Interestingly, the AgOTf-catalyzed reaction produces a mixture of bridgehead diastereoisomers, presumably due to the decreased rate of the reaction making the thermal version competitive; the thermal reaction is known to afford the *trans*-diastereoisomer preferentially. The significance of the formation of **40** is that it provides indirect evidence for the formation of the metallacycle **I**.

Nearly simultaneously, Gilbertson and Hoge reported similar findings utilizing an alternative catalyst system, $[Rh(DIPHOS)(CH_2Cl_2)_2]SbF_6$ [21, 22]. As illustrated in Tab. 12.3, this catalyst system is generally applicable to both carbon- and oxygen-tethered systems **42**, with the exception of the reaction carried out in acetone, which favors the conjugated product (entry 2). One of the major advantages of this catalyst system is the ability to employ less forcing conditions, while significantly increasing the reaction scope with the addition of oxygen-tethered substrates [23]. Additionally, the diene–ene variant **44** was investigated (Eq. 6).

Tab. 12.3 Intramolecular cyclization of dienyne fragments.

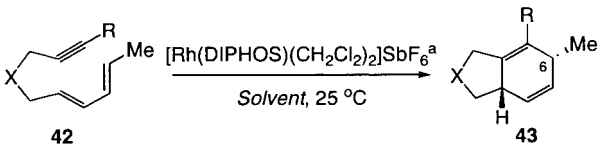

Entry	*X*	*R*	*Solvent*	*Yield (%)*
1	O	H	DCM	75
2	O	TMS	acetone	80 [b]
3	O	TMS	DCM	76
4	$(CO_2Et)_2C$	H	DCM	75
5	O	Et	DCM	65
6	O	H	DCM	41

a) The active catalyst was generated through treatment of the parent complex $[Rh(DIPHOS)(NBD)]SbF_6$ with H_2 in DCM.

b) The conjugated diene product was formed preferentially, resulting in the loss of the C6 stereocenter.

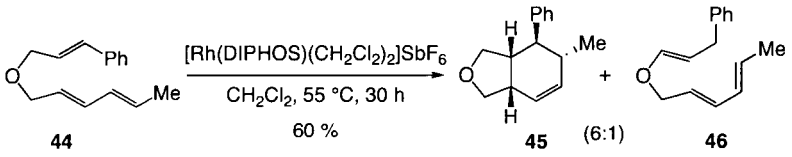

44 45 (6:1) 46 (6)

As previously mentioned, Chung and co-workers have also developed a highly efficient coordinatively unsaturated catalyst system, which has general applicability to multiple heteroatom tethers (Scheme 12.8) [7]. This was the first example of a single rhodium catalyst system capable of facilitating [4+2] annulations for all three of the most common tethers (O, N, and C), including some intermolecular examples.

This was followed by a report from the Zhang group, which provides the most comprehensive study of both steric and electronic factors associated with a variety of lig-

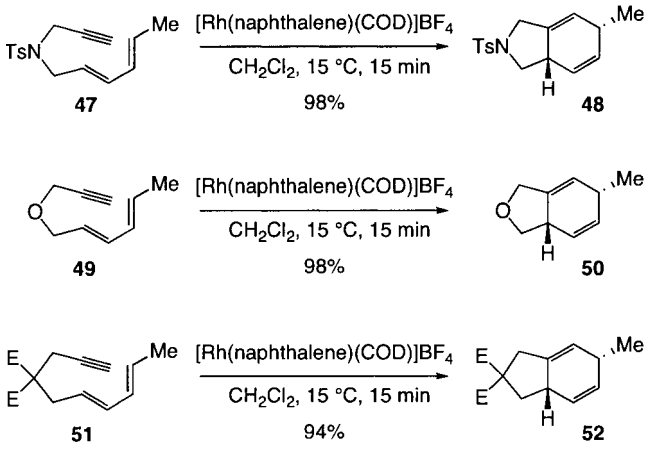

Scheme 12.8

Tab. 12.4 Expanded scope of the intramolecular [4+2] reaction.

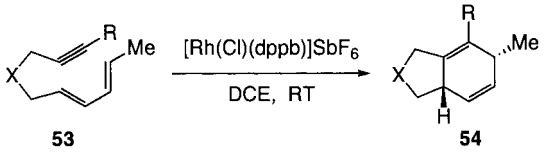

53 54

Entry	*X*	*R*	*Time*	*Yield (%)*
1	$PhSO_2N$	CH_3	1 h	95
2	$(CO_2Me)_2C$	"	3 h	99
3	O	"	10 min	90
4	O	H	10 min	75
5	O	Et	10 min	89
6	O	Ph	10 min	99
7	O	TMS	2 h	96

ands for the rhodium-catalyzed [4+2] carbocyclization reaction [24]. As illustrated in Tab. 12.4, this catalyst system is extremely robust, and can easily accommodate carbon, oxygen, and nitrogen tethers, in addition to a variety of substituents at the alkyne terminus. This was the first example of a catalyst that exhibits broad tether and alkyne substitution in the rhodium-catalyzed [4+2] reaction

12.2.4
Asymmetric Induction in Intramolecular Rhodium(I)-Catalyzed [4+2] Reactions

The enantioselective version was examined utilizing both diene–ene and diene–yne ether-tethered moieties, which probed the steric and electronic effects of various substituted bridging bidentate DIOP ligands. Additionally, the "bite angle" influence was investigated through modification of the 2-position of the 1,3-dioxolane ring [25]. These studies demonstrated that simple electronic effects alone could not be attributed to deviations in the asymmetric induction, as exemplified by comparison of the electron-deficient *bis*-3,5-(trifluoromethyl)phenylphosphine-modified ligand with DIOP. The highest degree of enantioselectivity for the diene–ene system was obtained with a terminally substituted olefin (Eq. 7), which was attributed to enhance steric differentiation. Alternatively, this substrate did not undergo cyclization with increasingly bulky ligands, suggesting that achieving a high degree of asymmetric induction may be ligand/substrate-dependent. The diene–yne systems were also examined, in which C_2-hindered DIOP-based ligands afforded the optimal enantioselectivity (Eq. 8).

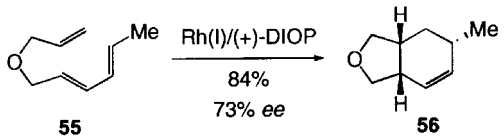

(7)

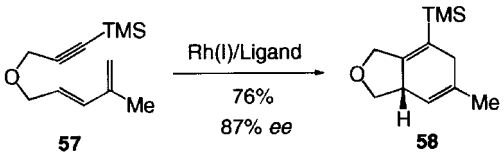

(8)

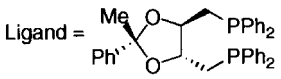

Gilbertson and co-workers conducted additional studies geared toward the asymmetric reaction with diene–ene and diene–ynes [26]. This examination revealed a catalyst system, $[Rh(ligand)(solvent)_2]SbF_6$, which was initially optimized for the corresponding diastereoselective transformation [21], and proved highly effective for the enantioselective version (Eqs. 9 and 10).

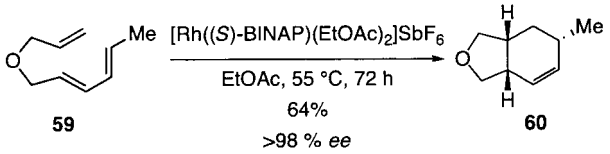

(9)

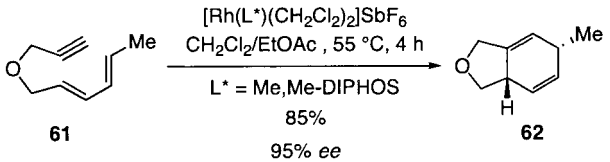

(10)

Moreover, the carbon-tethered derivative also proved applicable to the optimized reaction conditions (Eq. 11), which afforded the desired bicycle in a highly selective fashion. Hence, this improved catalyst system exhibits some degree of universal applicability [27].

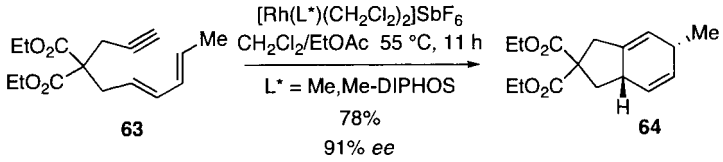

(11)

12.2.4.1 **Influence of Counter-Ion on Enantiosoelectivity**

Livinghouse also examined the effect of various counter-ions on enantioselectivity [18]. As illustrated in Tab. 12.5, both coordinatively saturated and cationic rhodium species are capable of effecting a highly selective and efficient transformation of **65** to **66**. The advan-

Tab. 12.5 Effects of counter-ions on enantioselectivity.

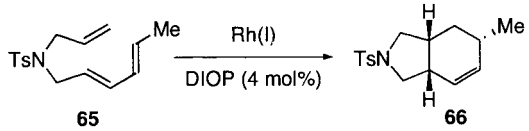

Anion (X)	*Additive*	*Solvent*	*Time (h)*	*Yield (%)*	*ee (%)*
Cl	none	DCE/TFE (1:1)	2	97	76
Br [a)]	none	DCE/TFE (1:1)	4	76	77
Br [a)]	none	DCE/TFE (1:1)	4	86	79
I	NaI	DCE/TFE (1:1)	4	trace	–
$SnCl_3$	$SnCl_2$	DCE/TFE (1:1)	4	trace	–
OTf	AgOTf	DCE/TFE (1:1)	2	84	61
SbF_6 [b)]	$AgSbF_6$	DCE (40 °C)	5	70	66
SbF_6 [c)]	H_2	DCE (40 °C)	45	96	68

a) $[Rh(COE)_2Br]_2$ (2 mol%).
b) $[Rh(COE)_2Cl]_2$ (1 mol%).
c) [Rh((+)-DIOP)(NBD)][SbF_6] (2 mol%).

tages of the coordinatively unsaturated rhodium complexes are that the reaction may be conducted at decreased temperature, and the use of polar solvents is avoided, albeit with slightly lower enantioselectivity. Livinghouse suggests that the increased reactivity of the hexafluoroantimonate catalyst system may be useful for highly substituted diene-containing substrates, as the coordinatively unsaturated species are less sensitive than the halogen-containing catalyst to olefin substitution. Combined, these catalyst systems allow for efficient carbocyclizations over a range of differentially substituted derivatives, with modest enantioselectivity.

12.3 Rhodium(I)-Catalyzed [4+2+2] Carbocyclization Reactions

12.3.1 Synthesis of Cyclooctanoids

The difficulty associated with the construction of eight-membered rings, coupled with their ubiquity in numerous diverse natural products, has prompted the development of a variety of methods for their construction [28, 29]. Since the introduction of the first transition metal-mediated synthesis of a cyclooctanoid by Wilke and co-workers in 1969 [30], many advances have been made to overcome the unfavorable entropic and enthalpic factors associated with the synthesis of medium rings [31b]. The most widely utilized of these methods is the intermolecular [4+4] cycloisomerization reaction, in which acyclic dienes undergo formal cycloaddition to afford eight-membered rings. Unfortunately, limitations associated with both regio- and diastereoselectivity when using unsymmetrical (nonequivalent) dienes severely limits the synthetic applicability of this method. Moreover, as many of the precursors used in the intramolecular variation of this reaction are synthetically challenging, the applicability of this method has not been widely adopted. Thus, alternative methods for the efficient and stereoselective construction of cyclooctanoids would be significant.

12.3.2 Rhodium(I)-Catalyzed Carbocyclization Reactions

Recently rhodium-catalyzed intramolecular annulation reactions have attracted significant attention due to their aforementioned synthetic versatility and selectivity. Other chapters within this book are dedicated to some of these milestones, which include the enyne cycloisomerization as well as [4+1], [4+2], [5+2], [5+2+1], and [6+2] carbocyclization reactions. The rhodium-catalyzed carbocyclizations of diene, enyne, and vinylallene derivatives for the synthesis of octanoid ring-systems presented herein are representative of the synthetic diversity of rhodium catalysis in the preparation of highly substituted mono- and bicyclic systems. Furthermore, it is rather intriguing that each of these transformations is related through the proposed intermediacy of a five-membered metallacycle. Hence, the selective formation of this metallacycle presents a common theme for understanding the origin of the selectivity in annulation reactions of this type, and provided the inspiration for the development of the rhodium-catalyzed [4+2+2] carbocyclization reaction. Although a few examples of both inter- and intramolecular [4+4] and [4+2+2] carbocyclization reactions are known, these have been

largely limited to nickel-, iron- and cobalt-catalyzed reactions [31–35]. To date, there have been two independently, yet simultaneously, developed rhodium-catalyzed [4+2+2] reactions. Both of these approaches are based on the highly selective and versatile nature of rhodium catalysis.

12.3.3
Development of the Rhodium(I)-Catalyzed [4+2+2] Carbocyclization Reactions

Gilbertson and co-workers developed a rhodium-catalyzed [4+2+2] carbocyclization reaction based on key observations and mechanistic insight gained during the pursuit of an asymmetric version of the rhodium-catalyzed [4+2] reaction [36]. In certain examples of the [4+2] reaction an additional equivalent of the starting substrate **67** was incorporated to yield a mixture of the [4+2] product **68** and dimer **69** (Eq. 12). It was this observation that provided the impetus to fully develop of the undesired side reaction into a selective method for the construction of eight-membered rings. Following extensive studies, it was found that the optimum catalyst for selective dimerization was $AgSbF_6$-modified $[Rh(NBD)Cl]_2$, using Me-DuPhOS as the ligand. As illustrated in Tab. 12.6, a highly regioselective crossed dimerization was obtained for multiple heteroatom-tethered dienyne synthons, yielding the desired cyclooctanoids in an efficient manner. Additionally, all the products were isolated as single diastereoisomers, by analogy with the proposed rationale described for the [4+2] reactions (entries 1 and 3). Interestingly, the dimerization using a nonsubstituted terminal dienynes (entry 2) produced a mixture of regioisomers, while formation of the corresponding [6.4.0] system was highly regioselective (entry 4).

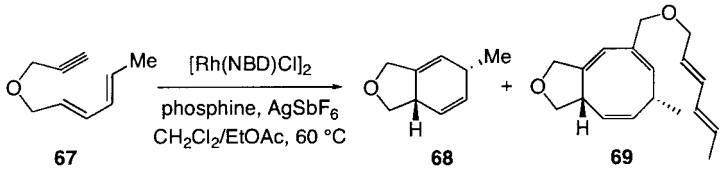

(12)

While the selective dimerization of dienynes is a significant step in fundamental advancement of this methodology with respect to the construction of medium rings, a truly practical method would possess the ability to selectively introduce other substituted alkynes. This was achieved as outlined in Tab. 12.7, using an excess of an external alkyne (5 equiv) to facilitate a highly regio- and diastereoselective cyclization (entries 1–4, 6, and 7). These examples exhibit broad substrate compatibility over both oxygen- and nitrogen-tethered systems. Furthermore, the ability to selectively introduce a range of protected propargyl alcohol derivatives, as well as simple alkyl- and heteroatom-substituted alkynes, is a considerable contribution in the synthesis of substituted cyclooctanoid systems.

Gilbertson and co-workers were also able to facilitate the rhodium-catalyzed [4+2+2] carbocyclization reaction with a substrate having an all-carbon tether (Eq. 13). This methodology has been extended to the asymmetric rhodium-catalyzed [4+2+2] reaction (Eq. 14). Although the exact origin of asymmetric induction was not discussed, the ability to accomplish the asymmetric rhodium-catalyzed [4+2+2] reaction provides a novel approach to eight-membered ring systems.

Tab. 12.6 Selective dimerization. [a)]

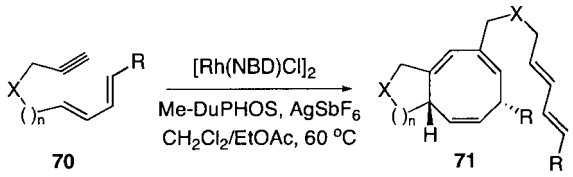

Entry	*Diene–yne*	*Yield (%)* [c)]	*Product*
1 [a)]	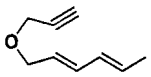	80	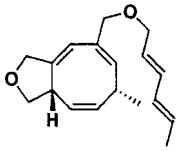
2 [a, d)]	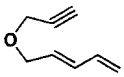	44	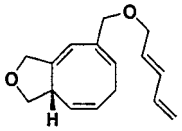
3 [b)]	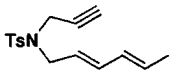	72	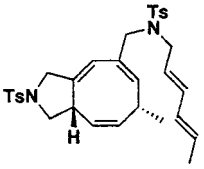
4 [b)]	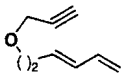	58	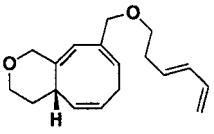

a) The catalyst was generated from a ratio of 1:2:1 of $[Rh(NBD)Cl]_2$/Me-DuPhos/$AgSbF_6$ and run in a 6:1 ratio of CH_2Cl_2/EtOAc. The reaction was run at RT for approximately 12 h.
b) The reaction was run at 60 °C for approximately 12 h.
c) Products isolated as single diastereoisomers.
d) A 1.5:1 mixture of regioisomers was obtained.

Tab. 12.7 [4+2+2] Cyclization with incorporation of a second alkyne.

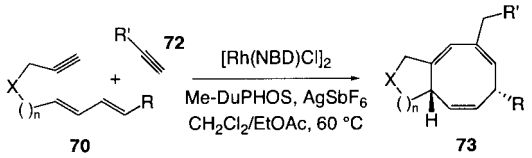

Entry	*Diene–yne*	*Alkyne*[b]	*Yield (%)*	*Product*
1[a]	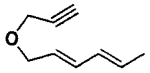	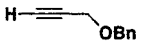	73[c]	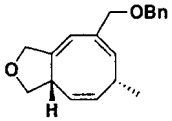
2[a]	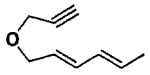	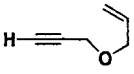	36[c]	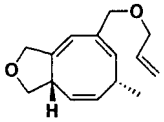
3[a]	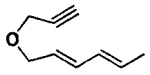	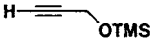	63[c]	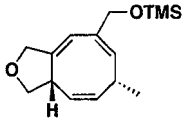
4[a]	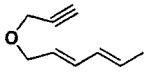	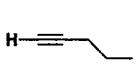	41[c]	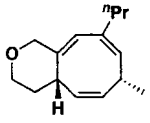
5[a,d]	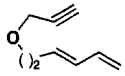	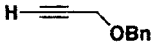	55	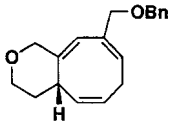
6[a]	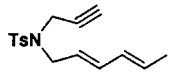	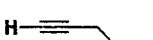	70[c]	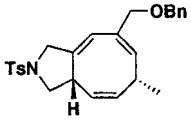
7[a]	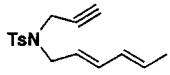	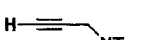	49[c]	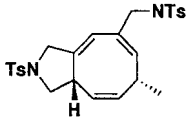
8[a,e]	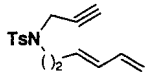	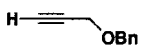	69	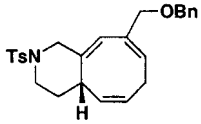

a) The catalyst was generated from a ratio of 1:2:1 of $[Rh(NBD)Cl]_2$/Me-DuPhos/$AgSbF_6$ and run in a 6:1 ratio of CH_2Cl_2:EtOAc. Reaction was run at 60 °C for approximately 12 h.
b) Reactions were run using 5 equiv alkyne.
c) Products isolated as single diastereoisomers.
d) A 2.9:1 mixture of regioisomers was obtained.
e) A 1.6:1 mixture of regioisomers was obtained.

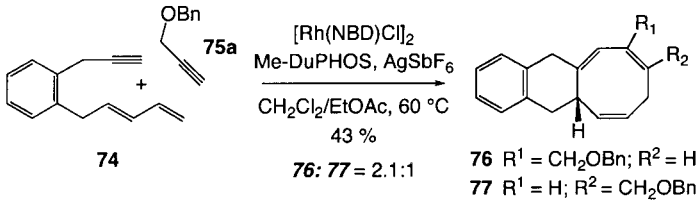

(13)

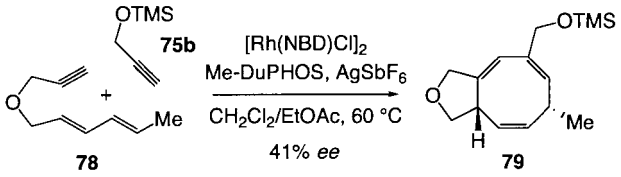

(14)

Evans and co-workers simultaneously developed of the rhodium-catalyzed [4+2+2] carbocyclization reaction through the identification of a novel mode of reactivity for the five-membered metallacycle intermediate [14, 37]. Evans proposed that 1,3 dienes should be amenable to addition to this intermediate, which would provide a new reaction pathway. The tethered enyne **80** (Scheme 12.9), was expected to afford the metallacycle **I**, which, upon sequential incorporation of a butadiene and reductive elimination, would afford the desired 5,8-fused product **81**. Additionally it was rationalized that this transformation should be highly diastereoselective, as outlined in Scheme 12.10. Treatment of the heteroatom-tethered enyne **I** under standard carbocyclization (Pauson–

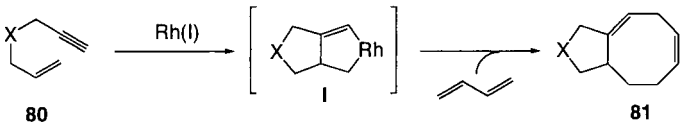

Scheme 12.9

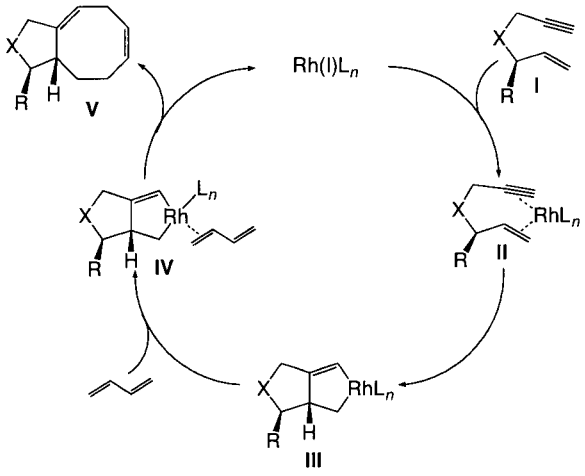

Scheme 12.10 Proposed catalytic cycle of the [4+2+2] carbocyclization reaction.

Tab. 12.8 Optimization of the rhodium-catalyzed [4+2+2] reaction [39].

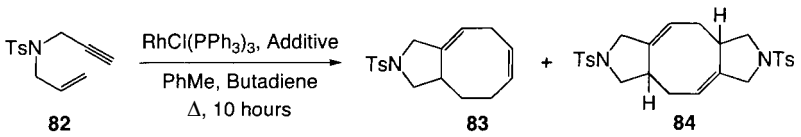

82 83 84

Entry[a]	*Additive*	*(83:84)*	*Yield (%)*		*Butadiene oligomers [mg] (COD)*[b]	*Yield (%) [2+2+2]*[c]
			83[b]	*84*[c]		
1	none	1:8	7	57	0 (0)	13
2	AgOTf	28:1	85	3	1.8 (4)	3
3	$AgBF_4$	11:1	74	7	5.6(0)	0
4	$AgPF_6$	2:1	49	27	14.7(2)	0
5	$AgSbF_6$	1:44	2	89	13.5(6)	0

a) All reactions were run using 10% catalyst, with 20 mol% silver salt as co-catalyst in each example, 0.1 M in touene.
b) GLC yield.
c) HPLC yield of [2+2+2] product.

Khand/[4+2]/[5+2]) conditions should facilitate the diastereoselective formation of the metallacycle **III**. Coordination of the diene **IV**, followed by migratory insertion and reductive elimination, should produce the preferred diastereoisomer **V**. The advantage of this system was the ability to significantly increase molecular complexity through the introduction of various rings and stereogenic centers using readily available fragments. Furthermore, it was rationalized that the significant electronic differences between the diene and enyne components would make it possible to completely suppress the undesired dimerization and oligomerization reactions.

Initial attempts at carbocyclization of the enyne **82** with Wilkinson's catalyst under an atmosphere of 1,3-butadiene in refluxing toluene furnished only trace amounts of product, which was attributed to the preference for the enyne to undergo homodimerization in a highly stereoselective manner (Tab. 12.8, entry 1; *ds* 19:1) [38]. Nonetheless, the coordinatively unsaturated (AgOTf-modified) catalyst furnished the [4+2+2] product in excellent yield (entry 2). The ability to alter the product distribution in this manner prompted further examination of various other silver salts.

As outlined in Tab. 12.8 (entries 2–5), additives that favor the formation of butadiene oligomers also produce a significant amount of the undesired enyne heterodimer product **84** (entries 4 and 5). This may be attributed to the increased rate of oligomerization of butadiene versus cross-coupling, thereby reducing the effective concentration of butadiene. This is consistent with the findings of Brookhart and co-workers, who demonstrated selective oligomerization of butadiene using similar catalyst systems [40]. Additionally, Wilkinson's catalyst is known to perform quite poorly for butadiene oligomerization, suggesting that such catalysts may proceed *via* alternative mechanisms to form **84**.

The understanding of the reactivity made possible the development of the rhodium-catalyzed [4+2+2] carbocyclization reaction as outlined in Tab. 12.9. This study demonstrated that nitrogen-, sulfur-, and oxygen-tethered enynes furnish the desired cycload-

Tab. 12.9 Scope of the intermolecular rhodium-catalyzed [4+2+2] carbocyclization reaction.

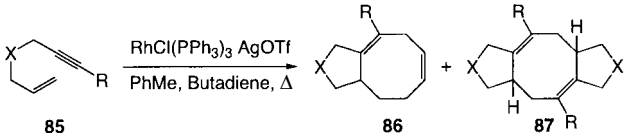

Entry[a]	*X*	*R*	*Product*	*Ratio of 86:87*[b]	*Yield of 86 (%)*[c]
1	TsN	H	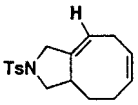	≥19:1	91
2	TsN	Me	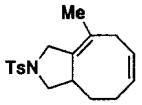	≥19:1	91
3	TsN	Ph	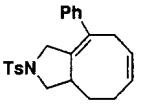	≥19:1	87
4	SO_2	H	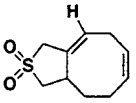	≥19:1	79
5	SO_2	Me	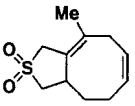	≥19:1	73
6	SO_2	Ph	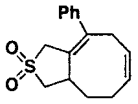	≥19:1	87
7	O	H	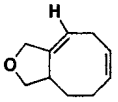	≥19:1	71
8	O	Me	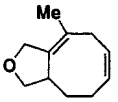	≥19:1	81
9	O	Ph	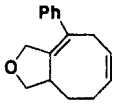	≥19:1	92

a) All reactions were carried out on a 0.5 mmol reaction scale using 10 mol% of Wilkinson's catalyst [$Rh(PPh_3)_3Cl$], modified with 20 mol% AgOTf, in toluene under an atmosphere of 1,3-butadiene.

b) Ratios of hetero- and homo-cycloadducts were determined by 400 MHz ^1H NMR with the exception of entry 1 (26:1 by crude GLC/HPLC).

c) Isolated yields.

ducts in excellent yield, with analogous selectivity. This reaction is tolerant of alkyl, aryl, and unsubstituted alkynes, producing only trace amounts of enyne cycloisomerization and olefin isomerization products. Additionally, the sulfones (entries 4–7) represent the first examples of this type of functionality used in a metal-catalyzed carbocyclization reaction [41]. Despite numerous attempts to facilitate carbocyclizations with a variety of geminally disubstituted and unsubstituted carbon derivatives, these reactions were largely unsuccessful, producing mainly the enyne cycloisomerization products [42].

12.3.4
Sequential Rhodium(I)-Catalyzed Allylic Substitution/[4 + 2 + 2] Carbocyclization

Based on previous success in the Pauson–Khand reaction [43], Evans demonstrated a sequential approach to the synthesis of eight-membered rings, which involved a rhodium-catalyzed allylic amination reaction followed by carbocyclization, to effect a three-component coupling (Scheme 12.11). To date, this transformation is only the second example of a sequential rhodium-catalyzed reaction in which only temperature is used to modulate catalytic activity.

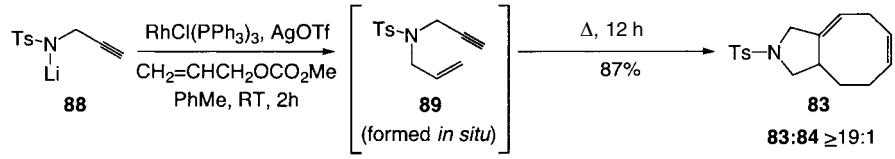

Scheme 12.11

12.3.5
Diastereoselective Rhodium-Catalyzed [4 + 2 + 2] Carbocyclization

Evans and co-workers were also successful in extending this methodology to the diastereoselective rhodium-catalyzed [4+2+2] reaction, which probed the influence of a C2-substituted tethered enyne (Eq. 15). Treatment of the substituted enyne **90**, under optimized conditions, furnished the 5,8-bicyclic product **91** in a highly efficient and diastereoselective manner. The observed stereoselectivity is in strong agreement with the selective formation of a single metallacycle intermediate as originally outlined.

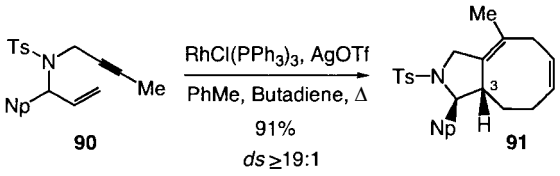

(15)

12.3.6 Conclusion

Recent advances in the rhodium-catalyzed [4+2] reactions have led to the development of the first highly regioselective intermolecular cyclization, providing access to new classes of carbocycles with both activated and unactivated substrates. The chemo- and stereoselective carbocyclizations of tethered diene-allene derivatives afford new classes of 5,6- and 6,6-bicyclic systems. Additionally, examination of a wide range of factors that influence both diastereo- and enantioselectivity has provided a significant advance in the understanding of catalyst requirements across these systems.

Evans and Gilbertson have developed the first intermolecular rhodium-catalyzed [4+2+2] carbocyclization reactions. The use of various tethered enynes with 1,3-butadiene, in addition to the dieneyne/alkyne version of this method, allows for exploration of multiple synthetic routes in the construction of eight-membered rings. These studies demonstrate that excellent selectivity can be obtained for the formation of either the homo- or crossed cycloadducts, through the judicious choice of additive, catalyst complex, and reaction stoichiometry. The asymmetric variant is also an impressive and significant development, as this represents the first example of asymmetric induction in the rhodium-catalyzed [4+2+2] carbocyclization reaction. The ability to accomplish a three-component annulation provides a versatile method for the construction of 5,8-systems, which circumvents the synthesis of enyne tether prior to cycloaddition. The high degree of stereoselectivity obtained in either variant should also provide an immensely powerful method for stereoselective construction of octanoid intermediates for target-directed synthesis.

12.4 References

1 For general reviews of the Diels–Alder Reaction see: (a) Lautens, M.; Klute, W.; Tam, W. *Chem. Rev.* **1996**, *96*, 49. (b) Danishefsky, S. *Aldrichimica Acta* **1986**, *19*, 59. (c) Oppolzer, W. *Comprehensive Organic Synthesis*; Trost, B.M., Fleming, I., Paquette, L.A., Eds. Pergamon: Oxford, **1991**; Vol. 5, p. 315. (c) Kagan, H.B.; Riant, O. *Chem. Rev.* **1992**, *92*, 1007. (d) Pindur, U.; Lutz, G.; Otto, C. *Chem. Rev.* **1993**, *93*, 741 and pertinent references therein.

2 For a detailed discussion of the various modes of complexation, as well as additional methods developed for the Diels–Alder reactions see ref. 1(a) and pertinent references therein.

3 Garratt, P.J.; Wyatt, M. *J. Chem. Soc., Chem. Commun.* **1974**, 251.

4 For lead references see: (a) Iron: Carbonaro, A.; Greco, A.; Dall'Asta, G. *J. Org. Chem.* **1968**, *33*, 3948. (b) Nickel: see ref. 3; Wender, P.A.; Jenkins, T.E. *J. Am. Chem. Soc.* **1989**, *111*, 6432. (c) Matsuda, I.; Shibata, M.; Sato, S.; Izumi, Y. *Tetrahedron Lett.* **1987**, *28*, 3361. (d) Pd: Grenouillet, P.; Neibecker, D.; Tkatchenko, I. *J. Chem. Soc., Chem. Commun.* **1983**, 542. (e) Ti: March, K.; Antropiusova, H.; Petrusova, L.; Turecek, F.; Hanus, V. *J. Organomet. Chem.* **1985**, *289*, 331 and pertinent references therein.

5 Matsuda, I.; Shibata, M.; Sato, S.; Izumi, Y. *Tetrahedron Lett.* **1987**, *28*, 3361.

6 (a) Genet, J.P.; Ficini, J. *Tetrahedron Lett.* **1979**, 1499. (b) Dieck, H.T.; Diercks, R. *Angew. Chem., Int. Ed. Engl.* **1983**, *22*, 778.

7 Paik, S.-J.; Son, S.U.; Chung, Y.K. *Org. Lett.* **1999**, *1*, 2045.

8 For a complete list of examples see: Murakami, M.; Ubukata, M.; Itami, K.; Ito, Y. *Angew. Chem., Int. Ed. Engl.* **1998**, *37*, 2248.

9 Jolly, R.S.; Luedtke, G.; Sheehan, D.; Livinghouse, T. *J. Am. Chem. Soc.* **1990**, *112*, 4965.

10 The first and only intramolecular transition metal-catalyzed reaction developed prior to this discovery was Ni(0)-catalyzed: Wender, P.A.; Jenkins, T.E. *J. Am. Chem. Soc.* **1989**, *111*, 6432.

11 The observed stereoselectivity matches that of the corresponding thermal reaction, for which only 20% product was observed after heating to 120 °C for 3 days. Additionally, simple acid catalyst effects were ruled out by exposing the starting ether (**21**) to 0.1 equiv HCl over 1 h under optimized reaction conditions, in the absence of rhodium catalyst. Under these conditions the starting material was recovered unchanged.

12 This intermediate is also often depicted as an η^3-type intermediate.

13 Pronounced rate and selectivity enhancements had previously been observed for Ni(0)-catalyzed cyclodimerizations as well as rhodium-catalyzed alkene hydroformylation reactions. For related references see: (Ni) van Leeuwen, P.W.N.M.; Roobeek, C.F. *Tetrahedron* **1981**, *37*, 1973. (Rh) van Leeuwen, P.W.N.M.; Roobeek, C.F. *J. Organomet. Chem.* **1983**, *258*, 343.

14 For a complete and detailed discussion see John.E. Robinson, Ph.D. thesis, University of Delaware, Newark, Delaware 19713, or "Recent advances in Rh-catalyzed carbocyclization reactions" John E. Robinson, *http://www.chem.wayne.edu/acs-organic-division/fellowships.html*.

15 Wender, P.A.; Jenkins, T.E.; Suzuki, S. *J. Am. Chem. Soc.* **1995**, *117*, 1843.

16 There are numerous examples of rhodacycle–propene type intermediates in the literature, suggesting that the modified Magnus–Buchwald type of transition state may be quite feasible. For lead references see: (a) Buckner, S.W.; Freiser, B.S. *Polyhedron* **1989**, *8*, 1401. (b) Chen, Y.-M.; Armentrout, P.B. *J. Am. Chem. Soc.* **1995**, *117*, 9291. (c) Tolbert, M.A.; Mandich, M.L.; Halle, L.F.; Beauchamp, J.L. *J. Am. Chem. Soc.* **86**, *108*, 5675 and references cited therein.

17 (a) Jolly, P.W.; Wilke, G. *The Organic Chemistry of Nickel*. Academic Press: New York, **1975**; Vol. 2, pp. 117–132. (b) Otsuka, S.; Nakamura, A. *Adv. Organomet. Chem.* **1976**, *14*, 245.

18 O'Mahony, D.J.R.; Belanger, D.R.; Livinghouse, T. *Synlett* **1998**, 443.

19 (a) RajanBabu, T.V.; Ayers, T.A.; Halliday, G.A.; You, K.K.; Calabrese, J.C. *J. Org. Chem.* **1997**, *62*, 6012. (b) Burk, M.J.; Feaster, J.E.; Nugent, W.A.; Harlow, R.L. *J. Am. Chem. Soc.* **1993**, *115*, 10 125.

20 Barnhart, R.W.; McMorran, D.A.; Bosnich, B. *Chem. Commun.* **1997**, 589.

21 Gilbertson, S.R.; Hoge, G.S. *Tetrahedron Lett.* **1998**, *39*, 2075.

22 This general strategy of activating the rhodium(I) complex through hydrogenation of the dialkene complex was previously utilized by Bosnich and co-workers to enhance the rate of hydroacylation in the corresponding rhodium(I)-catalyzed transformation. For lead references see ref. 15 and pertinent references therein.

23 This catalyst system was also applied to the [5+2] carbocyclization reactions, discussed at length in Chapter 13 of this book.

24 Wang, B.; Cao, P.; Zhang, X. *Tetrahedron Lett.* **2000**, *41*, 8041.

25 Livinghouse, T.; McKinstry, L. *Tetrahedron* **1994**, *50*, 6145.

26 Gilbertson, S.R.; Hoge, G.S.; Genov, D.G. *J. Org. Chem.* **1998**, *63*, 10077.

27 Livinghouse and co-workers report a similar carbocyclization, using a dimethyl malonate diene–ene derivative, in which they obtained 6% *ee* (69%) with a highly sterically hindered DIOP-based ligand (ref. 25). The unaltered DIOP ligand was also highly efficient (83%), but imparted poor enantiocontrol (10% *ee*).

28 To date there are more than 100 cyclooctanoid-containing natural products. For a lead reference concerning this statistic, see: Petasis, N.A.; Patane, M.A. *Tetrahedron* **1992**, *48*, 5757.

29 For recent review of metal-mediated synthesis of cyclooctanoids see: (a) Sieburth, S.McN.; Cunard, T. *Tetrahedron* **1996**, *52*, 6251. (b) Mehta, G.; Singh, V. *Chem. Rev.* **1999**, *99*, 881. (c) Yet, L. *Chem. Rev.* **2000**, *100*, 2963.

30 Brenner, W.; Heimbach, P.; Hey, H.; Mueller, E.W.; Wilke, G. *Justus Liebigs Ann. Chem.* **1969**, *727*, 161.

31 For lead references concerning the [4+4] intermolecular cyclizations see: (a) Jolly, P.W.; Wilke, G. in *The Organic Chemistry of Nickel*, Vol. 2. Academic Press, New York, **1975**. (b) Jolly, P.W., Tkatchenko, I., Wilke, G. *Angew. Chem., Int. Ed. Engl.* **1971**, *10*, 329. (c) Bogdanovic, B.; Heimbach, P.; Kröner, M.; Wilke, G.; Hoffmann, E.G.; Brandt, J. *Justus Liebigs Ann. Chem.* **1969**, *727*, 143.

32 Other transition metal complexes also catalyzed the dimerization of simple butadiene type substrates. For related examples see: (a) Bosch, M.; Brookhart, M.S.; Ilg, K.; Werner, H. *Angew. Chem., Int. Ed. Engl.* **2000**, *39*, 2304. (b) Itoh, K.; Masuda, K.; Fukahori, T.; Nakano, K.; Aoki, K.; Nagashima, H. *Organometallics* **1994**, *13*, 1020 and references cited therein.

33 For lead references on intramolecular [4+4] cyclization reactions see: (a) Wender, P.A.; Ihle, N.C. *J. Am. Chem. Soc.* **1986**, *108*, 4678. (b) Wender, P.A.; Snapper, M.L. *Tetrahedron Lett.* **1987**, *28*, 2221. (c) Wender, P.A.; Tebbe, M.J. *Synthesis* **1991**, *12*, 1089. (d) Wender, P.A.; Ihle, N.C.; Correia, C.R. *J. Am. Chem. Soc.* **1988**, *110*, 5904.

34 For lead references pertaining to iron- and cobalt-catalyzed [4+2+2] intermolecular cyclizations see: (a) Greco, A.; Carbonaro, A.; Dall'Asta, G. *J. Org. Chem.* **1970**, *35*, 271. (b) Carbonaro, A.; Cambisi, F.; Dall'Asta, G. *J. Org. Chem.* **1971**, *36*, 1443. (c) Lyons, J.E.; Myers, H.K.; Schneider, A. *Ann. N.Y. Acad. Sci.* **1980**, *333*, 273. (d) Lautens, M.; Tam, W.; Sood, C. *J. Org. Chem.* **1993**, *58*, 4513 and references cited therein.

35 For the cobalt-catalyzed [4+2+2] intramolecular cyclization see: Lautens, M.; Tam, W.; Lautens, J.C.; Edwards, L.G.; Crudden, C.M.; Smith, A.C. *J. Am. Chem. Soc.* **1995**, *117*, 6863.

36 Gilbertson, S.R.; DeBoef, B. *J. Am. Chem. Soc.* **2002**, *124*, 8784.

37 Evans, P.A.; Robinson, J.E.; Baum, E.W.; Fazal, A.N. *J. Am. Chem. Soc.* **2002**, *124*, 8782.

38 Attempts to assign the relative configuration of the homodimer were complicated due to the extreme instability of the compound. Additionally, due to the increased reactivity of this substrate for homodimerization, there was no noticeable concentration effect between 0.1 and 0.0626 M.

39 The following [2+2+2] product was isolated as a single regioisomer:

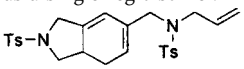

40 Bosch, M.; Brookhart, M.S.; Ilg, K.; Werner, H. *Angew. Chem., Int. Ed. Engl.* **2000**, *39*, 2304.

41 For the related use of a temporary sulfur tether in Pauson–Khand reactions see: Castro, J.; Moyano, A.; Pericas, M.A.; Riera, A. *J. Org. Chem.* **1998**, *63*, 3346.

42 The dimethyl malonate-tethered (R=H) enyne was the single example of a carbon-tethered enyne that did produce the desired product in trace amounts, albeit the isomerized product:

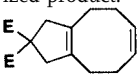

43 Evans, P.A.; Robinson, J.E. *J. Am. Chem. Soc.* **2001**, *123*, 4609.

13
Rhodium(I)-Catalyzed [5+2], [6+2], and [5+2+1] Cycloadditions: New Reactions for Organic Synthesis

Paul A. Wender, Gabriel G. Gamber, and Travis J. Williams

13.1
Introduction

Organic synthesis has played a major role in the advancement of modern science and technology by enabling the preparation of natural and designed targets of chemical, biological, medicinal, environmental, and materials importance [1]. This progress and its continuation toward products of even greater value are unique consequences of the design or discovery and development of fundamentally new reactions. New reactions give rise to new synthetic strategies, which in turn allow for more step-economical, if not ideal, approaches to molecules of interest [2]. The synthesis of silphinene (Scheme 13.1) illustrates how a target, requiring typically ten to twenty steps, can be prepared in only three steps based on a new strategy inspired by a new reaction, the arene–alkene cycloaddition [3]. New reactions also enable more rapid and efficient access to known and, more importantly, structurally novel chemical libraries. New reactions can also provide benefits in safety, cost, time, resource utilization, and environmental impact, while simultaneously introducing new mechanisms and opportunities for achieving synthetic selectivity (chemo-, regio-, stereo-, and enantioselectivity).

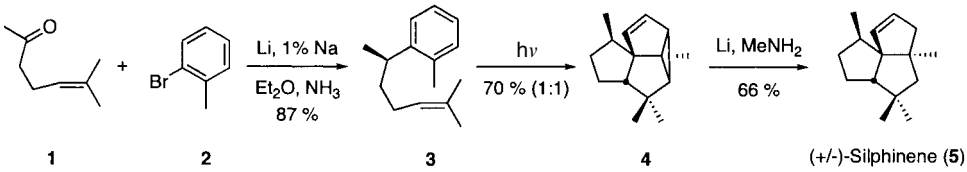

Scheme 13.1 New reactions and step economy: a three-step total synthesis of silphinene.

Among the classes of new reactions, cycloadditions are of unique value for increasing molecular complexity and thereby achieving step brevity [4]. They allow for the assembly of complex ring systems in a convergent and often selective fashion, generally from simple, readily available building blocks. The Diels–Alder cycloaddition (Scheme 13.2) [5] is illustrative of the enormous utility of such reactions in synthesis, providing a cycloadduct with up to four stereogenic centers in one step. This process has figured prominently in the synthesis of six-membered ring systems found in a wide array of molecules of theoretical, medicinal, and materials value.

Modern Rhodium-Catalyzed Organic Reactions. Edited by P. Andrew Evans

ISBN: 3-527-30683-8

Scheme 13.2 The Diels–Alder reaction: convergency and complexity increase to favor step economy.

Some time ago, prompted by the growing number of structurally novel targets with profound biological activities that incorporate seven- or eight-membered rings (Scheme 13.3) and the limited number of cycloaddition processes for their assembly, we initiated a program directed at the design and development of new reactions for the synthesis of medium-sized ring systems. A special emphasis was placed on the catalysis of reactions that in the absence of a catalyst would be difficult or impossible to achieve [6], a research strategy that favors the production of fundamentally new ways of thinking about synthetic problems.

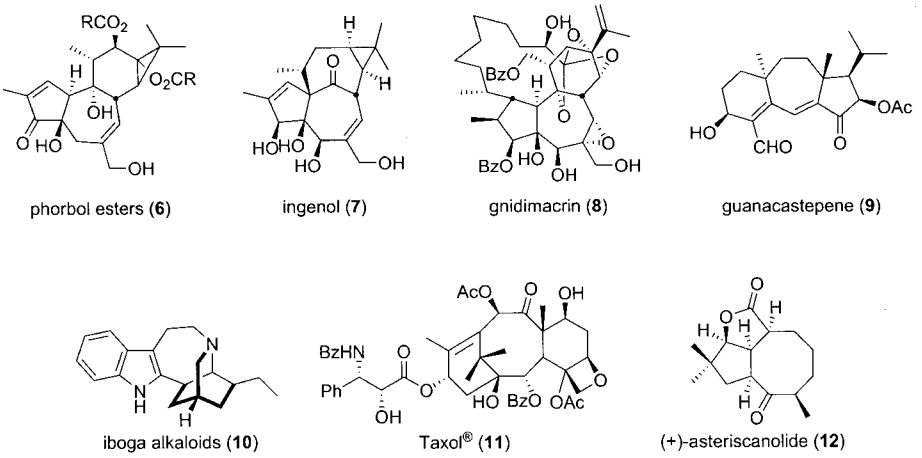

Scheme 13.3 Representative natural products incorporating medium-sized rings.

Our initial studies focused on the transition metal-catalyzed [4+4] cycloaddition reactions of bis-dienes. These reactions are thermally forbidden, but occur photochemically in some specific, constrained systems. While the transition metal-catalyzed intermolecular [4+4] cycloaddition of simple dienes is industrially important [7], this process generally does not work well with more complex substituted dienes and had not been explored intramolecularly. In the first studies on the intramolecular metal-catalyzed [4+4] cycloaddition, the reaction was found to proceed with high regio-, stereo-, and facial selectivity. The synthesis of (+)-asteriscanolide (**12**) (Scheme 13.4a) [8] is illustrative of the utility and step economy of this reaction. Recognition of the broader utility of adding dienes across π-systems (not just across other dienes) led to further studies on the use of transition metal catalysts to facilitate otherwise difficult Diels–Alder reactions [9]. For example, the attempted thermal cycloaddition of diene-yne **15** leads only

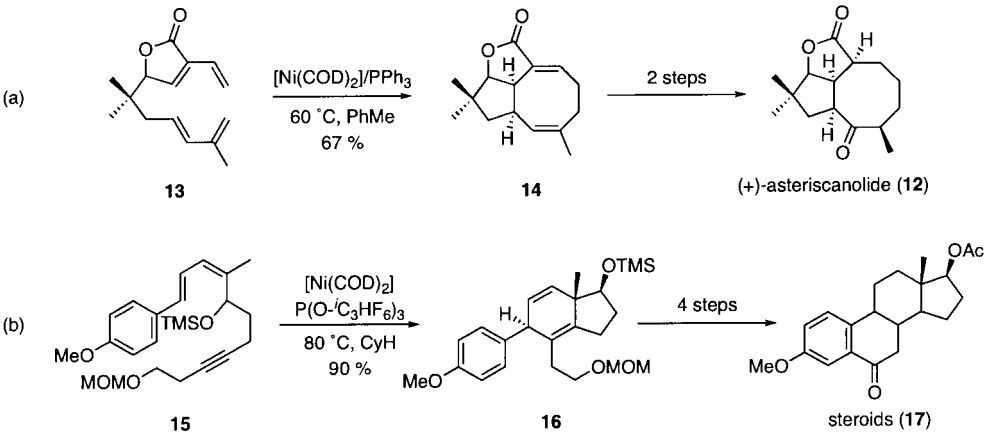

Scheme 13.4 Metal catalysis enables forbidden or difficult noncatalyzed reactions: [4+4] and [4+2] reactions of dienes.

to decomposition at 175 °C, but in the presence of a nickel(0) catalyst, the multi-step [4+2] cycloaddition proceeds at 80 °C and in 90% yield.

In this chapter we provide an overview of studies originating from the above work and directed at the design and development of three new metal-catalyzed cycloaddition reactions, namely the [5+2] cycloaddition of vinylcyclopropanes (VCPs) and π-systems, the [6+2] cycloaddition of vinylcyclobutanones and π-systems, and the three-component, [5+2+1] cycloaddition of VCPs, π-systems, and CO. These new reactions provide fundamentally new approaches to a range of problems in seven- and eight-membered ring synthesis.

13.2
Cycloaddition Approaches to Seven-Membered Rings

Thermal cycloaddition approaches to seven-membered rings [10] are principally limited to isoelectronic variants of the Diels–Alder cycloaddition. Thermal [4_π+2_π] cycloadditions involving allyl cations as 2π components in [4+3] cycloadditions (Scheme 13.5 a) [11] or pentadienyl cations as 4π components in [5+2] cycloadditions of oxidopyrylium zwitterions (Scheme 13.5 b) [12] have been developed into powerful methodologies for the construction of seven-membered rings and have been applied successfully to the syntheses of complex natural products. VCPs have been used formally as (2_π+2_σ) homodienes in thermal cycloadditions with dieneophiles (Scheme 13.5 c) [13], although mechanistically it is likely that these reactions proceed through initial ring opening to zwitterionic intermediates followed by dipolar cycloaddition. Due in part to the formidable activation barrier for the thermal opening of simple VCPs (~50 kcal/mol) [14], these processes have thus far been limited to heteroatom-activated VCPs that are constrained in bicyclic networks, such as homofurans and homopyrroles.

Complementing these purely thermal processes, transition metal-catalyzed reactions have also been used for the synthesis of seven-membered rings. For example, palla-

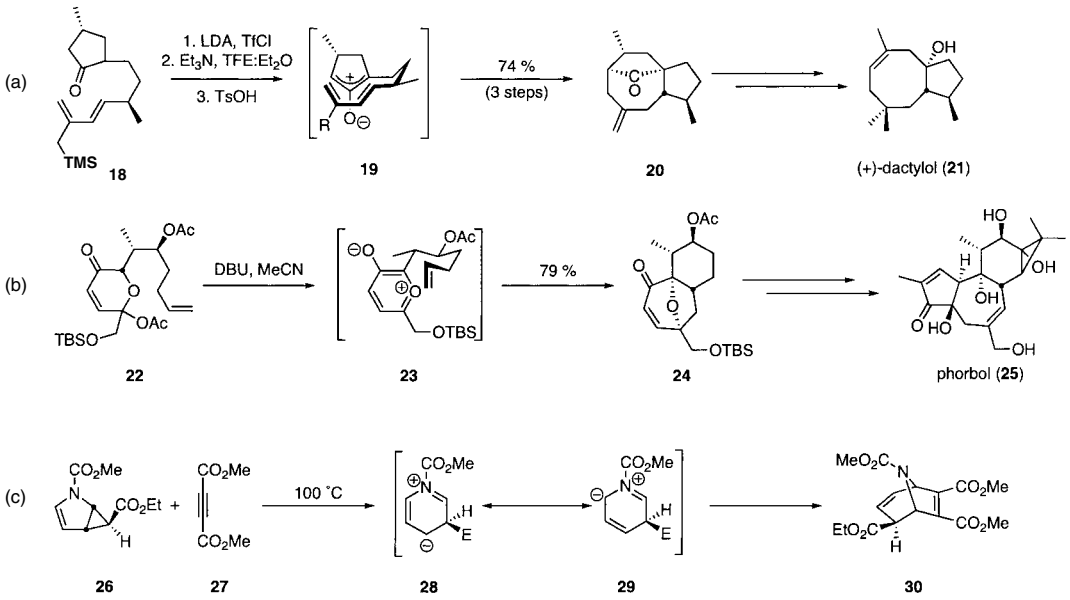

Scheme 13.5 Representative thermal cycloadditions for seven-membered ring synthesis.

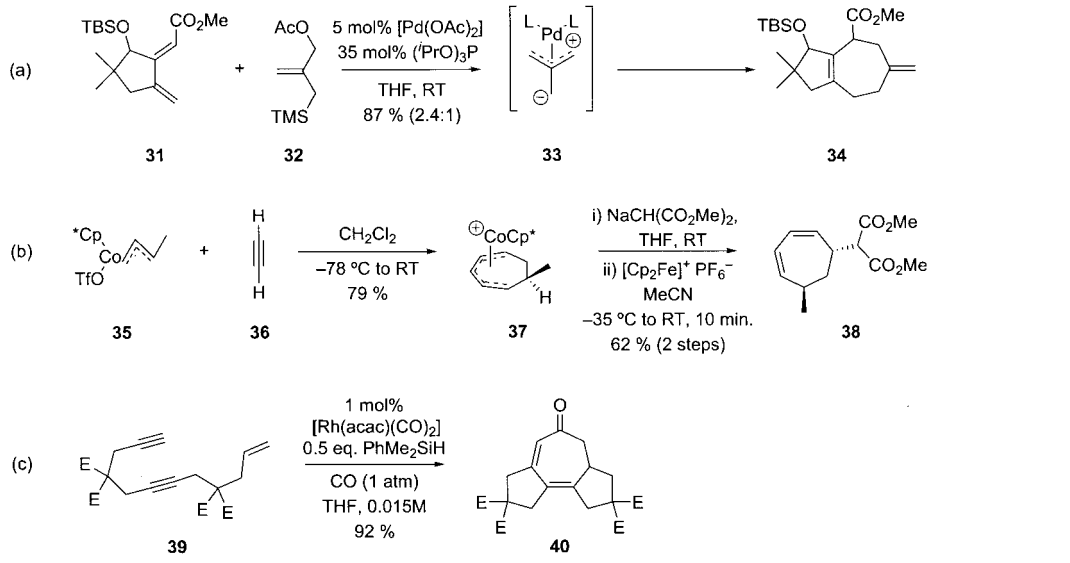

Scheme 13.6 Representative transition metal-mediated cycloadditions for seven-membered ring synthesis.

dium trimethylenemethane (TMM) complexes have been shown to react with constrained dienes in a [4+3] cycloaddition process (Scheme 13.6a) [15]. In a mechanistically intriguing process, stoichiometric iridium and cobalt π-allyl complexes have been used to form seven-membered rings through multi-component [3+2+2] cycloadditions (Scheme 13.6b) [16]. Rhodium(I) catalysts have been used in silylcarbocyclization (SiCaC) cascades of tethered 1-ene-6,11-diyne substrates in a formal [2+2+2+1] reaction (Scheme 13.6c) [17]. Section 13.3 provides an overview of another transition metal-catalyzed process, the [5+2] cycloaddition of VCPs and π-systems, which has been proven to be a robust, general, and efficient process for the synthesis of seven-membered rings.

13.3
Design of a Transition Metal-Catalyzed [5+2] Cycloaddition of Vinylcyclopropanes and π-Systems

The Diels–Alder reaction is an excellent model for the design of new reactions for the synthesis of medium-sized rings. In looking at a seven-membered ring as a homolog of a six-membered ring, it follows that the use of a homolog of either the diene or dienophile components of a Diels–Alder [4+2] cycloaddition could lead to a new reaction for seven-membered ring synthesis. Based on this analogy, the 5 C VCP system was selected as a homolog of a 4 C diene in our initial design of a transition metal-catalyzed approach to seven-membered rings (Scheme 13.7), as it is kinetically stable, provides a handle for metal coordination, and contains ring strain to drive C–C bond cleavage when activated.

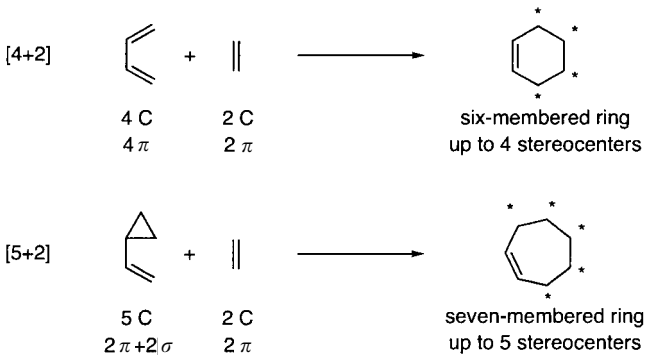

Scheme 13.7 The [5+2] cycloaddition: a conceptual homolog of the Diels–Alder reaction.

Drawing on our experiences with cycloaddition reactions of dienes, we set out to determine if a VCP could be used as a diene homolog in a fundamentally new approach to seven-membered ring synthesis. VCPs have been shown to undergo transition metal-mediated, strain-driven ring cleavage [18]. For example, various transition metals, including rhodium(I), catalyze the isomerization of VCPs to dienes and cyclopentenes (Scheme 13.8) [19]. These reactions probably proceed through initial coordination of the VCP, followed by reversible ring opening to a metallacyclohexene (**41** → **43**). Upon

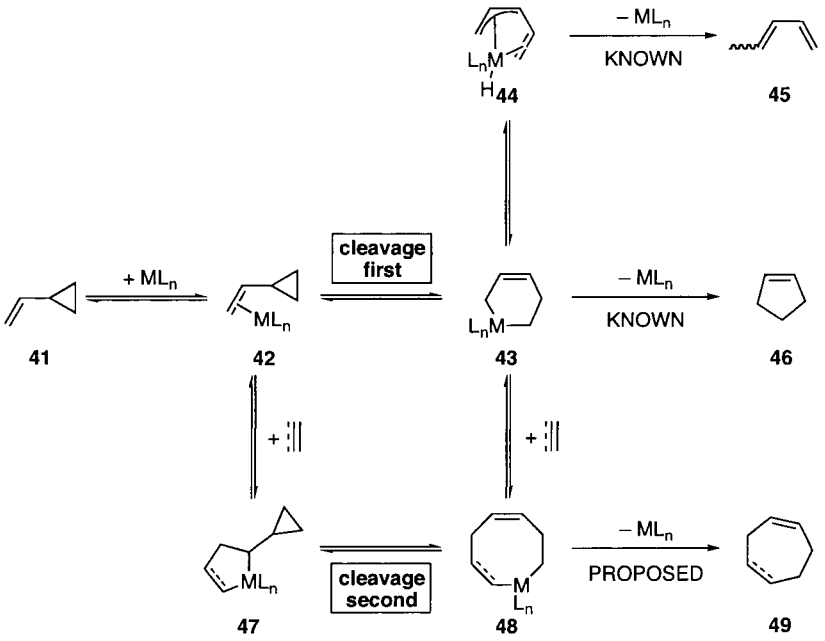

Scheme 13.8 Metal-catalyzed VCP isomerization and the design of a new reaction.

hydride transfer (**43** → **45**) or reductive elimination (**43** → **46**), this metallacycle produces a diene **45**, a cyclopentene **46**, or the starting VCP **41**. We reasoned that capture of intermediates of these reactions with suitable π-systems could produce a new [5+2] cycloaddition reaction (**41** → **49**).

Two possible mechanistic pathways for the [5+2] process arise from the above analysis. These differ only in the order of the bond formation and cyclopropane cleavage steps. If cleavage of the cyclopropane occurs first after initial VCP coordination, metallacyclohexene **43** would be formed (Scheme 13.8, "cleavage first"). Capture of this metallacycle with a 2π component would lead to ring-expanded metallacyclooctene **48**. Subsequent reductive elimination would produce a seven-membered ring **49**. It is also possible that coupling of the coordinated VCP **42** with a 2π-component proceeds first, to form metallacyclopentane **47**, followed by strain-driven cleavage of the adjacent cyclopropane by the carbon–metal bond (Scheme 13.8, "cleavage second"). This form of carbon–carbon bond activation has been observed in studies by Liebeskind, in which a cyclopropane-substituted rhodacycle **51** undergoes carbon–carbon bond cleavage to gen-

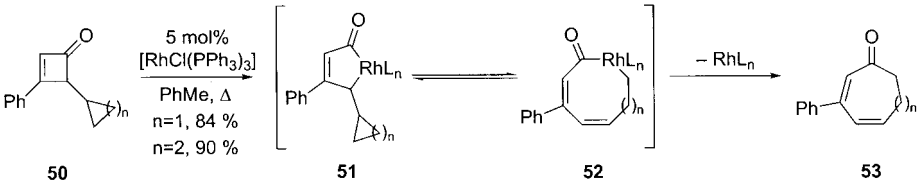

Scheme 13.9 Strain-driven cleavage of metal carbinyl cyclopropanes.

erate rhodacyclooctadiene **52**, from which a seven-membered ring **53** is obtained by reductive elimination (Scheme 13.9) [20]. The "cleavage second" mechanism leads to the same metallacyclooctene **48** as the "cleavage first" mechanism.

Other mechanistic possibilities also exist for the [5+2] cycloaddition reaction and cannot be ruled out at this point. In addition to the stepwise pathways depicted in Scheme 13.8, it is also possible that coordination of the 2π-component to **42** could lead directly to **48** through simultaneous insertion and cleavage. Variations on these events, such as direct insertion into the cyclopropane to form a metallacyclobutane, are also possible.

13.4 Intramolecular [5+2] Cycloadditions of VCPs

13.4.1 Reactions with Alkynes

The first examples of metal-mediated [5+2] cycloadditions between VCPs and tethered alkynes were reported in 1995 (Tab. 13.1) [21]. Initial success was obtained by treating alkyne-VCP **54** with Wilkinson's catalyst ([RhCl(PPh$_3$)$_3$]) in refluxing toluene for 48 h to produce cycloadduct **55** in 84% yield. Further investigations led to the development

Tab. 13.1 [5+2] cycloadditions of tethered alkyne-VCPs.

Entry	*Substrate*	*Catalyst* [a]	*Conditions* [b]	*Cycloadduct*	*Yield (%)*
1	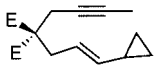 **54**	10 mol% [Rh]	110 °C, 48 h	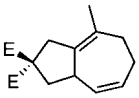 **55**	84
2		0.5 mol% [Rh]/ AgOTf	0.23 M, 110 °C, 20 min		83
3	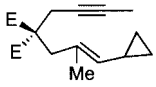 **56**	10 mol% [Rh]/ AgOTf	110 °C, 30 min	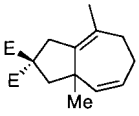 **57**	82
4	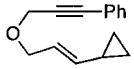 **58**	10 mol% [Rh]	110 °C, 90 min	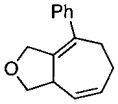 **59**	80
5	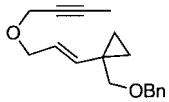 **60**	5 mol% [Rh]	0.01 M, 110 °C, 60 min	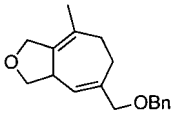 **61**	90

a) [Rh] = [RhCl(PPh$_3$)$_3$].
b) Concentrations refer to substrate concentration in toluene. E = CO_2Me.

of several reaction conditions that could facilitate this transformation. A solvent study found that replacing the nonpolar solvent toluene with the polar, protic solvent 2,2,2-trifluoroethanol (TFE) provided significant rate acceleration as well as an increased overall yield. This acceleration was attributed to the increased solvent polarity of TFE, which would favor dissociation of the chloride ligand, thereby opening a coordination site on the catalyst. Consistently with this view, an even more dramatic accelerating effect was achieved through the addition of silver triflate (1:1 mole ratio to rhodium), which precipitates silver chloride, leaving behind the weakly coordinating triflate counterion. In toluene at 110 °C, the reaction time was reduced from two days to just 45 min through the use of silver triflate. Most notably, these reactions are remarkably efficient and general, even allowing for the formation of quaternary centers (Tab. 13.1, entry 3). A wide range of alkyne substituents is acceptable, including –H, $–CO_2R$, –TMS, –alkyl, and –aryl groups. Cyclopropane substitution is also tolerated (entries 4 and 5) and will be discussed further in Section 13.4.5.

13.4.2
Reactions With Alkenes

Wilkinson's catalyst with silver triflate as an additive was also found to affect the [5+2] cycloaddition of tethered alkene-VCPs [22]. Investigations began with substrate **62** (Tab. 13.2). Treatment of this compound with a catalyst prepared from 0.1 mol% each of $[RhCl(PPh_3)_3]$ and silver triflate gives cycloadduct **63** in 86–90% isolated yield. Importantly, the *cis*-fused cycloadduct is the *single* diastereomer formed in the [5+2] reaction, which is consistent with the intermediacy of a metallabicyclo[3.3.0]octane. This reaction is equally effective on milligram to gram scales, and is expected to be suitable for even larger-scale reactions. In this context, it is noteworthy that the cycloaddition proceeds efficiently even at substrate concentrations of up to 5 M, in which case the solvent/substrate volume ratio is approximately 1:1. At concentrations above 5 M, yields are reduced due to competing oligomerization reactions. The reaction can also be effected in the absence of silver triflate, although such conditions generally require longer reaction times. Substitution of the VCP substrate is generally well tolerated [23]. Moreover, asymmetric induction has been achieved when the metal is modified by a chiral ligand. Initial results show that moderate enantioselectivity can be attained with the (–)-chiraphos ligand (Tab. 13.2, entry 2). More recent unpublished results have produced enantioselectivities of up to 99% [24].

13.4.3
Reactions with Allenes

In contrast to the efficient reactions illustrated above, the use of 1,2-disubstituted alkenes as the 2π-components in the [5+2] cycloaddition has resulted, thus far, in low cycloadduct yields and complex mixtures, putatively arising from an intermediate metallacycle through competitive β-hydride elimination. This limits access to the carbocyclic cores of some large and medicinally interesting natural product families (for example, those in Scheme 13.3). Introduction of an allene substrate, however, circumvents this limitation by installing the needed carbon–carbon bond while simultaneously leaving a handle for further functionalization (Scheme 13.10). For example, reduction of the *exo*-

Tab. 13.2 [5+2] cycloadditions of tethered alkene-VCPs.

Entry	*Substrate*	*Catalyst, solvent*	*Conditions*[b]	*Cycloadduct*	*Yield (%)*
1	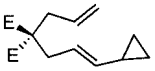 **62**	0.1 mol% [Rh][a]/ AgOTf	1.0 M, 110 °C, 15 h	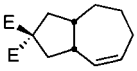 **63**	90
2		5 mol% $[Rh(CH_2{=}CH_2)_2Cl]_2$, 10 mol% AgOTf, 11 mol% (–)-chiraphos	0.001 M, 90 °C		80 63% *ee*
3	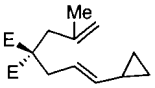 **64**	10 mol% [Rh][a]/ AgOTf	0.01 M, 110 °C, 1 h	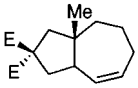 **65**	94
4	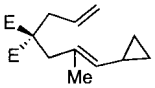 **66**	10 mol% [Rh][a]/ AgOTf	0.01 M, 110 °C, 1 h	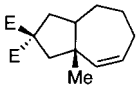 **67**	92
5	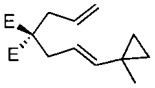 **68**	1 mol% [Rh][a]/ AgOTf	0.01 M, 110 °C 10 h	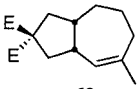 **69**	90

a) [Rh] = $[RhCl(PPh_3)_3]$.
b) Concentrations refer to substrate concentration in toluene. E = CO_2Me.

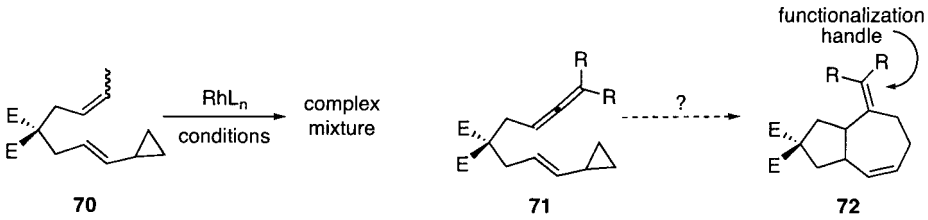

Scheme 13.10 2 C components: allenes as surrogates of 1,2-disubstituted alkenes.

cyclic alkene of an allene cycloadduct would provide the same product as would be obtained from cycloaddition of a 1,2-disubstituted alkene [25].

Allene **73** was used as a test substrate for the systematic investigation of reaction conditions required for allenyl-VCP [5+2] cycloadditions (Tab. 13.3). In the presence of 0.2 mol% $[RhCl(PPh_3)_3]$, allene-VCP **73** (0.1 M in toluene) gave, after 5 h at 110 °C, cycloadduct **74** in remarkably high isolated yield (96%). Importantly, only a *single* diastereomer was obtained, with addition proceeding to the internal alkene, away from the *tert*-butyl group, and with the formation of a *cis*-ring fusion. The product alkene geometry, with the *tert*-butyl group positioned in a more sterically encumbered orientation, is con-

Tab. 13.3 [5+2] cycloadditions of tethered allene-VCPs.

Entry	*Substrate*	*Catalyst, solvent* [a]	*Conditions* [b]	*Cycloadduct*	*Yield (%)*
1	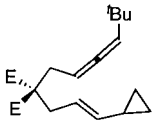 73	1 mol% [Rh] [c]	0.1 M, 110 °C, 5 h	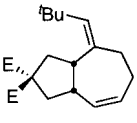 74	96
2		0.2 mol% [Rh] [c]	1.0 M, 100 °C, 6 h		90
3		1 mol% $\{[RhCl(CO)_2]_2\}$, DCE	0.1 M, 80 °C, 6 h		89
4	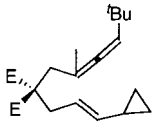 75	5 mol% [Rh] [c]/ AgOTf	0.01 M, 100 °C, 16 h	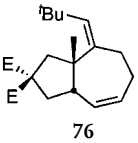 76	70
5	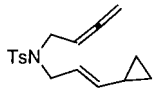 77	5 mol% [Rh] [c]/ AgOTf	0.01 M, 100 °C, 30 min	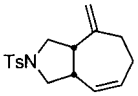 78	85
6		5 mol% $\{[RhCl(CO)_2]_2\}$	0.01 M, 100 °C, 45 min		90

a) Solvent is toluene, unless otherwise indicated. DCE = 1,2-dichloroethane. E = CO_2Me.
b) Concentrations refer to substrate concentration in solvent.
c) [Rh] = $[RhCl(PPh_3)_3]$.

sistent with a kinetically controlled process. The cycloaddition of **73** proceeds efficiently with substrate concentrations from 0.1 to 1.0 M and catalyst loadings from 0.2 to 1 mol% (Tab. 13.3). At concentrations higher than 1.0 M, competing oligomerization processes begin to dominate. For the transformation of allene-VCPs. $[RhCl(PPh_3)_3]$ and $\{[RhCl(CO)_2]_2\}$ work comparably well.

13.4.4
Other Catalyst Systems

In our initial studies on the [5+2] cycloaddition, several metal catalysts were screened. Rhodium(I) systems were found to provide the optimum yields *and* generality [26]. Since the introduction of this new reaction in 1995, our group and others have reported other catalyst systems that can effect the cycloaddition of tethered VCPs and systems. These new catalysts thus far include chlororhodium dicarbonyl dimer ($\{[RhCl(CO)_2]_2\}$) [27], bidentate phosphine chlororhodium dimers such as $\{[RhCl(dppb)]_2\}$ [28] and $\{[RhCl(dppe)]_2\}$ [29], and arene–rhodium complexes $[(arene)Rh(cod)]^+ SbF_6^-$ [30]. $[Cp^*Ru(NCCH_3)_3]^+ PF_6^-$ has also been demonstrated to be effective in the case of tethered alkyne-VCPs [31], but has not yet been extended to intermolecular systems or other 2π-components.

$\{[RhCl(CO)_2]_2\}$ was discovered early in our work as a new catalyst for the [5+2] cycloaddition of VCPs and alkynes. This catalyst proved to be impressively effective for many of the previously problematic cases and, more generally, allowed the reactions to proceed under mild conditions. Initial interest in $\{[RhCl(CO)_2]_2\}$ was prompted, in part, by the expectation that it would be less sterically encumbered than Wilkinson's catalyst.

The reaction of VCP **79** illustrates the performance of the rhodium(I) dimer (Tab. 13.4). For reference, attempts to effect [5+2] cycloadditions with this substrate (**79**) and $[RhCl(PPh_3)_3]$/silver triflate resulted only in the formation of complex product mixtures. In remarkable contrast, when this same substrate was treated with 5 mol% $\{[RhCl(CO)_2]_2\}$ for 20 min in toluene at 110 °C, the [5+2] cycloadduct **80** was obtained in 80% yield. Despite these significant advantages, tethered alkene-VCPs are not successfully converted with this catalyst.

In 2000 Xumu Zhang and co-workers reported a bisphosphine complex of rhodium, $\{[RhCl(dppb)]_2\}$, which, when used with silver hexafluoroantimonate, in some cases offers a rate advantage over the Wilkinson's catalyst/silver triflate system [28], allowing the reaction to be conducted at room temperature (Tab. 13.5). Scott Gilbertson and co-workers reported a related example, employing $[Rh(dppe)(CH_2Cl_2)_2]^+ SbF_6^-$ as a catalyst for the [5+2] reaction (Tab. 13.5, entry 5) [29].

Arene complexes of rhodium have also been proven to be effective pre-catalysts for the [5+2] reaction [30]. We had previously shown that intramolecular diene–alkyne (and

Tab. 13.4 [5+2] Cycloadditions with the $\{[RhCl(CO)_2]_2\}$ dimer.

Entry	*Substrate*	*Catalyst, solvent* [a]	*Conditions* [b]	*Cycloadduct*	*Yield (%)*
1	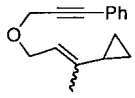	5 mol% $\{[RhCl(CO)_2]_2\}$	110 °C, 20 min	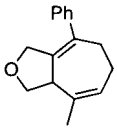	80
2	**79** *E*/*Z* 3.3:1	10 mol% [Rh][d]/ AgOTf	110 °C	**80**	0 [c]
3	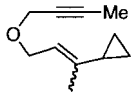	5 mol% $\{[RhCl(CO)_2]_2\}$	110 °C, 20 min	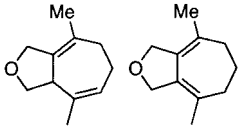	78 (**a**)
4	**81** *E*/*Z* 3.3: 1	10 mol% [Rh][d]/ AgOTf	110 °C, 17 h	**82a** **82b**	65 (**a**) 13 (**b**)
5	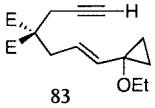 **83**	5 mol% $\{[RhCl(CO)_2]_2\}$, $CDCl_3$	0.074 M, 30 °C, 40 h	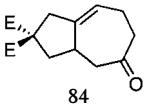 **84**	81
6	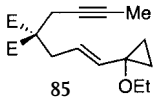 **85**	0.5 mol% $\{[RhCl(CO)_2]_2\}$, CH_2Cl_2	0.05 M, RT, 30 h	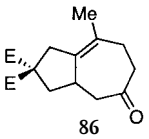 **86**	75

a) Solvent is toluene unless otherwise indicated.
b) Concentrations refer to substrate concentration in solvent.
c) Complex mixture of products.
d) [Rh] = $[RhCl(PPh_3)_3]$, E = CO_2Me.

Tab. 13.5 [5+2] Cycloadditions with $[Rh(dppb)]^+$ and $[Rh(dppe)(CH_2Cl_2)_2]^+$.

Entry	*Substrate*	*Catalyst, solvent*[a)]	*Conditions*[b)]	*Cycloadduct*	*Yield (%)*
1	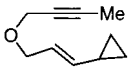	2.5 mol% $[Rh(dppb)]^+SbF_6^-$, DCE	0.1 M, RT, 1.5 h	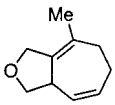	92
2[c)]	**87**	10 mol% [Rh],[c)] PhMe	110 °C, 1.5 h	**88**	88
3	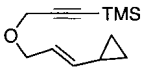	1.0 mol% $[Rh(dppb)]^+SbF_6^-$, DCE	0.1 M, RT, 2 h	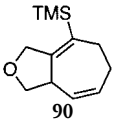	96
4[d)]	**89**	10 mol% [Rh],[c)] PhMe	110 °C, 3.5 h	**90**	83
5	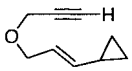	6.0 mol% [Rh(dppe)$(CH_2Cl_2)_2]^+SbF_6^-$, CH_2Cl_2	RT, 20 h	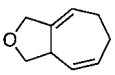	59[e)]
6[d)]	**91**	10 mol% [Rh],[c)] THF	100 °C, 1.5 h	**92**	50[e)]

a) $[Rh(dppb)]^+SbF_6^-$ is generated in situ by treatment of 1.25 mol% $\{[RhCl(dppb)]_2\}$ with 2.5 mol% $AgSbF_6$. DCE = 1,2-dichloroethane, THF = tetrahydrofuran.
b) Concentrations refer to substrate concentration in solvent.
c) [Rh] = $[RhCl(PPh_3)_3]$.
d) See ref. [21].
e) Low yield is due to product volatility.

diene–allene) [4+2] cycloadditions can be achieved with nickel, and later, rhodium catalysts [32]. Livinghouse showed that the rhodium(I) catalysts are effective for intramolecular diene–ene [4+2] cycloadditions [33]. Chung and co-workers subsequently reported a readily prepared, air-stable naphthalene complex of rhodium ($[(C_{10}H_8)Rh(COD)]^+$ BF_4^-),

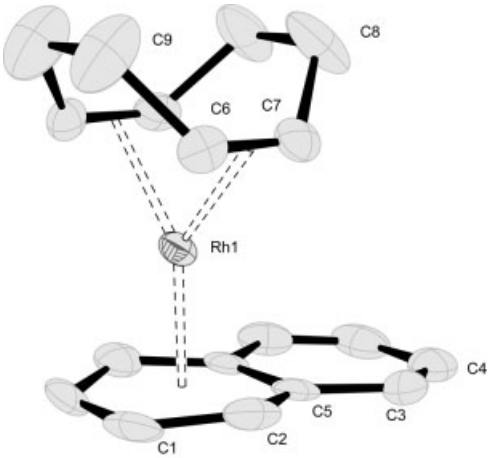

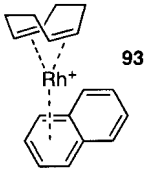

93

which is an efficient catalyst for [4+2] cycloaddition reactions of dienes and alkynes [34]. An analogous complex **93** ($[(C_{10}H_8)Rh(COD)]^+$ SbF_6^-) is prepared in a single step from commercially available $\{[RhCl(COD)]_2\}$ through a known procedure [35]. The complex is air-stable at room temperature for prolonged periods of time and retains its catalytic activity even after several months' storage.

Complex **93** was tested in a variety of [5+2] cycloaddition reactions and compared, where relevant, with some other effective catalysts (Tab. 13.6). Excellent results were obtained with VCPs tethered to terminal and internal alkynes, alkynoates, and alkenes.

Tab. 13.6 [5+2] Cycloaddition reactions with the naphthalene catalyst **93**.

Entry	*Substrate*	*Catalyst, solvent* [a]	*Conditions* [b]	*Cycloadduct*	*Yield (%)*
1	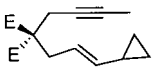 **54**	2 mol% **93**	0.15 M, RT, 15 min	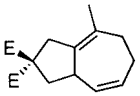 **55**	>99 [c]
2		10 mol% [Rh][a], PhMe	2.0 M, 110 °C, 3 h		89
3		1 mol% $\{[RhCl(CO)_2]_2\}$, TFE	0.01 M, 55 °C, 19 h		90–95
4	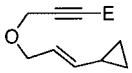 **94**	2 mol% **93** [d]	0.51 M, RT, 16 min	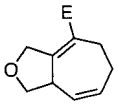 **95**	96
5	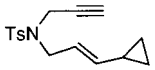 **96**	5 mol% **93** [d]	0.20 M, RT, 65 min	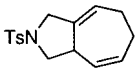 **97**	90 [e]
6	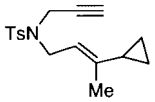 **98**	5 mol% **93**	0.03 M, 60 °C, 60 min	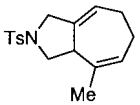 **99**	93
11	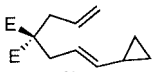 **62**	5 mol% **93**	0.05 M, 60 °C, 6 h	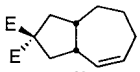 **63**	96
12		0.1 mol% [Rh][a]/ AgOTf, PhMe	0.01 M, 110 °C, 15 h		90
13	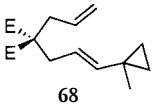 **68**	5 mol% **93**	0.01 M, 60 °C, 6.5 h	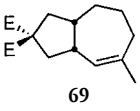 **69**	90
14		1 mol% [Rh][a]/ AgOTf, PhMe	0.01 M, 110 °C, 10 h		90
15	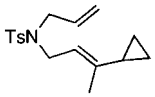 **100**	5 mol% **93**	0.03 M 60 °C, 19 h	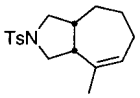 **101**	76

Tab. 13.6 (cont.)

Entry	*Substrate*	*Catalyst, solvent* [a)]	*Conditions* [b)]	*Cycloadduct*	*Yield (%)*
16	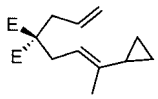	10 mol% **93**	0.03 M, 70 °C, 10 h	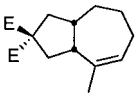	75 (**a**)
17		5 mol% [Rh][a)]/AgOTf, PhMe	0.01 M, 110 °C, 15 h		78 (**b**)
18	**102**	5 mol% [Rh][a)]/AgOTf, PhMe	0.01 M, 85 °C, 66 h	**103a**	67 (2.3:1 **a**:**b**)
				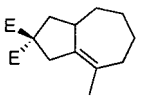	
				103b	

a) [Rh]=[RhCl(PPh$_3$)$_3$].
b) Unless otherwise indicated, each reaction was run in a tightly capped vial at the indicated temperature, catalyst loading, and concentration (refers to substrate) in 1,2-dichloroethane. E=CO_2Me.
c) Found 85% yield with BF_4^- anion.
d) Catalyst added in four aliquots.
e) 1 g scale, found 96% yield with BF_4^- anion, product structure verified by X-ray crystallography.

Substitution of the VCP is tolerated both on and adjacent to the cyclopropane ring. Diester-substituted and heteroatom (O, NTs) tethers are well tolerated. Reactions were conducted with 2–10 mol% catalyst at up to 0.20 M, as illustrated. Most importantly, reactions with the naphthalene catalyst were found to be more rapid than those with other catalysts. For example substrate **54** is readily converted in >99% yield to cycloadduct **55** in only 15 min at room temperature (entry 1). Complex **93** efficiently catalyzes the reactions of both alkynes and alkenes with VCPs, offering greater generality than thus far observed with non-rhodium catalysts. This catalyst is particularly advantageous in the cases of substrates **100** and **102**, for which the desired product is not formed cleanly with Wilkinson's catalyst due to product isomerization.

To survey the role of the arene, additional complexes, based on 1,4-dimethylnaphthalene, benzene, and hexamethylbenzene, were prepared (Tab. 13.7). The complexes were compared with each other and with the catalyst generated in situ by the treatment of {[RhCl(COD)]$_2$} with $AgSbF_6$ (Tab. 13.7, entry 1) using the conditions found to be optimal for conversion of substrate **54** with catalyst **93**. The trend is that increasing arene substitution with methyl groups results in lower yields, and that the extended arene system is not necessary for successful cycloaddition reaction. For example, benzene-ligated complex **105** was quite effective in mediating the intramolecular [5+2] reaction, while the hexamethylbenzene-ligated complex **106** was not a competent catalyst.

With an eye toward increasing efficiency and eliminating the atom-uneconomical solvent waste stream involved in most organic reactions, a reusable, water-soluble catalyst, using bidentate phosphine **107** as a ligand, has been developed [36]. The catalyst is prepared by treatment of {[RhCl(nbd)]$_2$} (nbd=norbornadiene) with $AgSbF_6$ in acetone, followed by introduction of the phosphine ligand [37]. In the presence of 10 mol% catalyst in water/methanol (1:1) at a catalyst concentration of 2.0 mM, **108** reacted efficiently at 70 °C to provide cycloadduct **109** after 12 h in 91% yield (GC analysis; Tab. 13.8). Notably, the yield and rate compare favorably to results obtained with Wilkinson's catalyst

Tab. 13.7 Synthesis and reactions of some [(arene)Rh(COD)]$^+$SbF$_6^-$ complexes.

Entry[a]	*Rhodium complex (yield)*		*Cycloadduct (55) yield (%)*[b]
1	{[RhCl(COD)]$_2$} + 2 AgSbF$_6$ Arene complex ([(Ar)Rh(COD)]$^+$SbF$_6^-$		90
2	**93** (70%)	Ar = 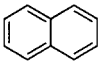	>99
3	**104** (67%)	Ar = 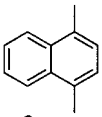	88
4	**105** (65%)	Ar = 	91
5	**106** (87%)	Ar = 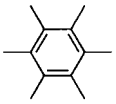	trace

a) Arene complexes prepared as with **93**.
b) Yield of the conversion of **54** to **55** with 2 mol% rhodium(I) in 1,2-dichloroethane (0.15 M) at room temperature in 15 min.

in THF at 65 °C (Tab. 13.8, entry 3) [22]. As illustrated, the water-soluble catalyst is effective with a variety of tethered alkynyl- and alkenyl-substrates. It is equally noteworthy that the reaction occurs readily in water as the only solvent. While the substrate is present as a neat liquid, these reactions occur under pseudo-high-dilution conditions, since only a small amount of substrate is dissolved in the aqueous layer and interacts with the water-soluble catalyst at any given time. This reduces the likelihood of competing oligomerization processes and consequently little byproduct formation is observed, even though the substrate is the major component of the organic phase.

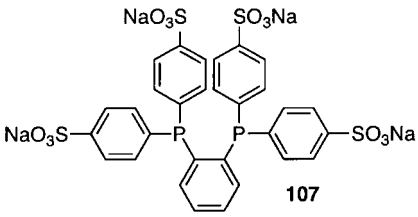

107

A further advantage of this catalytic system is that the organic cycloadducts can be easily separated from the aqueous phase, allowing the catalyst solution to be isolated and directly reused. The catalyst retains its activity for the cycloaddition through several separate uses. As illustrated for the conversion of **108** to **109**, the yield of the cycloaddition remained approximately constant for five reuses of the catalyst and decreased only with the sixth use (Tab. 13.9). With alkynoate substrate **94**, the experiment was repeated with rigorous deoxygenation (by freeze–pump–thaw cycles) of the catalyst solution between uses, and it was found to function cleanly after eight uses (Tab. 13.8, entry 4).

Tab. 13.8 Rhodium(I)-catalyzed [5+2] cycloadditions in water.

Entry	*Substrate*	*Catalyst, solvent* [a]	*Conditions* [b]	*Cycloadduct*	*Yield (%)*
1	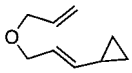	**A**, 50% MeOH/H_2O	2.0 mM, 70 °C, 12 h	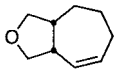	91 (GC)
2		**A**, H_2O	2.0 mM, 90 °C, 12 h		90 (GC)
3	**108**	**B**, THF	0.50 mM, 65 °C, 12 h	**109**	94 (GC)
4	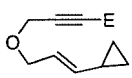	**A**, 20% MeOH/H_2O	5 mM, 90 °C, 1.5 h	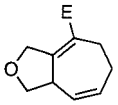	79 [c]
5		**A**, 30% MeOH/H_2O	0.5 mM, 90 °C, 3.5 h		79 [d]
6	**94**	**B**, PhMe, 5 mol%	0.25 mM, 110 °C, 1 h	**95**	81
7	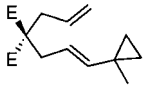	**A**, 20% MeOH/H_2O	2 mM, 70 °C, 12 h	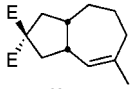	80
8		**B**, PhMe, 1 mol%	0.1 mM, 110 °C, 10 h		90
	68			**69**	
9	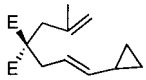	**A**, 20% MeOH/H_2O	2 mM, 70 °C, 12 h	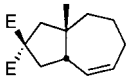	83
10		**B**, PhMe, 10 mol%	1 mM, 110 °C, 1 h		94
	64			**65**	

a) **A**: 10 mol% [Rh(nbd)(**107**)]$^+SbF_6^-$, **B**: [RhCl(PPh_3)$_3$]/AgOTf. E = CO_2Me.
b) Concentrations refer to *catalyst* concentration in solvent.
c) Eighth use of catalyst.
d) Millimole scale.

Tab. 13.9 Catalyst recyclability (unoptimized results).

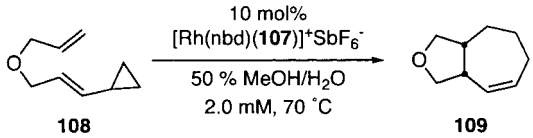

108 **109**

Catalyst use	*Time*	*Yield (GC) (%)*
1	12 h	91
2	12 h	88
3	12 h	84
4	14 h	85
5	24 h	81
6	48 h	65

13.4.5

Stereochemistry and Regiochemistry of the Intramolecular [5+2] Cycloaddition

In order to explore the regio- and stereochemistry of the intramolecular [5+2] cycloaddition, a series of compounds incorporating cyclopropyl substituents with differing steric and electronic properties were prepared (Tab. 13.10) [23, 38]. These substrates were exposed to two previously described catalytic systems: Wilkinson's catalyst ($[RhCl(PPh_3)_3]$) with silver triflate, and $\{[RhCl(CO)_2]_2\}$. For the protected hydroxymethyl substrate **110**, the regioisomer arising from cleavage of the less substituted cyclopropane bond predominated, giving preferentially or exclusively products of type **a** (**111a**). With modified Wilkinson's catalyst the regiocontrol is complete, while utilization of the rhodium(I) dimer catalyst leads to a mixture of regioisomers favoring type **b** cycloadducts (**111b**).

Mechanistic analysis of the reaction of substituted cyclopropanes reveals that each regioisomeric cycloadduct correlates uniquely with a metal–π-system complex (Scheme 13.11, **A** and **A′**). Metal coordination to either of the two vinyl π-system faces of **122** followed by oxidative coupling leads to diastereomeric metallacyclopentenes **B** or **B′** [39]. The subsequent formation of a *cis*-olefin in **C** and **C′** requires a *syn* alignment of the hydrogens along bond **a**. This analysis indicates that only one cyclopropane bond in **B** and **B′** could be cleaved. Each of the complexes (**B** or **B′**) aligns a different cyclopropane bond for cleavage, leading to the formation of different constitutional isomers **123** or **124**, respectively. As the substituent (R) in **122** is spatially removed from the vinyl fragment during the initial coordination, very little π-facial selectivity would be expected in the formation of diastereomeric complexes **A** and **A′** and their downstream intermediates and products. The observed high selectivity is thus a consequence of the reversibility of the initial mechanistic steps and cleavage proceeding preferentially

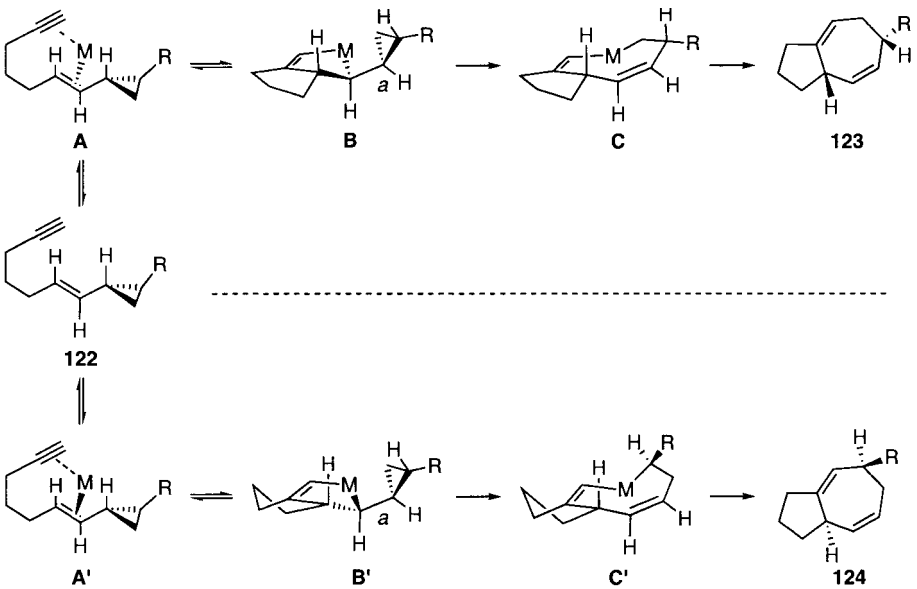

Scheme 13.11 Regiochemistry in the metallacyclopentene pathway.

Tab. 13.10 Regioselectivity and diastereoselectivity of the [5+2] cycloaddition.

Entry	*Substrate*	*Catalyst, solvent* [a]	*Conditions* [b]	*Cycloadduct(s)*		*Yield (%)*
1	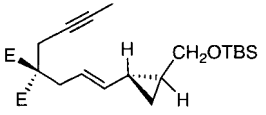	**A**	10 mM, 1 h	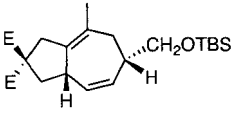	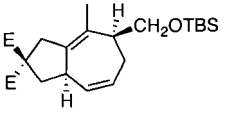	95 (a)
2		**B**	10 mM, 1 h			86 (3.1:1 **a**:**b**)
	110			**111a**	**111b**	
3	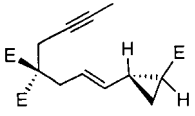	**A**	10 mM, 1 h	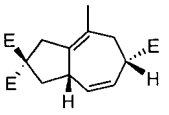	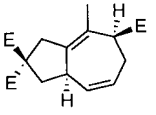	81 (20:1 **a**:**b**)
4		**B**	10 mM, 1 h			93 (1:11 **a**:**b**)
	112			**113a**	**113b**	
5	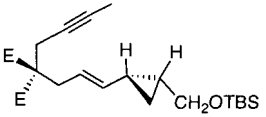	**A**	10 mM, 2 h	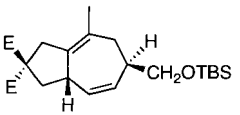	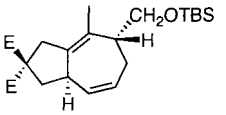	81 (a)
6		**B**	10 mM, 1 h			96 (a)
	114			**115a**	**115b**	

Entry	Substrate	Catalyst, solvent [a]	Conditions [b]	Cycloadduct(s)		Yield (%)
7	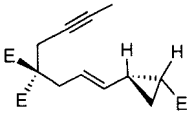	A	10 mM, 2 h	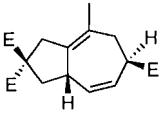	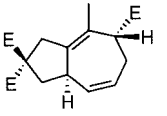	95 (6.4:1 **a**:**b**)
8	**116**	B	10 mM, 2 h	**117a**	**117b**	98 (1.5:1 **a**:**b**)
9	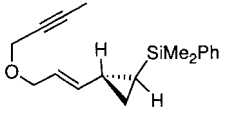	A	50 mM 30 min	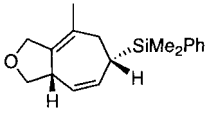		91
	118			**119**		
10	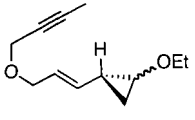	C	50 mM 30 min	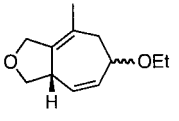		88
	120			**121**		

a) **A**: 10 mol% $[RhCl(PPh_3)_3]$/silver triflate in toluene, **B**: 5 mol% $\{[RhCl(CO)_2]_2\}$ in toluene, **C**: 10 mol% $\{[RhCl(CO)_2]_2\}$ in 1,2-dichloroethane. E = CO_2Me.

b) Concentrations refer to substrate concentration in solvent. Temperature is reflux (110 °C for toluene, 80 °C for DCE).

through **B** → **C**, the less substituted bond. It is noteworthy that the stereochemistry of the starting cyclopropane is conserved during the cycloaddition. Thus, *trans*-VCP **110** gives only *syn*-product **111a** with [RhCl(PPh$_3$)$_3$]/silver triflate and the *cis*-VCP **114** gives only the *anti*-cycloadduct **115a** under the same conditions. Importantly, by changing the catalyst one can also access the cycloadduct arising from cleavage of the more substituted cyclopropane bond (compare entries 3 and 4 in Tab. 13.10).

13.4.6 Applications to Natural Product Synthesis

The introduction of the [5+2] cycloaddition reaction has enabled new strategies and opened the door to shorter, more efficient syntheses of natural products containing seven-membered rings. One such example is found in the total synthesis of (+)-dictamnol (Scheme 13.12, **129**) [40], a trinor-guaiane sesquiterpene first isolated from the roots of *Dictamnus dascarpus*. While structurally quite simple, its core skeleton can also be found in much more complex natural product targets, such as the aforementioned phorbol esters (**6**) and gnidimacrin (**8**) (Scheme 13.3). As such, dictamnol presented an attractive target for an allene–VCP cycloaddition in a more complex framework. It also provided a system to evaluate stereocommunication between a pre-existing stereogenic center and those forming during the cycloaddition. When VCP **126**, available in homochiral form in just three steps from commercially available cyclopropane carboxaldehyde, is treated with {[RhCl(CO)$_2$]$_2$}, cycloadduct **127** is produced in 76% yield in a diastereomeric ratio greater than 9:1. In addition to the selectivity of this process, another noteworthy feature is that the reaction proceeds in the presence of an unprotected alcohol. Oxidation of **127**, which occurs with epimerization of the *α*-stereocenter, and exposure of the resultant product **128** to methylmagnesium bromide, gave (+)-dictamnol, along with the 8-*epi* product in 50% yield.

Another example of the use of the [5+2] cycloaddition as a strategy-level reaction is provided in the total synthesis of (+)-aphanamol I (**138**) [41], isolated in 1984 as a minor toxic principle of *Aphanamixis grandifolia*. This target presents an array of synthetic challenges that are addressed quite effectively using the allenyl [5+2] cycloaddition. In this case, the allenyl unit ultimately functions as a ketene equivalent in the

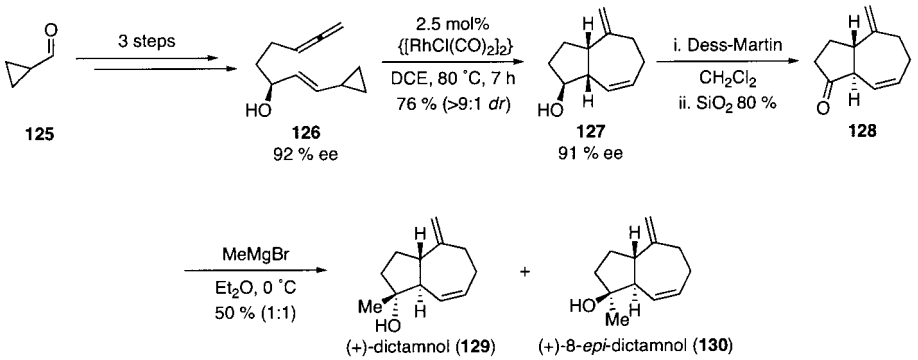

Scheme 13.12 Total synthesis of (+)-dictamnol.

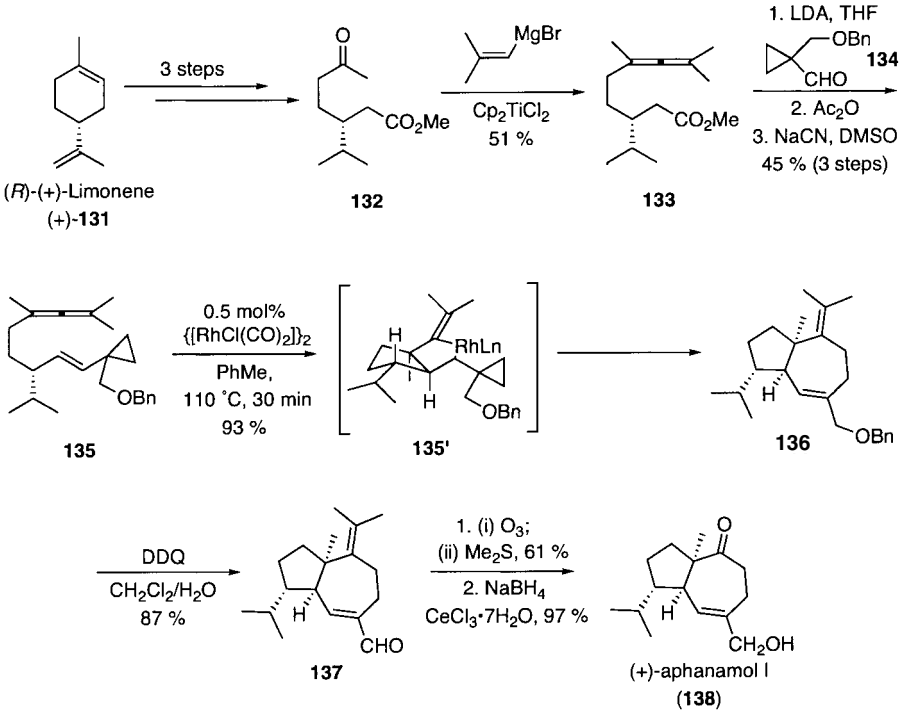

Scheme 13.13 Total synthesis of (+)-aphanamol.

cycloaddition. A synthetic approach to this compound based on the [5+2] cycloaddition allowed for the first investigation of the use of tetrasubstituted allenes and 1,1-disubstituted VCPs in the process, in addition to the evaluation of the degree of relative stereocontrol imparted by a pre-existing stereocenter in the cycloaddition (Scheme 13.13). The tetrasubstituted allene fragment **133**, containing a chiral isopropyl substituent and generated in four steps from (*R*)-(+)-limonene, was condensed with cyclopropyl aldehyde **134**. Acylation of the free hydroxyl followed by a novel decarboxylative dehydration reaction provided substrate **135** for the key [5+2] cycloaddition. Treatment of **135** with 0.5 mol% rhodium(I) dimer resulted in the formation of desired cycloadduct **136** in 93% yield with complete diastereoselectivity. Oxidative deprotection of the benzyl group, ozonolysis of the *exo*-olefin, and Luche reduction of enal **137** provided the target molecule in a total of 13 steps and 13.6% overall yield.

The structural complexity and biological activity of the cyathane family of diterpenes has stimulated considerable interest from synthetic chemists, as reflected in the number and diversity of approaches reported thus far [42]. Our own strategy for cyathane synthesis is based on a rhodium-catalyzed [5+2] cycloaddition. The precursor for this reaction was fashioned ultimately from commercially available and inexpensive (*S*)-(–)-limonene. Treatment of the ketone **139** with 5 mol% $\{[RhCl(CO)_2]_2\}$ in 1,2-dichloroethane gave cycloadduct **140** (Scheme 13.14) in 90% yield and in analytically pure form after simple filtration through a plug of neutral alumina [43].

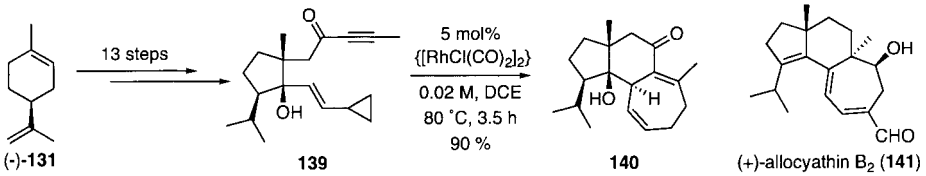

Scheme 13.14 Efficient assembly of the allocyathin core.

Tab. 13.11 The first examples of intermolecular [5+2] cycloadditions.

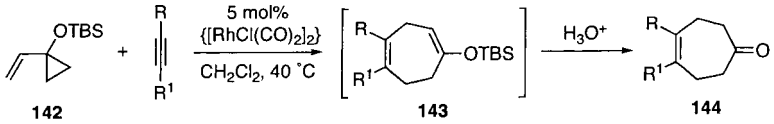

Entry	Alkyne	Time	Product	Yield (%)
1	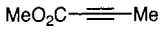 **145**	1.5 h	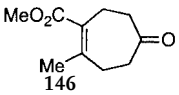 **146**	92
2	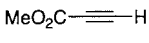 **147**	2 h	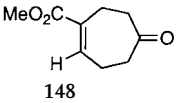 **148**	93
3	 **149**	2.5 h	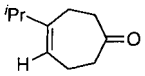 **150**	84
4	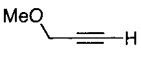 **151**	1.5 h	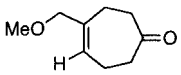 **152**	88
5	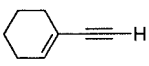 **153**	3 h	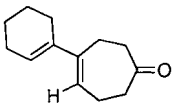 **154**	75
6	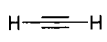 **36**	6 h	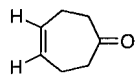 **155**	79

13.5
Intermolecular [5+2] Cycloadditions of VCPs and Alkynes

13.5.1
Oxygen-Substituted VCPs

The Wender group described the first examples of *intermolecular* metal-catalyzed [5+2] cycloadditions of VCPs and alkynes in 1998 [44]. Although earlier attempts to achieve this process with various VCPs and alkynes in the presence of $[RhCl(PPh_3)_3]$ failed [45], siloxy-VCP **142** was found to react efficiently in the presence of $\{[RhCl(CO)_2]_2\}$ under mild conditions. This is in line with observations that in *intramolecular* [5+2] cycloadditions, oxygen-substitution of the VCP facilitates the reaction and that $\{[RhCl(CO)_2]_2\}$ enables the cycloaddition of otherwise unreactive substrates (see, for example, Tab. 13.4, entries 5 and 6). The intermolecular [5+2] cycloaddition of siloxy-VCP **142** and alkynes was found to be remarkably general (Tab. 13.11). After hydrolysis of the initially formed enol ether **143**, cycloheptenones **144** were obtained in good to excellent yields with electron-poor, electron-rich, conjugated, internal, and terminal alkynes, including acetylene. This process benefits from the use of abundantly available alkyne feedstocks and produces products that have utility as building blocks in synthesis and as scaffolds for combinatorial chemistry. Ketoester **148**, for example, could be easily diversified through selective reductive aminations, Michael additions, or ester conversions.

The synthesis of VCP **142** involves four steps, including a reductive cyclization using sodium metal, and protection using TBSOTf (Scheme 13.15, Eq. 1) [46]. Although it is adequate for many applications, the synthetic potential of the [5+2] cycloaddition for cycloheptenone synthesis would be complemented by a short, scalable, economical, and safe synthesis of a five-atom reagent. Toward this end, a two-step synthesis of alkoxy-VCP **163** was developed (Scheme 13.15, Eq. 2) [47], which avoids the use of highly reactive metals and expensive protecting groups. This synthesis allows the facile construction of VCP **163** on multi-gram scale at one-tenth of the cost of the production of **142** [48].

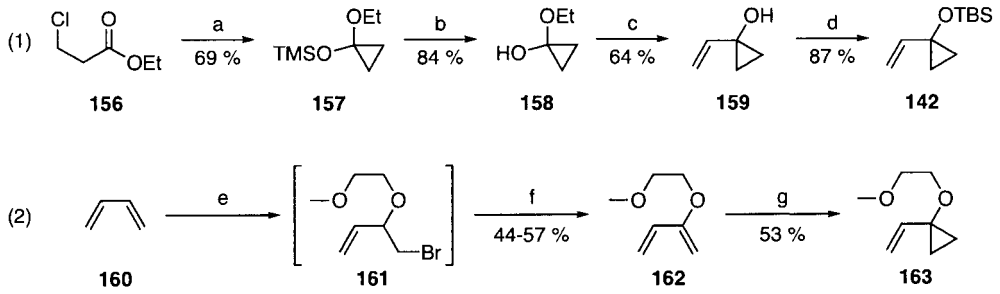

Scheme 13.15 Preparation of oxygen-substituted VCPs **142** (Eq. 1) and **163** (Eq. 2). Conditions: (a) Na metal, TMSCl, Et_2O, Δ; (b) MeOH, RT; (c) vinylmagnesium bromide, Et_2O, 0 °C to RT; (d) TBSOTf, 2,6-lutidine, CH_2Cl_2, RT; (e) *N*-bromosuccinimide, 2-methoxyethanol, –78 °C to RT; (f) KOH, RT to 90 °C; (g) 1.3 equiv. CH_2I_2, Zn metal, CuCl, AcCl, Et_2O, Δ.

Tab. 13.12 Intermolecular [5+2] cycloadditions with alkoxy-VCP **163**.

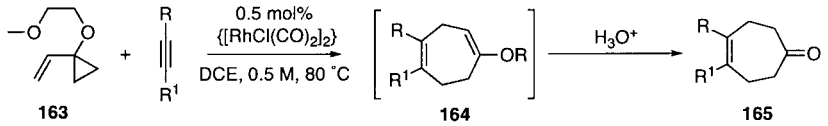

163 **164** **165**

Entry	*Alkyne*	*Time*	*Product*	*Yield (%)*
1	$EtO_2C{-}{\equiv}{-}CO_2Et$ **167**	1 h	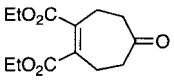 **168**	96
2	$MeO_2C{-}{\equiv}{-}H$ **147**	10 min	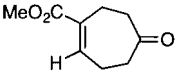 **148**	84
3	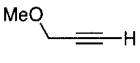 **151**	30 min	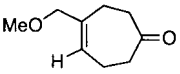 **152**	94[a]
4	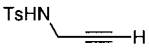 **169**	15 min	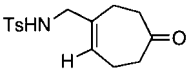 **170**	87
5	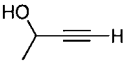 **171**	12 min	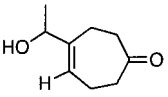 **172**	89
6	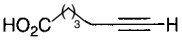 **173**	1.5 h	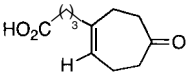 **174**	87
7	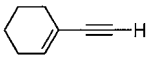 **153**	7 h[b]	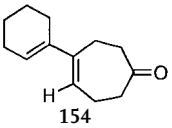 **154**	85
8	$H{-}{\equiv}{-}H$ **36**	2 h	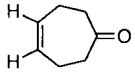 **155**	75

a) 100 mmol (14.20 g VCP **163**) scale.
b) Reaction carried out at room temperature.

Alkoxy-VCP **163** was found to be a very competent reagent in the intermolecular [5+2] cycloaddition (Tab. 13.12). With some minor optimization of the previous reaction conditions, namely the use of 1,2-dichloroethane (DCE) as solvent at a higher concentration (0.5 M) and reaction temperature (80 °C), the reaction was found to be complete in minutes in some cases with 0.5 mol% $\{[RhCl(CO)_2]_2\}$, while still providing good to excellent yields of cycloheptenone products. Significantly, reactive functionality, including unprotected alcohols and carboxylic acids, is tolerated in the reaction. The reaction is also readily scaled, with comparable isolated yields over a 100-fold increase in scale. The formation of products in minutes is of consequence, as such reactions allow for the more time-efficient realization of synthetic goals.

13.5.2
Serial [5+2]/[4+2] Cycloaddition Reactions

As illustrated by the reactions of conjugated ene-ynes (Tab. 13.11, entry 5, and Tab. 13.12, entry 7), the intermolecular [5+2] cycloaddition shows complete chemoselectivity for alkynes. Based on this selectivity, a serial [5+2]/[4+2] cycloaddition process was developed (Tab. 13.13) [49], in which VCP **163** is reacted with a conjugated ene-yne in 1,1,2,2-tetrachloroethane (TCE), yielding a diene that reacts in a thermal [4+2] cycloaddition with a dienophile. In this way a complex polycyclic compound with two new rings and up to four new stereocenters is formed from three simple starting materials *in one operation*. The synergistic effect of linking multiple cycloaddition steps on the increase in molecular complexity is a key to achieving greater complexity in synthesis. Significantly, by capturing the diene intermediate as it is formed in the reaction, higher yields are attained with the serial procedure than with the analogous procedure involving the uncoupled individual steps. This reaction is also readily scalable, with reactions of up to 100 mmol of **163** giving excellent yields of single diastereomer products.

13.5.3
Reactions of Simple, Alkyl-Substituted VCPs

While the facility and efficiency of the [5+2] cycloaddition of oxygen-substituted VCPs could be attributed solely to the electronic contribution of the heteroatom substituent, it could also be a consequence of its conformational influence. Substitution of a VCP, particularly at the 1-position, has been shown to reduce the difference in energy between the *s-cis* (local minimum) and *s-trans* (global minimum) conformations through steric effects [50]. Based on the proposed mechanisms for the [5+2] cycloaddition, only the *s-cis* conformations, **190** and **192**, can lead to productive reaction, so biasing intermediates toward this conformation could therefore accelerate the reaction (Scheme 13.16).

Indeed, in a study of reaction rate and efficiency as a function of geminal substitution of the VCP, it was found that heteroatom substitution was not required to activate the VCP for intermolecular [5+2] cycloaddition (Tab. 13.14) [51]. Substitution for –H at the 1-position of the cyclopropane with –Me, –TMS, or $-^{i}$Pr led to an acceleration of the reaction that correlated with size of the substituent. Significantly, good to excellent yields and high, if not complete, regioselectivities are observed with a variety of monosubstituted alkynes and simple, unactivated VCPs.

Tab. 13.13 Serial [5+2]/[4+2] cycloaddition reactions.

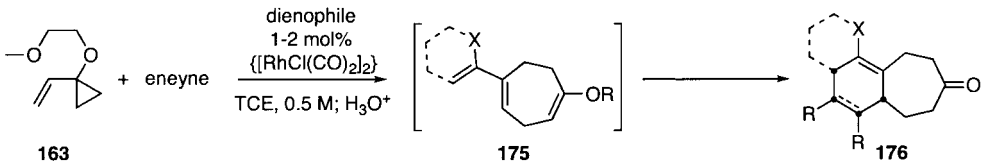

163 **175** **176**

Entry	*Ene-yne*	*Dienophile*	*Temp.*	*Time*	*Product* [a]	*Yield (%)*
1		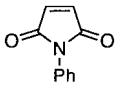	40 °C	24 h	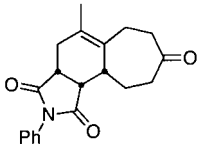	89
	177	**178**			**179**	
2	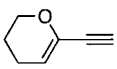	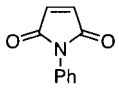	50 °C	36 h	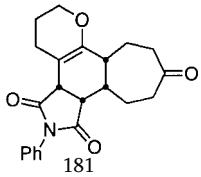	89
	180	**178**			181	
3	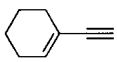	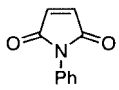	60 °C	5 h	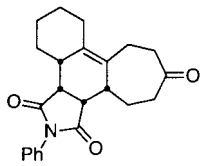	91
	153	**178**			**183**	
4	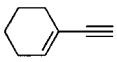	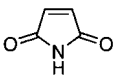	70 °C	6 h	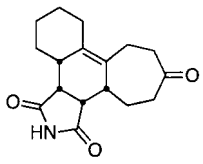	91 [b]
	153	**184**			**185**	
5	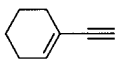	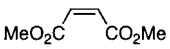	140 °C	21.5 h	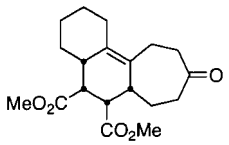	84
	153	**186**			**187**	
6 [c]	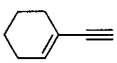	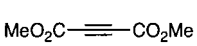	130 °C	24 h	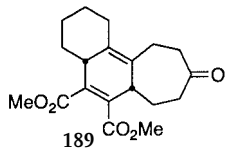	77
	153	**188**			**189**	

a) Relative stereochemistry indicated.
b) 100 mmol (14.20 g) VCP **163** scale.
c) 2-step serial procedure.

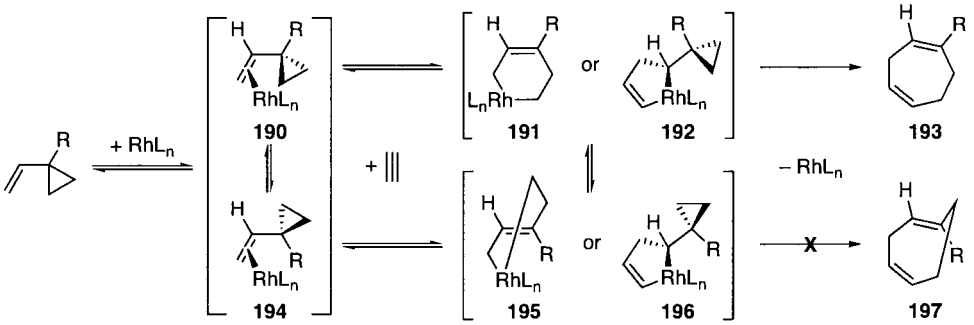

Scheme 13.16 Mechanistic effects of conformational bias of the VCP on the [5+2] cycloaddition.

13.5.4

Hetero-[5+2] Cycloadditions of Cyclopropylimines

It is instructive at this point to recall the powerful template, the Diels–Alder [4+2] cycloaddition, upon which the new [5+2] cycloaddition was designed. In so doing, one finds that the Diels–Alder cycloaddition enjoyed greatly expanded scope when it was realized that carbon atoms in both the 4- and 2-atom components could be replaced with heteroatoms [52]. It is expected that this could also be achieved with the [5+2] process. Indeed, recent studies have demonstrated that cyclopropyl imines can be used in place of VCPs, thereby expanding the scope of five-atom substrates and seven-membered ring products, through the development of a novel hetero-[5+2] approach to dihydroazepines via a rhodium(I)-catalyzed cycloaddition of cyclopropyl imines with alkynes (Scheme 13.17) [53]. Although the alkyne component is, thus far, limited to dimethyl acetylenedicaboxylate (DMAD, **188**), the reaction was shown to be very efficient with a variety of aldimines and ketimines, which can either be preformed or formed in situ in a serial imine formation/aza-[5+2] cycloaddition procedure, in up to multigram quantities. Substitution of the cyclopropane was also well tolerated in the reaction, leading to single regioisomeric products through cleavage of the less-substituted cyclopropyl bond.

Tab. 13.14 [5+2] cycloadditions of simple, unactivated VCPs.

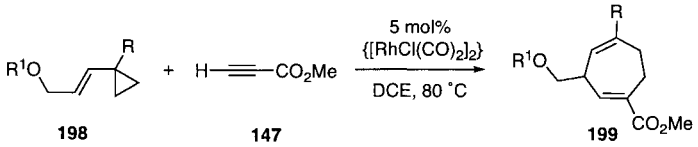

198 **147** **199**

Entry	*VCP*	*Time*	*Product*	*Yield (%)*
1	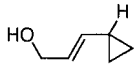 **200**	30 h	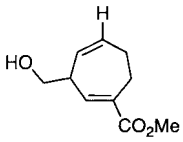 **201**	23
2	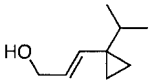 **202**	2 h	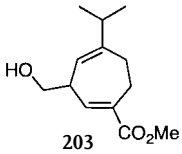 **203**	82
3	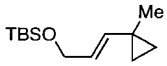 **204**	8 h	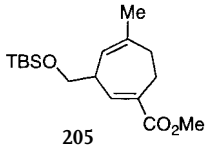 **205**	81
4	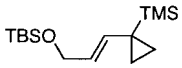 **206**	3 h	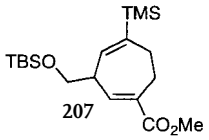 **207**	53
5	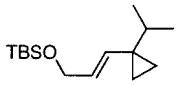 **208**	2 h	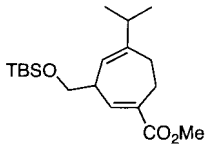 **209**	93

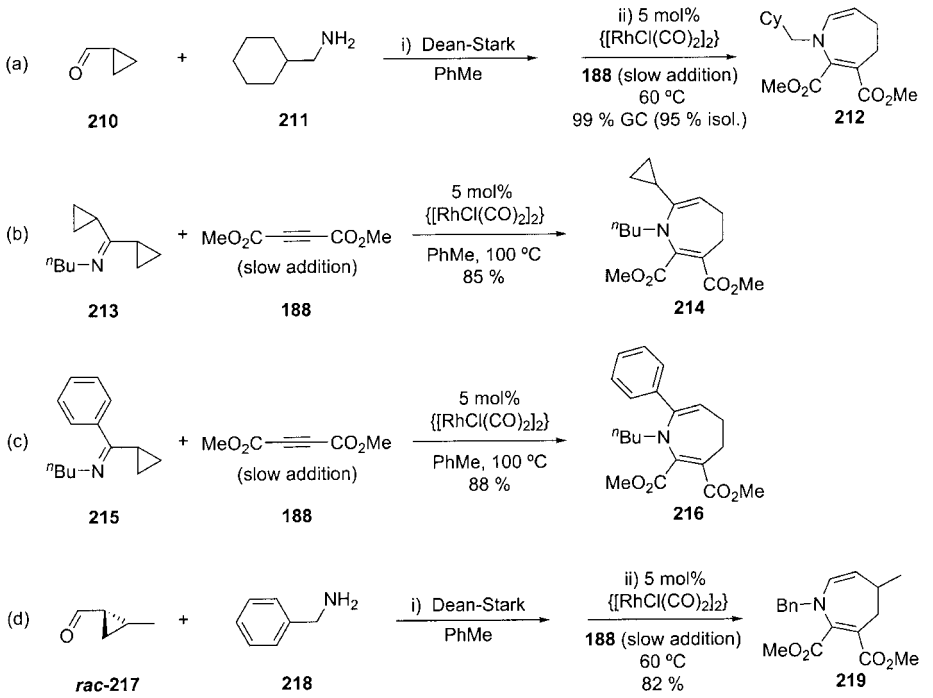

Scheme 13.17 The first examples of hetero-[5+2] cycloadditions.

13.6
Cycloaddition Approaches for Eight-Membered Ring Synthesis

As with seven-membered ring synthesis, there is a well-defined and significant need for cycloaddition methods for the formation of eight-membered rings [54]. Thermal [4+4] cycloadditions represent an attractive option but are forbidden in the ground state, and photochemical approaches are only usefully efficient in specific, constrained cases. Transition metal catalysis, however, has enabled several new processes for the formation of eight-membered rings, as exemplified in the development of the [4+4] cycloaddition of dienes (Scheme 13.4a) [7, 8]. Another approach, introduced by Reppe in the late 1940s, the [2+2+2+2] cycloaddition of ethyne in the presence of $NiBr_2/CaC_2$, represents a superb four-component route to cyclooctatetraene (COT). This reaction can also be catalyzed by $[Ni(acac)_2]$ or $[Ni(COT)_2]$, and has been used for the production of COT on an industrial scale (Scheme 13.18a) [55]. Iron [56] and, later, cobalt [57] catalysts have been use to effect [4+2+2] cycloadditions of norbornadienes with dienes (Scheme 13.18b). Rhodium(I) catalysts have recently been shown to enable multi-component [4+2+2] cycloadditions of ene-ynes with dienes (Scheme 13.18c) [58] and diene-ynes with alkynes (Scheme 13.18d) [59]. Chromium(0) complexes have been shown to facilitate efficient [6+2] cycloadditions of cycloheptatriene (CHT) with 2π-components (Scheme 13.18e) [60]. Some of these reactions are covered elsewhere in this book. The following sections provide an overview of the development of a novel [6+2] cycloaddition of vinylcyclobutanones and 2π-components in analogy to the [5+2] cycloaddition of

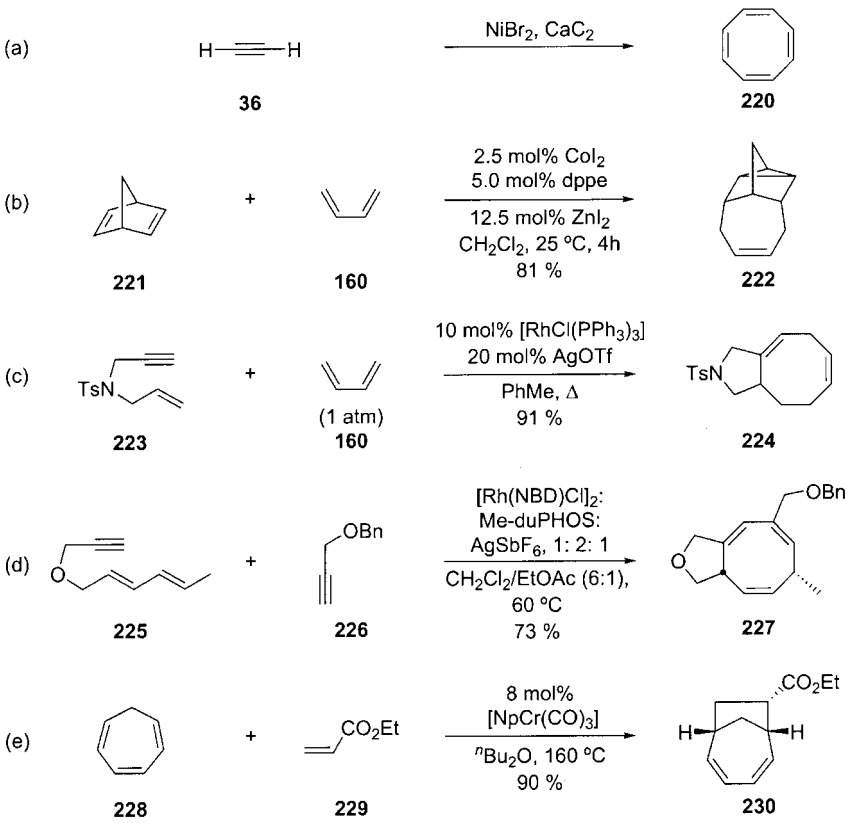

Scheme 13.18 Representative examples of transition metal-mediated cycloadditions for eight-membered ring synthesis.

VCPs and 2π-components and the subsequent development of the first [5+2+1] three-component cycloaddition approach to eight-membered ring synthesis.

13.7
Design and Development of [6+2] Cycloadditions of Vinylcyclobutanones

New reaction design is based on first principles and analogy. With the success of the VCP-based [5+2] cycloaddition, the idea was proposed that the process might work with vinylcyclobutanes, thereby providing a new [6+2] cycloaddition reaction (Scheme 13.19). This idea is not unreasonable at first glance, as the strain energies in a simple cyclopropane and cyclobutane are approximately equal (~27 kcal/mol and ~26 kcal/mol, respectively). Further, Liebeskind has shown that metal carbinyl cyclobutanes are equally adept at rhodium(I)-catalyzed strain-driven ring expansions to the cyclopropyl homologs (Scheme 13.9) [20]. Accordingly, an analogous mechanistic proposal can be written for a new reaction for the formation of eight-membered rings, involving the rhodium-catalyzed [6+2] cycloaddition of vinylcyclobutanes and π-systems [61].

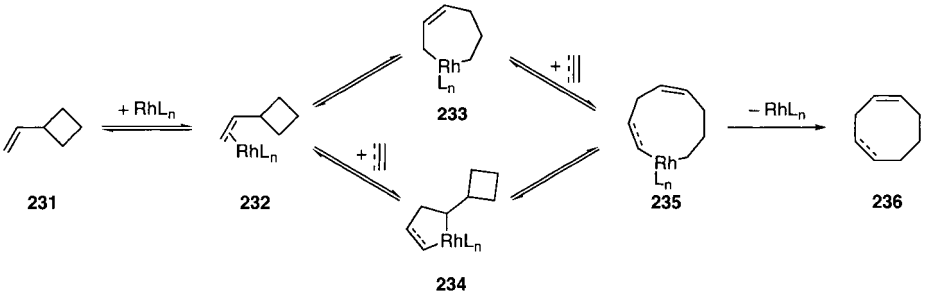

Scheme 13.19 Proposed mechanism for a [6+2] cycloaddition.

Initial attempts to effect the [6+2] cycloaddition with simple vinylcyclobutanes were unsuccessful. Either the substrates were unreactive or complex mixtures resulted. The work of Liebeskind (Scheme 13.9) [20] suggested that a vinylcyclobutanone might be a preferred 6 C component. Such systems are more strained and would be expected to encounter heteroatom-facilitated insertion.

With this revision in our original plans, both alkenes and allenes were found to undergo efficient cycloadditions to produce cyclooctenone products in a new [6+2] cycloaddition process. This novel cycloaddition has been shown to proceed efficiently with alkenes tethered with sulfonamide, ether, or geminal diester linkers (Tab. 13.15, see page 294). Isomerization of the olefin, a potential competing reaction in this process, is not observed. Methyl substitution of either alkene in the substrate is well tolerated, resulting in the facile construction of quaternary centers. Of mechanistic importance, in some cases cycloheptene byproducts were isolated from [6+2] cycloaddition reactions in addition to the expected cyclooctenone products (that is, entries 3 and 4).

13.8
Design and Development of Multi-component [5+2+1] Cycloadditions of VCPs, Alkynes, and CO

One of the major goals of organic synthesis is to produce target-relevant complexity with step economy. A relatively underdeveloped but highly significant approach to this goal is to develop multi-component reactions that allow the formation of many bonds from simple starting materials. Toward this goal, we speculated whether an intermediate in the previously described new two-component reactions could be trapped by additional components to produce an [*m*+*n*+*o*…(+*x*)] process. Ultimately, one could imagine very complex molecule synthesis being achieved in one operation by stitching together simple substrates on a multi-purpose catalyst or multi-catalyst ensemble.

In the course of our studies on the [6+2] cycloaddition, the formation of products arising from a [6+2–1] path was observed (Scheme 13.20). Conceptually, **249** produces the [6+2] cycloadduct **251**, but under certain conditions **49**, the [6+2–1] product, is observed, presumably arising through the conversion of **250** to **48**. Reflection on this observation suggests that one might start with VCP **41** and an alkyne and trap **48** with CO in the microscopic reverse of the **250**-to-**48** path to produce **251** by an overall three-component [5+2+1] cycloaddition. This idea worked.

Tab. 13.15 The first examples of [6+2] cycloadditions of vinylcyclobutanones.

Entry[a]	*Substrate*	*Catalyst, solvent*[b]	*Conditions*[c]	*Cycloadduct*		*Yield (%)*
1	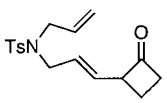 **237**	**A**	14 mM, 3 h	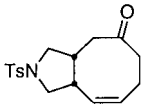 **238**		95
2	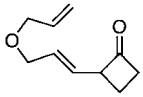 **239**	**B**	14 mM, 14 h	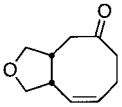 **240**		80
3	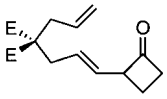 **241**	**B**	14 mM, 17 h	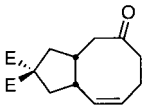 **242**	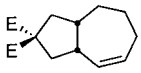 **63**	88 (10:1 **242**[d]/**63**)
4	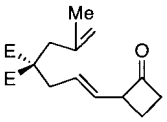 **243**	**B**	10 mM, 20 h	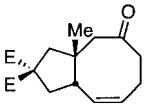 **244**	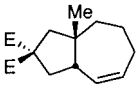 **65**	94 (4.5:1 **244**/**65**)
5	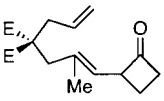 **245**	**B**	14 mM, 26 h	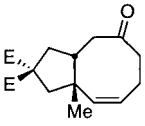 **246**		78
6	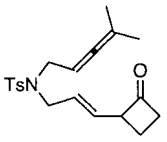 **247**	5 mol% {[RhCl(CO)$_2$]$_2$}	10 mM, 45 min	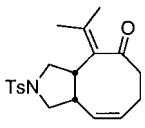 **248**		91

a) E = CO_2Me, Ts = *p*-toluenesulfonyl.
b) **A**: 10 mol% [RhCl(PPh_3)$_3$], 10 mol% silver triflate, **B**: 5 mol% {[RhCl(CO)$_2$]$_2$}, 10 mol% silver triflate, 10 mol% $^nBu_3P$; all reactions run in toluene.
c) Concentrations refer to substrate concentration in solvent; temperature is reflux (110 °C).
d) An additional 6% of *trans*-**242** was also collected.

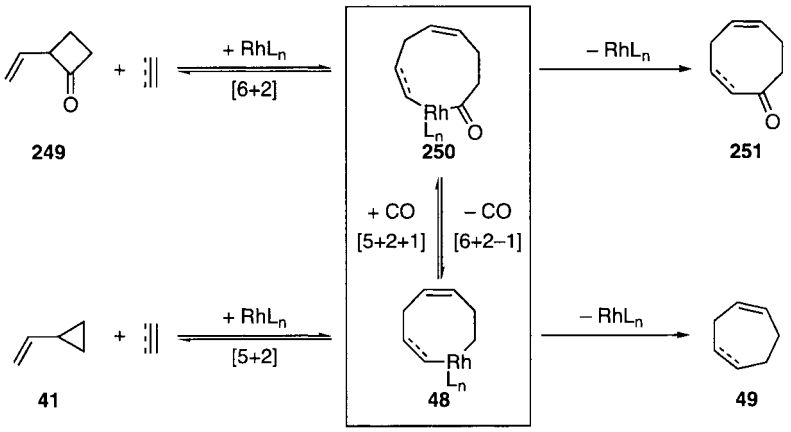

Scheme 13.20 Proposed mechanism of [6+2–1] and [5+2+1] cycloaddition reactions.

In accordance with the above mechanistic analysis, the first [5+2+1] cycloadditions of VCPs, alkynes, and CO have recently been reported [62]. The reaction proceeds in high yield and with high or exclusive regioselectivity with a variety of alkynes bearing carbonyl substituents, including alkynyl ketones, esters, amides, and even aldehydes. The regiochemistry of the cycloaddition is predictable, leading in all cases to CO insertion distal to the carbonyl substituent of the alkyne. Interestingly, the initially formed eight-membered ring products undergo a "bonus" transannular closure to give, after hydrolysis, bicyclo[3.3.0]octenone adducts (Tab. 13.16). These cycloadducts display diverse functional groups that are oriented in well-defined arrays as a result of the conformational inflexibility of the systems. As such they serve as new and superb scaffolds for combinatorial libraries and as building blocks for synthesis.

13.9 Conclusion

In this chapter we have described three new reactions that have been designed and advanced through the creativity and dedication of an exceptional group of co-workers. These new reactions represent only a portion of over 14 new processes that have arisen through the fusion of their efforts with the philosophical goal of achieving greater step economy. In closing, it is exciting to reflect on the origins of this program with the [4+4] and then [4+2] cycloadditions (still an under-exploited process that could solve many Diels–Alder cycloaddition problems), on the newly emerged [5+2], [6+2], and [5+2+1] processes, and on the emerging new two-, three-, and four-component processes, some of which will probably be appearing contemporaneously with this review.

Tab. 13.16 The first metal-catalyzed [5+2+1] cycloadditions.[a)]

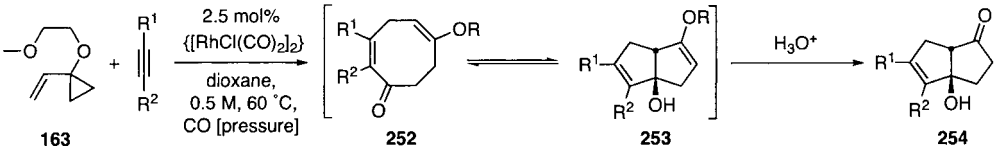

163 252 253 254

Entry	Alkyne	CO	Time	Product	Yield (%)
1	 255	2 atm	20 h	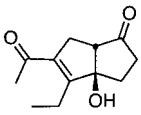 256	97
2	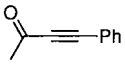 257	1 atm	26 h	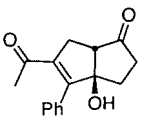 258	54
3	 259	1 atm	42 h	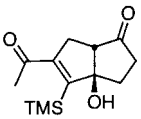 260	88
4	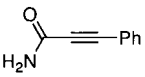 261	1 atm	40 h	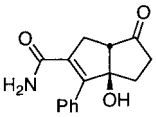 262	96
5	 263	2 atm	26 h	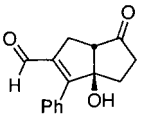 264	69[b)]
6	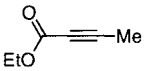 265	1 atm	20 h	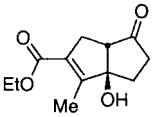 266	85[c)]

a) Relative stereochemistry indicated.
b) Also isolated 14% yield of [5+2] product.
c) Ratio of regioisomers 6:1 by ^{1}H-NMR.

13.10 References

1 (a) P.A. Wender, S.T. Handy, D.L. Wright, *Chem. Ind.* **1997**, 766; (b) P.A. Wender, *Chem. Rev.* **1996**, *96*, 1.

2 P.A. Wender, B.A. Miller, *Org. Synth. Theory Appl.* **1993**, *2*, 27.

3 P.A. Wender, R.J. Ternansky, *Tetrahedon Lett.* **1985**, *26*, 2625.

4 (a) C.P. Dell, *Contemp. Org. Synth.* **1997**, *4*, 87; (b) C.P. Dell, *J. Chem. Soc. Perkin Trans. 1* **1998**, 3873; (c) *Advances in Cycloaddition*; JAI Press: Greenwich, CT, **1988–1999**, Vols. 1–6; (d) W. Carruthers, *Cycloaddition Reactions in Organic Synthesis*; Pergamon: Elmsford, NY, **1990**.

5 (a) O. Diels, K. Alder, *Justus Liebigs Ann. Chem.* **1928**, *460*, 98. For representative reviews, see: (b) J.A. Norton, *Chem. Rev.* **1942**, *31*, 319; (c) J.G. Martin, R.K. Hill, *Chem. Rev.* **1961**, *61*, 537; (d) A. Wasserman, *Diels–Alder Reactions*; Elsevier: New York, **1965**; (e) G. Breiger, J.N. Bennett, *Chem. Rev.* **1980**, *80*, 63; (f) I. Fleming, in *Pericyclic Reactions*; Oxford University Press: Oxford, 1999, p. 7.

6 For reviews of transition metal-catalyzed cycloadditions, see: (a) C. Aubert, O. Buisine, M. Malacria, *Chem. Rev.* **2002**, *102*, 813; (b) L. Yet, *Chem. Rev.* **2000**, *100*, 2963; (c) I. Ojima, M. Tzamarioudaki, Z. Li, R. J. Donovan, *Chem. Rev.* **1996**, *96*, 635; (d) M. Lautens, W. Klute, W. Tam, *Chem. Rev.* **1996**, *96*, 49.

7 (a) P.W. Jolly, in *Comprehensive Organometallic Chemistry*, G. Wilkinson, F.G.A. Stone, E.W. Abel, Eds.; Pergamon: New York, **1982**, Vol. 8, pp. 613–797; (b) W. Keim, A. Behr, M. Roper, in *Comprehensive Organometallic Chemistry*, G. Wilkinson, F.G.A. Stone, E.W. Abel, Eds.; Pergamon: New York, **1982**, Vol. 8, pp. 371–461; (c) P.W. Jolly, G. Wilke, *The Organic Chemistry of Nickel*; Academic Press: New York, **1974–1975**, Vols. 1–2; (d) P. Heimbach, P.W. Jolly, G. Wilke, in *Advances in Organometallic Chemistry*, F.G.A. Stone, R. West, Eds.; Academic Press: New York, **1970**, Vol. 8, p. 29; (e) H. W. B. Reed, *J. Chem. Soc.* **1954**, 1931.

8 (a) P.A. Wender, N.C. Ihle, *J. Am. Chem. Soc.* **1986**, *108*, 4678; (b) P.A. Wender, N.C. Ihle, *Tetrahedron Lett.* **1987**, *28*, 2451; (c) P.A. Wender, N.C. Ihle, C.R.D. Correia, *J. Am. Chem. Soc.* **1988**, *110*, 5904; (d) P.A. Wender, M.L. Snapper, *Tetrahedron Lett.* **1987**, *28*, 2221; (e) P.A. Wender, M.J. Tebbe, *Synthesis* **1991**, 1089.

9 P.A. Wender, T.E. Smith, *Tetrahedron* **1998**, *54*, 1255.

10 For reviews of approaches to seven-membered ring synthesis, see: (a) P.A. Wender, J.A. Love, in *Advances in Cycloaddition*; JAI Press, Greenwich, **1999**, Vol. 5, pp. 1–45; (b) G. Dyker, *Angew. Chem.* **1995**, 107, 2407; *Angew. Chem. Int. Ed. Engl.* **1995**, *34*, 2223.

11 For reviews of [4+3] cycloadditions of allyl cations, see: (a) M. Harmata, *Acc. Chem. Res.* **2001**, *34*, 595; (b) J. Cha, J. Oh, *Curr. Org. Chem.* **1998**, *2*, 217; (c) J.H. Rigby, F.C. Pigge, *Org. React.* **1997**, *51*, 351; (d) M. Harmata, in *Advances in Cycloaddition*; M. Lautens, Ed; JAI Press: Greenwich, **1997**, Vol. 4, p. 41; (e) M. Harmata, *Tetrahedron* **1997**, *53*, 6235.

12 Recent examples include: (a) F. Lopez, L. Castedo, J.L. Mascareñas, *Org. Lett.* **2002**. *4*, 3683; (b) J.R. Rodriguez, A. Rumbo, L. Castedo, J.L. Mascareñas *J. Org. Chem.* **1999**, *64*, 4560; and references therein. For a review, see: A.R. Katrizky, N. Dennis, *Chem. Rev.* **1989**, *89*, 827; P.A. Wender, C.D. Jesudason, H. Nakahira, N. Tamura, A.L. Tebbe, Y. Ueno, *J. Am. Chem. Soc.* **1997**, *119*, 12 976.

13 (a) R. Herges, in *Chemical Structures*, W.A. Warr, Ed.; Springer-Verlag: Berlin, **1988**, pp. 385–398; (b) R. Herges, I. Ugi, *Chem. Ber.* **1986**, *119*, 829; (c) R. Herges, I. Ugi, *Angew. Chem.* 1985, 97, 596; *Angew. Chem. Int. Ed. Engl.* **1985**, *24*, 594; (d) M. Cristl, E. Brunn, F. Lanzendörfer, *J. Am. Chem. Soc.* **1984**, *106*, 373; (e) F.W. Fowler, *Angew. Chem.* **1971**, 87, 148; *Angew. Chem. Int. Ed. Engl.* **1971**, *24*, 135; (f) J.E. Baldwin, R.K. Pinschmidt, *Tetrahedron Lett.* **1971**, 935.

14 (a) D.K. Lewis, D.J. Charney, B.L. Kalra, A.-M. Plate, M.H. Woodard, S.J. Cianciosi, J.E. Baldwin, *J. Phys. Chem. A* **1997**, *101*, 4097; (b) D.G. Retzloff, B.M. Coull, J. Coull, *J. Phys. Chem.* **1970**, *74*, 2455; (c) C.A. Wellington, *J. Phys. Chem.* **1962**, *66*,

1671; (d) M.C. Flowers, H.M. Frey, *J. Chem. Soc.* **1961**, 3547.

15 (a) B.M. Trost, D.T. MacPherson, *J. Am. Chem. Soc.* **1987**, *109*, 3483; (b) B.M. Trost, S. Schneider, *Angew. Chem.* **1989**, *101*, 215; *Angew. Chem. Int. Ed. Engl.* **1989**, *28*, 213.

16 (a) K.E. Schwiebert, J.M. Stryker, *J. Am. Chem. Soc.* **1995**, *117*, 8275; (b) N. Etkin, T.L. Dzwiniel, K.E. Schweibert, J.M. Stryker, *J. Am. Chem. Soc.* **1998**, *120*, 9702; (c) T.L. Dzwiniel, N. Etkin, J.M. Stryker, *J. Am. Chem. Soc.* **1999**, *121*, 10 640.

17 I. Ojima, S.Y. Lee, *J. Am. Chem. Soc.* **2000**, *122*, 2385.

18 R.I. Khusnutdinov, U.M. Dzhemilev, *J. Organomet. Chem.* **1994**, *471*, 1.

19 For lead references, see: (a) M.P. Doyle, D. Van Leusen, *J. Org. Chem.* **1982**, *47*, 5326; (b) M.P. Doyle, D. Van Leusen, *J. Am. Chem. Soc.* **1981**, *103*, 5917; (c) R.G. Salomon, M.F. Salomon, J.L.C. Kachinski, *J. Am. Chem. Soc.* **1977**, *99*, 1043; (d) H.W. Voigt, J.A. Roth, *J. Catal.* **1974**, *33*, 91; (e) M.F. Salomon, R.G. Salomon *J. Chem. Soc., Chem. Commun.* **1976**, *3*, 89; (f) I. Ryu, K. Ikura, Y. Tamura, J. Maenaka, A. Ogawa, N. Sonoda, *Synlett* **1994**, 941.

20 (a) M.A. Huffman, L.S. Liebeskind, *J. Am. Chem. Soc.* **1991**, *113*, 2771; (b) M.A. Huffman, L.S. Liebeskind, W.T. Pennington, *Organometallics* **1992**, *11*, 255; M.A. Huffman, L.S. Liebeskind, *J. Am. Chem. Soc.* **1993**, *115*, 4895.

21 P.A. Wender, H. Takahashi, B. Witulski, *J. Am. Chem. Soc.* **1995**, *117*, 4720.

22 P.A. Wender, C.O. Husfeld, E. Langkopf, J.A. Love, *J. Am. Chem. Soc.* **1998**, *120*, 1940.

23 P.A. Wender, A.J. Dyckman, C.O. Husfeld, D. Kadereit, J.A. Love, H. Rieck, *J. Am. Chem. Soc.* **1999**, *121*, 10 442.

24 P.A. Wender, C.O. Husfeld, E. Langkopf, J.A. Love, N. Pleuss, *Tetrahedron* **1998**, *54*, 7203; P.A. Wender, L.O. Haustedt, J. Lim, J.A. Love, T.J. Williams, J.-Y. Yoon, Stanford University, unpublished results.

25 P.A. Wender, F. Glorius, C.O. Husfeld, E. Langkopf, J.A. Love, *J. Am. Chem. Soc.* **1999**, *121*, 5348.

26 Other metals screened include Fe, Co, Ni, Ru, Pd, Ir, and Pt.

27 P.A. Wender, D. Sperandio, *J. Org. Chem.* **1998**, *63*, 4164.

28 B. Wang, P. Cao, X. Zhang, *Tetrahedron Lett.* **2000**, *41*, 8041.

29 S.R. Gilbertson, G.S. Hoge, *Tetrahedron Lett.* **1998**, *39*, 2075.

30 P.A. Wender, T.J. Williams, *Angew. Chem.* **2002**, *114*, 4732; *Angew. Chem. Int. Ed.* **2002**, *41*, 4550.

31 (a) B.M. Trost, F.D. Toste, H. Shen, *J. Am. Chem. Soc.* **2000**, *122*, 2379; (b) B.M. Trost, H.C. Shen, *Org. Lett.* **2000**, *2*, 2523; (c) B.M. Trost, H.C. Shen, *Angew. Chem.* **2001**, *113*, 2375; *Angew. Chem. Int. Ed.* **2001**, *40*, 2313; (d) B.M. Trost, F.D. Toste, *Angew. Chem.* **2001**, *113*, 1148; *Angew. Chem. Int. Ed.* **2001**, *40*, 1114.

32 For examples see: (a) P.A. Wender, T.E. Jenkins, *J. Am. Chem. Soc.* **1989**, *111*, 6432; (b) P.A. Wender, T.E. Jenkins, S. Suzuki, *J. Am. Chem. Soc.* **1995**, *117*, 1843.

33 For examples see: (a) R.S. Jolly, G. Luedtke, D. Sheehan, T. Livinghouse, *J. Am. Chem. Soc.* **1990**, *112*, 4965; (b) L. McKinstry, T. Livinghouse, *Tetrahedron* **1994**, *50*, 6145.

34 S.-J. Paik, S.U. Son, Y.K. Chung, *Org. Lett.* **1999**, *1*, 2045.

35 M. Scotti, M. Valderrama, R. Ganz, H. Werner, *J. Organomet. Chem.* **1985**, *286*, 399. Other silver salts are known to be effective.

36 D.P. Fairlie, B. Bosnich, *Organometallics* **1988**, *7*, 936.

37 P.A. Wender, J.A. Love, T.J. Williams, *Synlett* **2003**, 1295.

38 P.A. Wender, A.J. Dyckman, *Org. Lett.* **1999**, *1*, 2089.

39 For brevity, only one mechanistic possibility is presented. An alternative set of mechanistic possibilities can be formulated around the initial formation of metallacyclohexenes followed then by coordination to the tethered alkyne and convergence on the advanced intermediates **E** and **E′**. Although differing in the timing of connections, the issues of regio- and stereoselectivity are treated similarly.

40 P.A. Wender, M. Fuji, C.O. Husfeld, J.A. Love, *Org. Lett.* **1999**, *1*, 137.

41 P.A. Wender, L. Zhang, *Org. Lett.* **2000**, *2*, 2323.

42 Reviewed in: D.L. Wright, C.R. Whitehead, *Org. Prep. Proc. Int.* **2000**, *32*, 307. For total syntheses of cyathane diterpenes, see: (a) B.B. Snider, N.H. Vo, S.V. O'Neil, B.M. Foxman, *J. Am. Chem. Soc.* **1996**, *118*,

7644; (b) M. Tori, N. Toyoda, S. Sono, *J. Org. Chem.* **1998**, *63*, 306; (c) E. Piers, M. Gilbert, K.L. Cook, *Org. Lett.* **2000**, *2*, 1407; (d) D.E. Ward, Y.Z. Gai, Q. Qiao, *Org. Lett.* **2000**, *2*, 2125. For synthetic approaches to cyathanes, see: (d) W.A. Ayer, D.E. Ward, L.M. Browne, L.T. Delbaere, Y. Hoyano, *Can. J. Chem.* **1981**, *59*, 2665; (e) D.E. Ward, *Can. J. Chem.* **1987**, *65*, 2380; (f) L.A. Paquette, K.R. Dahnke, *J. Org. Chem.* **1994**, *59*, 885; (g) P. Magnus, L. Shen, *Tetrahedron* **1999**, *55*, 3553; (h) D.L. Wright, C.R. Whitehead, H. Sessions, I. Ghiviriga, D.A. Frey, *Org. Lett.* **1999**, *1*, 1535; (i) K. Takeda, D. Nakane, M. Takeda, *Org. Lett.* **2000**, *2*, 1903.

43 P.A. Wender, F.C. Bi, M.A. Brodney, F. Gosselin, *Org. Lett.* **2001**, *3*, 2105.

44 P.A. Wender, H. Rieck, M. Fuji, *J. Am. Chem. Soc.* **1998**, *120*, 10976.

45 There is only a single published example of an intermolecular [5+2] cycloaddition catalyzed by Wilkinson's catalyst, in which a constrained VCP is reacted with acetylene: P. Binger, P. Wedmann, S.I. Kozhushkov, A.E. de Meijere, *J. Org. Chem.* **1998**, 113. This appeared after our initial report in 1995 (ref. 21).

46 Prepared by analogy to the methods in the following: (a) J. Salaün, J. Marguerite, *Org. Synth.* **1985**, *63*, 147; (b) H.H. Wasserman, M.J. Hearn, R.E. Cochoy, *J. Org. Chem.* **1980**, *45*, 2874.

47 P.A. Wender, A.J. Dyckman, C.O. Husfeld, M.J.C. Scanio, *Org. Lett.* **2000**, *2*, 1609.

48 On the basis of retail cost of reagents, **142** costs approximately ten-fold less than **163**.

49 P.A. Wender, G.G. Gamber, M.J.C. Scanio, *Angew. Chem.* **2001**, *113*, 4013; *Angew. Chem. Int. Ed.* **2001**, *40*, 3895.

50 (a) V.V. Plemenkov, O.J. Butenko, V.V. Zverev, L.V. Ermolaeva, V.M. Vakar, A.V. Ignatchenko, I.G. Bolesov, *J. Mol. Struct.* **1990**, *218*, 195; (b) G. De Mare, *J. Mol. Struct. (THEOCHEM)* **1987**, *153*, 341.

51 P.A. Wender, C.M. Barzilay, A.J. Dyckman, *J. Am. Chem. Soc.* **2001**, *123*, 179.

52 (a) D.L. Boger, S.M. Weinreb, *Hetero-Diels–Alder Methodology in Organic Synthesis*; Academic Press: New York, **1987**; (b) S.M. Weinreb, P.M. Scola, *Chem. Rev.* **1989**, *89*, 1525.

53 P.A. Wender, T.M. Pedersen, M.J.C. Scanio, *J. Am. Chem. Soc.* **2002**, *124*, 15 154.

54 (a) G. Mehta, V. Singh, *Chem. Rev.* **1999**, *99*, 881; (b) S. McN. Sieburth, N.T. Cunard, *Tetrahedron*, **1996**, *52*, 6251; (c) G. Illuminati, L. Mandolini, *Acc. Chem. Res.* **1981**, *14*, 95.

55 (a) W. Reppe, O. Schlichting, K. Klager, T. Toepel, *Justus Liebigs Ann. Chem.* **1948**, *560*, 1; (b) P.W. Jolly, in *Comprehensive Organometallic Chemistry*, G. Wilkinson, F.G.A. Stone, E.W. Able, Eds.; Pergamon: New York, **1982**; Vol. 8, p. 649.

56 A. Greco, A. Carbonara, G. Dall'Asta, *J. Org. Chem.* **1970**, *35*, 271.

57 (a) A. Carbonara, F. Cambisi, G. Dall'Asta, *J. Org. Chem.* **1971**, *36*, 1443; (b) M. Lautens, W. Tam, C. Sood, *J. Org. Chem.* **1993**, *58*, 4513; (c) M. Lautens, W. Tam, J.C. Lautens, L.G. Edwards, C.M. Crudden, A.C. Smith, *J. Am. Chem. Soc.* **1995**, *117*, 6863; (d) Y. Chen, J.K. Snyder, *J. Org. Chem.* **2001**, *66*, 6932.

58 P.A. Evans, J.E. Robinson, E.W. Baum, A.N. Fazal, *J. Am. Chem. Soc.* **2002**, *124*, 8782.

59 S.R. Gilbertson, B. DeBoef, *J. Am. Chem. Soc.* **2002**, *124*, 8784.

60 (a) J.H. Rigby, J.A. Henshilwood, *J. Am. Chem. Soc.* **1991**, *113*, 5122; (b) I. Fischer, F.-W. Grevals, J. Leitich, S. Özkar, *Chem. Ber.* **1991**, *124*, 2857; (c) K. Chaffee, J.B. Sheridan, A. Aistars, *Organometallics* **1992**, *11*, 18. For reviews of [6+2] cycloadditions: (d) J.H. Rigby, *Org. React.* **1997**, *49*, 331; (e) J.H. Rigby, *Tetrahedron*, **1999**, *55*, 4521.

61 P.A. Wender, A.G. Correa, Y. Sato, R. Sun, *J. Am. Chem. Soc.* **2000**, *122*, 7815.

62 P.A. Wender, G.G. Gamber, R.D. Hubbard, L. Zhang, *J. Am. Chem. Soc.* **2002**, *124*, 2876.

14
Rhodium(II)-Stabilized Carbenoids Containing Both Donor and Acceptor Substituents

Huw M. L. Davies and Abbas M. Walji

14.1
Introduction

The metal-catalyzed decomposition of diazo compounds has broad applications in organic synthesis [1–8]. Transient metal carbenoids provide important reactive intermediates that are capable of a wide variety of useful transformations, in which the catalyst dramatically influences the product distribution [5]. Indeed, the whole field of diazo compound decomposition was revolutionized in the early 1970s with the discovery that dirhodium tetracarboxylates **1** are effective catalysts for this process [9]. Many of the reactions that were previously low-yielding using conventional copper catalysts were found to proceed with unparalleled efficiency using this particular rhodium catalysis. The field has progressed extensively and there are some excellent reviews describing the breadth of this chemistry [5, 7, 10–17].

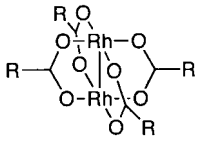

1

By far the most extensively used classes of rhodium carbenoids have been those derived from diazo compounds containing one or two electron-withdrawing groups [1, 2, 4, 12, 18–20]. These carbenoids are highly reactive and behave as very electrophilic species [5]. This chapter focuses on a different class of rhodium carbenoid intermediate, namely the donor/acceptor-substituted system **2**. Since the early 1980s we, and most recently others, have been exploring the chemistry of these donor/acceptor-substituted carbenoids, based on the discovery that they have a very different reactivity profile from that of the conventional carbenoids [15, 16, 21]. For example, donor/acceptor carbenoids undergo many types of highly chemoselective and stereoselective reactions due to the ability of the donor group to moderate the reactivity of the carbenoids [11, 22, 23]. Several reviews have been published on various reactions of donor/acceptor carbenoids [11, 13–15, 24, 25]. This chapter gives an overview of the major reactions of the donor/acceptor carbenoids and highlights the recent advances in the field.

Modern Rhodium-Catalyzed Organic Reactions. Edited by P. Andrew Evans

ISBN: 3-527-30683-8

donor/acceptor substituted carbenoid

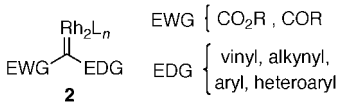

Section 14.2 describes the highly stereoselective cyclopropanation chemistry of the donor/acceptor-carbenoids (Fig. 14.1 a) [16]. This section introduces the range of vinyl, aryl, alkynyl, and heteroaryl functionalities that have been used as donor groups in this chemistry. Also, chiral auxiliaries and chiral catalysts that achieve high asymmetric induction in this chemistry are described [25]. The next two sections cover chemistry that is unique to the vinylcarbenoid system, namely [3+4] cycloaddition with dienes (Fig. 14.1 b; see also Section 14.3) [13] and [3+2] cycloaddition with vinyl

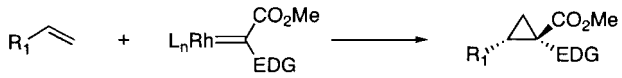

a Cyclopropanation

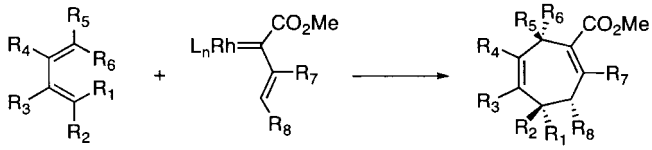

b [3+4] Cycloaddition

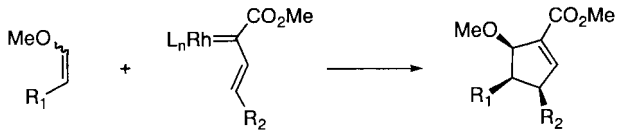

c [3+2] Cycloaddition

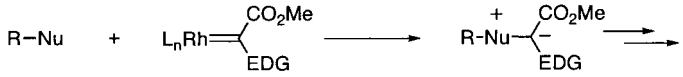

d Ylide Transformations

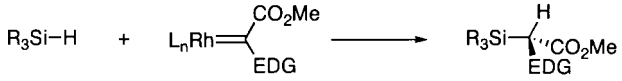

e Si-H Insertion

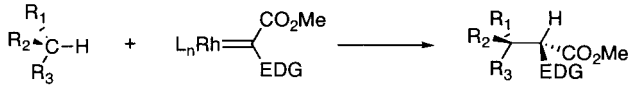

f C-H Activation

Fig. 14.1

ethers (Fig. 14.1 c; see also Section 14.4) [11, 26]. Both transformations can generate products containing multiple stereogenic centers with very high diastereo- and enantioselectivity. This is followed by an overview of the reactions of these carbenoids with various nucleophiles to generate transient ylides (Fig. 14.1 d; see also Section 14.5) [27]. Carbenoid insertion into nonpolar X–H bonds will be covered next with a separate section for Si–H insertion reactions (Fig. 14.1 e; see also Section 14.6) [28, 29]. Section 14.7 covers the spectacular C–H activation chemistry that is possible by means of the C–H insertion reactions of these carbenoids (Fig. 14.1 f) [14, 15, 17]. The enhanced stability of these carbenoids, in comparison to the traditional ones, is a crucial factor that has enabled the asymmetric intermolecular version of this chemistry to be developed into a highly practical reaction [17].

14.2 Cyclopropanation

The major challenge with the cyclopropanation chemistry of carbenoids derived from diazoacetates containing just an electron-acceptor group is the issue of diastereocontrol [16]. In general, the diastereoselectivity is very poor with virtually all catalysts, and reasonable results can only be obtained using diazoacetates possessing bulky esters [30]. Recently, diastereoselective examples with cobalt [31, 32] and ruthenium based catalysts have been reported [33, 34]. In contrast, reactions with the donor/acceptor carbenoids are routinely highly diastereoselective. The dramatic difference can be readily seen in comparing the rhodium acetate-catalyzed cyclopropanation of styrene with different carbenoid systems (Tab. 14.1). The reactions with phenyldiazoacetate **3** and phenylvinyldiazoacetate **4** are highly diastereoselective (>30:1) [22, 35–39], whereas poor diastereoselectivity (1.6:1) is observed in the reaction with ethyl diazoacetate **5** [2]. Hammett studies have shown that the cyclopropanation with the donor/acceptor-substituted carbenoids is much more chemoselective than cyclopropanation with either ethyl diazoacetate or methyl diazomalonate [39]. The diastereoselectivity of the cyclopropanation is dependent on the structure of the alkene, with electron-rich alkenes such as styrenes and vinyl ethers affording optimal results [35]. Another major distinction between the donor/acceptor-substituted carbenoids and those derived from unsubstituted diazoacetates is that they are much more sterically demanding. They can effectively cyclopropanate only 1-substituted, 1,1-disubstituted, and *cis*-1,2-disubstituted alkenes [16, 40], while ethyl diazoacetate is known to cyclopropanate even tetrasubstituted alkenes [41].

Tab. 14.1 Highly diastereoselective cyclopropanations by donor/acceptor-substituted carbenoids.

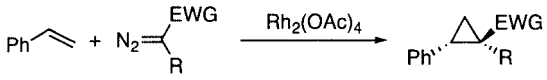

Diazo	*R*	*EWG*	*trans:cis*
3	Ph	CO_2Me	>30:1
4	CH=CHPh	CO_2Me	>50:1
5	H	CO_2Et	1.6:1

Tab. 14.2 Asymmetric cyclopropanation using (*R*)-pantolactone as the chiral auxiliary.

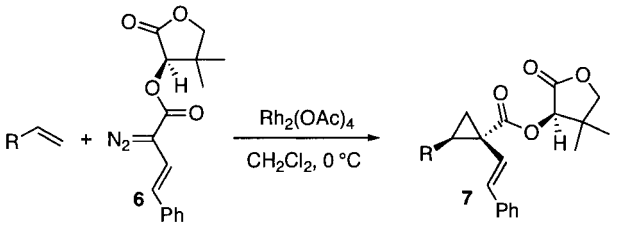

R	*Yield (%)*	*de (%)*
Ph	84	97
p-ClPh	92	95
p-OMePh	75	95
OEt	71	92
OAc	42	90

Tab. 14.3 Asymmetric cyclopropanation using rhodium prolinates as chiral catalysts.

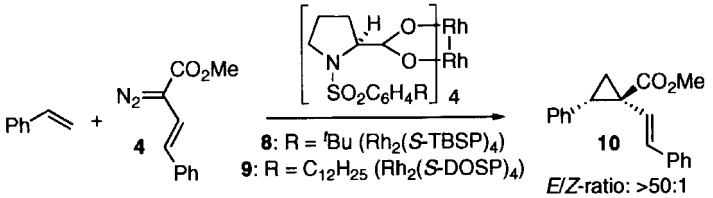

Catalyst	*Temp. °C*	*ee (5)*	
		Pentane	*CH_2Cl_2*
Rh_2(*S*-TBSP)$_4$	25	90	74
Rh_2(*S*-DOSP)$_4$	25	92	74
Rh_2(*S*-DOSP)$_4$	–78	98	–

The introduction of *β*-hydroxy esters as chiral auxiliaries for the cyclopropanation chemistry of the donor/acceptor carbenoids has been very successful [42]. The highest levels of asymmetric induction are obtained using (*R*)-pantolactone as a chiral auxiliary on the vinylcarbenoid **6** (Tab. 14.2). The carbonyl functionality of the auxiliary is proposed to have a major influence in controlling the facial selectivity of the ensuing cyclopropanation by interacting with the prochiral rhodium carbenoid [42]. This neighboring group participation has further implications for modulating the reactivity of the carbenoids, in addition to the asymmetric induction [43, 44].

An alternative strategy for achieving high asymmetric induction in these cyclopropanations has been the use of chiral catalysts. Dirhodium tetraprolinates have been shown to be exceptional catalysts for this chemistry, especially the hydrocarbon-soluble catalysts,

Tab. 14.4 Catalytic asymmetric cyclopropanation using methyl phenylvinyldiazoacetate.

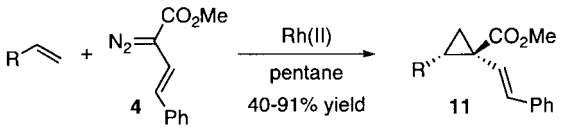

R	*ee at 25°C (%)* *Rh_2(S-TBSP)$_4$ (8)*	*ee at –78°C (%)* *Rh_2(S-DOSP)$_4$ (9)*
Ph	90	98
p-ClPh	89	>97
p-MeOPh	83	90
AcO	76	95
EtO	59	93
^{n}Bu	>90	–
Et	>95	–
^{i}Pr	95	–

Rh_2(*S*-TBSP)$_4$ **8** and Rh_2(*S*-DOSP)$_4$ **9** (Tab. 14.3) [40, 45]. A very unusual feature of the prolinate-catalyzed cyclopropanations is that the reactions proceed with much higher asymmetric induction when hydrocarbon solvents are used instead of dichloromethane [40, 45]. Room-temperature cyclopropanations of styrene with Rh_2(*S*-TBSP) or Rh_2(*S*-DOSP)$_4$ typically occur with 90–92% enantioselectivity, while the Rh_2(*S*-DOSP)$_4$-catalyzed reaction at –78°C occurs in 98% enantiomeric excess (Tab. 14.3) [40]. The rhodium prolinate catalysts are very easy to handle, being stable to air, heat, and moisture; although it has been reported that the enantioselectivity can decrease if the cyclopropanation is conducted in wet solvents [46].

The cyclopropanation utilizing donor/acceptor rhodium carbenoids can be extended to a range of monosubstituted alkenes, occurring with very high asymmetric induction (Tab. 14.4) [40]. Reactions with electron-rich alkenes, where low enantioselectivity was observed at room temperature, could be drastically improved using the more hydrocarbon-soluble Rh_2(*S*-DOSP)$_4$ catalyst at –78°C. The highest enantioselectivity is obtained when a small ester group such as a methyl ester is used [40], a trend which is the opposite to that seen with the unsubstituted diazoacetate system [16].

Carbenoids derived from the aryldiazoacetates are excellent donor/acceptor systems for the asymmetric cyclopropanation reaction [22]. Methyl phenyldiazoacetate **3** cyclopropanation of monosubstituted alkenes catalyzed by Rh_2(*S*-DOSP)$_4$ is highly diastereo- and enantioselective (Tab. 14.5) [22]. Higher enantioselectivities can be obtained when these reactions are performed at –78°C, as the catalyst maintains high solubility and activity at this temperature. The phenyldiazoacetate system has been evaluated using many popular rhodium(II) and copper catalysts; the rhodium(II) prolinates have proven to be superior catalysts for this class of carbenoids [37, 38].

The alkynyldiazoacetate **13** is a unique donor/acceptor system due to the linearity of the donor substituent. This allows the evaluation of the electronic influence on the stereoselectivity, by using alkyne as a donor group [47]. Indeed, the donor/acceptor combination is operative as phenylethynyldiazoacetate **13** maintains high diastereo- and enantioselec-

Tab. 14.5 Catalytic asymmetric cyclopropanation using methyl phenyldiazoacetate (**3**).

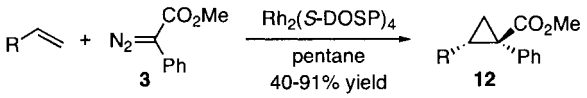

R	*ee at 25°C (%)*	*ee at –78°C (%)*
Ph	89	92
p-ClPh	85	88
p-MeOPh	88	–
EtO	66	86
^{n}BuO	64	89
^{n}Bu	80	84

Tab. 14.6 Catalytic asymmetric cyclopropanation using alkynyldiazoacetate **13**.

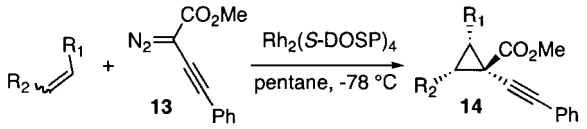

R_1	R_2	*Yield (%)*	*de (%)*	*ee (%)*
Ph	H	68	84	89
OBu	H	66	>94	87
OAc	H	61	>94	95
OEt	Ph	50	>94	45

tivity in cyclopropanation reactions catalyzed by Rh_2(*S*-DOSP)$_4$ (Tab. 14.6) [47]. A similar lack of reactivity with *trans*-alkenes was established in the reaction of **13** with a 1:1 mixture of *E*- and *Z*-methyl propenyl ethers. A single diastereomer was obtained in 45% enantiomeric excess, which demonstrates that the alkynylcarbenoids display similar diastereoselectivity to the vinyl- and phenylcarbenoid counterparts [47].

A further class of donor/acceptor-substituted carbenoids capable of highly diastereoselective cyclopropanations comprises heteroaryldiazoacetates **15** (Tab. 14.7) [48]. Both electron-rich and electron-deficient heterocycles are able to stabilize the resulting electrophilic carbenoid, and thus modulate its reactivity. Asymmetric cyclopropanation of styrene by **15** using Rh_2(*S*-DOSP)$_4$ as the catalyst gave high enantioselectivities, with the exception of methyl *N*-BOC-indolediazoacetate and methyl pyridinediazoacetate [48]. Even though alkanes are the optimum solvents for high asymmetric induction, cosolvents can be used, if required, to solubilize the heteroaryldiazoacetates [48]. Catalyst poisoning by strongly basic sites on the heteroaryldiazoacetates is a limitation; nonetheless, basic heterocycles such as pyridines are compatible with this chemistry.

A variety of chiral catalysts have been evaluated in intermolecular cyclopropanations of donor/acceptor carbenoid systems, but few come close to the levels of asymmetric induction furnished by the prolinate catalysts [11, 37, 38, 40, 49]. The only system that

Tab. 14.7 Catalytic asymmetric cyclopropanation using heteroaryldiazoacetates **15**.

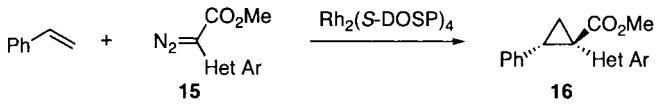

Product	*Yield (%)*	*de (%)*	*ee (%)*	*Product*	*Yield (%)*	*de (%)*	*ee (%)*
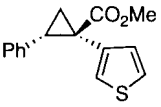	87	96	89	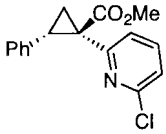	79	98	72
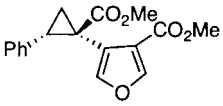	91	96	86	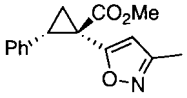	84	93	86
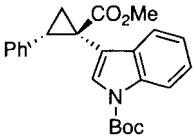	82	94	12	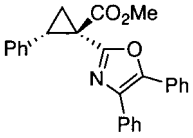	81	96	71
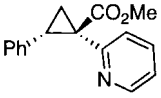	58	91	47	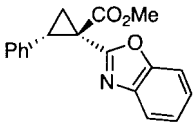	68	85	71

compares favorably with Rh_2(*S*-TBSP)$_4$ or Rh_2(*S*-DOSP)$_4$ is the bridged prolinate catalyst Rh_2(*S*-biTISP)$_2$ **17** [50]. Catalysts **17** and **18** were designed as rigid D_2-symmetric versions of the prolinate catalysts, and Rh_2(*S*-biTISP)$_2$ in particular is capable of very high asymmetric induction [50]. In certain respects, Rh_2(*S*-biTISP)$_2$ is superior to the tetraprolinate catalysts as it appears to be much more robust under conditions of high substrate-to-catalyst (S/C) ratios [51]. A spectacular example is the reaction of the phenyldiazoacetate **3** with styrene at a S/C ratio of 100 000 : 1 (Eq. 1). Only 3.7 mg of Rh_2(*S*-biTISP)$_2$ is required to catalyze the complete decomposition of 35 g of **3**. The crude cyclopropane **19** is initially formed in 92% yield with 85% enantiomeric excess, and after a single recrystallization **19** was enriched to 99.3% enantiomeric excess (75% yield) [51].

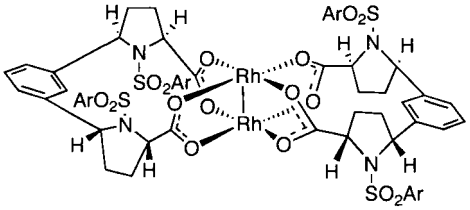

17: Rh_2(*S*-biTISP)$_2$: Ar = 2,4,6-tri-^{i}PrC$_6$H$_2$
18: Rh_2(*S*-biDOSP)$_2$: Ar = *p*-($C_{12}H_{25}$)C_6H_4

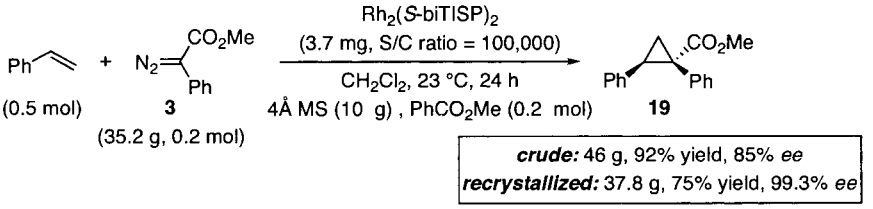

(1)

crude: 46 g, 92% yield, 85% *ee*
recrystallized: 37.8 g, 75% yield, 99.3% *ee*

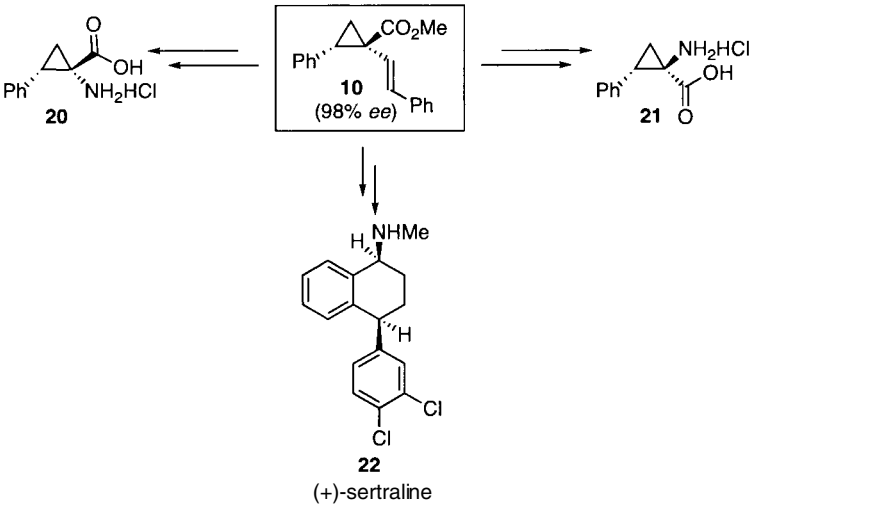

Scheme 14.1 Major transformations of donor/acceptor-substituted carbenoids.

The vinylcyclopropane **10** is a useful chiral building block for organic synthesis, as the vinyl group can be oxidatively cleaved if desired and further functionalized (Scheme 14.1). Either diastereomer **20** or **21** of the cyclopropane analog of phenylalanine can be readily prepared from **10** [40]. Corey has reported another elegant application of the vinylcyclopropane **10** in the asymmetric synthesis of the antidepressant (+)-sertraline **22** [52].

Another application of this chemistry is the asymmetric synthesis of the cyclopropane analog **25** of the breast cancer treatment agent tamoxifen **26** (Scheme 14.2) [53]. The Rh_2(*S*-DOSP)$_4$-catalyzed reaction of phenyldiazoacetate **3** with diarylethylene **23** at

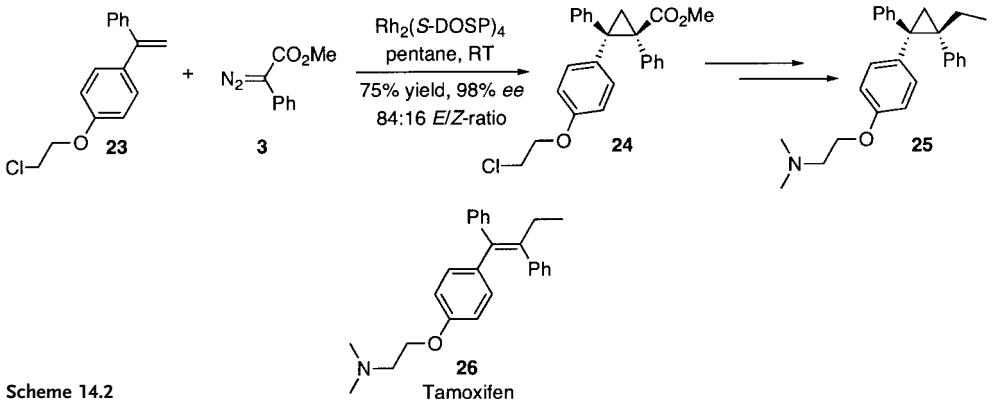

Scheme 14.2

room temperature generated the triarylcyclopropane **24** in 75% yield (68% *de*, 98% *ee*), which was easily converted to **25** using standard chemistry [53].

Solid-phase carbenoid chemistry is a relatively underdeveloped field within combinatorial chemistry. Only a few examples of heterogeneous carbenoid reactions in which the diazo compound is immobilized on a solid support have appeared in the literature [54–61]. The major difficulty is the high reactivity of the carbenoid intermediates, which precludes effective capture in heterogeneous reactions. The enhanced stability of the donor/acceptor-substituted carbenoids makes these systems much more effective for solid-phase reactions [62]. An example of this is the reaction of phenyldiazoacetate **3** with the immobilized diarylethylene **27**, in which the cyclopropane **28** was formed in 93% yield (Eq. 2). The importance of the donor/acceptor-substituted carbenoid for the success of this chemistry was convincingly demonstrated, since the corresponding reaction with ethyl diazoacetate gave very low conversions with the immobilized trapping reagent **27** [62].

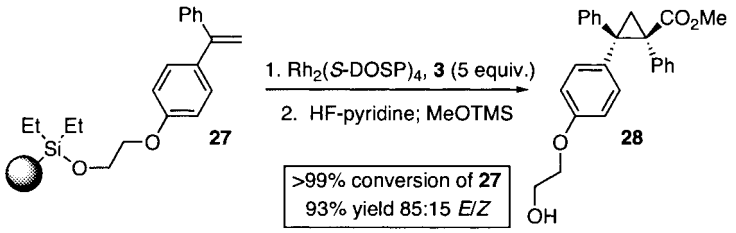

(2)

An interesting extension within solid-phase carbenoid chemistry is the development of the dirhodium tetraprolinates as reusable catalysts [63]. Several strategies have been developed for the immobilization of chiral catalysts for carbenoid chemistry, but very few heterogeneous catalysts maintain high stereoselectivity upon reuse [64–67]. The more stabilized nature of the donor/acceptor-substituted carbenoids is advantageous for ensuring that the catalysts are recoverable and reusable. By taking advantage of the dimeric nature of the rhodium(II) complexes, a novel noncovalent binding design has been proposed for attaching the complex to the solid support [63]. One rhodium metal

atom of the complex was coordinated to the polymer, while the other rhodium metal atom was involved in the catalytic reaction. Exceptional results have been obtained with immobilized bridged prolinate $Rh_2(S\text{-biTISP})_2$ **29**, when evaluated for the standard asymmetric cyclopropanation of methyl phenyldiazoacetate with styrene. The immobilized **29** was recycled 15 times, furnishing the cyclopropane **19** without loss in enantioselectivity (85–88% *ee*) and maintaining the yield (87–91%) (Eq. 3) [63].

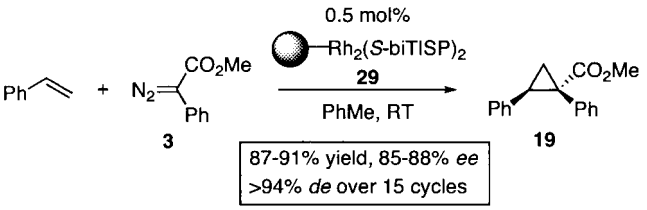

(3)

The high stereoselectivity obtained in the cyclopropanation reactions of the donor/acceptor carbenoids may be rationalized using the cyclopropanation model outlined in Fig. 14.2. A concerted, nonsynchronous mechanism has been proposed where charge build-up takes place in the transition state [40]. Evidence of the charge build-up has been established through the formation of products derived from zwitterionic intermediates [40]. A highly constricted approach of the alkene from over the electron-withdrawing group (EWG) in a side-on manner forces the alkene's substituents to point away from the catalyst. As a consequence *trans*-substituted alkenes are unable to approach the carbenoid and therefore do not react [40]. Cyclopropane formation is completed with the required bond rotation outward, which sets up the relative *cis*-stereochemistry between the R_1 group and the electron-donating group (EDG).

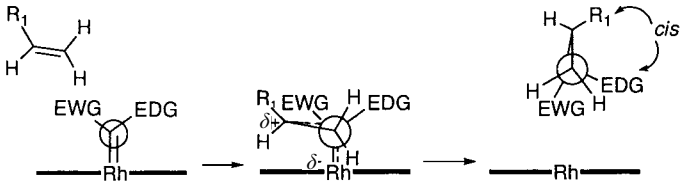

Fig. 14.2 Model for diastereoselection

The general model presented above has been very useful for rationalizing the asymmetric induction observed in reactions using chiral auxiliaries and catalysts. In the (*R*)-pantolactone auxiliary system, an electronic interaction between the lactone carbonyl and the carbenoid carbon locks the complex in conformation **30** (Fig. 14.3 a) [42]. This exposes the *si* face of the carbenoid for attack by the alkene, which, by applying the trajectory proposed in Fig. 14.2, forms the (1*R*, 2*R*) diastereomer predominantly [37, 42]. A similar hypothetical model has been proposed for the chiral prolinate catalysts. The most stable conformation of these catalysts is believed to have D_2 symmetry wherein the sulfonyl prolinate ligands are aligned in an "up–down–up–down" arrangement [25, 40]. Once the carbenoid is formed, its *si* face is protected by a sulfonyl ligand behaving as a blocking group **31** (Fig. 14.3 b). Approach of the alkene takes place over the elec-

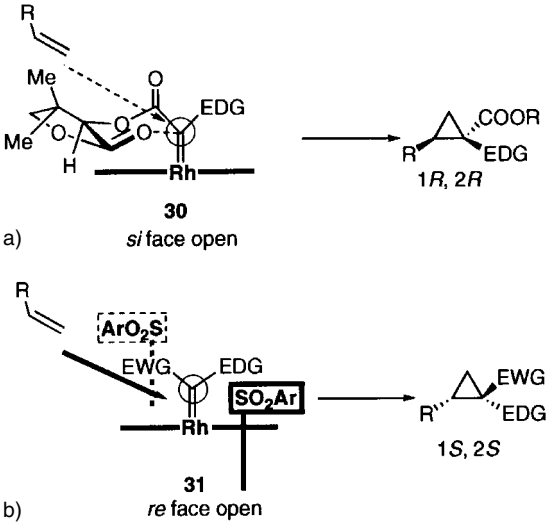

Fig. 14.3 Predictive models for asymmetric induction by (a) (*R*)-pantolactone as a chiral auxiliary; (b) (*S*)-prolinate dirhodium catalysts

tron-withdrawing group (EWG) from the *re* face, resulting in the formation of the (1*S*, 2*S*)-diastereomer [25, 40].

In contrast to the intermolecular cyclopropanation, the dirhodium tetraprolinates give modest enantioselectivities for the corresponding intramolecular reactions with the donor/acceptor carbenoids [68]. For example, the Rh_2(*S*-DOSP)$_4$-catalyzed reaction with allyl vinyldiazoacetate **32** gives the fused cyclopropane **33** in 72% yield with 72% enantiomeric excess (Eq. 4) [68]. The level of asymmetric induction is dependent upon the substitution pattern of the alkene; *cis*-alkenes and internally substituted alkenes afford the highest asymmetric induction. Other rhodium and copper catalysts have been evaluated for reactions with vinyldiazoacetates, but very few have found broad utility [42].

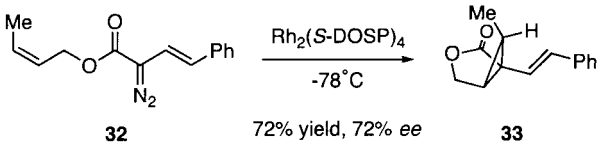

(4)

Recently, Doyle reported the use of dirhodium azetidinone carboxamidates as viable catalysts for the decomposition of aryl and vinyldiazoacetates [69]. Evaluation of several catalysts from the family of dirhodium tetracarboxamidates revealed that only the azetidinone-derived catalysts were effective for the intramolecular cyclopropanation of aryl- and vinyldiazoacetates (Tab. 14.8) [69]. Dirhodium azetidinone catalysts Rh_2(*S*-MEAZ)$_4$ **34** and Rh_2(*S*-IBAZ)$_4$ **35** generally gave better enantioselectivities than the prolinate catalysts, with the highest level of enantiocontrol being achieved in the reaction of allyl phenyldiazoacetate **36**, where the cyclopropane **37** was formed in 84% enantiomeric excess.

Tab. 14.8 Effect of catalyst on intramolecular cyclopropanation.

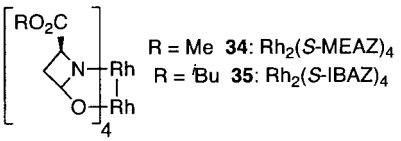

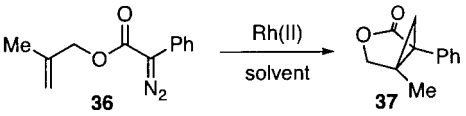

Catalyst	*Solvent*	*Yield (%)*	*ee (%)*
Rh_2(*S*-TBSP)$_4$	Pentane	77	51
Rh_2(*S*-MEAZ)$_4$	CH_2Cl_2	82	84
Rh_2(*S*-IBAZ)$_4$	CH_2Cl_2	80	68

14.3 [3+4] Cycloaddition of Vinyl Carbenoids

One of the most general transformations of the donor/acceptor-substituted carbenoids occurs between vinylcarbenoids and dienes, leading to an overall [3+4] cycloaddition (Scheme 14.3) [13, 21]. The cycloheptadienes formed in these reactions are very useful, since seven-membered rings are prevalent in many important natural products [70–72]. The reaction is applicable to a range of carbon- and heteroatom-functionalized dienes, providing entry into a variety of carbo- and heterocyclic systems [13]. The [3+4] cycloaddition occurs by initial cyclopropanation of the diene **39** by the vinylcarbenoid **38** followed by a Cope rearrangement of the divinylcyclopropane **40**. The Cope rearrangement of *cis*-divinylcyclopropanes takes place through a stereodefined boat-like transition state, which furnishes the cycloheptadienes **41** with full control of stereochemistry at three stereocenters [13]. The key to the success of this overall [3+4] cycloaddition process is a highly regio- and stereoselective cyclopropanation providing easy access to *cis*-divinylcyclopropanes. As described in Section 14.2, high asymmetric induction can be achieved in the cyclopropanation reaction using chiral auxiliaries and chiral catalysts [16]. Similarly, asymmetric intramolecular variants of the [3+4] cycloaddition have been developed, which provide highly functionalized bicyclic systems with excellent diastereo- and enantioselectivity [13].

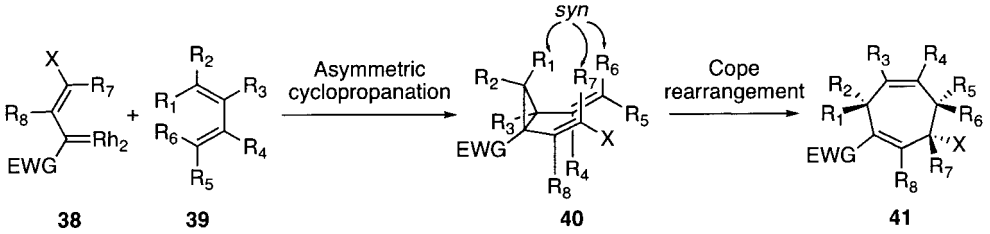

Scheme 14.3

One of the early examples demonstrating the efficiency of this chemistry was the [3+4] cycloaddition reaction of diazoglutaconate **42** with cyclopentadiene, in which the *endo*-isomer **43** is exclusively formed in 98% yield (Eq. 5) [73]. The intermediacy of a *cis*-divinylcyclopropane is consistent with the stereochemical outcome because it would rearrange to the *endo*-product. Indeed in the case of more highly functionalized vinyldiazoacetates, the *cis*-divinylcyclopropane was isolable, in which elevated temperatures were required for the Cope rearrangement [73].

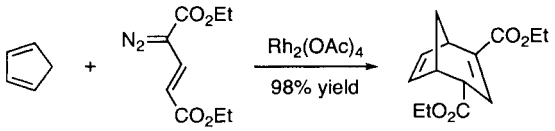

42 **43** (5)

Issues regarding regioselectivity arise when the chemistry is extended to unsymmetrical acyclic dienes. Selective cyclopropanation of a single double bond is required to generate the *cis*-divinylcyclopropane, which then undergoes the Cope rearrangement. With the carbenoid derived from diazoglutaconate **42** the regioselectivity is generally excellent, favoring the cyclopropanation of the less sterically hindered and/or most electron-rich alkene of the 1,3-dienes. The regioselectivity is far superior to that typically observed with ethyl diazoacetate [74]. The diastereoselectivity with this highly electrophilic vinylcarbenoid [39] was not optimal however, as illustrated in the reaction with 2,4-dimethylpenta-1,3-diene (Eq. 6) [75]. Even though the cycloheptadiene **44** predominates, the triene **45** derived from a 1,5-homodienyl rearrangement of the *trans*-divinylcyclopropane is also formed.

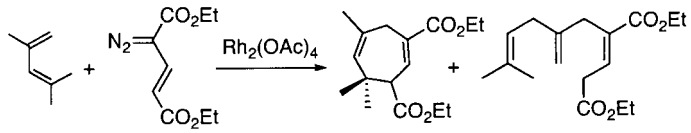

42 **44** 62% yield **45** 14% yield (6)

The diastereoselective formation of *cis*-divinylcyclopropane intermediates is greatly enhanced when the vinyl group of the vinylcarbenoid is more electron-rich. Once again, regiochemical discrimination is based on the extent of alkene substitution. Cyclopropanation of a geminally unsubstituted alkene is preferred over that of a *cis*-disubstituted alkene, whereas reaction with a *trans*-alkene is not observed [76]. These effects are illustrated in the [3+4] cycloadditions of vinyldiazoacetate **46** with 4-methyl-1,3-pentadiene (Eq. 7) and (*E*,*Z*)-2,4-hexadiene (Eq. 8) [75]. In these cases, the cycloheptadienes **47** and **48** are formed without any evidence of products derived from *trans*-divinylcyclopropanes. The formation of **48** as a single regio- and diastereoisomer is a striking example of the chemoselectivity of the donor/acceptor-substituted carbenoids, which is a result of selective cyclopropanation of the *Z*-olefin in the 1,3-diene. Excellent control of regio- and stereoselectivity is possible across a wide range of dienes [75].

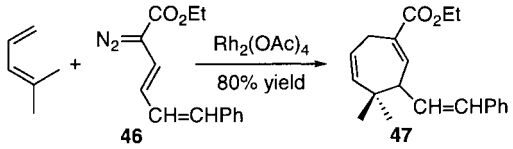

(7)

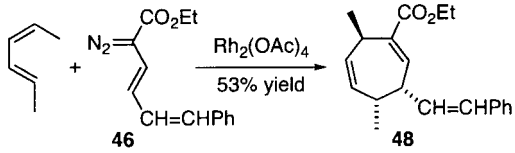

(8)

The reactivity profile of vinylcarbenoids derived from unsubstituted vinyldiazoacetates **49** is very different from those of other substituted vinylcarbenoids (Eq. 9) [77]. Reactions at the vinylogous position are possible, as indicated by the zwitterionic resonance form **51**. This effect is more prevalent in polar solvents [77]. Vinylogous reactivity is further enhanced by the use of electron-deficient catalysts such as rhodium(II) trifloroacetate, ($Rh_2(TFA)_4$) [77].

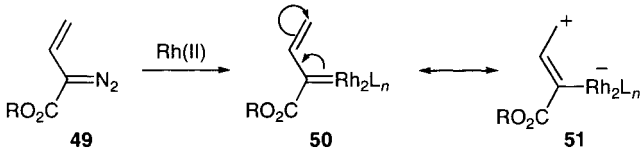

(9)

An example of the vinylogous reactivity is the reaction of **52** with cyclopentadiene (Tab. 14.9) [77]. Rhodium(II) acetate-catalyzed decomposition of **52** in dichloromethane, yields a 2:1 mixture of the bicyclic system **53** derived from the [3+4] cycloaddition, and the bicyclo[2.2.1]heptene **54** resulting from electrophilic attack at the vinylic position followed by ring closure. When $Rh_2(TFA)_4$ is used as the catalyst, bicyclo[2.2.1]heptene **54** becomes the dominant product, while the reactivity of the vinyl terminus is suppressed using a hydrocarbon solvent as observed in the $Rh_2(OOct)_4$-catalyzed reaction in pentane, which affords a 50:1 ratio of products favoring the [3+4] cycloadduct **53**.

Tab. 14.9 Carbenoid versus vinyl terminus reactivity.

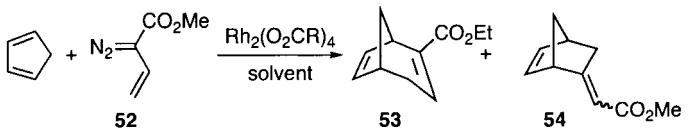

Catalyst/Solvent	*Ratio (53:54)*
$Rh_2(OAc)_4/CH_2Cl_2$	67:33
$Rh_2(TFA)_4/CH_2Cl_2$	32:68
$Rh_2(OOct)_4$/pentane	98:2

Oxygenated dienes are exceptional substrates for vinylcarbenoids [78]. In order to avoid side-products derived from zwitterionic intermediates, nonpolar solvents are typically employed. A short synthesis of nezukone **57** highlights the utility of the [3+4] cycloaddition for the synthesis of tropones (Scheme 14.4). The cycloaddition between the oxygenated butadiene **55** and **52** generates the cycloheptadiene **56** in 67% yield [78]. Treatment of **56** with MeLi followed by acid-induced dehydration completes a very short synthesis of nezukone **57**.

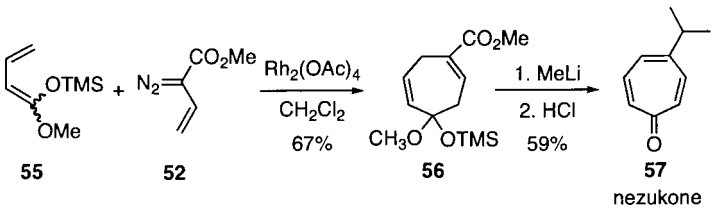

Scheme 14.4 Model for diastereoselection.

Tropolones are readily accessible from the [3+4] cycloadditions of vinylcarbenoids with the highly oxygenated diene **58**, as illustrated in Scheme 14.5 [79]. Treatment of the cyclic vinyldiazoacetate **59** with diene **58** in the presence of $Rh_2(OPiv)_4$ affords the fused cycloheptadiene product **60** in 68% yield. Deprotection followed by oxidation gives the single regioisomeric methyl tropolone **61** in 80% yield.

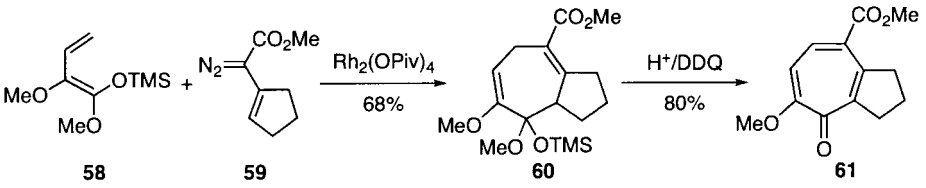

Scheme 14.5

A direct entry into hydroazulenes has also been achieved through [3+4] cycloaddition chemistry, using the more elaborate cyclic vinyldiazoacetate **62** and acetoxybutadienes **63** and **64** (Scheme 14.6) [80]. The tandem process is facile with the *trans*-isomer of butadiene **64** leading to the [3+4] cycloadduct **68** in 67% yield. Reaction with *cis*-acetoxybutadiene **63**, however, forms the isolable *cis*-divinylcyclopropane **65** (80% yield), which required forcing conditions to initiate the Cope rearrangement to form **67** [80].

The vinylcarbenoid [3+4] cycloaddition was applicable to the short stereoselective synthesis of (±)-tremulenolide A **73** and (±)-tremulenediol A **74** (Scheme 14.7) [81]. The key step is the cyclopropanation between the cyclic vinyldiazoacetate **69** and the functionalized diene **70**, which occurs selectively at the *cis*-double bond in **70**. Because of the crowded transition state for the Cope rearrangement of the divinylcyclopropane **71**, forcing conditions are required to form the fused cycloheptadiene **72**. The stereo-

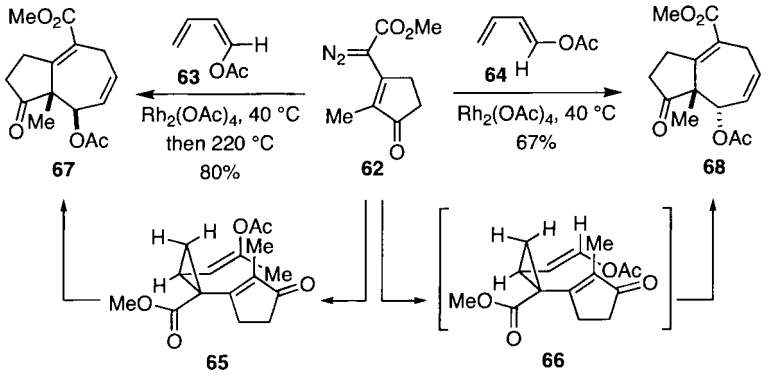

Scheme 14.6

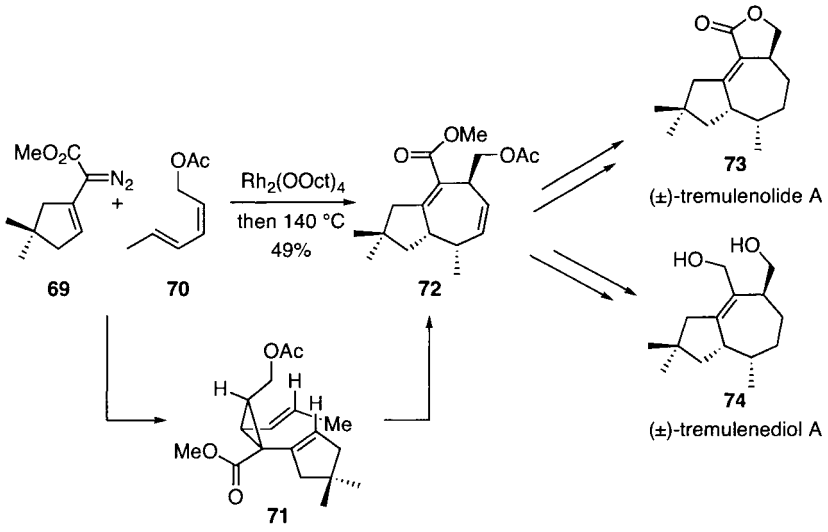

Scheme 14.7

chemistry of the three stereocenters is controlled in this step, with **72** being readily converted to the natural products **73** and **74** [81].

The asymmetric [3+4] cycloaddition is readily achieved using chiral auxiliaries or catalysts [16]. The efficiency of the chiral auxiliary approach is illustrated in the [3+4] cycloaddition with cyclopentadiene. The vinyldiazoacetate **6**, with (*R*)-pantolactone as the chiral auxiliary, generated the bicyclo[3.2.1]octadiene **75** in 87% yield and 76% diastereomeric excess (Eq. 10) [82]. Alternatively, the chiral rhodium prolinate Rh_2(*S*-DOSP)$_4$-catalyzed reaction of **4** generated the bicyclo[3.2.1]octadiene **76** in 77% yield and with 93% enantiomeric excess (Eq. 11) [83].

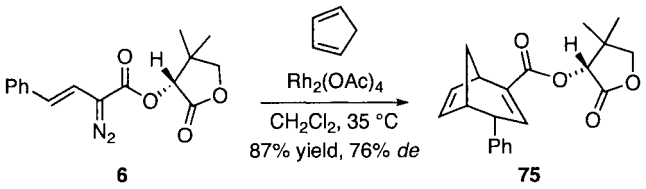

6 75 (10)

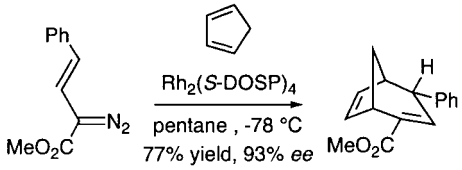

4 76 (11)

Rh_2(*S*-DOSP)$_4$ has been applied to the asymmetric [3+4] cycloaddition of a range of 1,3-dienes. The hydrocarbon-soluble Rh_2(*S*-DOSP)$_4$ is a very active catalyst and the reactions can be conducted at temperatures as low as –78°C to maximize the level of asymmetric induction. Representative examples are illustrated in Scheme 14.8 [83]. In addition to excellent asymmetric induction, these [3+4] cycloadducts **77–82** are formed with full control of the regio- and diastereoselectivity.

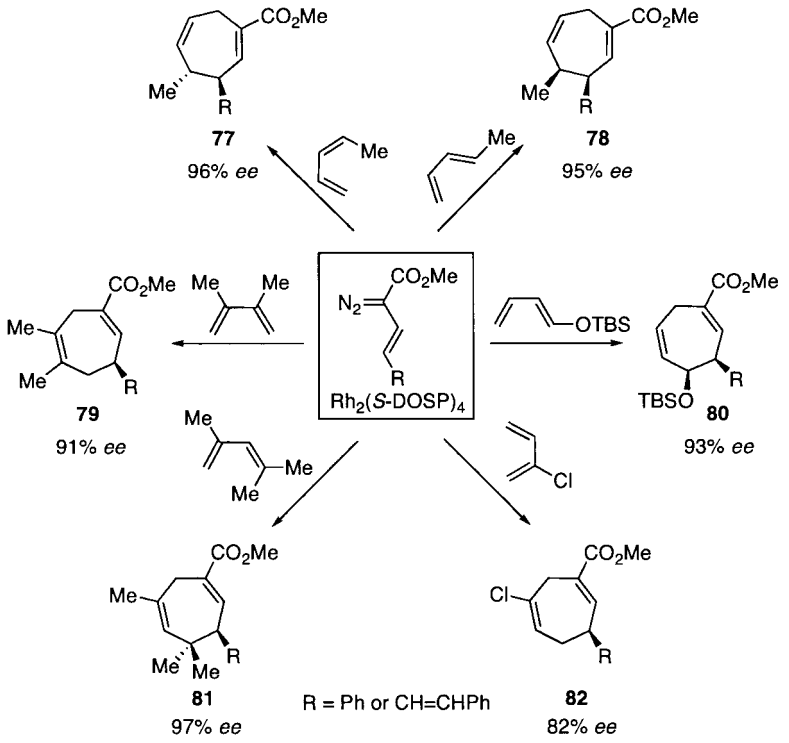

Scheme 14.8

Furans are also excellent substrates for the vinylcarbenoid [3+4] cycloadditions leading to the formation of 8-oxabicyclo[3.2.1]octadienes **86** (Scheme 14.12) [84]. However, the [3+4] cycloadduct **86** is not always the dominant product in this chemistry, due to a competing reaction that involves the ring opening of the furan ring to form the triene **84** [84, 85]. Competing triene formation is believed to occur through the dipolar intermediate **83**, wherein bond formation at the *α*-position of furan is more advanced than at the *β*-position. The ring system becomes prone to cleavage and opens to triene **84** [85] in competition with the divinylcyclopropane rearrangement to **86**. The ratio of **84** to **86** is dependent on the extent of charge build-up in the transition state. In contrast, when bond formation at the *β*-position is more advanced during the initial cyclopropanation (**85**), the Cope rearrangement to form **86** proceeds uneventfully [85].

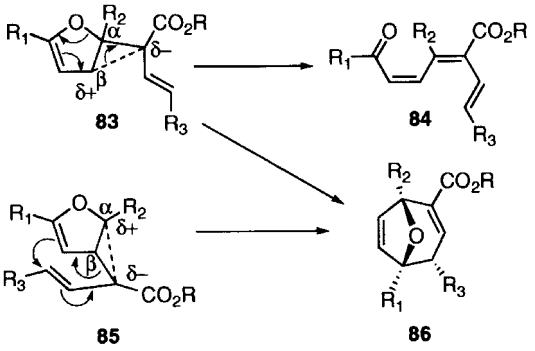

Scheme 14.9

The nature of the dipolar intermediate is crucial in the reaction with furans, since the product distribution is greatly influenced by the substituents present on the furan and vinylcarbenoid (Tab. 14.10) [84–86]. Electron-rich 2-methoxyfuran leads to exclusive formation of triene **89** with vinyldiazoacetate **42**, whereas the corresponding reaction with 2,5-dimethylfuran affords only the [3+4] cycloaddition product **88** in 70% yield.

Tab. 14.10 Reactions of vinylcarbenoids with furans.

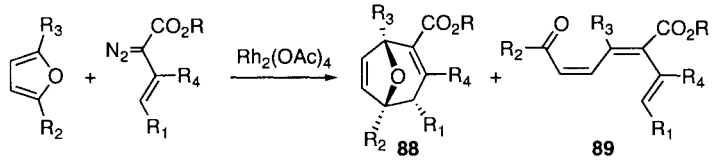

Diazo	*R*	*R_1*	*R_2*	*R_3*	*R_4*	*88, Yield (%)*	*89, yield (%)*
42	Et	CO_2Et	OMe	H	H	0	92
42	Et	CO_2Et	Me	Me	H	70	0
52	Me	H	H	H	H	51	15
87	Me	H	H	H	OTBS	90	0

The reaction with furan forms a mixture of the two products with a preference for the [3+4] cycloadduct **88**. Similarly, the reaction of furan with the vinylcarbenoid of siloxy-substituted vinyldiazoacetate **87** yields 90% of the [3+4] cycloaddition product with no triene formation.

The asymmetric synthesis of oxabicyclo[3.2.1]octanes has been explored using chiral catalysts and auxiliaries [86]. The extent of asymmetric induction is good (86% *ee*) using Rh_2(*S*-TBSP)$_4$ as the catalyst with 2,5-dimethylfuran giving a 95% yield of **90** (Eq. 12). Competing triene formation, however, is more prevalent with Rh_2(*S*-TBSP)$_4$ than with $Rh_2(OAc)_4$, as a result of the greater electrophilicity of the catalyst, which favors the intermediacy of charged transition states. The chiral auxiliary approach using siloxy-substituted vinyldiazoacetate **92** is very efficient for [3+4] cycloadditions with various 2- and 3-substituted furans **91** to form **93** (Eq. 13). This approach has found several applications in the preparation of synthetic intermediates for natural product synthesis [87–89].

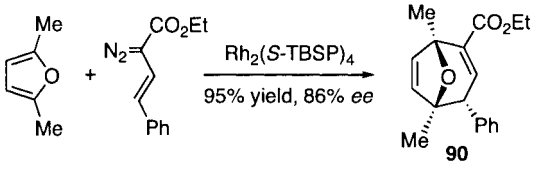

(12)

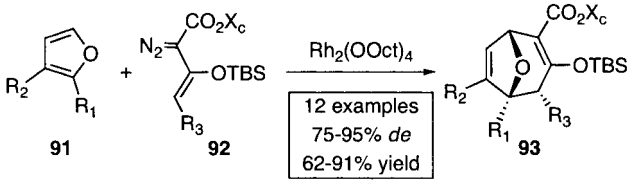

(13)

X_c = (*R*)-pantolactone or (*S*)-lactate

The complementary azabicyclic products can be prepared from the reactions of vinylcarbenoids with pyrroles, leading to a novel entry into the tropane skeleton [90]. Although the reaction of vinyldiazoacetate **42** and pyrrole leads to the alkylation product **94** (Eq. 14), placing an electron-withdrawing group on the nitrogen decreases its ability to stabilize positive charge build-up, enhancing formation of the desired [3+4] cycloadducts **97** [90]. Several carbamate protecting groups have been evaluated with the various vinylcarbenoids **96** (Eq. 15), which result in efficient reactions to afford the tropane systems **97** in 53–71% yield.

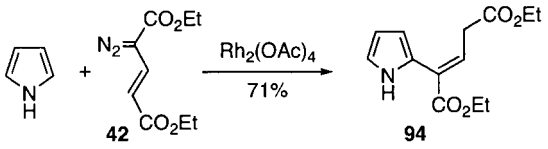

(14)

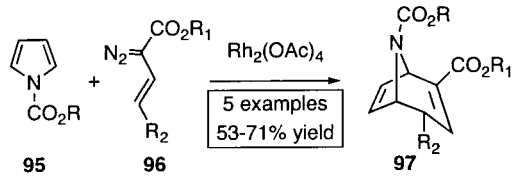

(15)

Tab. 14.11 Tropane formation versus vinylogous reactivity.

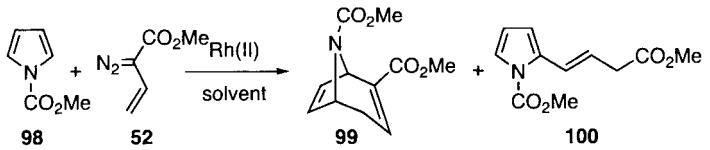

98 52 99 100

Reaction conditions	*Ratio 99:100*
$Rh_2(OAc)/CH_2Cl_2$	55:45
$Rh_2(OHex)_4/CH_2Cl_2$	15:85
$Rh_2(OHex)_4$/hexane	>95:5

Vinylogous electrophilic reactivity is once again observed in the reaction of acylated pyrrole **98** with unsubstituted vinyldiazoacetate **52** (Tab. 14.11) [91]. Under standard conditions with $Rh_2(OAc)_4$ and employing dichloromethane as solvent gave a mixture of the [3+4] cycloadduct **99** and the alkylated product **100**. Reactivity of the vinyl terminus could be enhanced by using a more electrophilic catalyst, and strongly suppressed using a nonpolar solvent, which gave optimal conditions for generating the tropane system **99**.

The chiral auxiliary approach was found to be most amenable to the asymmetric synthesis of a wide range of tropanes **102** (Eq. 16) [44]. Due to their electrophilic character, rhodium tetraprolinates such as Rh_2(*S*-TBSP)$_4$ give rise to the formation of side-products derived from zwitterionic intermediates and result in moderate enantioselectivities in the [3+4] cycloaddition reactions of pyrroles. Therefore, the use of an electron-rich catalyst with a chiral auxiliary is advantageous in providing stereoselectivity and control of carbenoid reactivity through an intramolecular stabilizing interaction between the lactone carbonyl of the auxiliary and the carbenoid carbon [13]. The [3+4] cycloaddition reactions of pyrroles has been extensively used for the synthesis of various biologically active tropanes [92–94]. These studies have led to the development of potential medications for cocaine addiction [95–97], molecular probes to study the neurobiology of addiction [98, 99], and neuroimaging agents [100].

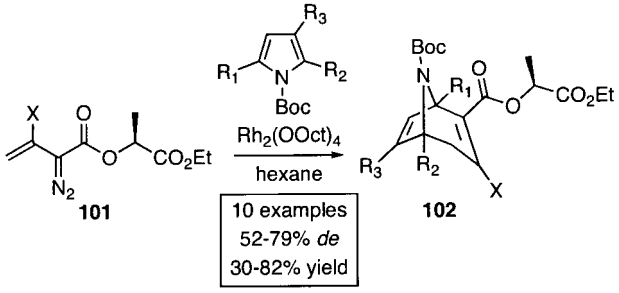

101 102 (16)

Kende described an impressive example of the use of the [3+4] cycloaddition in natural product synthesis (Scheme 14.10) [101]. A key nortropinone intermediate for the total synthesis of (±)-isostemofoline **105** was acquired through the tropane system **104**, which was formed from the [3+4] cycloaddition of pyrrole **103** and a siloxy-substituted vinylcarbenoid of **87** in 90% yield.

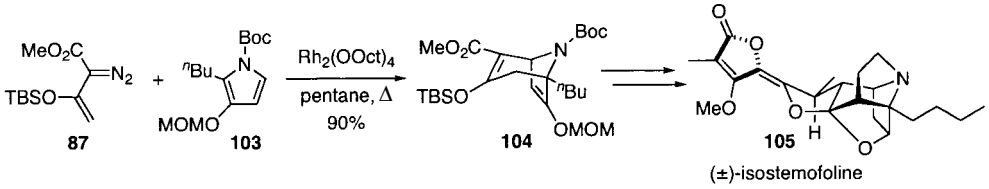

Scheme 14.10

Enantioselective syntheses of fused cycloheptadienes have been accomplished *via* the intramolecular variant of the asymmetric vinylcarbenoid [3+4] cycloaddition [81, 102]. The most notable example is the asymmetric synthesis of the tremulenolide skeleton **111** (Scheme 14.11) [81]. Using the *cis,trans*-dienyl system **106**, the *trans*-divinylcyclopropane **107** is formed with 93% enantiomeric excess. Under forcing conditions isomerization of **107** to the *cis*-divinylcyclopropane **108** occurred, which then underwent a Cope rearrangement to **110**. Although the approach using *trans,trans*-dienyl system **109** directly forms the fused cycloheptadiene **110**, the enantioselectivity of the direct reaction was lower (35% *ee*). Reduction of the unconjugated alkene of **110** *via* hydrogenation using Wilkinson's catalyst accomplished the asymmetric synthesis of (+)-5-*epi*-tremulenolide **111**.

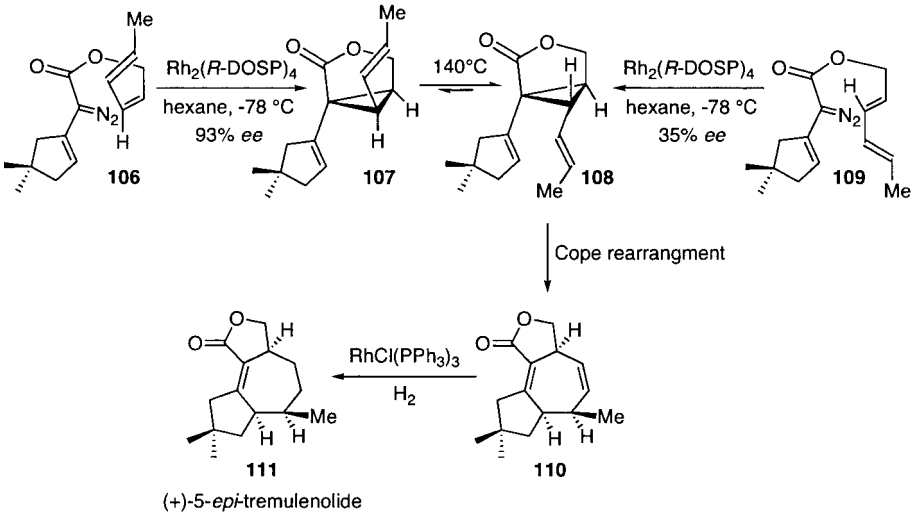

Scheme 14.11

An elegant application of the [3+4] cycloaddition methodology was showcased in model studies directed toward the synthesis of the core skeleton of CP-263 114 **115** (Scheme 14.12) [103]. The key step is the intramolecular [3+4] cycloaddition of furan with the siloxy-substituted vinyldiazoacetate in **112**. The oxabicyclic system **113** was obtained in 68% yield and was converted in eight steps to furnish the core structure **114** [103].

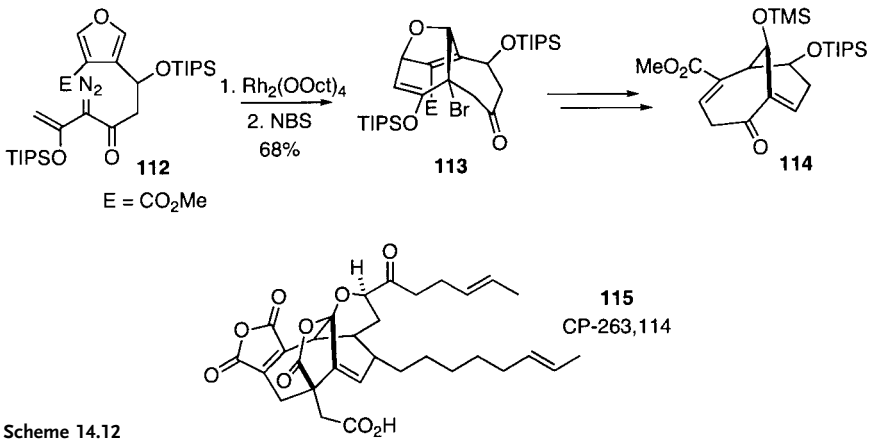

Scheme 14.12

14.4
[3+2] Cycloaddition of Vinyl Carbenoids

Rhodium-stabilized vinylcarbenoids are capable of undergoing a variety of [3+2] cycloadditions providing new synthetic routes to functionalized cyclopentenes [11]. The reactions are specific to the reactions of vinylcarbenoids with vinyl ethers, which either directly form cyclopentenes or form vinylcyclopropane intermediates that can rearrange to the five-membered ring products [104, 105]. A very effective two-step [3+2] cycloaddition is the cyclopropanation of vinyl ethers **116** with vinylcarbenoids **117** followed by a Lewis acid-catalyzed rearrangement of the vinylcyclopropane **118** (Scheme 14.13) [104, 105]. Owing to the presence of donor and acceptor groups on adjacent carbons in **118**, Lewis acid-catalyzed vinylcyclopropane rearrangement is very facile. Even though the rearrangement is likely to be a stepwise process, cyclopentene **119** is formed as a single diastereomer.

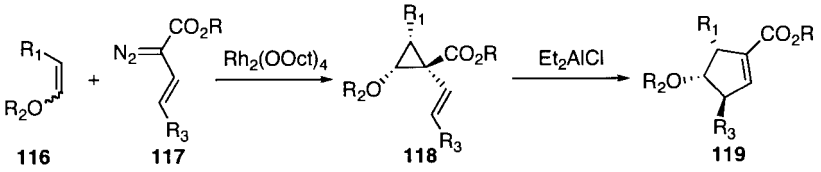

Scheme 14.13

The reactions of vinyl ethers with vinyldiazoacetates unsubstituted at the vinyl terminus result in a very interesting outcome because either regioisomer of the [3+2] cycloadduct can be obtained (Scheme 14.16) [104]. An example is the reaction with 2,3-dihydrofuran where regioisomer **122** is formed *via* the established ring-opening reaction of the donor/acceptor-substituted vinylcyclopropane **121** under Lewis acidic conditions (Scheme 14.14) [104, 105]. The cyclopropanation step has been optimized to

block reactivity at the vinylogous position using a nonpolar solvent. By this two-step process cyclopentene **122** was obtained in 66% yield as a single diastereomer. The formation of the other regioisomer **124** occurs by enhancing electrophilic attack at the vinyl terminus followed by ring closure to form the five-membered ring. The reaction is proposed to go through the zwitterionic intermediate **123**, which is stabilized in a polar solvent. By using a very bulky ester group on the vinyldiazoacetate **120** (BHT: 2,6-di(*tert*-butyl)hydroxytoluene) the vinylogous reactivity is enhanced so that regioisomer **124** is formed as the exclusive [3+2] cycloadduct.

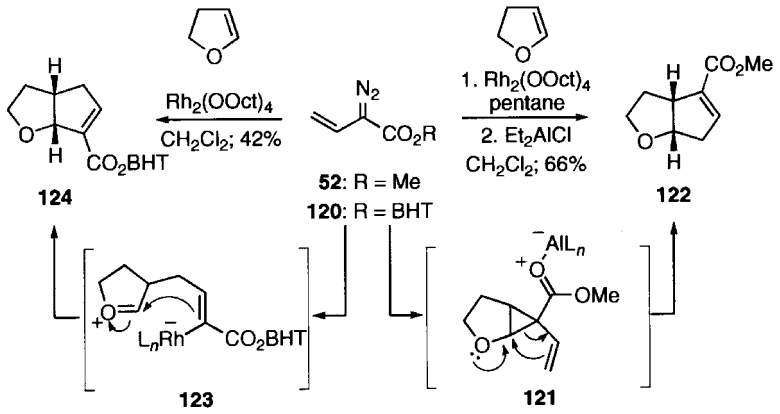

Scheme 14.14

Asymmetric induction is possible in the two-step [3+2] cycloaddition by starting the sequence with an asymmetric cyclopropanation (Scheme 14.15) [106]. The Rh_2(*S*-DOSP)$_4$-catalyzed reactions gave the desired vinylcyclopropanes **126** with high enantioselectivities [106]. Partial or complete racemization occurred in the vinylcyclopropane rearrangement of monocyclic vinylcyclopropanes, but the fused vinylcyclopropanes **128–133** rearrange to form **134–139** with virtually no racemization.

A third mechanistically distinct [3+2] cycloaddition between vinyl ethers and vinylcarbenoids was discovered and reported in 2001 [26]. This reaction is remarkable because when Rh_2(*S*-DOSP)$_4$ is used as the catalyst, the *cis*-cyclopentenes **142** are formed in up to 99% enantiomeric excess. The reaction occurs between vinylcarbenoids unsubstituted or alkyl-substituted at the vinyl terminus and vinyl ethers substituted with an aryl or vinyl group. Some illustrative examples are shown in Tab. 14.12. The reaction is considered to be a concerted process, which would be consistent with the highly stereoselective nature of the reaction [26]. Contrary to the [3+2] cycloaddition derived by means of vinylogous carbenoid reactivity, this latest [3+2] cycloaddition is not influenced by solvent effects. Due to steric demands on the carbenoid, the [3+2] cycloaddition *only* occurs with *cis*-vinyl ethers.

The cyclopentene products can be used as synthetic intermediates to generate highly functionalized cyclopentanes, in which the stereochemistry at every carbon within the ring may be controlled (Scheme 14.16) [26]. Using a double cuprate addition strategy on cyclopentene **143**, the pentasubstituted cyclopentane **145** can be generated, essentially as a single stereoisomer, in good overall yield.

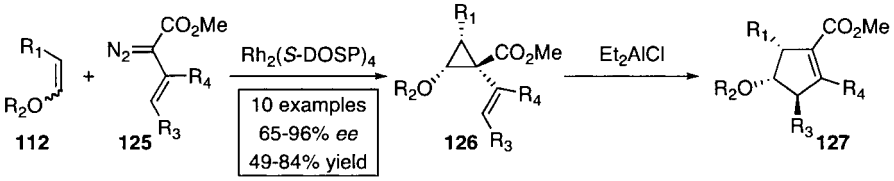

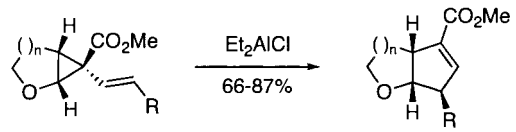

128: *n* =1, R = Ph 86% *ee*
129: *n* =1, R = Me 86% *ee*
130: *n* =2, R = Ph 88% *ee*
131: *n* =2, R = Me 87% *ee*

134: *n* =1, R = Ph 86% *ee*
135: *n* =1, R = Me 85% *ee*
136: *n* =2, R = Ph 82% *ee*
137: *n* =2, R = Me 84% *ee*

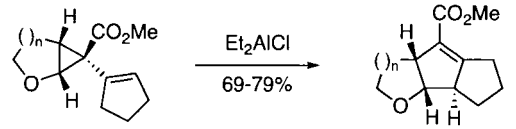

132: *n* =1, 76% *ee*
133: *n* =2, 88% *ee*

138: *n* =1, 74% *ee*
139: *n* = 2, 86% *ee*

Scheme 14.15

Tab. 14.12 Asymmetric [3+2]cycloaddition of vinyl ethers with vinyldiazoacetate **141**.

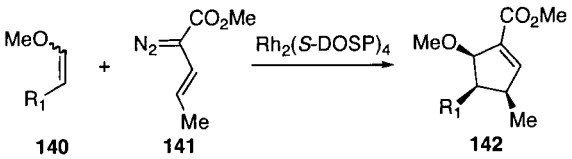

R_1	*Yield (%)*	*ee (%)*
Ph	79	98
p-BrPh	71	>99
E-CH=CHEt	49	99

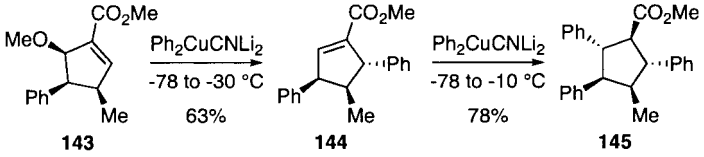

Scheme 14.16

The reaction of vinylcarbenoids with vinyl ethers can lead to other types of [3+2] cycloadditions. The symmetric synthesis of 2,3-dihydrofurans is readily achieved by reaction of rhodium-stabilized vinylcarbenoids with vinyl ethers (Scheme 14.17) [107]. In this case, (*R*)-pantolactone is used as a chiral auxiliary. The initial cyclopropanation proceeds with high asymmetric induction; upon deprotection of the silyl enol ether **146**, ring expansion occurs to furnish the dihydrofuran **147**, with no significant epimerization during the ring-expansion process.

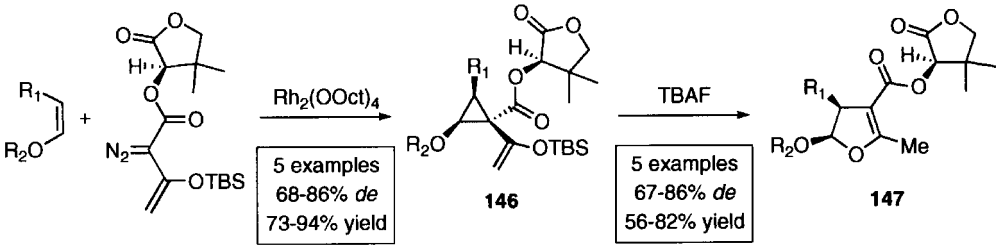

Scheme 14.17

Another unusual two-step [3+2] cycloaddition involves the ring expansion of *tert*-butyl-1-vinylcyclopropane-1-carboxylate **148** to the *α*-ethylidenebutyrolactone **149** (Scheme 14.18) [108]. When the reaction is catalyzed by boron tribromide the monocyclic product **149** is formed, but when the Lewis acidic oxidant $VOCl_2(OEt)$ is used, a very unusual dimeric product (**150**) is formed.

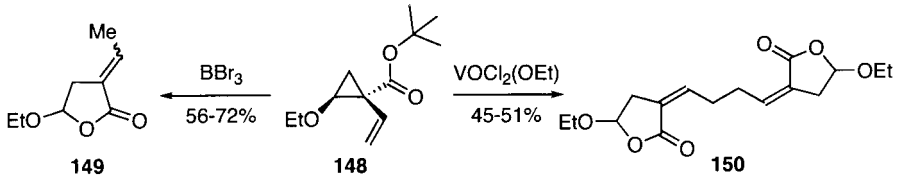

Scheme 14.18

An interesting application of the boron tribromide-induced rearrangement has been the synthesis of ether analogs of (±)-acetomycin **157** (Scheme 14.19) [76]. The rhodium(II) acetate-catalyzed reaction of vinyl ether **151** with vinyldiazoacetate **152** generated cyclopropane **153** as a single diastereomer. By an appropriate sequence of reactions, **153** can be converted stereoselectively to three ether analogs of (±)-acetomycin, **154–156**.

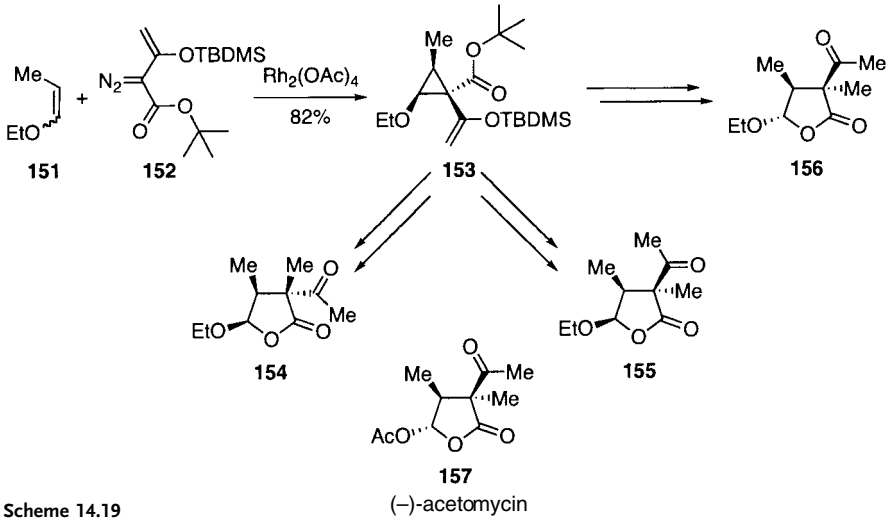

Scheme 14.19

14.5 Ylide Transformations

Numerous studies have been directed toward expanding the chemistry of the donor/acceptor-substituted carbenoids to reactions that form new carbon–heteroatom bonds. It is well established that traditional carbenoids will react with heteroatoms to form ylide intermediates [5]. Similar reactions are possible in the rhodium-catalyzed reactions of methyl phenyldiazoacetate (Scheme 14.20). Several examples of O–H insertions to form ethers **158** [109, 110] and S–H insertions to form thioethers **159** [111] have been reported, while reactions with aldehydes and imines lead to the stereoselective formation of epoxides **160** [112, 113] and aziridines **161** [113]. The use of chiral catalysts and pantolactone as a chiral auxiliary has been explored in many of these reactions but overall the results have been rather moderate. Presumably after ylide formation, the rhodium complex disengages before product formation, causing degradation of any initial asymmetric induction.

Vinyldiazoacetates are also capable of ylide transformations. Both N–H and O–H insertions to form **162** and **163** respectively have been reported, albeit with low asymmetric induction (Scheme 14.21) [28, 110]. Due to the presence of the vinyl groups, some novel rearrangements of the initially formed ylides are possible. The reaction of vinyldiazoacetates with imines preferentially forms dihydropyrroles **164** [114], whereas the reaction with unsaturated imines generates dihydroazepines [115]. The reaction with aldehydes generates dihydrofurans as byproducts [115]. A very intriguing reaction was observed with indole thioethers, in which the initially formed sulfur ylide underwent a 3,3-sigmatropic rearrangement to form **165** [116].

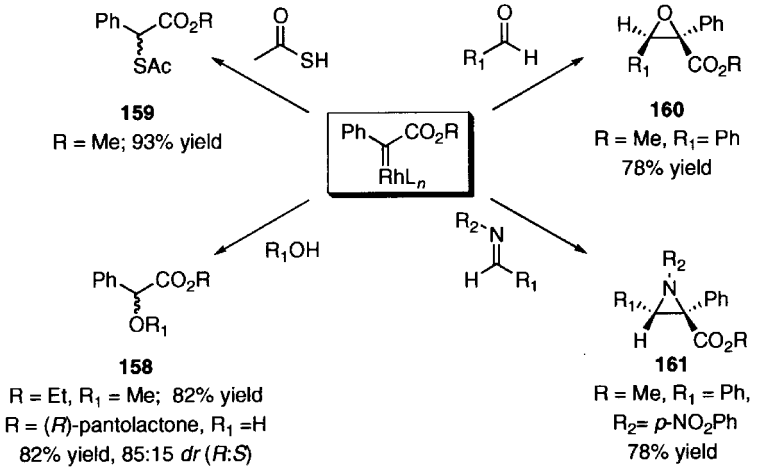

Scheme 14.20

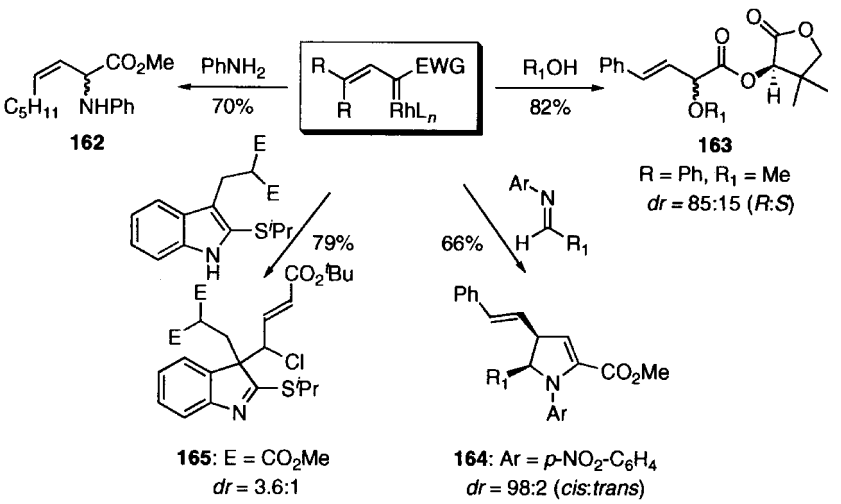

Scheme 14.21

14.6 Si–H Insertion

In addition to insertions into polar X–H bonds by means of ylide intermediates, carbenoids are capable of inserting into nonpolar bonds such as Si–H and C–H. The Si–H insertion by vinylcarbenoids has been developed as a novel method for the synthesis of allylsilanes **166** and **167** of defined geometry as illustrated in Eqs. (17) and (18) [28]. The alkene geometry of the vinyldiazoacetate is not altered during carbenoid formation or the subsequent Si–H insertion.

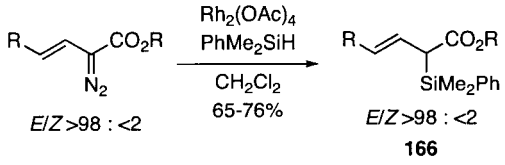

(17)

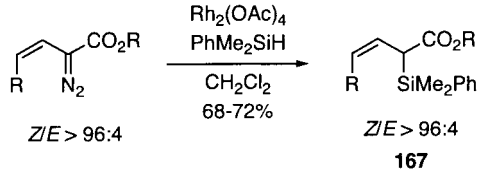

(18)

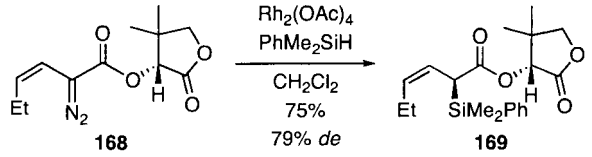

(19)

Considerable interest has been shown in developing asymmetric variants of the Si–H insertion. The chiral auxiliary (*R*)-pantolactone has performed quite well in this chemistry, as illustrated in the formation of **169** in 79% diastereomeric excess (Eq. 19) [28]. A wide variety of chiral catalysts have been explored for the Si–H insertion chemistry of methyl phenyldiazoacetate [29, 117–119]. The highest reported enantioselectivity to date was obtained with the rhodium prolinate catalyst Rh_2(*S*-DOSP)$_4$, which generated **170** with 85% enantiomeric excess (Eq. 20) [120].

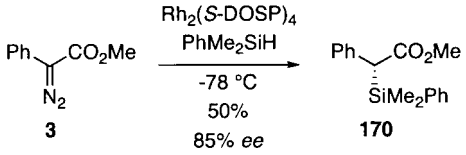

(20)

14.7
C–H Activation by Carbenoid-Induced C–H Insertion

The most spectacular application of the donor/acceptor-substituted carbenoids has been intermolecular C–H activation by means of carbenoid-induced C–H insertion [17]. Prior to the development of the donor/acceptor carbenoids, the intermolecular C–H insertion was not considered synthetically useful [5]. Since these carbenoid intermediates were not sufficiently selective and they were very prone to carbene dimerization, intramolecular reactions were required in order to control the chemistry effectively [17]. The enhanced chemoselectivity of the donor/acceptor-substituted carbenoids has enabled intermolecular C–H insertion to become a very practical enantioselective method for C–H activation. Since the initial report in 1997 [121], the field of intermolecular enantioselective C–H insertion has undergone explosive growth [14, 15]. Excellent levels of asymmetric induction are obtained when these carbenoids are derived

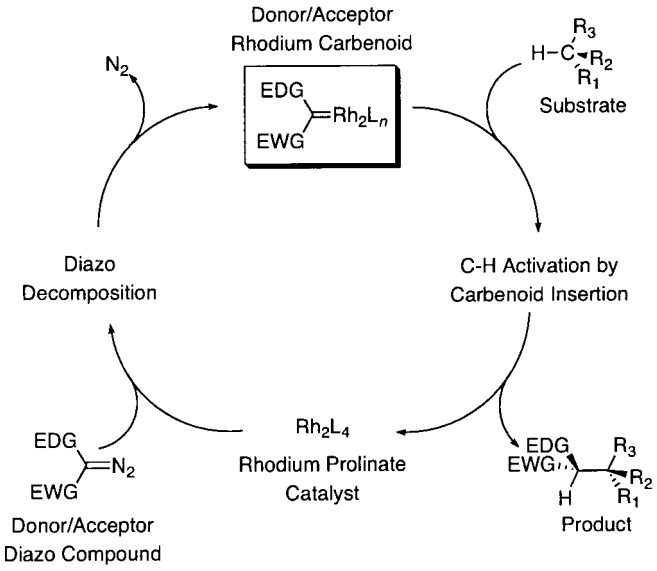

Scheme 14.22

from the dirhodium tetraprolinates. Numerous reviews have been published on this subject and, as will be illustrated here, this strategy has proven to be a versatile tool for target-oriented synthesis [14, 15, 17]. Furthermore, this methodology elegantly complements some of the classic C–C bond-forming reactions of organic chemistry, providing alternative methods for the preparation of target molecules with multiple stereogenic centers [14, 15, 17].

The challenge of functionalizing unactivated carbon–hydrogen bonds, especially those of hydrocarbons, has fascinated many synthetic organic and inorganic chemists [122, 123]. As a result, major advances have been made in this field using organometallic species as mediators for insertion into unactivated C–H bonds [122–128]. A complementary approach is the use of metal carbenoids, which accomplish C–H activation *via* insertion of the carbenoid across C–H bonds (Scheme 14.22) [128]. Donor/acceptor carbenoids of the Rh_2(*S*-DOSP)$_4$ catalyst have proven to be exceptional for this purpose, inducing C–H insertion into cyclic and acyclic hydrocarbons with high levels of enantioselectivity [17]. Recently, it has been reported that problems associated with one electron-acceptor carbenoids can be overcome using bulky copper pyrazolylborate catalysts [129]. These catalysts will be of interest for future developments in the area of C–H activation chemistry.

Highly enantioselective intermolecular C–H insertion into cyclohexane and cyclopentane is possible using the Rh_2(*S*-DOSP)$_4$ carbenoids generated from aryl diazoacetates **172** to form **173** (Eq. 21) [121, 130]. The enantioselectivity is enhanced when the reactions are conducted at lower temperatures, without any deleterious effect on the catalytic activity or product yield [130]. Extending the reaction to other cyclic and acyclic hydrocarbons has revealed a delicate balance required between the steric environment and the electronic state of the carbon undergoing C–H insertion [130]. The decreasing enantioselectivity and yield of C–H insertion into adamantane **174** (67% yield, 90% *ee*),

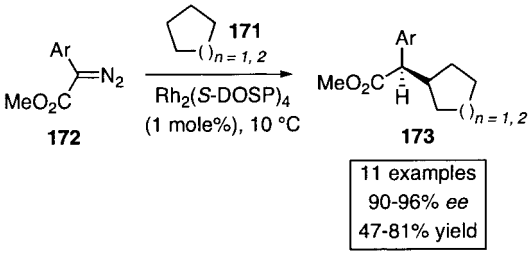

(21)

2-methylbutane **175** (60% yield, 69% *ee*), and 2,3-dimethylbutane **176** (27% yield, 66% *ee*) illustrates this effect (Scheme 14.23). In the event that a substrate like 2-methylpentane presents several sites for insertion, the carbenoid discriminates the tertiary and secondary sites from the primary site, and only two C–H insertion products, **177** and **178**, are formed. Tertiary sites are favored for insertion based on electronic grounds, but the least sterically encumbered secondary sites are favored due to the steric demands of the bulky Rh_2(*S*-DOSP)$_4$ carbenoids [130]. Primary insertion in the hydrocarbon series is rarely observed; however, in more electronically activated systems, as discussed later, C–H activation into a primary C–H bond can occur.

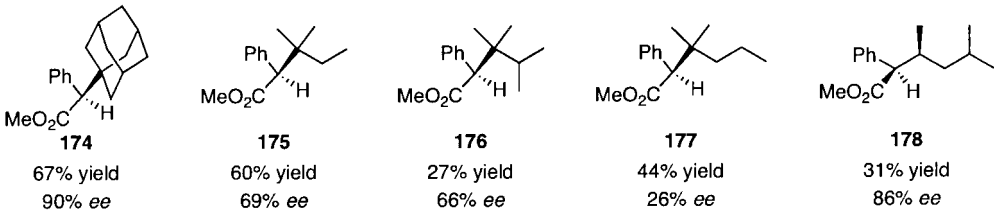

Scheme 14.23

The C–H activation of allylic and benzylic C–H bonds has considerable application in organic synthesis. Studies by Muller [131] and Davies [130] on reactions with cyclohexene revealed that Rh_2(*S*-DOSP)$_4$ in a hydrocarbon solvent is the optimum system for high asymmetric induction (Tab. 14.13). Although this particular example gives a mixture of the C–H activation product **179** and cyclopropane **180**, similar reactions with ethyl diazoacetate gave virtually no C–H activation product. Some of the other classic chiral dirhodium catalysts **181** and **182** were also effective in this chemistry, but the enantioselectivity with these catalysts (45% *ee* and 55% *ee*) [131] was considerably lower than with Rh_2(*S*-DOSP)$_4$ (93% *ee*) [130].

Asymmetric allylic C–H activation of cyclohexadiene systems has been used for the asymmetric synthesis of several compounds of pharmaceutical relevance. The key step in the asymmetric syntheses of the monoamine reuptake inhibitor (+)-indatraline **185** was the C–H insertion reaction of the aryldiazoacetate **183** with 1,4-cyclohexadiene (Scheme 14.24). The product **184**, obtained in 83% yield with 93% enantiomeric excess, is readily converted to (+)-indatraline using standard synthetic procedures [132].

The asymmetric synthesis of (+)-cetiedil **188** utilizes the thiophene ring as an alternative electron-donating group on the donor/acceptor carbenoid (Scheme 14.25) [133]. Activated substrates are able to trap the carbenoid from **186** and, using 1,4-cyclohexa-

Tab. 14.13 Effect of catalyst and solvent on stereoselectivity of C–H activation.

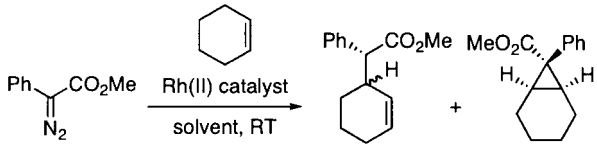

179 **180**

Catalyst	*Solvent*	*Ratio 179:180*	*Yield 179+180 (%)*	*ee 179 (%)*
$Rh_2(OAc)_4$	CH_2Cl_2	72:25	50	–
Rh_2(*S*-MEPY)$_4$	CH_2Cl_2	93:7	50	45
Rh_2(*S*-PTPA)$_4$	CH_2Cl_2	50:50	45	53
Rh_2(*S*-DOSP)$_4$	CH_2Cl_2	80:20	33	75
Rh_2(*S*-DOSP)$_4$	2,2-DMB	79:21	73	93

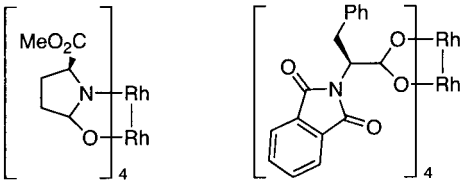

181: Rh_2(*S*-MEPY)$_4$ **182**: Rh_2(*S*-PTPA)$_4$

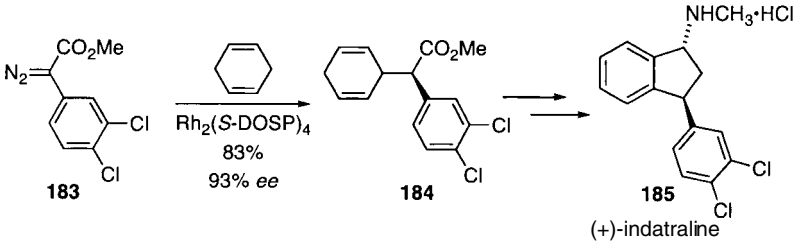

Scheme 14.24

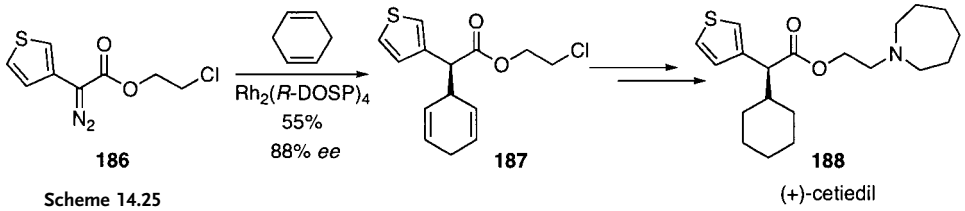

Scheme 14.25

diene, **187** can be obtained in 55% yield with 88% enantiomeric excess. The synthesis of (+)-cetiedil (**188**) from **187** is then completed in two steps.

The reaction of vinylcarbenoids with allylic C–H bonds leads to a remarkable transformation, a combined C–H insertion/Cope rearrangement, which is reminiscent of the tandem cyclopropanation/Cope rearrangement of vinylcarbenoids. An interesting application of this chemistry is the asymmetric synthesis of the antidepressant (+)-sertraline **191** (Scheme 14.26) [134]. The Rh_2(*S*-DOSP)$_4$-catalyzed reaction of the vinyldiazoacetate **189** with 1,3-cyclohexadiene generates the 1,4-cyclohexadiene **190** in 99% enantiomeric excess. The further conversion of **190** to (+)-sertraline **191** is then achieved using conventional synthetic transformations.

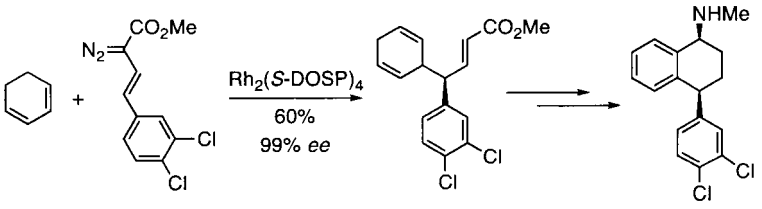

189 **190** **191**

(+)-sertraline

Scheme 14.26

Asymmetric allylic C–H activation of more complex substrates reveals some intrinsic features of the Rh_2(*S*-DOSP)$_4$ donor/acceptor carbenoids [135, 136]. Cyclopropanation of *trans*-disubstituted or highly substituted alkenes is rarely observed, due to the steric demands of these carbenoids [16]. Therefore, the C–H activation pathway is inherently enhanced at substituted allylic sites and the bulky rhodium carbenoid discriminates between accessible secondary sites for diastereoselective C–H insertion. As a result, the asymmetric allylic C–H activation provides alternative methods for the preparation of chiral molecules traditionally derived from classic C–C bond-forming reactions such as the Michael reaction and the Claisen rearrangement [135, 136].

The asymmetric allylic C–H activation of cyclic and acyclic silyl enol ethers furnishes 1,5-dicarbonyl compounds and represents a surrogate of the Michael reaction [136]. When sufficient size discrimination is possible the C–H insertion is highly diastereoselective, as in the case of acyclic silyl enol ether **193** (Eq. 22). Reaction of aryldiazoacetate **192** with **193** catalyzed by Rh_2(*S*-DOSP)$_4$ gives the C–H insertion product **194** (>90% *de*) in 84% enantiomeric excess. A second example is the reaction of the silyl enol ether **195** with **192** to form **196**, a product that could not be formed from the usual Michael addition because the necessary "enone" would be in its tautomeric naphthol form (Eq. 23).

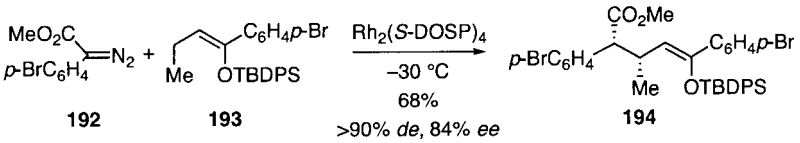

192 **193** **194** (22)

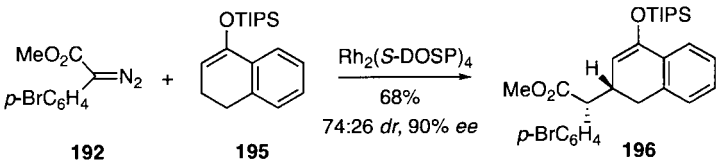

192 195 196 (23)

The Claisen rearrangement of allyl vinyl ethers is a classic method for the stereoselective synthesis of γ,δ-unsaturated esters. The allylic C–H activation is an alternative way of generating the same products [135]. Reactions with silyl-substituted cyclohexenes **197** demonstrate how the diastereoselectivity in the formation of **198** improves (40% to 88% *de*) for the C–H insertion reactions as the size of the silyl group increases (TMS to TBDPS) (Tab. 14.14). Indeed, in cases where there is good size differentiation between the two substituents at a methylene site, high diastereo- and enantioselectivity is possible in the C–H activation.

Tab. 14.14 Diastereocontrol achieved by size differentiation in allylic C–H activation.

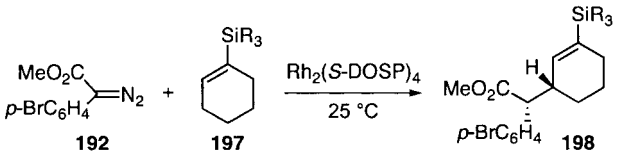

192 197 198

SiR$_3$	*Yield (%)*	*de (%)*	*ee (%)*
TMS	48	40	88
TBDPS	64	88	95

The reaction has been applied to many systems; an impressive example is the enantiomeric differentiation and kinetic resolution of α-pinene **199** (Tab. 14.15) [135]. The Rh_2(*S*-DOSP)$_4$-catalyzed reaction with (+)-α-pinene is the matched reaction, in which **200** is formed in 93% yield and with 96% diastereomeric excess. The corresponding re-

Tab. 14.15 Kinetic resolution in allylic C–H activation of α-pinene and Rh_2(*S*-DOSP)$_4$.

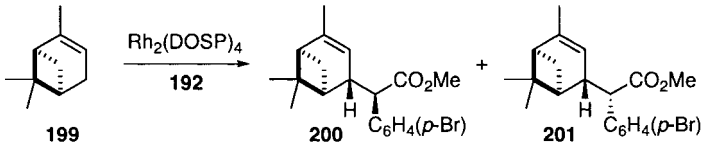

199 200 201

Substrate	*Catalyst*	*Yield (5)*	*Ratio 200:201*	*ee 200 (%)*
(+) (0.5 equiv)	Rh_2(*S*-DOSP)$_4$	93	98:2	–
(+) (0.5 equiv)	Rh_2(*R*-DOSP)$_4$	62	24:76	–
(±) (0.5 equiv)	Rh_2(*S*-DOSP)$_4$	52	88:12	99

action with Rh_2(*R*-DOSP)$_4$ is the mismatched reaction leading to a 24:76 diastereomeric mixture of **200** and **201**. Reaction with a racemic mixture of α-pinene forms **200** as the major diastereomer with 99% enantiomeric excess.

In systems where steric interference is not a factor, C–H insertion at a methylene site is strongly preferred over that at methyl sites. A striking example of this effect is the reaction with 4-ethyltoluene (Eq. 24) [137]. The only C–H activation product formed is **202**, derived from C–H insertion at the methylene site. A Hammett study on the benzylic C–H activation indicated that the transition-state build-up of positive charge at the benzylic position is stabilized by resonance.

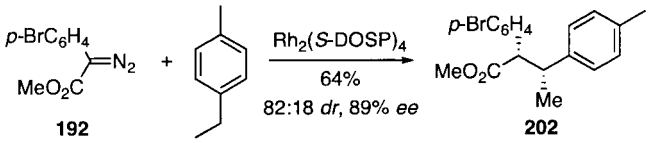

(24)

C–H activation at a primary benzylic site was the key step in very short syntheses of lignans **206** and **207** (Scheme 14.27) [138]. Even though both the substrate **203** and the vinyldiazoacetate **204** contain very electron-rich aromatic rings, C–H activation to form **205** (43% yield and 91% *ee*) is still possible because the aromatic rings are sterically protected from electrophilic aromatic substitution by the carbenoid. Reduction of the ester in (*S*)-**205** followed by global deprotection of the silyl ethers completes a highly efficient three-step asymmetric total synthesis of (+)-imperanene **206**. Treatment of (*R*)-**205** in a more elaborate synthetic sequence of a cascade Prins reaction/electrophilic substitution/lactonization results in the total synthesis of a related lignan, (–)-α-conidendrin **207**.

Highly stereoselective intermolecular C–H activation is possible at C–H bonds adjacent to nitrogen [130]. The ability of the nitrogen lone pair to stabilize charge buildup

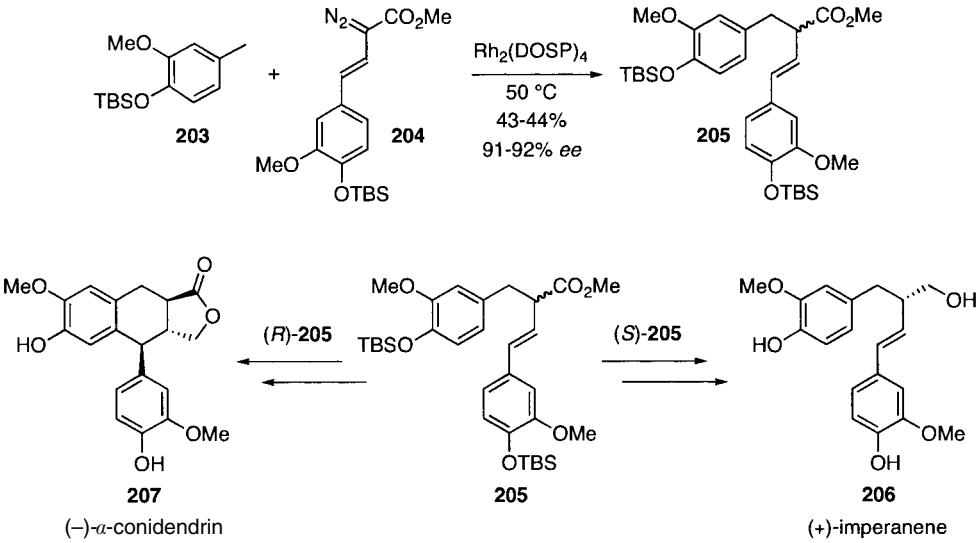

Scheme 14.27

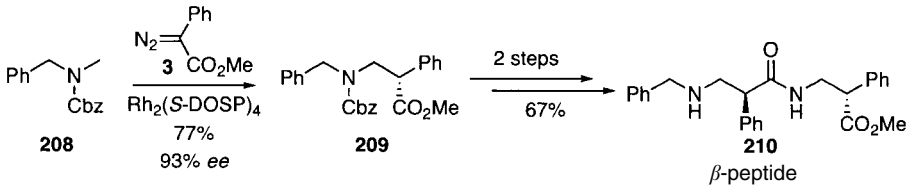

Scheme 14.28

in the transition state allows unprecedented insertions at primary sites [139]. Highly enantioselective C–H insertion at the *N*-methyl site of Cbz-protected benzylamine **208** has been utilized for the preparation of a novel *β*-peptide **210** (Scheme 14.28) [139].

Chiral cyclic *β*-amino esters have been prepared using the asymmetric C–H activation of *N*-Boc-pyrrolidine and *N*-Boc-piperidine [140]. Remarkable levels of diastereo- and enantioselectivity have been observed in the pyrrolidine systems [139]. Decomposition of methyl phenyldiazoacetate **3**, catalyzed by Rh_2(*S*-DOSP)$_4$ in the presence of **211**, generates the C–H insertion product **212** (92% *de*) with 94% enantiomeric excess (Eq. 25) [139]. Double C–H insertion was possible to form **213** when a further 4.5 equiv of methyl phenyldiazoacetate **3** was added to the reaction mixture (Eq. 26) [140]. This double C–H insertion sequence allows excellent control at four stereocenters, generating an elaborate C_2-symmetric amine. A more extensive study on the double stereodifferentiation and kinetic resolution of chiral cyclic pyrrolidines via C–H activation has been published [141]. The highlight of this study was the chemoselective C–H activation of **214** at the methylene position adjacent to nitrogen, essentially generating a single stereoisomer of **215** (>94% *de*, 98% *ee*) in 85% yield (Eq. 27).

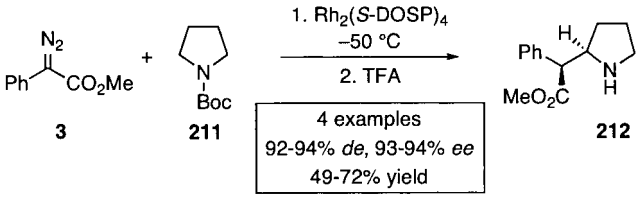

(25)

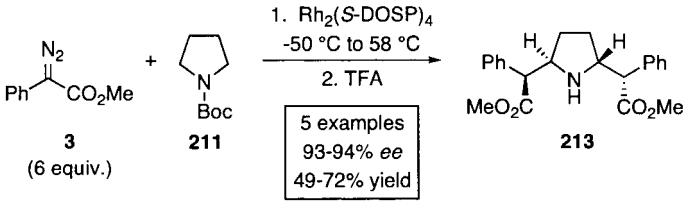

(26)

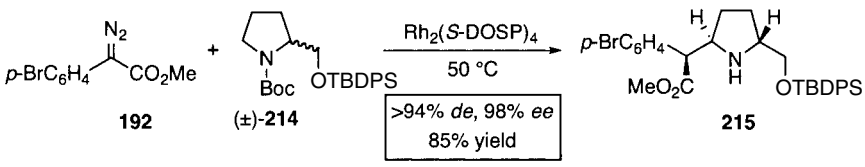

(27)

The full potential of this C–H activation process, as a surrogate Mannich reaction, was realized in the direct asymmetric synthesis of *threo*-methylphenidate (Ritalin) **217** (Eq. 28) [140]. C–H insertion of *N*-Boc-piperidine **216** using second-generation Rh_2-(*S*-biDOSP)$_2$ and methyl phenyldiazoacetate resulted in a 71:29 diastereomeric mixture, where the desired *threo*-diastereomer was obtained in 52% yield with 86% enantiomeric excess. Winkler and co-workers screened several dirhodium tetracarboxamidates and found Rh_2(*R*-MEPY)$_4$ to be the catalyst that gives the highest diastereoselectivity for this reaction [142].

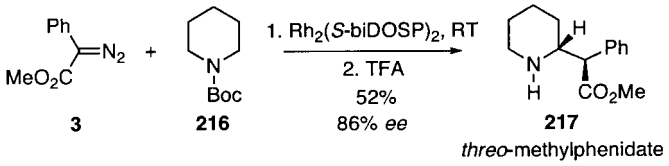

(28)

Highly efficient C–H insertion adjacent to oxygen atoms to generate *β*-hydroxy esters has been demonstrated [130, 143, 144]. Reactions with cyclic oxygenated systems have not been extensively explored with these carbenoids and only the reaction with tetrahydrofuran has been reported [130]. The major *syn*-diastereomer **218** from the reaction of methyl phenyldiazoacetate with tetrahydrofuran at –50 °C was obtained in 67% yield with 97% enantiomeric excess (Eq. 29).

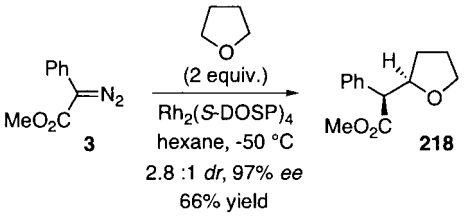

(29)

Extending the reaction to acyclic *trans*-allyl silyl ethers **220** results in the highly diastereoselective formation of *syn*-aldol products **221** (Eq. 30) [143]. Even higher stereoselectivity can be achieved with the tetraalkoxysilanes **222**, where both the diastereo- and enantioselectivity for the formation of **223** are exceptional (Eq. 31) [144]. C–H insertion into tetraethoxysilane **222** generates the *syn*-aldol product **223** in 70% yield (>94% *de*) with 95% enantiomeric excess.

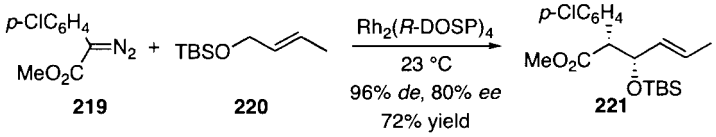

(30)

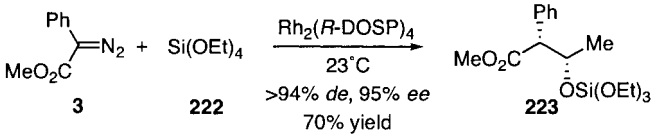

(31)

In summary, the chemistry of the donor/acceptor-substituted carbenoids represents a new avenue of research for metal-catalyzed decomposition of diazo compounds. The resulting carbenoids are more chemoselective than the conventional carbenoids, which allows reactions to be achieved that were previously inaccessible. The discovery of pantolactone as an effective chiral auxiliary, and rhodium prolinates as exceptional chiral catalysts for this class of rhodium-carbenoid intermediate, broadens the synthetic utility of this chemistry. The successful development of the asymmetric intermolecular C–H activation process underscores the potential of this class of carbenoids for organic synthesis.

14.8 References

1 Maas, G. *Top. Curr. Chem.* **1987**, *137*, 75.
2 Doyle, M.P. *Chem. Rev.* **1986**, *86*, 919.
3 Davies, H.M.L. In *Comprehensive Organic Synthesis*; Trost, B.M., Ed.; Pergamon Press: Oxford, **1991**; Vol. 4, pp. 1031–1068.
4 Ye, T.; McKervey, M.A. *Chem. Rev.* **1994**, *94*, 1091.
5 Doyle, M.P.; McKervey, M.A.; Ye, T. *Modern Catalytic Methods for Organic Synthesis with Diazo Compounds: From Cyclopropanes to Ylides*; Wiley: New York, **1998**.
6 Pfaltz, A. In *Comprehensive Asymmetric Catalysis I–III*; Jacobsen, E.N., Pfaltz, A., and Yamamoto, H., Eds.; Springer: New York, **1999**; Vol. 2, pp. 513–538.
7 Lydon, K.M.; McKervey, M.A. In *Comprehensive Asymmetric Catalysis I–III*; Jacobsen, E.N., Pfaltz, A., and Yamamoto, H., Eds.; New York, **1999**; Vol. 2, pp. 539–580.
8 Charette, A.B.; Lebel, H. In *Comprehensive Asymmetric Catalysis I–III*; Jacobsen, E.N., Pfaltz, A., and Yamamoto, H., Eds., **1999**; Vol. 2, pp. 581–603.
9 Paulissen, R.; Reimlinger, H.; Hayez, E.; Hubert, A.J.; Teyssie, P. *Tetrahedron Lett.* **1973**, 2233.
10 Padwa, A.; Weingarten, M.D. *Chem. Rev.* **1996**, *96*, 223.
11 Davies, H.M.L. *Curr. Org. Chem.* **1998**, *2*, 463.
12 Doyle, M.P.; Forbes, D.C. *Chem. Rev.* **1998**, *98*, 911.
13 Davies, H.M.L. In *Advances in Cycloaddition*; Haramata, M.E., Ed.; JAI Press: Greenwich, CT, **1999**; Vol. 5, pp. 119–164.
14 Davies, H.M.L.; Antoulinakis, E.G. *J. Organomet. Chem.* **2001**, *617–618*, 47.
15 Davies, H.M.L. *J. Mol. Catal. A: Chem.* **2002**, *189*, 125.
16 Davies, H.M.L.; Antoulinakis, E.G. *Org. Reactions* **2001**, *57*, 1.
17 Davies, H.M.L.; Beckwith, R.E.J. *Chem. Rev.* **2003**, *103*, 2861.
18 Peace, B.W.; Wulfman, D.S. *Synthesis* **1973**, 137.
19 Alonso, M.E.; Jano, P.; Hernandez, M.I.; Greenberg, R.S.; Wenkert, E. *J. Org. Chem.* **1983**, *48*, 3047.
20 Doyle, M.P. *Acc. Chem. Res.* **1986**, *19*, 348.
21 Davies, H.M.L. *Tetrahedron* **1993**, *49*, 5203.
22 Davies, H.M.L.; Bruzinski, P.R.; Fall, M.J. *Tetrahedron Lett.* **1996**, *37*, 4133.
23 Davies, H.M.L.; Hodges, L.M.; Matasi, J.J.; Hansen, T.; Stafford, D.G. *Tetrahedron Lett.* **1998**, *39*, 4417.
24 Davies, H.M.L. *Aldrichim. Acta* **1997**, *30*, 107.
25 Davies, H.M.L. *Eur.J. Org. Chem.* **1999**, 2459.
26 Davies, H.M.L.; Xiang, B.; Kong, N.; Stafford, D.G. *J. Am. Chem. Soc.* **2001**, *123*, 7461.
27 Hodgson, D.M.; Pierard, F.Y.T.M.; Stupple, P.A. *Chem. Soc. Rev.* **2001**, *30*, 50.
28 Bulugahapitiya, P.; Landais, Y.; Parra-Rapado, L.; Planchenault, D.; Weber, V. *J. Org. Chem.* **1997**, *62*, 1630.
29 Buck, R.T.; Coe, D.M.; Drysdale, M.J.; Ferris, L.; Haigh, D.; Moody, C.J.; Pearson, N.D.; Sanghera, J.B. *Tetrahedron: Asymmetry* **2003**, *14*, 791.
30 Doyle, M.P.; Bagheri, V.; Wandless, T.J.; Harn, N.K.; Brinker, D.A.; Eagle, C.T.; Loh, K.L. *J. Am. Chem. Soc.* **1990**, *112*, 1906.
31 Niimi, T.; Uchida, T.; Irie, R.; Katsuki, T. *Adv. Synth. Catal.* **2001**, *343*, 79.
32 Katsuki, T. *Adv. Synth. Catal.* **2002**, *344*, 131.

33 Nishiyama, H.; Itoh, Y.; Matsumoto, H.; Park, S.-B.; Itoh, K. *J. Am. Chem. Soc.* **1994**, *116*, 2223.

34 Nishiyama, H.; Itoh, Y.; Sugawara, Y.; Matsumoto, H.; Aoki, K.; Itoh, K. *Bull. Chem. Soc. Jpn.* **1995**, *68*, 1247.

35 Davies, H.M.L.; Clark, T.J.; Church, L.A. *Tetrahedron Lett.* **1989**, *30*, 5057.

36 Ressig, H.-U. In *Stereoselective Synthesis, Methods of Organic Chemistry (Houben-Weyl)*; Helmchen, G., Hoffmann, R.W., Mulzer, J., and Schaumann, E., Eds.; Georg Thieme Verlag: New York, **1995**; Vol. E21c, pp. 3179–3270.

37 Doyle, M.P.; Zhou, Q.-L.; Charnsangavej, C.; Longoria, M.A.; McKervey, M.A.; Garcia, C.F. *Tetrahedron Lett.* **1996**, *37*, 4129.

38 Starmans, W.A.J.; Thijs, L.; Zwanenburg, B. *Tetrahedron* **1998**, *54*, 629.

39 Davies, H.M.L. L.; Panaro, S.A. *Tetrahedron* **2000**, *56*, 4871.

40 Davies, H.M.L.; Bruzinski, P.; Hutcheson, D.K.; Kong, N.; Fall, M.J. *J. Am. Chem. Soc.* **1996**, *118*, 6897.

41 Doyle, M.P.; Dorow, R.L.; Buhro, W.E.; Griffin, J.H.; Tamblyn, W.H.; Trudell, M.L. *Organometallics* **1984**, *3*, 44.

42 Davies, H.M.L.; Huby, N.J.S.; Cantrell, W.R., Jr.; Olive, J.L. *J. Am. Chem. Soc.* **1993**, *115*, 9468.

43 Davies, H.M.L.; Matasi, J.J.; Thornley, C. *Tetrahedron Lett.* **1995**, *36*, 7205.

44 Davies, H.M.L.; Matasi, J.J.; Hodges, L.M.; Huby, N.J.S.; Thornley, C.; Kong, N.; Houser, J.H. *J. Org. Chem.* **1997**, *62*, 1095.

45 Davies, H.M.L.; Hutcheson, D.K. *Tetrahedron Lett.* **1993**, *34*, 7243.

46 Wynne, D.C.; Olmstead, M.M.; Jessop, P.G. *J. Am. Chem. Soc.* **2000**, *122*, 7638.

47 Davies, H.M.L.; Boebel, T.A. *Tetrahedron Lett.* **2000**, *41*, 8189.

48 Davies, H.M.L.; Townsend, R.J. *J. Org. Chem.* **2001**, *66*, 6595.

49 Davies, H.M.; Kong, N. *Tetrahedron Lett.* **1997**, *38*, 4203.

50 Davies, H.M.L.; Panaro, S.A. *Tetrahedron Lett.* **1999**, *40*, 5287.

51 Davies, H.M.L.; Chandrasekar, V. *Org. Lett.* **2003**, *5*, 1403.

52 Corey, E.J.; Gant, T.G. *Tetrahedron Lett.* **1994**, *35*, 5373.

53 Davies, H.M.L.; Nagashima, T.; Klino, J.L., III. *Org. Lett.* **2000**, *2*, 823.

54 Zaragoza, F.; Petersen, S.V. *Tetrahedron* **1996**, *52*, 5000.

55 Gowravaram, M.R.; Gallop, M.A. *Tetrahedron Lett.* **1997**, *38*, 6973.

56 Cano, M.; Camps, F.; Joglar, J. *Tetrahedron Lett.* **1998**, *39*, 9819.

57 Iso, Y.; Shindo, H.; Hamana, H. *Tetrahedron* **2000**, *56*, 5353.

58 Clapham, B.; Spanka, C.; Janda, K.D. *Org. Lett.* **2001**, *3*, 2173.

59 Clapham, B.; Reger, T.S.; Janda, K.D. *Tetrahedron* **2001**, *57*, 4637.

60 Lee, S.-H.; Clapham, B.; Koch, G.; Zimmermann, J.; Janda, K.D. *J. Comb. Chem.* **2003**, *5*, 188.

61 Lee, S.-H.; Clapham, B.; Koch, G.; Zimmermann, J.; Janda, K.D. *Org. Lett.* **2003**, *5*, 511.

62 Nagashima, T.; Davies, H.M.L. *J. Am. Chem. Soc.* **2001**, *123*, 2695.

63 Nagashima, T.; Davies, H.M.L. L. *Org. Lett.* **2002**, *4*, 1989.

64 Bergbreiter, D.E. In *Chiral Catalyst Immobilization and Recycling*; De Vos, D.E., Vankelecom, I.F.J., and Jacobs, P.A., Eds.; Wiley-VCH: New York, **2000**; pp. 43–80.

65 Rechavi, D.; Lemaire, M. *Chem. Rev.* **2002**, *102*, 3467.

66 Doyle, M.P.; Timmons, D.J.; Tumonis, J.S.; Gau, H.-M.; Blossey, E.C. *Organometallics* **2002**, *21*, 1747.

67 Doyle, M.P.; Yan, M.; Gau, H.-M.; Blossey, E.C. *Org. Lett.* **2003**, *5*, 561.

68 Davies, H.M.L.; Doan, B.D. *J. Org. Chem.* **1999**, *64*, 8501.

69 Doyle, M.P.; Davies, S.B.; Hu, W. *Org. Lett.* **2000**, *2*, 1145.

70 Vandewalle, M.; De Clercq, P. *Tetrahedron* **1985**, *41*, 1767.

71 Rigby, J.H. In *Studies in Natural Products Chemistry*; Rahman, A., Ed.; Elsevier: New York, **1988**; Vol. 1, pp. 545–576.

72 Heathcock, C.H.; Grahm, S.L.; Pirrung, M.C.; Plavac, F.; White, C.T. In *The Total Synthesis of Natural Products*; Simon, J., Ed.; Wiley: New York, **1980**; Vol. 5, pp. 333–384.

73 Davies, H.M.L.; Smith, H.D.; Korkor, O. *Tetrahedron Lett.* **1987**, *28*, 1853.

74 Doyle, M.P.; Wang, L.C.; Loh, K.L. *Tetrahedron Lett.* **1984**, *25*, 4087.

75 Davies, H.M.L.; Clark, T.J.; Smith, H.D. *J. Org. Chem.* **1991**, *56*, 3817.

76 Davies, H.M.L.; Hu, B. *Heterocycles* **1993**, *35*, 385.

77 Davies, H.M.L.; Hu, B.; Saikali, E.; Bruzinski, P.R. *J. Org. Chem.* **1994**, *59*, 4535.

78 Davies, H.M.L.; Clark, T.J.; Kimmer, G.F. *J. Org. Chem.* **1991**, *56*, 6440.

79 Davies, H.M.L.; Clark, T.J. *Tetrahedron* **1994**, *50*, 9883.

80 Cantrell, W.R., Jr.; Davies, H.M.L. *J. Org. Chem.* **1991**, *56*, 723.

81 Davies, H.M.L.; Doan, B.D. *J. Org. Chem.* **1998**, *63*, 657.

82 Davies, H.M.L.; Cantrell, W.R., Jr. *Tetrahedron Lett.* **1991**, *32*, 6509.

83 Davies, H.M.L.; Stafford, D.G.; Doan, B.D.; Houser, J.H. *J. Am. Chem. Soc.* **1998**, *120*, 3326.

84 Davies, H.M.L.; Clark, D.M.; Smith, T.K. *Tetrahedron Lett.* **1985**, *26*, 5659.

85 Davies, H.M.L.; Clark, D.M.; Alligood, D.B.; Eiband, G.R. *Tetrahedron* **1987**, *43*, 4265.

86 Davies, H.M.L.; Ahmed, G.; Churchill, M.R. *J. Am. Chem. Soc.* **1996**, *118*, 10774.

87 Padwa, A.; Kassir, J.M.; Xu, S.L. *J. Org. Chem.* **1991**, *56*, 6971.

88 Fattori, D.; Vogel, P. *Tetrahedron Lett.* **1993**, *34*, 1017.

89 Molander, G.A.; Swallow, S. *J. Org. Chem.* **1994**, *59*, 7148.

90 Davies, H.M.L.; Young, W.B.; Smith, H.D. *Tetrahedron Lett.* **1989**, *30*, 4653.

91 Davies, H.M.L.; Saikali, E.; Young, W.B. *J. Org. Chem.* **1991**, *56*, 5696.

92 Davies, H.M.L.; Saikali, E.; Huby, N.J.; Gilliatt, V.J.; Matasi, J.J.; Sexton, T.; Childers, S.R. *J. Med. Chem.* **1994**, *37*, 1262.

93 Davies, H.M.L.; Kuhn, L.A.; Thornley, C.; Matasi, J.J.; Sexton, T.; Childers, S.R. *J. Med. Chem.* **1996**, *39*, 2554.

94 Davies, H.M.L.; Gilliatt, V.; Kuhn, L.A.; Saikali, E.; Ren, P.; Hammond, P.S.; Sexton, T.; Childers, S.R. *J. Med. Chem.* **2001**, *44*, 1509.

95 Nader, M.A.; Grant, K.A.; Davies, H.M.L.; Mach, R.H.; Childers, S.R. *J. Pharmacol. Exp. Ther.* **1997**, *280*, 541.

96 Letchworth, S.R.; Smith, H.R.; Porrino, L.J.; Bennett, B.A.; Davies, H.M.L.; Sexton, T.; Childers, S.R. *J. Pharmacol. Exp. Ther.* **2000**, *293*, 686.

97 Freeman, W.M.; Yohrling, G.J.; Daunais, J.B.; Gioia, L.; Hart, S.L.; Porrino, L.J.; Davies, H.M.L.; Vrana, K.E. *Drug Alcohol Depend.* **2000**, *61*, 15.

98 Bennett, B.A.; Wichems, C.H.; Hollingsworth, C.K.; Davies, H.M.L.; Thornley, C.; Sexton, T.; Childers, S.R. *J. Pharmacol. Exp. Ther.* **1995**, *272*, 1176.

99 Bennett, B.A.; Hollingsworth, C.K.; Martin, R.S.; Childers, S.R.; Ehrenkaufer, R.E.; Porrino, L.J.; Davies, H.M.L. *Neuropharmacology* **1998**, *37*, 123.

100 Mach, R.H.; Nader, M.A.; Ehrenkaufer, R.L.; Gage, H.D.; Childers, S.R.; Hodges, L.M.; Hodges, M.M.; Davies, H.M.L. *Synapse* **2000**, *37*, 109.

101 Kende, A.S.; Smalley, T.L., Jr.; Huang, H. *J. Am. Chem. Soc.* **1999**, *121*, 7431.

102 Davies, H.M.L.; Doan, B.D. *Tetrahedron Lett.* **1996**, *37*, 3967.

103 Davies, H.M.L.; Calvo, R.L.; Townsend, R.J.; Ren, P.; Churchill, R.M. *J. Org. Chem.* **2000**, *65*, 4261.

104 Davies, H.M.L.; Hu, B. *Tetrahedron Lett.* **1992**, *33*, 453.

105 Davies, H.M.L.; Hu, B. *J. Org. Chem.* **1992**, *57*, 3186.

106 Davies, H.M.L.; Kong, N.; Churchill, M.R. *J. Org. Chem.* **1998**, *63*, 6586.

107 Davies, H.M.L.; Ahmed, G.; Calvo, R.L.; Churchill, M.R.; Churchill, D.G. *J. Org. Chem.* **1998**, *63*, 2641.

108 Davies, H.M.L.; Hu, B. *J. Org. Chem.* **1992**, *57*, 4309.

109 Moody, C.J.; Miller, D.J. *Tetrahedron* **1998**, *54*, 2257.

110 Doyle, M.P.; Yan, M. *Tetrahedron Lett.* **2002**, *43*, 5929.

111 Yao, W.; Liao, M.; Zhang, X.; Xu, H.; Wang, J. *Eur.J. Org. Chem.* **2003**, 1784.

112 Davies, H.M.L.; DeMeese, J. *Tetrahedron Lett.* **2001**, *42*, 6803.

113 Doyle, M.P.; Hu, W.; Timmons, D.J. *Org. Lett.* **2001**, *3*, 933.

114 Doyle, M.P.; Yan, M.; Hu, W.; Gronenberg, L.S. *J. Am. Chem. Soc.* **2003**, *125*, 4692.

115 Doyle, M.P.; Hu, W.; Timmons, D.J. *Org. Lett.* **2001**, *3*, 3741.

116 Novikov, A.V.; Kennedy, A.R.; Rainier, J.D. *J. Org. Chem.* **2003**, *68*, 993.

117 Buck, R.; Doyle, M.; Drysdale, L.; Ferris, L.; Forbes, D.; Haigh, D.; Moody, C.; Pearson, N.; Zhou, Q. *Tetrahedron Lett.* **1996**, *37*, 7631.

118 Buck, R.; Coe, D.; Drysdale, M.; Moody, C.; Pearson, N. *Tetrahedron Lett.* **1998**, *39*, 7181.

119 Dakin, L.A.; Schaus, S.E.; Jacobsen, E.N.; Panek, J.S. *Tetrahedron Lett.* **1998**, *39*, 8947.

120 Davies, H. M. L.; Hansen, T.; Rutberg, J.; Bruzinski, P. R. *Tetrahedron Lett.* **1997**, *38*, 1741.

121 Davies, H. M. L.; Hansen, T. *J. Am. Chem. Soc.* **1997**, *119*, 9075.

122 Arndtsen, B. A.; Bergman, R. G.; Mobley, T. A.; Peterson, T. H. *Acc. Chem. Res.* **1995**, *28*, 154.

123 Shilov, A. E.; Shul'pin, G. B. *Chem. Rev.* **1997**, *97*, 2879.

124 Arndtsen, B. A.; Bergman, R. G. *Science* **1995**, *270*, 1970.

125 Dyker, G. *Angew. Chem., Int. Ed.* **1999**, *38*, 1699.

126 Jones, W. D.; Kakiuchi, F.; Murai, S. *Activation of C–H Bonds: Stoichiometric Reactions*; Murai, S., Ed.; Springer: New York, **1999**, pp. 9–46.

127 Kakiuchi, F.; Murai, S. *Activation of C–H Bonds: Catalytic Reactions*; Murai, S., Ed.; Springer: New York, **1999**, pp. 47–79.

128 Jia, C.; Kitamura, T.; Murai, S. *Acc. Chem. Res.* **2001**, *34*, 633.

129 Diaz-Requejo, M. M.; Belderrain, T. R.; Nicasio, M. C.; Trofimenko, S.; Perez, P. J. *J. Am. Chem. Soc.* **2002**, *124*, 896.

130 Davies, H. M. L.; Hansen, T.; Churchill, M. R. *J. Am. Chem. Soc.* **2000**, *122*, 3063.

131 Muller, P.; Tohill, S. *Tetrahedron* **2000**, *56*, 1725.

132 Davies, H. M. L.; Gregg, T. M. *Tetrahedron Lett.* **2002**, *43*, 4951.

133 Davies, H. M. L.; Walji, A. M.; Townsend, R. J. *Tetrahedron Lett.* **2002**, *43*, 4981.

134 Davies, H. M. L.; Stafford, D. G.; Hansen, T. *Org. Lett.* **1999**, *1*, 233.

135 Davies, H. M. L.; Ren, P.; Jin, Q. *Org. Lett.* **2001**, *3*, 3587.

136 Davies, H. M. L.; Ren, P. *J. Am. Chem. Soc.* **2001**, *123*, 2070.

137 Davies, H. M. L.; Jin, Q.; Ren, P.; Kovalevsky, A. Y. *J. Org. Chem.* **2002**, *67*, 4165.

138 Davies, H. M. L.; Jin, Q. *Tetrahedron: Asymmetry* **2003**, *14*, 941.

139 Davies, H. M. L.; Venkataramani, C. *Angew. Chem., Int. Ed.* **2002**, *41*, 2197.

140 Davies, H. M. L.; Hansen, T.; Hopper, D. W.; Panaro, S. A. *J. Am. Chem. Soc.* **1999**, *121*, 6509.

141 Davies, H. M. L.; Venkataramani, C. *Org. Lett.* **2001**, *3*, 1773.

142 Axten, J. M.; Ivy, R.; Krim, L.; Winkler, J. D. *J. Am. Chem. Soc.* **1999**, *121*, 6511.

143 Davies, H. M. L.; Antoulinakis, E. G.; Hansen, T. *Org. Lett.* **1999**, *1*, 383.

144 Davies, H. M. L.; Antoulinakis, E. G. *Org. Lett.* **2000**, *2*, 4153.

15
Chiral Dirhodium(II) Carboxamidates for Asymmetric Cyclopropanation and Carbon–Hydrogen Insertion Reactions

Michael P. Doyle

15.1
Introduction

In 1989–1990 three groups published initial results relating to the development of dirhodium(II) catalysts for asymmetric transformations of diazo compounds [1–3]. Two focused on amino acid carboxylate ligands [1, 2], and one of them fortuitously found that prolinate ligands had unusual selectivity in reactions of diazoacetates and related substrates [2], even though the ligand's chiral centers lie far from the axial sites of dirhodium(II), which is where the carbene intermediate is formed. This discovery has led to very significant undertakings by Davies, particularly with aryl- and vinyldiazoacetates [4–8], but they have already been described in Chapter 14.

On the basis of reports by Bear and co-workers [10–12] and the discovery that carboxamidate ligands could be introduced onto dirhodium(II) by semi-automated methods [13], Doyle and co-workers began their development of carboxamidate ligands for dirhodium with oxazolidinones (for example, **1** and **2**), but with limited success in achieving high enantiocontrol [3]. Only when a carboxylate attachment, as in pyrrolidinone **3**, rather than an isopropyl or benzyl group, as in **1** or **2**, was placed in proximity to the reaction center, could high enantiocontrol be achieved [14]. The key developments here were: 1) the methodology for the semi-automated synthesis of dirhodium(II) carboxamidates by trapping acetic acid with sodium carbonate in a Soxhlet extraction apparatus (Eq. 1) [15]; and 2) the discovery of the high selectivity enhancement afforded by the carboxylate attachment [16].

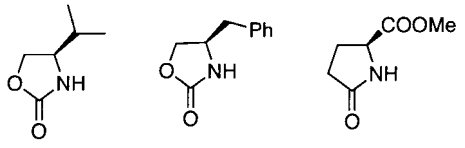

1 **2** **3**

$$Rh_2(OAc)_4 + 4LH \xrightarrow[\text{reflux}]{\text{PhCl}} Rh_2L_4 + 4HOAc \quad \text{(trapped by } Na_2CO_3\text{)} \qquad (1)$$

Modern Rhodium-Catalyzed Organic Reactions. Edited by P. Andrew Evans

ISBN: 3-527-30683-8

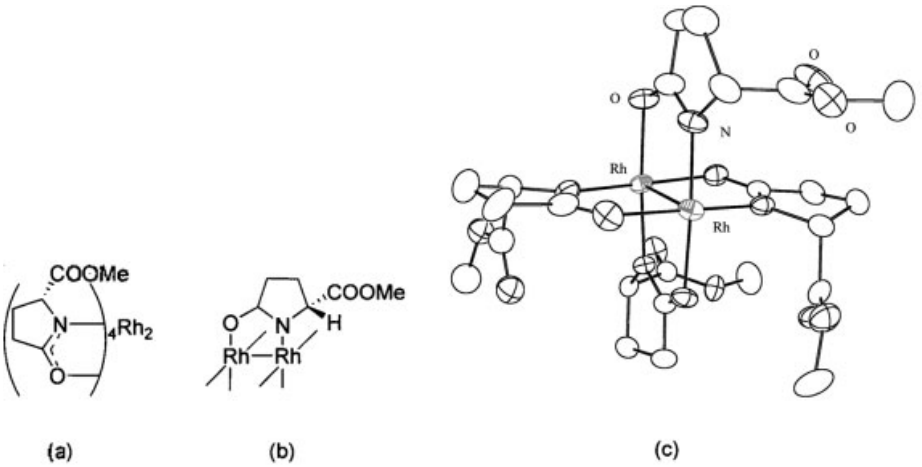

Fig. 15.1 Structural depictions of $Rh_2(5R\text{-MEPY})_4$:
(a) formula, (b) alternative depiction, (c) X-ray structure [14].

Dirhodium(II) carboxamidates are uniquely constructed with four bridging ligands in a paddlewheel fashion. Two nitrogen atoms and two oxygen atoms are bound to each rhodium and, as a result of coordination preferences [17], the nitrogens (or oxygens) are oriented *cis* to each other (Fig. 15.1). In these structures the ligands are tightly bound and undergo slow exchange only at temperatures at or above 80 °C [18]. If the COOMe "chiral attachment" is viewed as a chemical entity that occupies the space around rhodium, two adjacent quadrants of a four-quadrant circle are occupied, leaving two open access sites on the reaction center (for example, **4** and **5**). The accessibility of the electrophilic carbene center in these catalysts to approach by nucleophiles makes them especially advantageous for highly selective intramolecular metal carbene reactions of diazo compounds [19, 20], and due to the rigidity of the carboxamidate ligands, selectivities in metal carbene reactions are independent of solvent.

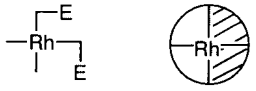

4: E = COOMe **5**

Broad selections of chiral ligands are now available and each has specific advantages [19–23]. Dirhodium(II) carboxamidates have been constructed from pyrrolidinones **6** [14, 15], oxazolidinones **7** [24], imidazolidinones **8** [25], and azetidinones **9** [26]. They differ in reactivities and selectivities for metal carbene reactions, on the basis of their steric and/or electronic influences. Because of the wider bite angle of the azetidinone OCN attachment, the rhodium–rhodium bond length is longer (2.53 Å versus 2.46 Å) in these complexes than in those constructed from five-membered ring lactams. The longer Rh–Rh distance imparts a greater electrophilic reactivity in these catalysts [27].

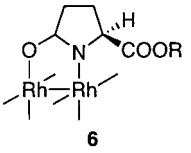

6

R = Me : Rh_2(5*S*-MEPY)$_4$
R = $(CH_2)_{17}CH_3$: Rh_2(5*S*-ODPY)$_4$

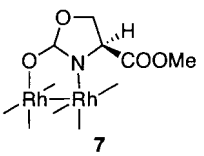

7

Rh_2(4*S*-MEOX)$_4$

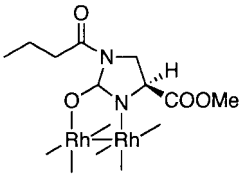

8

Rh_2(4*S*-MPPIM)$_4$

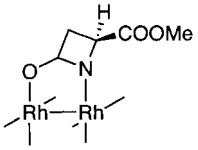

9

Rh_2(4*S*-MEAZ)$_4$

15.2
Catalytic Asymmetric Cyclopropanation and Cyclopropenation

15.2.1
Intramolecular Reactions

Chiral dirhodium(II) carboxamidates are preferred for intramolecular cyclopropanation of allylic and homoallylic diazoacetates (Eq. 2). The catalyst of choice is Rh_2(MEPY)$_4$ when R^c and R^i are H, but Rh_2(MPPIM)$_4$ gives the highest selectivities when these substituents are alkyl or aryl. Representative examples of the applications of these catalysts are listed in Scheme 15.1 according to the cyclopropane synthesized. Use of the catalyst with mirror image chirality produces the enantiomeric cyclopropane with the same enantiomeric excess [33]. Enantioselectivities fall off to a level of 40–70% *ee* when *n* is increased beyond 2 and up to 8 (Eq. 2) [32], and in these cases the use of the chiral bisoxazoline–copper complexes is advantageous.

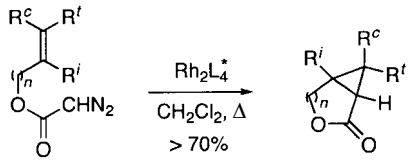

10 (n = 1,2) **11** (*n* = 1,2) (2)

"Kinetic resolution" (enantiomer differentiation) of cycloalkenyl diazoacetates has been achieved (for example, according to Eq. 3) [34]. In these cases one enantiomer of the racemic reactant matches with the catalyst configuration to produce the intramolecular cyclopropanation product in high enantiomeric excess, whereas the mismatched enantiomer preferentially undergoes hydride abstraction from the allylic position [35] to yield the corresponding cycloalkenone. With acyclic secondary allylic diazoacetates the hydride abstraction pathway is relatively unimportant, and diastereoselection becomes the means for enantiomer differentiation [31].

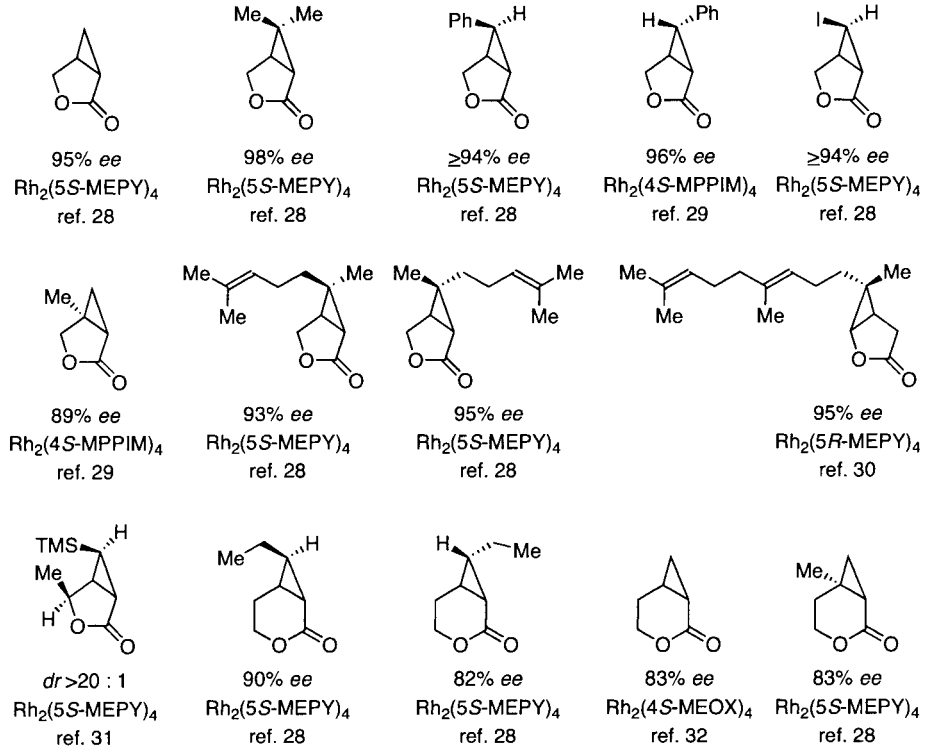

Scheme 15.1 Enantioselectivity for intramolecular cyclopropanation of diazoacetates.

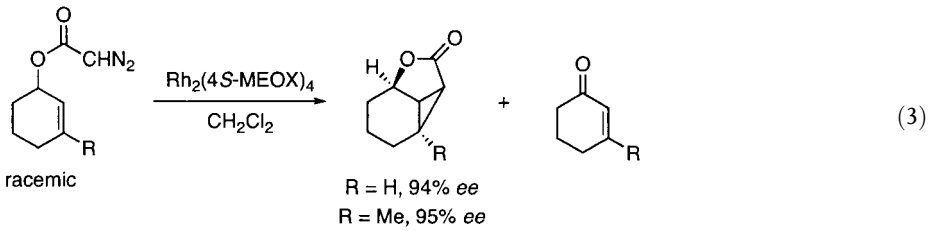

(3)

Diazoacetamides undergo intramolecular cyclopropanation with similarly high enantioselectivities (Eq. 4) [33, 36, 37]. In these cases, however, competition from intramolecular dipolar cycloaddition can complicate the reaction process. Therefore, the use of R^n = Me or ^{t}Bu has been required to achieve good yields of reaction products. Representative examples of applications of chiral dirhodium(II) carboxamidates for enantioselective intramolecular cyclopropanation of diazoacetamides are compiled in Scheme 15.2.

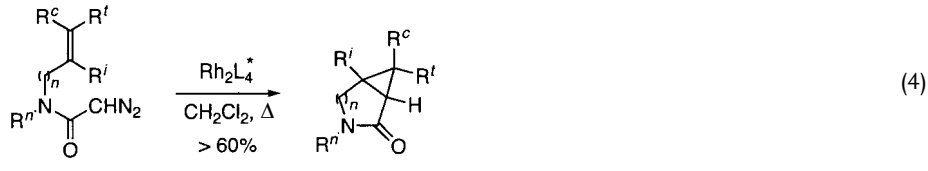

(4)

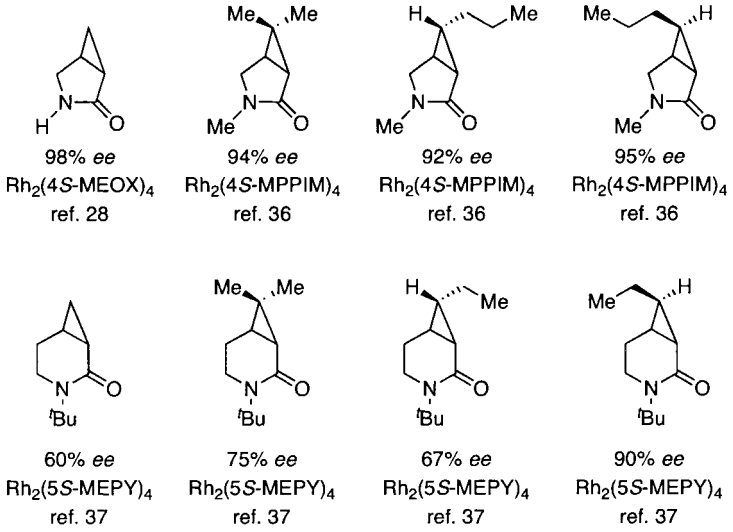

Scheme 15.2 Enantioselectivity for intramolecular cyclopropanation of diazoacetamides.

Dirhodium carboxamidates are less reactive toward diazo decomposition than are dirhodium(II) carboxylates [21]. This has usually meant that they could not be used for reactions with aryl- and vinyldiazoacetates or with diazomalonates. However, the azetidinone-ligated catalysts such as $Rh_2(4S\text{-MEAZ})_4$ **9** offer distinct advantages for rapid diazo decomposition and for achieving the highest levels of enantioselectivity reported (for example, according to Eq. 5) [27]. This catalytic system has been used to prepare milnacipran and its analogs [38]. In the case of the conversion of **16** to **17**, the $Rh_2(4S\text{-MEAZ})_4$ catalyst gave a turnover number of 10000 and a selectivity of 95% enantiomeric excess (Eq. 6). Further reactivity enhancement has been achieved with difluoro analogs of $Rh_2(5S\text{-MEPY})_4$ and the isobutyl and cyclohexyl esters of azetidinone **9** (see **18** and **19**); however, these catalysts did not enhance selectivities beyond those achieved with **6** or **9** [39]. As expected from the comparative reactivities of **6** and **9**, **19** is significantly more electrophilic in its reactions than is **18**.

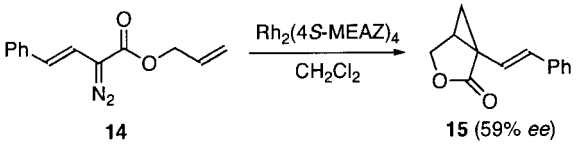

(5)

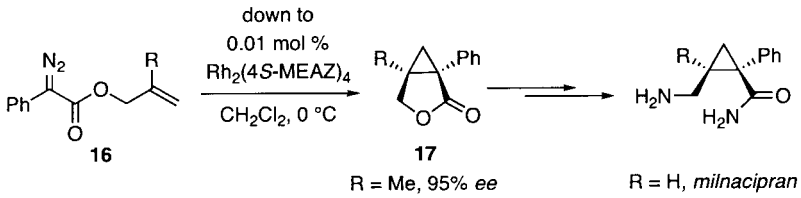

(6)

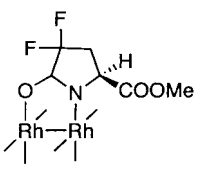

18

$Rh_2(5S\text{-dFMEPY})_4$

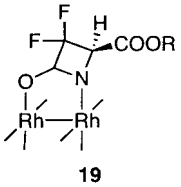

19

R= ^{t}Bu : $Rh_2(4S\text{-dFtBAZ})_4$

R= ^{c}Hex : $Rh_2(4S\text{-dFCHAZ})_4$

These chiral catalysts have also been linked to polymeric resins (Equation (7)) for multiple use/reuse without significant loss in enantiocontrol (Fig. 15.2) [40, 41]. Both Novasyn and Merrifield resins proved effective, and mixed ligand systems with enhanced electronic and steric characteristics could be produced by this methodology [41].

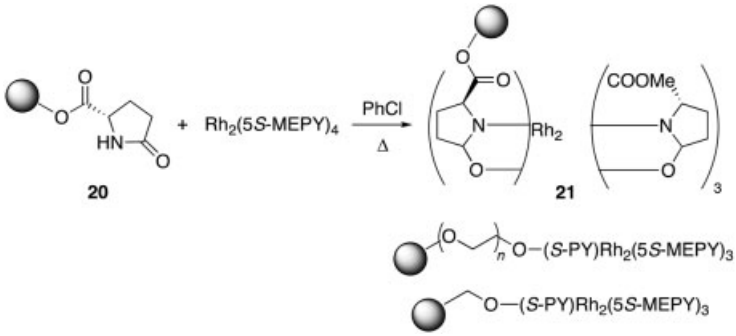

(7)

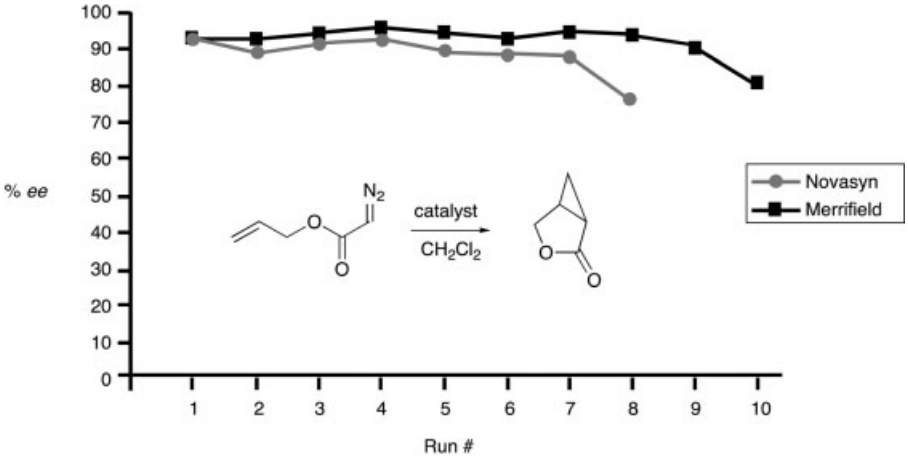

Fig. 15.2 Immobilized chiral dirhodium(II) pyrrolidinone-carboxylates and their application to intramolecular cyclopropanation of allyl diazoacetate [40].

15.2.2
Intermolecular Reactions

Dirhodium(II) catalysts do not offer many advantages over copper, ruthenium, or cobalt catalysts in stereoselective carbene additions from diazoacetates to simple alkenes [20, 23, 33, 42]. Diastereoselectivity is modest; however, the chiral catalysts with carboxamidate ligands show a propensity to form the *cis*-isomer in preference to the thermodynamically favored *trans*-isomer (for example, Eq. 8) [43]. Using an azetidinone with a menthyl-carboxylate attachment **22**, diastereoselectivities as high as 92:8 (*cis*/*trans*) were achieved in the synthesis of **23** [44]. This methodology has been applied to the synthesis of a cyclopropane-configured urea–PETT analog **24** that is an HIV-1 reverse transcriptase inhibitor (Eq. 9) [44]. Although the Katsaki catalysts [45, 46] exhibit virtually complete *cis*-selectivity for cyclopropanation of styrene, reactivities are problematic and they have not been examined with other substrates. The mechanism of the cyclopropanation reactions catalyzed by dirhodium(II) compounds is well established [19].

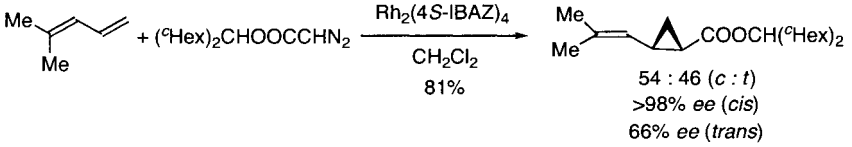

(8)

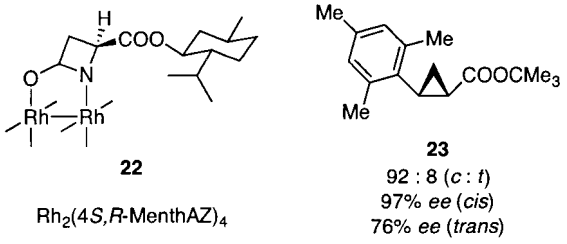

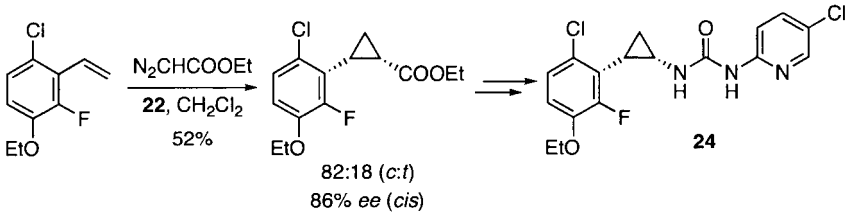

(9)

Cyclopropenation reactions are also effectively catalyzed by dirhodium(II) compounds, and high enantiocontrol has been achieved with the $Rh_2(MEPY)_4$ catalysts (Scheme 15.3) [47]. A striking example of the catalyst effect on selectivity is found in the behavior of substrate **25** toward $Rh_2(5S\text{-MEPY})_4$ and the more reactive $Rh_2(4S\text{-IBAZ})_4$ (Eq. 10) [48]. With the less reactive $Rh_2(5S\text{-MEPY})_4$ it preferentially undergoes allylic cyclopropanation with high chemoselectivity and enantiocontrol. With the more reactive $Rh_2(4S\text{-IBAZ})_4$ addition to the carbon–carbon triple bond is favored even though this involves construction of a ten-membered ring.

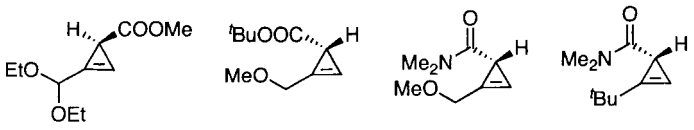

≥98% ee 78% ee ≥ 94% ee 89% ee

Scheme 15.3 Enantioselectivity for intermolecular cyclopropenation.

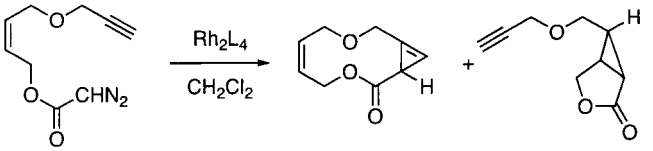

(10)

25	Rh_2(5*S*-MEPY)$_4$	4	96 (96% *ee*)
	Rh_2(4*S*-IBAZ)$_4$	84 (97% *ee*)	16 (88% *ee*)

15.3
Catalytic Asymmetric Carbon–Hydrogen Insertion

Intramolecular carbon–hydrogen insertion reactions have well known to be effectively promoted by dirhodium(II) catalysts [19–23]. Insertion into the γ-position to form five-membered ring compounds is virtually exclusive, and in competitive experiments the expected reactivity for electrophilic carbene insertion (3^o>2^o>>1^o) is observed [49], as is heteroatom activation [50]. A recent theoretical treatment [51] confirmed the mechanistic proposal (Scheme 15.4) that C–C and C–H bond formation with the carbene carbon proceeds in a concerted fashion as the ligated metal dissociates [52]. Chemoselectivity is dependent on the catalyst ligands [53].

Dirhodium(II) carboxamidates, and especially the Rh_2(MPPIM)$_4$ (**8**) catalysts, are exceptionally effective for highly enantioselective intramolecular insertion reactions of diazoacetates and diazoacetamides [19–23]. These reactions take place with high regioselectivity for γ-lactone (lactam) formation (Eq. 11) [54, 55], and enantioselectivities greater than 90% *ee* are commonly achieved. In the reaction of **25** to **26**, the *S*-configured catalyst yields the *S*-configured product, whereas the *R*-configured catalyst affords the *R*-enantiomer. Application of this methodology for the synthesis of a series of lignan lactones (Scheme 15.5) has been reported [55]. Recently, this methodology has been used for the synthesis of naturally occurring (*S*)-(+)-imperanene (Eq. 12) [56] and for the $GABA_b$ receptor agonist (*R*)-(–)-baclofen (Eq. 13) [57]. In all cases selectivities were high with less than 5% insertion into other C–H positions.

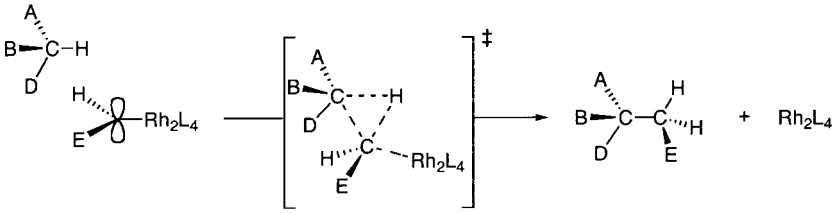

Scheme 15.4 Mechanism of metal carbene carbon–hydrogen insertion.

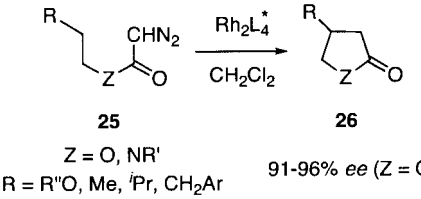

25 **26**

Z = O, NR'
R = R"O, Me, ^{i}Pr, CH_2Ar

91-96% *ee* (Z = O)

(11)

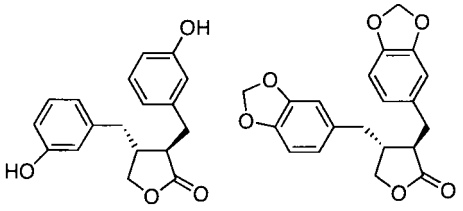

27 : (-)-enterolactone **28** : (-)-hinokinin

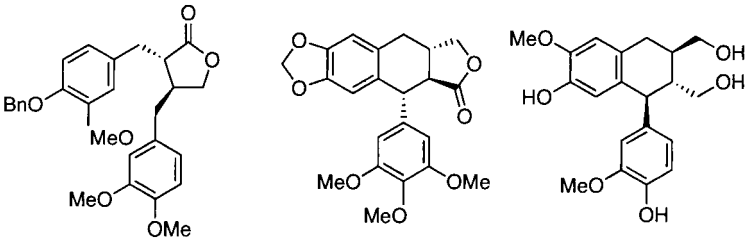

29 : (-)-arctigenin **30** : (+)-isodeoxypodophyllotoxin **31** : (+)-isolauricerisinol

Scheme 15.5 Synthesis of lignan lactones via C–H insertion.

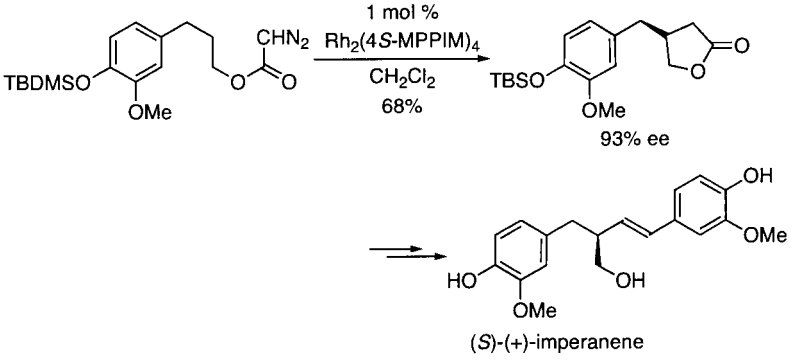

(12)

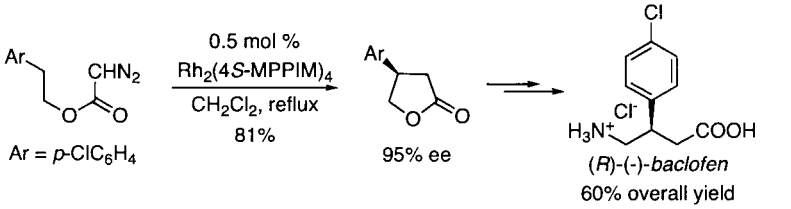

(13)

Because of the synthetic interest in their products, and the potential for control of both diastereo- and enantioselectivity in their C–H insertions, catalytic reactions of cycloalkyl diazoacetates have received a great deal of attention [58–61]. For example, although cyclohexyl diazoacetate could be converted to both *cis*- and *trans*-bicyclic products (Eq. 14), the ability to control both the diastereo- and enantioselectivity proved challenging.

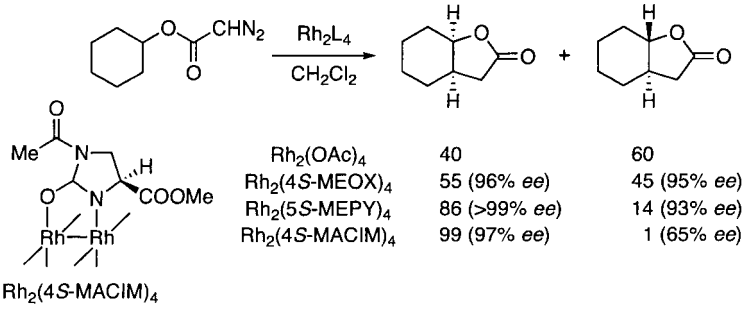

(14)

Use of $Rh_2(OAc)_4$ suggested that there was no inherent selectivity attributable to the coordinated carbene or to rhodium(II). However, modification of dirhodium(II) ligands to imidazolidinones provided exceptional diastereocontrol, obtained by influencing the conformational energies of the intermediate metal carbene [19, 23], as well as high enantiocontrol. Representative examples of products from these highly selective intramolecular C–H insertion reactions with cyclic systems is given in Scheme 15.6. Additional examples of effective insertions in systems from which diastereomeric products can result are illustrated in processes of the synthesis of 2-deoxyxylolactone (Scheme 15.7) [64, 65]. Here the conformation of the reactant metal carbene that is responsible for product formation is **32** rather than **33**. Other examples in non-heteroatom-bound systems (for example, as in Eq. 15) confirm this preference.

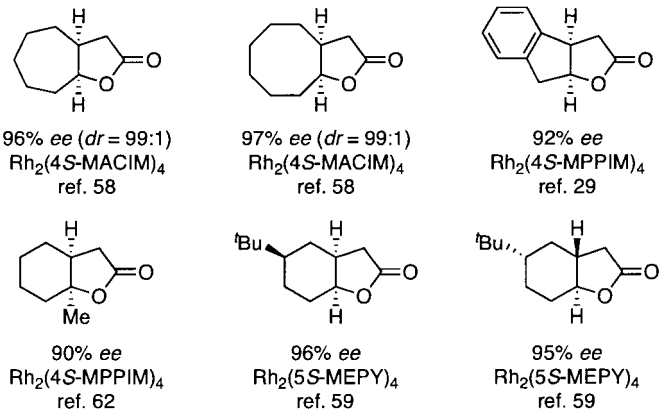

Scheme 15.6 nantioselectivity for intramolecular C–H insertion reactions.

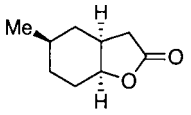

98% *ee* (*dr* >99:1)
Rh_2(4*S*-MEOX)$_4$
ref. 58

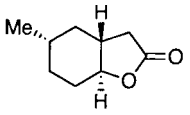

95% *ee* (*dr* = 90:10)
Rh_2(4*S*-MEOX)$_4$
ref. 58

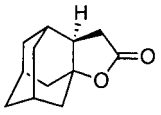

98% *ee*
Rh_2(4*S*-MEOX)$_4$
ref. 24

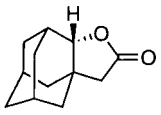

98% *ee*
Rh_2(4*S*-MEOX)$_4$
ref. 24

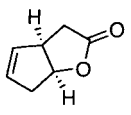

91% *ee*
Rh_2(4*S*-MPPIM)$_4$
ref. 62

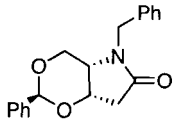

85% *ee*
Rh_2(4*S*-MEPY)$_4$
ref. 63

Scheme 15.6 (cont.)

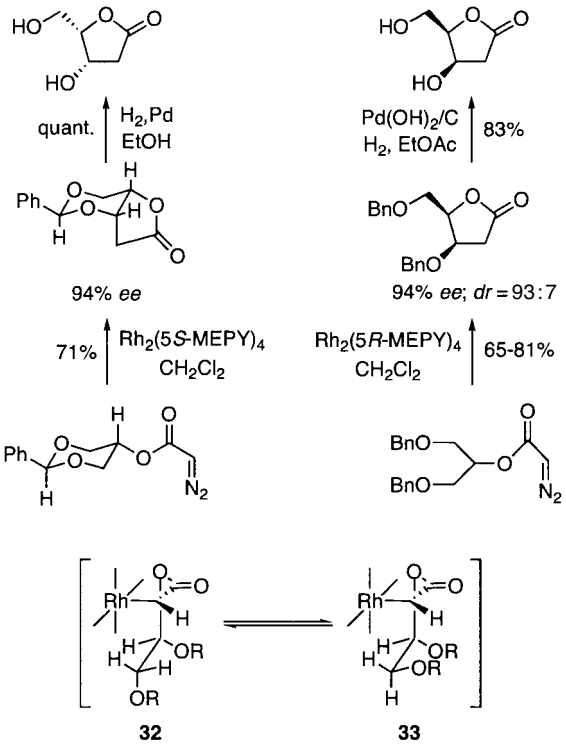

32 **33**

Scheme 15.7 Synthesis of 2-deoxyxylolactone.

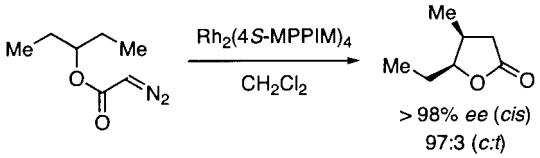

(15)

Configurational match/mismatch governs these reactions so that different products may be produced in high yield and selectivity when enantiomeric catalysts are applied to the same substrate [61, 62], as illustrated by the reaction processes in Scheme 15.8 [61]. Additional examples in the steroidal field have also been reported [66]. In these cases the formation of four-membered ring β-lactones is common.

Lactam systems have been synthesized by reliance on configurational matching, as exemplified in the synthesis of the pyrrolizidine alkaloid (–)-heliotridane (Scheme 15.9)

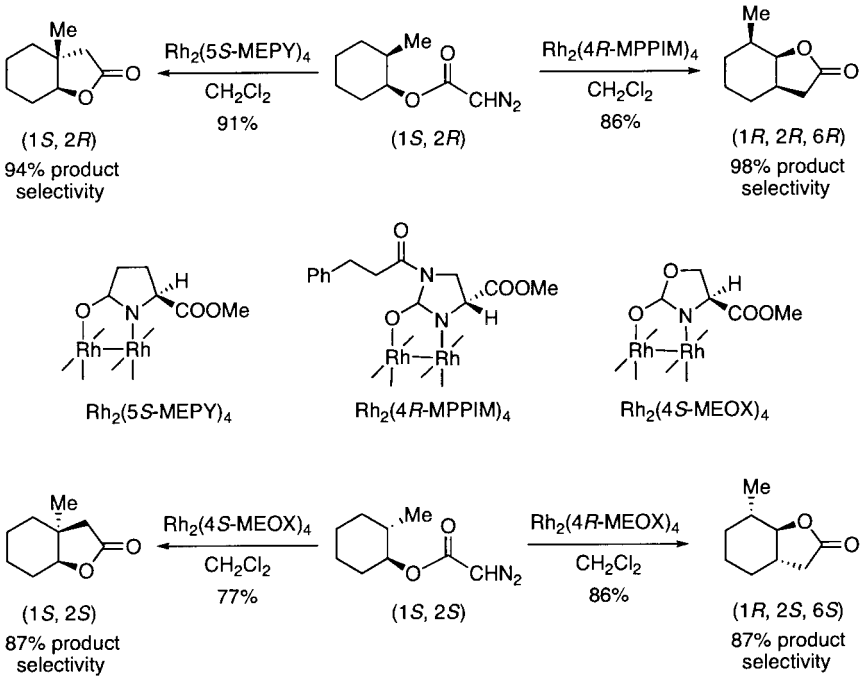

Scheme 15.8 Diastereocontrol in C–H insertion reactions with chiral dirhodium(II) carboxamidate catalysts.

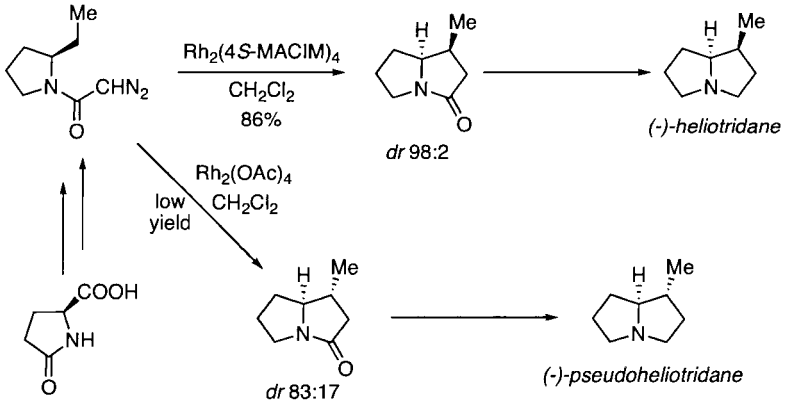

Scheme 15.9 Synthesis of (–)-heliotridane.

[67]. Interestingly, while the chiral $Rh_2(4S\text{-MACIM})_4$ catalyst gave the desired isomer from the C–H insertion reaction, the achiral $Rh_2(OAc)_4$ catalyst afforded the opposite diastereoisomer in low yield. The enantioselective preparation of *β*-lactams by C–H insertion has also been examined, and some like **34** and **35** are formed with high enantiocontrol [68], but the generality of this process has not yet been established.

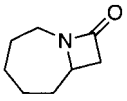

34: 97% ee
with $Rh_2(5S\text{-MEPY})_4$

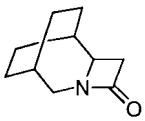

35: 96% ee
with $Rh_2(5S\text{-MEPY})_4$

15.4 Summary

Dirhodium(II) carboxamidates are highly selective catalysts for metal carbene transformations of diazoacetates and diazoacetamides. Intramolecular cyclopropanation of allylic and homoallylic systems occurs with the highest enantioselectivities when catalyzed by chiral dirhodium(II) carboxamidates, and in select cases turnover numbers of 10 000 have been achieved. Activated catalysts with chiral azetidinone ligands offer high *cis*-diastereoselection in intermolecular cyclopropanation reactions. Intramolecular insertion into a carbon–hydrogen bond is a facile process, occurring with enantioselectivities of greater than 90% *ee* and with high diastereocontrol. Although formation of a five-membered ring lactone or lactam is generally preferred, the formation of four-membered ring products is also well established. These catalysts have unique advantages in asymmetric synthesis, and their applications in total synthesis are increasingly visible, as they hold great potential for numerous stereocontrolled processes.

15.5 References

1 H. Brunner, H. Kluschanzoff, K. Wutz, *Bull. Soc. Chem. Belg.* **1989**, *98*, 63.
2 M. Kennedy, M.A. McKervey, A.R. Maguire, G.H.P. Roos, *J. Chem. Soc., Chem. Commun.* **1990**, 361.
3 M.P. Doyle, B.D. Brandes, A.P. Kazala, R.J. Pieters, M.B. Jarstfer, L.M. Watkins, C.T. Eagle, *Tetrahedron Lett.* **1990**, *31*, 6613.
4 H.M.L. Davies, Z.-Q. Peng, J.H. Houser, *Tetrahedron Lett.* **1994**, *35*, 8939.
5 H.M.L. Davies, P. Bruzinski, D.K. Hutcheson, M.J. Fall, *J. Am. Chem. Soc.* **1996**, *118*, 6897.
6 H.M.L. Davies, E.G. Antoulinakis, *Org. React.* **2001**, *57*, 1.
7 H.M.L. Davies, P. Ren, *J. Am. Chem. Soc.* **2001**, *123*, 2070.
8 M.P. Doyle, M.A. McKervey, *J. Chem Soc., Chem. Commun.* **1997**, 983.
9 H.M.L. Davies, B. Xiang, N. Kong, D.G. Stafford, *J. Am. Chem. Soc.* **2001**, *123*, 7461.
10 M.Q. Ahsam, I. Bernal, J.L. Bear, *Inorg. Chem.* **1986**, *25*, 260.
11 J.L. Bear, T.P. Zhu, T. Malinski, A.M. Dennis, K.M. Kadish, *Inorg. Chem.* **1984**, *23*, 674.
12 A.M. Dennis, J.D. Korp, I. Bernal, R.A. Howard, J. L. Bear, *Inorg. Chem.* **1983**, *22*, 1522.

13 M.P. Doyle, V. Bagheri, T.J. Wandless, N.K. Harn, D.A. Brinker, C.T. Eagle, K.-L. Loh, *J. Am. Chem. Soc.* **1990**, *112*, 1906.

14 M.P. Doyle, W.R. Winchester, J.A.A. Hoorn, V. Lynch, S.H. Simonsen, R. Ghosh, *J. Am. Chem. Soc.* **1993**, *115*, 9968.

15 M.P. Doyle, W.R. Winchester, M.N. Protopopova, A.P. Kazala, L.J. Westrum, *Org. Synth.* **1996**, *73*, 13.

16 M.P. Doyle, *Recl. Trav. Chim. Pays-Bas* **1991**, *110*, 305.

17 M.P. Doyle, C.E. Raab, G.H.P. Roos, V. Lynch, S.H. Simonsen, *Inorg. Chim. Acta* **1997**, *266*, 13.

18 M.P. Doyle, M.Y. Eismont, D.E. Bergbreiter, H.N. Gray, *J. Org. Chem.* **1992**, *57*, 6103.

19 M.P. Doyle, M.A. McKervey, T. Ye, *Modern Catalytic Methods for Organic Synthesis with Diazo Compounds*, John Wiley & Sons, New York, **1997**.

20 M.P. Doyle in *Catalytic Asymmetric Synthesis*, 2nd edition, I. Ojima, Ed., John Wiley & Sons, New York, **2000**, Chapter 5.

21 M.P. Doyle, T. Ren, *Prog. Inorg. Chem.* **2001**, *49*, 113.

22 M.P. Doyle in *Catalysis by Di- and Polynuclear Metal Cluster Complexes*, R.D. Adams, F.A. Cotton, Eds., VCH Publishers, New York, **1998**, Chapter 7.

23 M.P. Doyle, D.C. Forbes, *Chem. Rev.* **1998**, *98*, 911.

24 M.P. Doyle, A.B. Dyatkin, M.N. Protopopova, C.I. Yang, C.S Miertschim, W.R. Winchester, S.H. Simonsen, V. Lynch, R. Ghosh, *Recl. Trav. Chim. Pays-Bas* **1995**, *114*, 163.

25 M.P. Doyle, Q.-L. Zhou, C.E. Raab, G.H.P. Roos, S.H. Simonsen, V. Lynch, *Inorg. Chem.* **1996**, *35*, 6064.

26 M.P. Doyle, Q.-L. Zhou, S.H. Simonsen, V. Lynch, *Synlett* **1996**, 697.

27 M.P. Doyle, S.B. Davies, W. Hu, *Org. Lett.* **2002**, *2*, 1145.

28 M.P. Doyle, R.E. Austin, A.S. Bailey, M.P. Dwyer, A.B. Dyatkin, A.V. Kalinin, M.M.Y. Kwan, S. Liras, C.J. Oalmann, R.J. Pieters, M.N. Protopopova, C.E. Raab, G.H.P. Roos, Q.-L. Zhou, S.F. Martin, *J. Am. Chem. Soc.* **1995**, *117*, 5763.

29 M.P. Doyle, Q.-L. Zhou, A.B. Dyatkin, D.A. Ruppar, *Tetrahedron Lett.* **1995**, *36*, 7579.

30 D.H. Rogers, E.C. Yi, C.D. Poulter, *J. Org. Chem.* **1995**, *60*, 941.

31 S.F. Martin, M.R. Spaller, S. Liras, B. Hartmann, *J. Am. Chem. Soc.* **1994**, *116*, 4493.

32 M.P. Doyle, I.M. Phillips, *Tetrahedron Lett.* **2001**, *42*, 3155.

33 M.P. Doyle, M.N. Protopopova, *Tetrahedron* **1998**, *54*, 7919.

34 M.P. Doyle, A.B. Dyatkin, A.V. Kalinin, D.A. Ruppar, S.F. Martin, M.R. Spallar, S. Liras, *J. Am. Chem. Soc.* **1995**, *117*, 11 021.

35 M.P. Doyle, A.B. Dyatkin, C.L. Autry, *J. Chem. Soc., Perkin Trans. 1* **1995**, 619.

36 M.P. Doyle, A.V. Kalinin, *J. Org. Chem.* **1996**, *61*, 2179.

37 M.P. Doyle, M.Y. Eismont, M.N. Protopopova, M.M.Y. Kwan, *Tetrahedron* **1994**, *50*, 1665.

38 M.P. Doyle, W. Hu, *Adv. Synth. Catal.* **2001**, *343*, 299.

39 M.P. Doyle, W. Hu, I.M. Phillips, C.J. Moody, A.G. Pepper, A.M.Z. Slavin, *Adv. Synth. Catal.* **2001**, *343*, 112.

40 M.P. Doyle, D.J. Timmons, J.S. Tumonis, H.-M. Gau, E.C. Blossey, *Organometallics* **2002**, *21*, 1747.

41 M.P. Doyle, H.-M. Gau, E.C. Blossey, M. Yan, *Org. Lett.* **2003**, *5*, 561.

42 P. Müller, C. Baud, D. Ene, S. Motallebi, M.P. Doyle, B.D. Brandes, A.B. Dyatkin, M.M. See, *Helv. Chim. Acta* **1995**, *78*, 459.

43 M.P. Doyle, S.B. Davies, W. Hu, *J. Chem. Soc., Chem. Commun.* **2000**, 867.

44 W. Hu, D.J. Timmons, M.P. Doyle, *Org. Lett.* **2002**, *4*, 901.

45 T. Niimi, T. Uchida, R. Irie, T. Katsuki, *Tetrahedron Lett.* **2000**, *41*, 3647.

46 T. Uchida, R. Irie, T. Katsuki, *Tetrahedron* **2000**, *56*, 3501.

47 M.P. Doyle, M.N. Protopopova, P. Müller, D. Ene, E.A. Shapiro, *J. Am. Chem. Soc.* **1994**, *116*, 8492.

48 M.P. Doyle, D.G. Ene, C.S. Peterson, V. Lynch, *Angew. Chem., Int. Ed.* **1999**, *38*, 700.

49 D.F. Taber, R.E. Ruckle Jr., *J. Am. Chem. Soc.* **1986**, *108*, 7686.

50 P. Wong, J. Adams, *J. Am. Chem. Soc.* **1994**, *116*, 3296.

51 E. Nakamura, N. Yoshikai, M. Yamanaka, *J. Am. Chem. Soc.* **2002**, *124*, 7181.

52 M.P. Doyle, L.J. Westrum, W.N.E. Wolthius, M.M. See, W.P. Boone, V. Bagheri, M.M. Pearson, *J. Am. Chem. Soc.* **1993**, *115*, 958.

53 A. Padwa, D. J. Austin, A. T. Price, M. A. Semonis, M. P. Doyle, M. N. Protopopova, W. R. Winchester, A. Tran, *J. Am. Chem. Soc.* **1993**, *115*, 8669.

54 M. P. Doyle, A. van Oeveren, L. J. Westrum, M. N. Protopopova, T. W. Clayton Jr., *J. Am. Chem. Soc.* **1993**, *115*, 8669.

55 J. W. Bode, M. P. Doyle, M. N. Protopopova, Q.-L. Zhou, *J. Org. Chem.* **1996**, *61*, 9146.

56 M. P. Doyle, W. Hu, M. Valenzuela, *J. Org. Chem.* **2002**, *67*, 2954.

57 M. P. Doyle, W. Hu, *Chirality* **2002**, *14*, 169.

58 M. P. Doyle, A. B. Dyatkin, G. H. P. Roos, F. Cañas, D. A. Pierson, A. van Basten, P. Müller, P. Polleux, *J. Am. Chem. Soc.* **1994**, *116*, 4507.

59 P. Müller, P. Polleux, *Helv. Chim. Acta* **1994**, *77*, 645.

60 D. F. Taber in *Methods of Organic Chemistry*, 4th edition, G. Helmchen, R. W. Hoffman, J. Mulzer, E. Schaumann, Eds., G. Thieme Verlag, New York, **1995**, Chapter 12.1.2.

61 M. P. Doyle, A. V. Kalinin, D. G. Ene, *J. Am. Chem. Soc.* **1996**, *118*, 8837.

62 M. P. Doyle, A. J. Catino, *Tetrahedron: Asymmetry* **2003**, *14*, 925.

63 M. P. Doyle, M. Yan, I. M. Phillips, D. J. Timmons, *Adv. Synth. Catal.* **2002**, *344*, 91.

64 M. P. Doyle, A. B. Dyatkin, J. S. Tedrow, *Tetrahedron Lett.* **1994**, *35*, 3853.

65 M. P. Doyle, J. S. Tedrow, A. B. Dyatkin, C. J. Spaans, D. G. Ene, *J. Org. Chem.* **1999**, *64*, 8907.

66 M. P. Doyle, S. B. Davies, E. J. May, *J. Org. Chem.* **2001**, *66*, 8112.

67 M. P. Doyle, A. V. Kalinin, *Tetrahedron Lett.* **1996**, *37*, 1371.

68 M. P. Doyle, A. V. Kalinin, *Synlett* **1995**, 1075.

16
Cyclopentane Construction by Rhodium(II)-Mediated Intramolecular C–H Insertion

Douglass F. Taber and Pramod V. Joshi

16.1
Introduction

The development of general methods for the preparation of polycarbocyclic natural products with control of both relative and absolute configuration has been a longstanding challenge in organic synthesis. Controlling the relative configuration of a stereogenic center on a pendant side chain, relative to the ring to which it is attached, has proven particularly troublesome. The synthetic power of cyclopentane construction by rhodium-mediated intramolecular C–H insertion is illustrated w1] by the cyclization of enantiomerically pure **1** to give the nicely crystalline β-ketoester **2** (Scheme 16.1). The synthetic utility of **2** as a chiron was demonstrated through the preparation of physiologically active natural products, as exemplified by the conversion of **2** to the *anti*-proliferative marine secosteroid (–)-astrogorgiadiol **3** [2, 3].

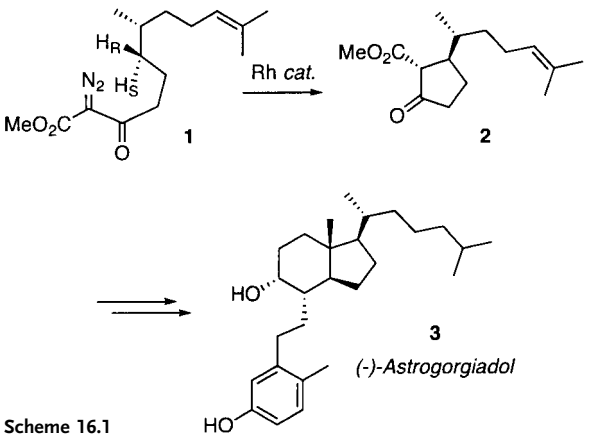

Scheme 16.1

16.2
Background: Cyclization versus Elimination

We initially observed [4, 5] that an α-diazo β-keto ester **5** would, on exposure to a catalytic amount of $Rh_2(OAc)_4$, undergo smooth cyclization to the cyclopentane derivative **6** (Scheme 16.2). The α-diazo β-keto ester **5** is readily prepared by diazo transfer [6] from

Modern Rhodium-Catalyzed Organic Reactions. Edited by P. Andrew Evans

ISBN: 3-527-30683-8

the corresponding β-keto ester **4**, which thereby provides a general strategy to highly substituted cyclopentanes. Subsequently, we observed [7] that $Rh_2(O_2CR)_4$ catalysts having more electron-donating carboxylic acids facilitate the efficient cyclization of simple α-diazo esters [8] such as **7** to the corresponding cyclopentanes with high diastereocontrol (Scheme 16.2). This observation set the stage for the work described herein.

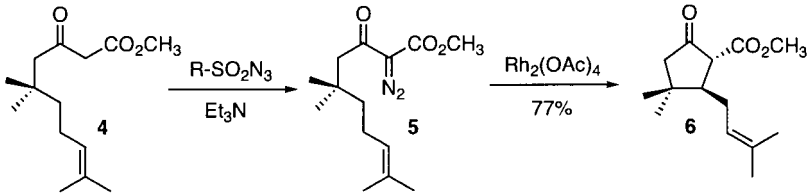

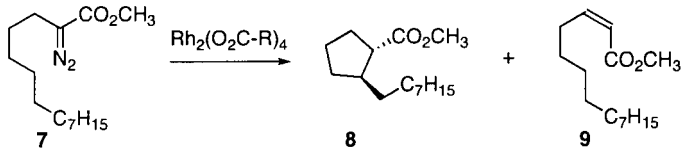

R	8	9
$-CH_3$	66	34
$-CF_3$	52	48
$-C(CH_3)_3$	85	15

Scheme 16.2

16.3 Beginnings of a Computational Approach

Any or all of the diastereomeric products **11–14** (Scheme 16.3) could have been formed by cyclization of the α-diazo ester **10**, in which only **12** was observed [9]. In an attempt to rationalize this result, we developed a computationally based model for the transition state of the C–H insertion.

An understanding of the mechanism [10] for rhodium-mediated intramolecular C–H insertion begins with the recognition that these α-diazo carbonyl derivatives can also be seen as stabilized ylides, such as **15** (Scheme 16.4). The catalytic rhodium(II) carboxylate **16** is Lewis acidic, with vacant coordination sites at the apical positions, as shown. The first step in the mechanism, carbene transfer from the diazo ester to the rhodium, begins with complexation of the electron density at the diazo carbon with an open rhodium coordination site, to give **17**. Back-donation of electron density from the proximal rhodium to the carbene carbon, with concomitant loss of N_2, then gives the intermediate rhodium carbene complex **18**.

The mechanism by which this intermediate rhodium carbene complex **18** reacts can be more easily understood if it is written as the inverted ylide **19**, as this species would clearly be electrophilic at carbon. We hypothesized that for bond formation to proceed, a transition state **20** in which the C–Rh bond is aligned with the target C–H bond

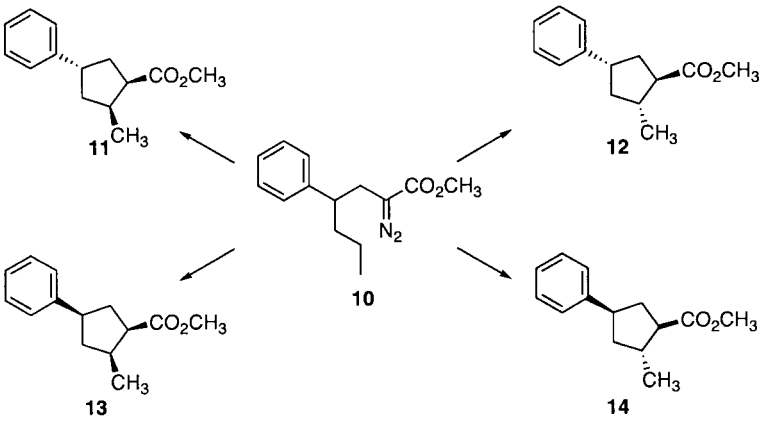

Scheme 16.3

would be required [11]. As the C–H insertion reaction proceeded, the electron pair in the C–H bond would be responsible for forming the new C–C bond, and the same time the electron pair in the C–Rh bond would slide over to form the new C–H bond. This would give the product **21** and release the initial rhodium species **16**, completing the catalytic cycle.

A central assumption of this mechanism is that the actual C–H insertion is concerted, and that it proceeds with retention of absolute configuration. We had already, in a related case [12], demonstrated that rhodium-mediated C–H insertion proceeds with retention of absolute configuration.

The actual product from a cyclization will be determined as the intermediate carbene *commits* to a particular diastereomeric transition state. If these diastereomeric transition states are indeed in full thermal equilibrium [13], then computational modeling of the diastereomeric transition states of **20** could allow us to predict which of them would be favored, and thus which diastereomeric product would be formed.

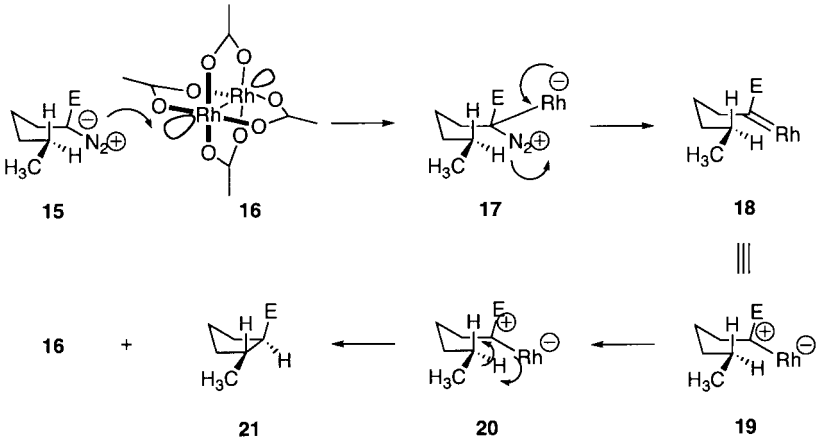

Scheme 16.4

16.3.1

Development of the Computational Model

To construct the transition states of **20**, we locked (Scheme 16.5) the Rh-Rh-C bond angle at 180°. To secure overlap between the C–Rh bond and the target C–H bond for modeling purposes, we established weak bonds (meaningful in Mechanics [14]) between the two incipiently bonding carbons, as well as between the target hydrogen and the proximal rhodium. As Mechanics tends to rehybridize weakly bonded carbons, we also found it necessary to lock the H-C-C-C dihedral angle of the target C–H at 60° (or, in the inverted transition state, –60°), to maintain sp^3 geometry.

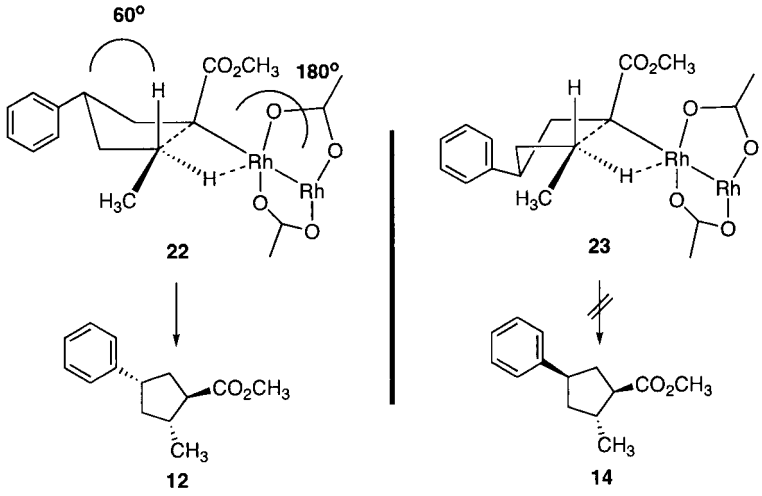

Scheme 16.5

On the basis of these parameters we determined two possible transition states, **22** and **23**. In transition state **22**, the rhodium carbene is pointed away from the flip of the incipient cyclopentane ring (a "chair-like" transition state, counting the five carbons and the rhodium in the six-membered ring), whereas in **23** the rhodium carbene is pointed toward the flip of the incipient cyclopentane ring (a "boat-like" transition state). As **10** (see Scheme 16.3) cyclizes to **12**, in which the methyl and the phenyl are on the same face of the cyclopentane, we concluded that at the point of commitment to product formation, the transition state leading to cyclization must be chair-like **22** rather than boat-like **23**.

Sterically (Mechanics), there is no significant energy difference between the competing transition states **22** and **23**. We therefore assume that the difference is electronic, and that conformation **22** makes electron density more readily available from the target C–H bond than does conformation **23**. This interplay between steric and electronic effects will be important throughout this discussion of rhodium-mediated intramolecular C–H insertion.

16.3.2
Application of the Computational Model

For the cyclization of **10**, there are four diastereomeric chair-like transition states, **22**, **24**, **25**, and **26** (Tab. 16.1), each leading to one of the four possible diastereomeric products. The minimization of the four transition states with Mechanics [14], using the angles and bonds as stated, demonstrated transition state **22** to be the lowest in energy, being 5.3 kcal mol^{-1} lower than the next most stable TS. This contrasts with the relative stability of the four diastereomeric *products*, **11**, **12**, **13**, and **14** (Tab. 16.1), which are quite comparable one to another.

Using this approach, we have successfully predicted the major product from the cyclization of more than 30 α-diazo esters and α-diazo β-keto esters [15]. Not all rhodium-mediated intramolecular C–H insertion reactions will proceed to give a single dominant diastereomer. Our interest in this initial investigation was to develop a model for the transition state that will allow us to discern those cyclizations that *will* proceed with high diastereoselectivity.

Tab. 16.1 Calculated relative energies of transition states and products for the cyclization of **10**.

Entry	*TS*	*Product*	*TS DE kcal mol^{-1}*	*Product DE kacl mol^{-1}*
1	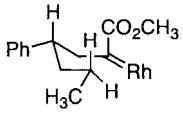 **22**	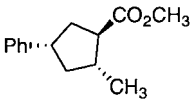 **12**	0.0	0.0
2	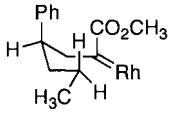 **24**	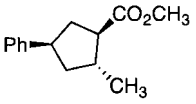 **14**	5.3	0.1
3	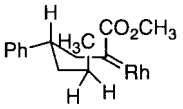 **25**	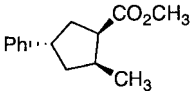 **11**	6.1	0.2
4	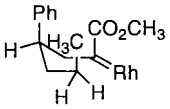 **26**	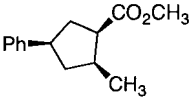 **13**	7.4	0.9

16.3.3
Chiral Auxiliary Control

Returning to the cyclization of a simple α-diazo ester (Scheme 16.6), we wanted to design [16] a chiral ester that would direct the cyclization preferentially to one absolute configuration of the product cyclopentane. In attempting to extend our computational approach to the design of such a chiral auxiliary, we found that we were missing a key piece of data, which was the dihedral angle between the ester carbonyl and the rhodium carbenoid at the point of commitment to cyclization (**28-syn** versus **28-anti**). We and others have speculated that the ester carbonyl and the rhodium carbenoid could be either *syn*, *anti* or *orthogonal* [10a, d, 17, 18], but no experimental or computational evidence in favor of any of these had been put forward. Since our computational approach did not allow us to answer this question directly, we devised an indirect approach based on the cyclization of α-diazoester **27**, derived from the naphthylborneol **31** [19].

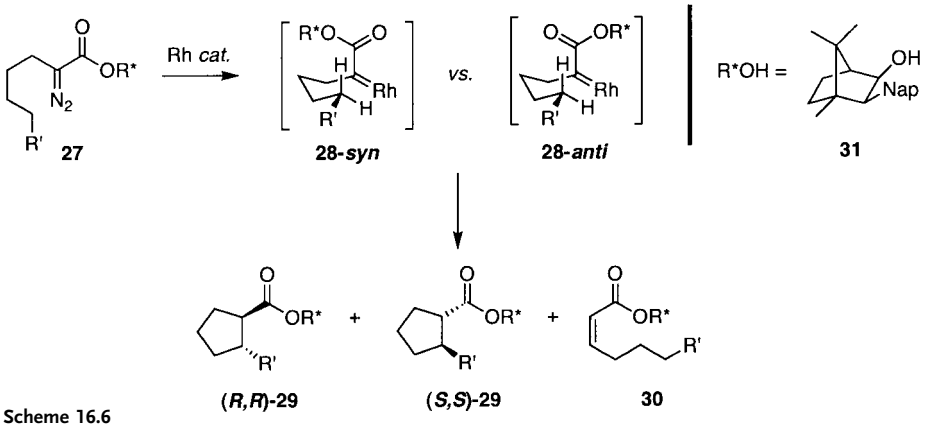

Scheme 16.6

The chiral diazo ester **27** was cyclized [16] with four commonly used rhodium carboxylate catalysts (Tab. 16.2), wherein the rhodium pivalate [20] (entry 4) was most efficient for forming the cyclopentanes, and the rhodium trifluoroacetate (entry 1) was optimum for forming alkenes [21]. Furthermore, it was demonstrated that the yield of the cyclization and the diastereoselectivity could be improved at lower temperature using the pivalate-derived catalyst (entry 5).

Tab. 16.2 Influence of the ligand bound to rhodium on the diastereoselectivity of the cyclization of ester **27**

Entry	*Ligand*	*rxn temp. (°C)*	*Yield (%)*	*(R,R)-29*		*(S,S)-29*		*30*
1	CF_3CO_2	18	89	1.5	:	1.0	:	4.2
2	CH_3CO_2	18	92	2.6	:	1.0	:	0.9
3	$^nC_7H_{15}CO_2$	18	82	3.8	:	1.0	:	0.7
4	$(CH_3)_3CCO_2$	18	99	8.4	:	1.0	:	1.0
5	$(CH_3)_3CCO_2$	–78	99	14	:	1.0	:	1.0

Tab. 16.3 Transition states and products resulting from cyclization of naphthylbornyl-2-diazoheptanoate **27**.

Possible diastereomeric TS	*Possible diasteromer*	*Relative energy of the transition state in kcal/mol*	
		syn	*anti*
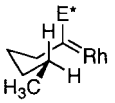	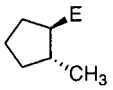 **(*R,R*)-29**	3.37	0.00
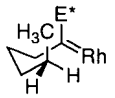	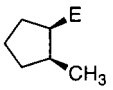 **(*R,S*)-29**	10.02	18.64
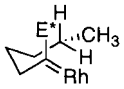	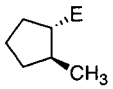 **(*S,S*)-29**	4.35	14.38
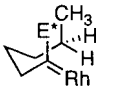	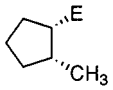 **(*S,R*)-29**	8.30	9.97

$E^* = CO_2R^*$

16.3.3.1 **Computational Analysis of the Naphthylbornyl-Derived Ester**

Assuming that the rhodium carbenoid and the ester carbonyl should be coplanar, the critical question, as we extended our computational analysis to the naphthylbornyl-derived ester **27**, was whether the rhodium carbenoid and the ester carbonyl would be *syn* or *anti* at the point of commitment to product formation. As illustrated in Tab. 16.3, there are four possible products, each of which could have come from either a *syn* or an *anti* transition state. Thus, there could be eight competing transition states leading to cyclization. We carried out, as outlined above, the minimizations for each of the corresponding eight "points of commitment". The minima, summarized in Tab. 16.3, were established using a meticulous grid search.

16.3.3.2 **Analysis**

The *syn* and the *anti* conformations leading to (*R,R*)-**29**, and illustrated in Tab. 16.3, are calculated (Mechanics) to be the two lowest energy transition states for the cyclization of **27**. Of the two, the *anti* conformation (rhodium carbene and carbonyl co-planar, but pointing in opposite directions) is the more stable by 3.37 kcal mol^{-1}. If steric factors alone governed the outcome of these cyclizations, we would expect that the *anti* transition state leading to (*R,R*)-**29** would compete with the *syn* transition state leading to (*S,S*)-**29**, with the former being favored by 4.35 kcal mol^{-1}. We have found that if the

difference in calculated transition state energies is greater than 2 kcal mol^{-1}, a single product is always formed in high (>95%) diastereomeric excess. We do not observe such high diastereoselectivity in the cyclization of **27**, so we conclude that steric factors *alone* do not govern the stereochemical outcome of this cyclization.

We propose that there is in fact a substantial electronic preference, not reflected in the Mechanics calculations, for the ester carbonyl and the C=Rh bond to be *syn* at the point of commitment to cyclization. This preference is strong enough to overcome the calculated steric preference (3.37 kcal mol^{-1}) for the *anti* transition state. The competition then, is between the *syn* transition state leading to (*R,R*)-**29**, and the *syn* transition state leading to (*S,S*)-**29**. The relative energies of these two transition states differ by slightly less than 1 kcal mol^{-1}, so we predict, and observe, low diastereoselectivity.

We posed this *syn*/*anti* question using a sterically demanding ester for which there is a significant conformational bias in favor of the *anti* transition state. We therefore believe that the conclusion – that there is a substantial preference for the ester carbonyl and the C=Rh bond to be *syn* at the point of commitment to cyclization – is general, and not limited to this particular case.

While we have had some success, we are aware of the limitations inherent in a transition state model for rhodium-mediated C–H insertion that attempts to predict product ratios on the basis of Mechanics calculations. Arbitrary decisions limiting the several degrees of freedom possible in the transition state could lead one to a model for the "point of commitment" to cyclization that would be far from reality. The work described herein is important because it offers *experimental* evidence for a key rotational degree of freedom in the dihedral angle between the ester carbonyl and the rhodium carbenoid.

Our initial objective, in this investigation, had been to design a useful chiral auxiliary. We were pleased to find that naphthylborneol **31**, upon optimization of the catalyst and the reaction temperature, served effectively. Until useful chiral catalysts are developed, naphthylborneol **31** will be of significant practical value for directing the absolute course of cyclopentane construction by rhodium-mediated intramolecular C–H insertion.

16.4
Comparing and Contrasting Rhodium Catalysts: Four Dimensions of Reactivity

It was apparent from the beginning (Scheme 16.7) that there were four potentially independent aspects of "reactivity": 1) the rate of bimolecular transfer of the diazo ester to the rhodium-complex [10a, 22]; 2) the ratio [21] of C–H insertion to β-H elimination [(**34**+**35** + **36** + **37**)/**33**]; 3) the chemoselectivity [(**34**+**35**)/(**36**+**37**)] [4]; and 4) the diastereoselectivity [9] of the insertion (**34**/**35** or **36**/**37**). As a prelude to the development of an effectively chiral catalyst, we felt that it was important to experimentally explore these aspects of reactivity.

The product esters could not be separated analytically, so we reduced the crude product from the cyclizations to the corresponding alcohols. We observed both diastereomers **39** and **40** of the methine insertion product, and three of the four possible diastereomers **41a**, **41b**, and **41c** of the methylene insertion product; interestingly alcohol **41d** was not detected. The five alcohols could be resolved by HPLC and by ^{1}H-NMR. While the HPLC ratios were more precise, the ^{1}H-NMR ratios tracked reasonably well, and could be sufficient if a new rhodium(II) catalyst was to be characterized.

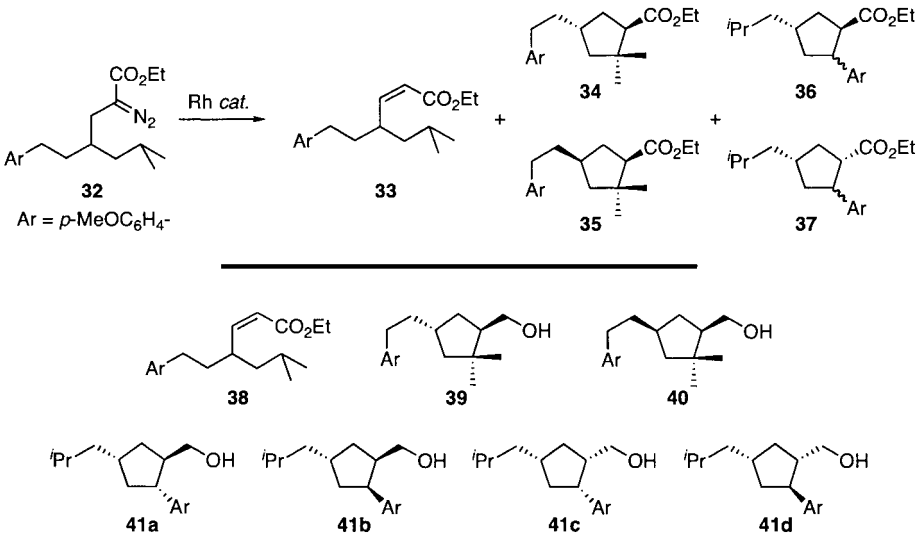

Scheme 16.7

16.4.1
Results from the Cyclizations

We selected a series of rhodium(II) carboxylates, rhodium(II) carboxamidate [5d] (Doyle catalysts **42h**, **42i**, **42j**), and the bridged rhodium(II) carboxylate (Lahuerta catalyst) **42g**, as representatives of the various rhodium(II) catalysts generally utilized. Most of the carboxylate and Doyle catalysts were commercially available and were purified by silica gel chromatography prior to use. The Lahuerta catalyst was prepared according to the literature procedure [23].

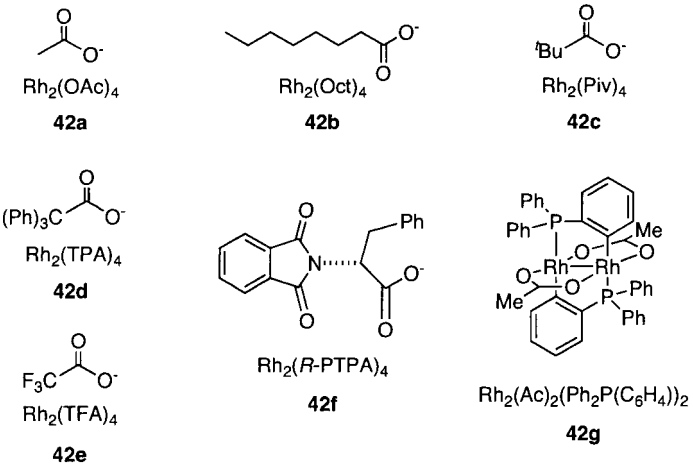

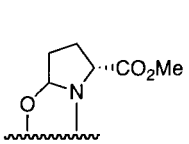

$Rh_2(5R\text{-MEPY})_4$

42h

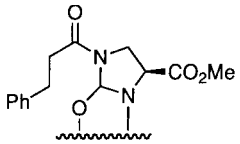

$Rh_2(4S\text{-MPPIM})_4$

42i

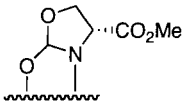

$Rh_2(4S\text{-MeOX})_4$

42j

16.4.1.1 Observed First-Order Rate Constants

Pirrung, Liu, and Morehead [22] have elegantly demonstrated the application of saturation kinetics (Michaelis–Menten) to the rhodium(II)-mediated insertion reactions of *α*-diazo *β*-keto esters and *α*-diazo *β*-diketones. Their method used the Eadie–Hofstee plot of reaction velocity (v) versus v/[S] to give k_{cat} and K_s, the equilibrium constants for the catalytic process. However, they were unable to measure the Michaelis constant (K_m) for the insertion reactions of *α*-diazo esters because they proved to be too rapid.

We determined the first-order rate constants for the disappearance of diazo ester **34** with the several rhodium(II) catalysts. The rate of disappearance of the diazo ester **34** upon exposure to each of the catalysts was monitored at 27±1°C, by following the UV absorbance at $\lambda = 265$ nm. The decrease in absorbance of the starting material was plotted versus time. The approximately linear portion of this direct plot, from 80% to 20% of the absorbance, was used to calculate the first-order rate constant for the disappearance of the diazo ester (Tab. 16.4).

The observed first-order rate constants, K_{obs} (s^{-1}) for the reaction of the rhodium(II) complexes with diazo ester **34** varied over a range of $>10^7$, in which the pivalate catalyst (entry 3) was almost two orders of magnitude faster than any of the other catalysts studied. The carboxamidate catalysts (entries 8–10) were slower than all the carboxylates, while the bridged phosphine catalyst (entry 7) behaved like most of the other carboxylates.

Tab. 16.4 Observed first-order rate constants for the insertion to elimination ratios for the reaction of the rhodium(II) catalysts with diazo ester **32.**

Entry	*Catalyst*	K_{obs} ($\times 10^4$) (s^{-1})
1	$Rh_2(OAc)_4$ **42a**	2.66
2	$Rh_2(Oct)_4$ **42b**	7.19
3	$Rh_2(Piv)_4$ **42c**	1728
4	$Rh_2(TPA)_4$ **42d**	14.8
5	$Rh_2(TFA)_4$ **42e**	28.6
6	$Rh_2(R\text{-PTPA})_4$ **42f**	12.2
7	$Rh_2(Ac)_2(Ph_2P(C_6H_4))_2$ **42g**	10.4
8	$Rh_2(5R\text{-MEPY})_4$ **42h**	3.6×10^{-5}
9	$Rh_2(4S\text{-MPPIM})_4$ **42i**	3.8×10^{-3}
10	$Rh_2(4S\text{-MeOX})_4$ **42j**	6.5×10^{-1}

16.4.1.2 **Cyclization *versus* Elimination**

The ratio of the insertion (Tab. 16.5) to the β-hydride elimination product (I/A) was determined for each of the catalysts. Two factors are believed to govern the ratio of insertion to elimination: (1) the "earliness" versus "lateness" of the transition state, and (2) the steric bulk of the ligand on the rhodium carbenoid.

A *reactive* carbenoid would have an early transition state, favoring β-H elimination over 1,5-insertion. We expect that the increased proportion of elimination observed with rhodium trifluoroacetate (entry 5) is due to the electron-withdrawing nature of the ligand, which makes the carbene carbon more electron-deficient and thus more reactive.

The steric effects become clear on inspecting the Newman projections of the transition states. The conformation **43a** leads to cyclopentane formation, while the conformation **43b** would give β-H elimination. As the rhodium carbenoid becomes larger, conformation **43b** is increasingly favored. Thus, as the steric bulk of the ligands on the Rh carbenoid increases on going from acetate (entry 1) to the TPA catalyst (entry 4), there is a significant increase in the proportion of β-hydride elimination.

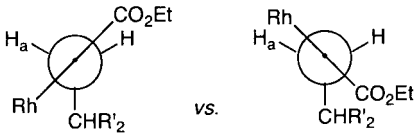

43a **43b**

In the carboxamidate class of complexes, the MeOX catalyst (entry 10) showed more β-elimination than the MEPY catalyst (entry 8), while the MPPIM amide analog (entry 9) showed the least β-elimination product. We were concerned that the application of an enantiomerically pure catalyst to a racemic substrate might bias the results, so we repeated one of the cyclizations using "racemic" (1:1 R/S) catalyst. The resulting product ratios (entry 11) were equivalent to those observed for the enantiomerically pure catalyst.

Tab. 16.5 Ratio of insertion to alkene (I/A) for the reaction of the rhodium(II) catalysts with diazo ester **34**.

Entry	*Catalyst*	*Isolated yield (%)*	*I/A*	
			HPLC	*NMR*
1	$Rh_2(OAc)_4$ **42a**	99	15.4	16.4
2	$Rh_2(Oct)_4$ **42b**	87	31.3	27.8
3	$Rh_2(Piv)_4$ **42c**	91	16.9	20.8
4	$Rh_2(TPA)_4$ **42d**	94	4.02	4.05
5	$Rh_2(TFA)_4$ **42e**	96	2.87	3.13
6	$Rh_2(R\text{-PTPA})_4$ **42f**	96	43.5	52.6
7	$Rh_2(Ac)_2(Ph_2P(C_6H_4))_2$ **42g**	94	32.1	26.2
8	$Rh_2(5R\text{-MEPY})_4$ **42h**	92	1.65	1.75
9	$Rh_2(4S\text{-MPPIM})_4$ **42i**	96	10.3	10.3
10	$Rh_2(4S\text{-MeOX})_4$ **42j**	95	0.83	1.05
11	*rac*-$Rh_2(4\text{-MeOX})_4$	94		1.1

The α-diazo ester **32** with its γ-branching was designed to minimize β-hydride elimination. The reaction of α-diazo methyl undecylenate **44** (Eq. 1) with $Rh_2(Oct)_4$ (**42b**) gave an I/A ratio of 2.8, while reaction with $Rh_2(MPPIM)_4$ (**42i**) gave only the β-hydride elimination product **45**.

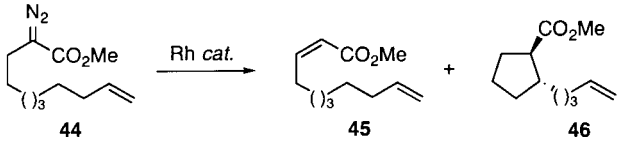

44 **45** **46** (1)

16.4.1.3 **Methine to Methylene Selectivity**

We believe that the selectivity of methine (CH) insertion over methylene (CH_2) insertion (Tab. 16.6) is a reflection of the polarizability of the rhodium carbenoid. As the carbenoid approaches the target C–H, the methine C–H is more electron-rich than the methylene C–H. A more easily polarized carbenoid would respond more fully to this and give proportionally more of the methine insertion product. Our design of the α-diazo ester **32** included the *p*-methoxy group on the benzene ring, so that the reactivity of the methylene benzylic C–H would approach that of the methine. Statistically, due to geometric constraints, only one of the two benzylic methylene C–H groups is available for the insertion necessary for the cyclization to **36/37**.

In the carboxylate series, the TPA catalyst (entry 4) was the most selective for methine over methylene insertion. Should this remarkable chemoselectivity prove to be general, this complex may add a possibility for high chemoselectivity not previously observed with rhodium(II) catalysts. The other carboxylate catalysts show less preference for CH over CH_2 insertion. We expect that the CH/CH_2 ratios would be more pronounced with a less carefully balanced substrate. In the carboxamidate class, MPPIM catalyst (entry 9) was more selective than the corresponding MeOX catalyst (entry 10), with the MEPY catalyst (entry 8) being the least discriminating for CH over CH_2 insertion.

Tab. 16.6 CH/CH_2 ratio for the reaction of the rhodium(II) catalysts with diazo ester **32.**

Entry	*Catalyst*	*CH/CH_2*	
		HPLC	*NMR*
1	$Rh_2(OAc)_4$ **42a**	1.09	1.03
2	$Rh_2(Oct)_4$ **42b**	1.57	1.46
3	$Rh_2(Piv)_4$ **42c**	1.77	1.67
4	$Rh_2(TPA)_4$ **42d**	10.9	CH- only
5	$Rh_2(TFA)_4$ **42e**	2.23	2.11
6	Rh_2(*R*-PTPA)$_4$ **42f**	2.73	2.66
7	$Rh_2(Ac)_2(Ph_2P(C_6H_4))_2$ **42g**	0.94	0.93
8	Rh_2(5*R*-MEPY)$_4$ **42h**	1.15	1.18
9	Rh_2(4*S*-MPPIM)$_4$ **42i**	2.67	2.84
10	Rh_2(4*S*-MeOX)$_4$ **42j**	2.01	2.18
11	*rac*-Rh_2(4-MeOX)$_4$	–	2.11

16.4.1.4 Distance at the Point of Commitment

For the cyclization of diazo ester **32** there are four competing diastereomeric chair transition states leading to CH_2 insertion products. In the transition state, the Rh–C bond is aligned with the target C–H bond leading to C–C bond formation. The two most stable of these transition states are depicted in Scheme 16.8. The actual product from cyclization is determined as the intermediate carbenoid commits to a particular diastereomeric transition state. If the C–C distance is short at the point of commitment (tight transition state), there will be a substantial steric interaction between the arene and the ester, and **32b** will be disfavored. If the C–C distance is longer, this interaction will not be as severe and more of **32a** will be formed. Thus, it seems reasonable that the ratio of **3a** to **36b** is a measure of the C–C bond distance at the point of commitment of the rhodium carbenoid.

The major diastereomer seen with each of the rhodium(II) catalysts surveyed was **36a**, leading to **41a** (Tab. 16.7). For the TFA catalyst (entry 5) a significant proportion

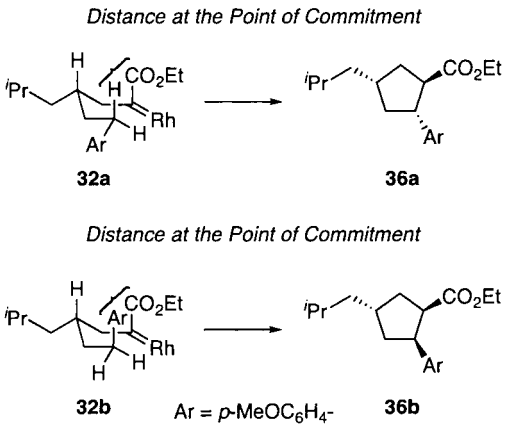

Scheme 16.8 Transition states for the CH_2 insertion. The distances at the point of commitment are indicated by braces.

Tab. 16.7 Ratio of CH_2 insertion products for the reaction of the rhodium(II) catalysts with diazo ester **32**.

Entry	*Catalyst*	*CH_2(41a/41b/41c)*
1	$Rh_2(OAc)_4$ **42a**	831:1:0
2	$Rh_2(Oct)_4$ **42b**	9.1:1:0
3	$Rh_2(Piv)_4$ **42c**	5.0:1:0.4
4	$Rh_2(TPA)_4$ **42d**	20.7:1:0
5	$Rh_2(TFA)_4$ **42e**	2.1:1:0.06
6	Rh_2(*R*-PTPA)$_4$ **42f**	1.7:1:0.09
7	$Rh_2(Ac)_2(Ph_2P(C_6H_4))_2$ **42g**	1438:1:4.2
8	Rh_2(5*R*-MEPY)$_4$ **42h**	15.8:1:0.9
9	Rh_2(4*S*-MPPIM)$_4$ **42i**	1.6:1:0.07
10	Rh_2(4*S*-MeOX)$_4$ **42j**	208:1:0
11	*rac*-Rh_2(4-MeOX)$_4$	**41a** only

of the *cis*-diastereomer **36b** was obtained, leading to **41b**. This suggests a longer C–C distance at the point that the rhodium carbenoid committed to C–C bond formation. Among the other carboxylate catalysts, the acetate catalyst (entry 1) and the bridged catalyst (entry 7) generated rhodium carbenoids that committed late to bond formation, and hence showed remarkable selectivity for the diastereomer **36a**. In the carboxamidate (Doyle) series, the MeOX catalyst (entry 10) shows excellent selectivity for the diastereomer **36a**, again reflecting a late commitment to bond formation. The MPPIM catalyst (entry 9) was the least selective.

16.4.1.5 Conclusions: Implications for the Design of an Effectively Chiral Catalyst

Changing the ligand on the rhodium carboxylate made striking changes (Tab. 16.5 to 16.7) in the product distribution from the cyclization of **32**. It has been consistently observed that the ligands exert substantial electronic control over the reactivity of the intermediate carbenoid. It is apparent that a strongly electron-withdrawing ligand will result in a more reactive carbenoid and that, with such a ligand, commitment to product formation will occur while the carbenoid carbon and the target C–H are still some distance apart. With a less reactive catalyst, the carbenoid carbon and the target C–H will be closer at the point of commitment, bringing the chiral ester in tighter proximity to the reaction center, where it can better influence the product distribution by the handedness of its steric bulk. An effective chiral catalyst, then, will have to direct the reaction sterically, and at the same time be electron-donating enough to have a late, tight "point of commitment".

We had expected that we might observe some correlation between two or more of these four measures of reactivity, but in fact plots of one versus the other showed no such correlation. We project that the study outlined here will lay the basis for a more detailed understanding of the mechanism of rhodium-mediated intramolecular C–H insertion.

16.5 Design of an Enantioselective Catalyst

With these results in hand, we turned our attention to the rational design of enantiomerically pure complexes [23, 24] that might direct the *absolute* sense of the cyclization of **47** to **48** (Eq. 2). The best catalyst reported to date for the cyclization of a *β*-keto *methyl* ester such as **47** is that of Hashimoto [25], which effects C–H insertion with up to 24% enantiomeric excess.

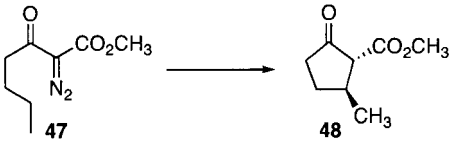

(2)

There are two competing transition states for C–H insertion, **49** and **50**. In transition state **49**, insertion is taking place into H_a, whereas in transition state **50**, insertion is taking place into the enantiotopic H_b. The challenge is to design a chiral rhodium cata-

lyst such that transition state **49** is favored over transition state **50** by *at least* the 2.5 kcal mol^{-1} we have observed is necessary to expect substantial diastereoselectivity in the C–H insertion reaction.

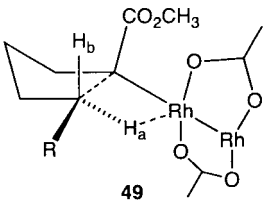

49

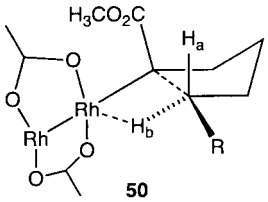

50

In cartoon form, what is needed is a ligand that will extend sterically to set up the local C_2-symmetry around the apical position of the rhodium, where the carbene binds and where the C–H insertion reaction is taking place. The resulting chiral environment would then favor transition state **52**, leading to one enantiomer, over transition state **53**, leading to the competing enantiomer.

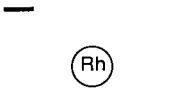

51

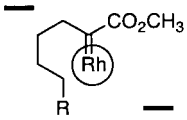

lower energy

52

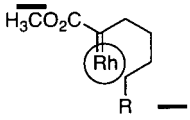

higher energy

53

We used our computationally based model to design and assess a series of chiral rhodium(II) carboxylates. It was quickly apparent that although others achieved some success with chiral monocarboxylates [24, 25], designs based on simple monocarboxylates were too flexible to allow rational design. We are therefore pursuing two complementary strategies: (1) the use of *ortho*-metallated head-to-tail triarylphosphine complexes, and (2) the use of bridging diacids.

16.5.1
Computational Design: Bridging the Dirhodium Core

In approaching the design of a chiral catalyst, the first question was whether or not our computational approach would allow prediction of the conformation of the ligands around the Rh–Rh core. Although several hundred tetrakiscarboxylato metal–metal dimers were known [20], there had been no report of a dicarboxylic acid that would bridge two positions on such a dimer [21]. We reasoned that the best chance for success would be with a dicarboxylic acid that was specifically designed to fit across the 5.4 Å gap between the carboxylate ligands.

To approach the design of a dicarboxylate ligand that would effectively bridge the Rh–Rh core, we first optimized the parent $Rh_2(CF_3CO_2)_4$ using ZINDO [14]. This structure was locked and then bridged by two of the trifluoroacetate methyl groups with an increasing number of methylenes, with the strain energy of the resulting (hypothetical) complexes evaluated using Mechanics [14]. As expected, the initial very

high strain energy for a zero-methylene bridge decreased rapidly with increasing bridge length, until the bridge reached four carbons. After that, the strain energy did not significantly decrease with increasing bridge length. Recognition that entropy considerations would favor bridging by a *convergent* bidentate ligand then led us to *m*-benzenedipropanoic acid **54** (Eq. 3) as a likely candidate [28, 29].

A priori, there was cause to be concerned that exchange of a tetrakiscarboxylato metal–metal dimer with a dicarboxylic acid would lead only to oligomers. Fortunately, heating **54** in dichloroethane with tetrakis(trifluoroacetato)dirhodium **42e** (Eq. 3) led to smooth exchange to give the emerald-green complex **55**, which was easily purified by silica gel chromatography. However, prolonged heating of the reaction mixture led to more polar materials. X-ray diffraction of the derived bisacetone adduct confirmed the structure of **55**. The calculated structure for the bisacetone adduct was exactly superimposable [30] on the X-ray structure. These results provided additional support for the computational approach to designing the three-dimensional shape of a catalyst.

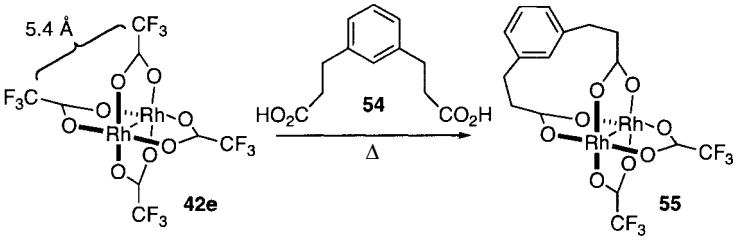

(3)

A key question was whether or not the bridged dimer would effectively catalyze the C–H insertion reaction. We were pleased to observe that complex **55** is in fact an efficient catalyst (1610 turnovers) for the cyclization of **47** to **48** (Eq. 2).

16.5.2 Triarylphosphine-Derived Catalysts

16.5.2.1 Construction of the Catalysts

All approaches to the design of enantiomerically pure rhodium(II) catalysts had depended on the attachment of enantiomerically pure ligands to the rhodium core. In collaboration with Professor Pascual Lahuerta of the University of Valencia, Spain, we undertook a complementary strategy, the preparation of rhodium(II)-dimers (*P*)-**56** and its enantiomer (*M*)-**56**, having backbone chirality [23]. Using the approach outlined above, we calculated that the transition state **52** should be favored over the transition state **53** by 4.2 kcal mol^{-1}.

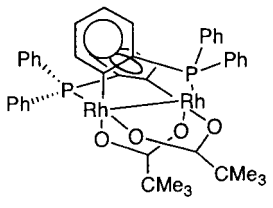

(*P*)-**56**

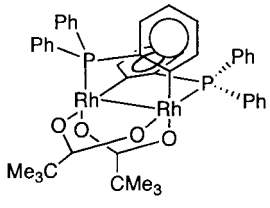

(*M*)-**56**

Motivated by this possibility, we considered strategies by which complexes such as (*P*)-**56** and (*M*)-**56** might be obtained as single enantiomers. A practical solution to this problem was separation of the diastereoisomers of $[Rh_2(PC)_2(O_2CR^*)_2]$, which were derived through the replacement of the achiral acetates with chiral carboxylates. Treatment of a mixture (*P*)-**57** and (*M*)-**57** with the inexpensive *N*-(4-methylphenyl)sulfonyl-L-proline **58** (Scheme 16.9) afforded the expected 1:1 mixture of diastereomers **59a** and **59b**, which were separable by silica gel chromatography (10% Et_2O/CH_2Cl_2). The two enantiomerically enriched complexes (*P*)-**60** and (*M*)-**60** were obtained *via* ligand exchange of **59a** and **59b** (separately) with trifluoroacetic acid. Further exchange with pivalic acid then gave (*M*)-**56** and (*P*)-**56**.

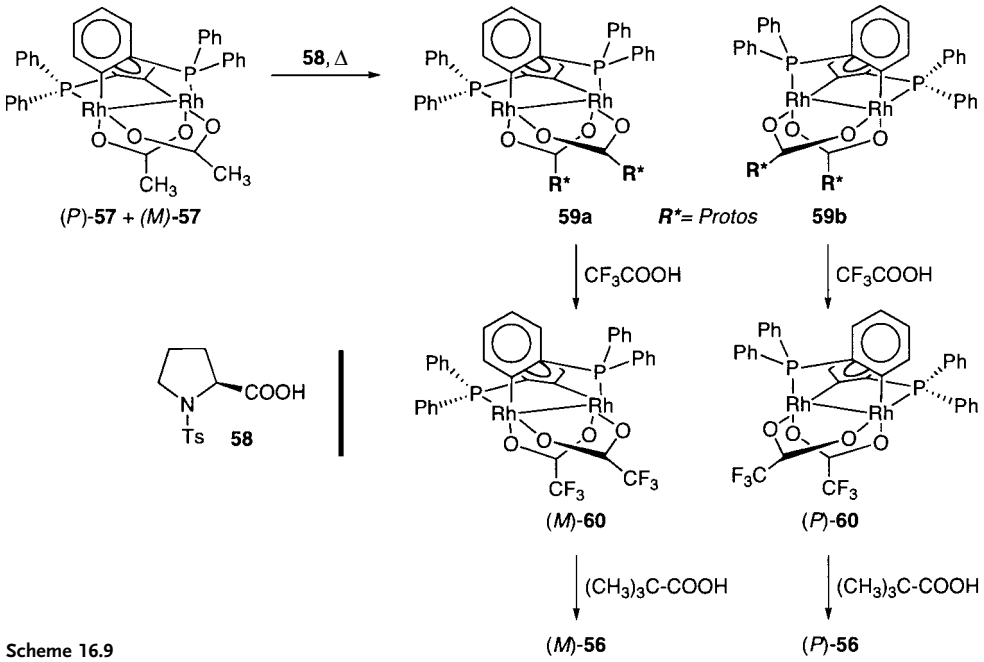

Scheme 16.9

16.5.2.2 Assessment of Catalyst Reactivity

This work predated the studies summarized in Section 16.4 above, but it was apparent even at that time that a highly reactive catalyst was not likely to be highly selective. Electron donation from the target C–H bond and concomitant commitment to bond formation would be too early, with the target C–H at too great a distance to feel the chirality of the ligands on rhodium. Therefore the *relative* reactivity of these new rhodium catalysts needed to be established. We had observed [6] that on exposure to rhodium tetrakis(trifluoroacetate), **61** (Eq. 4) gave only the eliminated product **63**, whereas the rhodium tetrakispivalate, on the other hand (pivalate is the most electron-donating ligand we have yet found), furnished an 8:1 ratio of **62** to **63**. Rhodium tetrakisacetate afforded a ratio of about 2.3:1 of **62** to **63**, and rhodium tetrakisoctanoate a 4:1 ratio. It was apparent that by this measure, the *ortho*-metallated triphenylphosphine catalysts were somewhat more reactive than the tetrakiscarboxylates.

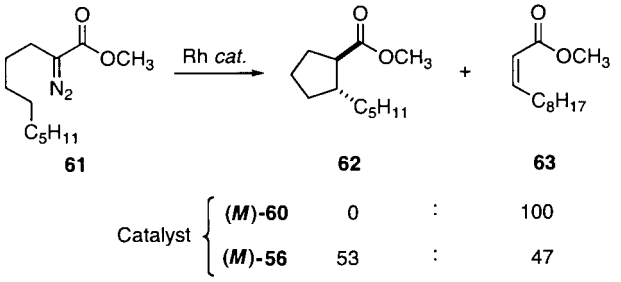

Catalyst				
	(*M*)-**60**	0	:	100
	(*M*)-**56**	53	:	47

(4)

16.5.2.3 Enantiomeric Excess

We knew from the cyclization/elimination ratio that the rhodium carbenes derived from (*P*)-**60** and (*P*)-**56** were very reactive, and so we did not expect them to be highly selective. We were delighted to observe that even these very reactive catalysts afforded significant enantiomeric excess. It is noteworthy that each of the three-substrate types, **61**, **64**, and **66** (Scheme 16.10), demonstrated about the same degree of enantioselectivity. It was especially encouraging that the major enantiomer observed in each case was that predicted by our computational model. In hindsight, the origin of the enantioselectivity can now be understood. The data in Tab. 16.7 (Section 16.4.1.4) suggest that the transition states for these *ortho*-metallated complexes are much tighter than those for the [tetrakis]carboxylates.

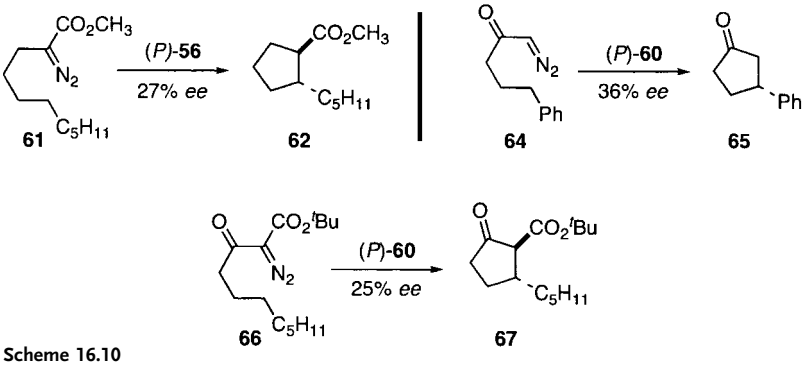

Scheme 16.10

16.5.2.4 More Electron-Donating Ligands

It is apparent from the results with the cyclization of **61** to **62** versus **63** (Eq. 4) that more electron-withdrawing ligands on the rhodium make the derived carbene more reactive. These results suggest that more electron-donating phosphines would be the optimum ligands for the preparation of analogs of (*M*)-**60** and (*M*)-**56**. Unfortunately, all attempts to prepare such derivatives have failed at the *ortho*-metallation stage.

16.5.3
Design of an Enantiomerically Pure Bridging Biscarboxylate

In a parallel approach, we have also pursued the design and preparation of enantiomerically pure biscarboxylates. Electronically, it is important that the carboxylate ligand on rhodium be as electron-donating as possible. In practice, this means that *α,α,α*-trialkylated carboxylates are likely to be the most effective. Combination of this concept with the bridged design **55** (Eq. 3), and the need to make the ligand usefully chiral, led to the ligand **68**. We envision that as **68** makes an equatorial belt around the Rh–Rh core to give **69**, the spiro cyclohexane rings will be perpendicular to that belt. The phenyl substituents will then project upward and downward, creating local C_2 symmetry around the apical position of the rhodium, where the carbene will be located. The preparation of **68** and **69** are currently under investigation.

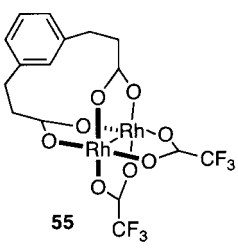

55

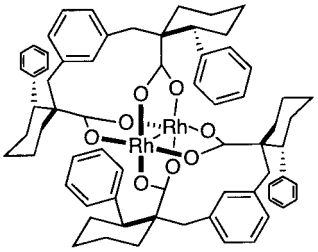

69

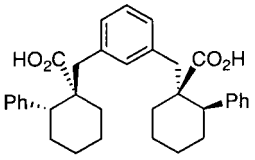

68

16.5.4
Development of an Alternative Diazo Ketone Substrate

Returning to Scheme 16.4, it is apparent that for the intermediate rhodium carbene **18** to be selective, it will be important to attenuate the reactivity. Rather than have two electron-withdrawing groups on the carbene, as with **47** (Eq. 2), a substrate having an electron-withdrawing group and an electron-donating group on the carbene [32] would seem most likely to cyclize with the highest enantioselectivity. We are therefore planning to investigate the preparation and cyclization of *α*-diazo *benzyl* ketones such as **70** (Eq. 5).

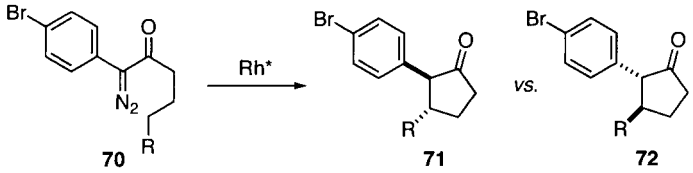

70 **71** **72** (5)

16.6
Conclusion

Cyclopentane construction by rhodium-mediated intramolecular C–H insertion has been established as a powerful tool for the construction of carbocyclic systems, but there is much yet to be learned about the factors governing selectivity in the C–H insertion process [33]. We look forward to exciting developments in this area in years to come.

16.7 References

1 For the synthesis of astrogorgiadiol, see Taber, D. F.; Malcolm, S. C. *J. Org. Chem.* **2001**, *66*, 944.

2 For the isolation, structure and biological activity of (–)-astrogorgiadiol, see Fusetani, N.; Nagata, H.; Hirota, H.; Tsuyuki, T. *Tetrahedron Lett.* **1989**, *30*, 7079.

3 For an alternative synthesis of (–)-astrogorgiadiol from vitamin D, see Della Sala, G.; Izzo, I.; De Riccardis, F.; Sodano, G. *Tetrahedron Lett.* **1998**, *39*, 4741.

4 (a) Taber, D. F.; Petty, E. H. *J. Org. Chem.* **1982**, *47*, 4808. (b) Taber, D. F; Ruckle, R. E., Jr. *J. Am. Chem. Soc.* **1986**, *108*, 7686.

5 For general reviews of rhodium mediated C–H insertions, see (a) Taber, D. F. *Comprehensive Organic Synthesis*; Pattenden G., Ed., Pergamon Press: Oxford, **1991**; Vol. 3, pp. 1045–1062. (b) Padwa, A.; Austin, D. J. *Angew. Chem., Int. Ed. Engl.* **1994**, *33*, 1797. (c) Ye, T.; McKervey, M. A. *Chem. Rev.* **1994**, *94*, 1091. (d) Doyle, M. P.; McKervey, M. A.; Tao, T. *Modern Catalytic Methods for Organic Synthesis with Diazo Compounds*; John Wiley & Sons: New York, **1998**.

6 Taber, D. F.; Ruckle, Robert E., Jr.; Hennessy, M. J. *J. Org. Chem.* **1986**, *51*, 4077.

7 Taber, D. F.; Hennessy, M. J.; Louey, J. P. *J. Org. Chem.* **1992**, *57*, 436.

8 Taber, D. F.; You, K.; Song, Y. *J. Org. Chem.* **1995**, *60*, 1093.

9 Taber, D. F.; You, K. K.; Rheingold, A. L. *J. Am. Chem. Soc.* **1996**, *118*, 547.

10 For related analyses of transition states for rhodium carbene insertions, see (a) Doyle, M. P.; Westrum, L. J.; Wolthius, W. N. E.; See, M. M.; Boone, W. P.; Bagheri, V.; Pearson, M. M. *J. Am. Chem. Soc.* **1993**, *115*, 958. (b) Brown, K. C.; Kodadek, T.; *J. Am. Chem. Soc.* **1992**, *114*, 8336. (c) Pirrung, M. C.; Morehead, A. T., Jr. *J. Am. Chem. Soc.* **1994**, *116*, 8991. (d) Davies, H. M. L.; Huby, N. J. S.; Cantrell, W. R., Jr.; Olive, J. L. *J. Am. Chem. Soc.* **1993**, *115*, 9468.

11 Alternatively, the initial complex of the electron-deficient carbon with the electron density in the target C–H could be depicted as a three-center, two-electron bond (ref. 9). We initially took this approach computationally, but found that the results did not correlate with the diastereoselectivity observed for the reaction. More recent computational work by Nakamura has confirmed the four-center nature of the transition state for Rh-mediated C–H insertion: Nakamura, E.; Yoshikai, N.; Yamanaka, M. *J. Am. Chem. Soc.* **2002**, *124*, 7181.

12 Taber, D. F.; Petty, E. H.; Raman, K. *J. Am. Chem. Soc.* **1985**, *107*, 196.

13 For reversible Rh-complexation with a C–H bond, see (a) Weiller, B. H.; Wasserman, E. P.; Bergman R. G.; Moore, C. B.; Pimentel, G. C. *J. Am. Chem. Soc.* **1989**, *111*, 8288. (b) Wasserman, E. P.; Moore, C. B.; Bergman. R. G. *Science* **1992**, *255*, 315.

14 Mechanics and ZINDO were used as implemented on the Tektronix CAChe workstation. Although our initial work (ref. 6) included minimizing the Rh–Rh core with ZINDO, we have subsequently found that this approach works just as well with Mechanics alone. The CAChe workstation is particularly well suited to the sort of analysis outlined here, as its superb three-dimensional visualization facilitates understanding of the competing transition states.

15 Taber, D. F.; You, K. *J. Am. Chem. Soc.* **1995**, *117*, 5757.

16 Taber, D. F.; Malcolm, S. C. *J. Org. Chem.* **1998**, *63*, 3717.

17 Doyle, M. P. *Chem. Rev.* **1986**, *86*, 919.

18 (a) Doyle, M. P.; Westrum, L. J.; Wolthuis, W. N. E.; See, M. M.; Boone, W. P.; Bagheri, V.; Pearson, M. M. *J. Am. Chem. Soc.* **1993**, *115*, 958. (b) Doyle, M. P. *Recl. Trav. Chim. Pays-Bas* **1991**, *110*, 305. (c) Davies, H. M. L.; Huby, N. J. S.; Cantrell, W. R., Jr.; Olive, J. L. *J. Am. Chem. Soc.* **1993**, *115*, 9468.

19 Taber, D. F.; Raman, K.; Gaul, M. D. *J. Org. Chem.* **1987**, *52*, 28.

20 Rhodium pivalate {dirhodium tetrakis[μ-(2,2-dimethylpropanato-O:O′)]} was synthesized by heating commercially available rhodium trifluoroacetate in 8 equiv pivalic acid for 24 h followed by removal of excess acid by heating under vacuum. The crude catalyst was purified by flash chromatogra-

phy using an MTBE/petroleum ether gradient. TLC R_f (10% MTBE/petroleum ether) = 0.52. For leading references to the preparation of other rhodium carboxylates, see Felthouse, T. R. *Prog. Inorg. Chem.* **1982**, *29*, 73.

21 Taber, D. F.; Herr, R. J.; Pack, S. K.; Geremia, J. M. *J. Org. Chem.* **1996**, *61*, 2908.

22 (a) Pirrung, M. C.; Morehead, A. T. *J. Am. Chem. Soc.* **1996**, *118*, 8162. (b) Pirrung, M. C.; Liu, H.; Morehead, A. T. *J. Am. Chem. Soc.* **2002**, *124*, 1014.

23 Taber, D. F.; Malcolm, S. C.; Bieger, K.; Lahuerta, P.; Sanau, M.; Stiriba, S.-E.; Perez-Prieto, J.; Angeles-Monge, M. *J. Am. Chem. Soc.* **1999**, *121*, 860.

24 (a) For the development of DOSP by Davies, see Davies, H. M. L. *Eur. J. Org. Chem.* **1999**, 2459. (b) For the development of BiTISP by Davies, see Davies, H.aM. L.; Panaro, S. A. *Tetrahedron Lett.* **1999**, *64*, 5287. The development of enantiomerically pure bridging biscarboxylates by Davies was independent of our efforts.

25 (a) Hashimoto, S.-i.; Watanabe, N.; Ikegami, S. *Tetrahedron Lett.* **1990**, *31*, 5173. (b) Hashimoto, S.-i.; Watanabe, N.; Sato, T.; Shiro, M.; Ikegami, S. *Tetrahedron Lett.* **1993**, *34*, 5109. Much higher enantioselectivities were observed using other esters, especially with insertion into allyic and benzylic C–H groups.

26 Tetrakis(carboxylato)dimetal complexes have been prepared from Cr, Cu, Mo, Re, Rh, Ru, Tc, and W. For leading references, see Cotton, F. A.; Walton, R. A. *Multiple Bonds Between Metal Atoms*; John Wiley and Sons: New York, **1982**.

27 Chisholm has reported diacids that can connect two tungsten (or molybdenum) dimers, to make tetramers: Cayton, R. H.; Chisholm, M. H.; Huffman, J. C.; Lobkovsky, E. B. *J. Am. Chem. Soc.* **1991**, *113*, 8709.

28 Diacid **54** was prepared by coupling α-α'-dibromo-*m*-xylene with allylmagnesium chloride, followed by RuO_4-mediated cleavage of the resultant diene [29]. Diacid **54**, prepared by an alternative route, was already a known compound: Ruggli, P.; Bucheler, P. *Helv. Chim. Acta* **1947**, *30*, 2048.

29 (a) Carlsen, P. H. J.; Katsuki, T.; Martin, V. S.; Sharpless, K. B. *J. Org. Chem.* **1981**, *46*, 3936. (b) Caron, M.; Carlier, P. B.; Sharpless, K. B. *J. Org. Chem.* **1983**, *53*, 5185. (c) Stock, L. M.; Tse K. W.-T. *Fuel* **1983**, *62*, 974.

30 Taber, D. F.; Meagley, R. P.; Louey, J. P.; Rheingold, A. L. *Inorg. Chim. Acta.* **1995**, *239*, 25.

31 Estevan, F.; Herbst, K.; Lahuerta, P.; Barberis, M.; Perez-Prieto, J. *Organometallics* **2001**, *20*, 950.

32 For the application of this push–pull stabilization principle to intermolecular C–H insertion, see Davies. H. M. L.; Hansen, T. *J. Am. Chem. Soc.* **1997**, *119*, 9075.

33 For a recent example, see Taber, D. F.; Green, J. H.; Zhang, W.; Song, R. *J. Org. Chem.* **2000**, *65*, 5436.

17
Rhodium(II)-Catalyzed Oxidative Amination

Christine G. Espino and Justin Du Bois

17.1
Introduction

The advancement of new chemical methods for C–N bond formation is stimulated by the widespread occurrence of synthetic and natural molecules having nitrogen-based functional groups. Strategies typically employed for assembling C–N centers follow principally two types of reaction pathways: (1) nucleophilic addition to carbonyl derivative, and (2) S_N2 displacement with amines or amine equivalents [1, 2]. A third, less common approach to C–N bond construction is based on the formation of *N*-centered electrophilic oxidants capable of reacting with both σ- and π-bonds [3–6]. Nitrenes represent one class of such oxidants, long recognized for their ability to aminate both saturated and unsaturated hydrocarbons [5]. In practice, nitrene generation is typically performed through photolytic or thermal extrusion of dinitrogen from an azide precursor [7, 8]. Nitrenes produced in this manner exist initially in a singlet state but relax rapidly to a favored ground-state triplet [9]. Triplet nitrenes, having two unpaired electrons, display reactivity characteristic of a biradical. By contrast, singlet nitrenes function as two-electron oxidants and effect the stereospecific amination of organic molecules. Consequently, reactions of singlet nitrenes and either substituted olefins or asymmetric carbon centers proceed with complete stereochemical fidelity. In spite of the desirable properties of nitrenes for C–N bond formation, the highly reactive and indiscriminate nature of such species has greatly limited their role in fine chemicals synthesis. Accordingly, the ability to modulate and to direct the oxidizing power of nitrenes could lead to versatile new strategies for establishing C–N bonds from existing C–H centers. The combination of transition metal catalysts with nitrene equivalents has made possible the formulation of such methods. Such protocols capitalize on the unique reaction chemistry of nitrenes and enable the expeditious preparation of highly functionalized nitrogen-containing materials [10–12].

17.2
Background

Work originally described by Kwart and Khan is often cited as the first example of a nitrene reaction performed under the influence of a transition metal ion [13, 14]. In these experiments, benzenesulfonyl azides were heated in the presence of copper pow-

Modern Rhodium-Catalyzed Organic Reactions. Edited by P. Andrew Evans

ISBN: 3-527-30683-8

der and hydrocarbons to afford small amounts of products arising from C–H insertion and alkene aziridination (Scheme 17.1). Generation of a Cu–nitrenoid intermediate was postulated but never established for this process. In general, azides are rarely employed as *N*-atom sources in catalytic metal-mediated amination processes. Moreover, the few protocols that combine such starting materials with metal catalysts likely operate through radical reaction pathways rather than stereospecific nitrene transfer [15–18].

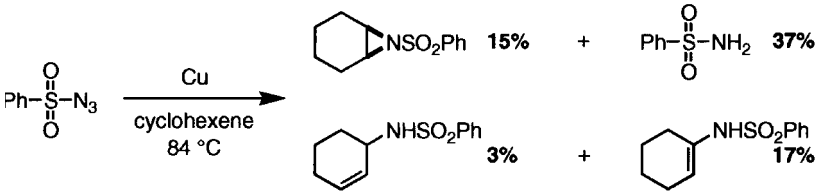

Scheme 17.1 Copper-catalyzed decomposition of arylsulfonyl azides.

Seminal findings by Breslow and Mansuy recognized the value of *N*-arenesulfonyl iminoiodinanes ($ArSO_2N{=}IPh$) as nitrene precursors for metal-catalyzed *N*-atom transfer [19–24]. A particularly intriguing report by Breslow and Gellman demonstrated the efficacy of the dimeric complex $Rh_2(OAc)_4$ for promoting intramolecular C–H amination (Scheme 17.2) [25]. This singular result is extraordinary, considering the high yield of sultam produced (86% by HPLC), and hints at the potential for future development of C–N bond-forming processes of this type. As noted by the authors, the effectiveness of $Rh_2(OAc)_4$ has a clear parallel to the established chemistry of metal–carbene C–H in-

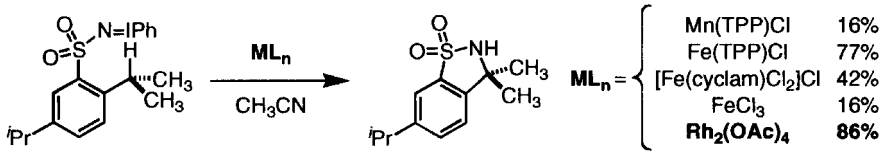

Scheme 17.2 Intramolecular C–H amination of an iminoiodinane.

sertion reactions, for which rhodium(II) dimers are considered superior catalysts [26]. Additional studies established the viability of manganese(III)– and iron(III) porphyrin complexes as promoters for intermolecular C–H amination reactions with *p*-$CH_3C_6H_4SO_2N{=}IPh$ (TsN=IPh) and simple hydrocarbon substrates such as 2-hexene (Scheme 17.3) [20–22]. In these experiments stereospecific oxidation was not observed, and a mechanism involving C–H abstraction by a high-valent manganese intermediate followed by rapid trapping of the incipient radical (radical rebound) was inferred (Scheme 17.4) [22, 27]. Such findings contrast with rhodium-catalyzed reactions of $ArSO_2N{=}IPh$ in which a metallo-nitrene mechanism is thought to be operative (*vide infra*).

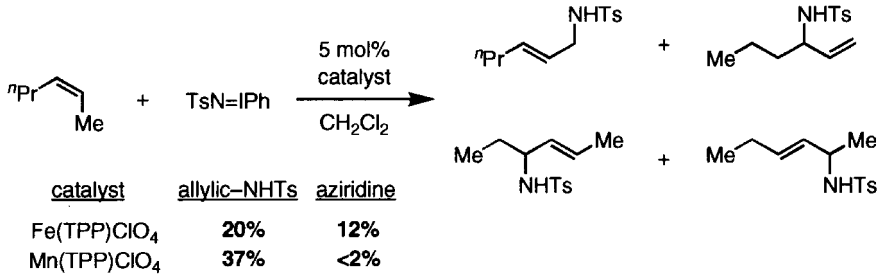

Scheme 17.3 Metal porphyrin-catalyzed allylic amination.

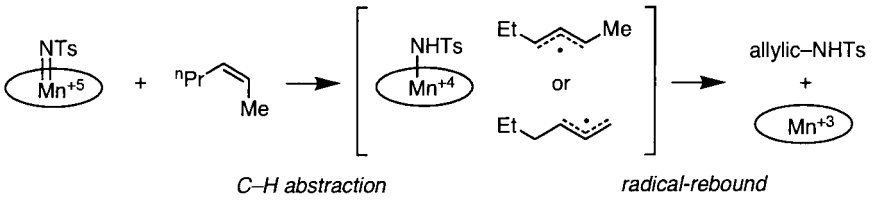

Scheme 17.4 C–H amination by a radical-rebound mechanism.

Interest in $ArSO_2N$=IPh reagents originates principally from their application in metal-catalyzed alkene aziridination [11, 28, 29]. One of the foremost reports, by Evans, highlighted the exceptional efficacy of both copper(I) and (II) salts for inducing transfer of the $ArSO_2N$– group to a broad range of olefin substrates [30]. Subsequent to this finding, intensive effort has focused on the identification of new achiral and chiral transition metal complexes that serve competently to mediate this event [10, 31]. Interestingly, a problem generally encountered with metal-catalyzed aziridination results from competing allylic C–H insertion, often observed for cyclopentene and cyclohexene substrates [32]. The elements of the catalyst structure and substrate that bias π-bond functionalization over allylic C–H insertion remain ambiguous. With respect to copper catalysis, it is reasonable to speculate that a concerted, two-electron *N*-atom transfer pathway occurs in parallel to a C–H abstraction/rebound process [33]. The degree to which one of these mechanisms is operative is likely a function of the redox properties of the metal complex and/or the spin state of the putative metallo-nitrene adduct. In this regard, it seems of all the metals known to catalyze atom transfer with RSO_2N=IPh reagents, rhodium(II) complexes appear to be principally effective for C–H insertion.

17.3
Intermolecular C–H Amination with Rhodium(II) Catalysts

Intermolecular amination experiments described by Müller using $O_2NC_6H_4SO_2N$=IPh (NsN=IPh) as the nitrene source underscore the value of certain rhodium(II) catalysts for C–H insertion (Scheme 17.5) [12, 34–36]. In accord with Breslow's finding, dirhodium carboxylates were demonstrated to catalyze the amination of allylic, benzylic, and adamantyl substrates. Notably, structurally related tetracarboxamide dimers fail to give

isolable amounts of insertion products. Although the synthetic utility of Müller's oxidation process is limited in scope and hampered by the requirement for excess hydrocarbon substrate (5–20 equiv), these studies comprise the first systematic mechanistic examination of rhodium-mediated C–H amination. Data collected from this work support a metallo-nitrene transfer event through a concerted three-centered transition state, as has been suggested for the analogous rhodium-catalyzed carbene insertion [37, 38]. Details from these experiments are described below.

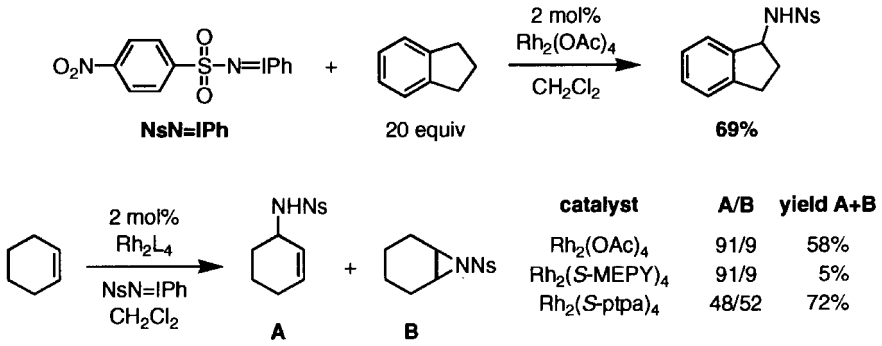

Scheme 17.5 Rhodium-catalyzed N-atom transfer using NsN=IPh.

The stereochemical course of the rhodium-catalyzed amination reaction was investigated using optically pure (*R*)-2-phenylbutane **1** as a substrate (Scheme 17.6). Though amination of this material with NsN=IPh gave only 3% of the product **2**, analysis showed that **2** did form with complete retention of configuration. Such a finding mirrors the stereospecific insertion of singlet nitrenes at enantiopure ternary centers and is consistent with a concerted transition state model [39, 40]. This singular result, however, does not discount a stepwise C–H abstraction/rebound mechanism in which radical recombination occurs faster than C–C bond rotation [41–43].

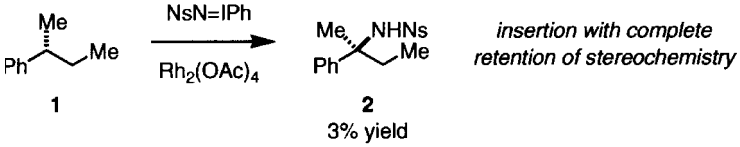

Scheme 17.6 Stereospecific C–H amination under rhodium-catalyzed conditions.

Müller has used cyclopropyl clock experiments to test for the possible intermediacy of radical species prior to C–N bond formation (Scheme 17.7). The diphenylcyclopropane derivative **3**, which fragments at a rate of $2\times10^{10}\ s^{-1}$, affords nosylated amine **4**; no product from ring opening is observed. Such a result mitigates the viability of a productive stepwise oxidation process, though it is important to note that sulfonamide **4** is formed in only 5% yield.

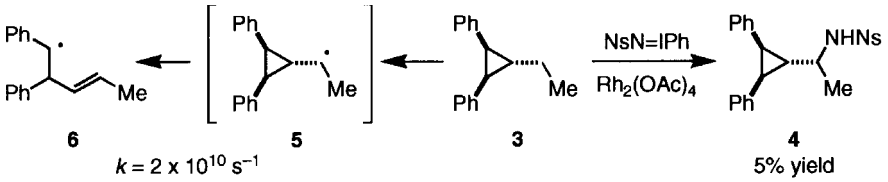

Scheme 17.7 Radical clock study of metallo-nitrene C–H insertion.

Additional data in support of a nitrene-type oxidant follows from a Hammett correlation analysis using *para*-substituted ethylbenzene derivatives. These experiments give a calculated ρ of –0.90, indicative of a transition state having only partial cationic charge development at the benzylic center. Such a result is in accordance with a concerted, albeit asynchronous, amination event. By contrast, a measured kinetic isotope effect (KIE) of 3.5 ± 0.2 using a deuterated adamantyl substrate is larger than expected for a presumed rhodium–nitrene mechanism. KIE values of ~ 1.5 have been recorded for reactions of singlet nitrenes, a number that is often cited as evidence for a nonlinear transition state [44, 45]. Thus, the KIE of 3.5 for the rhodium-catalyzed adamantyl insertion is rather perplexing and differs from the balance of experimental data that suggests a concerted, nitrene insertion pathway.

Müller has explored enantioselective C–H insertion using optically active rhodium complexes, NsN=IPh as the oxidant, and indane **7** as a test substrate (Scheme 17.8) [35]. Chiral rhodium catalysts have been described by several groups and enjoy extensive application for asymmetric reactions with diazoalkanes [46–48]. In C–H amination experiments, Pirrung's binaphthyl phosphate-derived rhodium system was found to afford the highest enantiomeric excess (31%) of the product sulfonamide **8** (20 equiv indane **7**, 71% yield).

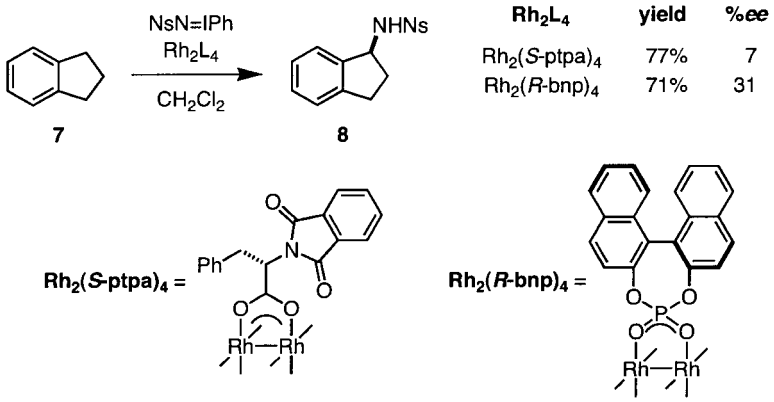

Scheme 17.8 Intermolecular C–H insertion by chiral rhodium catalysts.

Hashimoto has noted improved enantioselectivities for C–H insertion of indane and tetralin substrates using dirhodium tetrakis(*N*-phthaloyl-*tert*-butylleucinate)-based catalysts (Scheme 17.9) [49]. In the best of these examples, 84% *ee* was obtained with 1,1-dimethyltetralin **9** (5 equiv) and NsN=IPh. Despite the modest enantiomeric ex-

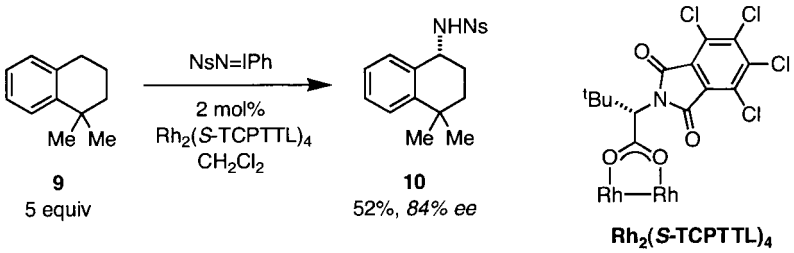

Scheme 17.9 Recent developments in asymmetric C–H amination.

cesses recorded by both Müller and Hashimoto, the transfer of asymmetry from catalyst to product offers compelling mechanistic data in support of a rhodium–substrate complex as the active oxidant in this process.

Collectively, the work of Breslow and Müller has established rhodium(II) dimers as effective catalysts for C–H amination reactions. Intermolecular C–H insertion can be of value for preparing nitrobenzene sulfonamides from simple hydrocarbon starting materials when it is reasonable to employ large excesses of substrate. Catalyst turnover numbers are generally low in these reactions and 10 mol% of the expensive dimeric rhodium complexes is often employed. Product yields also vary substantially over a limited substrate scope. Irrespective of these practical limitations, the mechanistic details of the rhodium-catalyzed amination process are significant and distinct from other metals (*vide supra*), and suggestive of the great potential for such methodology in synthesis.

17.4
Intermolecular C–H Amination with Other Metals

Manganese and iron porphyrins have been employed for intermolecular C–H amination with allylic, benzylic, and some saturated hydrocarbons using $ArSO_2N$=IPh reagents [20, 22]. The preponderance of mechanistic data collected with these systems strongly implicates a radical abstraction/rebound mechanism for C–N bond formation [22, 27]. Such findings contrast with the work of Müller for analogous reactions using rhodium catalysts. Other metal salts and coordination complexes have since been demonstrated to promote C–H insertion with $ArSO_2N$=IPh oxidants. These systems include ruthenium(II) porphyrin, –bipyridine, and –tris-amine complexes, copper(I)–diamine adducts, and manganese(III)–salen derivatives [50–53]. Elegant mechanistic studies by Che using ruthenium-based catalysts give compelling evidence for a radical abstraction/rebound event leading to sulfonamidated products [54]. A similar pathway appears to be followed for allylic and benzylic amination reactions with chiral manga-

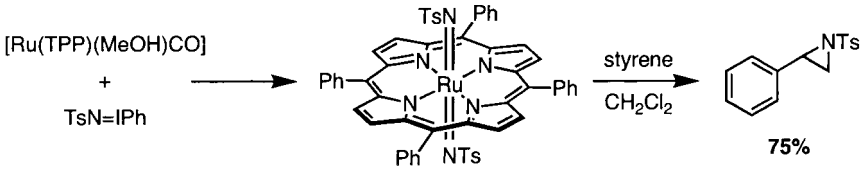

Scheme 17.10 Ruthenium porphyrin-promoted azirdination.

nese–salen systems, as shown by Katsuki [52]. With ruthenium(II) porphyrins and TsN=IPh, the reactive oxidant is assigned as a *bis*(tosylimido)Ru(VI) intermediate, having been spectroscopically characterized (Scheme 17.10) [55].

In an important advance, Che has demonstrated that $PhI(OAc)_2$ and $TsNH_2$ can replace the capricious TsN=IPh reagent for C–H insertion reactions with manganese and ruthenium porphyrins (Scheme 17.11) [56]. A similar discovery was made contemporaneously by Espino and Du Bois for intramolecular C–H amination of carbamate and sulfamate esters with rhodium(II) catalysts (*vide infra*) [57]. Reactions catalyzed by ruthenium- and manganese-complexes under these so-called "*in-situ*" conditions operate through a radical rebound mechanism, thus precluding stereospecific C–H bond functionalization of optically pure 3° substrates. Additionally, product regiocontrol is often unpredictable for oxidations with dissymmetrically substituted allylic units. Nevertheless, product yields are, in general, much higher using ruthenium and manganese porphyrin catalysts than for corresponding intermolecular reactions with rhodium(II) dimers. Turnover numbers with the former systems also vastly exceed the rhodium complexes. In all, the procedures outlined by Che and Katsuki make available a number of allylic and benzylic sulfonamides from inexpensive, unfunctionalized starting materials. Breslow and Che have both demonstrated the utility of ruthenium- and manganese catalysts for the intermolecular amination of steroids, though improvements to the efficiency of such reactions are still required [54, 58, 59].

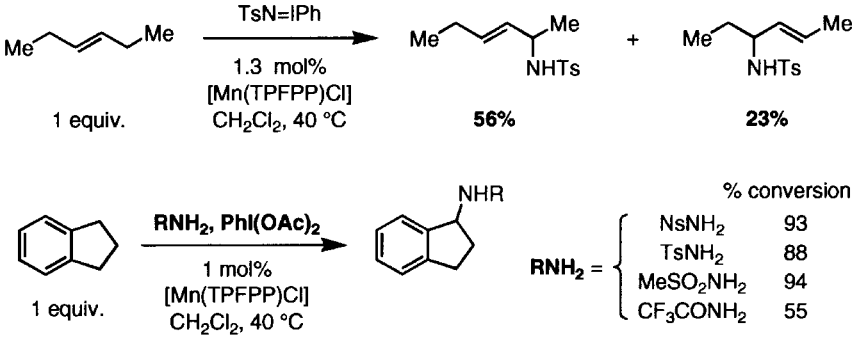

Scheme 17.11 Allylic and benzylic amination using $PhI(OAc)_2$.

17.5
Intramolecular C–H Amination with Rhodium(II) Catalysts

17.5.1
Carbamate Esters

Intramolecular C–H insertion by an iminoiodinane reagent as described by Breslow and Gellman remained for many years the singular example of such a process until a report by Espino and Du Bois [57]. By employing 1° carbamate esters **11** with $PhI(OAc)_2$ and catalytic $Rh_2(OAc)_4$, oxidative cyclization could be promoted to furnish the corresponding oxazolidin-2-one **13** (Scheme 17.12). This process was envisioned to proceed through a mechanism involving: (1) *in-situ* formation of a carbamoyl imino-

iodinane **12**; (2) metallo-nitrene formation; and (3) selective intramolecular C–H insertion at the β-position of the carbamate side chain. Though the original experiments provided only 10–15% of the desired heterocycle using 5 mol% catalyst loading, a dramatic improvement in the product yield was realized with the addition of MgO. Final optimization with **11** afforded a convenient set of conditions that employ 1 equiv of carbamate, a slight excess of oxidant, and MgO to generate the indanol-derived *cis*-oxazolidinone **13** in 86% isolated yield. The function of the MgO additive in this reaction is presumed to be as an AcOH scavenger. Accordingly, substitution of MgO with 2,6-di-*tert*-butyl-4-methylpyridine has proven effective in certain instances (*vide infra*), though it is interesting that other bases such as K_2CO_3 or Na_2HPO_4 are entirely ineffective at promoting catalyst turnover. Alternative metal oxides, including CaO, BaO, and ZnO, gave mixed results and do not display general utility.

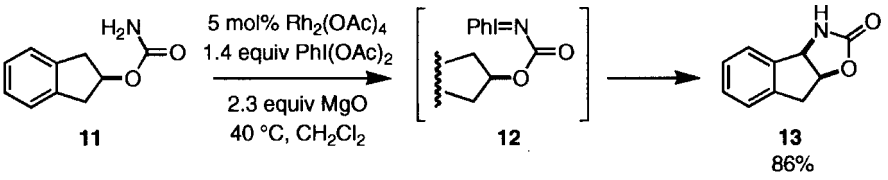

Scheme 17.12 Oxidative cyclization of carbamate esters.

Preliminary efforts to examine the mechanism of C–H amination proved inconclusive with respect to the intermediacy of carbamoyl iminoiodinane **12**. Control experiments in which carbamate **11** and $PhI(OAc)_2$ were heated in CD_2Cl_2 at 40°C with and without MgO gave no indication of a reaction between substrate and oxidant by NMR. In line with these observations, synthesis of a carbamate-derived iodinane has remained elusive. The inability to prepare iminoiodinane reagents from carbamate esters precluded their evaluation in catalytic nitrene transfer chemistry. By employing the $PhI(OAc)_2$/MgO conditions, however, 1° carbamates can now serve as effective N-atom sources. The synthetic scope of metal-catalyzed C–H amination processes is thus expanded considerably as a result of this invention. Details of the reaction mechanism for this rhodium-mediated intramolecular oxidation are presented in Section 17.8.

Oxidative cyclization of 1° carbamates has been shown to encompass a broad range of disparate substrates (Table 17.1). In addition to indanol **11**, other benzylic (entry 2) and allylic (entries 1 and 5) C–H centers react efficiently to give oxazolidinone products. The reactivity of these C–H groups toward oxidation is well documented and consistent with either a concerted- or radical rebound-type mechanism. Of perhaps greater significance, carbamate insertions occur smoothly at saturated 2° and 3° sites. Such findings attest to the potent nature of the oxidizing species generated in this process and are suggestive of a nitrene-type pathway. The trends evidenced from the body of recorded data parallel quite remarkably that of intramolecular C–H insertions of diazocarbonyls catalyzed by rhodium(II) dimers, which are widely believed to proceed through electrophilic metal–carbene intermediates [37, 38, 60]. Accordingly, attachment of an electron-withdrawing group to a carbon center deactivates the corresponding C–H bonds toward oxidation [61]. This conclusion is highlighted with entry 8, wherein amination occurs exclusively on the cyclohexane ring to afford the oxazolidinone as a

Tab. 17.1 C–H amination of 1° carbamate esters.

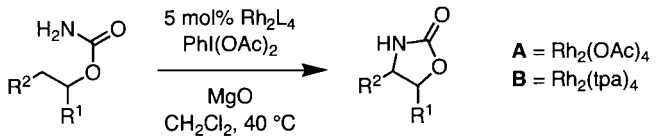

Entry	Substrate		Product	Entry	Substrate		Product
1	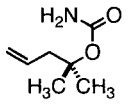	A, 82%	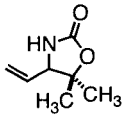	5	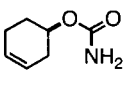	B, 55%	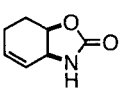
2	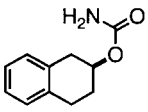	B, 74%	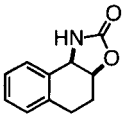	6	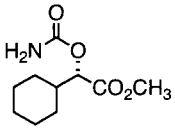	A, 60%	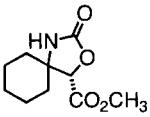
3	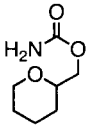	A, 79%	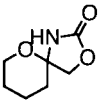	7	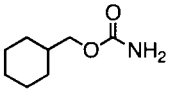	A, 77%	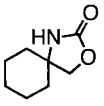
4	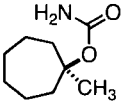	A, 83%	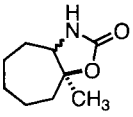 8:1 cis/trans	8	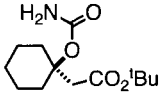	A, 83%	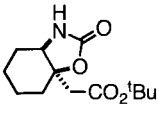 single regio- and stereisomer

single diastereomer. No product from insertion into the α-center of the ester unit is observed.

Oxidation of 3° C–H substrates provides an invaluable tool for exploring both fundamental and practical elements of the amination method (Scheme 17.13). An experiment performed with optically pure (*S*)-2-methylbutyl carbamate **14** first demonstrated that C–H insertion is stereospecific (75% yield). The observed results match the chemistry of carbamoylnitrenes, which insert into 3° sites with complete retention of stereochemical configuration [39, 40]. In practice, the stereospecific amination of C–H bonds has significant consequence. Access to enantiomeric tetrasubstituted C–N centers is made available from optically pure 3° starting materials. Such stereochemical elements are particularly difficult to fashion using modern asymmetric methods [62–65]. By employing the C–H amination protocol, product stereocontrol is absolute and obtained without recourse to chiral catalysis. Preparation of 4° α-amino acids is just one of many possible applications for this new technology.

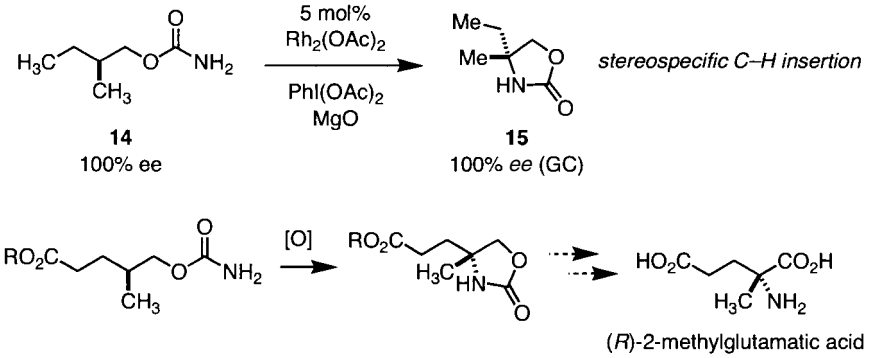

Scheme 17.13 Stereospecific oxidation of 3° C–H centers.

Chiral 3° alkanol-derived carbamates have been used to examine the influence of catalyst structure on product regio- and diastereoselectivity (Eq. 1). Initial reactions conducted with **16** and 5 mol% $Rh_2(OAc)_4$ indicate that amination of 3° C–H site is preferred over the 2° methylene with an 8:1 bias. The product of methyl oxidation is not detected. A change to the more sterically hindered tetrakis(triphenylacetate) rhodium dimer, $Rh_2(tpa)_4$, erodes the 3°/2° product ratio to 1:1 [66]. Though the variance in selectivity between these two examples is modest, the results implicate a role for the rhodium complex in the key C–N bond-forming event. These conclusions are reinforced through experiments with carbamate **19** (Eq. 2), for which use of two different catalyst structures is found to reverse the ratio of diastereomeric oxazolidinone products **20** and **21**. The small, albeit distinguishable, differences in selectivity further implicate a rhodium–substrate complex as the reactive intermediate. Such findings lend support to future prospects of developing chiral rhodium catalysts for diastereo- and enantioselective C–H amination.

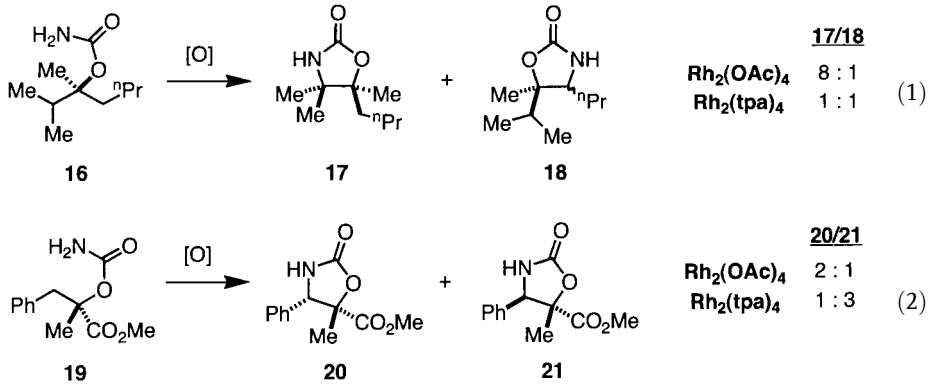

A current limitation of the amination methodology is encountered with carbamate esters derived from 2° alcohols (that is, **22** and **24** in Scheme 17.14). With some notable exceptions, substrates in this class often give only small amounts (~0–20%) of oxazolidinone, and instead afford the corresponding ketones in variable yields. A similar observation has been made by Doyle for C–H insertion reactions with 1-indanol diazo-

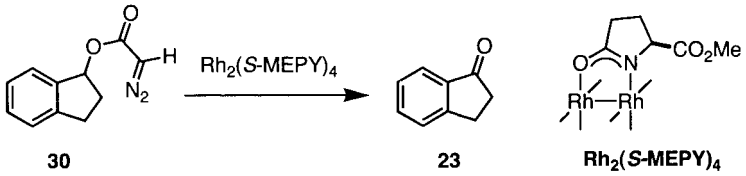

(3)

ester **30** (Eq. 3) [67]. Kinetic isotope data obtained from this work suggest that indanone **23** formation follows through a mechanism involving hydride abstraction by the intermediate rhodium–carbene. An analogous pathway (that is, **26** → **27**) can be drawn for carbamate ester oxidations (Scheme 17.14). Alternatively, C–H insertion into the α-C–H bond of **29** would generate a four-membered ring species **28** that could spontaneously extrude HN=C=O or CO_2 to afford ketone **27**. The detailed steps of this undesired side reaction aside, problems associated with select 2° and 1° alkanol-based carbamates can be alleviated by employing the $Rh_2(tpa)_4$ catalyst. In general, this complex has been particularly useful in situations where $Rh_2(OAc)_4$ or $Rh_2(oct)_4$ give suboptimal yields of oxazolidinone. Other known rhodium–carboxamidate complexes (for example, $Rh_2(acam)_4$, $Rh_2(cap)$, $Rh_2(MEOX)_4$) have found limited application for the amination chemistry despite their effectiveness in carbene C–H insertion reactions.

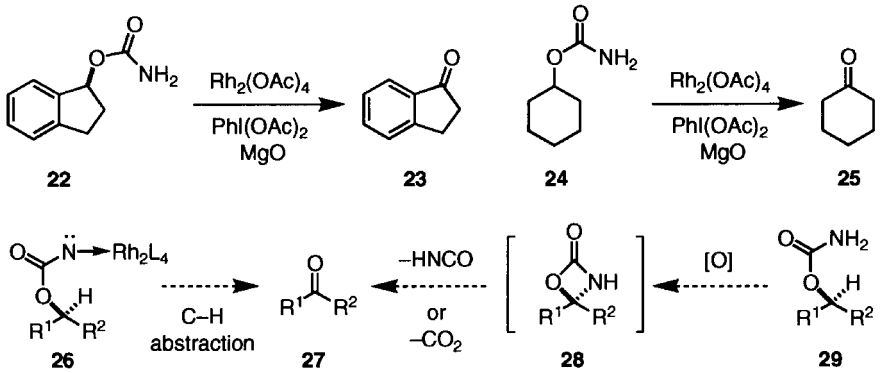

Scheme 17.14 Ketone formation by 2° alcohol-derived carbamates.

Intramolecular rhodium-catalyzed carbamate C–H insertion has broad utility for substrates fashioned from most 1° and 3° alcohols. As is typically observed, 3° and benzylic C–H bonds are favored over other C–H centers for amination of this type. Stereospecific oxidation of optically pure 3° units greatly facilitates the preparation of enantiomeric tetrasubstituted carbinolamines, and should find future applications in synthesis (*vide infra*). Importantly, use of $PhI(OAc)_2$ as a terminal oxidant for this process has enabled reactions with a class of starting materials (that is, 1° carbamates) for which iminoiodinane synthesis has not proven possible. Thus, by obviating the need for such reagents, substrate scope for this process and related aziridination reactions is significantly expanded (*vide infra*). Looking forward, the versatility of this method for C–N bond formation will be advanced further with the advent of chiral catalysts for diastero- and enantiocontrolled C–H insertion. In addition, new catalysts may increase the range of 2° alkanol-based carbamates that perform as viable substrates for this process.

17.5.2 Sulfamate Esters

Advances in amination methodology have seen great progress with the identification of sulfamate esters **32** as effective starting materials for both intra- and intermolecular *N*-atom transfer reactions (Scheme 17.15) [68, 69]. Sulfamates are readily accessed from 1° and 2° alcohols (for example, **31**) using $ClSO_2NH_2$, a convenient reagent that is prepared from inexpensive $ClSO_2NCO$ and HCO_2H [70, 71]. These compounds are often crystalline and, as with carbamate esters, are stable to prolonged storage. Oxidative cyclization of sulfamates occurs smoothly with $PhI(OAc)_2$, MgO, and 1–2 mol% $Rh_2(OAc)_4$ or $Rh_2(Oct)_4$ to furnish the [1,2,3]oxathiazinane-2,2-dioxide heterocycles **33**. The reduced catalyst loadings used with this process vis-à-vis the carbamate reaction are in accordance with the faster turnover rates witnessed for sulfamate substrates. A competition experiment performed with equimolar amounts of sulfamate **35** and carbamate **34** shows exclusive consumption of the former starting material (Eq. 4).

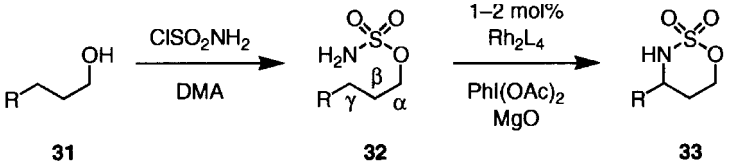

Scheme 17.15 Sulfamate esters as substrates for oxidative cyclization.

In addition to their having improved efficiency, the range of sulfamate structures that may be employed with this amination method is greater than with carbamates (Table 17.2). Substrates prepared from most 1° and 2° alkanols will react to furnish oxathiazinane products. The few exceptions include 3°, benzylic, and allylic sulfamates, which are intrinsically unstable as starting materials due to the activating nature of the sulfamoyl group for elimination and/or nucleophilic displacement. Importantly, C–H amination occurs with exceptional selectivity at the γ-position on the sulfamate side chain to afford the six-membered ring heterocycles. A comparison of the sulfamate ester **37** N-S-O bond angle from X-ray crystallography with that of an oxathiazinane **38** and a five-membered sulfamidate **39** displays almost an exact match between the acyclic sulfamate **37** and the larger-ring product **38** (Scheme 17.16) [72, 73]. Though speculative, this analysis suggests that selectivity for oxathiazinane production is favored through a transition state in which the sulfamate unit remains relatively undistorted. As will be highlighted in a subsequent section (Section 17.11.2), the unique oxathiazinane products of the amination reaction have value as electrophiles and make available other important 1,3-difunctionalized amine derivatives.

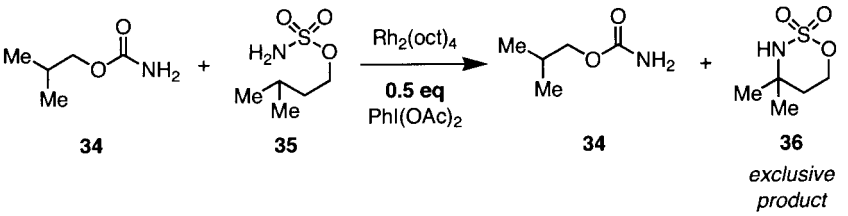

(4)

Tab. 17.2 Rhodium-catalyzed insertion of sulfamates.

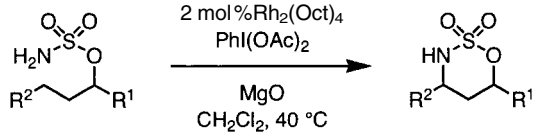

Entry	Product	Yield	Entry	Product	Yield
1	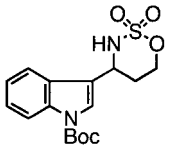	78	2	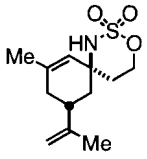	80
3	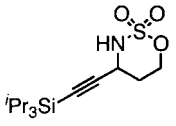	75	4	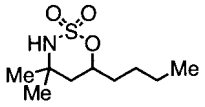	90
5	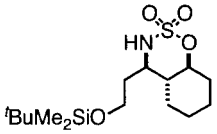	75	6	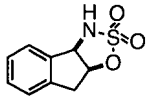	60

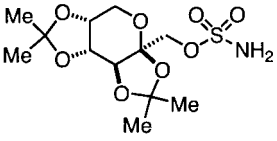

37

S–N: 1.58 Å
S–O: 1.58 Å
–N-S-O: 103°

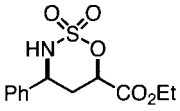

38

S–N: 1.61 Å
S–O: 1.60 Å
–N-S-O: 104°

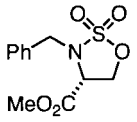

39

S–N: 1.61 Å
S–O: 1.57 Å
–N-S-O: 95°

Scheme 17.16 X-ray crystallographic analysis of sulfamate derivatives.

Sulfamate esters **40** prepared from enantiopure alcohols having 3° γ-C–H centers insert stereospecifically and with exceptional efficiency to generate optically pure oxathiazinanes **41** (Scheme 17.17). This same finding has been demonstrated with carbamates and offers a powerful new strategy for synthesizing chiral, tetrasubstituted carbinolamines (*vide supra*). In addition, the ability to perform amination reactions with sulfamates from 2° alcohols makes possible investigations in stereoselective C–H insertion (Table 17.3) [74]. The use of such substrates (entries 1–4) reveals an extraordinary substituent effect on product selectivity. In this small series of compounds, the phenyl derivatives (entries 3 and 4) perform optimally to furnish the product oxathiazinane in

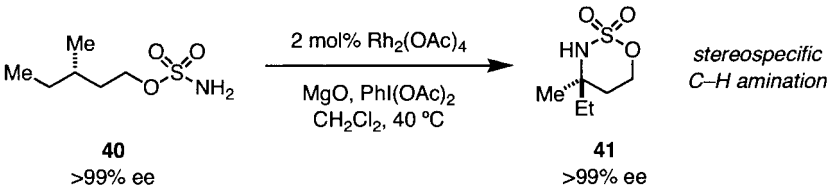

40
>99% ee

41
>99% ee

Scheme 17.17 Synthesis of optically pure oxathiazinanes through C–H insertion.

Tab. 17.3 Diastereoselective sulfamate ester oxidation.

Entry	*Product*	*syn/anti*	*Yield*	*Entry*	*Product*	*syn/anti*	*Yield*
1	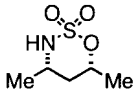	3:1	88	5	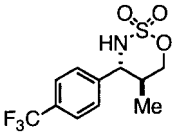	20:1	70
2	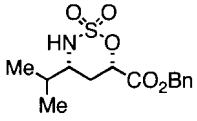	8:1	55	6	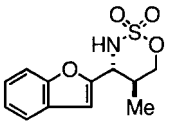	20:1	65
3	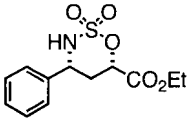	15:1	91	7	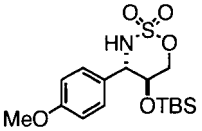	10:1	77
4	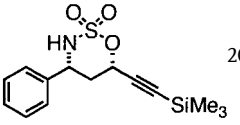	20:1	62	8	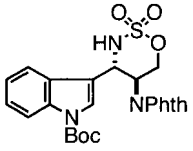	12:1	85

high yield (91%) and with ≥15:1 *syn/anti* selectivity. A general preference for the *syn*-stereoisomer exists for sulfamates having this type of substitution pattern. By contrast, the sulfamates prepared from *β*-branched 1° alcohols are formed with exceptional diastereocontrol in the *anti*-configuration (entries 5–8). To account for these apparently divergent outcomes, a stereochemical model of the transition state has been formulated (Scheme 17.18). Placement of the sulfamate side chain in a cyclohexane chair-like arrangement staggers R^1, R^2, and R^3 groups to minimize *gauche* interactions. Subsequent insertion into the equatorially aligned C–H bond generates a product in a low-energy chair conformation. Although speculative, this construct serves as a useful predictive tool and accounts for all of the stereochemical data collected thus far.

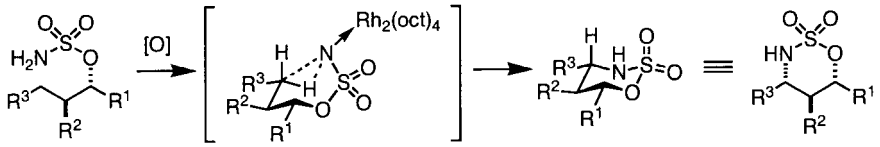

Scheme 17.18 Predictive model for stereoselective C–H insertion.

The preference for amination reactions at 3° sites is a general property of both sulfamate and carbamate oxidations. Competition experiments with dissymmetrically substituted sulfamates demonstrate that 3° C–H insertion is favored over benzylic and 2° centers and that catalyst structure can largely influence reaction regioselectivity (Scheme 17.19) [75]. In one example, cyclization of **42** with $Rh_2(OAc)_4$ yields a mixture of products having only a small bias for **43**, the product of 3° C–H insertion. Conversely, employment of the $Rh_2(tpa)_4$ catalyst with this same substrate affords 12:1 selectivity for **43**. The change in product ratio may result from destabilizing substrate–catalyst interactions between the phenyl moiety of **42** and the sterically bulky $Rh_2(tpa)_4$ complex. The rate of C–H amination at the benzylic center is thus slowed relative to the 3° position, and selectivity is improved. In many other examples, the triphenylacetate complex is found to be a poor catalyst for oxidations of benzylic C–H bonds. Further evidence to support a proposed steric model for regiocontrol has been obtained with sulfamate **45**. This starting material gives oxathiazinane **46** exclusively (>20:1) when $Rh_2(OAc)_4$ is employed; however, product selectivity erodes to ~4:1 with the $Rh_2(tpa)_4$ catalyst. Steric repulsion between the isopropyl unit in **47** and the triphenylacetate ligands presumably destabilizes the transition state for this insertion pathway and results in a less discriminating process. Additional data continue to give useful insight for predicting site selectivity between sterically and electronically disparate C–H bonds in these oxidative processes. Moreover, the effect of catalyst structure on product control is viewed as strong evidence for the involvement of the metal in the C–N bond forming event (that is, metal-bound nitrene formation), and should have significant practical consequence.

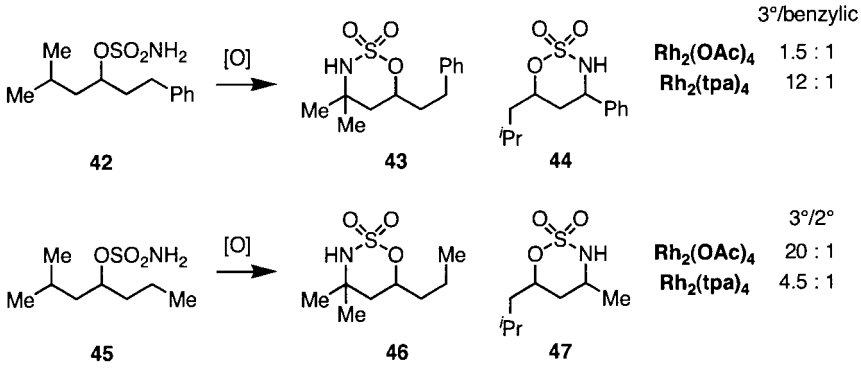

Scheme 17.19 Influence of rhodium catalysts on product distribution.

The established activity of ethereal α-C–H bonds toward carbene and nitrene insertion has evoked new applications for sulfamate oxidation [76–78] In principle, a C–H center to which an alkoxy group is attached should be a preferred site for amination irrespective of the additional functionality on the sulfamate ester backbone (Scheme 17.20). Such a group can thus be used to control the regiochemistry of product formation. The *N,O*-acetal products generated are iminium ion surrogates, which may be coupled to nucleophiles under Lewis acid-promoted conditions [79]. This strategy makes available substituted oxathiazinanes that are otherwise difficult to prepare in acceptable yields through direct C–H amination methods [80].

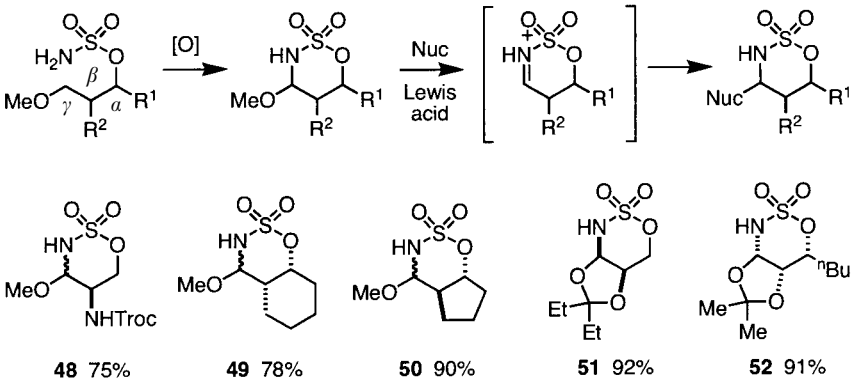

Scheme 17.20 Oxathiazinane *N,O*-acetals as iminium ion surrogates.

Oxidation reactions with γ-OMe-derived sulfamates efficiently produce the desired oxathiazinanes (**48**–**50**, Scheme 17.20). The somewhat acid-labile *N,O*-acetals are furnished cleanly and may be employed in coupling reactions without prior purification. Though these compounds are typically formed as epimeric mixtures, it is inconsequential given their subsequent use. Unlike their MeO– counterparts, *N,O*-acetals **51** and **52** are quite robust and easily isolated. The reaction of sulfamate **53** underscores the regiodirecting effect of the γ-OMe substituent (Scheme 17.21). In combination with $Rh_2(tpa)_4$, the observed selectivity for the *N,O*-acetal product **54** is >10:1. Catalysts such as $Rh_2(OAc)_4$ also favor insertion at the ethereal C–H bond, though regiocontrol is significantly diminished.

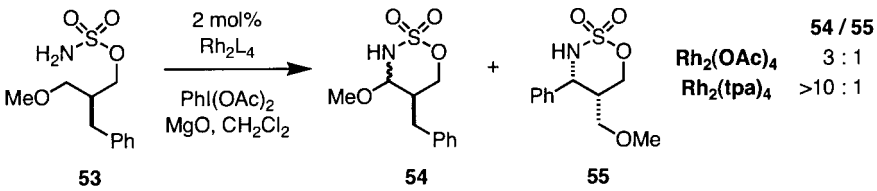

Scheme 17.21 Selective formation of *N,O*-acetals under catalyst and substrate control.

Nucleophilic addition reactions to oxathiazinane *N,O*-acetals proceed smoothly with allylsilane, alkynylzinc, silyl enol ether, and silylketene acetal reagents (Scheme 17.22)

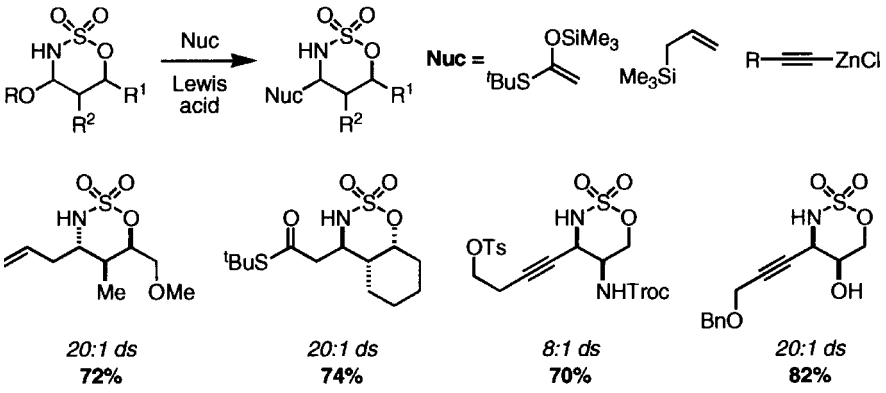

Scheme 17.22 Nucleophilic additions to *N,O*-acetal heterocycles.

[80, 81]. Both stoichiometric $BF_3 \cdot OEt_2$ and catalytic $Sc(OTf)_3$ (5–10 mol%) function as effective Lewis acids for these reactions. Coupling to the putative iminium ion intermediate occurs with good to excellent levels of diastereocontrol and in yields ranging from 60 to 95%. The stereochemical outcome from this process has been rationalized through a hybrid model of Stevens (for related reactions of tetrahydropyridinium ions) superimposed with that of Felkin, Ahn, and Eisenstein (for additions to α-substituted carbonyls) [75, 80, 82, 83]. Overall, the application of C–H amination methodology to generate novel *N,O*-acetals, together with their subsequent use as iminium ion equivalents, greatly expands the number of oxathiazinane structures that can be constructed from sulfamate starting materials. The versatility of this chemistry should create numerous opportunities for its use in synthesis (*vide infra*).

17.5.3
Sulfamides and Sulfonamides

The discovery of high-yielding, catalytic methods for C–H insertion of carbamate and sulfamate esters has prompted efforts to identify additional functional groups that serve as viable substrates for such processes. Sulfamides appear an obvious choice, though initial reactions performed with the simplest monoalkylated derivatives were unexpectedly problematic. In control experiments, a reaction between sulfamide and $PhI(OAc)_2$ was found to consume partially both reagents and to produce as-yet unassigned side products. The addition of $Rh_2(OAc)_4$ had little influence on this reaction outcome. A simple modification of the sulfamide moiety, however, inhibits the unproductive reaction with $PhI(OAc)_2$ and makes possible efficient C–H amination. These substrates (for example, **56**) can be prepared conveniently using $BocHNSO_2NH_2$, a crystalline starting material easily accessed from $ClSO_2NCO$ (Scheme 17.23) [84]. Using this reagent, the treatment of 1° and 2° alcohols (such as **31**) with diisopropyl azodicarboxylate (DIAD) and PPh_3 affords the *N*-Boc sulfamide products in respectable yields. Though few sulfamides have been tested so far, their performance appears to equal that of sulfamates. Six-membered ring heterocycles are formed selectively and product yields range from 80 to 85% [85]. These novel compounds may have utility as medicinally active agents and/or as precursors to complex 1,3-diamines and derivatives thereof [86–89].

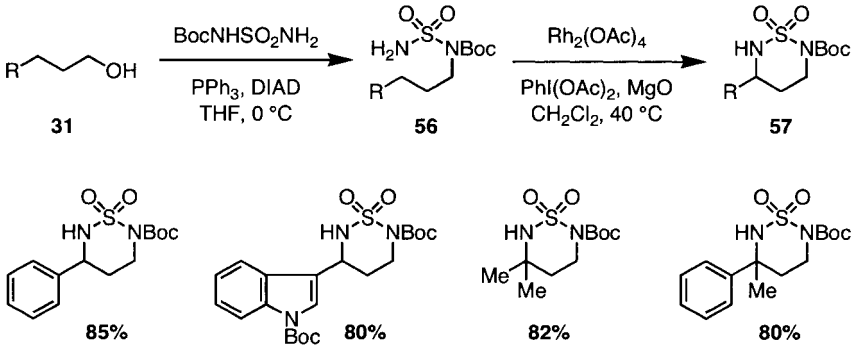

Scheme 17.23 Sulfamide substrates for rhodium-catalyzed C–H amination.

Prior studies by Breslow, Che, and Dauban and Dodd suggested that sulfonamides would function as suitable starting materials for rhodium-catalyzed intramolecular cyclization [25, 59, 90] In practice, substrates such as **59** and **60** react smoothly to generate six-membered heterocycles (Scheme 17.24) [91]. Isolable amounts of γ-sultam **58B**, however, are obtained from oxidation of **58**. The poorer regiocontrol found with insertion reactions of sulfonamides vis-à-vis sulfamate esters is rather surprising, but may be possible to improve using different catalyst structures. In addition, the large bias for reactions to occur at 3° and benzylic centers makes possible the design of substrates that are predisposed for site-selective insertion. Sultam products obtained from this process have value in synthesis [92].

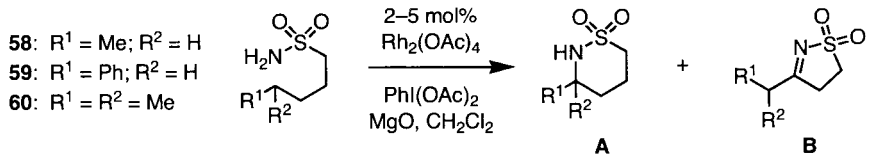

Scheme 17.24 Oxidative cyclization of sulfonamides.

17.6
Rhodium(II)-Catalyzed Olefin Aziridination

17.6.1
Carbamate Esters

Intramolecular π-bond functionalization under rhodium catalysis has been explored using allyl carbamate ester **61** (Eq. 5). The reaction with 5 mol% $Rh_2(OAc)_4$, $PhI(OAc)_2$, and MgO affords oxazolidinone **63**, a product presumed to arise through acetate-opening of an intermediate aziridine **62**. Rojas has described a related process using D-allal-derived carbamate **64** (Scheme 17.25) [93]. Oxidation of this substrate with catalytic $Rh_2(OAc)_4$ and $PhI(OAc)_2$ gives an anomeric mixture of the C2-amidoglycosylated product. A mechanism involving glycal aziridination followed by nucleophilic ring opening with acetate is postulated. By employing PhI=O as the oxidant, glycosyl

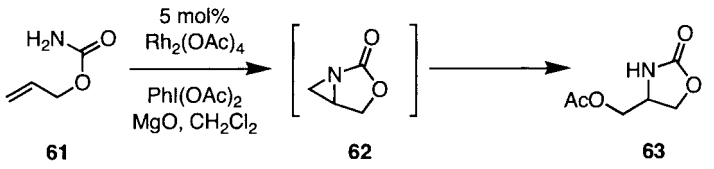

(5)

acceptors (1° and 2° alcohols) can be included in the reaction mixture to trap the putative aziridine. The coupled products are formed with high β-anomer selectivity using 5 equivalents of the added alcohol and 10 mol% $Rh_2(OAc)_4$. Following earlier observations made by Dauban and Dodd, Rojas has also established that $Cu(MeCN)_4PF_6$ and $Cu(acac)_2$ catalyze the amidoglycosylation with PhI=O as the oxidant [94]. Product yields for the copper-catalyzed reactions (38–49%), however, are less than those recorded with $Rh_2(OAc)_4$ (47–75%).

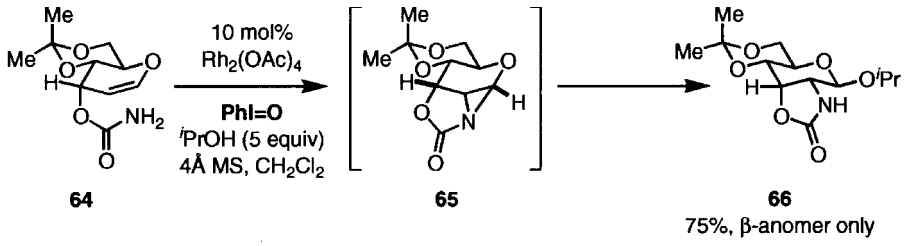

Scheme 17.25 Aminoglycoside synthesis through intramolecular aziridination.

Padwa has shown that rhodium-catalyzed oxidation of indolyl carbamate **67** employing either $PhI(OAc)_2$ or PhI=O follows a path similar to that of the D-allal carbamate (Scheme 17.26) [95]. In principle, indole attack of the putative rhodium–nitrene generates zwitterion **68**, which is trapped subsequently by an exogenous nucleophile. Spirooxazolidinone products (for example, **69**) are isolated as single diastereomers in yields ranging from 50 to 85%. As an intriguing aside, Padwa has found that certain carbamates react with PhI=O in the absence of any metal catalyst to furnish oxazolidinone products. This result may have implications for the mechanism of the rhodium-catalyzed process, although it should be noted that control experiments by Espino and Du Bois confirm the essential role of the metal catalyst for C–H amination [57].

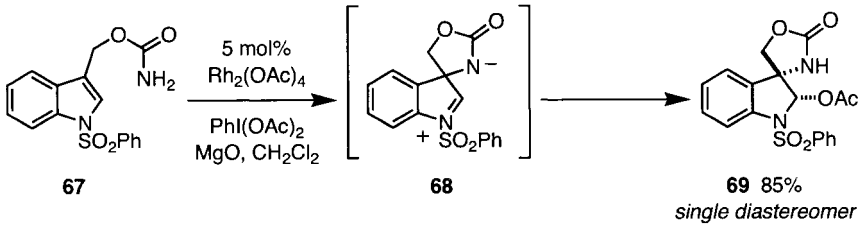

Scheme 17.26 Generation of a novel spirocyclic structure by indole oxidation.

17.6.2
Sulfamate Esters

Oxidative functionalization of π-bonds using sulfamate ester starting materials has been explored for both intra- and intermolecular reaction development. Cyclizations of homoallyl sulfamates occur at reduced temperatures (–20°C) and are exceptionally efficient, irrespective of the electronic properties of the alkene (Scheme 17.27) [69, 74]. In general, aziridination takes place in preference to C–H insertion. Importantly, the reaction is both stereospecific with respect to olefin geometry and stereoselective under rhodium catalysis. A number of chiral homoallyl sulfamates (**71–73**) have been found to give oxathiazinane products with moderate levels of stereocontrol. Preliminary results suggest that the structure of the rhodium complex may be used to improve diastereoselectivity within this substrate class. Such findings would be of value, given the unique reactivity and potential utility of the isolable bicyclic aziridines. Accordingly, these compounds react as electrophiles with alcohols, carboxylates, thiols, amines, N_3^-, and CN^- to generate seven-membered [1,2,3]oxathiazepane-2,2-dioxides [96]. In one rather remarkable example, displacement at a tetrasubstituted γ-center occurs stereospecifically and in preference to attack at the less hindered δ-site (Scheme 17.28) [74]. The product heterocycles can be treated with a second nucleophile to promote ring opening, thereby yielding 1,4-polyfunctionalized amines.

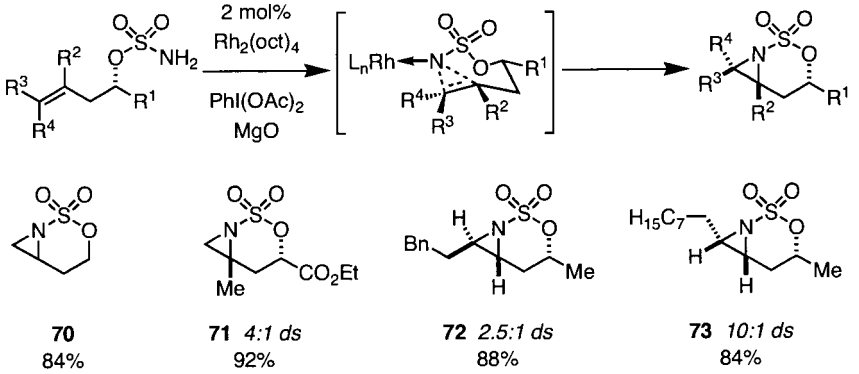

Scheme 17.27 Bicyclic aziridine synthesis from homoallyl sulfamates.

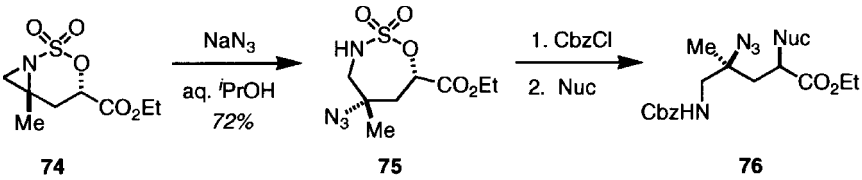

Scheme 17.28 Aziridines as precursors to polyfunctionalized amines.

Homoallyl sulfamate azirdination can be promoted using conditions developed by Dauban and Dodd, which employ 10 mol% $Cu(MeCN)_4PF_6$ and PhI=O (Eq. 6) [96]. As with $Rh_2(O_2CR)_4$, the copper-catalyzed aziridination is stereospecific and bicyclic

oxathiazinane products are delivered in high yields. This method holds promise for enantioselective catalysis, considering the number of chiral copper complexes that have been utilized successfully for intermolecular aziridination reactions.

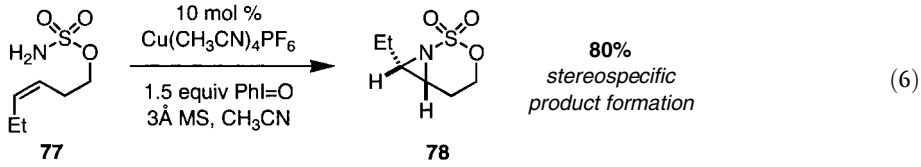

77 78 (6)

Guthikonda and Du Bois have outlined a protocol for intermolecular alkene amination that uses trichloroethylsulfamate **79**, $PhI(OAc)_2$, and MgO with 1–2 mol% $Rh_2(HNCOCF_3)_4$ (Table 17.4) [69]. Alkoxylsulfonyl aziridines are synthesized in moderate to high yields under these conditions. Of the catalysts screened, $Rh_2(HNCOCF_3)_4$ is particularly effective for promoting chemoselective alkene functionalization in preference to C–H insertion. By contrast to other protocols for intermolecular aziridination, reactions under these conditions are performed with alkene as the limiting reagent. The range of substrates that display efficacy includes both aliphatic (entries 1 and 4) and styrenyl systems (entries 2 and 3). Oxidation of *cis*-2-decene (entry 1) and *cis*-*β*-methylstyrene (entry 2) gives exclusively *cis*-configured aziridines, evidence that nitrogen transfer is stereospecific. Finally, this new procedure has been successfully extrapolated to include other sulfamate esters **80** (entry 5) and phosphoramidates **81** (entry 6). Following aziridine ring opening, the resultant trichloroethoxy sulfonylated amines may be deprotected using mild reductive protocols (for example, with Zn/AcOH). By avoiding use of capricious $ArSO_2N{=}IPh$ re-

Tab. 17.4 $Rh_2(HNCOCF_3)_4$-promoted intermolecular aziridination.

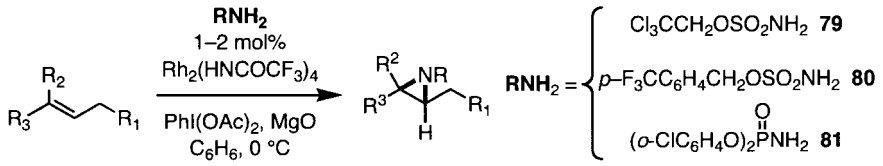

Entry	Product	Yield	Entry	Product	Yield
1	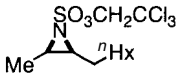	72	4	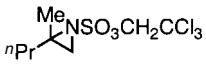	72
2	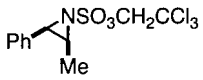	85	5	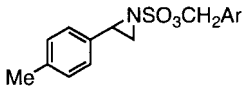	91
3	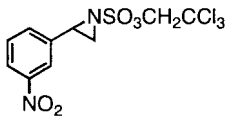	95	6	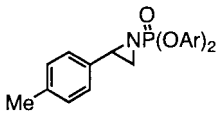	33

agents, a convenient and easily scalable method for accessing important aziridine materials is made available.

17.6.3 Sulfonamides

Recent advances in rhodium-catalyzed amination methodology have obviated use of iminoiodinane oxidants, replacing them instead with stable amine derivatives and $PhI(OAc)_2$. In a similar display, Dauban and Dodd have shown that preformed iminoiodinane reagents are not required for copper-mediated oxidative amination (Table 17.5) [94]. By employing PhI=O as the terminal oxidant in combination with 10 mol% $Cu(MeCN)_4PF_6$, molecular sieves, and sulfonamide substrates, both intra- and intermolecular alkene aziridination is possible. Intermolecular reactions may be conducted with limiting amounts of olefin, and typically afford 40–70% yields of aziridine products. The addition of a chiral bisoxazoline (box) ligand to a reaction mixture containing styrene, PhI=O, and $TsNH_2$ leads to a modest enantiomeric excess (59% *ee*). In one intriguing though somewhat anomalous result, $Cu(MeCN)_4PF_6$ catalyzed the intramolecular allylic C–H insertion of arylsulfonamide **84** (Eq. 7), to afford sultam **85** in 51% yield, with the apparent exclusion of any of the bicyclic aziridine. There exist, however, only a limited number of examples of C–H amination reactions promoted by copper salts, almost all of which appear with cyclohexene or other allylic substrates [32, 53].

Tab. 17.5 N-atom transfer under copper-catalyzed conditions.

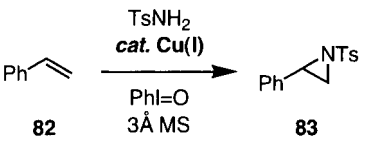

82 **83**

Cu(I)/ligand	*Solvent*	*Yield*	*%ee*
$Cu(MeCN)_4PF_6$	CH_3CN	75	n/a
Cu(OTf)/(*S*,*S*)-t-Bu-box]	C_1H_6	86	59%

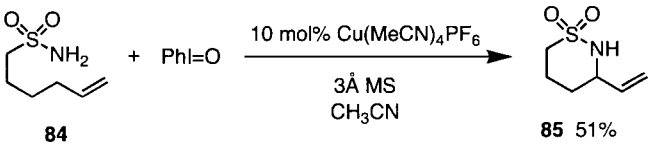

84 **85** 51% (7)

Che has reported that both achiral and chiral rhodium catalysts function competently for intramolecular aziridination reactions of alkyl- and arylsulfonamides (Scheme 17.29) [59, 97]. Cyclized products **87** are isolated in ~90% yield using 2 mol% catalyst, $PhI(OAc)_2$, and Al_2O_3. Notably, reactions of this type can be performed with catalyst loadings as low as 0.02 mol% and display turnover numbers in excess of 1300. In addition, a number of chiral dimeric rhodium systems have been examined for this process, with some encouraging results. To date, the best data are obtained using Doyle's $Rh_2(MEOX)_4$ complex. At 10 mol% catalyst and with a slight excess of PhI=O, the iso-

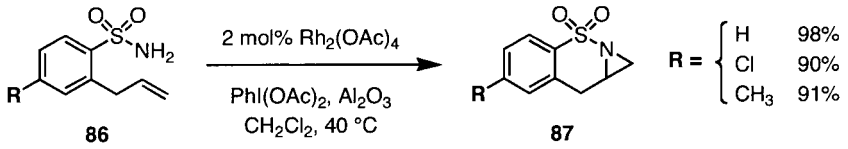

86 87

Scheme 17.29 Oxidative cyclization of unsaturated sulfonamides.

lated sultams display enantiomeric excesses ranging between 55 and 60% [97]. Nonetheless, conversion of the starting material to product is quite variable (22–95%), thus leaving opportunity available for future developments in this area.

17.7
Enantioselective C–H Insertion with Sulfamate Esters

Asymmetric C–H insertion using chiral rhodium catalysts has proven rather elusive (Scheme 17.30). Dimeric complexes derived from functionalized amino acids **90** and **91** efficiently promote oxidative cyclization of sulfamate **88**, but the resulting asymmetric induction is modest at best (~50% *ee* with **90**). Reactions conducted using Doyle's asymmetric carboxamide systems **92** and **93** give disappointing product yields (~5–10%) and negligible enantiomeric excesses. In general, the electron-rich carboxamide rhodium dimers are poor catalysts for C–H amination. Low turnover numbers with these systems are ascribed to catalyst oxidation under the reaction conditions.

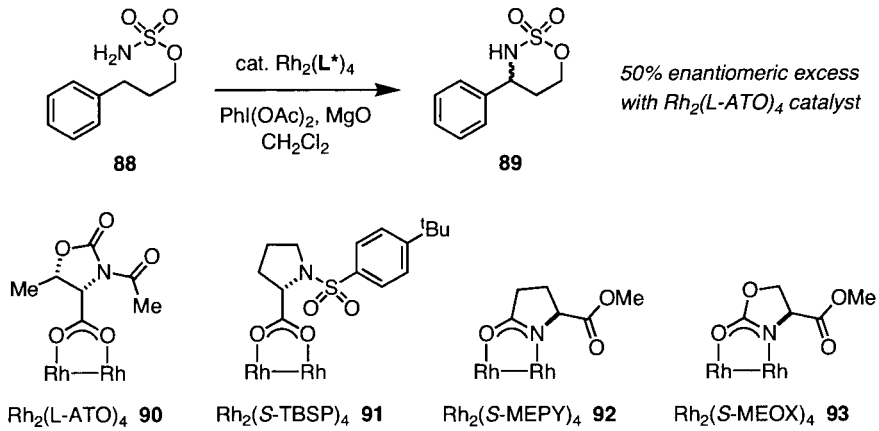

88 89

Scheme 17.30 Preliminary investigations of asymmetric C–H amination.

Asymmetric C–H amination has progressed through the application of ruthenium(II) porphyrin catalysts. Che has employed fluorinated ruthenium porphyrin complexes with added Al_2O_3 (in place of MgO) to catalyze sulfamate ester insertion (Scheme 17.31) [98]. These systems show exceptional catalyst activity (>300 turnovers) and afford product yields that are comparable to rhodium tetracarboxylate-promoted reactions. Of perhaps greater significance is that the use of the chiral ruthenium complex

95 generates optically enriched sulfamidates and select oxathiazinanes with enantiomeric excesses from 70 to 87%. As Che has demonstrated, an iminoiodinane made from a sulfamate substrate and $PhI(OAc)_2$ reacts with **95** to furnish the product in comparable yield and optical purity to that recorded under the "in-situ" conditions. Such a result convincingly establishes iminoiodinanes as chemically competent intermediates on the reaction pathway. The continued development of chiral catalysts along with added mechanistic insight will undoubtedly lead to improved product enantioselectivities in sulfamate ester oxidation.

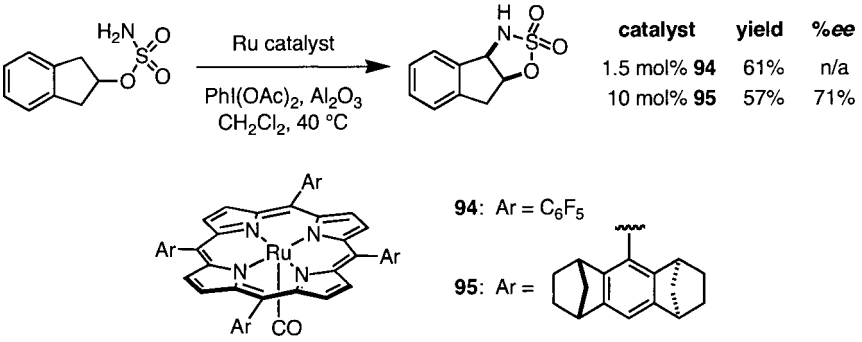

Scheme 17.31 Enantioselective sulfamidate synthesis using ruthenium catalysis.

17.8 Mechanistic Investigations

Several lines of inquiry have been explored to address key mechanistic issues in the rhodium-catalyzed C–H insertion of carbamates and sulfamates (Scheme 17.32) [99]. A pathway involving initial condensation between substrate **96** and $PhI(OAc)_2$ to form iminoiodinane **97** was envisioned in the original design of this chemistry. Coordination of **97** to an axial site on the rhodium dimer would promote nitrene formation and the ensuing C–H insertion event. Surprisingly, control experiments with $PhI(OAc)_2$ and sulfamate **96** (or analogous carbamates) give no indication for a reaction between these two components.

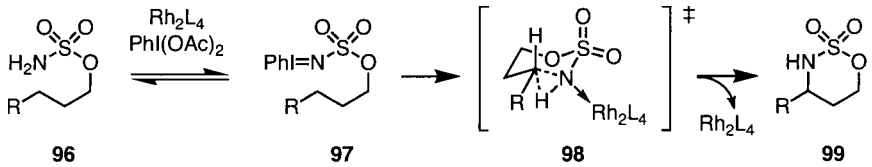

Scheme 17.32 Proposed catalytic cycle for rhodium-catalyzed C–H insertion.

To examine further the possible intermediacy of iminoiodinane **101**, a compound having this presumed structure was prepared (Scheme 17.33) [91]. Support for the assignment of **101** was obtained upon treatment with Ph_3P, which leads rapidly to the formation of iminophosphorane **102**. The putative iodinane **101** also reacts with 2 mol%

$Rh_2(OAc)_4$ to afford ~60% of oxathiazinane **103** and ~40% of recovered sulfamate **100**. Although the yield for this process is significantly below that obtained under conditions employing $PhI(OAc)_2$ and MgO, this result does establish **101** as a chemically competent intermediate. From these data, it is reasonable to conclude that a small concentration of iodinane **101** may exist in equilibrium when $PhI(OAc)_2$ and substrate are combined. This material is rapidly converted by the rhodium catalyst to oxathiazinane **103**. Such a proposal would explain the absence of any detectable amount of **101** (or a related species) in the aforementioned control experiments.

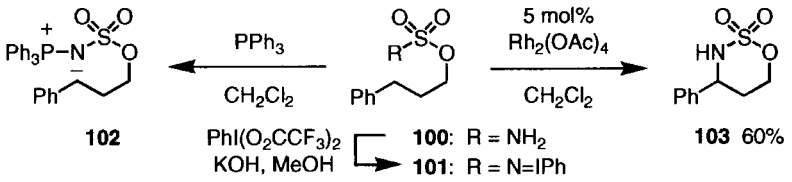

Scheme 17.33 Investigating the reactivity of alkoxysulfonyl iminoiodinanes.

Studies designed to interrogate the nature of the active oxidant provide compelling support for a rhodium–nitrene. Stereospecific C–H insertion with optically active 3° substrates gives strong indications for a nitrene-type pathway (*vide supra*). Additional experiments conducted with a cyclopropyl clock substrate **104** furnish in 91% yield the corresponding oxathiazinane **105** with no evidence of radical-rearranged products (Eq. 8). In light of the rapid rate constant for cyclopropyl carbinyl radical fragmentation ($\sim 10^{11}\ s^{-1}$), this observation provides further support for a concerted C–H insertion mechanism and significantly reduces the likelihood of a stepwise C–H abstraction/radical-rebound pathway [100].

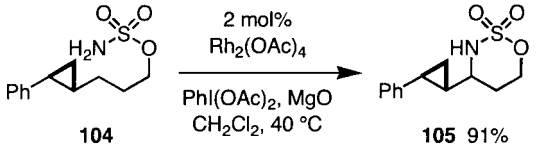

(8)

Analysis of the reaction KIE using monodeuterated sulfamate **106** reinforces the proposed rhodium–nitrene model (Eq. 9). The ratio of H/D products **107**/**108** is a direct measure of the KIE and has been found to equal 1.5±0.2 by integration of the ^{13}C NMR spectrum. An equivalent value is obtained for nitrene C–H insertion upon photolysis of a carbamoyl azide, and is taken as evidence for a nonlinear transition state. As noted previously, Müller's use of NsN=IPh with partially deuterated adamantane gives

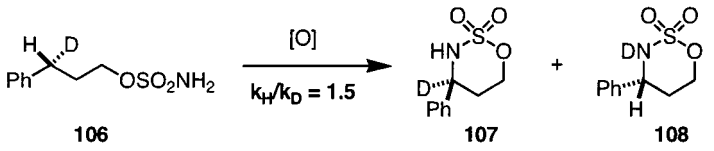

(9)

a KIE of 3.5±0.2 [35]. The disparity in these independent measurements is rather surprising for two reactions that are thought to proceed *via* analogous rhodium–nitrene intermediates. However, the low product yields obtained by Müller mitigate to some extent the validity of the adamantane result. Conversely, Hammett analysis using *para*-substituted diaryl sulfamates **109** gives a ρ value of –0.8, which matches closely the value recorded for intermolecular C–H amination with NsN=IPh (Table 17.6) [101]. The picture of a reaction transition state having little charge separation is thus inferred from this small, negative ρ value. Such a conclusion is in complete accordance with nitrene-like C–H insertion, which proceeds through a three-centered concerted, albeit asynchronous, pathway.

Tab. 17.6 Hammett analysis of sulfamate insertion.

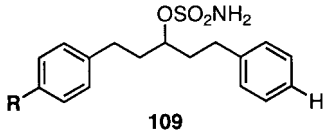

109

R=	σ_p	*Ratio Ph/Ar$_R$*
OCH_3	–0.27	1.0:3.0
CH_3	–0.17	1.0:1.7
Br	0.23	1.1:1.0
CF_3	0.54	1.5:1.0
NO_2	0.78	3.0:1.0

Examination of the structure and bonding of dimeric rhodium(II) carboxylates provides insight into their unparalleled utility as catalysts for nitrenoid (and carbenoid) reactions. The electronic configuration of the dinuclear rhodium complex is uniquely disposed to bind and to stabilize a ligated nitrene [38, 102, 103]. To understand why, it is useful to consider a simplified molecular orbital representation of these D_4-symmetric lantern complexes, generated by admixing the ten metal d-orbitals (Scheme 17.34). The 14 valence electrons from the two d^7 Rh^{2+} centers thus occupy a $\sigma^2\pi^4\delta^2\pi^{*4}\delta^{*2}$ ground state. Such an orbital diagram is in agreement with computational and experimental data that establish a Rh–Rh single bond for these dimeric structures [102]. Moreover, this picture suggests that a ligand coordinated along the

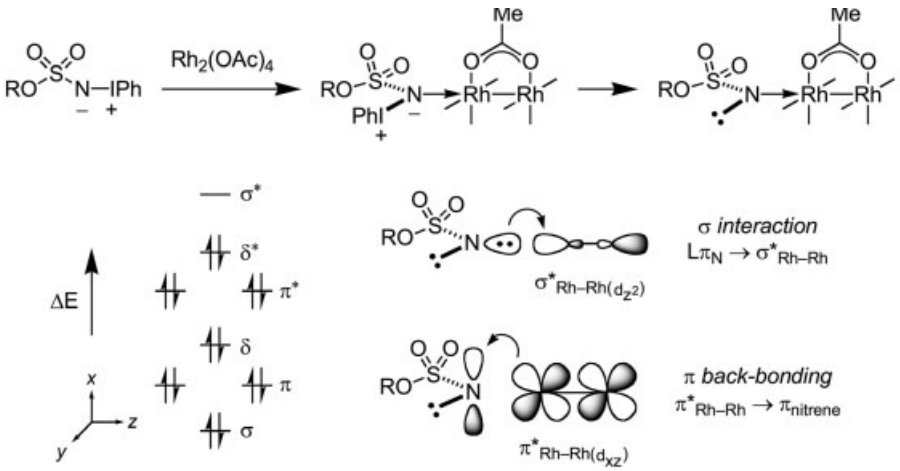

Scheme 17.34 Molecular orbital analysis of putative metallo-nitrene.

Rh–Rh vector may donate electron density to the empty Rh–Rh σ^*-orbital and/or overlap through back-bonding with either of the filled π^* MOs [103]. Infrared measurements of Rh_2L_4–CO adducts demonstrate clearly a red shift in the C=O stretching frequency relative to unligated carbon monoxide [104]. These results are consistent with electron delocalization from the Rh–Rh π^* into the low-lying σ^*_{CO}. Similarly, back-bonding from the rhodium π^* into the σ^*_{N-I} can occur upon coordination of an iminoiodinane to the rhodium dimer (Scheme 17.34). Subsequent loss of PhI is thus facilitated, and the resulting nitrene ligand is stabilized through both σ-bonding ($Lp_N \rightarrow \sigma^*_{Rh-Rh}$) and π back-bonding ($\pi^*_{Rh-Rh} \rightarrow p_N$) interactions. This model for metal–nitrene bonding essentially mirrors that proposed for diazoalkane activation and metal–carbene coordination by dinuclear rhodium(II) catalysts [37, 60, 104, 105].

The kinetic profile of the intramolecular amination process has been explored using substrates **110**, **111**, and **114** (Scheme 17.35). Reactions performed with equimolar mixtures of sulfamates **110** and **111** run to varying conversions (ca. 10–50%) afford 1:1 mixtures of the product oxathiazinanes. These data diverge significantly from those obtained with sulfamate **114**, a substrate in which the intrinsic selectivity between 3° and 2° C–H bonds is measured directly. The conclusion is therefore reached that the product-forming step (that is, rhodium–nitrene C–H insertion) is not rate-determining in the overall reaction pathway. When coupled to more recent findings that suggest a zero-order dependence on [catalyst] and a first-order dependence on both [substrate] and [$PhI(OAc)_2$], the following mechanistic postulate evolves: (1) rate-determining condensation between $PhI(OAc)_2$ and substrate; (2) reaction of the oxidant–substrate complex with $Rh_2(OAc)_4$; (3) rhodium–nitrene generation; and (4) C–H insertion with concomitant regeneration of the catalyst. Though elements of this scheme remain speculative, future experimentation should resolve a number of unanswered questions. Importantly, identification of the inactive rhodium species and/or rhodium decomposition products that arrest turnover will provide a deeper understanding of metal–nitrene reactivity. Altogether, the mechanistic insights gathered from these efforts may provide a springboard to new, more efficient catalyst systems that promote both intra- and intermolecular C–H amination.

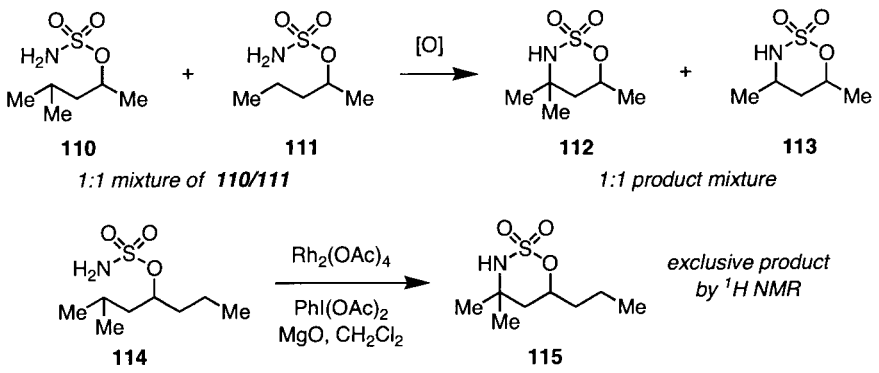

Scheme 17.35 Divergent outcomes of inter- and intramolecular competition studies.

17.9
Summary and Outlook for Rhodium(II)-Catalyzed Nitrene Transfer

Oxidative amination of carbamates, sulfamates, and sulfonamides has broad utility for the preparation of value-added heterocyclic structures. Both dimeric rhodium complexes and ruthenium porphyrins are effective catalysts for saturated C–H bond functionalization, affording products in high yields and with excellent chemo-, regio-, and diastereocontrol. Initial efforts to develop these methods into practical asymmetric processes give promise that such achievements will someday be realized. Alkene aziridination using sulfamates and sulfonamides has witnessed dramatic improvement with the advent of protocols that obviate use of capricious iminoiodinanes. Complexes of rhodium, ruthenium, and copper all enjoy application in this context and will continue to evolve as both achiral and chiral catalysts for aziridine synthesis. The invention of new methods for the selective and efficient intermolecular amination of saturated C–H bonds still stands, however, as one of the great challenges.

17.10
Rhodium(II)-Catalyzed Olefin Diamination

Selective methods for the direct conversion of alkenes to vicinal diamines are exceedingly scarce. Both osmium- and selenium-based reagents have been demonstrated to promote this transformation, but application in synthesis is limited by the stoichiometric nature of these processes and by an abridged substrate scope [106–108]. Li has described a rhodium-catalyzed diamination reaction of alkenes using $TsNCl_2$ as the terminal oxidant (Scheme 17.36) [109]. Optimized reactions are reported for electron-deficient *α,β*-unsaturated ketones and esters in combination with excess $TsNCl_2$ (2.5 equiv), 2 mol% $Rh_2(O_2CC_3F_7)_4$, and 4 mol% Ph_3P in acetonitrile. The product imidazolines **118** are isolated in yields ranging from 45 to 82% and may be hydrolyzed in a subsequent step under strongly acidic conditions to afford differentially protected 1,2-diamines. With *trans*-alkene substrates, high selectivity (>20:1) for the *anti*-imidazoline stereoisomer is always observed. The choice of acetonitrile as a solvent for this process is essential, based on mechanistic considerations that posit a Ritter-type reaction of a chloroaziridinium species **117**. Only a single equivalent of $TsNCl_2$ is thus incorporated into the resulting heterocycle **118**. The mixture of $Rh_2(O_2CC_3F_7)_4$ and Ph_3P presumably functions to catalyze aziridinium ion formation, though the mechanistic details of such an event remain unclear. Interestingly, imidazoline synthesis may be promoted with similar efficiency using 20 mol% of a 2:1 $Ph_3P/FeCl_3$ complex [110,

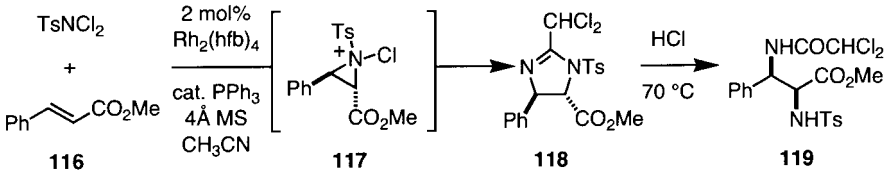

Scheme 17.36 Catalytic olefin diamination.

111]. Although currently confined to a small window of substrates, future investigations of this type of methodology would seem fruitful for discovery.

17.11 Applications of C–H Amination in Synthesis

17.11.1 Carbamate Ester Amination

Methods for C–H amination have been applied successfully to the preparation of deoxyamino sugars. Such structures appear with frequency in Nature as component parts of peptidyl, macrolide, steroidal, and other natural product aglycon skeletons. Rojas has shown that intramolecular glycal amination with D-allal carbamate **64** can be achieved under either rhodium- or copper-catalyzed amination conditions (see Scheme 17.25) [93]. The putative aziridine **65** is trapped *in situ* with various alcohols to give 2-deoxyamine-derived products **66**. Alternative methods for the synthesis of 2-amino pyranoses from protected glycals involve aziridine formation through intermolecular *N*-atom transfer (Eq. 10). The reactive aziridine intermediate couples selectively with oxygen nucleophiles at the anomeric position. Use of stoichiometric manganese nitride reagents with $(CF_3CO_2)O$ has demonstrated efficacy in this context [112, 113]. Reaction of D-glucal **120** with trichloroethyl sulfamate, $PhI(OAc)_2$, MgO, and catalytic $Rh_2(Oct)_4$ is also an effective method for preparing the C2-deoxyamino glucosyl acetate **121**.

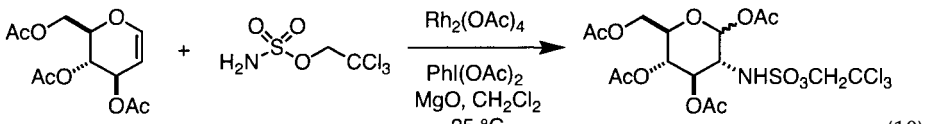

120 **121** (10)

Though intra- or intermolecular aziridination affords convenient access to C2-deoxyamino sugars, related approaches to C3- and C4-amine derivatives have not evolved. Instead, C–H insertion may hold greater potential as a tool for constructing these types of unique monosaccharide targets. Two recent, independent syntheses of methyl-L-callipeltose **122** by Trost and Panek nicely illustrate such a strategy (Scheme 17.37). Callipeltose is a modified C4-deoxyamino sugar found in the macrolide natural product, callipeltoside A. The oxazolidinone moiety embedded within **122** together with the stereochemical substitution pattern of the desired target makes oxidative cyclization of the C3-carbamate **124** optimally suited as a method for installing the C4-carbinolamine. Accordingly, Trost has employed a hetero-Diels–Alder reaction to assemble pyranone **123**, which was processed through four additional steps to carbamate **124** [114]. Oxidative C4 insertion using 10 mol% $Rh_2(OAc)_4$, $PhI(OAc)_2$, and MgO in dichloromethane (40°C) furnished methyl-L-callipeltose **122** in 57% yield (~20% of unreacted **124**). A slight improvement in the reaction efficiency was noted by substituting MgO with 2,6-di-*tert*-butyl-4-methylpyridine (DTBMP). Switching the catalyst from $Rh_2(OAc)_4$ to the $Rh_2(tpa)_4$ complex did not affect the reaction outcome. The preparation of racemic callipeltose was thus accomplished in six steps and 17% overall yield.

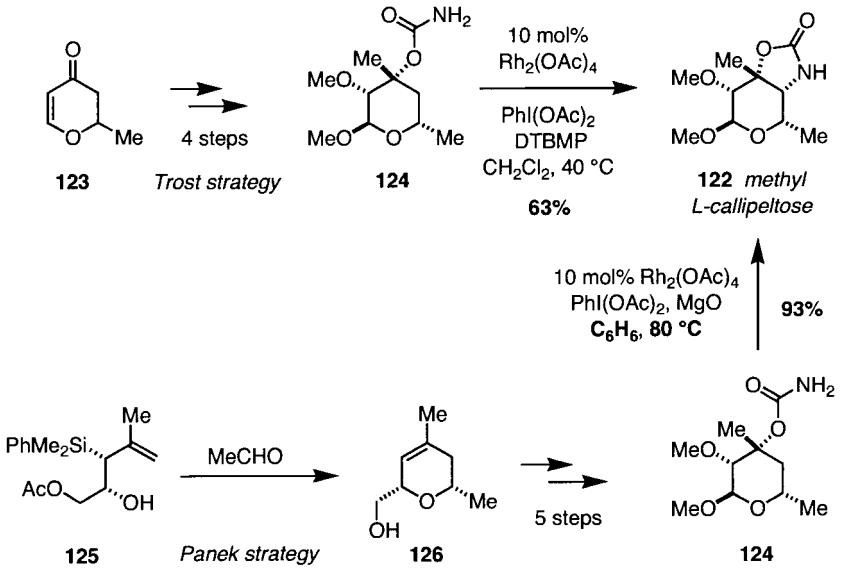

Scheme 17.37 Carbamate oxidation for the synthesis of methyl-L-callipeltose.

The synthesis of methyl-L-callipeltose as described by Panek also capitalizes on C3-carbamate **124** insertion to fashion the requisite oxazolidinone (Scheme 17.37) [115]. Assembly of the desired pyran **126** is performed using a novel [4+2] annulation reaction between optically pure allylsilane **125** and MeCHO. Carbamate **124** is then accessed following a straightforward, five-step sequence. Panek has shown that the product yield from the oxidative cyclization of **124** can be improved to 93% by employing 10 mol% $Rh_2(OAc)_4$, $PhI(OAc)_2$, and MgO in refluxing benzene. This useful modification of the original protocol (CH_2Cl_2, 40 °C) is quite possibly of general value for reactions with other carbamate substrates. Panek's asymmetric synthesis of methyl L-callipeltose **122** totals eight steps from allysilane **125** and proceeds in 23% overall yield.

Parker has outlined an elegant, enantioselective synthesis of L-vancosamine derivatives commencing from noncarbohydrate precursors (Scheme 17.38) [116]. This approach features a diastereoselective allenylstannane addition and $W(CO)_6$-catalyzed cycloisomerization to construct the pyranose core. Oxidative cyclization of the C4-carbamate **128** is performed with 10 mol% $Rh_2(OAc)_4$ and proceeds stereospecifically to give the crystalline oxazolidinone **129** (86%). All told, synthesis of this useful L-vancosamine glycal equivalent covers seven steps from (*S*)-(–)-ethyl lactate **127** and is accomplished in 44% overall yield.

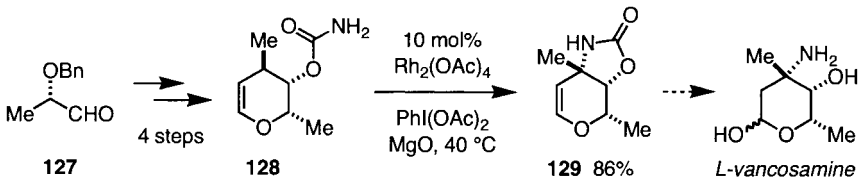

Scheme 17.38 Stereospecific C–H oxidation affords L-vancosamine equivalent.

A recent preparation of (–)-tetrodotoxin (TTX), the poisonous constituent of the Japanese *fugu*, stands as perhaps the signature application for carbamate C–H amination in synthesis (Scheme 17.39) [117]. The intricate structure of tetrodotoxin is comprised of unique hemi-orthoacid and guanidine-aminal functional groups on a heavily oxygenated cyclohexane core. Rhodium-catalyzed carbamate oxidation makes possible the formulation of a synthetic plan in which installation of the guanidine (more specifically the C8a-carbinolamine center) is postponed until the late stage of development. The assembly of tetrodotoxin is thereby simplified to a problem involving stereocontrolled synthesis of a monocyclic structure with oxygen-based groups at almost every carbon. A compound **130** of this type, having a suitable collection of protecting groups, has been prepared over a 25-step sequence commencing from D-isoascorbic acid **131**. This intermediate **130** properly configures the C9-carbamate and the C8a-methine for the critical oxidative cyclization event. Initial reactions performed under conditions that employed $Rh_2(OAc)_4$, gave moderate yields (~50%) of the desired oxazolidinone **132**. Subsequent experimentation with alternative catalyst complexes, however, has afforded a more favorable outcome. The reaction of **130** with 10 mol% $Rh_2(HNCOCF_3)_4$, $PhI(OAc)_2$, and MgO in C_6H_6 solvent furnishes a 77% yield of the insertion product **132**. In addition, ~15% of the C9-ketone **133** is produced. Successful application of C–H amination at this stage of the synthesis enables complete assembly of (–)-tetrodotoxin in six additional steps from oxazolidinone **132**.

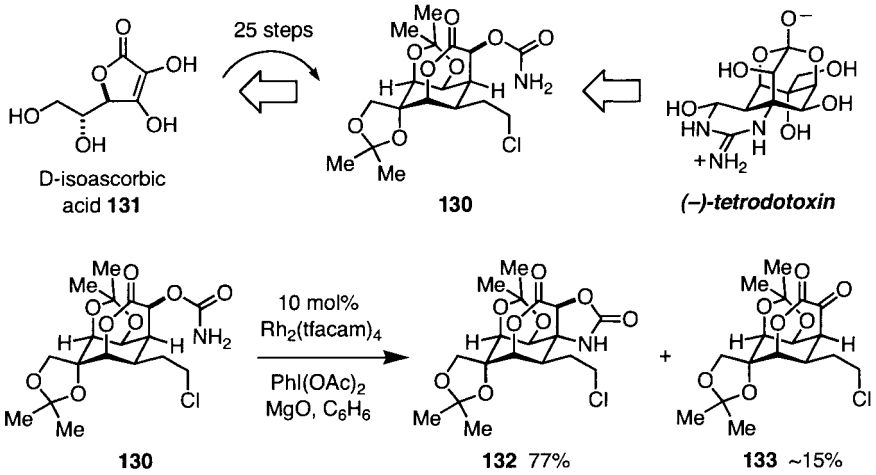

Scheme 17.39 Asymmetric synthesis of (–)-tetrodotoxin.

17.11.2 Sulfamate Ester C–H Insertion

17.11.2.1 1,2,3-Oxathiazinane-2,2-dioxides as Tools in Synthesis

The advent of sulfamate ester oxidative cyclization makes available a myriad of oxathiazinane derivatives from simple alcohol precursors. These unusual heterocycles have enjoyed only sparing use despite their potential as electrophilic azetidine equivalents. By contrast, five-membered ring sulfamidates and cyclic sulfates are broadly recog-

nized as important functional surrogates of aziridines and epoxides, respectively [118–121]. However, the facility by which such heterocycles undergo nucleophilic ring opening is in no way mirrored by the robust oxathiazinanes. Two early reports of oxathiazinane ring opening seemed to indicate that only forcing conditions could promote C–O bond cleavage in these materials [122, 123]. Fortunately, as both Du Bois and Lubell have shown, modification of the N–H moiety on the oxathiazinane ring with either acyl or alkyl groups (that is, to form 9-fluorenyl) can have a dramatic influence on the reactivity of these heterocycles [68, 121, 124]. As an example, ring opening of *N*-CBz-oxathiazinane **134** occurs smoothly between 25 and 40 °C with nucleophiles that include CN^-, N_3^-, thiolates, carboxylates, metal enolates, alcohols, and H_2O (Scheme 17.40). Solvolytic displacement of **135** using aqueous acetonitrile (~40°C) is most efficient and can be conducted to access either the 1,3-amino alcohol or the corresponding *β*-amino acid. By capitalizing on the stereospecificity of C–H insertion and a "one-pot" ring-opening/oxidation sequence, access to optically pure *β*,*β*-disubstituted *β*-amino acids is greatly simplified (*vide infra*).

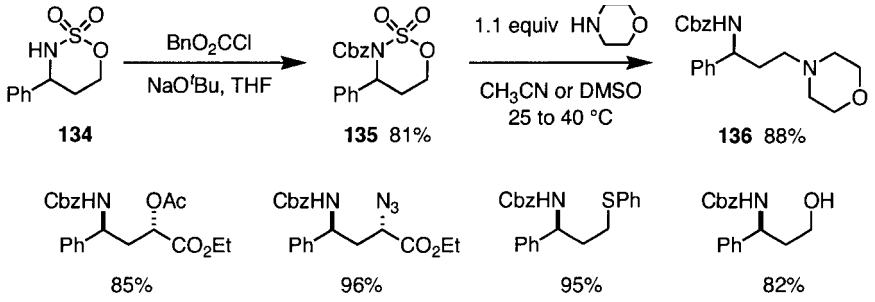

Scheme 17.40 Nucleophilic ring opening of *N*-acylated oxathiazinanes.

Phenolic sulfamates **137** serve as useful starting materials for both intramolecular C–H insertion and alkene aziridination (Scheme 17.41). Products furnished from these reactions are structurally unique and may be employed for subsequent nickel-catalyzed cross-coupling to Grignard reagents [125]. Under the action of $Ni(dppp)Cl_2$, biaryl and alkyl-substituted arene adducts such as **139** are furnished conveniently and in good yields (75–95%). Related palladium-catalyzed boronic acid couplings have also proven viable, though further screening of reaction conditions and ligand groups is warranted for process optimization.

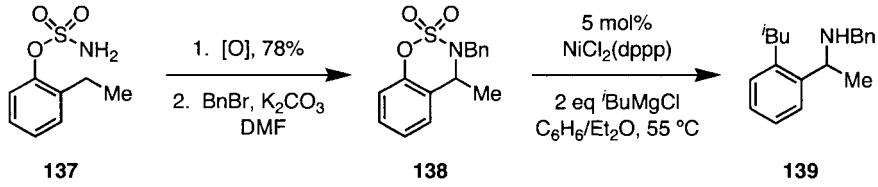

Scheme 17.41 Nickel-catalyzed cross-coupling of phenol-derived sulfamate esters.

This brief discussion on the synthetic utility of oxathiazinanes is only intended to highlight the versatility of these reagents. Readers who seek a more detailed review on the chemistry of sulfamidites and sulfamidates are referred to a recent, comprehensive account by Lubell [121]. Applications for these unusual heterocyclic building blocks should see continued growth with the oxidative amination technologies now available for their preparation.

17.11.2.2 **Synthetic Applications of Sulfamate Ester Oxidation**

Methods for C–H amination using sulfamate esters are beginning to find application in the arena of complex molecular synthesis. The generation of large quantities of oxathiazinanes is readily reduced to practice, due to the simplicity of performing sulfamate oxidations on scale. Optically pure oxathiazinanes fashioned through stereospecific C–H insertion are particularly useful building blocks for preparing β-amino acids, as highlighted in the synthesis of β-isoleucine **142** (Scheme 17.42). The short sequence of steps commencing from (*S*)-3-methylpentan-1-ol sulfamate **140** facilitates the preparation of >1.8 g of **142** in a single throughput [68].

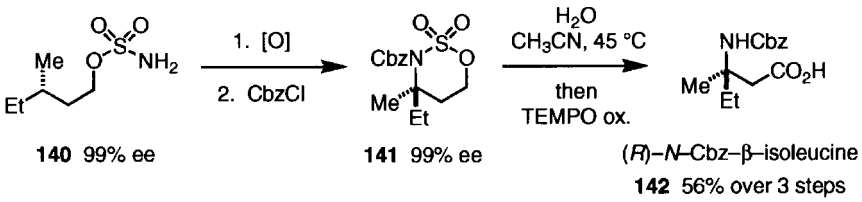

Scheme 17.42 Stereospecific preparation of β,β-disubstituted β-amino acids.

A strategy for the synthesis of bromopyrrole alkaloids, manzacidin A and C, was conceived using epimeric oxathiazinanes **143** and **144** *en route* to optically active α,γ-diaminoester derivatives **145** and **146**, respectively (Scheme 17.43) [126]. These functionalized diamines comprise the requisite framework of this unique class of natural products. Access to such intermediates is achieved using an asymmetric Evans ene reaction followed by directed olefin hydrogenation. In this way, both C6 antipodes are prepared from a common precursor, **147**. Oxidative cyclization of sulfamate **148** gives the corresponding oxathiazinane as a stereoisomerically pure product (85%); the same conditions employing epimeric substrate function with comparable effectiveness. The electrophilicity of the oxathiazinane core is then exploited to install the desired *N*-formyl amine. Three subsequent manipulations afford the target structures. In all, more than 300 mg of each compound has been furnished using this efficient ten-step reaction sequence.

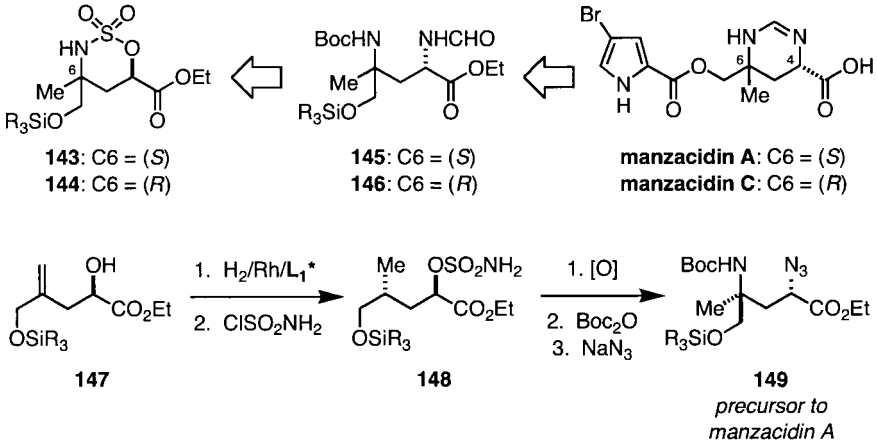

Scheme 17.43 Bromopyrrole alkaloid assembly, highlighting sulfamate ester oxidation.

Coupling of alkynylzinc reagents to oxathiazinane *N,O*-acetals yields heterocyclic structures that have exceptional versatility as synthetic intermediates [80]. Crystalline tosylate **151** is one such compound that can be easily transformed to select polyhydroxylated indolizidine alkaloids and related molecules of interest. An example of such a synthesis is illustrated in Scheme 17.44. Accordingly, alkyne semi-hydrogenation and subsequent tosylate displacement afford the bicyclic compound **152**. Catalytic dihydroxylation of **152** with OsO_4 generates the vicinal diol as a single stereoisomer, which is treated with NaCN (^{i}PrOH/H_2O, 55°C) to effect oxathiazinane ring opening. The rather mild aqueous conditions used to promote displacement of the C–O bond may be of general utility for such reactions and are in contrast to other protocols for nucleophilic addition to *N*-alkyloxathiazinanes that require high temperatures and long reaction times. The entire route to **153** totals six steps from the sulfamate ester (34% overall) and has been performed without recourse to any protecting groups. Structurally analogous indolizidine alkaloids should be available from either **150** or alternative *N,O*-acetal starting materials.

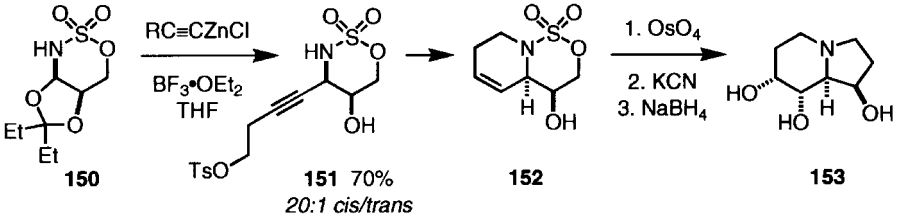

Scheme 17.44 Oxathiazinane *N,O*-acetals as useful tools in synthesis.

17.12 Conclusion

Metal-mediated C–H amination, though first described as long ago as the 1960s, remains in a formative stage as methodology for synthesis. Recent advances have provided high-yielding and selective methods for intramolecular C–H oxidation with carbamate, sulfamate, sulfamide, and sulfonamide starting materials. The ability to perform such reactions is possible only with the discovery of new experimental protocols based on combinations of catalyst, the inexpensive commercial oxidant $PhI(OAc)_2$, and metal oxide additives (that is, MgO, Al_2O_3). These findings have increased dramatically the substrate scope by avoiding use of capricious iminoiodinane reagents, most of which are not stable to isolation. Conditions employing catalyst, $PhI(OAc)_2$, and metal oxide also extend to intra- and intermolecular π-bond functionalization and furnish important aziridine derivatives. Collectively, use of these new chemistries for the preparation of natural products, pharmaceutical agents, and other materials should continue to flourish, given the demonstrated value of the product heterocycles. The sustained evolution of catalyst systems that influence chemo-, regio-, and stereocontrolled C–N bond formation will undoubtedly foster additional applications for these methods. The challenge, however, to find a selective process of general function for the *inter*molecular amination of C–H bonds still stands. The complexity of such a problem is formidable, but a solution of inestimable reward.

Acknowledgments

We are indebted to our co-workers, whose intellectual contributions, tireless efforts, and tremendous enthusiasm for science have made possible the writing of this chapter. C.G.E. is grateful for pre-doctoral fellowships from the NSF (1999–2002), Pfizer (2002), and the ACS Division of Organic Chemistry, sponsored by Merck Research Laboratories (2002–2003). Research has been supported by the National Science Foundation, the National Institutes of Health, and the Beckman Foundation, and by generous contributions from Abbott, Boehringer Ingelheim, Bristol–Myers Squibb, Eli Lilly, GlaxoSmithKline, Johnson Matthey, Merck, and Pfizer.

17.13 References

1 C.M. Marson, A.D. Hobson in *Comprehensive Organic Functional Group Transformations Vol. 2* (Ed.: A.R. Katritzky, O. Meth-Cohn, C.W. Rees), Elsevier Science, Oxford, **1995**, pp. 297.
2 *Modern Amination Methods* (Ed. A. Ricci), Wiley-VCH, Weinheim, **2000**.
3 I.D.G. Watson, A.K. Yudin, *Curr. Opin. Drug Discov. Develop.* **2002**, *5*, 906.
4 R.S. Atkinson, *Tetrahedron* **1999**, *55*, 1519.
5 C.J. Moody in *Comprehensive Organic Synthesis Vol. 7* (Ed.: B.M. Trost, I. Fleming), Pergamon Press, Oxford, **1993**, pp. 21–38.
6 S. Andreae, E. Schmitz, *Synthesis* **1991**, 327.
7 *Azides and Nitrenes. Reactivity and Utility* (Ed. E.F.V. Scriven), Academic Press, Orlando, **1984**.
8 O. Meth-Cohn, *Acc. Chem. Res.* **1987**, *20*, 18.

9 C. Buron, M.S. Platz, *Org. Lett.* **2003**, *5*, 3383.
10 P. Müller, C. Fruit, *Chem. Rev.* **2003**, *103*, 2905.
11 P. Dauban, R.H. Dodd, *Synlett* **2003**, 1571.
12 P. Müller in *Advances in Catalytic Processes Vol. 2* (Ed.: M. P. Doyle), JAI Press, Greenwich, **1997**, pp. 113–151.
13 H. Kwart, A.A. Khan, *J. Am. Chem. Soc.* **1967**, *89*, 1951.
14 D.S. Breslow, M.F. Sloan, *Tetrahedron Lett.* **1968**, 5349.
15 Y. Tamura, T. Uchida, T. Katsuki, *Tetrahedron Lett.* **2003**, *44*, 3301.
16 K. Omura, M. Murakami, T. Uchida, R. Irie, T. Katsuki, *Chem. Lett.* **2003**, *32*, 354.
17 F. Ragaini, A. Penoni, E. Gallo, S. Tollari, C. Li Gotti, M. Lapadula, E. Mangioni, S. Cenini, *Chem. Eur. J.* **2003**, *9*, 249.
18 T. Bach, B. Schlummer, K. Harms, *Chem. Eur. J.* **2001**, *7*, 2581.
19 Y. Yamada, T. Yamamoto, M. Okawara, *Chem. Lett.* **1975**, 361.
20 R. Breslow, S. H. Gellman, *J. Chem. Soc., Chem. Commun.* **1982**, 1400.
21 J.P. Mahy, G. Bedi, P. Battioni, D. Mansuy, *Tetrahedron Lett.* **1988**, *29*, 1927.
22 J.-P. Mahy, G. Bedi, P. Battioni, D. Mansuy, *New J. Chem.* **1989**, *13*, 651.
23 D. Mansuy, *Pure Appl. Chem.* **1990**, *62*, 741.
24 D. Mansuy, *Coord. Chem. Rev.* **1993**, *125*, 129.
25 R. Breslow, S.H. Gellman, *J. Am. Chem. Soc.* **1983**, *105*, 6728.
26 M.P. Doyle, M.A. McKervey, T. Ye, *Modern Catalytic Methods for Organic Synthesis with Diazo Compounds: From Cyclopropanes to Ylides*, John Wiley and Sons, New York, **1998**.
27 J.-P. Mahy, G. Bedi, P. Battioni, D. Mansuy, *J. Chem. Soc., Perkin Trans. 2* **1988**, 1517.
28 G.F. Koser in *Topics in Current Chemistry Vol. 224* (Ed.: T. Wirth), Springer-Verlag, Heidelberg, **2002**, pp. 137–172.
29 V.V. Zhdankin, P.J. Stang, *Chem. Rev.* **2002**, *102*, 2523.
30 D.A. Evans, M.M. Faul, M.T. Bilodeau, *J. Am. Chem. Soc.* **1994**, *116*, 2742.
31 E.N. Jacobsen in *Comprehensive Asymmetric Catalysis Vol. 2* (Ed.: E.N. Jacobsen, A. Pfaltz, H. Yamamoto), Springer-Verlag, Berlin, **1999**, pp. 607–618.
32 D.P. Albone, P.S. Aujla, P.C. Taylor, S. Challenger, A.M. Derrick, *J. Org. Chem.* **1998**, *63*, 9569.
33 P. Brandt, M.J. Södergren, P.G. Andersson, P.-O. Norrby, *J. Am. Chem. Soc.* **2000**, *122*, 8013.
34 P. Müller, C. Baud, I. Nägeli, *J. Phys. Org. Chem.* **1998**, *11*, 597.
35 I. Nägeli, C. Baud, G. Bernardinelli, Y. Jacquier, M. Moran, P. Müller, *Helv. Chim. Acta* **1997**, *80*, 1087.
36 P. Müller, C. Baud, Y. Jacquier, M. Moran, I. Nägeli, *J. Phys. Org. Chem.* **1996**, *9*, 341.
37 E. Nakamura, N. Yoshikai, M. Yamanaka, *J. Am. Chem. Soc.* **2002**, *124*, 7181.
38 M.P. Doyle, T. Ren in *Prog. Inorg. Chem. Vol. 49* (Ed.: K.D. Karlin), John Wiley & Sons, New York, **2001**, pp. 113–168.
39 G. Smolinsky, B.I. Feuer, *J. Am. Chem. Soc.* **1964**, *86*, 3085.
40 S. Terashima, S.-I. Yamada, *Chem. Pharm. Bull.* **1968**, *16*, 1953.
41 M. Newcomb, *Tetrahedron* **1993**, *49*, 1151.
42 M. Newcomb, P.H. Toy, *Acc. Chem. Res.* **2000**, *33*, 449.
43 M.-H. Baik, M. Newcomb, R.A. Friesner, S. J. Lippard, *Chem. Rev.* **2003**, *103*, 2385.
44 W. Lwowski, T.J. Maricich, *J. Am. Chem. Soc.* **1965**, *87*, 3630.
45 I.H. Williams, *Chem. Soc. Rev.* **1993**, *22*, 277.
46 H.M.L. Davies, R.E.J. Beckwith, *Chem. Rev.* **2003**, *103*, 2861.
47 C.A. Merlic, A.L. Zechman, *Synthesis* **2003**, 1137.
48 H. Lebel, J.-F. Marcoux, C. Molinaro, A.B. Charette, *Chem. Rev.* **2003**, *103*, 977.
49 M. Yamawaki, H. Tsutsui, S. Kitagaki, M. Anada, S. Hashimoto, *Tetrahedron Lett.* **2002**, *43*, 9561.
50 S.-M. Au, S.-B. Zhang, W.-H. Fung, W.-Y. Yu, C.-M. Che, K.-K. Cheung, *Chem. Commun.* **1998**, 2677.
51 S.-M. Au, J.-S. Huang, C.-M. Che, W.-Y. Yu, *J. Org. Chem.* **2000**, *65*, 7858.
52 Y. Kohmura, T. Katsuki, *Tetrahedron Lett.* **2001**, *42*, 3339.
53 M. M. Díaz-Requejo, T. R. Belderraín, M.C. Nicasio, S. Trofimenko, P.J. Pérez, *J. Am. Chem. Soc.* **2003**, *125*, 12 078.
54 J.-L. Liang, J.-S. Huang, X.-Q. Yu, N. Zhu, C.-M. Che, *Chem. Eur. J.* **2002**, *8*, 1563.
55 S.-M. Au, J.-S. Huang, W.-Y. Yu, W.-H. Fung, C.-M. Che, *J. Am. Chem. Soc.* **1999**, *121*, 9120.

56 X.-Q. Yu, J.-S. Huang, X.-G. Zhou, C.-M. Che, *Org. Lett.* **2000**, *2*, 2233.

57 C.G. Espino, J. Du Bois, *Angew. Chem. Int. Ed. Engl.* **2001**, *40*, 598.

58 J. Yang, R. Weinberg, R. Breslow, *Chem. Commun.* **2000**, 531.

59 J.-L. Liang, S.-X. Yuan, P.W.H. Chan, C.-M. Che, *Org. Lett.* **2002**, *4*, 4507.

60 M.C. Pirrung, H. Liu, A.T.J. Morehead, *J. Am. Chem. Soc.* **2002**, *124*, 1014.

61 G. Stork, K. Nakatani, *Tetrahedron Lett.* **1988**, *29*, 2283.

62 J.A. Ellman, T.D. Owens, T.P. Tang, *Acc. Chem. Res.* **2002**, *35*, 9845.

63 A. G. Steinig, D.M. Spero, *Org. Prep. Proced. Int.* **2000**, *32*, 205.

64 S. Kobayashi, H. Ishitani, *Chem. Rev.* **1999**, *99*, 1069.

65 D. Enders, U. Reinhold, *Tetrahedron: Asymmetry* **1997**, *8*, 1895.

66 S.-i. Hashimoto, N. Watanabe, S. Ikegami, *Tetrahedron Lett.* **1992**, *33*, 2709.

67 M.P. Doyle, A.B. Dyatkin, C.L. Autry, *J. Chem. Soc., Perkin Trans. 1* **1995**, 619.

68 C.G. Espino, P.M. Wehn, J. Chow, J. Du Bois, *J. Am. Chem. Soc.* **2001**, *123*, 6935.

69 K. Guthikonda, J. Du Bois, *J. Am. Chem. Soc.* **2002**, *124*, 13672.

70 J.W. Timberlake, W.J. Ray, Jr., E.D. Stevens, C.L. Klein, *J. Org. Chem.* **1989**, *54*, 5824.

71 M. Okada, S. Iwashita, N. Koizumi, *Tetrahedron Lett.* **2000**, *41*, 7047.

72 P. Gritsonie, M. Pilkington, J.D. Wallis, D.C. Povey, *Acta Crystallogr., Sect. C: Cryst. Struct. Commun.* **1994**, *C50*, 763.

73 B.E. Maryanoff, M.J. Costanzo, S.O. Nortey, M.N. Greco, R.P. Shank, J.J. Schupsky, M.P. Ortegon, J.L. Vaught, *J. Med. Chem.* **1998**, *41*, 1315.

74 P.M. Wehn, J. Lee, J. Du Bois, *Org. Lett.* **2003**, *5*, 4823.

75 K.W. Fiori, J. Du Bois, unpublished results.

76 P. Wang, J. Adams, *J. Am. Chem. Soc.* **1994**, *116*, 3296.

77 D.M. Spero, J. Adams, *Tetrahedron Lett.* **1992**, *33*, 1143.

78 H.M.L. Davies, T. Hansen, M.R. Churchill, *J. Am. Chem. Soc.* **2000**, *122*, 3063.

79 W.N. Speckamp, M.J. Moolenaar, *Tetrahedron* **2000**, *56*, 3817.

80 J.J. Fleming, K.W. Fiori, J. Du Bois, *J. Am. Chem. Soc.* **2003**, *125*, 2028.

81 K.W. Fiori, J.J. Fleming, J. Du Bois, *Angew. Chem. Int. Ed. Engl.* **2004**, *43*, 4349.

82 R.V. Stevens, *Acc. Chem. Res.* **1984**, *17*, 289.

83 N.T. Ahn, O. Eisenstein, *Tetrahedron Lett.* **1976**, 155.

84 Y. Iso, T. Irie, T. Iwaki, M. Kii, Y. Sendo, K. Motokawa, Y. Nishitani, *J. Antibiot.* **1996**, *49*, 478.

85 C. G. Espino, J. Du Bois, unpublished results.

86 V.J. Arán, P. Goya, C. Ochoa in *Advances in Heterocyclic Chemistry Vol. 44* (Ed.: A.R. Katritzky), **1988**, pp. 81–197.

87 A. Casini, A. Scozzafava, C.T. Supuran, *Expert Opin. Ther. Patents* **2002**, *12*, 1307.

88 Z. Régania, J.-Y. Winum, F.-Z. Smaine, L. Toupet, N.-E. Aouf, J.-L. Montero, *Tetrahedron* **2003**, *59*, 6051.

89 K.C. Nicolaou, D.A. Longbottom, S.A. Snyder, A.Z. Nalbanadian, X. Huang, *Angew. Chem. Int. Ed.* **2002**, *41*, 3866.

90 P. Dauban, R.H. Dodd, *Org. Lett.* **2000**, *2*, 2327.

91 C.M. Older, J. Du Bois, unpublished results.

92 Z. Liu, Y. Takeuchi, *Heterocycles* **2002**, *56*, 693.

93 E. Levites-Agababa, E. Menhaji, L.N. Perlson, C. M. Rojas, *Org. Lett.* **2002**, *4*, 863.

94 P. Dauban, L. Sanière, A. Tarrade, R.H. Dodd, *J. Am. Chem. Soc.* **2001**, *123*, 7707.

95 A. Padwa, T. Stengel, *Org. Lett.* **2002**, *4*, 2137.

96 F. Duran, L. Leman, A. Ghini, G. Burton, P. Dauban, R.H. Dodd, *Org. Lett.* **2002**, *4*, 2481.

97 J.-L. Liang, S.-X. Yuan, P.W.H. Chan, C.-M. Che, *Tetrahedron Lett.* **2003**, *44*, 5917.

98 J.-L. Liang, S.-X. Yuan, J.-S. Huang, W.-Y. Yu, C.-M. Che, *Angew. Chem., Int. Ed.* **2002**, *41*, 3465.

99 C.G. Espino, B.H. Brodsky, J. Du Bois, in preparation.

100 M. Newcomb, C.C. Johnson, M.B. Manek, T.R. Varick, *J. Am. Chem. Soc.* **1992**, *114*, 10915.

101 B.H. Brodsky, J. Du Bois, unpublished results.

102 T.R. Felthouse, *Prog. Inorg. Chem.* **1982**, *29*, 73.

103 A.L. Sargent, M.E. Rollog, C.T. Eagle, *Theor. Chem. Acc.* **1997**, *97*, 283.

104 M.C. Pirrung, A.T.J. Morehead, *J. Am. Chem. Soc.* **1994**, *116*, 8991.

105 S.M. Sheehan, A. Padwa, J.P. Snyder, *Tetrahedron Lett.* **1998**, *39*, 949.

106 A.O. Chong, K. Oshima, K.B. Sharpless, *J. Am. Chem. Soc.* **1977**, *99*, 3420.

107 M. Bruncko, T.-A.V. Khuong, K. B. Sharpless, *Angew. Chem., Int. Ed. Engl.* **1996**, *35*, 454.

108 K. Muiz, M. Nieger, *Synlett* **2003**, 211.

109 G. Li, H.-X. Wei, S.H. Kim, M.D. Carducci, *Angew. Chem. Int. Ed.* **2001**, *40*, 4277.

110 H.-X. Wei, S.H. Kim, G. Li, *J. Org. Chem.* **2002**, *67*, 4777.

111 D. Chen, C. Timmons, H.-X. Wei, G. Li, *J. Org. Chem.* **2003**, *68*, 5742.

112 J. Du Bois, C.S. Tomooka, J. Hong, E.M. Carreira, *J. Am. Chem. Soc.* **1997**, *119*, 3179.

113 J. Du Bois, C.S. Tomooka, J. Hong, E.M. Carreira, *Acc. Chem. Res.* **1997**, *30*, 364.

114 B.M. Trost, J.L. Gunzner, O. Dirat, Y.H. Rhee, *J. Am. Chem. Soc.* **2002**, *124*, 10396.

115 H. Huang, J.S. Panek, *Org. Lett.* **2003**, *5*, 1991.

116 K.A. Parker, W. Chang, *Org. Lett.* **2003**, *5*, 3891.

117 A. Hinman, J. Du Bois, *J. Am. Chem. Soc.* **2003**, *125*, 11510.

118 Y. Gao, K.B. Sharpless, *J. Am. Chem. Soc.* **1988**, *110*, 7538.

119 H.-S. Byun, L. He, R. Bittman, *Tetrahedron* **2000**, *56*, 7051.

120 B. Lohray, V. Bhushan in *Advances in Heterocyclic Chemistry Vol. 68* (Ed.: A.R. Katritzky), Academic Group, San Diego, **1997**, pp. 89–180.

121 R.E. Meléndez, W.D. Lubell, *Tetrahedron* **2003**, *59*, 2581.

122 T.A. Lyle, C.A. Magill, S.M. Pitzenberger, *J. Am. Chem. Soc.* **1987**, *109*, 7890.

123 N. Meunier, U. Veith, V. Jäger, *Chem. Commun.* **1996**, 331.

124 M. Atfani, L. Wei, W. D. Lubell, *Org. Lett.* **2001**, *3*, 2965.

125 P.M. Wehn, J. Du Bois, in preparation.

126 P.M. Wehn, J. Du Bois, *J. Am. Chem. Soc.* **2002**, *124*, 12950.

18
Rearrangement Processes of Oxonium and Ammonium Ylides Formed by Rhodium(II)-Catalyzed Carbene Transfer

Frederick G. West

18.1
Introduction

Rhodium(II) carboxylate dimers and their carboxamide counterparts have been demonstrated to be exceptionally useful catalysts for carbene transfer processes involving diazocarbonyl substrates [1]. Doyle's seminal work identified $Rh_2(OAc)_4$ as the catalyst of choice for a variety of cyclopropanation, C–H insertion, and ylide rearrangement transformations using diazoketones or diazoesters [2]. Important contributions by Taber [3], Padwa [4], and Davies [5] further established the superior catalytic activity of dirhodium catalysts and the excellent selectivity of rhodium–carbenes.

Pirrung and Johnson published back-to-back articles in 1986, describing the use of $Rh_2(OAc)_4$ for the generation of cyclic oxonium ylides by way of an intramolecular addition of electron-deficient rhodium carbenes to pendant ethers (Scheme 18.1) [6]. If a suitable group was attached to the resulting oxonium oxygen, efficient rearrangement by a [2,3]- or [1,2]-shift occurred, affording either cyclic ethers **1** or ring-contracted cyclobutanones **2** respectively. In contrast to ammonium or sulfonium ylides, oxonium ylides are not easily formed by stepwise alkylation/deprotonation methods due to facile dealkylation of the intermediate oxonium salts. Thus, direct generation from carbenoid precursors offers the only viable way to access these highly reactive species. Prior work had demonstrated that transient oxonium ylides could be formed from ethers with subsequent rearrangement, by utilizing free carbenes generated thermally [7] or photochemically [8]. Alternatively, the analogous transformation could be accomplished using the metal carbene produced with the requisite copper catalyst [9]. The importance of the Pirrung and Johnson results lay in the mildness of the reaction conditions and the generally high yields of the overall process. Subsequently, Padwa also described the efficient generation and [2,3]-shift of an oxonium ylide under $Rh_2(OAc)_4$ catalysis [10].

Around the same time, our group became interested in exploring the [1,2]-shift chemistry of oxonium ylides and the related ammonium ylides. The Stevens [1,2]-shift is a mechanistically fascinating process [11] (Scheme 18.2), in which orbital symmetry considerations forbid a direct concerted rearrangement. Nonetheless, the observation of partial retention of configuration by chiral migrating centers offered some support for a concerted mechanism. Stevens favored a stepwise ion-pair mechanism, and solvent polarity effects on the reaction rate seemed to support this postulate [12]. However, careful work by the Ollis group throughout the 1970s and 1980s established

Modern Rhodium-Catalyzed Organic Reactions. Edited by P. Andrew Evans

ISBN: 3-527-30683-8

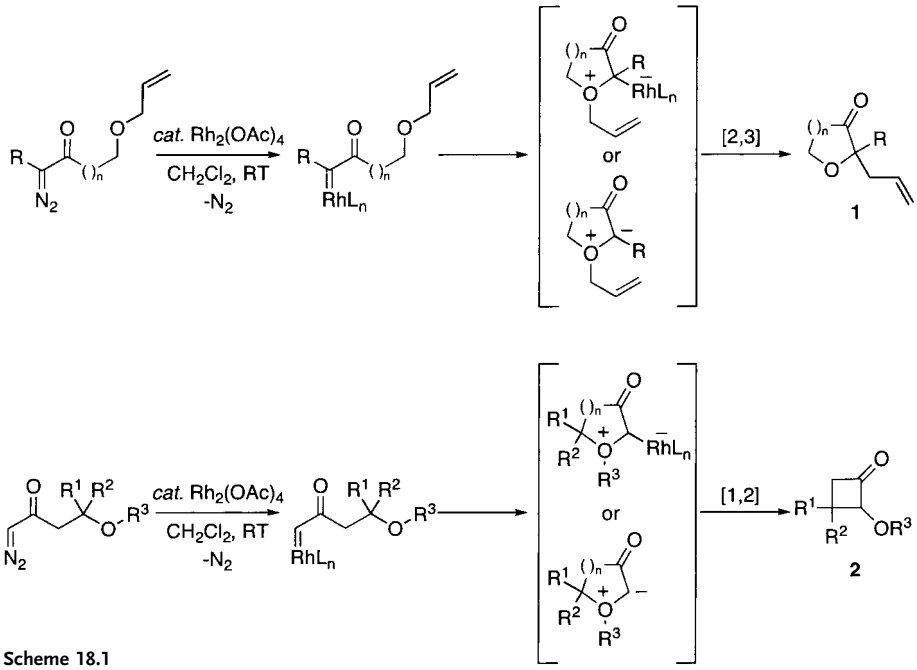

Scheme 18.1

Concerted Mechanism:

Stepwise Mechanism (Ion Pair):

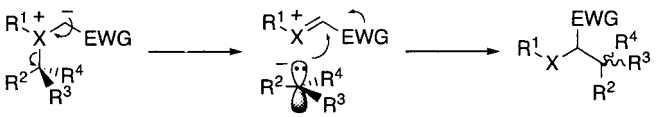

Stepwise Mechanism (Radical Pair):

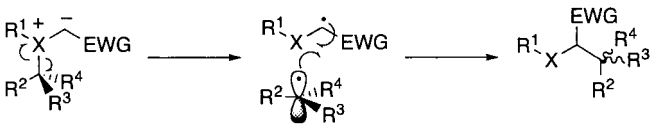

(X = O, S or NR)

Scheme 18.2

strong evidence for stepwise rearrangement *via radical pair* intermediates in the case of ammonium ylides [13]. Of course, these studies were carried out using standard quaternization/deprotonation conditions. Ylides generated by transition metal catalysis might follow a different course, and the intervention of a metal-associated ylide (as indicated in Scheme 18.1) could not be ruled out. Indeed, Roskamp and Johnson proposed a mechanism involving participation of a C–Rh bond for the formation of cyclobutanones **2** from five-membered oxonium ylides [6b]. Regardless of the mechanistic subtleties, use of metal-catalyzed carbene transfer methodology was attractive from a pragmatic perspective as mild conditions should permit greater selectivity, and direct ylide generation removed any ambiguity as to the site of the ylide carbon (in contrast to deprotonation of onium salts).

18.2 Oxonium Ylides

Initial efforts focused on the generation of oxonium ylides possessing migrating groups deemed capable of undergoing a [1,2]-shift (Scheme 18.3) [14]. A series of benzyl ethers **3a–3f** possessing pendant diazoketones were prepared and subjected to the standard conditions for $Rh_2(OAc)_4$-mediated carbene transfer (Scheme 18.3). In the event, we found that moderate to good yields of cyclic ether products **4a–4e** could be realized from the corresponding diazoketones. In contrast to 4-benzyloxy-1-diazobutan-2-ones **3a–3c**, the homologous substrate **3f** furnished very little of the corresponding pyranone product **4f**; instead, cyclopentanone **5** was the major product, resulting from an alternative C–H insertion process. This outcome is not unexpected, given the high reactivity of C–H bonds adjacent to alkoxy groups toward insertion processes with rhodium–carbenes [15]. Importantly, a phenacyl group also underwent migration (**3g→4g**), demonstrating that this process was not limited to benzyl migrating groups, although the yield was disappointing. An additional important observation was the isolation in several cases of dimeric products **6** and **7**, providing strong evidence for at least some partitioning *via* a radical-pair mechanism.

Subsequent work employed substrates **i** in which the ether oxygen was constrained within a pre-existing ring (Scheme 18.4) [16]. This variation results in the formation of an intermediate fused bicyclic oxonium ylide **iii**. With the appropriate choice of substituents adjacent to the ether oxygen, such an ylide would be expected to undergo [1,2]-shift to give a bridged bicyclic product **iv**. As a consequence of this transformation, the outer carbon periphery would be spliced together, affording a medium-sized carbocycle from the starting heterocyclic scaffold. The bridging ether in such products could then serve as a suitable precursor to sites of oxygenation around the carbocyclic ring, offering a convenient entry to functionalized medium-ring carbocycles.

The phenyl-substituted substrates **8a–8d** were prepared from the corresponding lactones and subjected to catalytic $Rh_2(OAc)_4$ (Scheme 18.5). Diastereomeric tetrahydrofurans **8a**, **8b** underwent conversion to the ether-bridged cycloheptanones **11a**, **11b** in good yield, in which each diastereomer afforded both products in varying ratios. This result is consistent with the intervention of intermediate biradicals **10** which undergo partial stereochemical randomization. Importantly, both **8a** and **8b** showed net retention of configuration by the migrating center, indicating that the rate of radical recom-

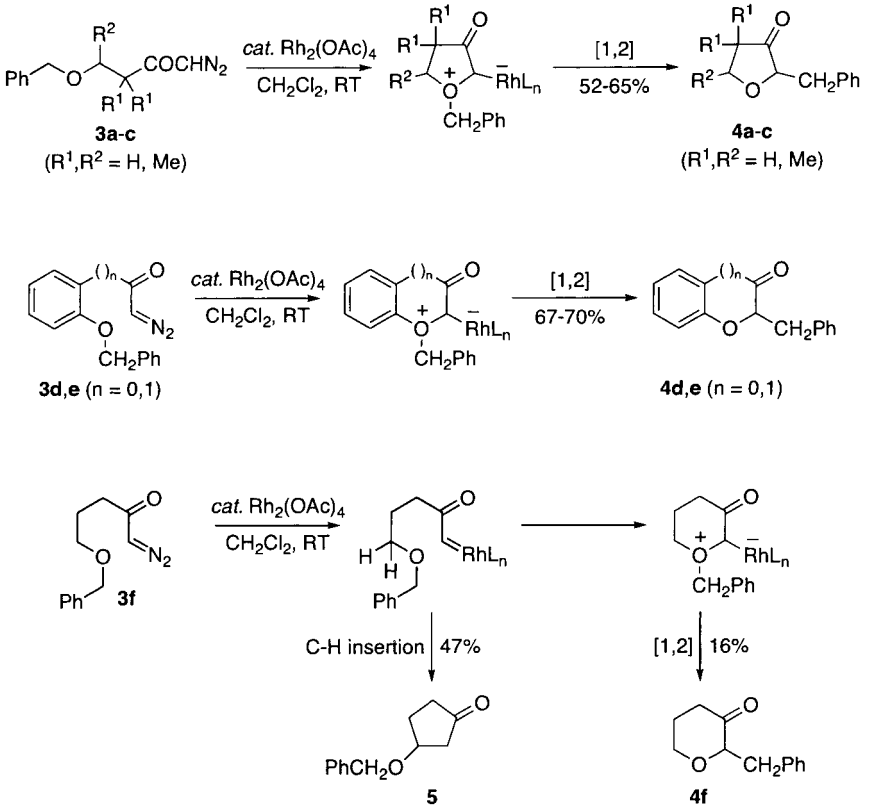

Scheme 18.3

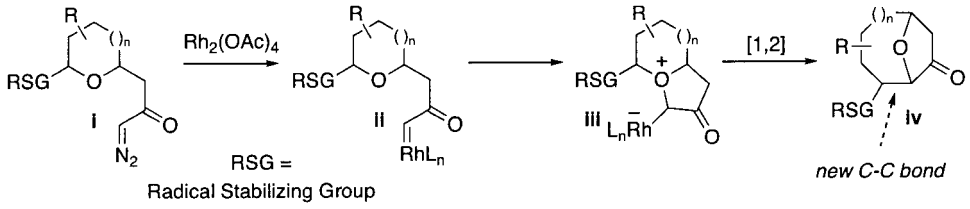

Scheme 18.4

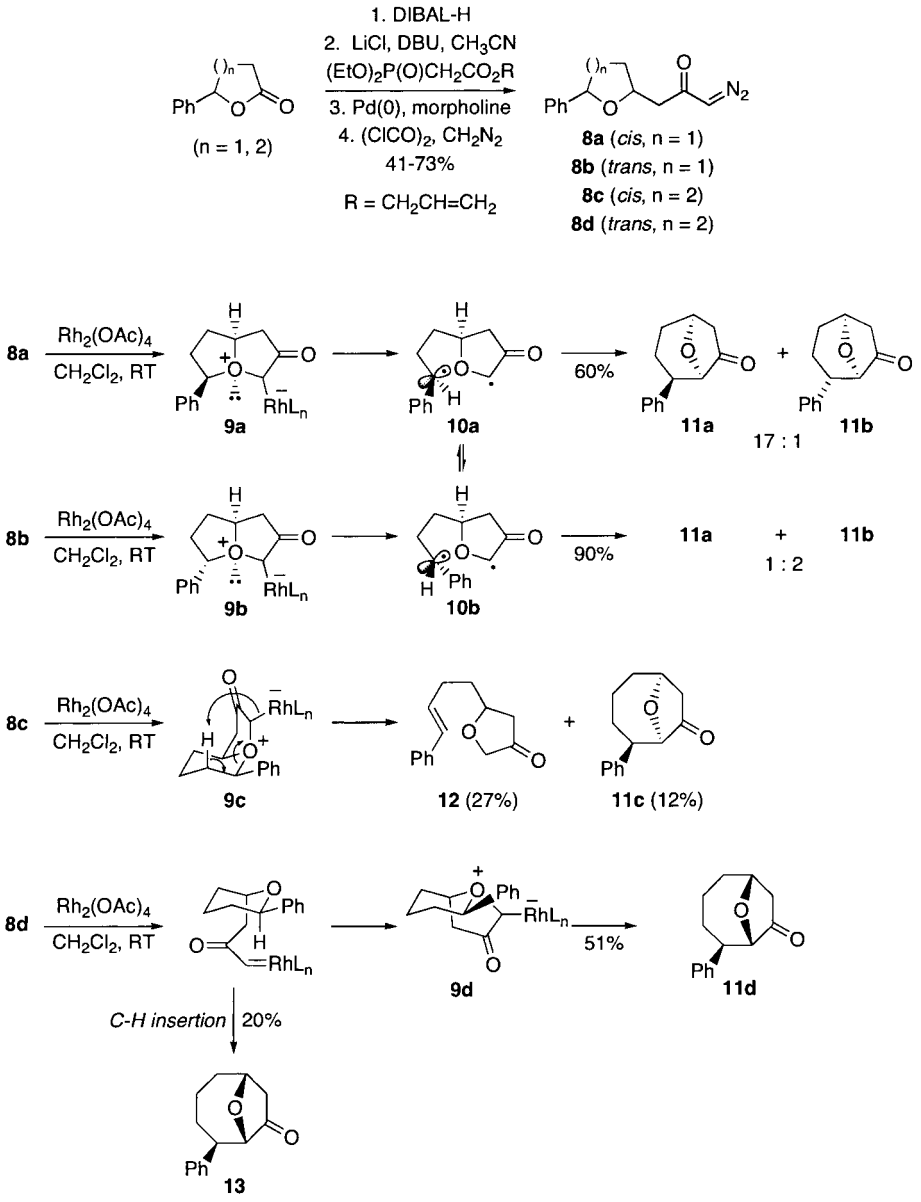

Scheme 18.5

bination is comparable to that of bond rotation. Tetrahydropyran substrates **8c**, **8d** showed much greater mechanistic diversity than **8a**, **8b**. The *cis*-diastereomer **8c** furnished only small amounts of cyclooctanone **11c**. Among a plethora of side products, the major component proved to be furanone **12**, which may arise from an alternative α',β-fragmentation pathway for ylide **9c**, although disproportionation of radical-pair **10c** is also possible. The *trans*-diastereomer **8d** afforded greater quantities of the desired [1,2]-shift product **11d**, along with the isomeric cyclooctanone **13**. This product is

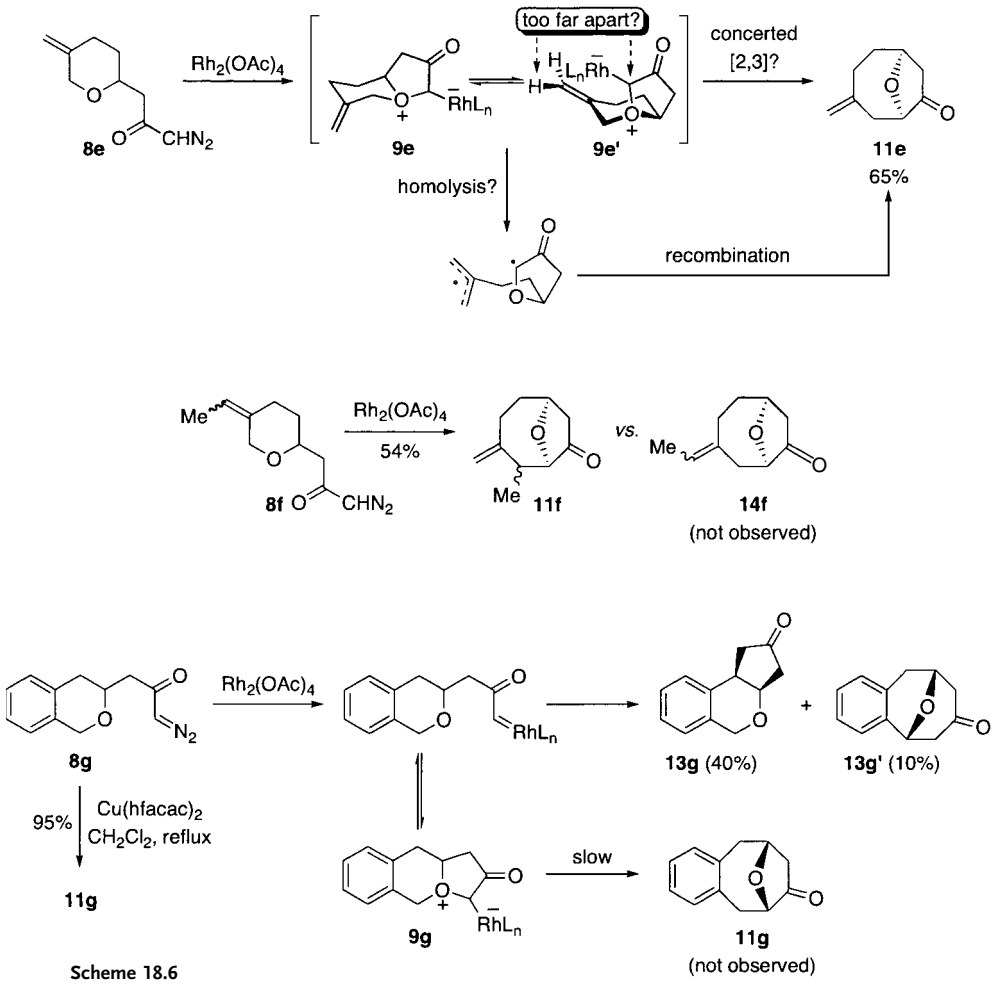

Scheme 18.6

presumed to be the result of a competing transannular C–H insertion by the initially formed rhodium–carbene. The stereospecific reactivity seen with **8c**, **8d** presumably arises as a consequence of the conformational preferences of the two diastereomers. In the case of **8c**, a diequatorial disposition of the two substituents assures delivery of the metallocarbene to the axial lone pair, resulting in fused bicyclic ylide **9c**, in which the fragmentation is permitted by the proximity of the basic ylide carbon with the *β*-proton. The *trans*-isomer **8d** can exist in one of two roughly equivalent conformers. Axial disposition of the carbene-containing side chain leads to ylide **9d** that is incapable of undergoing a fragmentation process analogous to that seen with **9c**; however, this conformation does permit the transannular C–H insertion, as observed. It is interesting to note that [1,2]-shift products **11c**, **11d** were formed with complete stereoselectivity.

Allyl ether substrate **8e** was also examined and found to undergo efficient conversion to cyclooctanone **11e** (Scheme 18.6). In this case there was some ambiguity as to whether the reaction occurs via a stepwise [1,2]- or concerted [2,3]-shift. Examination of

models of the putative ylide intermediate **9e** suggested that the separation of the termini might be too great to permit the concerted process [17]. Allylic stabilization of the intermediate radical-pair should make the alternative mechanism involving a [1,2]-shift energetically feasible. To clarify this question, ethylidene homolog **8f** was prepared and subjected to the standard reaction conditions. In this case, *only* the diastereomeric cyclooctanone **11f** was isolated, with none of the isomeric **14f** being observed. Complete allylic inversion in this case argues strongly for a concerted rearrangement *via* the [2,3]-shift mechanism. The benzo-fused substrate **8g** did not furnish any of the expected [1,2]-shift product **11g**, giving instead C–H insertion products **13g** and **13g′**. It was speculated that homolytic cleavage of ylide **9g** might be slow due to poor benzylic overlap, thereby permitting reversion to the metallocarbene and preferential reaction *via* that intermediate. Evidence for equilibration between ylide and carbene intermediates has been observed in related examples [18]. It is notable that the same substrate was converted to **11g** in near-quantitative yield using $Cu(hfacac)_2$ as the carbene transfer catalyst, suggesting a fundamental difference in the reactivity of rhodium- and copper-derived oxonium ylides [19].

Cyclic acetals could be subjected to a similar sequence to furnish O-bridged medium-sized cyclic ethers (Scheme 18.7) [20]. The necessary substrates were readily prepared from the corresponding 1,2- and 1,3-diol precursors. Given their close analogy to ethers **8a–8d**, it was not surprising that benzylidene acetals **15a–15c** underwent efficient ring-expansion to **16a–16c**. Interestingly, the stereochemical outcome was different in this case as **16a** predominated regardless of whether starting diazoketone **15a** or **15b** was used. This suggests that the diastereoselectivity is derived from an inherent kinetic preference for recombination of the intermediate. In other words, in these cases C–C bond formation is slow relative to bond rotation, allowing partial or complete erosion of the starting stereochemical information at the migrating center. The corresponding acetonides **15d**, **15e** also rearranged to **16d**, **16e**. This result was notable, as it was the first example of an efficient [1,2]-shift by a migrating group devoid of any conjugative stabilization. Apparently, the combination of geminal dimethyl substitution and the electron-donating oxygen confers sufficient stability to permit formation of a radical center at the acetonide carbon. The importance of the acetonide methyl groups was supported by the fact that the methylene acetal **15f** gave none of the desired product **16f**. It must be acknowledged, however, that an alternative heterolytic mechanism *via* ion pair **17** cannot be discounted on the basis of current evidence. The issue of competing C–H insertion adjacent to oxygen was seen in the case of **15d**, which gave comparable amounts of **16d** and cyclopentanone **18**. Catalysis with $Cu(hfacac)_2$ led to greatly improved yields of ylide-derived product **16d**.

Most recently, we have investigated the use of iterative oxonium ylide [1,2]- or [2,3]-shifts as a convenient approach to the polypyran domains often found in the marine polyether ladder toxins (Scheme 18.8) [21]. Initial studies indicated that [1,2]-shifts of *O*-benzyl oxonium ylides such as **19a** or **19b** were inefficient. Alternative metallocarbene processes including C–H insertion and dimerization were found to predominate in these cases, again suggesting that carbene–ylide equilibration may occur [21b]. On the rationale that concerted [2,3]-shifts of the corresponding *O*-allyl oxonium ylides might occur more readily, the allyl ethers **19c**, **19d** were then examined. These examples were much more effective, especially in conjunction with the optimized catalyst $Cu(tfacac)_2$ [21a]. However, rhodium(II) triphenylacetate ($Rh_2(tpa)_4$) [22] was found to

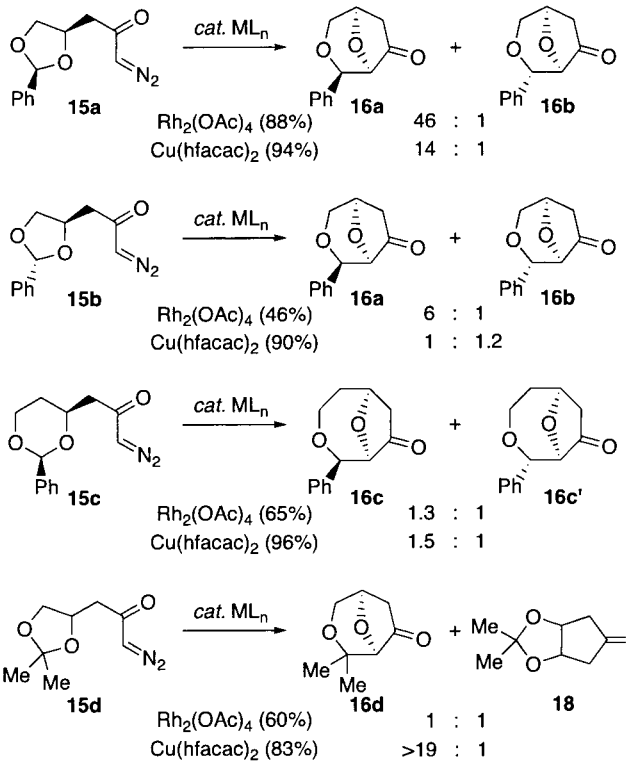
cat. ML_n
15a
16a
16b
$Rh_2(OAc)_4$ (88%) 46 : 1
$Cu(hfacac)_2$ (94%) 14 : 1
15b
$Rh_2(OAc)_4$ (46%) 6 : 1
$Cu(hfacac)_2$ (90%) 1 : 1.2
15c
16c
16c'
$Rh_2(OAc)_4$ (65%) 1.3 : 1
$Cu(hfacac)_2$ (96%) 1.5 : 1
15d
16d
18
$Rh_2(OAc)_4$ (60%) 1 : 1
$Cu(hfacac)_2$ (83%) >19 : 1

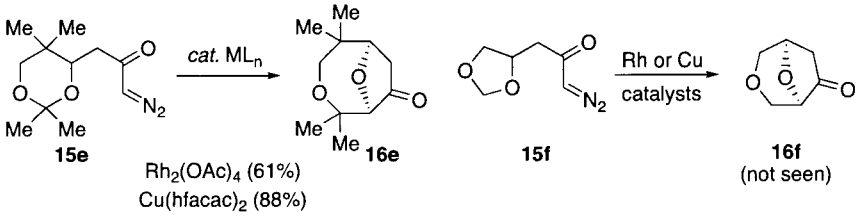
cat. ML_n
15e
16e
$Rh_2(OAc)_4$ (61%)
$Cu(hfacac)_2$ (88%)
15f
Rh or Cu
catalysts
16f
(not seen)

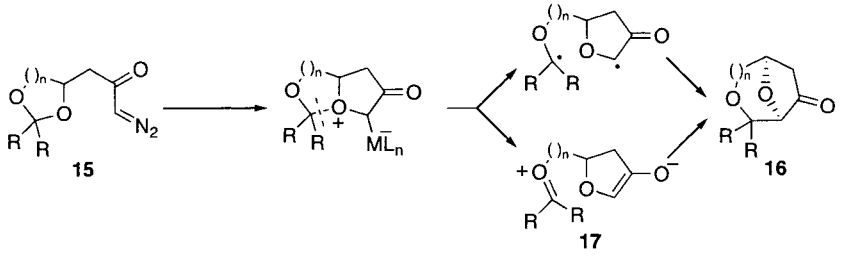
15
16
17

Scheme 18.7

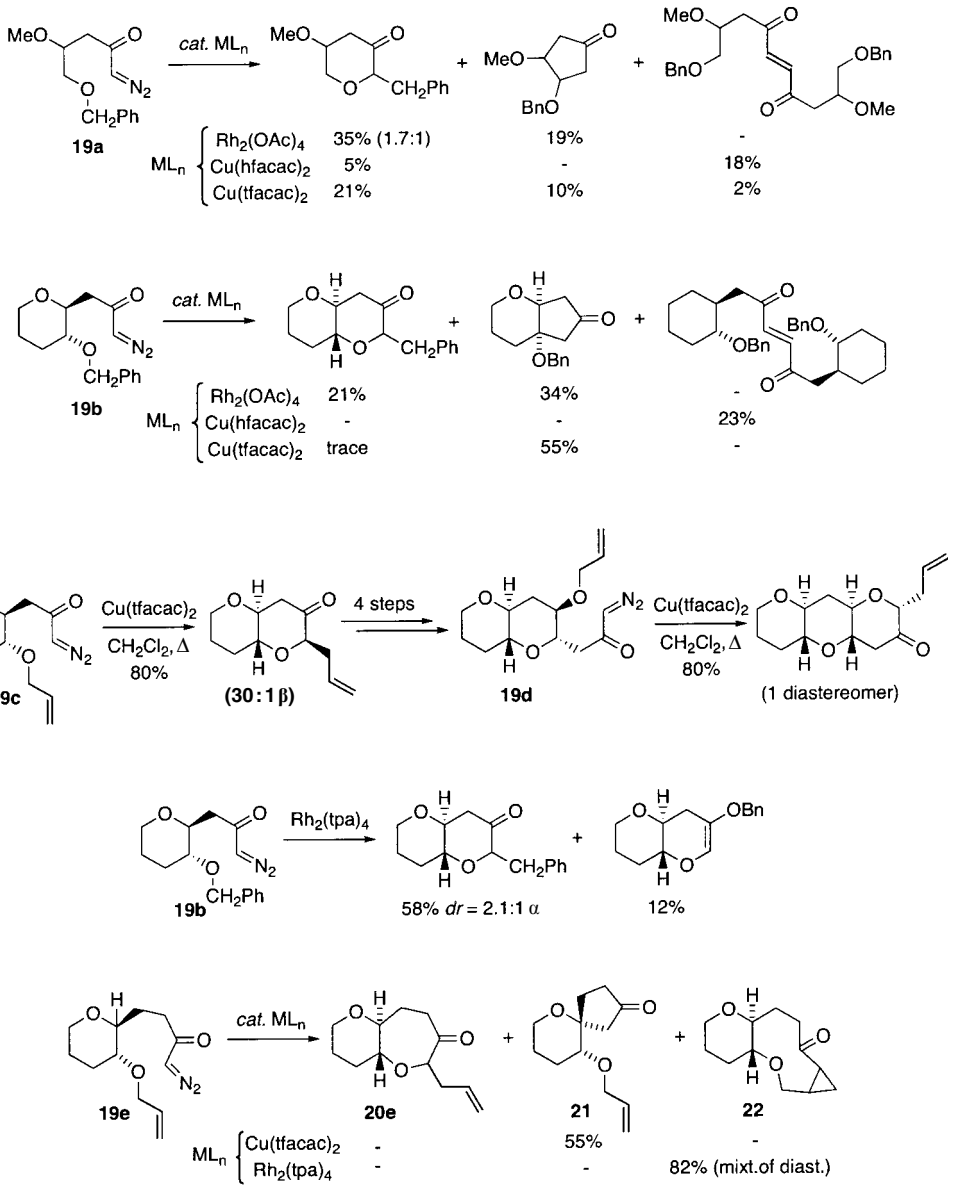

Scheme 18.8

be a highly effective catalyst for the [1,2]-shift of previously unreactive substrates such as **19b**. Homologous allyl ether substrate **19e** was also examined. Under the optimized $Cu(tfacac)_2$ conditions, this substrate had furnished spirocycle **21** instead of the desired oxepane [2,3]-shift product **20e**. With $Rh_2(tpa)_4$, a high yield of cyclopropane **22** was obtained. Cyclopropanation with concomitant generation of a nine-membered ring was quite surprising, and suggests that this catalyst may be especially suitable for metallocarbene reactions involving difficult medium and large ring-closures.

18.3
Ammonium Ylides

There was very little known about metallocarbene routes to ammonium ylides when we first began to explore the nitrogen variant of this chemistry. Doyle had demonstrated that $Rh_2(OAc)_4$ catalyzed the intermolecular addition of ethyl diazoacetate to an allylamine, with the resulting ammonium ylide undergoing a [2,3]-shift [2]. However, related work suggested that compounds containing a basic nitrogen could bind tightly to rhodium(II) carboxylate dimers, with a consequent loss of catalytic activity [23]. In fact, attempts to undertake the intermolecular addition of various diazocarbonyl compounds to simple tertiary amines failed under rhodium catalysis, necessitating the use of copper powder [24]. To our surprise, however, we found that a variety of *N*-benzyl-5-amino-1-diazopentan-2-ones **23a–e** could be efficiently converted to *N*-substituted piperidines **24a–e** in good to excellent yield, without resorting to high dilution or slow addition techniques (Scheme 18.9) [25]. Glycyl derivative **23f** also underwent clean rearrangement, as did diazo ester **23g** [26] and aromatic substrate **23h**. However, various homologues of **23** seemed to be prone to alternative reactivity (C–H insertion or ylide decomposition pathways) under these conditions. The soluble copper(II) catalyst $Cu(acac)_2$ was found to be superior in these cases [19]. Given the greater stability of ammonium ylides relative to their oxonium counterparts, involvement of a metal-associated ylide is considered less likely in these cases.

This methodology was applied to a concise synthesis of the alkaloid epilupinine (Scheme 18.10) [27]. *N*-alkylation of proline benzyl ester with bromo diazoketone **25** gave substrate **26**. Treatment with either $Rh_2(OAc)_4$ or various copper-based catalysts

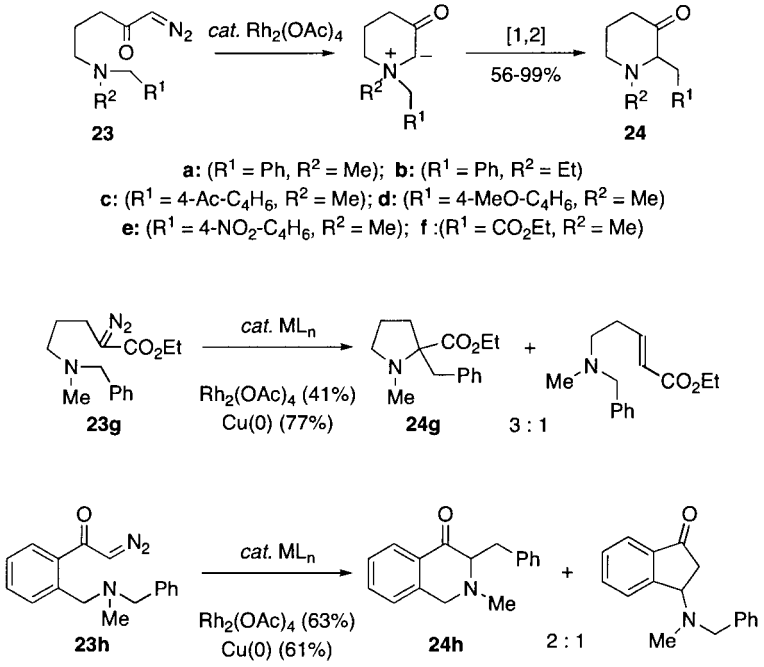

Scheme 18.9

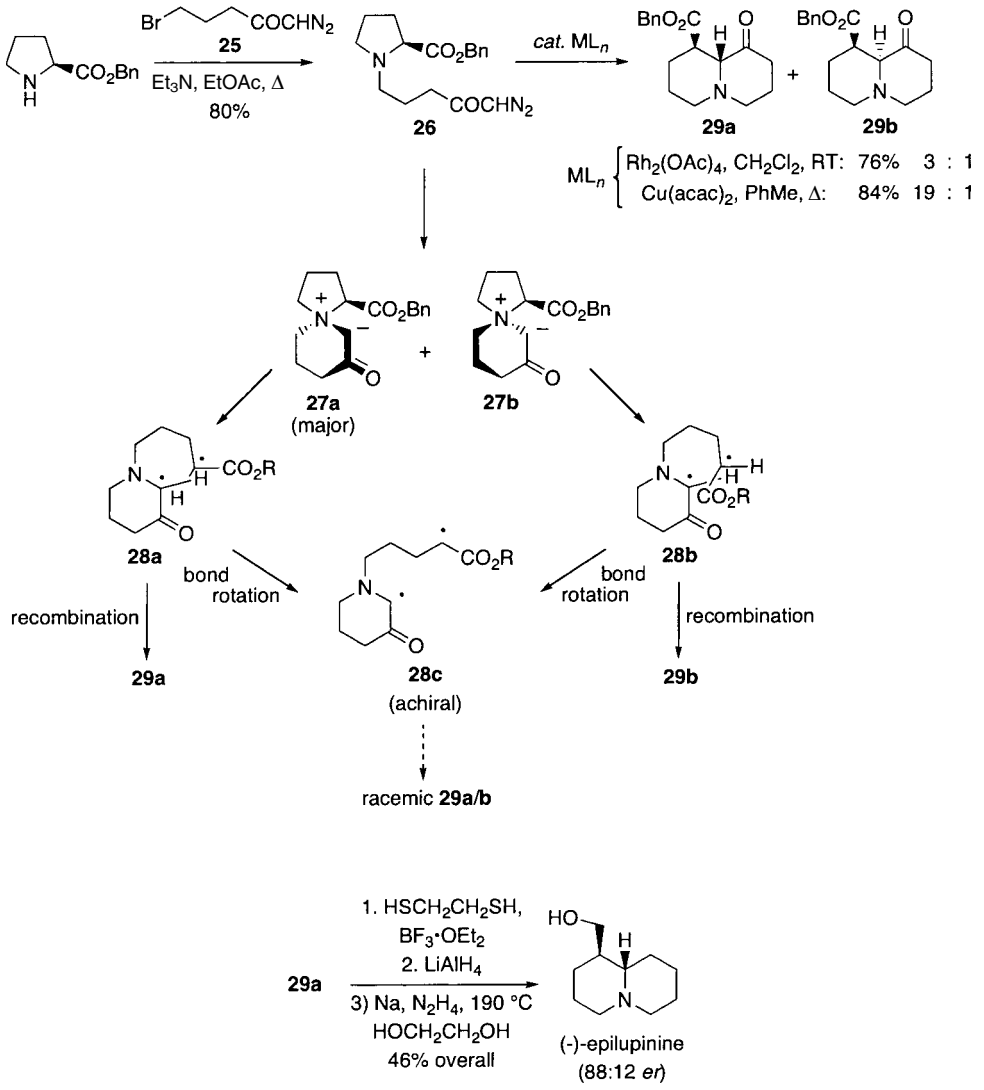

Scheme 18.10

afforded a mixture of diastereomeric quinolizidines **29a**/**29b** in good yield. Enantiomeric ratios of the major diastereomer **29a** of up to 88:12 indicated that the intermediate ylides underwent rearrangement mainly with retention of configuration. Had the intermediate biradical **28a** suffered complete randomization to achiral **28c**, a racemic mixture of products would have been formed. Thus, the diastereoselectivity of the major isomer arises from the preferential formation of the spirocyclic ylide **27a** over its diastereomer **27b**, followed by a [1,2]-shift with retention of configuration. Erosion of optical purity suggested a minor amount of randomization *via* **28c** was also occurring. A simple three-step reductive sequence then provided the natural product in five steps overall from the proline ester.

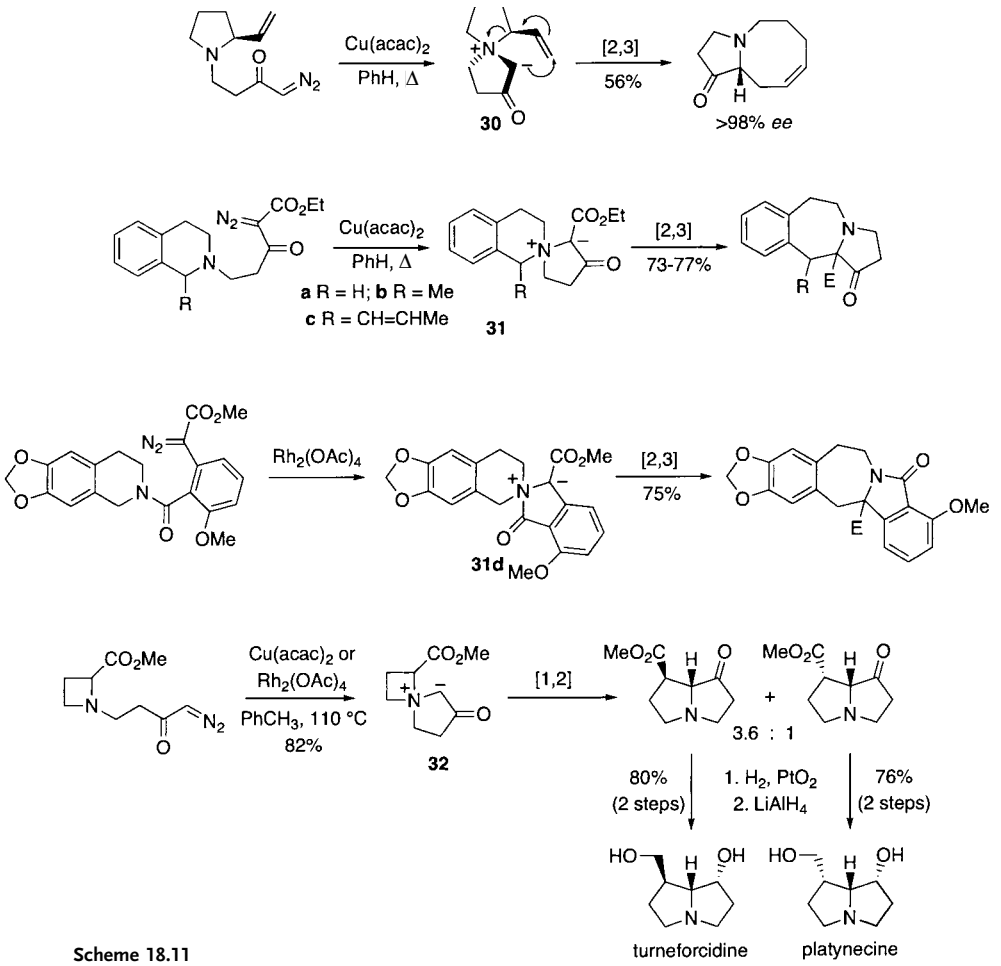

Scheme 18.11

More recent work with other ring sizes has allowed facile entry to indolizidines and related skeletons, by demonstrating that directing groups other than esters (for example, R_3Si) can be used in the [1,2]-shift step [28]. Related strategies were applied by Clark and Padwa, although catalysis was restricted in most cases to the soluble copper(II) salts (Scheme 18.11). Thus, Clark assembled the bicyclic core of the manzamines, via a highly stereospecific [2,3]-shift of the spirocyclic ammonium ylide **30** [29]. Padwa used the [1,2]-shift of spirocyclic ammonium ylides **31** in a clever and direct approach to the cephalotaxine and isoindolobenzazepine ring skeletons [30]. Smaller ring systems can also be prepared using this approach, as seen in our route to the pyrrolizidine alkaloids turneforcidine and platynecine *via* spirocyclic ylide **32**, which is generated from readily available azetidinecarboxylate [31].

18.4 Conclusion

Since Doyle's original reports in the 1980s concerning the use of $Rh_2(OAc)_4$ for catalyzing carbene transfer processes to generate transient ylides, a great deal has been learned regarding the scope and limitations of this methodology. Other ylide-mediated processes aside from the [1,2]- and [2,3]-shift processes discussed above have been developed [32]. The electronic effects arising from the bridging carboxylate or carboxamide ligands of rhodium dimers have been shown to significantly modulate the chemoselectivity of the intermediate metallocarbenes [33], and in some cases the subsequently formed ylides [34]. Perhaps most importantly, asymmetric catalysis in the formation and rearrangement of oxonium ylides has been achieved using various catalysts possessing enantiomerically pure bridging ligands [35]. Future work in this area ideally will add to our understanding of the importance of metal-associated ylides in the rearrangement processes and the exact role-played by the metal in facilitating [1,2]- or [2,3]-shift reactions. This in turn will permit the application of these strategically important transformations in increasingly complex systems en route to important target structures.

18.5 References

1 Reviews: (a) Doyle, M. P. *Chem. Rev.* **1986**, *86*, 919–939. (b) Adams, J.; Spero, D. M. *Tetrahedron* **1991**, *47*, 1765. (c) Padwa, A.; Krumpe, K. E. *Tetrahedron* **1992**, *48*, 5385. (d) Ye, T.; McKervey, M. A. *Chem. Rev.* **1994**, *94*, 1091. (e) Doyle, M. P.; Forbes, D. C. *Chem. Rev.* **1998**, *98*, 911. (f) For a comprehensive overview, see: Doyle, M. P.; McKervey, M. A.; Ye, T. *Modern Chemical Methods for Organic Synthesis with Diazo Compounds: From Cyclopropanes to Ylides*; John Wiley: New York; **1998**.

2 (a) Doyle, M. P.; Tamblyn, W. H.; Bagheri, V. *J. Org. Chem.* **1981**, *46*, 5094. (b) Doyle, M. P.; Griffin, J. H.; Chinn, M. S.; van Leusen, D. *J. Org. Chem.* **1984**, *49*, 1917. (c) See also: Paulissen, R.; Reimlinger, E.; Hayez, E.; Hubert, A. J.; Teyssié, P. *Tetrahedron Lett.* **1973**, 2233.

3 (a) Taber, D. F.; Petty, E. H. *J. Org. Chem.* **1982**, *47*, 4808. (b) Taber, D. F.; Ruckle, R. E. *J. Am. Chem. Soc.* **1986**, *108*, 7686. (c) Taber, D. F.; Stiriba, S. E. *Chem. Eur. J.* **1998**, *4*, 990. Review: (d) Sulikowski, G. A.; Cha, K. L.;Sulikowski, M. M. *Tetrahedron: Asymmetry* **1998**, *9*, 3145.

4 Reviews: (a) Padwa, A.; Hornbuckle, S. F. *Chem. Rev.* **1991**, *91*, 263. (b) Padwa, A.; Weingarten, M. D. *Chem. Rev.* **1996**, *96*, 223.

5 Reviews: (a) Davies, H. M. L. *Curr. Org. Chem.* **1998**, *2*, 463. (b) Davies, H. M. L. *J. Mol. Catal. A – Chem.* **2002**, *189*, 125.

6 a) Pirrung, M. P.; Werner, J. A. *J. Am. Chem. Soc.* **1986**, *108*, 6060. (b) Johnson, C. R.; Roskamp, E. J. *J. Am. Chem. Soc.* **1986**, *108*, 6062.

7 Iwamura, H.; Imahashi, Y.; Kushida, K. *Tetrahedron Lett.* **1975**, *16*, 1401.

8 (a) Ando, W.; Kondo, S.; Nakayama, K.; Ichibori, K.; Kohoda, H.; Yamato, H.; Imai, I.; Nakaido, S.; Migita, T. *J. Am. Chem. Soc.* 1972, *94*, 3870. (b) Friedrich, K.; Jansen, U.; Kirmse, W. *Tetrahedron Lett.* **1985**, *26*, 193. (c) Kirmse, W.; Chiem, P. V. *Tetrahedron Lett.* **1985**, *26*, 197.

9 Nozaki, H.; Takaya, H.; Moriuti, S.; Noyori, R. *Tetrahedron* 1968, *24*, 3655.

10 Padwa, A.; Hornbuckle, S. F.; Fryxell, G. E.; Stull, P. D. *J. Org. Chem.* **1989**, *54*, 817.

11 Reviews: (a) Pine, S. H. *Org. React. (N.Y.)* 1970, *18*, 403. (b) Lepley, A. R.; Giumanini, A. G. In *Mechanisms of Molecular Migrations,*

Thygarajan, B.S., Ed.; Interscience: New York, **1971**; Vol. 3, pp 297–440. (c) Markó, I.E. In *Comprehensive Organic Synthesis*; Trost, B.M.; Fleming, I., Eds.; Pergamon: Oxford, **1991**; Vol. 3, pp 913–973.

12 (a) Stevens, T.S.; Creighton, E.M.; Gordon, A.B.; MacNicol, M. *J. Chem. Soc.* 1928, 3193. (b) Stevens, T.S.; *J. Chem. Soc.* **1930**, 2107. (c) Thomson, T.; Stevens, T.S. *J. Chem. Soc.* **1932**, 55. (d) Dunn, J.L.; Stevens, T.S. *J. Chem. Soc.* **1932**, 1926. (e) Dunn, J.L.; Stevens, T.S. *J. Chem. Soc.* **1934**, 279.

13 Ollis, W.D.; Rey, M.; Sutherland, I.O. *J. Chem. Soc., Perkin Trans. 1* **1983**, 1009, and references therein.

14 Eberlein, T.H.; West, F.G.; Tester, R.W. *J. Org. Chem.* **1992**, *57*, 3479.

15 (a) Adams, J.; Poupart, M.A.; Grenier, L.; Schaller, C.; Ouimet, N.; Frenette, R. *Tetrahedron Lett.* **1989**, *30*, 1749. (b) Wang, P.; Adams, J. *J. Am. Chem. Soc.* **1994**, *116*, 3296. (c) Davies, H.M.L.; Antoulinakis, E.G.; Hansen, T. *Org. Lett.* **1999**, *1*, 383. (d) Davies, H.M.L.; Hansen, T.; Churchill, M.R. *J. Am. Chem. Soc.* **2000**, *122*, 3063.

16 (a) West, F.G.; Eberlein, T.H.; Tester, R.W. *J. Chem. Soc., Perkin Trans. 1* **1993**, 2857. (b) For a related oxonium ylide-based route to medium-sized carbocycles, see: Clark, J.S.; Bate, A.L.; Grinter, T. *Chem. Commun.* **2001**, 459.

17 [1,2]-Shift of *N*-allylammonium ylides geometrically constrained or sterically impeded from [2,3]-sigmatropic rearrangement is precedented: (a) Ollis, W.D.; Rey, M.; Sutherland, I.O. *J. Chem. Soc., Chem. Commun.* **1978**, 675. (b) West, F.G.; Naidu, B.N. *J. Org. Chem.* **1994**, *59*, 6051.

18 (a) Pirrung, M.C.; Brown, W.L.; Rege, S.; Laughton, P. *J. Am. Chem. Soc.* **1991**, *113*, 8561. (b) Oku, A.; Murai, N.; Baird, J. *J. Org. Chem.* **1997**, *62*, 2123. (c) Mori, T.; Taniguchi, M.; Suzuki, F.; Doi, H.; Oku, A. *J. Chem. Soc., Perkin Trans. 1* **1998**, 3623.

19 West, F.G.; Naidu, B.N.; Tester, R.W. *J. Org. Chem.* **1994**, *59*, 6892.

20 Tester, R.W.; West, F.G. *Tetrahedron Lett.* **1998**, *39*, 4631.

21 a) Marmsäter, F.P.; West, F.G. *J. Am. Chem. Soc.* **2001**, *123*, 5144. (b) Marmsäter, F.P.; Vanecko, J.A.; West, F.G. *Tetrahedron* **2002**, *58*, 20270. Review: (c) Marmsäter, F.P.; West, F.G. *Chem. Eur. J.* **2002**, *8*, 4346.

22 Hashimoto, S.; Watanabe, N.; Ikegami, S. *Tetrahedron Lett.* **1992**, *33*, 2709. (b) Hashimoto, S.; Watanabe, N.; Ikegami, S. *J. Chem. Soc., Chem. Commun.* **1992**, 1508. (c) Hashimoto, S.; Watanabe, N.; Anada, M.; Ikegami, S. *J. Synth. Org. Chem. Jpn.* **1996**, *54*, 988.

23 Felthouse, T.R. *Prog. Inorg. Chem.* **1982**, *29*, 73.

24 West, F.G.; Glaeske, K.W.; Naidu, B.N. *Synthesis* **1993**, 977.

25 West, F.G.; Naidu, B.N. *J. Am. Chem. Soc.* **1993**, *115*, 1177.

26 Naidu, B.N. *The Stevens Rearrangement of Ammonium Ylides and Its Applications to the Synthesis of Azaheterocycles, α-Amino Acid Derivatives and Optically Active (–)-Epilupinine*; Ph.D. Dissertation, University of Utah, **1994**.

27 (a) West, F.G.; Naidu, B.N. *J. Am. Chem. Soc.* **1993**, *115*, 8420. (b) Naidu, B.N.; West, F.G. *Tetrahedron* **1997**, *53*, 16565.

28 (a) Vanecko, J.A.; West, F.G. *Org. Lett.* **2002**, *4*, 2813. (b) Vanecko, J.A. *Novel Transformations in the Stevens Rearrangment of Ammonium Ylides and Their Application Toward Synthesis of Alkaloid Natural Products*; Ph.D. Dissertation, University of Utah, **2003**.

29 (a) Clark, J.S.; Hodson, P.B. *Tetrahedron Lett.* **1995**, *36*, 2519. (b) Clark, J.S.; Hodgson, P.B.; Goldsmith, M.D.; Blake, A.J.; Cooke, P.A.; Street, L.J. *J. Chem. Soc., Perkin Trans. 1* **2001**, 3325.

30 Padwa, A.; Beall, L.S.; Eidell, C.K.; Worsencroft, K.J. *J. Org. Chem.* **2001**, *66*, 2414.

31 Vanecko, J.A.; West, F.G. submitted for publication.

32 (a) Oku, A.; Ohki, S.; Yoshida, T.; Kimura, K. *Chem. Commun.* **1996**, 1077. (b) Oku, A.; Murai, N.; Baird, J. *J. Org. Chem.* **1997**, *62*, 2123. (c) Oku, A.; Numata, N. *J. Org. Chem.* **2000**, *65*, 1899. (d) Sawada, Y.; Mori, T.; Oku, A. *Chem. Commun.* **2001**, 1086.

33 (a) Padwa, A.; Austin, D.J. *Angew. Chem., Int. Ed. Engl.* **1994**, *33*, 1797. (b) Pirrung, M.C.; Morehead, A.T. *J. Am. Chem. Soc.* **1994**, *116*, 8991. (c) Doyle, M.P.; Ren, T. *Prog. Inorg. Chem.* **2001**, *49*, 113.

34 (a) Karche, N.; Jachak, S.M.; Dhavale, D.D. *J. Org. Chem.* **2001**, *66*, 6323. (b) Marmsäter, F.P.; Vanecko, J.A.; West, F.G. *Org. Lett.* **2004**, *6*, 1657.

35 (a) McCarthy, N.; McKervey, M.A.; Ye, T.; McCann, M.; Murphy, E.; Doyle, M.P. *Tetrahedron Lett.* **1992**, *33*, 5983. (b) Doyle, M.P.; Ene, D.G.; Forbes, D.C.; Tedrow, J.S. *Tetrahedron Lett.* **1997**, *38*, 4367. (c) Doyle, M.P.; Forbes, D.C.; Vasbinder, M.M.; Peterson, C.S. *J. Am.* Chem. Soc. **1998**, *120*, 7653. (d) Hodgson, D.M.; Petroliagi, M. *Tetrahedron: Asymmetry* **2001**, *12*, 877. (e) Kitigaki, S.; Yanamoto, Y.; Tsutsui, H.; Anada, M.; Nakajima, M.; Hashimoto, S. *Tetrahedron Lett.* **2001**, *42*, 6361.

19
Rhodium(II)-Catalyzed 1,3-Dipolar Cycloaddition Reactions

Ruben M. Savizky and David J. Austin

19.1
Rhodium(II) in 1,3-Dipole Formation

19.1.1
Introduction

The rhodium(II)-catalyzed formation of 1,3-dipoles has played a major role in facilitating the use of the dipolar cycloaddition reaction in modern organic synthesis. This is apparent from the increasing number of applications of this chemistry for the construction of heterocyclic and natural product ring systems. This chapter initially focuses on those aspects of rhodium(II) catalysis that control dipole formation and reactivity, and concludes with a sampling of the myriad examples that exist in the literature today.

As with any modern review of the chemical literature, the subject discussed in this chapter touches upon topics that are the focus of related books and articles. For example, there is a well recognized tome on the 1,3-dipolar cycloaddition reaction that is an excellent introduction to the many varieties of this transformation [1]. More specific reviews involving the use of rhodium(II) in carbonyl ylide cycloadditions [2] and intramolecular 1,3-dipolar cycloaddition reactions have also appeared [3, 4]. The use of rhodium for the creation and reaction of carbenes as electrophilic species [5, 6], their use in intramolecular carbenoid reactions [7], and the formation of ylides *via* the reaction with heteroatoms have also been described [8]. Reviews of rhodium(II) ligand-based chemoselectivity [9], rhodium(II)-mediated macrocyclizations [10], and asymmetric rhodium(II)–carbene transformations [11, 12] detail the multiple aspects of control and applications that make this such a powerful chemical transformation. In addition to these reviews, several books have appeared since around 1998 describing the catalytic reactions of diazo compounds [13], cycloaddition reactions in organic synthesis [14], and synthetic applications of the 1,3-dipolar cycloaddition [15].

19.1.2
The First Examples of Transition Metal-Mediated 1,3-Dipole Formation

The cycloaddition reaction of dipoles has been known since the late eighteenth century; however, before Huisgen's introduction of the concept of a 1,3-dipole, these reactions were considered to proceed *via* a diradical mechanism [16]. One of the earliest examples of metal-catalyzed 1,3-dipole formation involved the controlled decomposition of an α-dia-

Modern Rhodium-Catalyzed Organic Reactions. Edited by P. Andrew Evans

ISBN: 3-527-30683-8

zo ketone in the presence of a catalytic amount of copper(II) acetylacetonate [Cu(acac)$_2$] [17]. It was later established that these α-diazo ketone decomposition products were indeed 1,3-dipoles and could undergo cycloaddition reactions with dipolarophiles [18, 19]. While these early examples utilized copper as the metal species, they set the stage for the evaluation of additional transition metals capable of catalyzing this transformation. The earliest example of a rhodium(II)-catalyzed α-diazo ketone decomposition to form a 1,3-dipole was described by Bien (Scheme 19.1) [20]. In this paper, the authors reported that the cyclopropanation gave **2** and **3** as the major products when palladium was used as the catalyst; however, rhodium catalysis provided cycloaddition adduct **5** as the predominant product. These early issues with selectivity formed the basis for much later work, which in combination with the ability to control product distribution through modification of the ligands within the rhodium(II) complex, ultimately led to the widespread use of this metal over palladium or copper (*vide infra*).

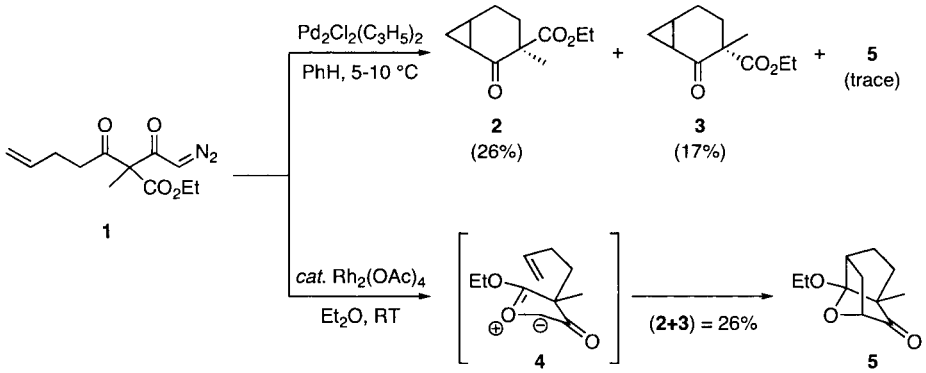

Scheme 19.1

Despite this promising beginning, and its growing use for the generation of electrophilic carbenes [5, 6], it was not until many years later that rhodium(II) was used generally for the formation of 1,3-dipoles. Padwa and Stull reported the use of rhodium(II) acetate [Rh$_2$(OAc)$_4$] in the successful formation of a six-membered ring carbonyl ylide (Scheme 19.2) [21]. This work was quickly followed by the use of rhodium(II) for the generation of

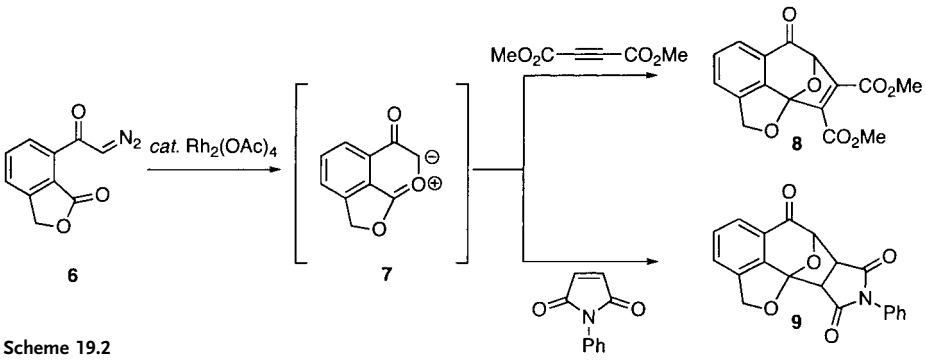

Scheme 19.2

furans *via* a [3+2] cycloaddition [22], and the generation of sulfonium and sulfoxonium ylides [23, 24]. The general synthetic utility of these transformations was greatly advanced by the demonstration of dipole formation and cycloaddition in the 1-diazo-2,5-pentanedione system [25], which was later applied to the synthesis of the natural product brevicomin [26]. This sequential cyclization–cycloaddition process, as it has become known, has since been applied to many ring systems [27].

19.1.3 Rhodium(II) Catalysts Used in 1,3-Dipole Formation

Rhodium(II) forms a dimeric complex with a lantern structure composed of four bridging ligands and two axial binding sites. Traditionally rhodium catalysts fall into three main categories: the carboxylates, the perfluorinated carboxylates, and the carboxamides. Of these, the two main bridging frameworks are the carboxylate **10** and carboxamide **11** structures. Despite the similarity in the bridging moiety, the reactivity of the perfluorinated carboxylates is demonstrably different from that of the alkyl or even aryl carboxylates. Solid-phase crystal structures usually have the axial positions of the catalyst occupied by an electron donor, such as an alcohol, ether, amine, or sulfoxide. By far the most widely used rhodium(II) catalyst is rhodium(II) acetate [$Rh_2(OAc)_4$], but almost every variety of rhodium(II) catalyst is commercially available.

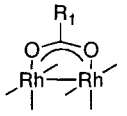

10

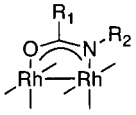

11

Rhodium(II) carboxylate Rhodium(II) carboxamide

R_1 = alkyl, aryl, fluro-alkyl, sulfoxyl
R_2 = H, alkyl

Rhodium(II) carbenoids are electrophilic species that have the ability to undergo insertion (C–H, N–H, O–H, and so on), cyclopropanation, cyclopropenation, and dimerization, in addition to dipole formation [5, 6]. By far the largest role that the rhodium metal plays in the formation of 1,3-dipolar cycloadditions is stabilization of the intermediate carbene [5, 6], as a rhodium carbenoid. A second benefit afforded with rhodium catalysts, which makes them preferable to those based on copper or palladium, is the ease with which the bridging ligands may be modified together with the dramatic change in reactivity that is observed from these modifications [9]. Alternatively, carbenes generated by either acidic [28] or photochemical [29] methods suffer from being overly reactive.

One of the most significant additions to the modern rhodium(II) catalyst ligand family was the development of the hybrid catalysts that combined the carboxamide bridging ligands with the enhanced reactivity of perfluoroalkyl substituents. In this series, rhodium(II) trifluoroacetamidate [$Rh_2(tfa)_4$] was the first described [30]. In addi-

tion to having enhanced reactivity, this molecule was initially described as an effective mediator of the O–H insertion reaction. Subsequent studies using $Rh_2(tfa)_4$ and the related rhodium(II) perfluorobutyramidate [$Rh_2(pfbm)_4$] demonstrated an additional propensity for oxindole [31] and indole formation [32] *via* C–H insertion, in addition to the formation of isomünchnones [33]. The enhanced reactivity of the perfluorinated carboxamides was also observed by Doyle *et al.* [34]; however, no increase in enantioselectivity was noted with the chiral variants of these catalysts. The use of rhodium(II) ligand modifications to mediate carbenoid chemoselectivity (Section 19.2.1) [9], as well as the many recent advances in the generation and use of chiral rhodium(II) catalysts [35] (Section 19.2.3), are discussed later in the chapter.

Despite the widespread use of rhodium(II) catalysis, the exact mechanism and nature of the rhodium carbenoid is not completely understood. In an effort to better understand the mechanism of rhodium(II)-mediated carbene reactivity, Pirrung [36] demonstrated that the reaction obeys saturation kinetics, which is consistent with the second step after complexation being rate-determining. This result is analogous with an earlier model for copper-catalyzed diazo decomposition [37]. Pirrung has also reported the ability of these catalysts to be inhibited by Lewis bases, and has further demonstrated their Michaelis–Menten behavior [38]. The first structural insight into the rhodium carbenoid was provided by the isolation and subsequent X-ray crystallographic analysis of a stable metal–carbene complex [39]. The structure showed an increased Rh–Rh bond distance relative to the uncomplexed structure, in addition to a long and presumably weak Rh–C bond, favoring decomplexation as suggested by reactivity.

19.1.4
Dipoles Created Using Rhodium(II) Catalysis

Many different types of 1,3-dipoles have been described [1]; however, those most commonly formed using transition metal catalysis are the carbonyl ylides and associated mesoionic species such as isomünchnones. Additional examples include the thiocarbonyl, azomethine, oxonium, ammonium, and nitrile ylides, which have also been generated using rhodium(II) catalysis [8]. The mechanism of dipole formation most often involves the interaction of an electrophilic metal carbenoid with a heteroatom lone pair. In some cases, however, dipoles can be generated *via* the rearrangement of a reactive species, such as another dipole [40], or the thermolysis of a three-membered heterocyclic ring [41].

Carbonyl ylides were the first, and remain the most prolific, form of 1,3-dipole formed using rhodium(II) catalysis [27]. This is due, in part, to their ease of formation and the utility of the oxygen-containing dipole cycloaddition product (*vide infra*). In addition, by changing the character of the carbonyl group that interacts with the rhodium carbenoid, the nature of the dipole and subsequent product formation can vary widely [42]. Examples include the cycloaddition with aldehydes [43] and their generation from diazo imides [44]. The isomünchnones, which can be considered a subclass of carbonyl ylides, have also been described [45, 46] and widely explored [47]. Specific examples include bimolecular cycloaddition [48], cycloaddition with heteroatomic π-systems [49], and the formation of polyheterocyclic ring systems [50]. The intramolecular cycloaddition of isomünchnones **13** [51, 52] has yielded a number of complex polyheterocyclic and multibridged ring systems (Eq. 1) [53]. Thiocarbonyl ylides **15** are particularly valuable since

they can be used to form thiol-containing heterocycles (Eq. 2) [54, 55], as well as molecules without sulfur following thermal extrusion [56]. The formation of oxiranes and dihydrofurans utilizing ylides possessing pendant functional groups that enhance reactivity, such as vinylcarbonyl ylides, has also been explored [57].

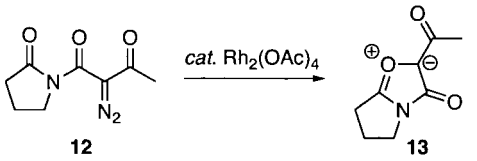

12 13 (1)

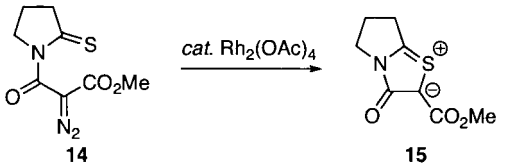

14 15 (2)

In addition to the carbonyl and thiocarbonyl ylides, additional rhodium(II)-generated 1,3-dipoles have been described such as the azomethine ylide **17**, which can generate a rich ensemble of nitrogen-containing hetero- and polyheterocycles (Eq. 3) [58–62]. The oxonium [63] and ammonium ylides **19** [64, 65] have been used to generate a number of heterocyclic ring systems (Eq. 4), and are the subject of a 2002 review [66]. In some cases, the decomposition of an *α*-diazo ketone containing an amide can access either a carbonyl or ammonium ylide [67]. Rhodium(II)-generated nitrile ylides **21**, normally acyl-substituted, can be a convenient source of both pyrroles and oxazoles (Eq. 5) [68, 69].

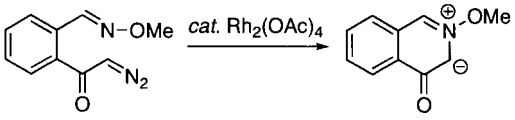

16 17 (3)

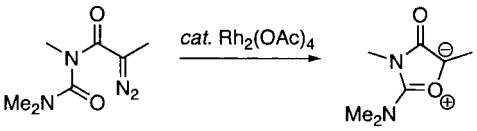

18 19 (4)

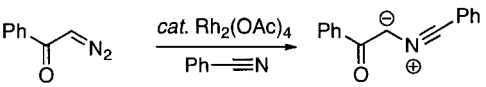

20 21 (5)

1,3-Dipoles can also be generated from rearrangements that take place after the formation of an initial rhodium carbenoid product [40, 70, 71]. One example of this type of transmutation, also known as a dipole cascade process, involves the formation of an azomethine ylide *via* the initial formation of a carbonyl ylide [72]. This process was

successfully applied to other systems such as diazo ketoamides [73, 74], diazo-substituted pyrrolidines [60], and 2-diazo-3-oxobutanoates [59] to form a variety of hetero- and polyheterocyclic systems. Dipoles have also been generated from rearrangement reactions to give aromatic heterocycles [75], *N*-acylium ions [71], and hydroxypyridones [76]. More recently, Doyle has reported the conversion of epoxides and aziridines, formed *via* a rhodium(II)-mediated cyclopropanation, to 1,3-dipoles [41, 77].

19.2
Chemical Aspects of Rhodium-Mediated 1,3-Dipolar Cycloaddition

19.2.1
Aspects of Rhodium(II) Catalysis that Affect Chemoselectivity

The potential for ligand-induced chemoselectivity of rhodium(II)-mediated carbenoid transformations is one of the primary factors in the selection of this catalyst which has resulted in its widespread utilization [9]. A major concern for 1,3-dipolar cycloaddition reactions is that dipole formation takes place over other potential reaction pathways such as insertion or cyclopropanation. Once the dipole has formed, however, the role of the rhodium metal is not clear. Thus the catalyst and reaction conditions employed must be optimized for each molecular system investigated. As described previously, dipoles have the ability to eliminate [19] or rearrange [71] in order to form a more stable species, and the inductive effect of rhodium on the dipole will depend on its tendency to undergo dissociation from this complex. In some cases, suppression of unwanted dipole reactivity, such as elimination, can be avoided by an alternative design of the dipole substituents [78]. Undesired rhodium carbenoid-based reactivity is more difficult to suppress, since this reactivity can occur with a pendant C–H, a group that would not normally be considered reactive under most experimental conditions. Early reports suggested that the tendency toward dipole formation and cycloaddition was dependent on the electrophilicity of the rhodium carbenoid intermediate [79]; however, conformational control of selectivity can dominate product distribution [63, 80]. One of the first investigations of controlled rhodium ligand chemoselectivity demonstrated that, within equal conformational constraints, the perfluorinated acetates, such as rhodium(II) perfluorobyturate [$Rh_2(pfb)_4$], prefer insertion over cyclopropanation and cyclopropanation over carbonyl ylide formation. Alternatively the acetamide catalysts, for example rhodium(II) caprolactam [$Rh_2(cap)_4$], prefer cyclopropanation and carbonyl ylide formation over insertion, while the alkyl acetates, such as rhodium(II) acetate [$Rh_2(OAc)_4$], are capable of forming each of the potential products equally [81, 82].

While the perfluorinated acetates do prefer insertion, they are still capable of forming 1,3-dipoles and have demonstrated interesting effects on the regioselectivity of intramolecular cycloaddition reactions, presumably through Lewis acid-mediated effects on the dipolarophile [83]. Other chemoselectivity effects have been noted in the intramolecular cycloaddition reactions and may or may not be partially induced by conformation and sterics [84]. It was further demonstrated that, when possible, O–H insertion is the predominant outcome over other types of insertion for rhodium(II)–carbenes, independently of the catalyst. However, cycloaddition reactions have been demonstrated to be ligand-dependent [85].

The perfluoroacetamide catalysts, rhodium(II) trifluoroacetamidate [$Rh_2(tfm)_4$] and rhodium(II) perfluorobutyramidate [$Rh_2(pfbm)_4$], are interesting hybrid molecules that combine the features of the amidate and perfluorinated ligands. In early studies, these catalysts were shown to prefer insertion over cycloaddition [30]. They also demonstrated a preference for oxindole formation *via* aromatic C–H insertion [31], even over other potential reactions [86]. In still another example, rhodium(II) perfluorobutyramidate showed a preference for aromatic C–H insertion over pyridinium ylide formation, in the synthesis of an indole nucleus [32]. Despite this demonstrated propensity for aromatic insertion, the perfluorobutyramidate was shown to be an efficient catalyst for the generation of isomünchnones [33]. The chemoselectivity of this catalyst was further demonstrated in the cycloaddition with ethyl vinyl ethers [87] and its application to diversity-oriented synthesis [88]. However, it was demonstrated that while diazo imides do form isomünchnones under these conditions, the selectivity was completely reversed from that observed with rhodium(II) acetate [89, 90].

19.2.2
Aspects of Rhodium(II) Catalysis that Affect Regio- and Diastereoselectivity

The regioselectivity of 1,3-dipolar cycloaddition reactions is largely controlled by the electronic/orbital nature of the dipole and dipolarophile [1], and is not affected by changes to the rhodium ligands [9]. Diastereoselectivity is achieved by controlling the orientation of the dipolarophile as it approaches the dipole, resulting in either an *exo*- or *endo*-cycloaddition product [47]. In the case of intramolecular cycloadditions, in the absence of electronic effects, the *exo*/*endo* ratio is mainly controlled by steric factors [49, 91, 92]. In the case of intermolecular cycloaddition reactions with electron-deficient dipolarophiles, low selectivities are observed and the *exo*/*endo* ratios are largely case-dependent [47, 87]. Interestingly, the intermolecular cycloaddition of electron-rich dipolarophiles with mesoionic dipoles provides exclusively the *endo*-cycloaddition product [87]. There is little evidence that the rhodium(II) catalyst plays a role in the *exo*/*endo* selectivity; however, it has been reported that addition of 10 mol% ytterbium triflate [$Yb(OTf)_3$] to a rhodium(II)-mediated 1,3-dipolar cycloaddition reaction with *N*-substituted maleimides produced cycloadducts with high *endo*-selectivity [93]. *Exo*/*endo* selectivity does seem to be dipolarophile-dependent, since the same additive led to a high level of *exo*-selectivity with aromatic aldehydes [94]. In both cases no selectivity was observed in the absence of the rare earth metal complex.

19.2.3
Aspects of Rhodium(II) Catalysis that Affect Facial Selectivity

There have been two main approaches to the development of dipolarophile facial selectivity: (1) the use of chiral substrates, templates, and auxiliaries; and (2) the use of chiral rhodium catalysts [35]. In one of the earliest examples of chiral substrate selectivity, Pirrung and Lee reported a selective hydroxy-directed cycloaddition with chiral hydroxy-substituted vinyl ethers [95]. This effort was followed by a number of chiral template approaches to diastereocontrol, including the use of (*R*)- or (*S*)-phenylglycinol to form a cyclic phenyloxazinone for the facially selective cycloaddition of isomünchnones [96, 97]. Padwa and Prein demonstrated acyclic diastereofacial control in the cycloaddi-

tion of isomünchnones, using *N*-substituted α-diazo imides based on amino acids [98]. Most recently, Savinov and Austin have reported the modular design of a chiral template that can be easily cleaved, allowing the chiral group to function as an auxiliary for isomünchnone cycloadditions [99] and as a selective cleavage reagent in solid-phase organic synthesis [88].

Despite the potential dissociation of the rhodium(II) metal from newly formed dipoles, a number of the chiral rhodium(II) catalysts have been developed that demonstrated the ability to induce enantioselectivity in 1,3-diploar cycloaddition reactions (**22**–**34**) [11, 35, 100, 101]. One of the earliest examples of a chiral rhodium(II)-induced enantioselective cycloaddition was described by Pirrung and Zhang [102] using a novel bisnaphtholphosphate ligand-containing catalyst **22** in the construction of the dihydrofuro[2,3-*b*]furan ring system. Ishitani and Achiwa later applied chiral *N*-benzoylpyrrolidine carboxylate catalysts **23** to the same transformation, with enantioselectivities ranging from 93 to 98% [103]. Moody described the development of new chiral phthalate ester- and pyrrole-based catalysts, and their application to the formation of oxonium ylides, which subsequently undergo sigmatropic rearrangement [100]. Hodgson [104] applied chiral induction in an intramolecular cycloaddition of a carbonyl ylide using Davies' [105] chiral *N*-arylsulfonyl prolinate rhodium(II) catalyst **24**. Other chiral catalysts were later applied to this [106, 107] and other systems [101, 108–111], with enantioselectivities of up to 92% being achieved. Hashimoto developed the *N*-phthaloyl-(*S*)-amino acid-based chiral dirhodium catalysts **28** and **29**, which have been successfully used in the enantioselective 1,3-dipolar cycloaddition of carbonyl ylides to obtain enantioselectivities of up to 93% [112, 113]. Davies has reported an asymmetric [3+2]-cycloaddition for the formation of cyclopentenes [114].

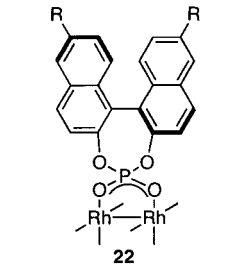

22

R = H Rh_2(*R*-BNP)$_4$

R = $C_{12}H_{25}$ Rh_2(*R*-DDBNP)$_4$

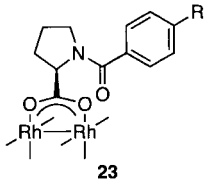

23

R = H, OMe, NMe_2, F, CF_3

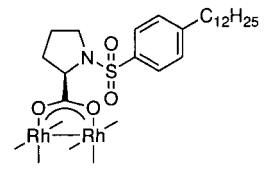

24

Rh_2(*S*-DOSP)$_4$

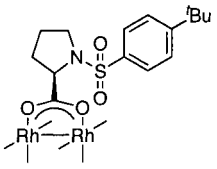

25

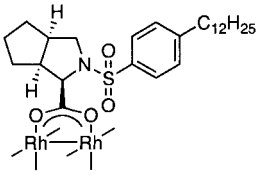

26

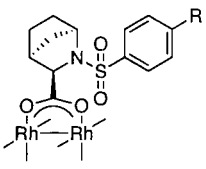

27

R = ^{t}Bu, $C_{12}H_{25}$

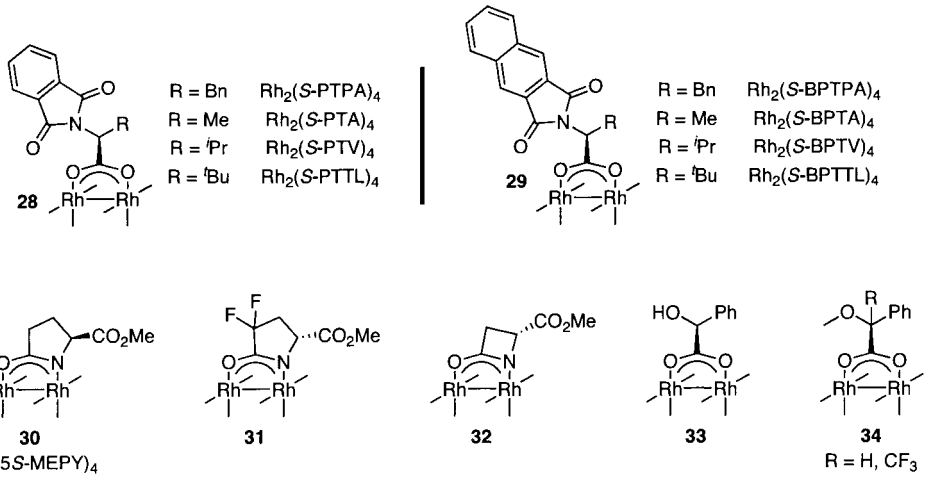

19.3
Applications of Rhodium(II)-Mediated 1,3-Dipolar Cycloaddition

19.3.1
Heterocyclic Synthesis and Novel Ring Systems

One of the earliest uses for rhodium(II)-catalyzed dipoles was demonstrated in Davies' furan synthesis [22]. Isomünchnones were also shown to produce substituted furans [115]. Additional furan syntheses have been described using silylacetates [116], unsaturated esters [117], and fluoroalkyl diazo acetates [118]. The synthesis of furofuranones and indenofuranones **35** from α-diazo ketones having pendant alkynes has also been reported (Eq. 6) [119]. Other fused heterocyclic systems include furo[3,4-*c*]furans [120, 121] furo[2,3-*b*]furans [122] as well as thiobenzofurans [123], and benzoxazoles[124] have also been synthesized with this methodology.

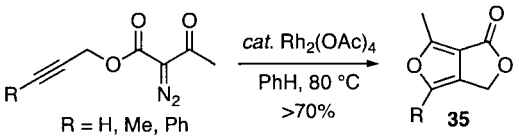

(6)

Additional heterocyclic ring systems, such as benzofurans [125], dihydropyrroles and dihydroazepines [41], piperidines and dihydropyrimidines **36** [126], and fused oxazole derivatives [127], have been described (Eq. 7). The formation of epoxides and aziridines, formally emanating from ylides, was recently reported by Doyle *et al.* [77]. Rhodium(II)-catalyzed isomünchnone cycloaddition followed by Lewis acid-mediated ring opening has been used as an entry into the protoberberine azapolycyclic ring structure [128].

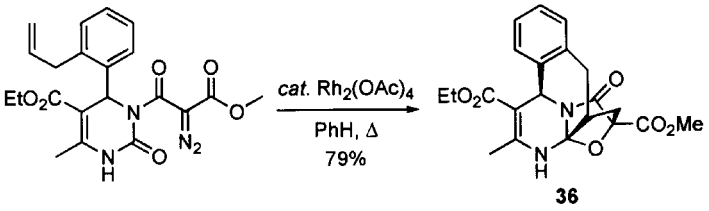

(7)

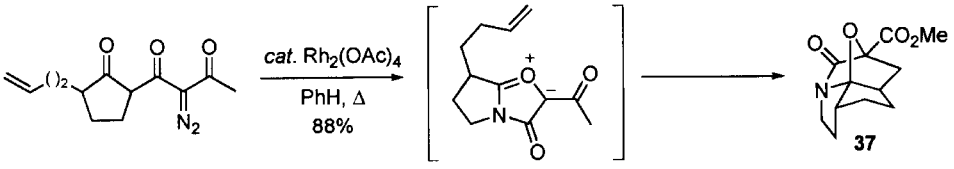

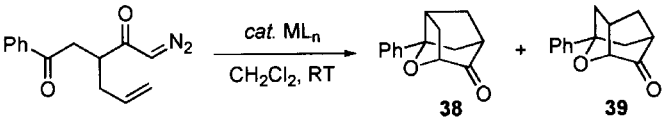

ML_n		38	39
	$Rh_2(OAc)_4$	10%	47%
	$Rh_2(tfa)_4$	34%	12%
	$Rh_2(cap)_4$	12%	52%

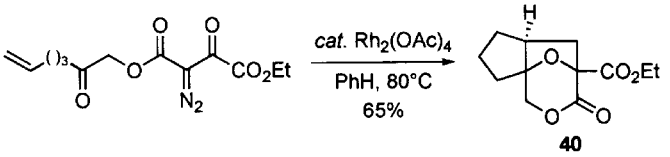

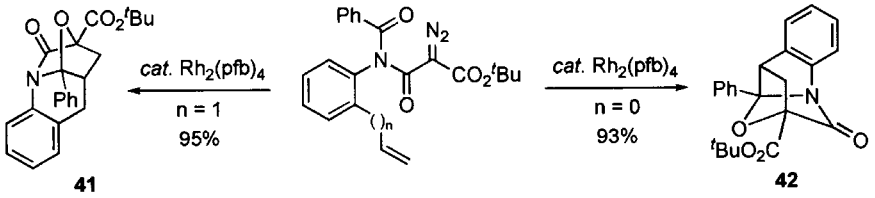

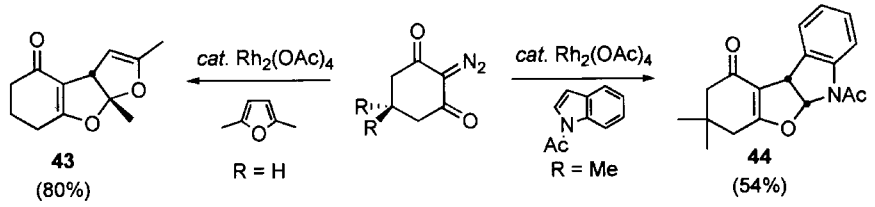

Scheme 19.3

A number of bridged heterocyclic compounds have been prepared using the intramolecular cycloaddition of rhodium(II)-generated isomünchnones [51–53, 84, 129], as exemplified by the complex structure **37** [49, 53] and the tricyclic derivatives **38** and **39** (Scheme 19.3) [92]. In addition, several oxabicyclic **40** [43, 67, 79] and azaoxabicyclic systems **41** and **42** [44, 50] have been reported. Other complex ring systems have also been described, such as oxathioles and oxazolones [130], spiro-oxo molecules [129], oxatricyclic compounds [131], and spiroxindole like structures [132–135]. The synthesis of fused ring structures **43** and **44** via the cycloaddition with quinone and quinone-like dipolarophiles was independently described by Pirrung [75, 136, 137], Muthusamy [138, 139], and Nair [140]. Stereoselective studies have generated *syn*-facial bridged norbornane structures [141, 142].

A rhodium-mediated carbonyl ylide approach to di- and tetrahydrofurans (Scheme 19.4) has been reported [143]. Interesting substrate-based selectivity was demonstrated with the dipolarophiles **45** and **47** in the carbonyl ylide cycloaddition to afford **46** and **48**, wherein different selectivities and efficiencies were achieved, based on the presence or absence of the cobalt complex.

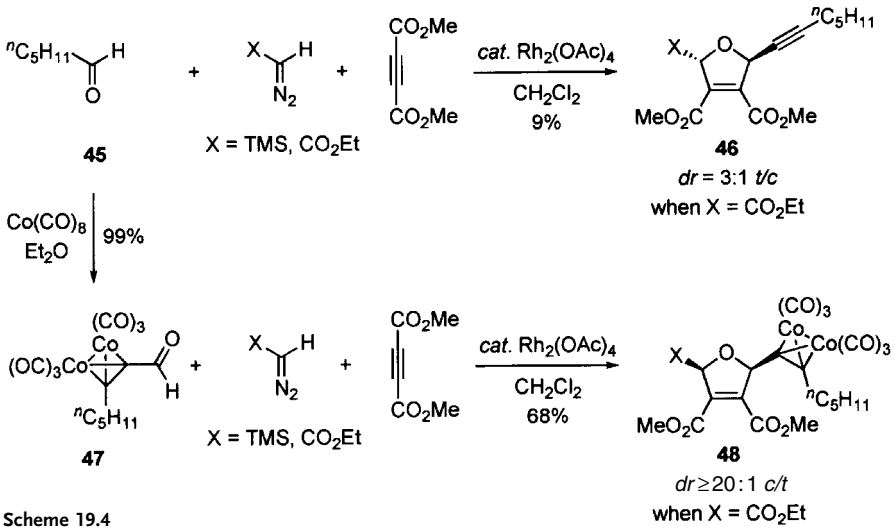

Scheme 19.4

19.3.2 Natural Product Synthesis and Core Structures

Perhaps the most intriguing aspect of rhodium(II)-mediated 1,3-dipolar cycloadditions is the plethora of natural products and natural product core structures that have been accessed using this methodology. A dipolar cycloaddition approach to the fungal metabolite benzotropolone **49** was first put forward by Plüg and Freidrichsen [144] using an intramolecular cycloaddition of a carbonyl ylide containing a terminal alkyne **50** to afford **51** (Scheme 19.5). Baldwin later used this methodology for the construction of the tropolone precursor **53**, in his biomimetic approach to the natural products pycnidione and epolone B [145].

A carbonyl ylide approach to the tigliane natural product phorbol **54** was demonstrated by Dauben, in which a convergent intramolecular cycloaddition was used to

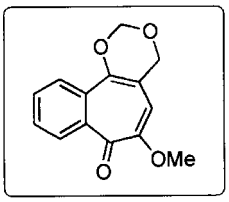

Benzotropolone **49**

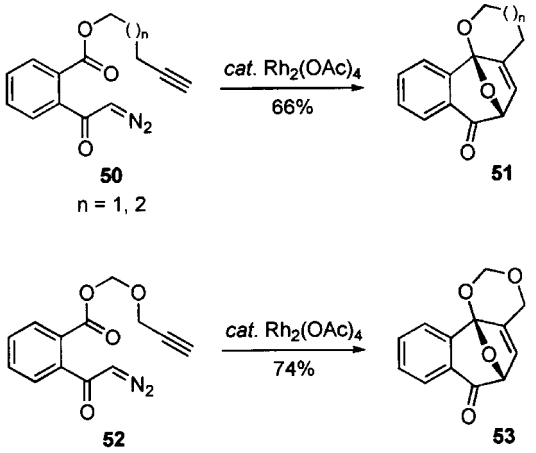

Scheme 19.5

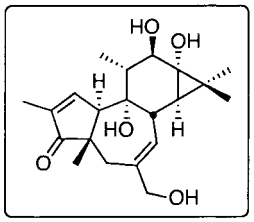

Phorbol **54**

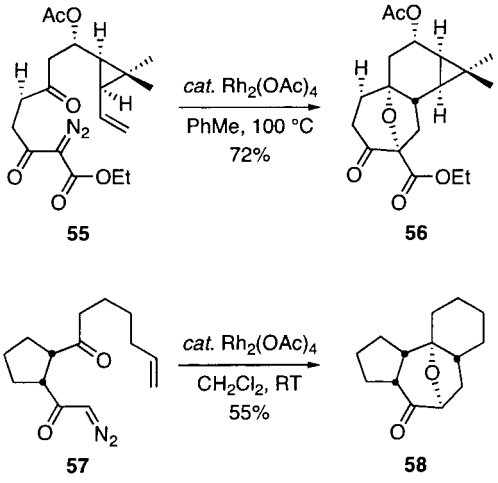

Scheme 19.6

form the oxo-bridged BCD-ring system **56** (Scheme 19.6) [146]. McMills built upon this approach with the construction of the oxo-bridged species **58**, from the diazo ketone **57**, to install the ABC rings of phorbol **54** [147].

Zaragozic acid A **59** is perhaps the most complex ring structure that has been attempted with the 1,3-dipolar cycloaddition reaction (Scheme 19.7). Koyama [148] reported the first approach using **60** with a silyl vinyl ether as the dipolarophile to furnish the requisite skeleton **61**, albeit in low yield. Hashimoto and co-workers [149] used a similar carbonyl ylide route, in which **62** was employed to generate the core **63** in their second-generation approach to this molecule. Hodgson also reported a carbonyl ylide pathway to the zaragozic acids [150], but disconnected the ring system in order to take advantage of its inherent chirality, in the intermolecular reaction of **64** with methyl glyoxalate to furnish **65** [151, 152].

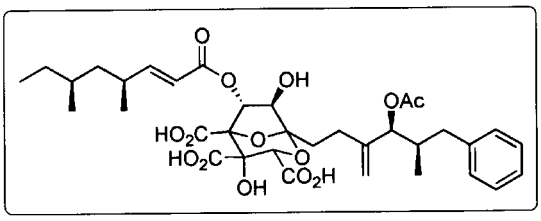

Zaragozic Acid A **59**

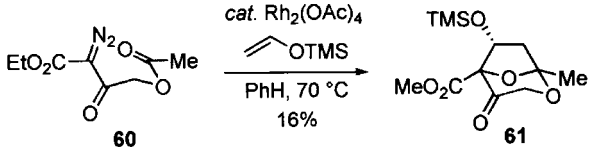

60 **61**

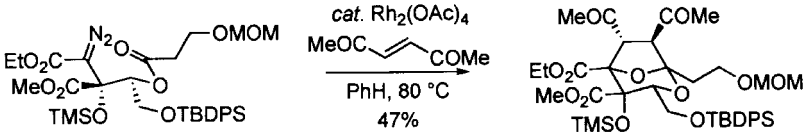

62 **63**

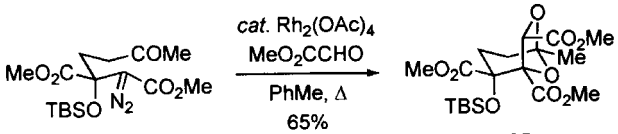

64 **65**

Scheme 19.7

Pirrung [153] has described the synthesis of (±)-pongomol **66** via the rhodium(II)-mediated reaction of the diazacyclohexane dione **67**, to afford the fused bicyclic ketone **68** (Scheme 19.8). Moreover, this group [154] also detailed a similar approach in their synthesis of (±)-isoeuparin **69** (Scheme 19.9). Pirrung and Lee [155] expanded their rhodium(II)-mediated dihydrofuran cycloaddition strategy, for the conversion of the

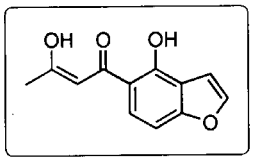

Pongamol **66**

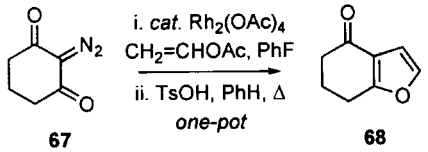

67 **68** (69%)

Scheme 19.8

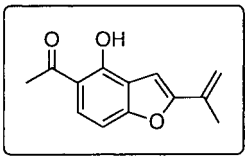

Isoeuparin **69**

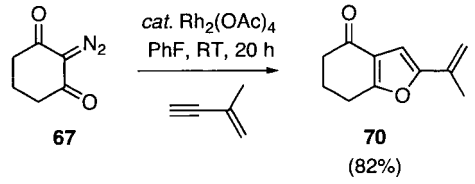

67 **70** (82%)

Scheme 19.9

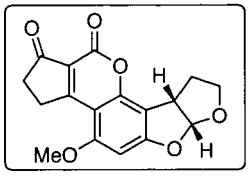

Aflatoxin B_2 **71**

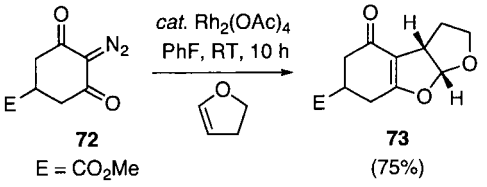

72 E = CO_2Me **73** (75%)

Scheme 19.10

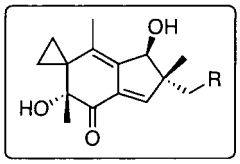

Illudin M (R=H)
Illudin S (R=OH) } **74**

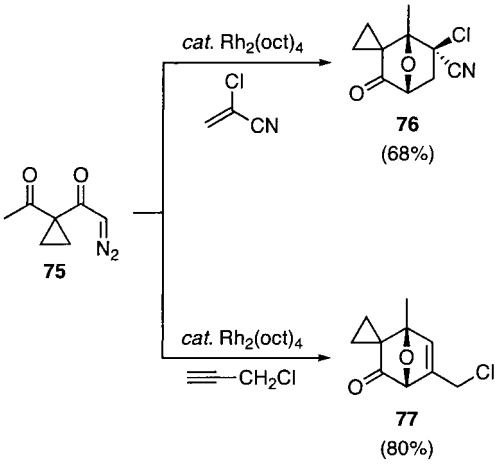

75 **76** (68%) **77** (80%)

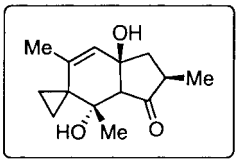

Ptaquilosin **78**

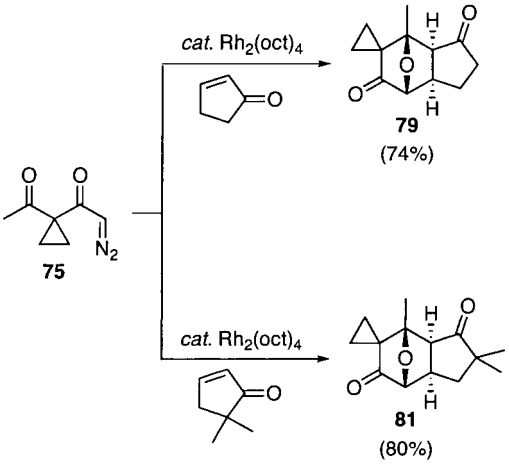

75 **79** (74%) **81** (80%)

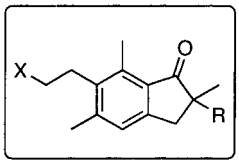

Pterosins **80**
(R=H, Me ; X=OH,OMe,Cl)

Scheme 19.11

diazo β-diketone **72** to the tricyclic ketone **73**, for a formal total synthesis of the natural product (±)-aflatoxin B_2 **71** (Scheme 19.10).

Padwa has reported a 1,3-dipolar cycloaddition approach to the illudin **74** and ptaquilosin **78** family of natural products (Scheme 19.11) [156]. Shortly thereafter, Kinder and Bair reported the total synthesis of illudin M using a similar approach [157]. Further studies demonstrated the versatility of this approach for the construction of the spirocyclic cores **76** and **77**, applicable to the natural products, from the common diazo ketone **75** [158, 159]. The 1,3-dipolar cycloaddition was also demonstrated for pterosin **80** [160] and the pterosin family [161]. McMorris [162] used this approach to the illudin ring system in order to synthesize a number of acylfulvene derivatives with potential antitumor activity. In addition, Pirrung and Kaliappan demonstrated the cycloaddition with *p*-quinones as an entry into this system [137]. The synthesis of the erythrinane ring system *via* a sequential dipolar cycloaddition of an isomünchnone followed by a Lewis acid-induced Mannich cyclization has been described [163]. An isomünchnone approach to the (±)-lycopodine precursor **84** was also outlined (Scheme 19.12) [164]. Lysergic acid has been the subject of a isomünchnone synthetic approach by Padwa [165], and Moody [166] has described the synthesis of dehydrogliotoxin analogs *via* thioisomünchnone intermediates.

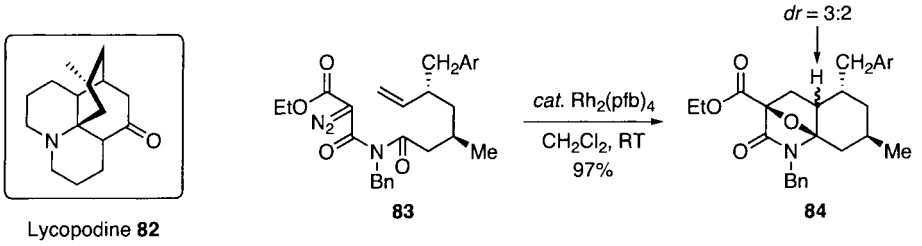

Scheme 19.12

In more recent work, Chiu and co-workers [167, 168] have reported an intramolecular 1,3-dipolar cycloaddition approach toward the pseudolaric acids **85**, in which the dipolarophile is an unactivated 1,1-disubstituted alkene. Hence, treatment of the diazo ketone **86** with catalytic $Rh_2(OAc)_4$ furnished a mixture of tricyclic products **87** and **88** in nearly equal proportions (Scheme 19.13). The synthesis of 2-pyridones [169] and their application to the ipalbidine core [170] has been described. The pentacyclic skeleton of the aspidosperma alkaloids was prepared *via* the cycloaddition of a push–pull carbonyl ylide [171]. The dehydrovindorosine alkaloids **89** have also been investigated, in which the α-diazo-β-ketoester **90** undergoes a facile cycloaddition to furnish **91** in

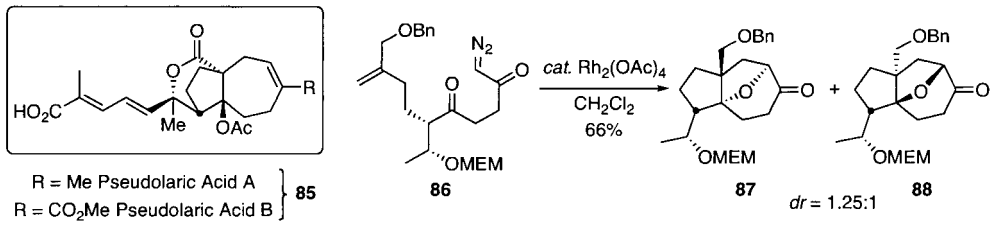

Scheme 19.13

95% yield (Scheme 19.14) [172]. Kissel and Padwa [173] have utilized the push–pull carbonyl ylide cycloaddition for the conversion of the α-diazo-β-ketoester **93** to the bicyclic heterocycle **94**, which represents a key intermediate in their approach toward the lycorine ring structure **92** (Scheme 19.15). Angiotensin-converting enzyme (ACE) inhibitor A58365A **95** and related 2-pyridones can be synthesized *via* isomünchnone intermediates, as exemplified by the conversion of **96** to **97** (Scheme 19.16) [169].

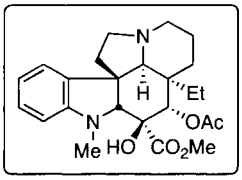

Dehydrovindirosin **89**

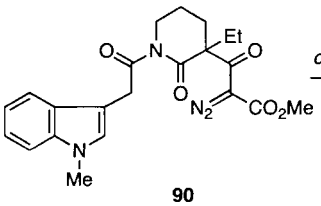

90

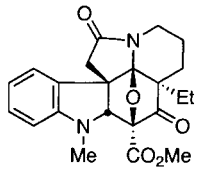

91

Scheme 19.14

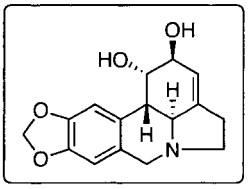

Lycorine **92**

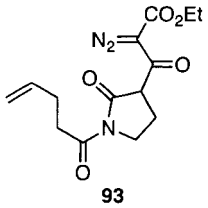

93

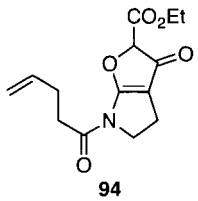

94

Scheme 19.15

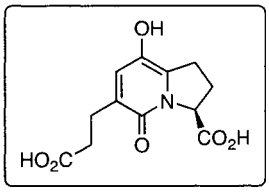

A58365A **95**

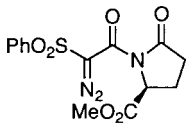

96

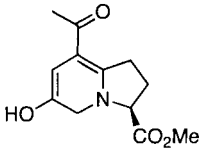

97

Scheme 19.16

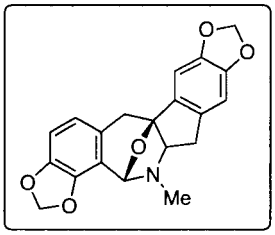

Ribasine **98**

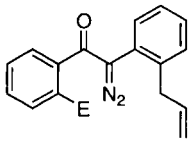

99
E = CO_2Et

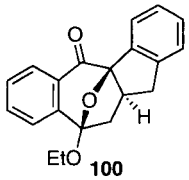

100

Scheme 19.17

Padwa has reported an approach to the ring system of the ribasine alkaloids **98** [174], using an intramolecular 1,3-dipolar cycloaddition of the *α*-diazo ketone **99** to produce the pentacyclic skeleton **100** (Scheme 19.17). Wood [175] used an intermolecular 1,3-dipolar cycloaddition of a carbonyl ylide for the total synthesis of (±)-epoxysorbicillinol **101** (Scheme 19.18). The key cycloaddition in this approach is the conversion of **102** to the natural product core **103**, which sets the substitution pattern around the entire ring system in a single step.

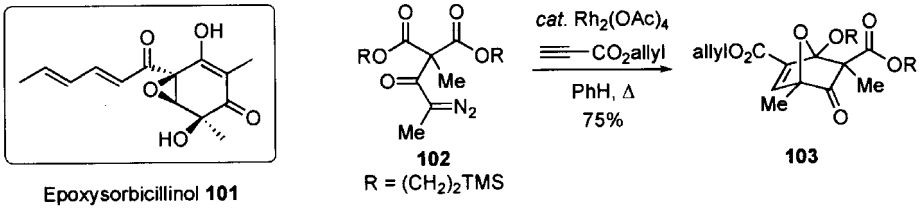

Epoxysorbicillinol **101**

Scheme 19.18

19.3.3
Combinatorial Chemistry and Solid-Phase Organic Synthesis

The isomünchnone cyclization/isocyanate cycloreversion process for substituted furan synthesis has been well studied, as exemplified by the conversion of **104** to **106** (Scheme 19.19). In a solid-phase adaptation of this transformation, two groups independently utilized this reaction to establish a traceless self-cleaving method for the synthesis of substituted furans [176, 177]. Further investigation of the thermal requirements of this cycloreversion led to its application in the split-pool synthesis of a small library of amides [178].

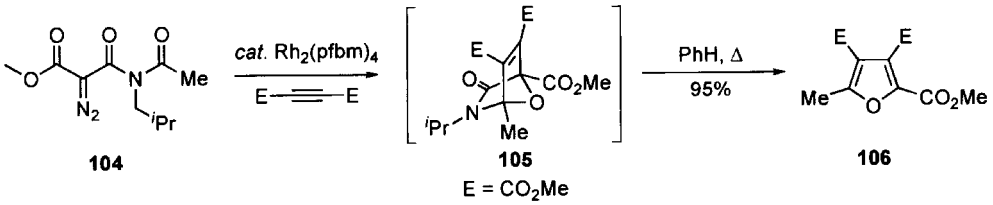

Scheme 19.19

The solid-phase synthesis of bridged bicyclic molecules **109–113**, based on the *endo*-selective cycloaddition of ethyl vinyl ethers with the isomünchnone [87] derived from **107** has also been reported [88]. In addition to good yields and high diastereofacial selectivity imparted through the use of a chiral auxiliary [99], the authors reported the ability to selectively cleave the cycloadduct **108** from the solid support through treatment with nucleophilic amines (Scheme 19.20). This result is based on the lability of the ester linkage between the bicyclic ring and the auxiliary. This dipolar synthetic approach to bicycles was further demonstrated in the construction of a small panel of adenosine mimics [179].

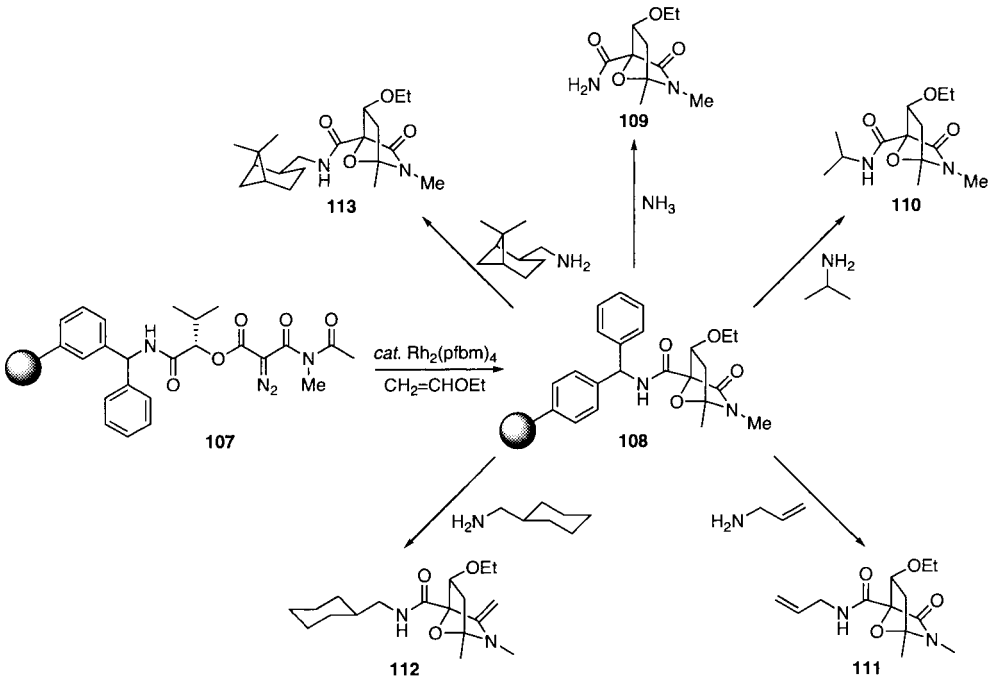

Scheme 19.20

19.4 Conclusion

The ability to produce 1,3-dipoles, through the rhodium-catalyzed decomposition of diazo carbonyl compounds, provides unique opportunities for the accomplishment of a variety of cycloaddition reactions, in both an intra- and intermolecular sense. These transformations are often highly regio- and diastereoselective, making them extremely powerful tools for synthetic chemistry. This is exemplified in the number of applications of this chemistry to the construction of heterocyclic and natural-product ring systems. Future developments are likely to focus on the enantioselective and combinatorial variants of these reactions.

19.5 References

1 Houk, K.; Yamaguchi, K. In *1,3-Dipolar Cycloaddition Chemistry*; Padwa, A., Ed.; Wiley: New York, **1984**; Vol. 2, pp. 407–450.
2 Padwa, A. *Trends Org. Chem.* **1993**, *4*, 139.
3 Padwa, A. *Angew. Chem., Int. Ed. Engl.* **1976**, *88*, 131.
4 Padwa, A.; Schoffstall, A. M. In *Advances in Cycloaddition*; Curran, D. P., Ed.; JAI Press: Greenwich, **1990**; Vol. 2, pp. 1–89.
5 Doyle, M. P. *Chem. Rev.* **1986**, *86*, 919.
6 Doyle, M. P. *Acc. Chem. Res.* **1986**, *19*, 348.
7 Padwa, A.; Krumpe, K. E. *Tetrahedron* **1992**, *48*, 5385.
8 Padwa, A.; Hornbuckle, S. F. *Chem. Rev.* **1991**, *91*, 263.
9 Padwa, A.; Austin, D. J. *Angew. Chem., Int. Ed. Engl.* **1994**, *106*, 1881.
10 Doyle, M. P.; Hu, W. *Synlett* **2001**, 1364.

11 Davies, H. M. L. *Eur. J. Org. Chem.* **1999**, 2459.

12 Kitagaki, S.; Hashimoto, S. *Yuki Gosei Kagaku Kyokaishi* **2001**, *59*, 1157.

13 Doyle, M. P.; McKervey, M. A.; Ye, T. *Modern Catalytic Methods for Organic Synthesis with Diazo Compounds: From Cyclopropanes to Ylides*; Wiley-Interscience: New York, **1998**.

14 Kobayashi, S.; Jorgensen, K. A., Eds. *Cycloaddition Reactions in Organic Synthesis*; Wiley-VCH: Weinheim, **2002**.

15 Padwa, A.; Pearson, W. H., Eds. *Synthetic Applications of 1,3-Dipolar Cycloaddition Chemistry Toward Heterocycles and Natural Products*; JohnWiley & Sons: Hoboken, **2003**.

16 Huisgen, R. In *1,3-Dipolar Cycloaddition Chemistry*; Padwa, A., Ed.; Wiley: New York, **1984**; Vol. 1, pp. 1–176.

17 Takebayashi, M.; Ibata, T.; Ueda, K. *Bull. Chem. Soc. Jpn.* **1970**, *43*, 1500.

18 Takebayashi, M.; Ibata, T.; Ueda, K.; Ohashi, T. *Bull. Chem. Soc. Jpn.* **1970**, *43*, 3964.

19 Bien, S.; Gillon, A. *Tetrahedron Lett.* **1974**, 3073.

20 Gillon, A.; Ovadia, D.; Kapon, M.; Bien, S. *Tetrahedron* **1982**, *38*, 1477.

21 Padwa, A.; Stull, P. D. *Tetrahedron Lett.* **1987**, *28*, 5407.

22 Davies, H. M. L.; Romines, K. R. *Tetrahedron* **1988**, *44*, 3343.

23 Moody, C. J.; Taylor, R. J. *Tetrahedron Lett.* **1988**, *29*, 6005.

24 Moody, C. J.; Slawin, A. M. Z.; Taylor, R. J.; Williams, D. J. *Tetrahedron Lett.* **1988**, *29*, 6009.

25 Padwa, A.; Fryxell, G. E.; Zhi, L. *J. Org. Chem.* **1988**, *53*, 2875.

26 Padwa, A.; Chinn, R. L.; Zhi, L. *Tetrahedron Lett.* **1989**, *30*, 1491.

27 Padwa, A. *Acc. Chem. Res.* **1991**, *24*, 22.

28 Philip, Bro. H.; Lowery, M. K.; Havel, J. *Tetrahedron Lett.* **1967**, *8*, 5049.

29 Tomioka, H. *Photomed. Photobiol.* **1984**, *6*, 23.

30 Cox, G. G.; Kulagowski, J. J.; Moody, C. J.; Sie, E. R. H. B. *Synlett* **1992**, 975.

31 Brown, D. S.; Elliott, M. C.; Moody, C. J.; Mowlem, T. J.; Marino, J. P., Jr.; Padwa, A. *J. Org. Chem.* **1994**, *59*, 2447.

32 Moody, C. J.; Miah, S.; Slawin, A. M. Z.; Mansfield, D. J.; Richards, I. C. *Tetrahedron* **1998**, *54*, 9689.

33 Brodney, M. A.; Padwa, A. *J. Org. Chem.* **1999**, *64*, 556.

34 Doyle, M. P.; Hu, W.; Phillips, I. M.; Moody, C. J.; Pepper, A. G.; Slawin, A. M. Z. *Adv. Synth. Cat.* **2001**, *343*, 112.

35 Doyle, M. P. *Pure Appl. Chem.* **1998**, *70*, 1123.

36 Pirrung, M. C.; Morehead, A. T., Jr. *J. Am. Chem. Soc.* **1996**, *118*, 8162.

37 Yates, P. *J. Am. Chem. Soc.* **1952**, *74*, 5376.

38 Pirrung, M. C.; Liu, H.; Morehead, A. T., Jr. *J. Am. Chem. Soc.* **2002**, *124*, 1014.

39 Snyder, J. P.; Padwa, A.; Stengel, T.; Arduengo, A. J., III; Jockisch, A.; Kim, H.-J. *J. Am. Chem. Soc.* **2001**, *123*, 11 318.

40 Padwa, A.; Weingarten, M. D. *Chem. Rev.* **1996**, *96*, 223.

41 Doyle, M. P.; Hu, W.; Timmons, D. J. *Org. Lett.* **2001**, *3*, 3741.

42 Padwa, A.; Zhang, Z. J.; Zhi, L. *J. Org. Chem.* **2000**, *65*, 5223.

43 Padwa, A.; Chinn, R. L.; Hornbuckle, S. F.; Zhi, L. *Tetrahedron Lett.* **1989**, *30*, 301.

44 Padwa, A.; Hertzog, D. L.; Chinn, R. L. *Tetrahedron Lett.* **1989**, *30*, 4077.

45 Hamaguchi, M.; Ibata, T. *Chem. Lett.* **1975**, 499.

46 Ibata, T.; Hamaguchi, M.; Kiyohara, H. *Chem. Lett.* **1975**, 21.

47 Osterhout, M. H.; Nadler, W. R.; Padwa, A. *Synthesis* **1994**, 123.

48 Padwa, A.; Hertzog, D. L. *Tetrahedron* **1993**, *49*, 2589.

49 Padwa, A.; Hertzog, D. L.; Nadler, W. R. *J. Org. Chem.* **1994**, *59*, 7072.

50 Padwa, A.; Austin, D. J.; Price, A. T. *Tetrahedron Lett.* **1994**, *35*, 7159.

51 Padwa, A.; Hertzog, D. L.; Nadler, W. R.; Osterhout, M. H.; Price, A. T. *J. Org. Chem.* **1994**, *59*, 1418.

52 Padwa, A.; Austin, D. J.; Price, A.; Weingarten, M. D. *Tetrahedron* **1996**, *52*, 3247.

53 Hertzog, D. L.; Austin, D. J.; Nadler, W. R.; Padwa, A. *Tetrahedron Lett.* **1992**, *33*, 4731.

54 Padwa, A.; Kinder, F. R.; Nadler, W. R.; Zhi, L. *Heterocycles* **1993**, *35*, 367.

55 Mloston, G.; Romanski, J.; Heimgartner, H. *Pol. J. Chem.* **2002**, *76*, 551.

56 Padwa, A.; Kinder, F. R.; Zhi, L. *Synlett* **1991**, 287.

57 Hamaguchi, M.; Matsubara, H.; Nagai, T. *Tetrahedron Lett.* **2000**, *41*, 1457.

58 Padwa, A.; Dean, D. C. *J. Org. Chem.* **1990**, *55*, 405.

59 Padwa, A.; Dean, D. C.; Hertzog, D. L.; Nadler, W. R.; Zhi, L. *Tetrahedron* **1992**, *48*, 7565.

60 Padwa, A.; Dean, D.C.; Zhi, L. *J. Am. Chem. Soc.* **1992**, *114*, 593.

61 Padwa, A.; Austin, D.J.; Precedo, L.; Zhi, L. *J. Org. Chem.* **1993**, *58*, 1144.

62 Padwa, A.; Dean, D.C.; Osterhout, M.H.; Precedo, L.; Semones, M.A. *J. Org. Chem.* **1994**, *59*, 5347.

63 Padwa, A.; Hornbuckle, S.F.; Fryxell, G.E.; Stull, P. D. *J. Org. Chem.* **1989**, *54*, 817.

64 Kappe, C.O. *Tetrahedron Lett.* **1997**, *38*, 3323.

65 Padwa, A.; Snyder, J.P.; Curtis, E.A.; Sheehan, S.M.; Worsencroft, K.J.; Kappe, C.O. *J. Am. Chem. Soc.* **2000**, *122*, 8155.

66 Doyle, M.P.; Forbes, D. C. In *Nitrogen, Oxygen, and Sulfur Ylide Chemistry*, Clark, J. S., Ed.; Oxford University Press: Oxford, **2002**; Chapter 2.3, pp. 141–152.

67 Curtis, E.A.; Worsencroft, K.J.; Padwa, A. *Tetrahedron Lett.* **1997**, *38*, 3319.

68 Fukushima, K.; Ibata, T. *Bull. Chem. Soc. Jpn.* **1995**, *68*, 3469.

69 Ibata, T.; Fukushima, K. *Chem. Lett.* **1992**, 2197.

70 Padwa, A. *Top. Curr. Chem.* **1997**, *189*, 121.

71 Padwa, A. *Chem. Commun.* **1998**, 1417.

72 Padwa, A.; Dean, D.C.; Zhi, L. *J. Am. Chem. Soc.* **1989**, *111*, 6451.

73 Padwa, A.; Zhi, L. *J. Am. Chem. Soc.* **1990**, *112*, 2037.

74 Padwa, A.; Price, A.T.; Zhi, L. *J. Org. Chem.* **1996**, *61*, 2283.

75 Pirrung, M.C.; Zhang, J.; McPhail, A.T. *J. Org. Chem.* **1991**, *56*, 6269.

76 Padwa, A.; Hasegawa, T.; Liu, B.; Zhang, Z. *J. Org. Chem.* **2000**, *65*, 7124.

77 Doyle, M.P.; Hu, W.; Timmons, D.J. *Org. Lett.* **2001**, *3*, 933.

78 Padwa, A.; Chinn, R.L.; Hornbuckle, S.F.; Zhang, Z.J. *J. Org. Chem.* **1991**, *56*, 3271.

79 Dean, D.C.; Krumpe, K.E.; Padwa, A. *J. Chem. Soc., Chem. Commun.* **1989**, 921.

80 Doyle, M.P.; Pieters, R.J.; Taunton, J.; Pho, H.Q.; Padwa, A.; Hertzog, D.L.; Precedo, L. *J. Org. Chem.* **1991**, *56*, 820.

81 Padwa, A.; Austin, D.J.; Hornbuckle, S.F.; Semones, M.A.; Doyle, M.P.; Protopopova, M.N. *J. Am. Chem. Soc.* **1992**, *114*, 1874.

82 Padwa, A.; Austin, D.J.; Price, A.T.; Semones, M.A.; Doyle, M.P.; Protopopova, M.N.; Winchester, W.R.; Tran, A. *J. Am. Chem. Soc.* **1993**, *115*, 8669.

83 Padwa, A.; Austin, D.J.; Hornbuckle, S.F. *J. Org. Chem.* **1996**, *61*, 63.

84 Padwa, A.; Hornbuckle, S.F.; Fryxell, G.E.; Zhang, Z. J. *J. Org. Chem.* **1992**, *57*, 5747.

85 Cox, G.G.; Moody, C.J.; Austin, D.J.; Padwa, A. *Tetrahedron* **1993**, *49*, 5109.

86 Miah, S.; Slawin, A.M.Z.; Moody, C.J.; Sheehan, S. M.; Marino, J.P.,Jr.; Semones, M.A.; Padwa, A.; Richards, I.C. *Tetrahedron* **1996**, *52*, 2489.

87 Savinov, S.N.; Austin, D.J. *Chem. Commun.* **1999**, 1813.

88 Savinov, S.N.; Austin, D.J. *Org. Lett.* **2002**, *4*, 1419.

89 Prein, M.; Padwa, A. *Tetrahedron Lett.* **1996**, *37*, 6981.

90 Prein, M.; Manley, P.J.; Padwa, A. *Tetrahedron* **1997**, *53*, 7777.

91 Padwa, A. In *1,3-Dipolar Cycloaddition Chemistry*, Padwa, A., Ed.; Wiley: New York, **1984**; Vol. 2, pp. 277–406.

92 Padwa, A.; Austin, D. J.; Hornbuckle, S.F.; Price, A.T. *Tetrahedron Lett.* **1992**, *33*, 6427.

93 Suga, H.; Ishida, H.; Ibata, T. *Tetrahedron Lett.* **1998**, *39*, 3165.

94 Suga, H.; Kakehi, A.; Ito, S.; Inoue, K.; Ishida, H.; Ibata, T. *Org. Lett.* **2000**, *2*, 3145.

95 Pirrung, M.C.; Lee, Y.R. *J. Chem. Soc., Chem. Commun.* **1995**, 673.

96 Angell, R.; Drew, M.G.B.; Fengler-Veith, M.; Finch, H.; Harwood, L.M.; Jahans, A.W.; Tucker, T.T. *Tetrahedron Lett.* **1997**, *38*, 3107.

97 Angell, R.; Fengler-Veith, M.; Finch, H.; Harwood, L.M.; Tucker, T.T. *Tetrahedron Lett.* **1997**, *38*, 4517.

98 Padwa, A.; Prein, M. *Tetrahedron* **1998**, *54*, 6957.

99 Savinov, S.N.; Austin, D.J. *Org. Lett.* **2002**, *4*, 1415.

100 Ferris, L.; Haigh, D.; Moody, C.J. *Tetrahedron Lett.* **1996**, *37*, 107.

101 Hodgson, D.M.; Stupple, P.A.; Pierard, F.Y.T.M.; Labande, A.H.; Johnstone, C. *Eur. J. Chem.* **2001**, *7*, 4465.

102 Pirrung, M.C.; Zhang, J. *Tetrahedron Lett.* **1992**, *33*, 5987.

103 Ishitani, H.; Achiwa, K. *Heterocycles* **1997**, *46*, 153.

104 Hodgson, D.M.; Stupple, P.A.; Johnstone, C. *Tetrahedron Lett.* **1997**, *38*, 6471.

105 Davies, H.M.L.; Bruzinski, P.; Hutcheson, D.K.; Kong, N.; Fall, M.J. *J. Am. Chem. Soc.* **1996**, *118*, 6897.

106 Hodgson, D.M.; Stupple, P.A.; Johnstone, C. *Chem. Commun.* **1999**, 2185.

107 Hodgson, D.M.; Petroliagi, M. *Tetrahedron: Asymmetry* **2001**, *12*, 877.

108 Hodgson, D.M.; Glen, R.; Redgrave, A.J. *Tetrahedron Lett.* **2002**, *43*, 3927.

109 Hodgson, D.M.; Labande, A.H.; Pierard, F.Y.T.M. *Synlett* **2003**, 59.

110 Hodgson, D.M.; Glen, R.; Grant, G.H.; Redgrave, A.J. *J. Org. Chem.* **2003**, *68*, 581.

111 Hodgson, D.M.; Labande, A.H.; Glen, R.; Redgrave, A.J. *Tetrahedron: Asymmetry* **2003**, *14*, 921.

112 Kitagaki, S.; Anada, M.; Kataoka, O.; Matsuno, K.; Umeda, C.; Watanabe, N.; Hashimoto, S.-I. *J. Am. Chem. Soc.* **1999**, *121*, 1417.

113 Kitagaki, S.; Yasugahira, M.; Anada, M.; Nakajima, M.; Hashimoto, S. *Tetrahedron Lett.* **2000**, *41*, 5931.

114 Davies, H.M.L.; Xiang, B.; Kong, N.; Stafford, D.G. *J. Am. Chem. Soc.* **2001**, *123*, 7461.

115 Maier, M.E.; Schoeffling, B. *Chem. Ber.* **1989**, *122*, 1081.

116 Alt, M.; Maas, G. *Tetrahedron* **1994**, *50*, 7435.

117 Lee, Y.R. *Synth. Commun.* **1998**, *28*, 865.

118 Wang, Y.; Zhu, S. *Tetrahedron* **2001**, *57*, 3383.

119 Kinder, F.R.; Padwa, A. *Tetrahedron Lett.* **1990**, *31*, 6835.

120 Padwa, A.; Kinder, F.R. *J. Org. Chem.* **1993**, *58*, 21.

121 Padwa, A.; Straub, C.S. *Org. Lett.* **2000**, *2*, 2093.

122 Pirrung, M.C.; Zhang, J.; Lackey, K.; Sternbach, D.D.; Brown, F. *J. Org. Chem.* **1995**, *60*, 2112.

123 Lee, Y.R. *Bull. Kor. Chem. Soc.* **1996**, *17*, 579.

124 Kim, H.-S.; Lee, J.-Y.; Koh, Y.K.; Kwon, I.-C.; Choi, J.-H.; Suk, J.Y.; Lee, Y.R. *Bull. Kor. Chem. Soc.* **1997**, *18*, 1222.

125 Murphy, P.V.; O'Sullivan, T.J.; Kennedy, B.D.; Geraghty, N.W.A. *J. Chem. Soc., Perkin 1* **2000**, 2121.

126 Jauk, B.; Belaj, F.; Kappe, C.O. *J. Chem. Soc., Perkin Trans. 1* **1999**, 307.

127 Muthusamy, S.; Gunanathan, C. *Chem. Commun.* **2003**, 440.

128 Nair, V.; Santhi, V.; Sheela, K.C.; Radhakrishnan, K.V.; Rath, N.P. *Synthesis* **2003**, 1559.

129 Padwa, A.; Carter, S.P.; Nimmesgern, H.; Stull, P.D. *J. Am. Chem. Soc.* **1988**, *110*, 2894.

130 Bien, S.; Kimmel, T.; Tirosh, N. *Acta Chem. Scand.* **1993**, *47*, 218.

131 Muthusamy, S.; Arulananda Babu, S.; Gunanathan, C.; Suresh, E.; Dastidar, P.; Vir Jasra, R. *Tetrahedron* **2000**, *56*, 6307.

132 Nair, V.; Sheela, K.C.; Radhakrishnan, K.V.; Rath, N.P. *Tetrahedron Lett.* **1998**, *39*, 5627.

133 Muthusamy, S.; Babu, S.A.; Gunanathan, C. *Tetrahedron Lett.* **2000**, *41*, 8839.

134 Nair, V.; Sheela, K.C.; Sethumadhavan, D.; Bindu, S.; Rath, N.P.; Eigendorf, G.K. *Synlett* **2001**, 272.

135 Nair, V.; Sheela, K.C.; Sethumadhavan, D.; Dhanya, R.; Rath, N.P. *Tetrahedron* **2002**, *58*, 4171.

136 Pirrung, M.C.; Blume, F. *J. Org. Chem.* **1999**, *64*, 3642.

137 Pirrung, M.C.; Kaliappan, K.P. *Org. Lett.* **2000**, *2*, 353.

138 Muthusamy, S.; Babu, S.A.; Gunanathan, C.; Suresh, E.; Dastidar, P.; Jasra, R.V. *Tetrahedron* **2001**, *57*, 7009.

139 Muthusamy, S.; Babu, S.A.; Gunanathan, C.; Suresh, E.; Dastidar, P. *Bull. Chem. Soc. Jpn.* **2002**, *75*, 801.

140 Nair, V.; Rajesh, C.; Dhanya, R.; Vinod, A.U. *Tetrahedron Lett.* **2001**, *42*, 2045.

141 Muthusamy, S.; Babu, S.A.; Gunanathan, C.; Ganguly, B.; Suresh, E.; Dastidar, P. *J. Org. Chem.* **2002**, *67*, 8019.

142 Muthusamy, S.; Babu, S.A.; Gunanathan, C. *Tetrahedron Lett.* **2002**, *43*, 5981.

143 Skaggs, A.J.; Lin, E.Y.; Jamison, T.F. *Org. Lett.* **2002**, *4*, 2277.

144 Plüg, C.; Friedrichsen, W. *Tetrahedron Lett.* **1992**, *33*, 7509.

145 Baldwin, J.E.; Mayweg, A.V. W.; Neumann, K.; Pritchard, G.J. *Org. Lett.* **1999**, *1*, 1933.

146 Dauben, W.G.; Dinges, J.; Smith, T.C. *J. Org. Chem.* **1993**, *58*, 7635.

147 McMills, M.C.; Zhuang, L.; Wright, D.L.; Watt, W. *Tetrahedron Lett.* **1994**, *35*, 8311.

148 Koyama, H.; Ball, R.G.; Berger, G.D. *Tetrahedron Lett.* **1994**, *35*, 9185.

149 Kataoka, O.; Kitagaki, S.; Watanabe, N.; Kobayashi, J.-I.; Nakamura, S.-I.; Shiro, M.; Hashimoto, S.-I. *Tetrahedron Lett.* **1998**, *39*, 2371.

150 Hodgson, D.M.; Bailey, J. M.; Harrison, T. *Tetrahedron Lett.* **1996**, *37*, 4623.

151 Hodgson, D.M.; Bailey, J.M.; Villalonga-Barber, C.; Drew, M.G.B.; Harrison, T. *J. Chem. Soc., Perkin Trans. 1* **2000**, 3432.

152 Hodgson, D.M.; Villalonga-Barber, C. *Tetrahedron Lett.* **2000**, *41*, 5597.

153 Pirrung, M.C.; Lee, Y.R. *Tetrahedron Lett.* **1994**, *35*, 6231.

154 Pirrung, M.C.; Zhang, J.; Morehead, A.T., Jr. *Tetrahedron Lett.* **1994**, *35*, 6299.

155 Pirrung, M.C.; Lee, Y.R. *Tetrahedron Lett.* **1996**, *37*, 2391.

156 Padwa, A.; Sandanayaka, V.P.; Curtis, E.A. *J. Am. Chem. Soc.* **1994**, *116*, 2667.

157 Kinder, F.R., Jr.; Bair, K.W. *J. Org. Chem.* **1994**, *59*, 6965.

158 Padwa, A.; Curtis, E.A.; Sandanayaka, V.P.; Weingarten, M.D. *Electronic Conference on Trends in Organic Chemistry [CD-ROM]* **1996**, http://www.ch.ic.ac.uk/ectoc/papers/01/.

159 Padwa, A.; Curtis, E.A.; Sandanayaka, V.P. *J. Org. Chem.* **1997**, *62*, 1317.

160 Padwa, A.; Curtis, E.A.; Sandanayaka, V.P. *J. Org. Chem.* **1996**, *61*, 73.

161 Padwa, A. *Farmaco* **1997**, *52*, 303.

162 McMorris, T.C.; Yu, J.; Hu, Y. *J. Org. Chem.* **1997**, *62*, 3015.

163 Padwa, A.; Brodney, M.A.; Marino, J.P., Jr.; Osterhout, M.H.; Price, A.T. *J. Org. Chem.* **1997**, *62*, 67.

164 Padwa, A.; Brodney, M.A.; Marino, J.P., Jr.; Sheehan, S.M. *J. Org. Chem.* **1997**, *62*, 78.

165 Marino, J.P., Jr.; Osterhout, M.H.; Padwa, A. *J. Org. Chem.* **1995**, *60*, 2704.

166 Moody, C.J.; Slawin, A.M.Z.; Willows, D. *Org. Biomol. Chem.* **2003**, *1*, 2716.

167 Chiu, P.; Chen, B.; Cheng, K.F. *Org. Lett.* **2001**, *3*, 1721.

168 Chen, B.; Ko, R.Y.Y.; Yuen, M.S.M.; Cheng, K.-F.; Chiu, P. *J. Org. Chem.* **2003**, *68*, 4195.

169 Padwa, A.; Sheehan, S.M.; Straub, C.S. *J. Org. Chem.* **1999**, *64*, 8648.

170 Sheehan, S.M.; Padwa, A. *J. Org. Chem.* **1997**, *62*, 438.

171 Padwa, A.; Price, A.T. *J. Org. Chem.* **1995**, *60*, 6258.

172 Padwa, A.; Price, A.T. *J. Org. Chem.* **1998**, *63*, 556.

173 Kissel, W.S.; Padwa, A. *Tetrahedron Lett.* **1999**, *40*, 4003.

174 Padwa, A.; Precedo, L.; Semones, M.A. *J. Org. Chem.* **1999**, *64*, 4079.

175 Wood, J.L.; Thompson, B.D.; Yusuff, N.; Pflum, D.A.; Matthaeus, M.S.P. *J. Am. Chem. Soc.* **2001**, *123*, 2097.

176 Gowravaram, M.R.; Gallop, M.A. *Tetrahedron Lett.* **1997**, *38*, 6973.

177 Whitehouse, D.L.; Nelson, K.H., Jr.; Savinov, S.N.; Austin, D.J. *Tetrahedron Lett.* **1997**, *38*, 7139.

178 Whitehouse, D.L.; Nelson, K.H., Jr.; Savinov, S.N.; Lowe, R.S.; Austin, D.J. *Bioorg. Med. Chem.* **1998**, *6*, 1273.

179 Liu, F.; Austin, D.J. *Org. Lett.* **2001**, *3*, 2273.

Subject Index

Modern Rhodium-Catalyzed Organic Reactions. Edited by P. Andrew Evans

ISBN: 3-527-30683-8